AFOSR   SCEEE

USAF RESEARCH INITIATION PROGRAM
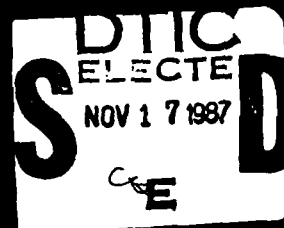
1984

RESEARCH REPORTS

VOLUME I

CONDUCTED BY

THE SOUTHEASTERN CENTER FOR

ELECTRICAL ENGINEERING EDUCATION

PROF. WARREN D. PEELE

PROGRAM DIRECTOR, SCEEE

MAJ. AMOS OTIS

PROGRAM MANAGER, AFOSR

REPORT DOCUMENTATION PAGE

Form Approved
OMB No. 0704-0188

1a. REPORT SECURITY CLASSIFICATION UNCLASSIFIED	1b. RESTRICTIVE MARKINGS
2a. SECURITY CLASSIFICATION AUTHORITY	3. DISTRIBUTION/AVAILABILITY OF REPORT
2b. DECLASSIFICATION/DOWNGRADING SCHEDULE	Approved for public release; distribution unlimited.

4. PERFORMING ORGANIZATION REPORT NUMBER(S)	5. MONITORING ORGANIZATION REPORT NUMBER(S) AFOSR-TR- 87-1720

6a. NAME OF PERFORMING ORGANIZATION The Southeastern Center for Electrical Engineering Education	6b. OFFICE SYMBOL (If applicable)	7a. NAME OF MONITORING ORGANIZATION Air Force Office of Scientific Research/XOT
6c. ADDRESS (City, State, and ZIP Code) 11th & Massachusetts Ave. St. Cloud, Florida 32769		7b. ADDRESS (City, State, and ZIP Code) Building 410 Bolling AFB, DC 20332

8a. NAME OF FUNDING/SPONSORING ORGANIZATION AFOSR	8b. OFFICE SYMBOL (If applicable) XOT	9. PROCUREMENT INSTRUMENT IDENTIFICATION NUMBER F49620-82-C-0035

8c. ADDRESS (City, State, and ZIP Code)	10. SOURCE OF FUNDING NUMBERS			
Building 410 Bolling AFB, DC 20332	PROGRAM ELEMENT NO. 61102F	PROJECT NO. 2301	TASK NO D5	WORK UNIT ACCESSION NO.

11. TITLE (Include Security Classification)

USAF Research Initiation Program - Volume 1

12. PERSONAL AUTHOR(S)
Prof. Warren D. Peele

13a. TYPE OF REPORT Interim	13b. TIME COVERED FROM _____ TO _____	14. DATE OF REPORT (Year, Month, Day) May 86	15. PAGE COUNT

16. SUPPLEMENTARY NOTATION

17. COSATI CODES			18. SUBJECT TERMS (Continue on reverse if necessary and identify by block number)
FIELD	GROUP	SUB-GROUP	

19. ABSTRACT (Continue on reverse if necessary and identify by block number)

(SEE REVERSE)

20. DISTRIBUTION/AVAILABILITY OF ABSTRACT ☒ UNCLASSIFIED/UNLIMITED ☐ SAME AS RPT ☐ DTIC USERS	21 ABSTRACT SECURITY CLASSIFICATION UNCLASSIFIED
22a NAME OF RESPONSIBLE INDIVIDUAL Amos Otis, Major, Program Manager	22b TELEPHONE (Include Area Code) (202) 767-4971	22c OFFICE SYMBOL XOT

DD Form 1473, JUN 86   Previous editions are obsolete   SECURITY CLASSIFICATION OF THIS PAGE

Research Initiation Program - 1984

AFOSR·TR· 87 - 1720

For several years prior to 1983, AFOSR conducted a special follow-on funding program for Summer Faculty Research Program (SFRP) participants; this was popularly known as the AFOSR Minigrant Program. That program was superceded in 1983 by the Research Initiation Program conducted by SCEEE.

To compete for a 1984 Research Initiation Program award, SFRP participants must submit a complete proposal .and proposed budget either during or promptly after their SFRP appointment periods. Awards to the 1984 participants may extend through 15 December 1985.

Each proposal was evaluated for technical excellence, with special emphasis on relevance to continuation of the SFRP effort, as determined by the Air Force laboratory/center. The final selection of awards was the responsibility of AFOSR.

The most effective proposals were those which were closely coordinated with the SFRP Effort Focal Point and which followed the SFRP effort with proposed research having strong prospects for later sustained funding by the Air Force laboratory/center.

The maximum award under the Research Initiation Program is $12,000 plus cost-sharing up to a matching total amount.

The mechanics of applying for a Research Initiation Program award are as follows:

(1) Research Initiation Program proposals of $12,000 plus cost-sharing were to be submitted after August 1, 1984 but no later than November 1, 1984.

(2) Proposals were evaluated and the final award decision was the responsibility of AFOSR after consultation with the Air Force Laboratory/center.

(3) The total available funding limited the number of awards to approximately half the number of 1984 SFRP participants.

(4) Subcontracts were negotiated with the employing institution, designating the SFRP participant as Principal Investigator, with the period of award having a start date no earlier than September 1, 1984 and a completion date no later than December 15, 1985.

Employing institutions were encouraged to cost-share since the program was designed as a research initiation procedure. Budgets included, where applicable, Principal Investigator time, graduate assistant and support effort, equipment and expendable supplies, travel and per diem costs, conference fees, indirect costs, and computer charges.

Volumes I, II, III, and IV of the 1984 Research Initiation Program Report contain copies of reports on the 89 subcontract efforts awarded under this program.

AFOSR-TR- 87-1720

①

DTIC
ELECTE
NOV 1 7 1987
S
D
E

87

1984 USAF/SCEEE RESEARCH INITIATION PROGRAM

Conducted by

Southeastern Center for

Electrical Engineering Education

under

USAF Contract Number F49620-82-C-0035

RESEARCH REPORTS

Volume I of IV

submitted to

Air Force Office of Scientific Research

Bolling Air Force Base

Washington, DC

BY

Southeastern Center for
Electrical Engineering Education

May 1986

AN ANALYTICAL STUDY OF
TWO-STAGE LIGHT GAS GUN PERFORMANCE

by

Dr. Robert W. Courter, Associate Professor
Michael D. Champagne, Graduate Student
Raymond M. Patin, Graduate Student

Department of Mechanical Engineering
Louisiana State University

October 31, 1985

PREFACE

The work presented in this report was initiated in the Summer of 1984 as part of a summer research program sponsored by the Southeastern Center for Electrical Engineering Education and the United States Air Force. Professor R. W. Courter and his graduate student, Raymond M. Patin, worked with members of the technical staff at the Aeroballistics Branch of the Armament Laboratory at Eglin AFB, Florida, to formulate the basic model.

The work was continued during the following year under subcontract to SCEEE as part of Air Force Contract Number F49620-82-C-0035. During that year the basic analysis was expanded and refined into a simple, but effective, simulation model of a two-stage light gas gun with deformable piston. An interactive microprocessor-based computer program and a report describing the model were delivered to the Air Force Armament Laboratory in May of 1985. This work constitutes the major portion of the contract work and is included as Part 1 of this present report.

One of the possible inconsistencies inherent in the Patin model is the treatment of the pump tube flow as one dimensional, isentropic flow of an ideal gas. The second part of this report addresses deviations from this model. Graduate student Michael Champagne has worked to incorporate a finite difference treatment of the pump tube flow to account for pressure variations between piston and projectile which are not considered in the Patin model and to include a real gas equation of state. Part 2 of the present report documents this work. The complete work will appear in the form of a thesis in May, 1986.

PART 1:   A Mathematical Model
                              of a Two-State Light Gas Gun
                                with a Jeformable Piston

Raymond M. Patin
Robert W. Courter

ABSTRACT

A time-dependent model of the internal ballistics of a two-stage light
gas gun is derived which predicts internal pressures and the kinematics of
the piston and the projectile. The method of analysis used is to model
each of the four physical processes which occur separately and then to link
them together using the thermodynamic and kinematic relationships for the
gases involved. The interior ballistics model for the first stage of the
gun is based on a formulation developed by O. K. Heiney. Piston and
projectile kinematics are determined from Newton's equation of motion, in
which firctional effects are included. The pressure-volume relationships
in the second (light gas) stage of the gun are assumed to be isentropic.
Piston extrusion effects in the transition section of the gun are accounted
for by including in the analysis an extrusion force which represents all of
the losses incurred as the piston extrudes. Comparisons of model perfor-
mance predictions with experimental data generated at Eglin AFB, Florida,
indicate that the model correlates well with the actual processes which
occur in the light gas gun. Additional work is suggested in defining the
pressure distribution between the piston face and the projectile base to
enable the model to match a wide range of experimental data.

INTRODUCTION

Ballistic testing in an instrumented free-flight range is an important part of the broad field of experimental aerodynamics. The flight conditions of the model being tested are determined by the launcher being used. It is important in ballistic testing, therefore, to have the capability of predicting the launcher performance so that a test program can be planned. The planning of a test program for models requires predictable muzzle velocities to provide the proper model flight regime, and knowledge of acceleration profiles to ensure that fragile models will not be damaged.

In the introduction, the topics to be covered are as follows: First, a few of the aspects of basic gun theory will be discussed. Then, some of the types of compressed gas launchers which exist will be described. This discussion will be followed by a detailed description of the two-stage light gas gun which is being modeled, along with the research objectives, and finally, the literature which was used in the course of this work will be reviewed.

1.1 BASIC GUN THEORY

A gun may be defined as a mechanical device in which the transfer of energy provides for the propulsion of projectiles toward specified targets. Internal ballistics

is the study of the processes which occur within the gun system, from the point of ignition to the time the projectile leaves the barrel of the gun. Through an analysis of the interior ballistics of a gun system, one attempts to predict the gun performance. This entails predictions of the projectile velocity, gas pressures, and the kinetics involved. The essential factors which dictate the velocity of the projectile may be determined by applying Newton's second law to a projectile. A schematic diagram of a projectile during its travel down the barrel of a conventional powder gun is shown in figure 1. In the application of Newton's law to the projectile, if frictional forces and the air resistance ahead of the projectile are neglected, the projectile velocity may be determined to be[1]

$$\dot{X}_s = \sqrt{2P_{av}A_bL_bg_c/m_s} \tag{1.1}$$

where, the value P_{av} represents the average pressure of the propellant gas, which is defined by[1]

$$P_{av} = \frac{1}{L_b} \int_0^{L_b} P_{sb} \, dX_s \tag{1.2}$$

In order to increase the velocity of the projectile, the term under the radical in equation (1.1) must be increased. The cross-sectional area of the barrel, A_b, along with the length of the barrel, L_b, are usually fixed for a particular gun system; therefore, these parameters normally cannot be

1.5

altered. The velocity of the projectile can therefore be varied by changing either the projectile mass or the average pressure of the propellant gas. For a specified gun system and projectile mass, the projectile velocity can be increased only by increasing the average pressure of the propellant gases. In a conventional gun, which is shown in figure 1, the propellant gas pressure is effectively increased by increasing the mass of the powder charge used. The powder charge in a gun system consists of a smokeless powder, which is also known as the gun propellant, since this substance produces the gases which propel the projectile. The smokeless powder contains one or more explosive ingredients mixed with additives which stabilize the mixture and produce the desired burning characteristics. The smokeless powder charge is a solid, and it may be formed into various shapes. Upon ignition of the gun system, the solid propellant charge begins to burn, and chemical energy is transformed into heat energy as hot gases are produced. Higher projectile velocities can be achieved by increasing the mass of the powder charge used which, in turn, increases the average pressure of the propellant gases. The increase in projectile velocity achieved with increases in the mass of the powder charge, however, is not unlimited. The limiting factor involved is the large mass of the propellant gases themselves. A qualitative explanation of this is as follows: The gases produced by the burning of the smokeless powder charge are extremely heavy. The molecular weight of

1.6

these gases is approximately 23 (the molecular weight will vary with the type of powder charge used). At high levels of gun performance, considerable energy is required to accelerate these heavy gases down the barrel of the gun; thus, less energy is available for the acceleration of the projectile. Due to the inertia of the propellant gases, the maximum velocity attainable with specially strengthened conventional guns, using low mass projectiles, is approximately 12,000 ft/s[1].

From the previous discussion, it can be deduced that in order to achieve higher projectile velocities, a "light gas", which has a lower inertia, must be used. Less energy will be required to accelerate a light gas down the barrel of a gun; therefore, more energy is available for the acceleration of the projectile. This results in the attainment of higher projectile velocities. The acoustic impedance plays the role of the inertia of the gas, and it is equal to the sound speed of the gas times its density. A gas such as hydrogen or helium satisfies the requirements of a light gas, and either one of these gases may be used in a gun to achieve higher projectile velocities. An analytical treatment of the discussion, which is given above, can be found in reference 1, pages 16 through 20.

The method by which the light gas is heated to attain high pressures and temperatures constitutes the different types of high performance launchers which exist. Some of these are discussed in the following section.

1.2 TYPES OF HIGH PERFORMANCE LAUNCHERS

In the firing sequence of the gun, energy must be input into the light gas, and a portion of this energy will in turn be imparted to the projectile. Some of the ways in which the light gas may be energized are described below.

One method of heating the light gas is by means of a chemical reaction. The energy released from the chemical reaction is transferred to the light gas raising the pressure and temperature of the gas. The reactants which are commonly used in the chemical reaction are hydrogen and oxygen.

The light gas may be heated by means of electrical energy. This technique is termed electrical arc heating and is accomplished with high inputs of electrical energy.

Another method by which the light gas may be heated is with the use of shock waves. This technique is called shock heating. The passage of shock waves compresses the gas, causing increases in its pressure and temperature. The generation of shock waves may be accomplished in two ways. The first method by which shock waves may be generated is with the failure of a diaphragm, which isolates the propellant chamber in the rear of the gun from the light gas. The second method is to use a light piston which travels at high velocities. As the piston attains high velocities with respect to the sound speed of the light gas, compression waves coalesce to form a shock wave which

1.8

compresses the gas ahead of the piston. A high performance launcher in which a piston is used as the means of energy transfer is called a two-stage gun. The type of two-stage gas gun described above is known as a shock-compression gun, and the second type of two-stage gun is an isentropic-compression gun. An isentropic-compression gun operates with a heavy, slow moving piston. No shock wave forms ahead of the piston, and the compression process is assumed to be isentropic.

This completes the discussion on several of the types of high performance launchers which have been developed. A detailed discussion of the light gas gun which is modeled in the present study will be given below.

1.3 THE TWO-STAGE LIGHT GAS GUN

A schematic diagram of the two-stage light gas gun which is being modeled is shown in figure 2. The term two-stage implies the presence of two separate gas chambers in the gun. The first chamber contains energetic gases which are produced by the burning of a smokeless powder charge. This gas will be termed the propellant gas due to its application in conventional guns. The second chamber contains the light gas which is used to accelerate the projectile. Energy is transferred from the propellant gases to the light gas by means of a free piston. The piston used in the gun which is being modeled is a deformable piston made of polypropylux. The piston is shown schematically in figure 3. The mass of the piston is varied by the addition

of lead pellets to a chamber in the rear of the piston. The rubber O-rings and the cupped face on the piston act as seals which prevent the leakage of the propellant gas and/or the light gas from occurring at the piston/pump tube interface. The piston motion is restrained up to a certain propellant gas pressure by the flared cap at its base. This pressure is called the shot-start pressure of the piston. A flat, scored, metal diaphragm isolates the projectile from the light gas up to a specified pressure. As the diaphragm fails, the projectile is subjected to the high pressure light gas which accelerates the projectile down the launch tube of the gun. In this paper, the term projectile refers to two separate components: the free-flight model and its carrier, which is called the sabot. The model is the part of interest, and free-flight tests are conducted with different model sizes and configurations. The use of a sabot allows the testing of oddly shaped models to be conducted since the model configuration is not restricted to the shape or size of the launch tube bore. The base of the projectile is termed the obturator, and its purpose is twofold. It acts to seal the bore of the launch tube, preventing any leakage of the light gas at the projectile/launch tube interface. The obturator also provides a foundation for distributing the propelling force onto the base of the model. The obturator may be an integral part of the sabot or it may be a separate entity, depending upon the design. A schematic diagram of a projectile is shown in figure 4. With the

1.10

components of the two-stage light gas gun described, the events which occur as the gun is fired will now be discussed.

The firing of the two-stage gas gun is initiated with the ignition of a primer charge. The primer is simply a small propellant charge, and it may be ignited by means of electrical heating or by the mechanical crushing of a small explosive in the primer. As the primer burns, hot gases and particles are released into the powder charge. The individual pieces of propellant charge are called granules. As the hot primer gases flow into the propellant charge, heat transfer to the propellant granules occurs mainly by conduction and radiation. As the surface temperature of the propellant granules increases, they ignite and hot gases evolve as the propellant granules burn. These hot gases begin to spread through the combustion chamber, igniting more of the propellant granules. As this occurs, pressure waves develop which pass through the propellant and reflect off the sides of the chamber of the gun. These pressure fluctuations tend to cause uneven burning of the powder charge. The propellant gases continue to be produced as long as the charge is still burning. Piston motion will not begin until the shot-start pressure of the piston is attained by the propellant gases. At the shot-start pressure, the flared skirt at the base of the piston extrudes into the pump tube, and piston motion proceeds. As the piston travels into the pump tube, the light gas ahead

1.11

of the piston is compressed to high pressures and temperatures. The entire propellant charge is consumed after the piston has traveled only a short distance. However, enough energy will have been imparted to the piston so that the shot may be completed. As the pressure of the light gas reaches the failure strength of the diaphragm, the diaphragm bursts, and the projectile base is subjected to the energized light gas. The light gas now provides the propelling force which accelerates the projectile down the launch tube. As the projectile is traveling in the launch tube, the deformable piston continues its forward motion. The piston eventually enters the transition section of the gun, where it undergoes plastic deformation. For the purpose of internal ballistics, the shot is completed once the projectile has left the launch tube and the piston has come to rest in the transition section of the gun. With the gun system and the firing sequence defined, the objectives may now be set forth.

The objective of this work is to develop a mathematical model for the two-stage light gas gun shown in figure 2 which will accurately predict the internal ballistics of the gun for a given set of loading conditions. The literature used in the course of this analysis will be reviewed in the following section.

1.12

1.4 LITERATURE REVIEW

The first successful two-stage light gas gun was developed in 1946 at the New Mexico School of Mines[2]. Since that time, much work has been done in the analysis of guns of this type (References 2 and 11 through 17).

The processes which occur in the first stage of the two-stage light gas gun are identical to those which occur in a conventional powder gun. These processes in turn, are dependent upon the type of propellant used and its characteristics (References 3,4, and 18 through 22).

The extrusion of the deformable piston in the transition section of the gun is based on information provided from the analysis performed in metal working processes (References 5 and 6). Material properties of the piston material were obtained from Reference 7.

The pressure at which the diaphragm fails is based on design considerations. The diaphragm design will ultimately affect its opening characteristics (References 8 and 9).

The present method of gas gun modeling involves successive analysis of the first-stage processes, piston kinetics, and projectile kinetics. The governing equations are then obtained by linking together these relationships using the thermodynamic and kinematic relationships for the gases involved (References 23 & 24).

The final step in the development of a model involves the creation of a computer program which numerically integrates four ordinary, non-linear differential equations

1.13

simultaneously (Reference 10).

This completes the literature review and also the introductory chapter. The next chapter covers the analysis of the gun in detail.

ANALYSIS

The firing sequence of the two-stage light gas gun which is being modeled consists of four separate physical processes. These processes are the burning of the powder charge, the time rate of change of the propellant gas pressure, piston kinetics, and projectile kinetics. Each of these distinct physical processes is modeled individually. The relations which are obtained are linked together with the thermodynamic and kinematic relationships for the gases involved. This results in a set of four coupled, non-linear, ordinary differential equations. These equations are the governing equations which model the physical processes that occur in the gas gun. The analysis of each of the processes involved, along with the assumptions made, is presented below.

2.1 THE INTERIOR BALLISTIC EQUATION

The first stage of the light gas gun consists of gases at high pressures and temperatures which are produced by the burning of a smokeless powder charge. The process by which the gases are produced from the powder charge and the rate at which the pressure changes are identical to the processes which occur in a conventional gun. Therefore, the modeling of the first stage in the light gas gun is based on a formulation developed by Heiney[3], in which the interior

ballistics for a conventional gun are determined.

As the powder charge burns, chemical energy is converted into heat energy. The principle of conservation of energy is used to define the distribution of the energy released by the powder charge

$$E_1 = E_2 + E_3 + E_4 \tag{2.1}$$

In equation (2.1), the term E_2, defines the translational energy of the piston. This term is expressed mathematically as

$$E_2 = \frac{1}{2} \frac{m_p}{g_c} \dot{x}_p^2 \tag{2.2}$$

The term E_3, in equation (2.1), describes the heat loss from the propellant gases to inner surfaces of the gun. This loss is accounted for by means of an adjustment factor, which is applied to the translational kinetic energy term, in which the piston mass has been artificially increased. The combination of these terms in the kinetic energy relation results in a reduction of the total energy available for acceleration of the piston. The heat loss term is thus defined as

$$E_3 = \frac{1}{2} \beta \frac{m_a}{g_c} \dot{x}_p^2 \tag{2.3}$$

The adjustment factor, β, in equation (2.3) is the heat loss factor, and the corrected piston mass term is called

I.16

the pseudo-mass of the piston, denoted by m_a. The piston
pseudo mass is defined as

$$m_a = m_p + \frac{C_w}{3} \qquad (2.4)$$

The final term in equation (2.1) is the energy required
to accelerate the propellant gases and the unburned
propellant granules down the pump tube of the gun. The
energy required for this process is accounted for by means
of a kinetic energy term in which only a fraction of the
mass of propellant gases and unburned granules is considered
to be accelerated into the bore of the gun. The energy lost
in accelerating the propellant gases and unburned propellant
granules is therefore defined by

$$E_4 = \frac{1}{2} \frac{C_w}{3 g_c} \dot{x}_p^2 \qquad (2.5)$$

In equation (2.5), the factor 3, is the density
distribution factor. This factor dictates that only a
portion of the propellant gases and granules will be
accelerated into the pump tube of the gun. The value of the
density distribution factor is constant and is approximately
equal to three. This implies that only a third of the
propellant gases are assumed to be accelerated into the pump
tube of the gun.

In order to obtain the interior ballistic equation,
which defines the pressure of the gases produced by the

burning of the propellant charge, an equation of state is required along with some of the characteristic properties of the powder charge used. An equation of state is a relationship which expresses the intensive parameters in terms of the extensive parameters. The equation of state used to describe the propellant gases is the Nobel-Able equation of state

$$P_{av}(V_c - nN_b) = N_b R_p T_o \qquad (2.6)$$

The Nobel-Able equation of state is a simplified form of the Van der Waal's equation of state. However, the term which accounts for the effect of molecular attractive forces has been omitted. In the Nobel-Able equation of state, only the effect of molecular volume is considered.

The temperature at which the propellant charge burns is known as the flame temperature, and it is related to the impetus of the propellant. The impetus, or force constant, of the propellant is a characteristic quantity of each type of propellant which defines the amount of energy a certain mass of propellant is capable of releasing. It is defined as

$$F_p = R_p T_o \qquad (2.7)$$

The impetus is used to define E_1, the total energy released by the powder charge.

· The expressions in equations (2.2) through (2.7) are used to solve for the interior ballistic equation which models the processes that occur in the first stage of the

1.18

gas gun. The ballistic equation is obtained from equation (2.1), and the differential form of this equation, which is used in the present model, is

$$\frac{dP_{av}}{dt} \left[V_c + X_p A_{pt} - \frac{(C_w - N_b)}{\rho_p} - \eta N_b \right] =$$

$$\frac{dN_b}{dt} F_p - (\gamma_p - 1)(1 + \beta) \frac{m_a}{g_c} \frac{d\dot{X}_p}{dt} \frac{dX_p}{dt} - P_{av} A_{pt} \dot{X}_p$$

(2.8)

In the above formulation, the gases which are produced by the burning of the powder charge are considered to be a homogeneous mixture. The interior ballistic equation given above, therefore, defines only the average pressure of the propellant gases, and this pressure occurs at all points in the propellant gas.

In order to completely define the interior ballistic equation given in (2.8), the functions which describe the rate at which the propellant gas is produced (dN_b/dt) and the acceleration of the piston must be defined. The time rate of propellant gas production is considered next.

The rate at which the powder charge is consumed is equal to the rate at which propellant gases are produced. This term is expressed as[3]

$$\frac{dN_b}{dt} = r S_b \rho_p$$

(2.9)

In equation (2.9), r defines the rate of reduction in size

1.19

of the propellant granules as burning proceeds. This parameter is known as the burning rate. Typically, the burning rate of the propellant is obtained by fitting the burn rate vs pressure data obtained in closed vessel test firings of the propellant to Vielle's equation, which relates the burning rate to the propellant gas pressure. Vielle's equation is defined as

$$r = BP_{av}^{N} \tag{2.10}$$

The burning of the propellant in closed vessel tests, however, does not simulate the burning conditions which actually occur in the gun system. In order to account for the dynamic effects that the burning propellant charge actually experiences, such as erosive burning, several modified forms of Vielle's equation have evolved[4]. The burn rate equation used in the present model is as follows

$$r = BP_{av}^{N} + K_v \dot{X}_p \tag{2.11}$$

In the burn rate equation given above, the coefficient K_v, is an adjustable constant which accounts for the effects of erosive burning. Erosive burning is defined as follows: As the velocity of the propellant gases near the surface of the granules increases, the heat transfer into the propellant granules also increases. The additional transfer of heat acts to increase the rate at which the propellant granules burn or regress. In the present model, the propellant erosive constant K_v, is defined by the ratio of the volume

of the powder charge to the volume of the breech, times 0.31. With the propellant erosion constant defined in this manner, the value of the constant will be different for shots in which different charge weights are used.

The final term to be defined in equation (2.9) is the exposed burning surface of the propellant granules. Propellant granules are formed into many different shapes and sizes. The expression, which defines the surface area of the propellant granules as burning proceeds, depends on the initial configuration of the propellant granules. The only propellant configuration which has been used in the gas gun to date is a single perforation type of propellant. Therefore, the present model considers only this particular configuration of propellant granules. The burning surface area of a single perforation propellant granule, in which the length is greater than the diameter, is defined by[3]

$$S_b = \frac{2 \ C_w}{c_p \ w_o} \tag{2.12}$$

The rate at which the propellant charge is consumed may now be defined with the use of equations (2.11) and (2.12) as

$$\frac{dN_b}{dt} = (B P_{av}{}^N + K_v \dot{X}_p) \ \frac{2 \ C_w}{w_o} \tag{2.13}$$

The remaining term to be defined in the interior ballistic equation of the first stage is that of the piston

1.21

acceleration. The acceleration of the piston deals with piston kinetics and will therefore be discussed in the next section. However, before proceeding with the analysis of piston kinetics, the assumptions made thus far in the modeling of the first stage of the gas gun will be summarized :

1) At time equals zero, all of the propellant granules have been ignited simultaneously and uniformly.

2) The effects of pressure oscillations which occur in the breech upon ignition are neglected.

3) All of the propellant granules are of the same size and are of uniform shape.

4) The gases produced from the powder charge are described by the Nobel-Able equation of state.

5) Dissociation of the main constituents of the propellant gas is negligible.

6) The heat loss from the propellant gases to the gun surface is accounted for by adjustment factors which reduce the energy available for acceleration of the piston.

7) There is no leakage of gases at the breech of the gun, around the piston, or at any of the connection points.

The analysis involved in determining the piston dynamics will now be examined.

2.2 PISTON KINETICS

The type of piston used in the light gas gun, which is being modeled, is a deformable piston which is made out of polyproxylux (figure 3). The piston is made such that lead pellets may be placed in a cavity in the back of the piston. This permits variations in the mass of the piston. During the firing sequence, four different types of forces will act on the piston. The high pressure and temperature propellant gas, which is generated by the burning powder charge, produces a force which propels the piston into the pump tube. As piston motion proceeds, a frictional force occurs at the contact surface of the piston and the pump tube which acts to retard the piston motion. As the piston travels into the pump tube, the light gas ahead of the piston is compressed, and this gas pressure produces a retarding force on the piston. The final force which acts on the piston is an extrusion force. As the piston enters the transition region of the gun, it undergoes deformations. The forces which cause this deformation are called the extrusion forces. The analysis of each of these forces will now be considered.

The interior ballistic equation, which models the processes in the first stage of the light gas gun, considers the propellant gas to be a homogenous mixture. The value of the propellant gas pressure which is computed from equation (2.8) is, therefore, only an average value, and this pressure is taken to exist at all points in the gas. The

1.23

pressure which is computed from equation (2.8) will not accurately model the pressure which acts on the base of the piston, since in actuality, a pressure gradient exists in the propellant gas. The existence of a pressure gradient implies that the gas pressure at the breech of the gun will be higher than the gas pressure at the piston base. To account for the effects of the pressure gradient, an expression which relates the piston base pressure to the average pressure is used[3]

$$P_{pb} = P_{av}\left[1 + \frac{\gamma_p - 1}{2\,\Phi}\,\frac{\dot{x}_p^2}{.7g_c\gamma_p F_p}\right]^{-\frac{\gamma_p}{\gamma_p - 1}} \qquad (2.14)$$

In equation (2.14) the temperature of the propellant gases is needed to define the gas sound speed. During the firing sequence the gas temperature changes constantly. However, the gas temperature is approximated as $.7T_o^3$.

With the base pressure on the piston known, the force on the piston due to the propellant gas is simply the pressure multiplied by the cross sectional area of the pump tube

$$FP_1 = P_{pb} \times A_{pt} \qquad (2.15)$$

As mentioned previously, the average value of the propellant gas pressure in equation (2.14) is defined by equation (2.8) to the point of diaphragm failure. After the diaphragm

1.24

fails, the rate of change of the average gas pressure is described using the following relation

$$\frac{dP_{av}}{dt} = -P_{av_o} \gamma_p \dot{X}_p A_{pt} \Psi_p^{\gamma_p} (\Psi_p - A_{pt} X_p)^{-(\gamma_p - 1)} \qquad (2.16)$$

Equation (2.16) is simply the differential form of the isentropic pressure relationship. The reason for using this equation to define P_{av} after the diaphragm has failed, instead of equation (2.8), is as follows: At the time of diaphragm failure, the entire powder charge has been consumed ($dN_b/dt = 0$), and the piston is decelerating rapidly, which implies a negative value for the acceleration. As this takes place, the rate of change of the propellant gas pressure will become positive, and the propellant gas pressure, as defined by equation (2.8), will begin to increase, even though the gas is continuing to expand. Since this does not occur in reality, and since a rise in propellant gas pressure would have adverse effects on the extrusion calculations, equation (2.16) is used to define the propellant gas pressure after the diaphragm fails.

The force on the piston due to the propellant gases has been defined. The next force which will be considered is the friction force which acts on the piston.

Piston motion does not begin until the propellant gas pressure reaches a certain value. The pressure at which the

motion begins is called the shot-start pressure. As the
shot start pressure is reached, the flared portion of the
piston extrudes into the pump tube, and piston motion
begins. The initial magnitude of the friction force which
acts on the piston is assumed to be the force which must be
overcome at the shot start pressure. This force is defined
by

$$FR_1 = (P_{sp} - P_{He_1}) A_{pt} \tag{2.17}$$

As the piston motion proceeds, its velocity increases and
the flared skirt and the rubber O-rings experience wear. It
is therefore assumed that the friction on the piston varies
with respect to the velocity. The friction force which acts
on the piston is thus defined as

$$FP_2 = FR_1 - \dot{X}_p FR_2 \tag{2.18}$$

In equation (2.18), FR_2 is the velocity decay coefficient.
This coefficient is determined by taking the ratio of FR_1 to
the maximum possible value of the piston velocity, $\dot{X}_{max}$.
This is expressed mathematically as

$$FR_2 = \frac{FR_1}{\sqrt{2F_p C_w q_c / m_p}} \tag{2.19}$$

In equation (2.19), $\dot{X}_{max}$, which is the term in the
denominator, is calculated by equating the total energy
released by the mass of powder charge used to the kinetic
energy of the piston, and then solving for the piston

1.26

velocity. With the velocity decay coefficient, FR_2, defined
in this fashion, the friction force term will always be a
positive number (i.e., for any shot, the actual piston
velocity will never be greater than $\dot{X}_{max}$). During the
firing sequence, the piston will decelerate and eventually
come to rest. As this occurs, equation (2.19) predicts that
the frictional force will begin to increase back to the
initial value FR_1, since the friction varies directly with
respect to the velocity. The increase in the friction force
at the time of piston deceleration may be justified
qualitatively as follows: The piston deceleration is
initiated by the high pressures which occur in the light
gas. It is assumed that these high pressures will expand
the cupped portion of the piston face. This will produce
large forces on the inner bore of the pump tube which will,
in turn, increase the friction force which acts on the
piston.

With the friction force on the piston defined, the
force on the piston due to the helium gas will now be
determined.

The second stage of chamber of the gas gun contains the
light gas which propels the projectile. As the piston is
forced down the pump tube by the propellant gas, the helium
is compressed. The velocity of the piston during its motion
down the pump tube is low compared with the sound speed of
the helium gas. Therefore, it is assumed that no shock waves
are formed ahead of the piston. The shock-free compression

is adequately modeled as an isentropic process. The pressure rise in the helium up to the point of diaphragm failure is thus defined as

$$P_{He} = P_{He_i} \left[\frac{V_{He_i}}{V_{He_i} - X_p A_{pt}} \right]^{\gamma_{He}} \tag{2.20}$$

Equation (2.20) is the isentropic pressure relationship. Usage of this relation implies that the light gas is assumed to be an ideal gas with constant specific heats. The pressure which is calculated from the relation given above exists at all points in the gas. In actuality, a pressure gradient exists in the light gas. Therefore, the pressure at the piston face is higher than the pressure at the diaphragm. In order to account for this effect, the isentropic stagnation pressure relationship is used to relate the average helium pressure to the helium pressure on the piston face

$$P_{pf} = P_{He} \left[1 + \frac{\gamma_{He}-1}{2} \frac{\dot{X}_p^2}{g_c \gamma_{He} R_{He} T_{He}} \right]^{\frac{\gamma_{He}}{\gamma_{He}-1}} \tag{2.21}$$

The temperature of the helium in equation (2.21) is defined by the following isentropic relation

1.28

$$T_{He} = T_{He_i} \left[\frac{P_{He}}{P_{He_i}} \right]^{\frac{\gamma_{He} - 1}{\gamma_{He}}} \qquad (2.22)$$

With the pressure of the helium on the piston face now defined, the force on the piston due to the light gas is computed by multiplying the result of equation (2.21) by the area of the piston face. This is expressed as

$$FP_3 = P_{pf} \times A_{pf} \qquad (2.23)$$

The final forces which act upon the piston are the extrusion forces. These forces are considered next.

As the piston enters the transition region of the gun, it undergoes deformations, and a flow pattern is developed. If the flow pattern is known, the strain rates involved in the deformation can be determined. In the current model, it is assumed that the piston flow field can be described by a spherical velocity field. In a spherical velocity field, all of the material in the deformation region is assumed to flow toward the apex of the cone. The spherical velocity field is shown in figure 5[5]. In Figure 5, ZONE I is the region where plastic deformation of the piston occurs. As the piston material enters and exits the transition region, the direction of the flow of the piston changes. These changes in flow direction cannot be described mathematically; therefore, they are described as velocity discontinuities which occur along surfaces Γ_1 and Γ_2. With

1.29

the velocity field described, the strain rate field of the material may be defined in spherical coordinates. The piston material is assumed to be perfectly plastic and obey von Mises' yield criterion. It is also assumed that the piston material is incompressible. With these assumptions, the internal power of deformation of the piston material may now be defined as[6]

$$\dot{W}_i = 2\pi\sigma V_0 R_0^2 \ln(R_0/R_e) \qquad (2.24)$$

Power is also spent in overcoming the velocity discontinuities at surfaces Γ_1 and Γ_2. The relations which define the power spent at these surfaces are[6]

$$\dot{W}_{S1} = \frac{1}{\sqrt{3}}\pi\sigma V_e R_e^2\left[\frac{1}{\sin^2\alpha} - \cot\alpha\right] \qquad (2.25)$$

$$\dot{W}_{S2} = \frac{1}{\sqrt{3}}\pi\sigma V_0 R_0^2\left[\frac{\alpha}{\sin^2\alpha} - \cot\alpha\right] \qquad (2.26)$$

As the piston extrudes into the conical section of the gun, frictional resistance must be overcome along surface Γ_3. The power required to overcome this resistance is given by[6]

$$\dot{W}_{S3} = \frac{2}{\sqrt{3}}\pi m V_0 R_0^2 \cot(\alpha)\ln(R_0/R_e) \qquad (2.27)$$

Since the extrusion process proceeds at a very high rate, the inertia effects must be accounted for. The inertia power term for an extrusion process is defined by[5]

$$\dot{W}_k = \frac{1}{2} \frac{\dot{\rho}_{pm}}{g_c} \tau V_o R_o^2 (V_e^2 - V_o^2) \qquad (2.28)$$

Equations (2.24) through (2.28) define the power absorbed by the piston as it extrudes into the transition region of the gun. Equations (2.24), (2.26), (2.27), and (2.28) apply throughout the entire extrusion process, while equation (2.25) is applicable only when the piston begins to extrude into the launch tube (in other words, only when the piston face has crossed the surface Γ_1). Since we are interested in the forces which act on the piston, the extrusion force must be extracted from the power terms given above. In the present model, the extrusion force is determined by multiplying the summation of the power terms by the ratio of the time of the extrusion, to the distance of the extrusion. The extrusion distance is simply the distance measured from the apex of the cone to the face of the piston.

The extrusion process has been described above. However, before the equations can be applied, the properties of the piston material must be known. The material properties of polypropylux are unavailable; therefore, the properties of polypropylene, a similar material, are used. These values are obtained from reference 7. In some shots, the face of the piston may extrude far into the launch tube, and parts of the piston may separate and be launched down range. In such cases of severe extrusion, the lead packing in the base of the piston will influence the extrusion

process and may even begin to extrude itself. In the present model, it is assumed that lead material will begin to extrude once the piston has filled the transition region and is beginning to extrude into the launch tube. The same extrusion equations apply for the extrusion of lead as were used for the polypropylux. Only the values of the material properties are different.

With all of the forces which act on the piston defined, the acceleration of the piston is obtained by applying Newton's second law of motion to the piston. It yields

$$\frac{d^2x_p}{dt^2} = (FP_1 - FP_2 - FP_3 - FP_4)g_c/m_p \qquad (2.28)$$

With the piston acceleration defined, all of the terms in the interior ballistic equation, equation (2.8), are now known. The assumptions made in determining the piston acceleration will now be summarized :

1) A modified form of the isentropic stagnation pressure equation is used to relate the average pressure of the propellant gas to the piston base pressure.

2) The initial friction force is the force which must be overcome at the piston shot-start pressure.

3) The friction force on the piston will vary with respect to the velocity of the piston.

4) The light gas is treated as an ideal gas with constant specific heats, and the effects of heat

transfer are considered negligible.

5) Compression of the light gas is taken as an isentropic process.

6) The pressure on the piston face is related to the average pressure by the isentropic stagnation pressure equation.

7) The flow field of the piston material in the transition region is defined by a spherical velocity field.

8) The piston material is assumed to be incompressible.

9) The piston material is assumed to be perfectly plastic and obey von Mises' yield criterion.

At this point, the gun firing cycle is completely modeled up to the point of diaphragm failure. The events which occur at and after diaphragm failure will now be explained.

2.3 PROJECTILE KINETICS

In the two-stage light gas gun, a flat, scored diaphragm isolates the projectile from the propellant gas up to the point of diaphragm failure. The pressure at which the diaphragm fails is also known as the projectile release pressure, since it is assumed that the projectile motion begins as soon as the diaphragm fails. This section of the analysis will deal with the projectile motion and the

ensuing forces which are involved.

As the diaphragm failure pressure is reached, the petals of the scored diaphragm begin to open. The actual time required for the diaphragm to open completely depends on the material used and the depth to which the diaphragm is scored. While the opening times vary, an estimate for the average opening time involved would be on the order of several hundred micro-seconds (references 8 and 9). In the present model, it is assumed that the diaphragm opens instantaneously. The justification for this assumption is as follows: After several hundred micro-seconds, the projectile has traveled only a short distance. This fact is shown in table 2, where the computed results of only the projectile motion for a typical shot are presented (Note : the starting postion of the projectile in the launch tube is one inch). Since the projectile moves only a small distance during the time that it takes for the diaphragm to open, the increase in volume behind the projectile is negligible, compared with the volume change due to the piston advancement. This implies that the pressure rise on the projectile base will be very rapid for the case of considering the diaphragm opening time. Therefore, the instantaneous pressure rise associated with the assumption of an instantaneous diaphragm opening will not deviate greatly from the process which actually occurs.

As the diaphragm fails, a shock wave is propagated toward the projectile base, and an expansion wave is

1.34

propagated toward the piston. In the present analysis, these effects are not accounted for. It is assumed that the light gas can still be considered as an ideal gas with constant specific heats and that isentropic relations can describe the changes which occur in the physical properties.

Up to the point of diaphragm failure, the average value of the helium pressure is determined by means of an isentropic relation in which the volume change is dependent only on the piston motion. The change in helium pressure at this stage in the firing cycle is dependent on the motion of the piston and the projectile and is now defined by

$$P_{He} = P_{He_i} \left[\frac{\Psi_{He_i}}{\Psi_{He_i} - X_p A_{pt} + X_s A_{1t}} \right]^{\gamma_{He}} \qquad (2.29)$$

The pressure of the helium gas, which is evaluated from equation (2.29), is only an average value. Due to the presence of a pressure gradient, the pressure on the piston face will be higher than the average value calculated, and the pressure on the projectile base will be lower than the average value calculated. The pressure on the piston face was determined by means of the isentropic stagnation pressure relation which is given in equation (2.21). The pressure on the projectile base is determined in a similar fashion, and is defined by

1.35

$$P_{sb} = P_{He} \left[1 + \frac{\gamma_{He}-1}{2} \frac{\dot{X}_s^2}{\gamma_{He}g_c R_{He} T_{He}} \right]^{-\frac{\gamma_{He}}{\gamma_{He}-1}} \qquad (2.\,\cdot\,$$

where, the helium temperature is calculated from the isentropic relationships.

With the projectile base pressure defined, the propelling force on the projectile is defined as follows

$$FS_1 = P_{sb} \times A_{lt} \qquad (2.31)$$

There are two remaining forces which act on the projectile. They are the force due to the compression of the air ahead of the projectile and the frictional force which acts on the sabot. These forces will now be analyzed.

In the gas gun which is being modeled, the launch tube may be open to the atmosphere or it may be evacuated. In either case, there will still be some air ahead of the projectile. As the projectile accelerates down the launch tube, compression waves will coalesce to form a normal shock wave ahead of the projectile. According to Siegel[1], the normal shock wave forms almost immediately after the onset of projectile motion. The pressure and velocity of the air directly behind the shock, and of the the air in front of the projectile, equalize very quickly. Thus, the pressure which occurs on the face of the projectile may be approximated by the pressure which exists immediately behind the normal shock wave. The relation which defines this is[1]

$$P_{sf} = P_{lt} \left[1 + \left| \frac{\dot{x}_s}{a_1} \right|^2 \frac{\gamma_1(\gamma_1+1)}{4} + \right.$$

$$\left. \frac{\gamma_1 \dot{x}_s}{a_1} \sqrt{1 + \left| \frac{\gamma_1+1}{4} \right|^2 \left| \frac{\dot{x}_s}{a_1} \right|^2} \right]$$

(2.32)

The retarding force produced by the air ahead of the projectile may now be computed by multiplying the pressure which acts on the projectile face by the cross-sectional area of the launch tube

$$FS_2 = P_{sf} \times A_{lt}$$

(2.33)

The final force which acts on the projectile is the friction force, which is considered next.

As the projectile travels down the launch tube, frictional resistance must be overcome. The free-flight model is encased by the polypropylux petals of the sabot, and the helium is prevented from leaking past the projectile by means of a polypropylux obturator. It is assumed that the obturator undergoes radial expansion as the propellant gas acts on its base. The radial expansion produces a normal force on the inner surface of the launch tube, and this force is related to friction that acts on the projectile. A free-body equilibrium approach, in cylindrical coordinates, is used to determine the pressure which is exerted on the inner surface of the launch tube.

1.37

The resultant friction force is modeled by means of Coulomb friction, and the relation which defines the friction force on the projectile is given by

$$FS_3 = \tau_w m (D_{1t})^2 P_{sb} \qquad (2.34)$$

The calculation of the friction force, which acts on the projectile, is given in Appendix A.

The change in the helium pressure during a shot has been defined only for the case in which the projectile is still in the launch tube, and it is based on the change in volume which occurs due to the motion of the piston and the projectile. Evaluation of the helium pressure in this fashion is correct as long as the projectile is in the launch tube. There are cases, however, for which the projectile has left the launch tube, and the piston is still in motion. The rate at which the helium pressure changes for this case must be determined, because the calculation proceeds up to the point where the piston stops, so that the piston extrusion distance may be determined. Determination of the drop in the helium pressure for this case deals with intermediate ballistics. The flow field and the analysis in this regime are extremely complex; however, the muzzle velocity of the projectile has already been determined. Since the projectile is out of the range of influence of the external flow field at this point, gross simplifying assumptions have been made to obtain a "crude" approximation of the helium pressure ahead of the piston once the

1.38

projectile has left the launch tube. The relation which describes the drop in the helium pressure is as follows with a derivation given in Appendix B :

$$P_{He} = P_{He_0} \exp^{-\left|\frac{\dot{X}_s A_{1c}}{\Psi_{He_0}}\right| t}$$

(2.35)

All of the forces which act on the projectile have been defined; therefore, the acceleration of the model, according to Newton's second law of motion, is given by

$$\frac{d^2 X_s}{dt^2} = (FS_1 - FS_2 - FS_3) g_c/m_s$$

(2.36)

The analysis on the kinetics of the projectile are now complete, and the assumptions which were made will now be summarized :

1) The projectile motion begins at the pressure at which the diaphragm fails.

2) The diaphragm opens instantaneously.

3) The shock and expansion waves which occur at diaphragm failure are neglected.

4) The light gas (helium), is treated as an ideal gas with constant specific heats, and the processes which occur are assumed to be isentropic.

5) A form of the isentropic stagnation pressure

1.39

relation is used to relate the average helium gas pressure to the projectile base pressure.

6) The air pressure on the projectile face is approximated by the pressure which occurs behind a normal shock which moves ahead of the projectile.

7) It is assumed that the normal shock ahead of the projectile forms instantaneously and that the air between the shock and the projectile equalizes quickly.

8) The friction on the projectile is a function of the pressure of the helium gas which acts on the base of the projectile.

9) The friction force which exists between the projectile and the bore of the launch tube is proportional to the force exerted on the bore by the obturator. The proportionality factor is assumed to be constant and is called the Coulomb coefficient of friction.

1J) No leakage of gases occurs at the projectile/launch tube interface.

This completes the analysis of the physical processes that occur in the firing of the two-stage light gas gun which is being modeled. The governing differential equations are presented on the following page.

1.40

$$\frac{dP_{av}}{dt} \left[V_c + A_{pt}X_p - \frac{(C_w - N_b)}{\rho_p} - \eta N_b \right] =$$

(2.3)

$$\frac{dN_b}{dt} \, \varepsilon_p - (\gamma_p - 1)(1 + \beta) \, \frac{m_a}{g_c} \, \frac{d\dot{X}_p}{dt} \, \frac{dX_p}{dt} - P_{av}A_{pt}\dot{X}_p$$

$$\frac{dN_b}{dt} = (B P_{av}{}^N + K_.\dot{X}_p) \, \frac{2 \, C_w}{w_o}$$

(2.13)

$$\frac{d^2 X_p}{dt^2} = (FP_1 - FP_2 - FP_3 - FP_4)g_c/m_p$$

(2.28)

$$\frac{d^2 X_{(p)}{}^S}{dt^2} = (FS_1 - FS_2 - FS_3)g_c/m_s$$

(2.36)

With the analysis of the processes which occur during the firing sequence of the gas gun completed, a method of solution is required .o numerically integrate the equations obtained. This topic is discussed in the following chapter.

NUMERICAL SOLUTION OF THE EQUATIONS

Now that the equations which model the gun have been defined, the numerical method used to obtain an approximate solution to the governing equations will be discussed.

3.1 SELECTION OF A NUMERICAL METHOD

A solution for the mathematical model of the two-stage light gas gun requires the numerical integration of four simultaneous differential equations, two of which are of second order. A numerical solution provides an approximation of the true solution. The difference between the numerical solution and the exact solution at any given step is the total error. The total error results from three conditions. The first condition is that of roundoff error which is introduced whenever arithmetic operations are performed. The second condition is the truncation error which results from the use of approximate formulas in the calculation of a given step. The third and final condition which contributes to the total error is a cumulative error, which is present at each step, due to errors in the preceding steps.

The roundoff error which is encountered can be controlled with the use of double-precision arithmetic. The truncation error may be minimized with the use of a small step size and/or with the use of a numerical integration

technique which employs a formula having a truncation error of high order.

The integration of the ordinary differential equations which model the two-stage light gas gun is an initial-value problem, and it will involve a large number of steps. Since a large number of steps will be required, a numerical method which has a small per-step truncation error is required in order to minimize the cumulative error. A numerical method which satisfies these requirements, and which is also stable, is Hamming's method[13]. Therefore, Hamming's method is the numerical method used to integrate the differential equations obtained in Chapter 2. Hammings method, however, has the disadvantage of not being self-starting. In the present calculation, a fourth-order Runge-Kutta method, which has the same truncation error as Hamming's method, is used to start the integration. The fourth-order Runge-Kutta scheme could be used to carry out the entire integration. However, Hamming's method was chosen because the required computation time is less.

With the numerical method having been decided upon, the method and the algorithms used will be discussed below.

3.2 HAMMING'S METHOD

Hamming's method is a predictor-corrector method. The solution is obtained by first applying a fourth-order Runge-Kutta scheme which generates the starting values required for use in Hamming's method. As mentioned previously, the

1.43

differential equations which are to be solved are of first
and second order. Hamming's method employs two separate
algorithms for each of these cases, and they are presented
below.

<u>Algorithm for first order ordinary differential equations :</u>

(predictor for y)

$$P(Y_{i+1}) = Y_{i-3} + (2Y'_i - Y'_{i-1} + 2Y'_{i-2})(4h/3)$$

(modifier for y)

$$M(Y_{i+1}) = P(Y_{i+1}) - [P(Y_i) - C(Y_i)](112/121)$$

(differential equation)

$$M(Y'_{i+1}) = f[M(Y_{i+1})]$$

(corrector for y)

$$C(Y_{i+1}) = \{9Y_i - Y_{i-2} + 3h[M(Y'_{i+1}) + 2Y'_i - Y'_{i-1}]\}(1/8)$$

(final value of y)

$$F(Y_{i+1}) = C(Y_{i+1}) + [P(Y_{i+1}) - C(Y_{i+1})](9/121)$$

(final value of y')

$$F(Y'_{i+1}) = f[F(Y_{i+1})]$$

Algorithm for second order ordinary differential equations :

(predictor for y')

$$P(y'_{i+1}) = y'_{i-3} + [2y''_i - y''_{i-1} + 2y''_{i-2}](4h/3)$$

(modifier for y')

$$M(y'_{i+1}) = P(y'_{i+1}) - [P(y'_i) - C(y'_i)](112/121)$$

(predictor for y)

$$P(Y_{i+1}) = \{9y_i - y_{i-2} + 3h[M(y'_{i+1}) + 2y'_i - y'_{i-1}]\}(1/8)$$

(differential equation)

$$M(y''_{i+1}) = f[P(Y_{i+1}), M(y'_{i+1})]$$

(corrector for y')

$$C(y'_{i+1}) = \{9y'_i - y'_{i-2} + 3h[M(y''_{i+1}) + 2y''_i - y''_{i-1}]\}(1/8)$$

(final value of y')

$$F(y'_{i+1}) = C(y'_{i+1}) + [P(y'_{i+1}) - C(y'_{i+1})](9/121)$$

(final value of y)

$$F(Y_{i+1}) = \{9y_i - y_{i-2} + 3h[F(y'_{i+1}) + 2y'_i - y'_{i-1}]\}(1/8)$$

(final value of y'')

$$F(y''_{i+1}) = f[F(Y_{i+1}), F(y'_{i+1})]$$

An interactive computer program which uses the above algorithms to obtain a solution has been developed. A listing of this BASIC program is presented in Appendix C. The results are presented in the following chapter.

RESULTS

In the two-stage light gas gun which is being modeled, no pressure sensors have been installed in the pump tube or in the launch tube. Therefore, measurements of the propellant gas pressure, the helium gas pressure, piston position and velocity, and projectile position and velocity during the firing cycle are not available. The only measurable data which can be extracted from the gun are the muzzle velocity of the projectile and the distance that the piston extrudes into the transition region and/or the launch tube.

A comparison of the model predictions with the valid data obtained from actual gun firings is presented in table 2. The maximum deviation of the model prediction of the projectile muzzle velocity occurred for shot 4, in which the percent error is -11.67%. The smallest deviation of the model prediction of the projectile muzzle velocity from the actual velocity was for shot 3, in which the percent error is -1.67%. In comparing the actual piston extrusion distance with the model predictions, the largest error incurred was for shot 1, in which the percent is -71.82%. The most accurate predictions of the piston extrusion was for shot 2, in which the percent error is 11.31%. The computer model has the capability of plotting the results

1.45

which are calculated, and some of these are discussed next.

The burning powder charge generates the propellant gas which drives the piston into the pump tube. The average value of the propellant gas as a function of time is shown in figure 6. The mass of powder burned as a function of time is shown in figure 7.

The piston motion is dependent on the propellant gas, the light gas, friction, and the extrusion forces. The piston velocity as a function of time is shown in figure 8. The corresponding friction and extrusion forces which act on the piston as a function of piston displacement are shown in figure 9.

The forward motion of the piston will compress the light gas. The average value of the helium gas pressure is shown in figure 10. When the pressure of the helium exceeds the strength of the diaphragm, failure occurs, and projectile motion proceeds due to the action of the high pressure light gas. The helium gas base pressure on the projectile as a function of the projectile displacement is shown in figure 11. The velocity of the projectile as a function of the projectile displacement is presented in figure 12.

The motion of the projectile is retarded by friction forces and by the compression of the air ahead of the projectile. These results are shown in figures 13 and 14 respectively. The resultant force which acts on the projectile as it travels down the launch tube is shown in

figure 15.

In order to achieve the desired projectile muzzle
velocity with allowable acceleration forces, six of the
loading parameters may be varied. These parameters are as
follows :

1) The mass of the powder charge.

2) The mass of the piston.

3) The initial helium pressure.

4) The pressure at which the diaphragm fails.

5) The mass of the projectile.

6) The air pressure in the launch tube.

The results of a study which show the effects of varying
each of these parameters will now be presented.

Instead of using the complete set of equations given in
Chapter 2 to explain some of the results which are obtained
in the parametric runs, only one equation is needed, and
this equation defines the rate of change of the helium
pressure after the diaphragm has failed. In the initial
stages of the launching of the projectile, the projectile
motion is negligible (table 1). Therefore, the time rate of
change of the helium pressure may be defined with respect to
the piston motion only. The helium pressure rate may be
obtained by differentiating the isentropic pressure
relationship, which is as follows[2]

$$\frac{dP_{He}}{dt} = \frac{\gamma_{He} A_{pt} \dot{X}_p}{V_{He_i}} \, P_{He} \left| \frac{P_{He}}{P_{He_i}} \right|^{(1-\gamma_{He})} \qquad (4.1)$$

Equation (4.1) defines the time rate of change of the helium
pressure and is also known as the pumping rate. The results
of the parametric runs show how the projectile muzzle
velocity, the projectile maximum base pressure, and the
piston extrusion distance are affected by changes in the
loading parameters.

The effect of varying the mass of the powder charge is
shown in figures 16 through 18. Figure 16 indicates that
the projectile muzzle velocity is very sensitive to
variations in the mass of the powder charge. Higher
projectile velocities can be attained by increasing the mass
of the powder charge. The reasoning for this is that as the
mass of the powder charge is increased, more energy is
available for accelerating the piston, and the piston
velocity is increased. Greater piston velocities provide for
a larger pumping rate (equation (4.1)), which results in the
higher projectile base pressures required to yield higher
projectile velocities. The result of attaining higher
projectile base pressures with increases in the mass of the
powder charge is shown in figure 17.   In general, the
greater the piston velocity, the greater the piston
extrusion distance, because the piston enters the transition
section of the gun with more kinetic energy. This result is

1.48

shown in figure 18.

The effect of varying the mass of the piston is shown in figures 19 through 21. Figure 19 indicates that the projectile velocity is not very sensitive to changes in the mass of the piston. The maximum base pressure on the projectile is also quite insensitive to variations in the mass of the piston (figure 20). Figure 21, however, shows that the piston extrusion distance is very sensitive to the mass of the piston. Heavier pistons will possess greater inertia and are harder to stop; therefore, the extrusion distance is greater. Large extrusion distances are undesirable for two reasons. First, the piston is difficult to remove, which increases the turn-around time for a shot; and secondly, pieces of the piston may be launched down-range where they could cause damage to the free-flight range. What these results indicate is that lighter pistons may be used to achieve the desired projectile muzzle velocity with the added benefit of not producing excessive extrusion distances.

The effects of varying the initial helium pressure are shown in figures 22 through 24. Figure 22 indicates the initial helium pressure has considerable effect on the projectile velocity. The lower the value of the initial helium pressure, the higher the projectile velocity. The reason for this is twofold. First, the lower initial pressure produces a larger pumping rate (equation (4.1)), which results in higher projectile base pressures. Second,

1.49

the compression ratio is higher for lower values of initial helium pressure. This results in higher gas temperatures which also serves to increase performance. The result of higher projectile base pressures at lower initial helium pressures is shown in figure 23. Figure 23 indicates that low values of initial helium pressures, in conjunction with high mass projectiles, may produce dangerously high helium pressures, due to large pumping rate and inertia of the projectile. The effects of the initial helium pressure on the piston extrusion distance are presented in figure 24. According to the model predictions, high levels of helium gas pressures will result in a mass of helium which is greater than the shot requires. The effect of this is that the piston rebounds off the cushion of the "extra" helium gas and travels back toward the breech of the gun before ultimately coming to rest in the transition section.

The effects of variations in the pressure at which the diaphragm fails are shown in figures 25 through 27. Figure 25 indicates that the projectile velocity is relatively insensitive to the pressure at which the diaphragm fails, especially for heavy projectiles. This result is so, based on the following factors: At low diaphragm failure pressures, the initial base pressure on the projectile is low, and the inertia of the model is the dominating factor. At high diaphragm failure pressures, the initial base pressure is high, and the inertia of the model is overcome more easily. Throughout a range of diaphragm failure

1.50

pressures, these two factors "balance" out during the launching of the projectile due to the effect of the pumping rate. This behavior produces little change in the projectile muzzle velocity. Figure 26 indicates that low projectile base pressures can be achieved with low diaphragm failure pressures. Lower diaphragm failure pressures result in a lower initial pumping rate (equation (4.1)), and this accounts for the lower projectile base pressures. As the diaphragm failure pressure is decreased, the average helium pressure generated during the compression will also decrease. This results in greater extrusion distances (figure 27) since the helium gas is the primary contributor in the deceleration of the piston. A batch of identical diaphragms will invariably fail at different pressures. These results indicate that shot repeatability will not be linked to the failure pressure of the diaphragm.

The effects of varying the mass of the projectile are shown in figures 28 through 30. Figure 28 represents the effect of variations in the projectile mass on the projectile velocity. As would be expected, the lower the mass of the projectile, the higher the muzzle velocity. The reason for this is, the lower the inertia of the projectile, the easier it is accelerated. A lighter projectile will have greater motion in the initial stages of the launching, and this results in a more rapid expansion of the helium gas which, in turn, produces lower projectile base pressures (figure 29). As a result of lower helium pressures, piston

1.51

deceleration by the helium is not as great; therefore, the piston enters the transition section at higher velocities and is harder to bring to rest. This results in greater extrusion distances (figure 30).

The final initial parameter which can be varied to achieve the desired gun performance is the pressure in the launch tube. The gas gun which is being modeled has a cover assembly which may be placed over the end of the launch tube. This allows for the air in the launch tube to be evacuated by means of a vacuum pump. The effects of varying the pressure in the launch tube are shown in figures 31 through 33. Variations in the launch tube pressure have negligible influence on the projectile velocity (figure 31), the projectile maximum base pressure (figure 32), and the piston extrusion distance (figure 33). These results imply that minimal improvements in performance are obtained from the time and effort invested in the procedure of evacuating the launch tube.

This completes the discussion on all of the results which were obtained. The conclusions and recommendations are presented in the following chapter.

CONCLUSIONS AND RECOMMENDATIONS

From the results presented in table 2, predicted muzzle velocities show good agreement with the actual data, with the largest percent error being -11.67%. The predicted piston extrusion distances do not correlate as well, with the largest percent error being -71.82 %. However, based on the order of magnitude of the figures, the predictions show the general trends. It is concluded, therefore, that the current mathematical model can be used as a tool in the prediction of the performance of a two-stage light gas gun, which incorporates a deformable piston, for modest levels of gun performance. The absence of experimental data at high levels of performance prohibits an evaluation of the effectiveness of the model over a wide range of velocities. It is also concluded that the parametric runs which are presented can be useful in determining the optimum loading parameters for a desired projectile launch history.

In order to improve the accuracy and effectiveness of the present model over a wider range of gun performance, it is recommended that the following enhancements be carried out: The pressure distribution between the piston and the projectile should be defined. The real gas effects of the light gas should be included. The compressibility and viscous effects of the polypropylux piston in the extrusion

1.53

analysis should be determined. Finally, the gun should be configured with the capability of obtaining internal data such as pressures, velocities, and displacements. The availability of such data would allow for the development of a more reliable mathematical model.

TABLES

1.55

Table 1. Computed results of projectile motion for a typical shot.

TIME (sec)	PR PRESS (psi)	He PRESS (psi)	PIST POS (in)	PIST VEL (ft/s)	PROJ POS (in)	PROJ VEL (ft/s)
0.017550	2,833.47	13,857.77	214.60	1,736.42	1.01	51.79
0.017650	2,801.77	16,065.40	216.66	1,695.52	1.29	389.14
0.017750	2,772.93	18,709.67	218.66	1,647.09	1.98	764.44
0.017850	2,745.89	21,846.28	220.61	1,589.71	3.14	1,194.38
0.017950	2,720.45	25,498.68	222.47	1,521.85	4.87	1,687.94
0.018050	2,696.62	29,615.58	224.25	1,442.01	7.22	2,250.18
0.018150	2,674.52	34,014.35	225.93	1,349.08	10.29	2,880.40
0.018250	2,654.28	38,328.95	227.49	1,242.76	14.16	3,569.59
0.018350	2,636.04	42,010.95	228.91	1,124.15	18.88	4,298.16
0.018450	2,619.90	44,442.04	230.18	996.15	24.48	5,036.36
0.018550	2,605.89	45,156.24	231.30	863.36	30.95	5,749.02
0.018650	2,593.99	44,051.07	232.25	731.24	38.25	6,403.54
0.018750	2,584.10	41,426.83	233.05	604.89	46.29	6,977.27
0.018850	2,576.07	37,826.85	233.71	488.07	54.96	7,460.61
0.018950	2,569.70	33,814.60	234.25	384.34	64.16	7,855.28
0.019050	2,564.70	29,848.27	234.72	303.31	73.78	8,170.32
0.019150	2,560.78	26,195.66	235.12	237.37	83.74	8,418.06
0.019250	2,557.74	22,962.30	235.46	183.38	93.96	8,610.83
0.019350	2,555.42	20,162.39	235.74	138.71	104.39	8,759.49
0.019450	2,553.69	17,765.24	235.95	101.37	114.97	8,873.05
0.019550	2,552.46	15,448.66	236.11	69.77	120.31	8,918.98
0.019650	2,551.65	14,288.52	236.22	43.05	120.31	8,918.98
0.019750	2,551.20	13,215.41	236.28	19.43	120.31	8,918.98
0.019850	2,551.07	12,222.82	236.30	0.37	120.31	8,918.98
0.019950	2,551.10	11,754.81	236.30	-7.27	120.31	8,918.98

1.56

Table 2.   Comparison of model predictions with actual gun
data.

SHOT NO.	1	2	3	4	5
POWDER CHARGE (grams)	600	1250	700	650	700
PISTON MASS (grams)	3175	5625	3400	2500	3401
HELIUM PRESS. (psi)	200	250	200	200	300
DIAPHRAGM PRESS. (psi)	12000	12000	12000	6000	12000
PROJECTILE MASS (grams)	68	30	55	60	50
BARREL PRESS. (psi)	0	0	0	0	0
MUZZLE VELOCITY (ft/s)	7800	11300	9800	9800	9500
PREDICTED VEL. (ft/s)	8108	12496	9636	8565	8918
% ERROR IN VEL. PRED.	3.95	10.85	-1.67	-11.67	-6.12
EXTRUSION DIST. (in.)	6.85	30.85	*	*	3.43
PREDICTED EXT. (in.)	1.93	34.34	16.91	7.65	2.55
% ERROR IN EXT. PRED.	-71.82	11.31	N/A	N/A	-25.55

* - No measurement taken

FIGURES

1.58
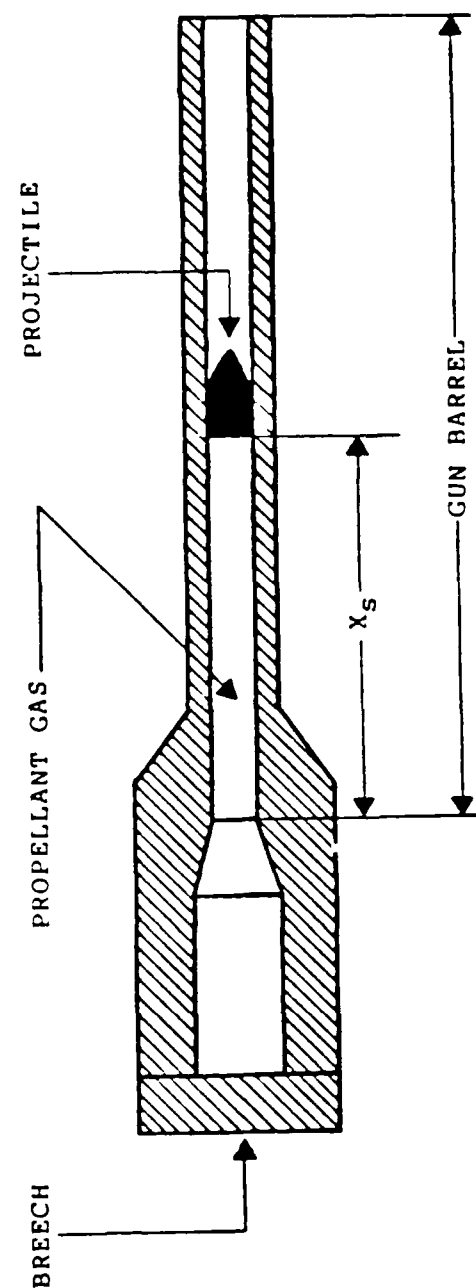
Figure 1. Schematic diagram of projectile motion in a conventional powder gun.

1.59
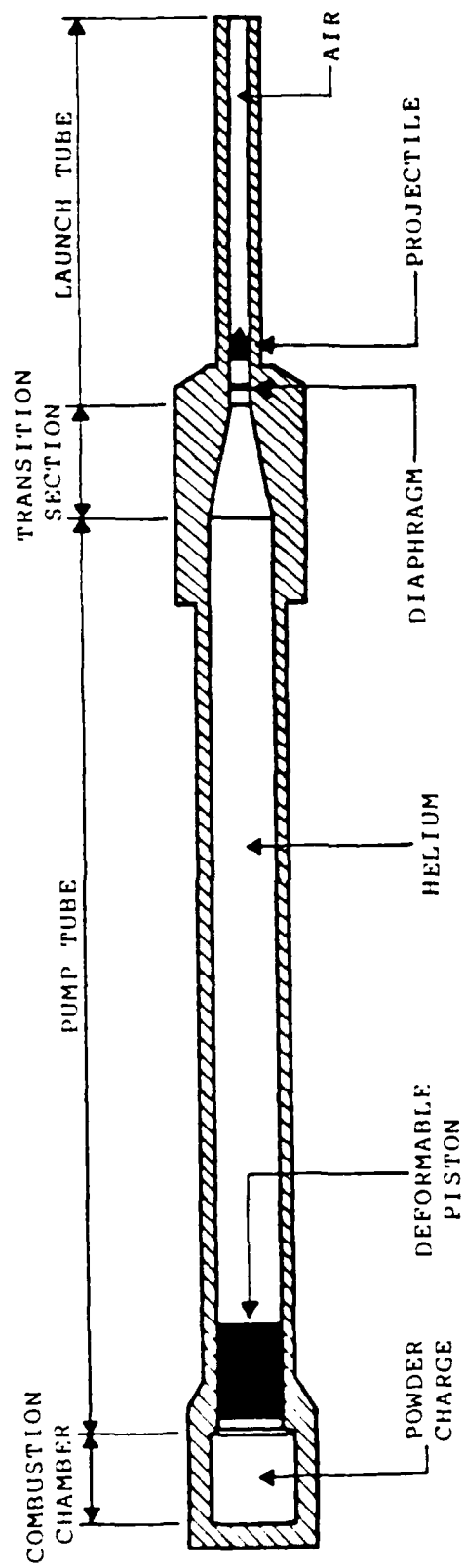
Figure 2. Schematic diagram of a two-stage light gas gun with a deformable piston.

1.60

RUBBER
O-RINGS

POLYPROPYLUX SPACERS

LEAD PACKING

TAPERED CAP
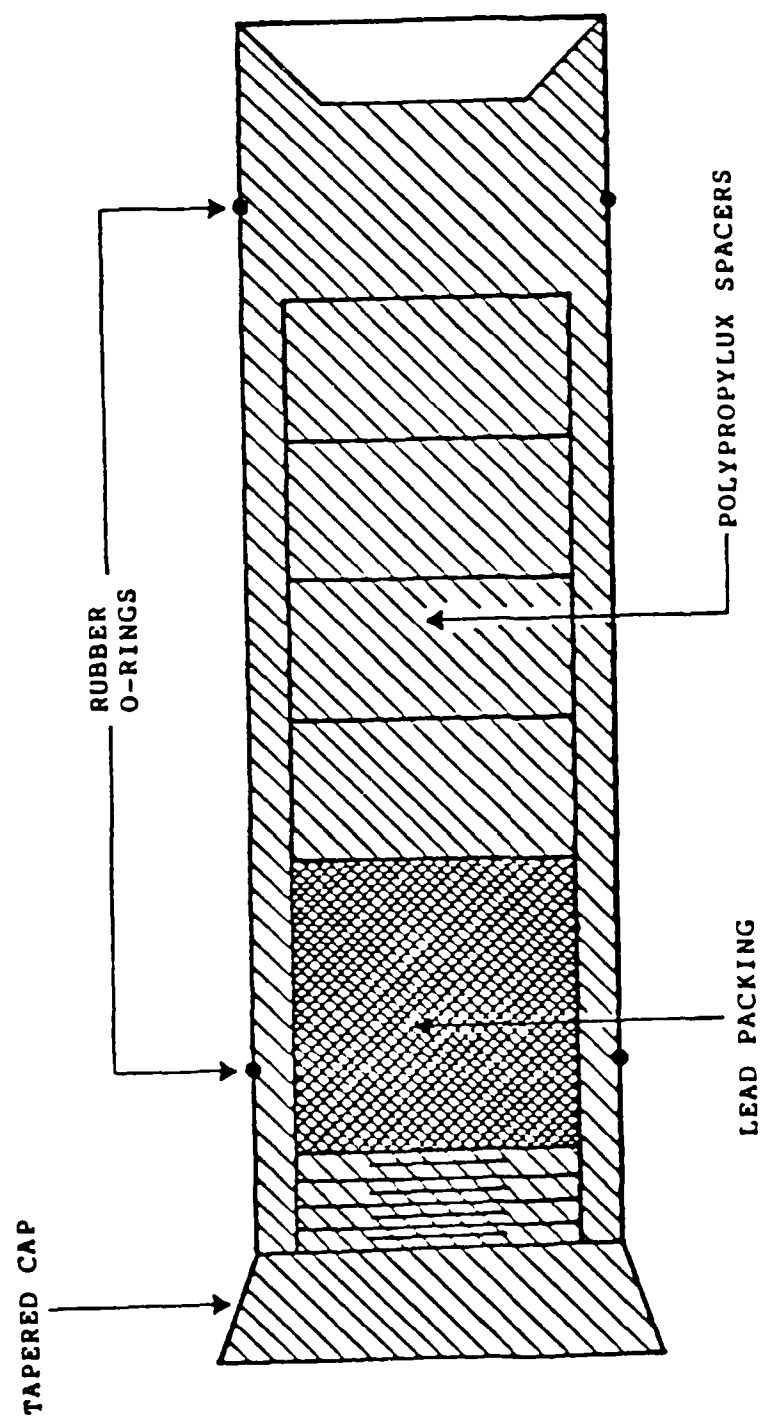
Figure 3. Schematic diagram of the lead packed polypropylux piston.

1.61
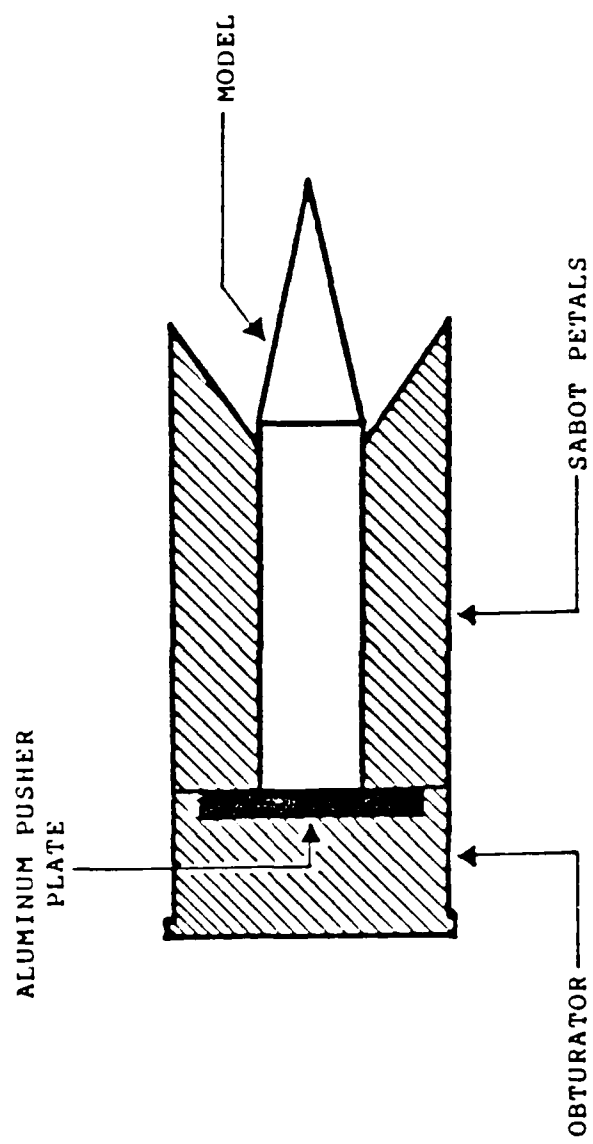
Figure 4. Schematic diagram of projectile.

1.62
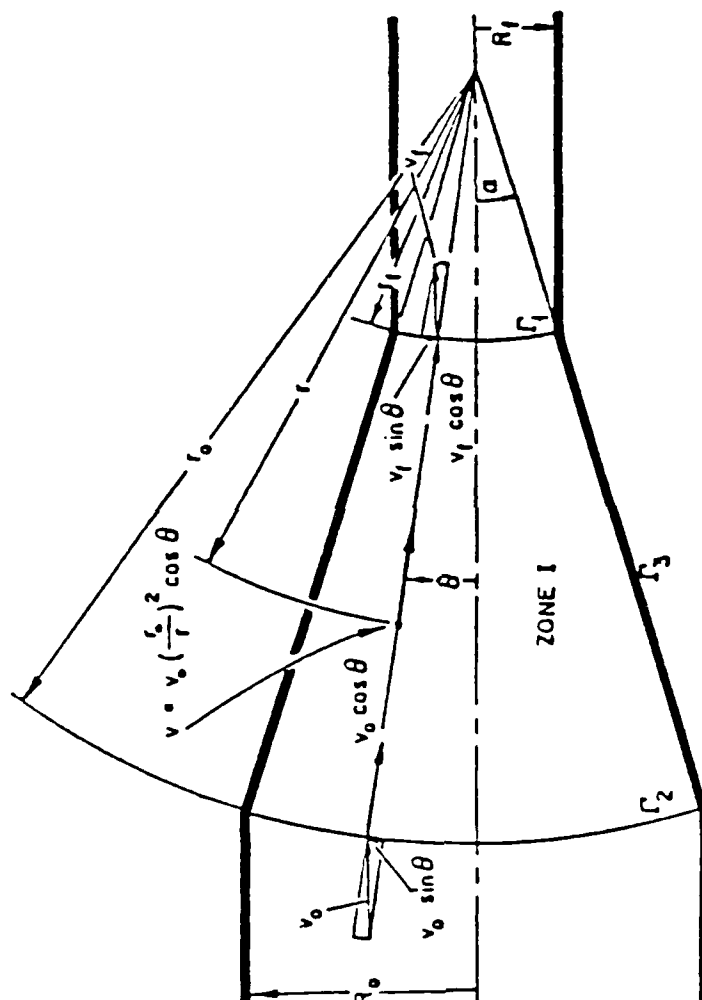
Figure 5. The spherical velocity field.

1.63
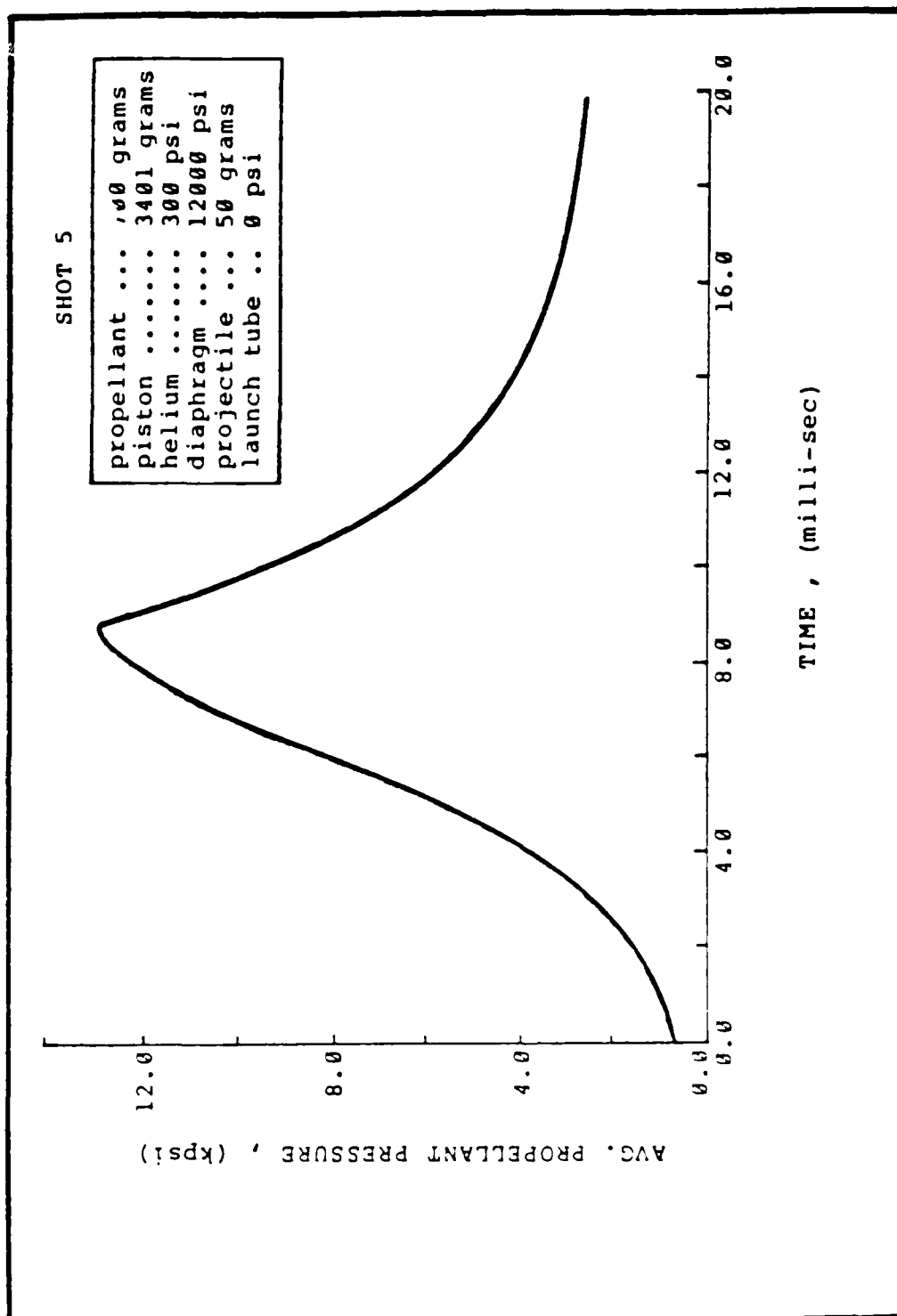
Figure 6. The average propellant pressure vs. time.

SHOT 5

propellant ...:	700 grams
piston ......:	3401 grams
helium ......:	300 psi
diaphragm ...:	12000 psi
projectile ...:	50 grams
launch tube ..:	0 psi

PROPELLANT BURNED , (kg)

TIME , (mill-sec)
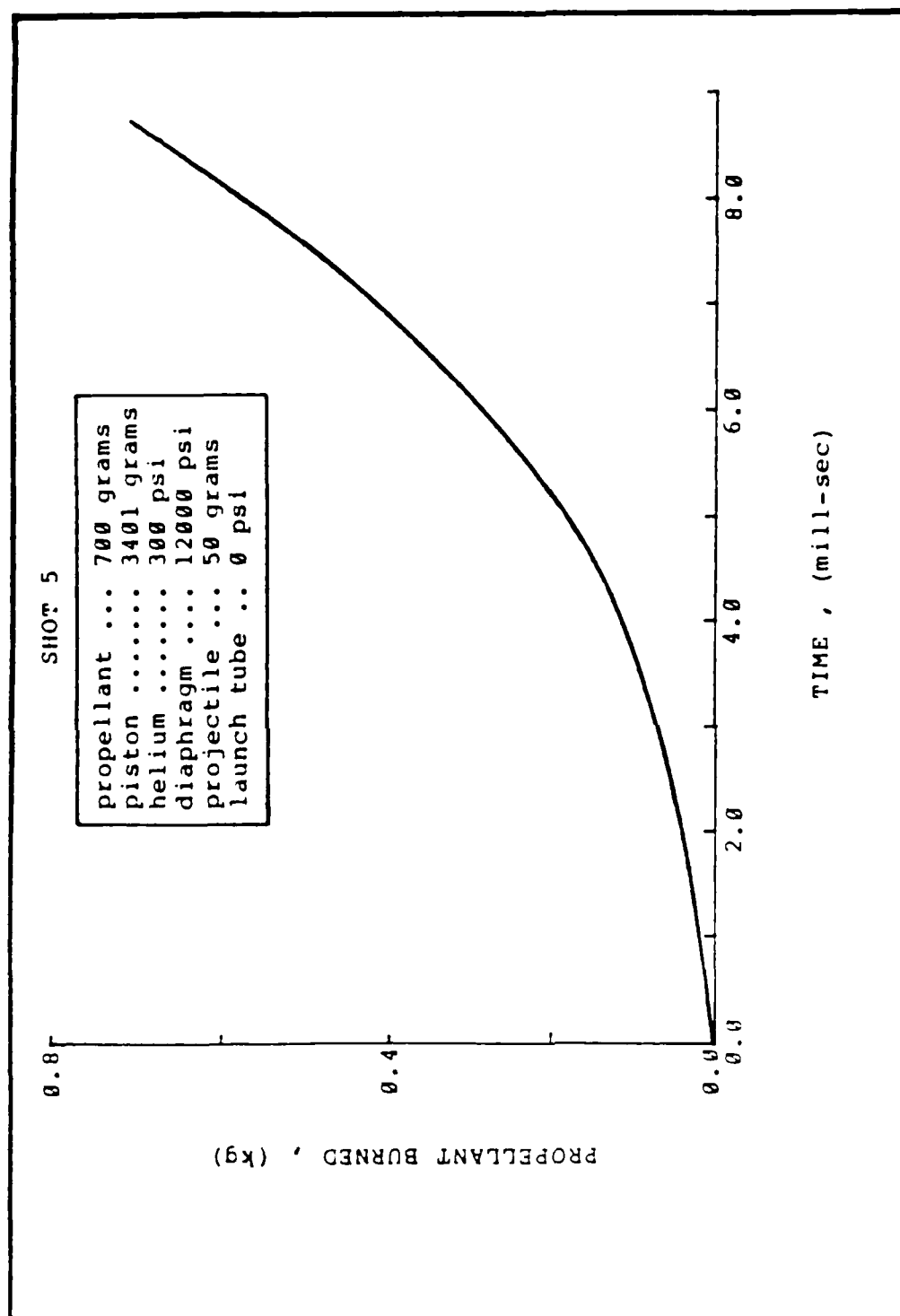
Figure 7.   The mass of propellant burned vs. time.

SHOT 5

propellant	...	700 grams
piston	...	3401 grams
helium	...	300 psi
diaphragm	...	12000 psi
projectile	...	50 grams
launch tube	...	0 psi

PISTON VELOCITY , (kft/s)

TIME , (milli-sec)
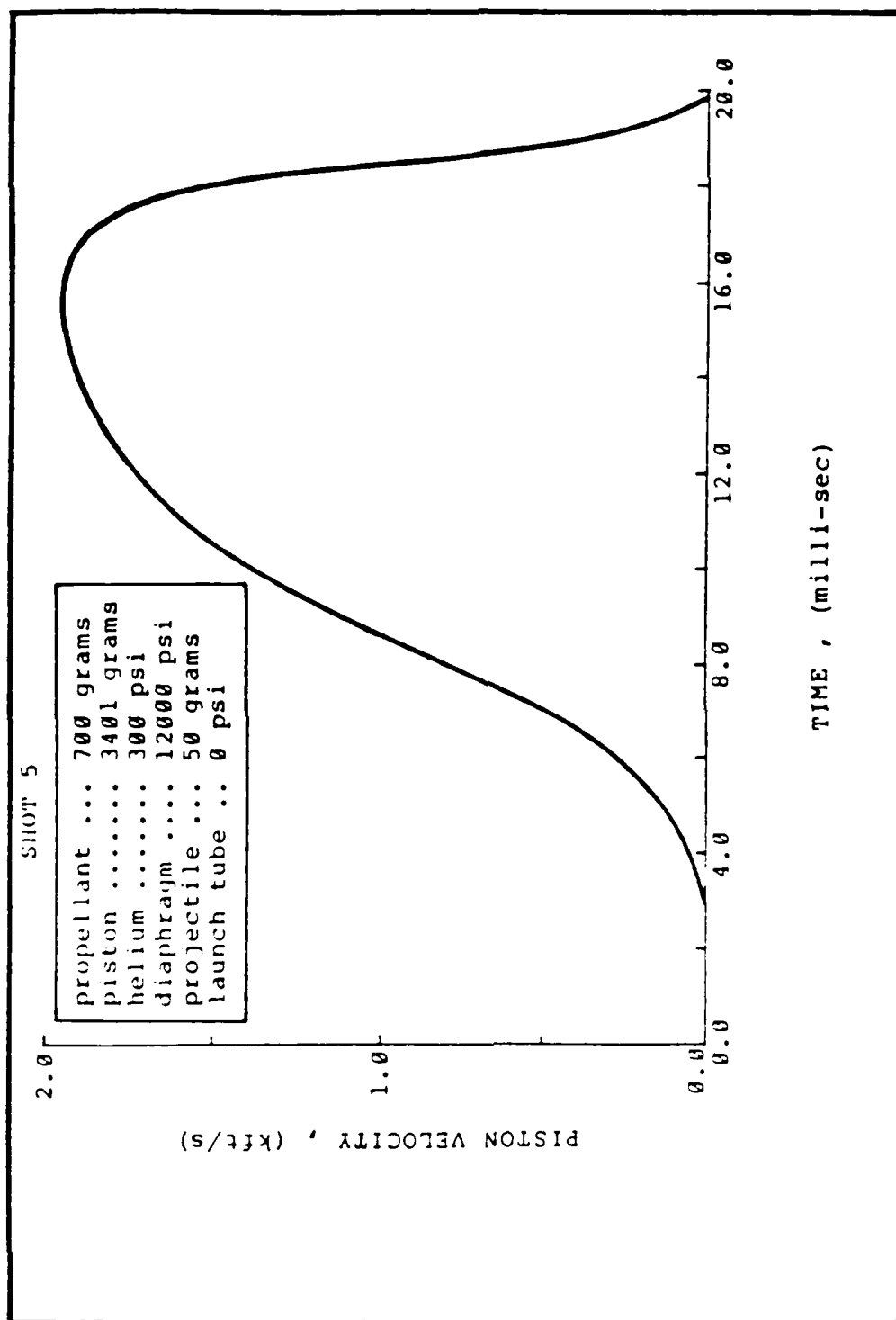
Figure 8. The piston velocity vs. time.

1.66
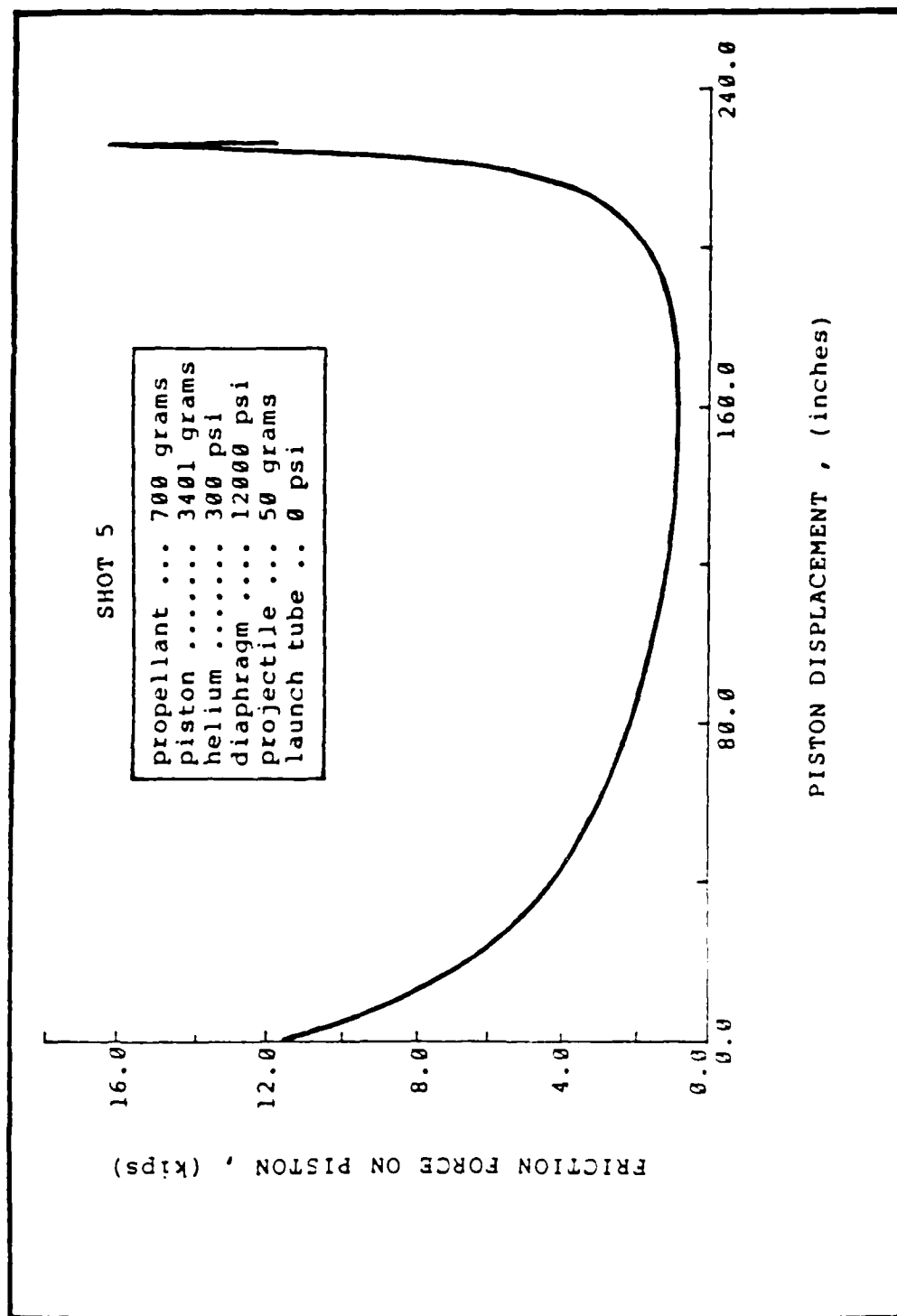
Figure 9. The piston friction and extrusion forces vs piston displacement.

1.67
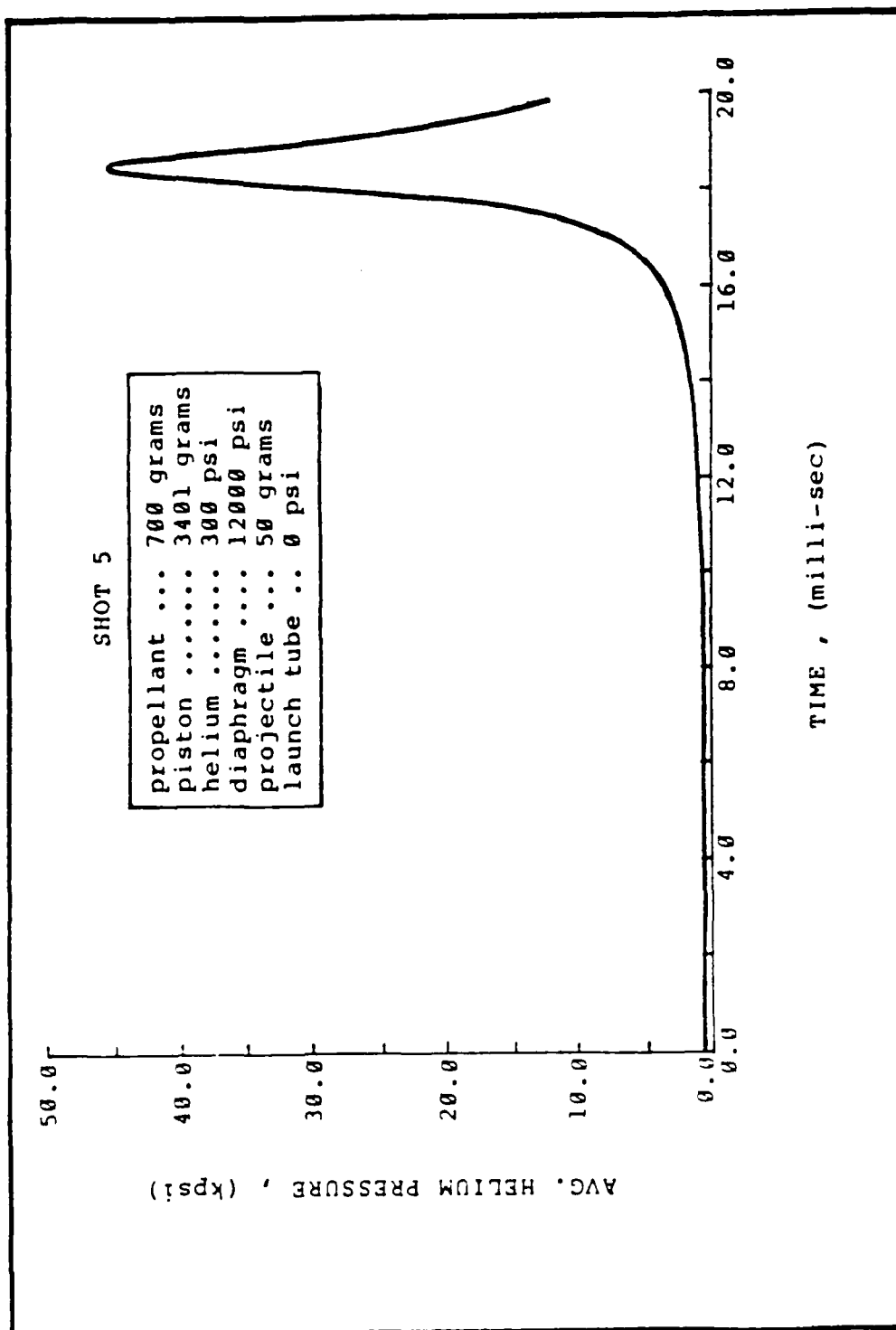
Figure 10. The helium pressure vs. time.

1.68
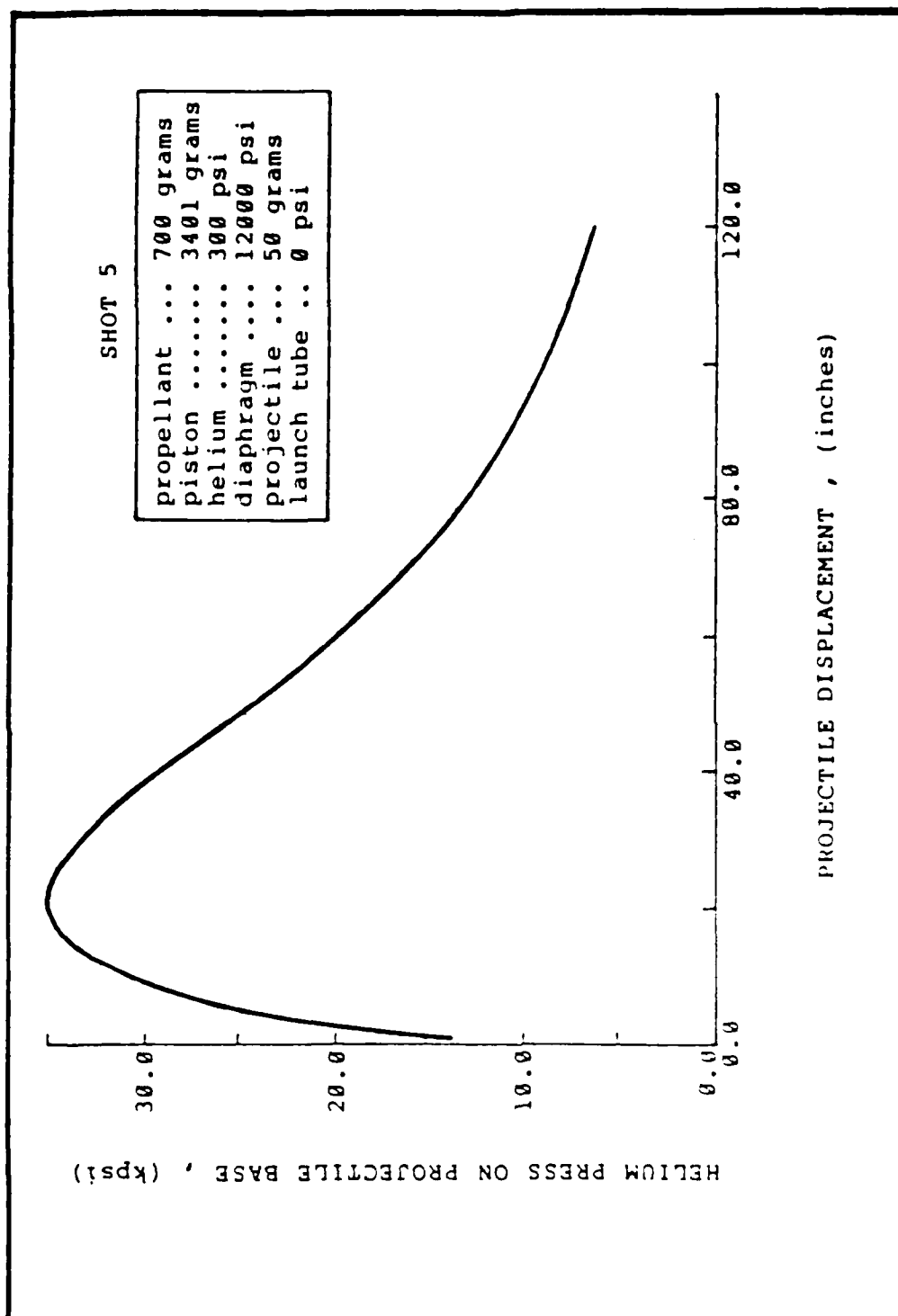
Figure 11. The helium base pressure on the projectile vs. projectile displacement.
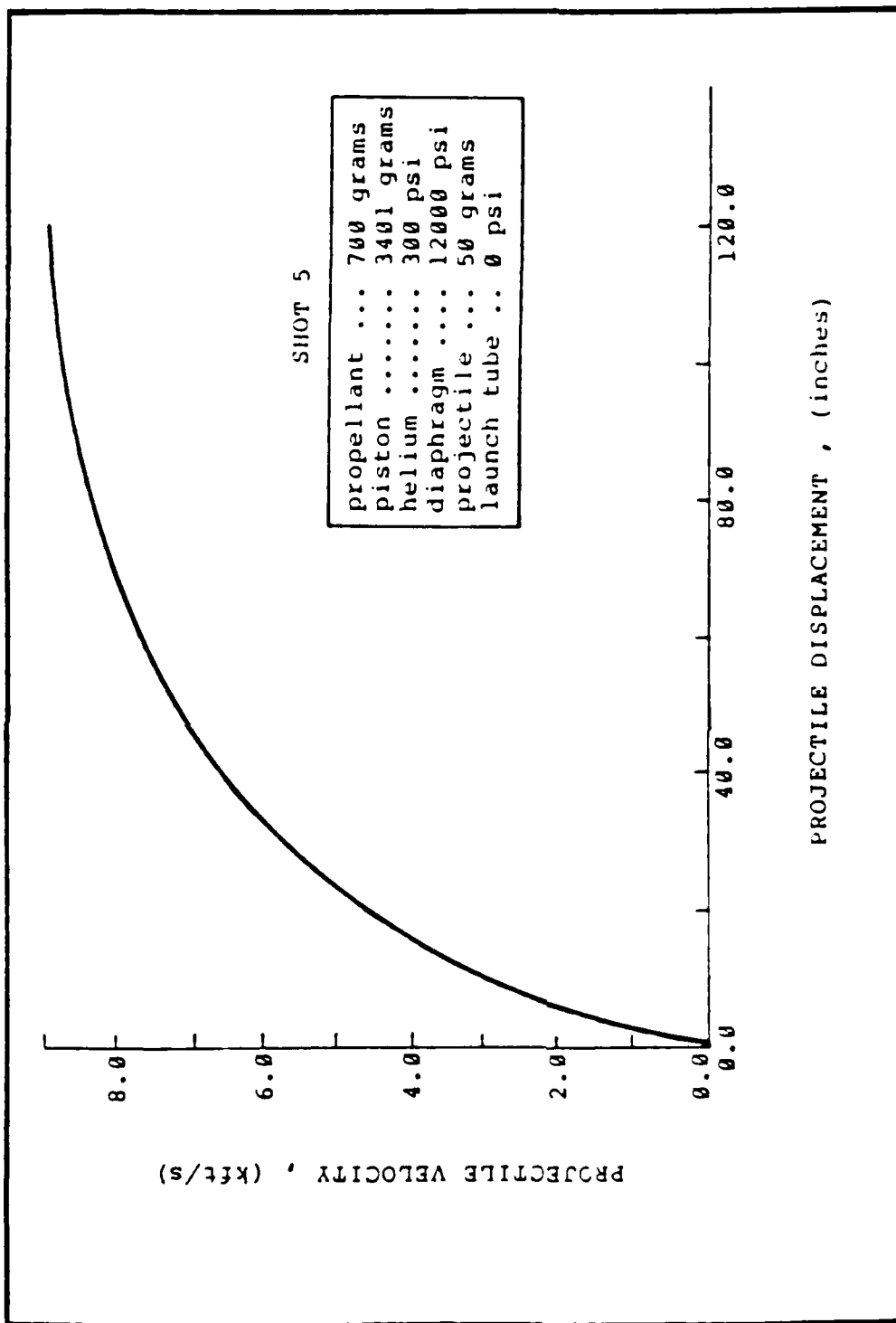
Figure 12. The velocity of the projectile vs. projectile displacement.

1.70

SHOT 5

propellant	....	700 grams
piston	......	3401 grams
helium	......	300 psi
diaphragm	....	12000 psi
projectile	....	50 grams
launch tube	..	0 psi

PROJECTILE DISPLACEMENT , (inches)

FRICTION FORCE ON THE PROJECTILE , (kips)
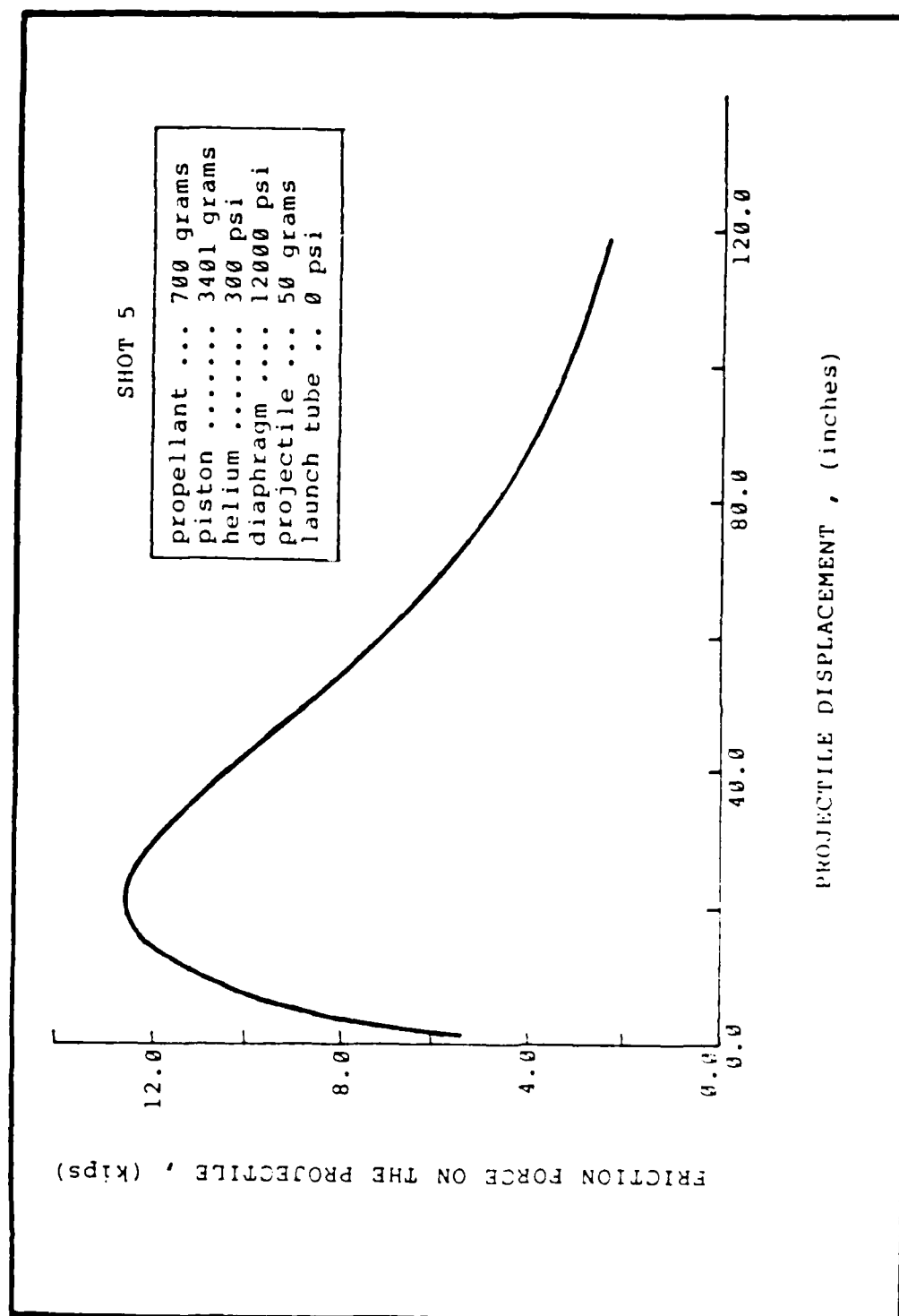
Figure 13.   The frictional force on the projectile vs. projectile displacement.

1.71

PROJECTILE DISPLACEMENT , (inches)

PRESSURE ON PROJECTILE FACE , (kpsi)

SHOT 5

propellant .... 700 grams
piston .... 3401 grams
helium .... 300 psi
diaphragm ..... 12000 psi
projectile .... 50 grams
launch tube ... 0 psi
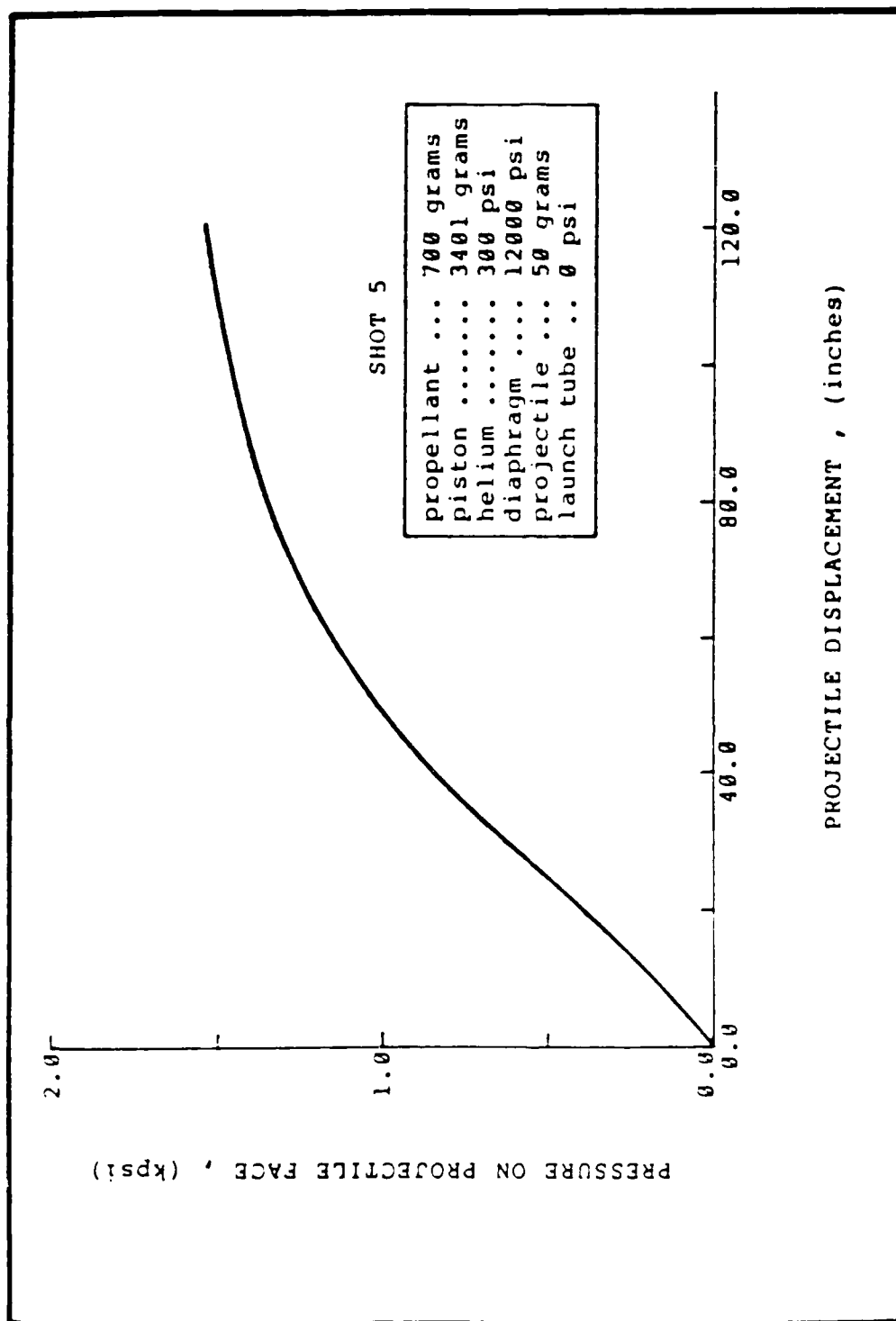
Figure 14. The air pressure on the projectile face vs. projectile displacement.

1.72
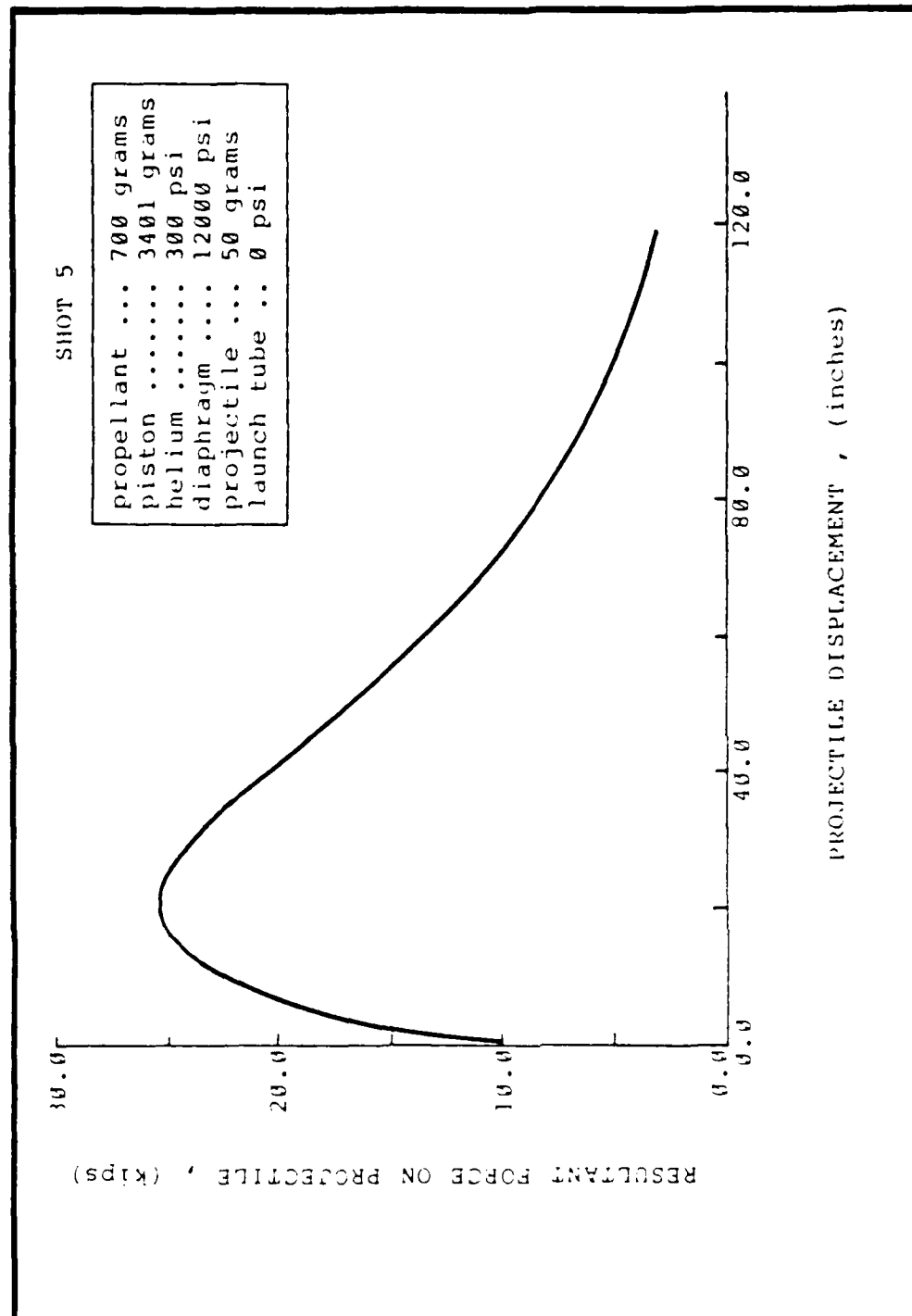
Figure 15. The resultant force on the projectile vs. projectile displacement.

SHOT 5

propellant	...	700 grams
piston	...	3401 grams
helium	...	300 psi
diaphragm	...	12000 psi
projectile	...	50 grams
launch tube	...	0 psi

PROJECTILE DISPLACEMENT , (inches)

RESULTANT FORCE ON PROJECTILE , (kips)

1.73
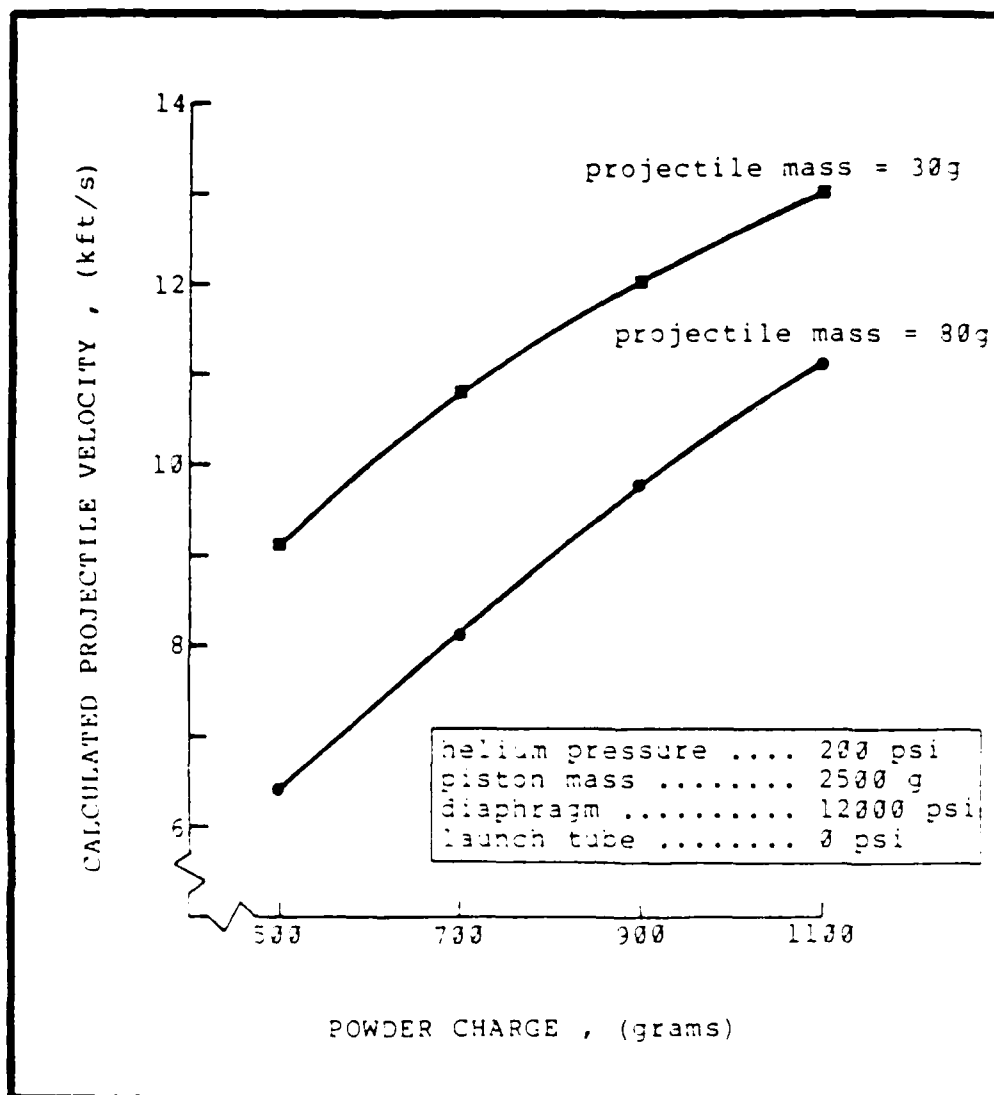
Figure 16. The effect of variations in powder charge on the projectile velocity.

1.74

CALCULATED MAX. BASE PRESSURE ON PROJECTILE , (kpsi)

helium pressure .... 200 psi
piston mass .... 2500 g
diaphragm .... 12000 psi
launch tube .... 0 psi

projectile mass = 30 g

projectile mass = 20 g

180

140

100

60

20

500   700   900   1100

POWDER CHARGE , (grams)
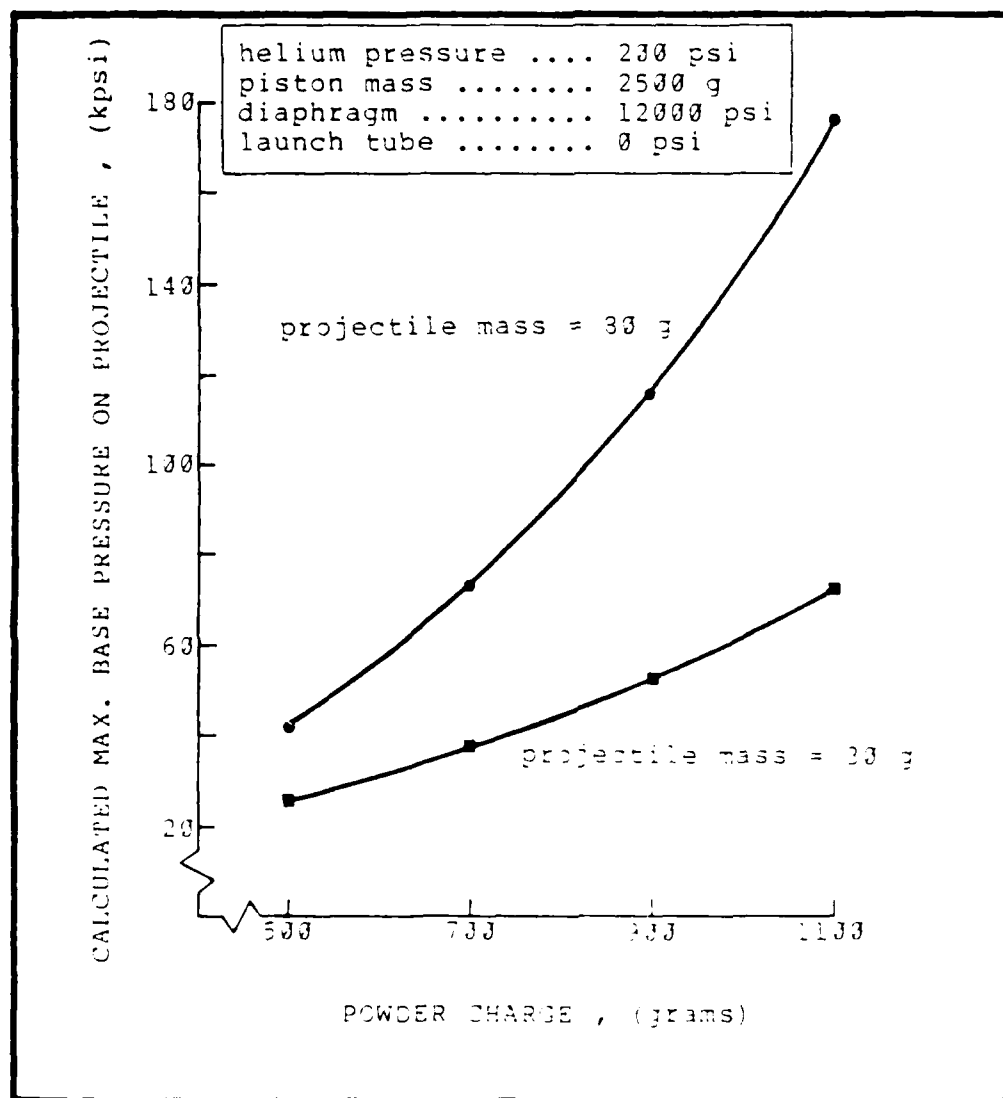
Figure 17. The effect of variations in powder charge on the projectile maximum base pressure.

1.75
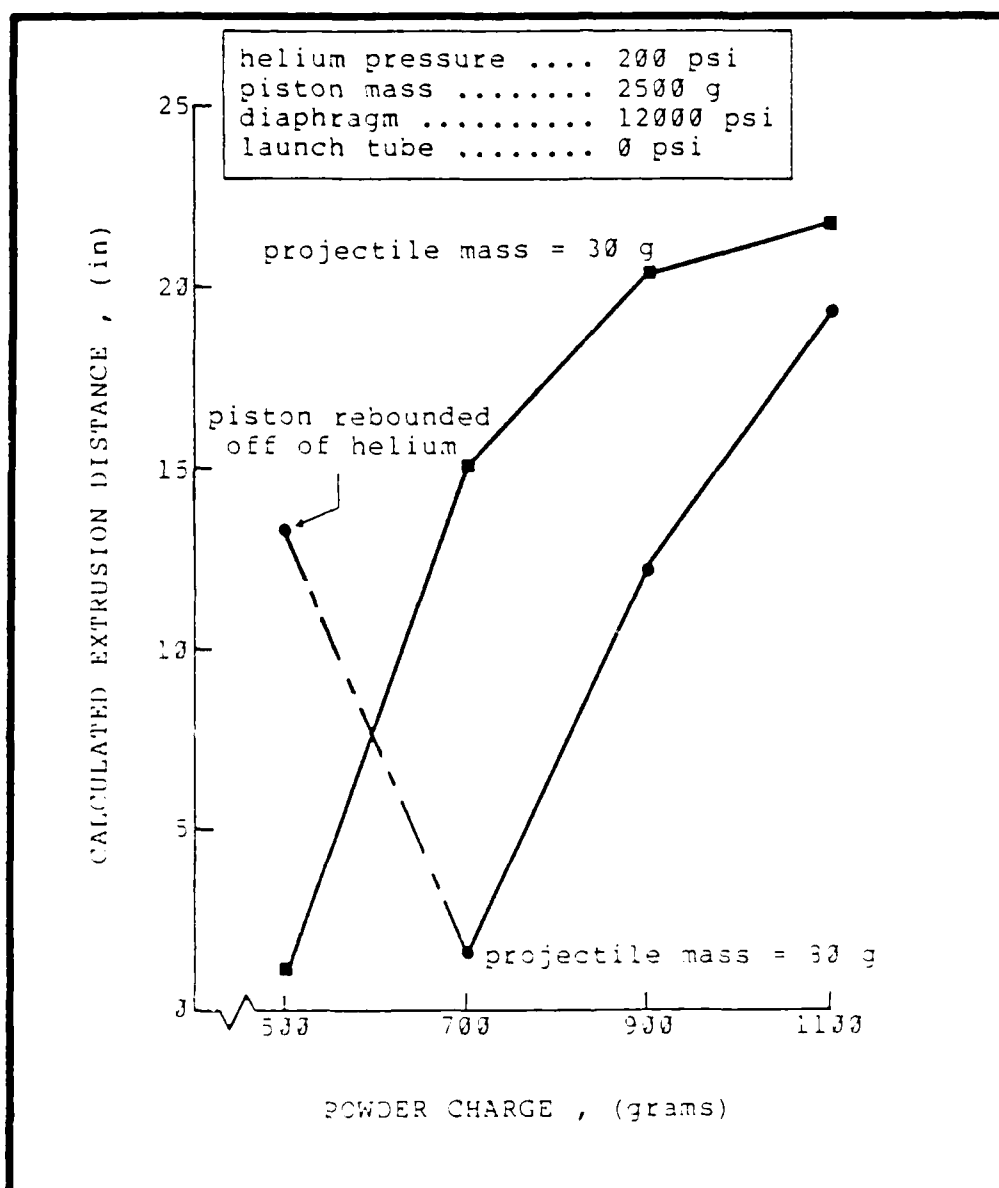
Figure 18. The effect of variations in powder charge on the piston extrusion distance.

1.76

helium pressure .... 200 psi
powder charge ...... 700 g
diaphragm .... 12000 psi
launch tube .... 0 psi

CALCULATED PROJECTILE VELOCITY , (kft/s)

11

projectile mass = 30g

13

9

projectile mass = 80g

8

2.5   3.5   4.5   5.5
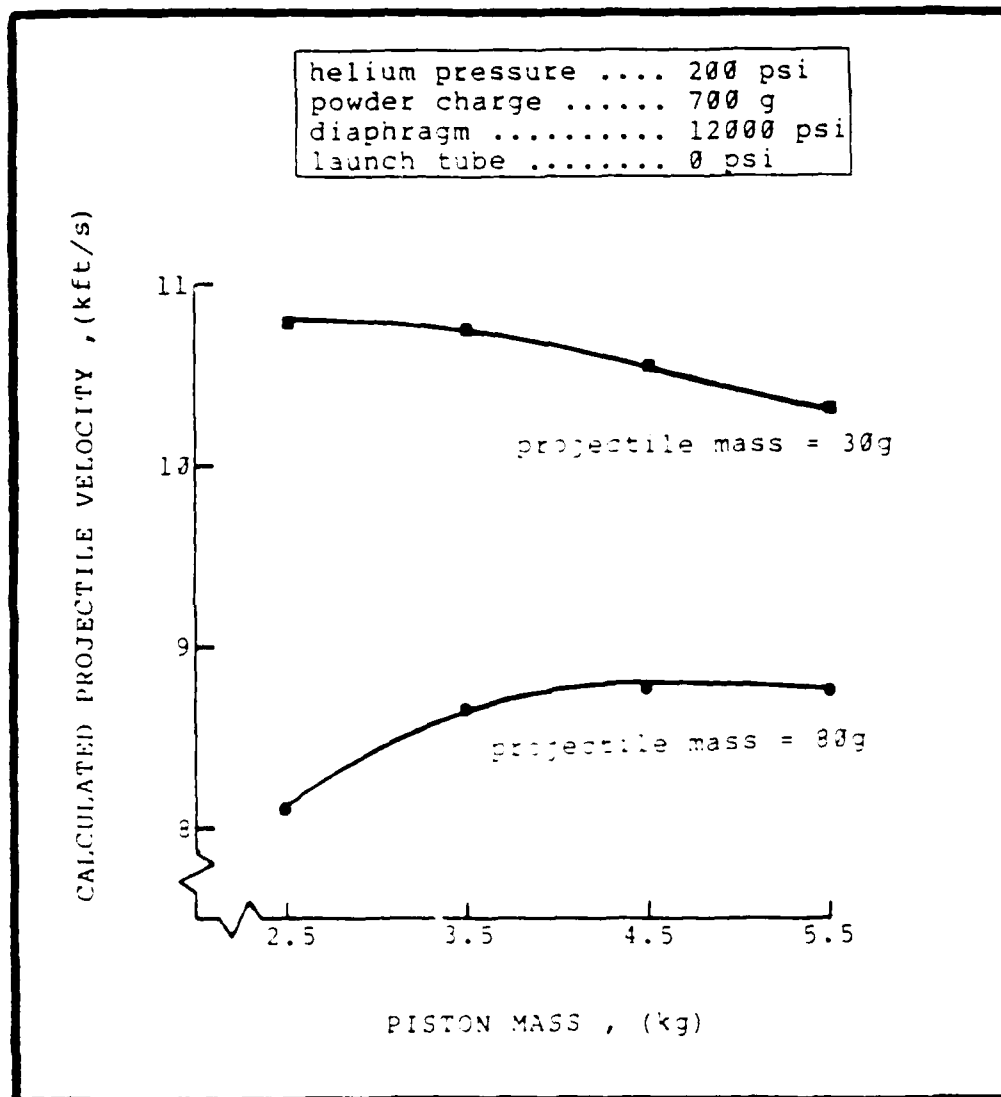
PISTON MASS , (kg)

Figure 19. The effect of variations in the piston mass on the projectile velocity.

1.77
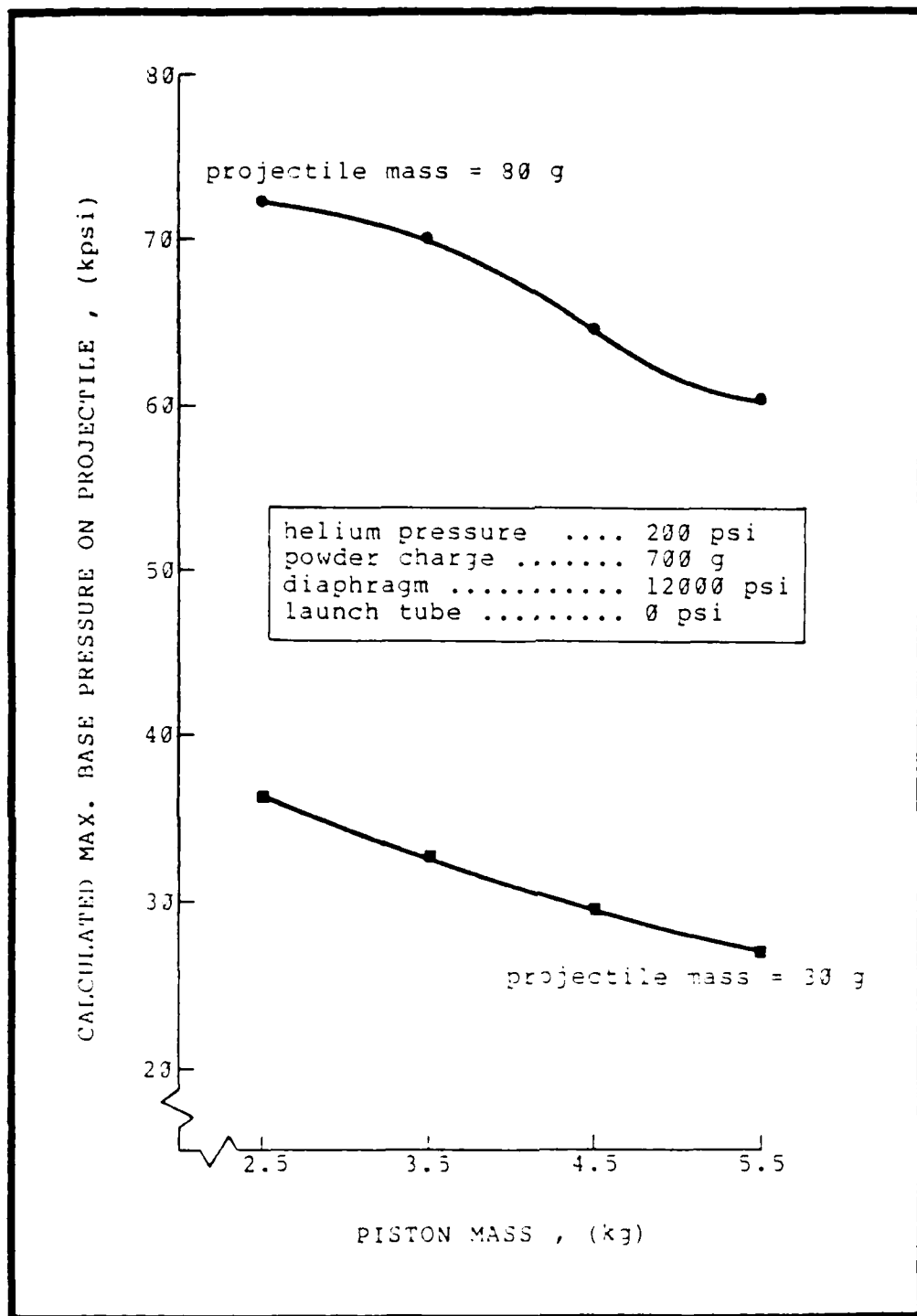
Figure 20. The effect of variations in the piston mass on
the projectile maximum base pressure.

1.78
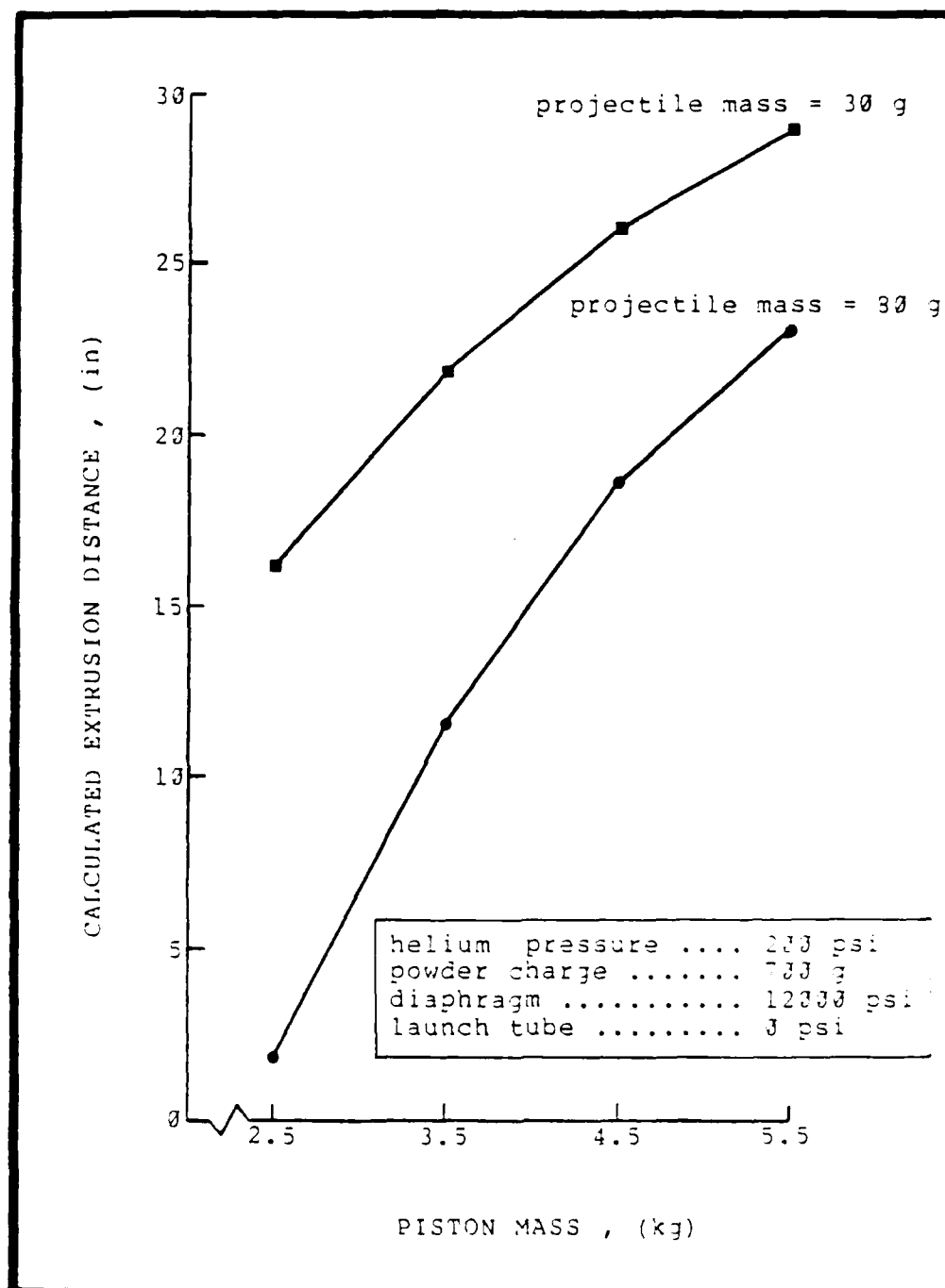
Figure 21. The effect of variations in the piston mass on the piston extrusion distance.

1.79
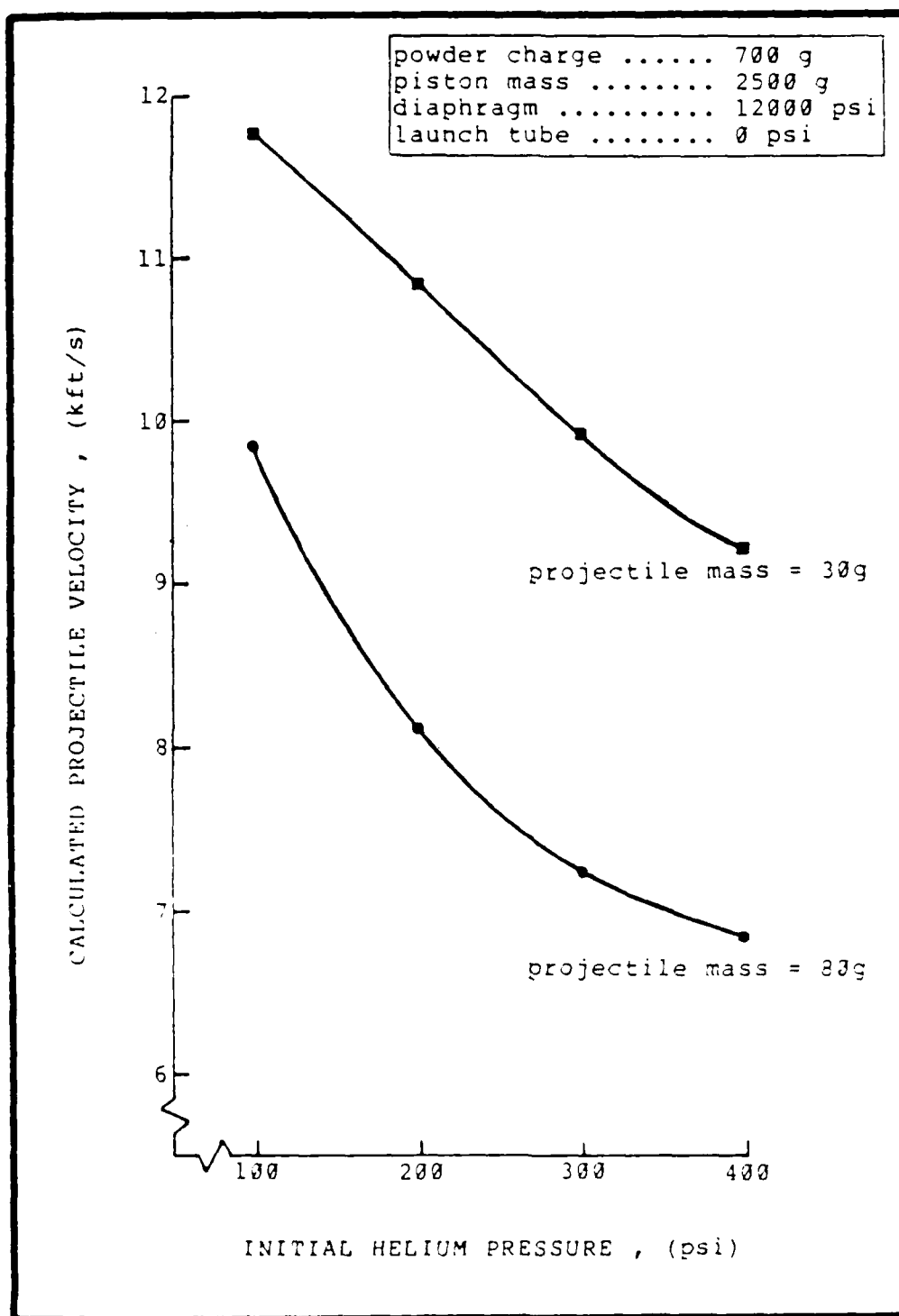
Figure 22.   The effect of variations in the initial helium
             pressure on the projectile velocity.

1.80
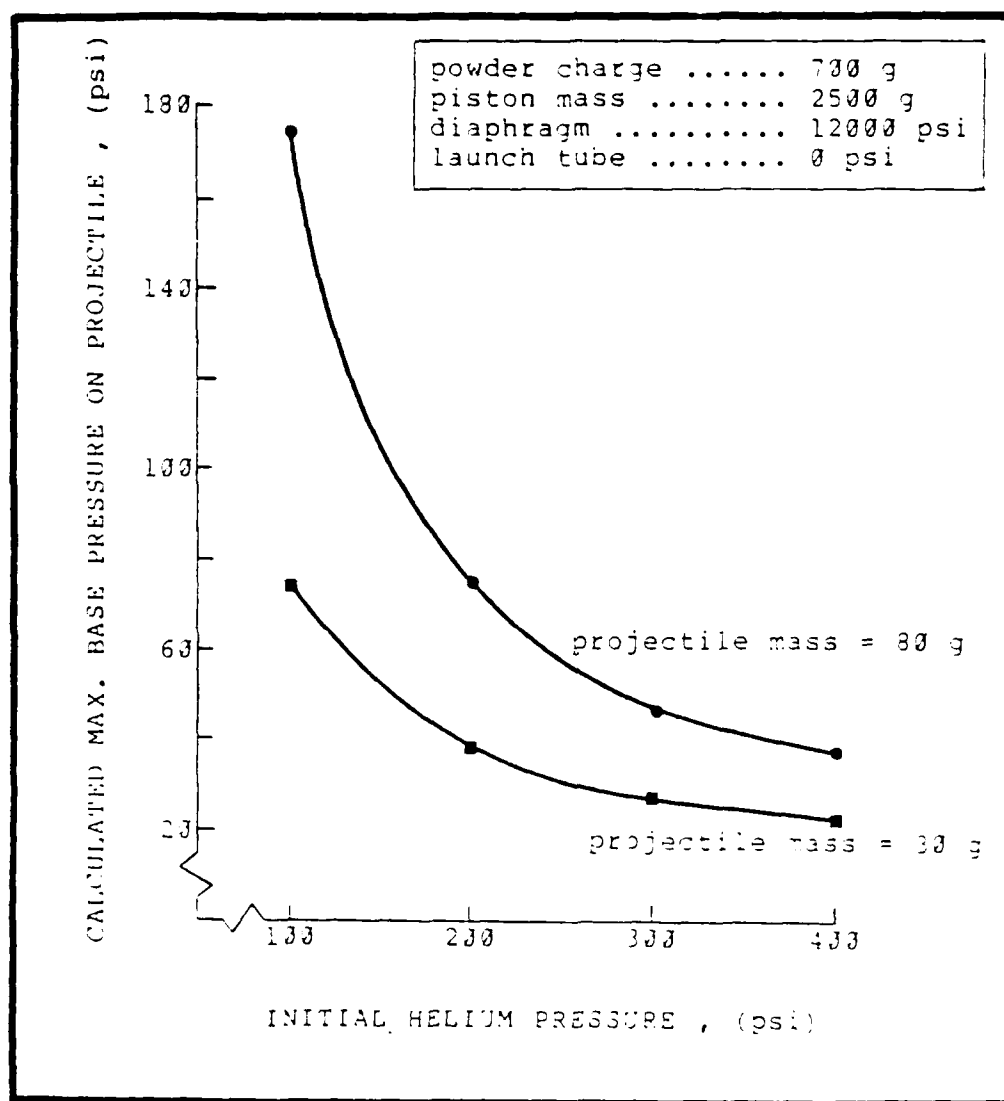
Figure 23. The effect of variations in the initial helium pressure on the projectile maximum base pressure.

powder charge ...... 700 g
piston mass .... 2500 g
diaphragm .... 12000 psi
launch tube .... 0 psi

CALCULATED EXTRUSION DISTANCE , (in)

20

15

10

5

0

piston rebounded
off of helium

piston rebounded
off of helium

projectile
mass
= 30 g

projectile mass = 30 g

100   200   300   400

INITIAL HELIUM PRESSURE , (psi)
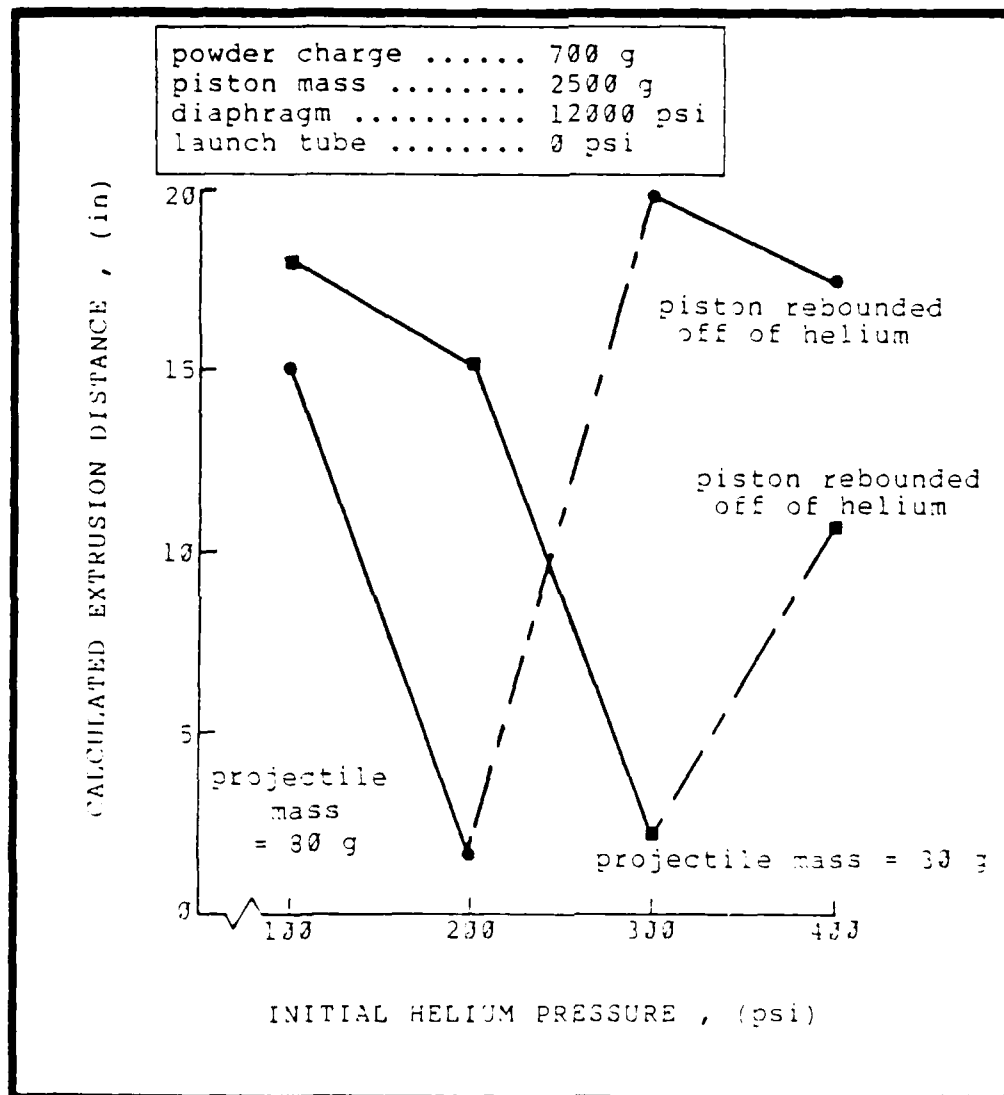
Figure 24.   The effect of variations in the initial helium
pressure on the piston extrusion distance.

1.82
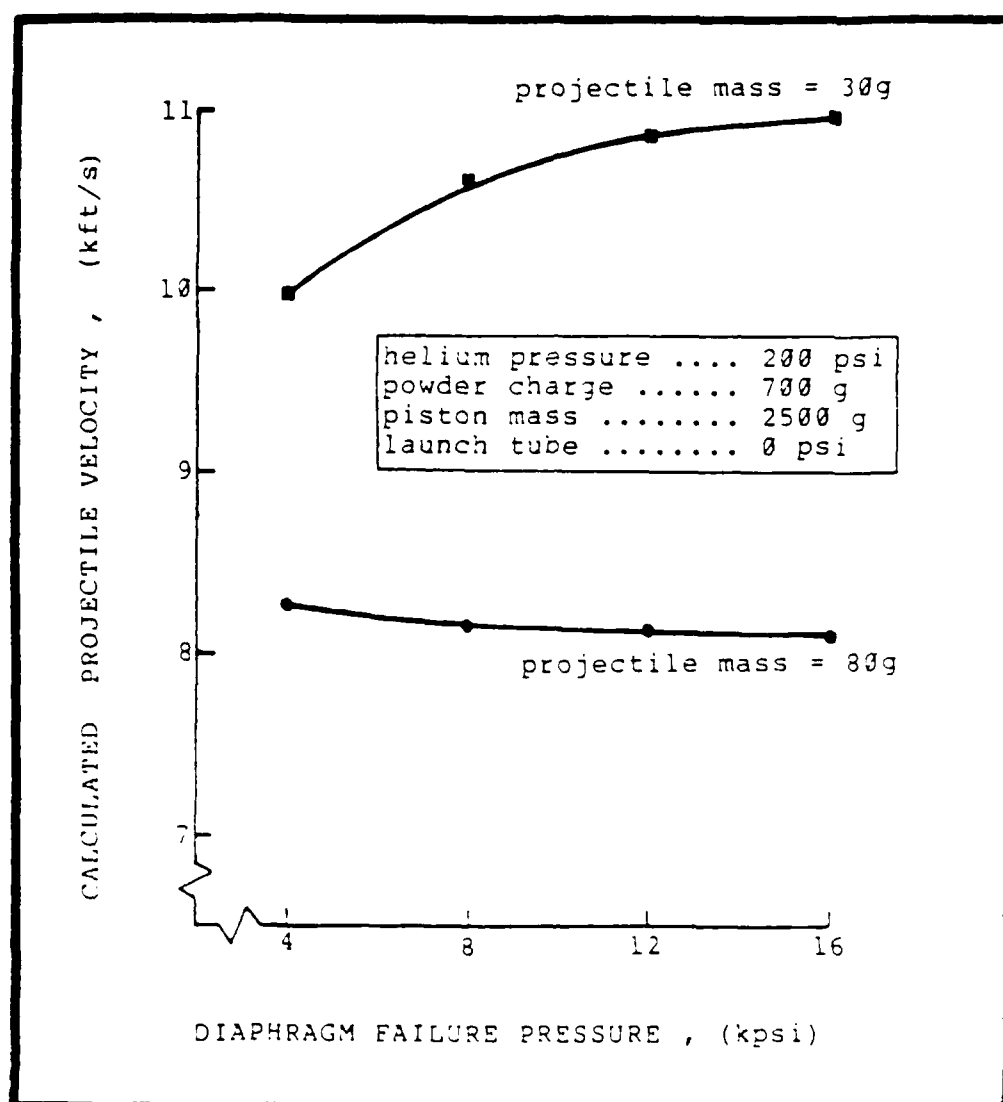
Figure 25. The effect of variations in the diaphragm failure pressure on the projectile velocity.

1.83
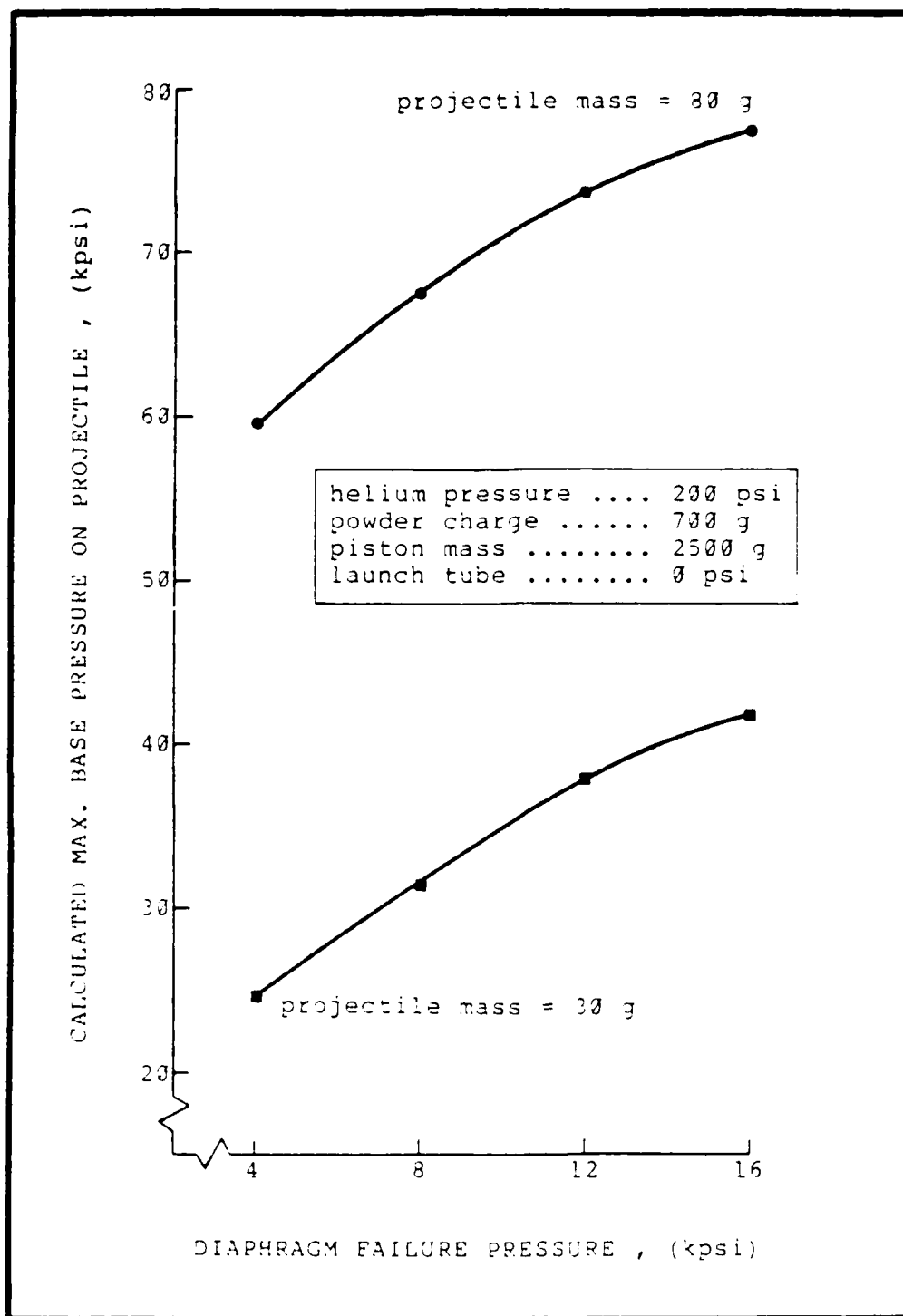
Figure 26. The effect of variations in the diaphragm failure pressure on the projectile maximum base pressure.
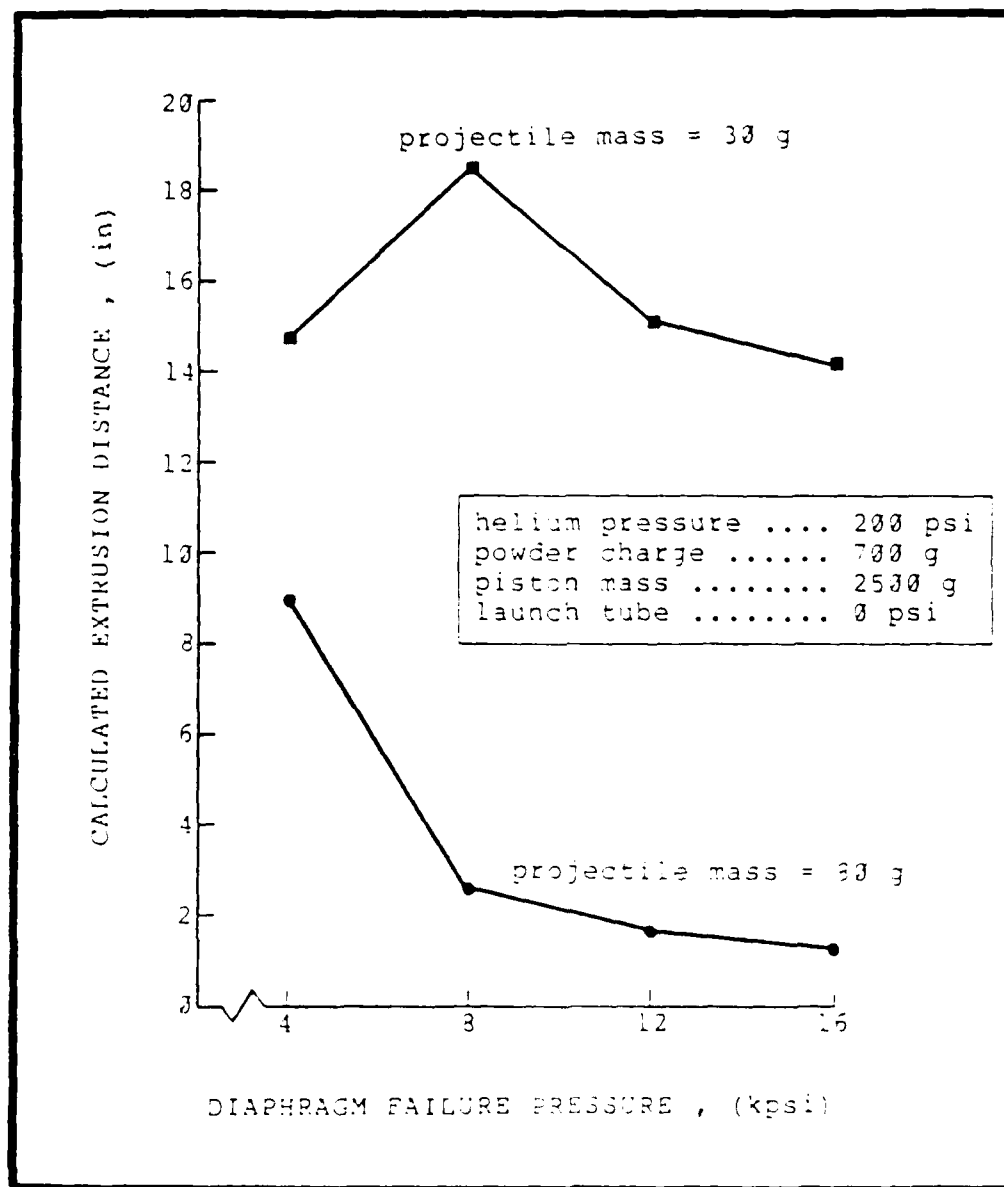
Figure 27. The effect of variations in the diaphragm failure pressure on the piston extrusion distance.
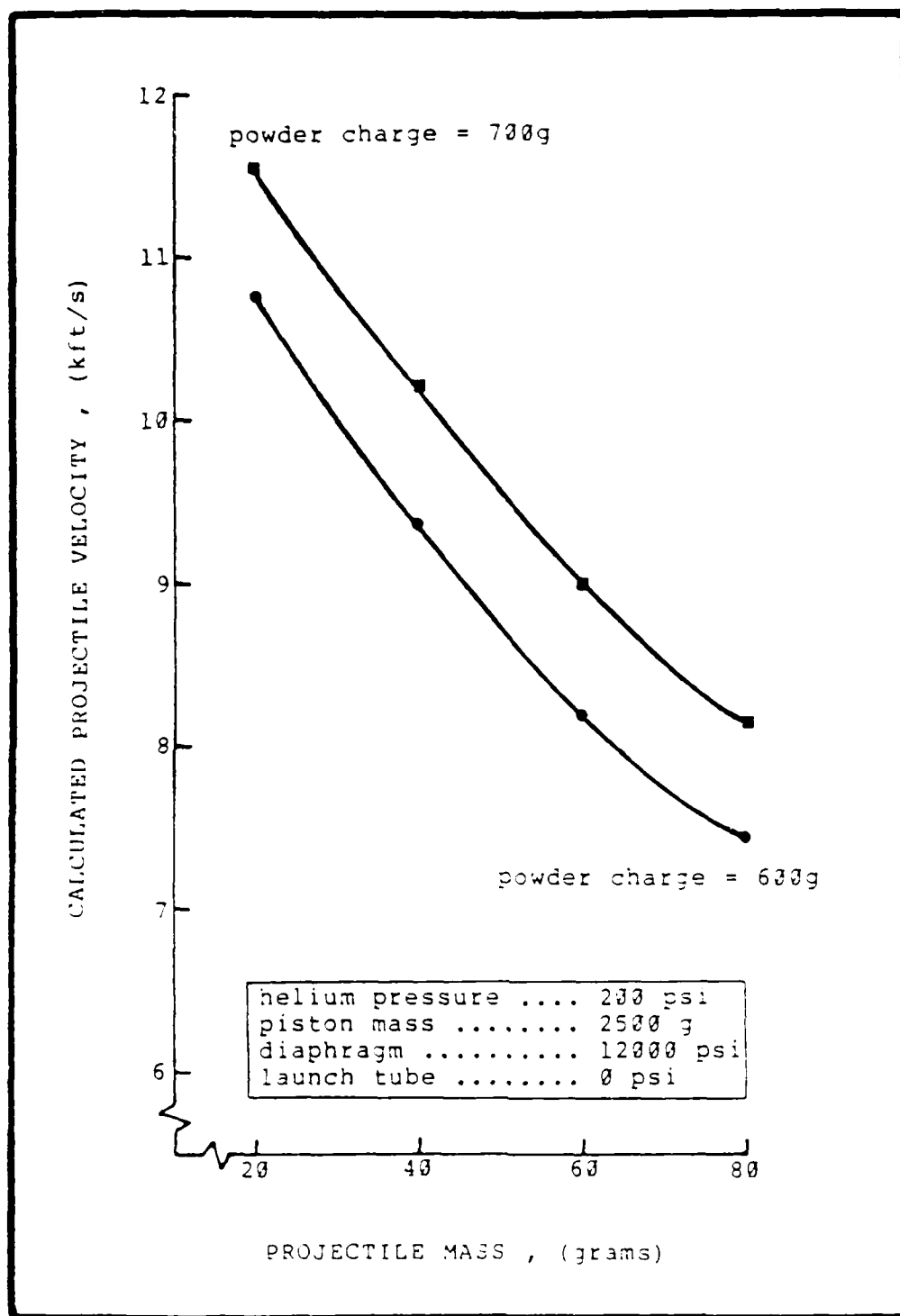
Figure 28. The effect of variations in the mass of the projectile on the projectile velocity.

1.86
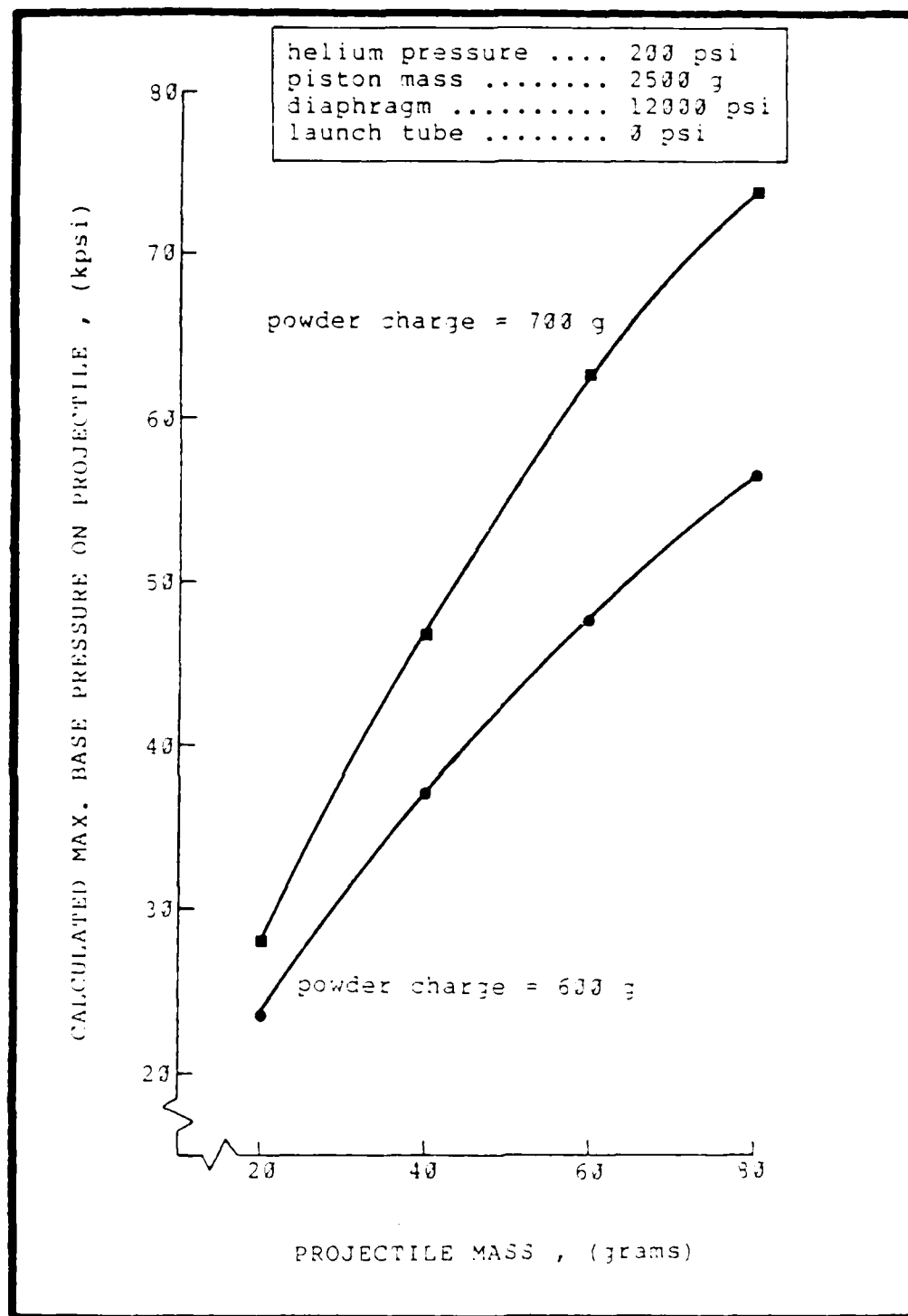
Figure 29. The effect of variations in the mass of the projectile on the projectile maximum base pressure.
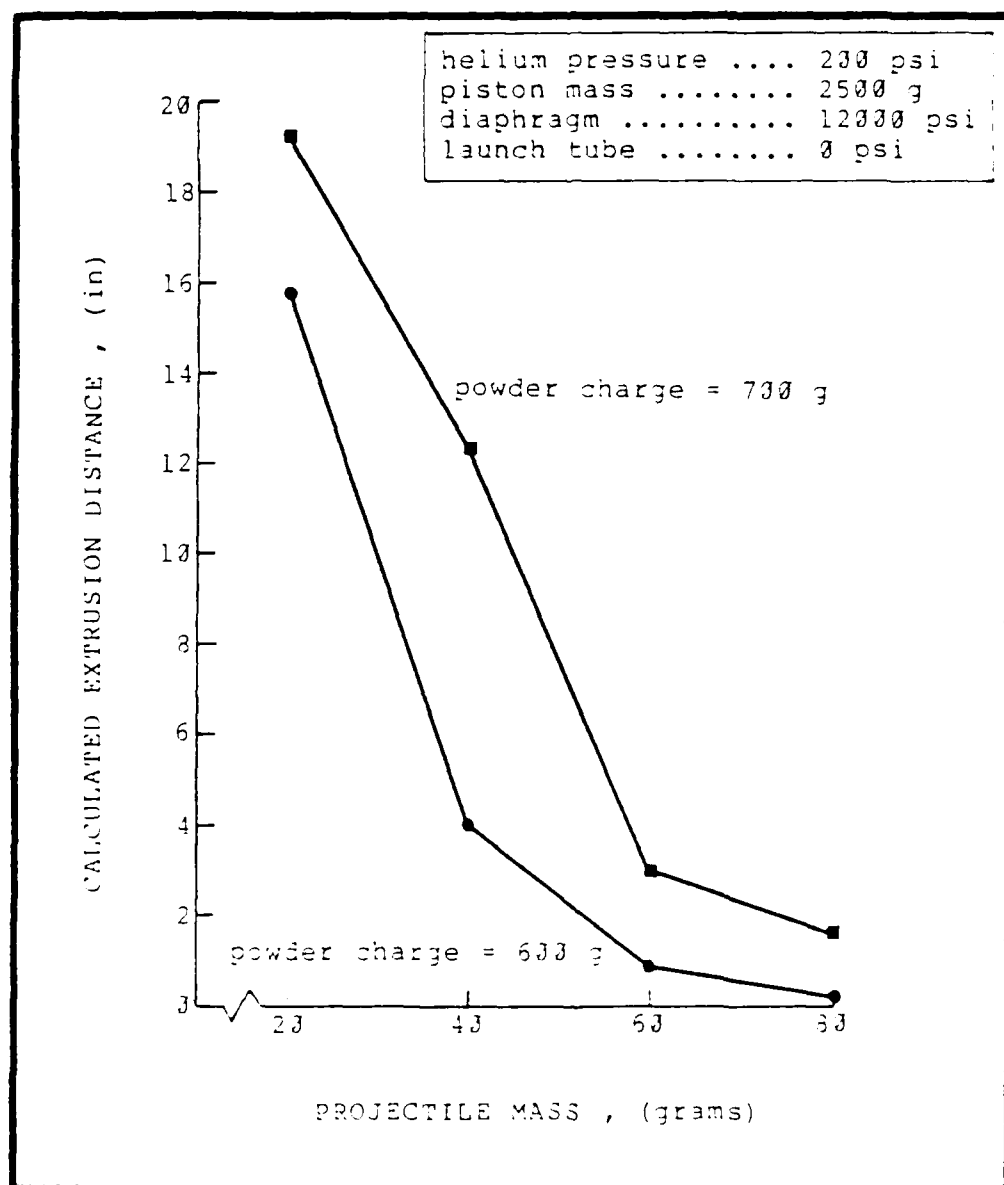
Figure 30. The effect of variations in the mass of the projectile on the piston extrusion distance.

1.88

helium pressure .... 200 psi
powder charge ...... 700 g
piston mass .... 2500 g
diaphragm .... 12000 psi

CALCULATED PROJECTILE VELOCITY , (kft/s)

12

11

10

9

8

projectile mass = 30g

projectile mass = 83g

0   5   10   15

LAUNCH TUBE PRESSURE , (psia)
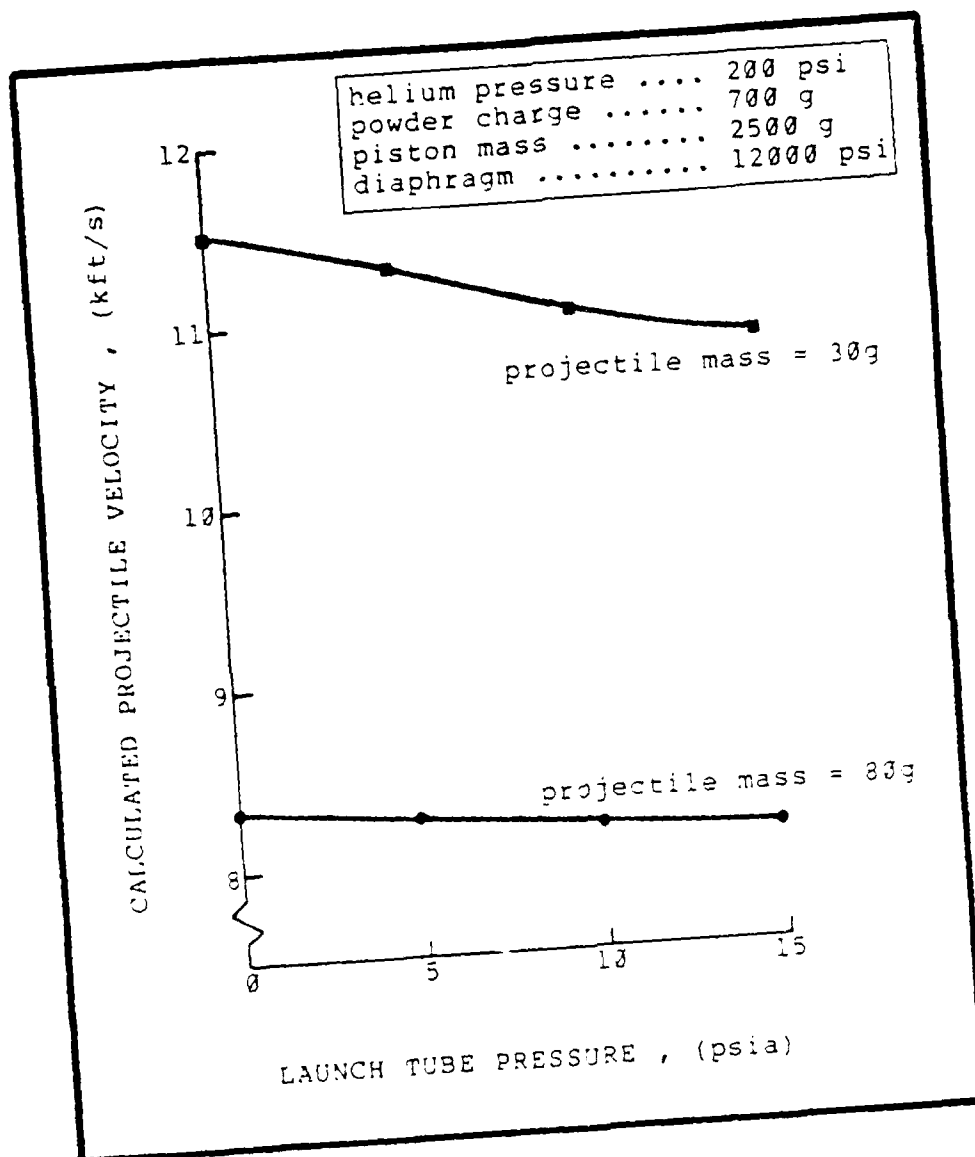
Figure 31.   The effect of variations in the launch tube
pressure on the projectile velocity.

1.89
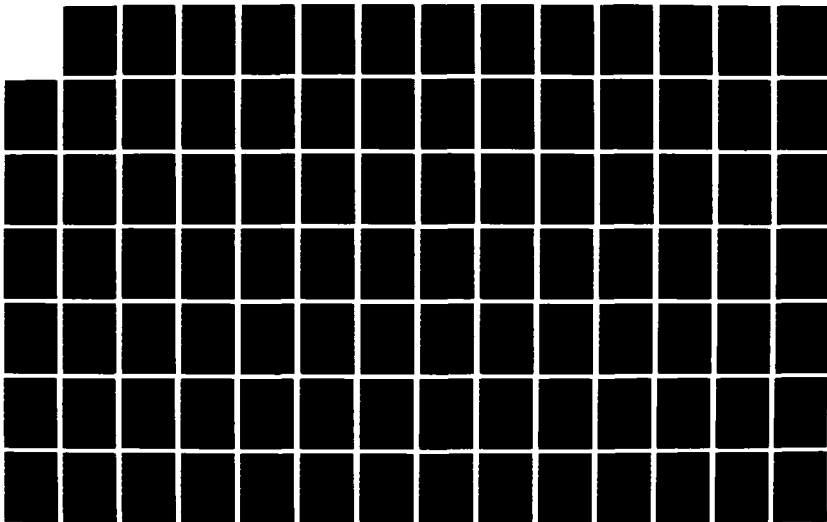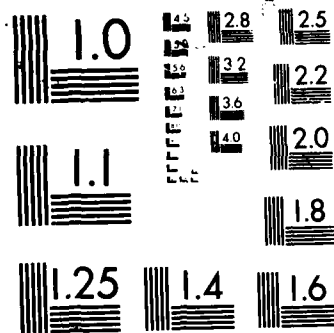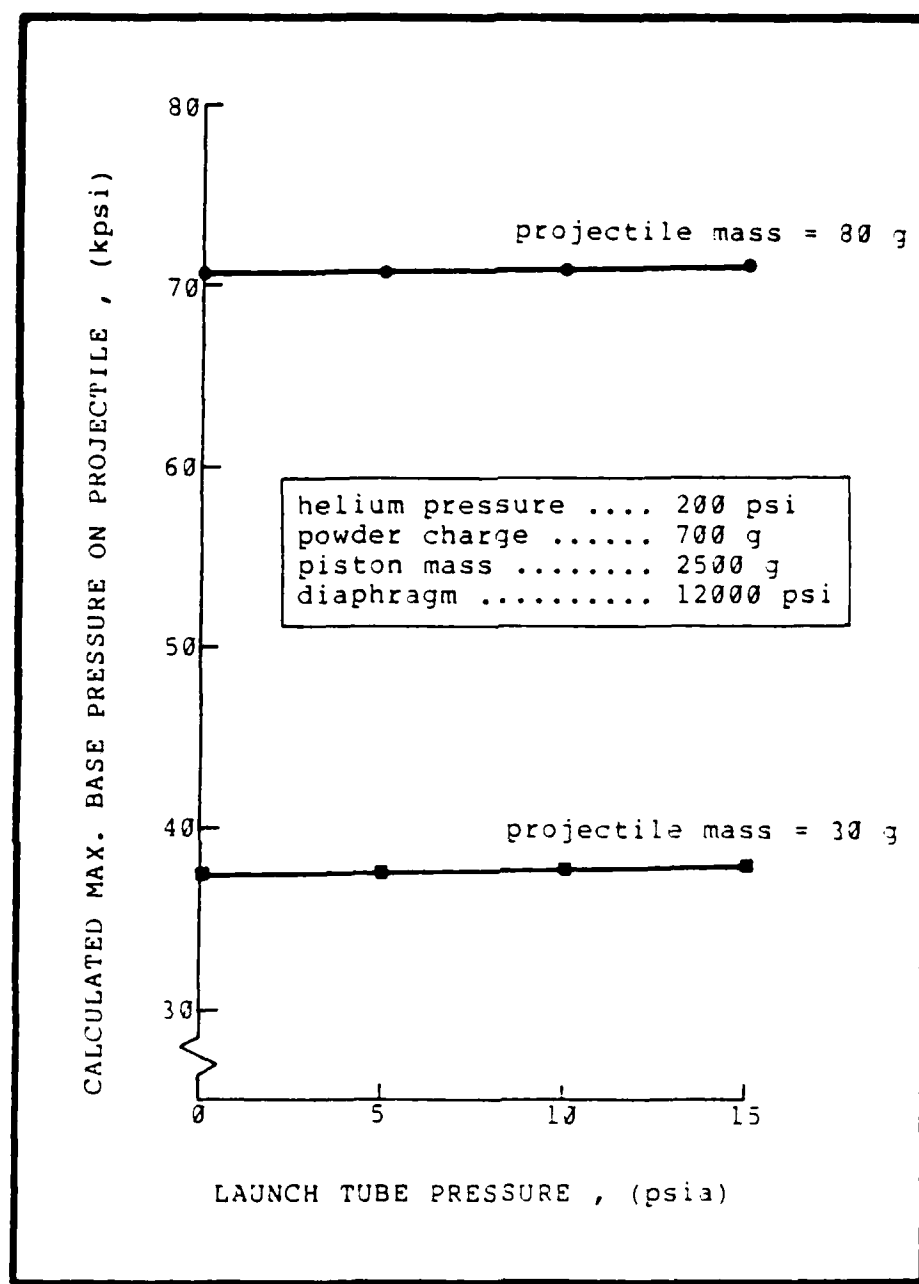
Figure 32. The effect of variations in the launch tube pressure on the projectile maximum base pressure.
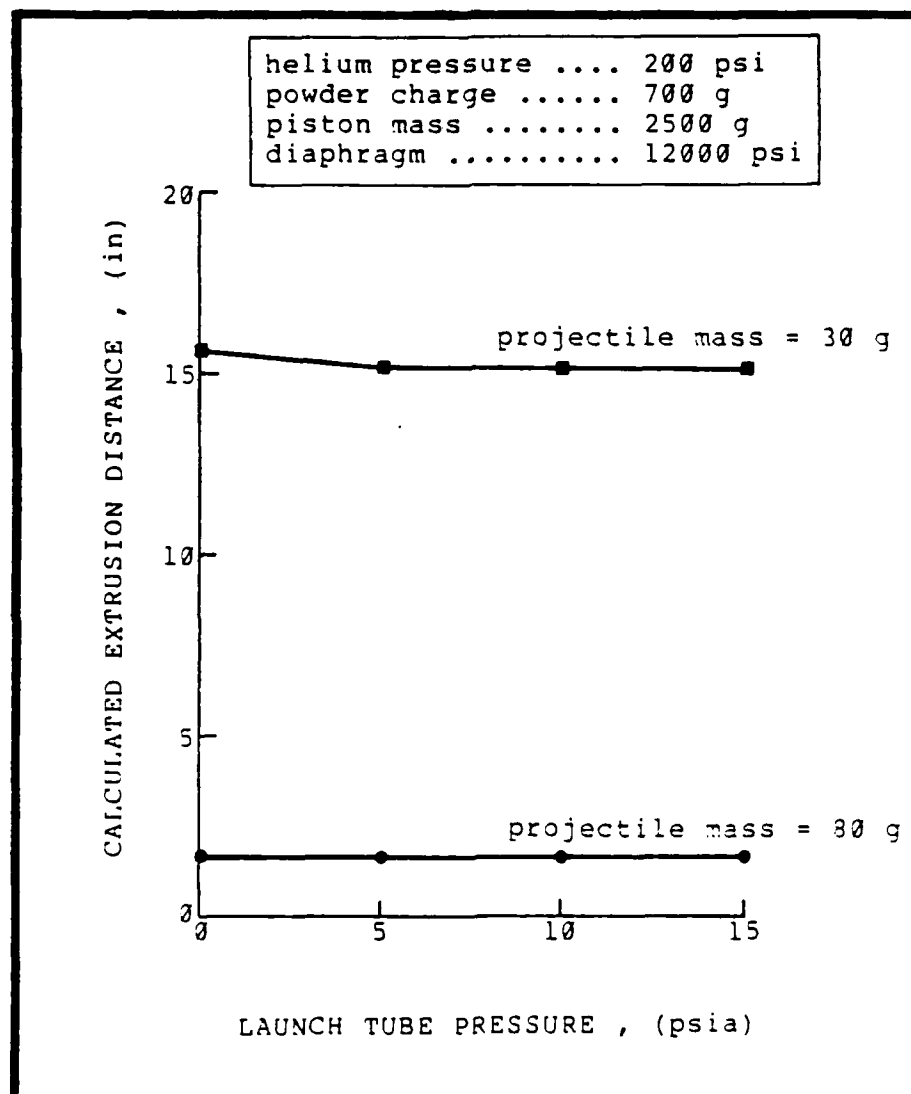
Figure 33. The effect of variations in the launch tube pressure on the piston extrusion distance.

1.91

REFERENCES

1. Siegel, A.E., The Theory of High Speed Guns, North Atlantic Treaty Organization Advisory Group for Aerospace Reasearch and Development, AGARDograph 91, May 1965.

2. Berggren, R.E., and Reynolds, R.M., "The Light-Gas-Gun Model Launcher", Ballistic Range Technology, ed. by Canning, T.N., Sief, A., and James, S.J., North Atlantic Treaty Organization Advisory Group for Aerospace Research and Development, AGARDograph 138, August 1970.

3. Heiney, O.K., "Interior Ballistics, Muzzle Flash and Gas Gradients of Aircraft Cannon", Air Force Armament Laboratory Report AFATL-TR-76-34, Eglin AFB, Flordia, March 1976.

4. Baer, P.G., "Practical Interior Ballistic Analysis of Guns", Interior Ballistics of Guns, ed. by H.Krier and M. Summerfield, Progress in Astronautics and Aeronautics Series, vol. 66, 1979.

5. Betzalel Avitzur, "Handbook of Metal-Forming Processes", John Wiley & Sons, 1983.

6. Betzalel Avitzur, "Metal Forming: Processes and Analysis", Robert E. Krieger Publishing Company, Huntington, New York, 1979.

7. "PLASTICS edition 5, desk-top data bank, Book A", ed. by M.J. Howard, The International Plastics Selector, Inc., 1980.

8. Rast, J.J., "The Design of Flat-Scored High-Pressure Diaphragms for Use in Shock Tunnels and Gas Guns", U.S. Naval Ordnance Laboratory Report NAVORD 6865, White Oak, Maryland, January 1961.

9. Yamaki, Y., and Rooker, J.R., "Experimental Investigation of Circular, Flat, Grooved and Plain Steel Diaphragms Bursting Into A 30.5-Centimeter-Square Section", NASA Technical Memorandum, NASA TM X-2549, Langley Reasearch Center, Hampton, Virginia, May 1972.

10. James, M.L.,Smith, G.M., and Wolford,J.C., "Applied Numerical Methods for Digital Computation with FORTRAN and CSMP, second edition", Harper & Row Publishers, 1977.

11. Munson, D.E., and May, R.E., "Interior Ballistics of a Two-Stage Light Gas Gun", Sandia Laboratory Report Sand 75-0323, Albuquerque, New Mexico, July 1975.

12. Hardy, R.D., "A Program to Predict Performance of a Gas Gun", Sandia Laboratory Report Sand 81-2546, Albuquerque, New Mexico, December 1981.

13. Jeelani, S., Kelly, J.J., Whitfield, J.K., Douglas, R.A. "Two-Stage Light Gas Gun Installation For Hypervelocity Impact Studies", North Carolina State University, Technical Report 73-3, September 1973.

14. Mitchell, A.C., and Nellis, W.J., "The Lawrence Livermore Laboratory Two-Stage Light Gas Gun", Lawrence Livermore Laboratory Preprint VCRL-83334, September 1979.

15. Otten, M.G., "Development of a 7-in Air Gun For Use in Interior Ballistics Simulation", Harry Diamond Laboratory Report HDL-TM-75-13, October 1975.

16. Heiney, O.K., "Simplified Analytic and Experimental Interior Ballistics of Light Gas Guns", Air Force Armament Laboratory Report AFATL-TR-74-32, Eglin AFB, Florida, January 1974.

17. Murphy, J.R.B., Badhwar, L.K.,and Lavoie, G.A., "Interior Ballistics Calculation Systems For Light Gas Guns and Conventional Guns", The Fluid Dynamic Aspects of Ballistics, AGARD Conference Proceedings No. 10, September 1966.

18. Krier, H., and Adams, M.J., "An Introduction to Gun Interior Ballistics and a Simplified Ballistic Code", Interior Ballistics of Guns, ed. by H. Krier and M. Summerfield, Progress in Astronautics and Aeronautics Series, vol. 66, 1979.

19. Ludwig Stiefel, "Gun Propellants", Interior Ballistics of Guns, ed. by H. Krier and M. Summerfield, Progress in Astronautics and Aeronautics Series, vol. 66, 1979.

20. Farrar, C.L., and Leeming, D.W., "Military Ballistics - A Basic Manual", Brassey's Publishers Ltd, 1983.

21. Goad, K.J.W., and Halsey, D.H.J. "Ammunition (including grenades and mines)", Brassey's Publishers Ltd, 1982.

22. Ryan, J.W., "Guns, Mortars and Rockets", Brassey's Publishers ltd, 1982.

23. Zucrow, M.J., and Hoffman, J.D., "Gas Dynamics, vol. I", John Wiley & Sons, 1976.

24. Callen, H.B., "Thermodynamics", John Wiley & Sons, 1963.

APPENDICES

1.95

APPENDIX A

ANALYSIS OF FRICTION FORCE ON THE PROJECTILE

It is assumed that only the obturator contributes to the frictional force on the projectile. It is also assumed that the obturator is thin enough so that the pressure in the axial direction is constant over the thickness of the obturator. The pressure exerted on the inner bore of the launch tube is determined using a free-body equilibrium approach :
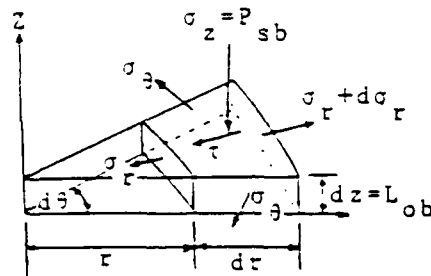
Figure A-1. Differential element of obturator in cylindrical coordinates.

Summation of forces in the radial direction yields :

$$\sigma_r r d\theta dz - (\sigma_r + d\sigma_r)(r + dr)d\theta dz + 2\tau r d\theta dr + 2\sigma_\theta dr dz \frac{d\theta}{2} = 0$$

Neglect higher order terms to get :

$$-\sigma_r dr dz - r d\sigma_r dz + \sigma_\theta dr dz + 2\tau r dr = 0$$

Assume σ_r and σ_θ are equal, and the shear stress τ will be related to the base pressure by mP_{sb}, to obtain :

$$L_{ob} d\sigma_r - 2m\sigma_z dr = 0$$

1.96

Integration yields :

$$\int d\sigma_r = \frac{2mP_{sb}}{L_{ob}} \int dr \quad ; \quad \sigma_r = \frac{2mrP_{sb}}{L_{ob}} + C$$

Apply the following boundary conditions to solve for the constant of integration :

B.C. ,   @ $r = 0$, $\sigma_r = 0$
          @ $r = r_{1t}$, $\sigma_r = P_{b1t}$

This yields :

$$\sigma_r = P_{b1t} = \frac{2mr_{1t}P_{sb}}{L_{ob}}$$

The normal force on the inner bore is thus defined as :

$$P_{b1t} = \pi 2mP_{sb}r_{1t}D_{1t}$$

The resultant friction force is related to the normal force by a constant of proportionality, μ , which is called the Coulomb coefficient of friction; thus :

$$FS_3 = \mu\pi m (D_{1t})^2 P_{sb}$$

1.97

APPENDIX B

ANALYSIS OF PRESSURE DROP ONCE PROJECTILE EXITS LAUNCH TUBE

The integral form of the continuity equation is defined as :

$$\frac{\partial}{\partial t}\int_{\forall} \rho\, d\forall + \int_{S} \rho \vec{V} \cdot d\vec{A} = 0$$

It will be assumed that the velocity of the gas exiting the launch tube is a constant and is equal to the velocity of the projectile. It will also be assumed that the effects of temperature and volume changes in the gas can be neglected. With these assumptions, the continuity equation yields :

$$\forall \frac{dP_{He}}{dt} + P_{He}\dot{X}_s A_{1t} = 0$$

The result of integration yields :

$$\int_{P_{He_0}}^{P_{He}} (1/P_{He})\, dP_{He} = -\frac{\dot{X}_s A_{1t}}{\forall_{He_0}}\int_{0}^{t} dt \quad ; \quad \ln\left|\frac{P_{He}}{P_{He}}\right| = -\frac{\dot{X}_s A_{1t}}{\forall_{He_0}} t$$

The decay in helium pressure after the projectile has exited the launch, as a function of time, is therefore defined as :

$$P_{He} = P_{He_0} \exp^{-\left|\frac{\dot{X}_s A_{1t}}{\forall_{He_0}}\right| t}$$

APPENDIX C

A listing of the computer program which was developed is provided. The program is coded in BASIC and is written specifically for the Zenith Z-100 computer.

```
1000 CLS
1010 '
1020 '    -----------------------------------------
1030 '    -  The variable types are declared.
1040 '    -----------------------------------------
1050 '
1060 DEFDBL A-Z
1070 DEFSNG I-K,R
1080 DEFSTR X-Z
1090 '
1100 '    -----------------------------------------
1110 '    -  The arrays are dimensioned.
1120 '    -----------------------------------------
1130 '
1140 OPTION BASE 0
1150 DIM R(500,16),F(16),NB(3,2),PR(3,2),U(4,2),XT(16),XU(16),IPLOT(2)
1160 '
1170 '    -----------------------------------------
1180 '    -  The data on gun geometry, material properties, and plotting
1190 '    -  information are read in from file DATA.GUN .
1200 '    -----------------------------------------
1210 '
1220 OPEN "I",#1,"DATA.GUN"
1230 INPUT#1,LBR,DBR,LPT,DPT,LNOZ,EDN,LHPS,LLT,DLT,VST,LP,SIGMA,M,DPP
1240 INPUT#1,SIGMAL,ML,DL,CF,FP,CPG,SHRP,DP,PGF,HLF,DDF,WT
1250 INPUT#1,BRC,BRI,SHRH,GCH,SHRA,GCA,PAV,PB,PISTX
1260 INPUT#1,PISTV,PISTP,SPP,PROJV,PROJX,PROJP,C1,C2,C3,PI,PATM,GC
1270 INPUT#1,XT(0),XU(0),XT(1),XU(1),XT(2),XU(2),XT(3),XU(3),XT(4),XU(4)
1280 INPUT#1,XT(5),XU(5),XT(6),XU(6),XT(7),XU(7),XT(8),XU(8),XT(9),XU(9)
1290 INPUT#1,XT(10),XU(10),XT(11),XU(11),XT(12),XU(12),XT(13),XU(13),XT(14)
1300 INPUT#1,XT(14),XT(15),XU(15),XT(16),XU(16),F(0),F(1),F(2),F(3),F(4),F(5)
1310 INPUT#1,F(6),F(7),F(8),F(9),F(10),F(11),F(12),F(13),F(14),F(15),F(16)
1320 CLOSE#1
1330 '
1340 '    -----------------------------------------
1350 '    -  The following subroutine displays the program heading.
```

```
1360  '  -----------------------------------------------------------
1370  '
1380  GOSUB 5190
1390  '
1400  '  -----------------------------------------------------------
1410  '  The following subroutine is for the input of the shot parameters.
1420  '  -----------------------------------------------------------
1430  '
1440  GOSUB 5470
1450  '
1460  '  -----------------------------------------------------------
1470  '  The cone angle, apex, and extrusion distance required
1480  '  to fill the cone are computed.
1490  '  -----------------------------------------------------------
1500  '
1510  ALPHA=ATN((DPT/2-EDN/2)/LNOZ)
1520  APEX=LNOZ/(1-EDN/DPT)
1530  EXT1=APEX*(1-(EDN/DPT)^3)/3
1540  '
1550  '  -----------------------------------------------------------
1560  '  The cross sectional area of each region in the gun is computed.
1570  '  -----------------------------------------------------------
1580  '
1590  ABR  =  PI*(DBR^2)/4
1600  APT  =  PI*(DPT^2)/4
1610  AHPS  =  PI*(EDN^2)/4
1620  ALT  =  PI*(DLT^2)/4
1630  '
1640  '  -----------------------------------------------------------
1650  '  The volume of each region in the gun is computed.
1660  '  -----------------------------------------------------------
1670  '
1680  VBR  =  ABR*LBR-VST
1690  VPT  =  APT*(LPT-LP)
1700  VNOZ  =  (APEX*(DPT/2)^2-(APEX-LNOZ)*(EDN/2)^2)*PI/3
1710  VHPS  =  AHPS*LHPS
```

1.101

```
1720   VTOT = VPT+VNOZ+VHPS
1730 :
1740 : -------------------------------------
1750 :      Mass is converted into lbm.
1760 : -------------------------------------
1770 :
1780   CW = CW/C3
1790   MP = MP/C3
1800   PMP = MP+CW/DDF
1810   MS = MS/C3
1820 :
1830 : -------------------------------------
1840 :      Initial pressures and tempuratures are converted to absolute values.
1850 : -------------------------------------
1860 :
1870   PHE1 = PHE1+PATM : PHE2 = PHE1 : PHEAVG = PHE1 : MAXPS = PATM
1880   PLT = PLT+PATM
1890   PAV = PAV+PATM
1900   THE1 = TA+C2 : THE2 = THE1
1910 :
1920 : -------------------------------------
1930 :      The mass of helium is computed.
1940 : -------------------------------------
1950 :
1960   MHE = (PHE1*VTOT)/(GCH*THE1)
1970 :
1980 : -------------------------------------
1990 :      The force to overcome at shot start (FC1), the max. vel. of the
2000 :      piston (VMAX), and the coefficient (FC2) are computed.
2010 : -------------------------------------
2020 :
2030   FC1 = APT*(SPP-PHE1)
2040   VMAX = SQR(2*GC*FP*CW/MP)
2050   FC2 = FC1/VMAX
2060 :
2070 : -------------------------------------
```

1.102

```
2080 '     The propellant erosion constant (PEC) and the sound speed
2090 '     of the air (SS1) are computed.
2100 '     ------------------------------------------------------------
2110 '
2120 PEC = .01*CW/(DP*VBR)
2130 SS1 = SQR(GC*SHRA*GCA*(TA+C2))
2140 '
2150 '     ------------------------------------------------------------
2160 '     A1 thru A11 are constants which are used in the governing eqns.
2170 '     ------------------------------------------------------------
2180 '
2190 A1 = (SHRP-1)/(2*PGF*SHRP*FP*GC*.7)
2200 A2 = -SHRP/(SHRP-1)
2210 A3 = (SHRP-1)*(1+HLF)*PMP/GC
2220 A4 = SHRH/(SHRH-1)
2230 A5 = (SHRH-1)/(2*SHRH*GCH*GC)
2240 A6 = SHRA*(SHRA+1)/4
2250 A7 = 2*PI*SIGMA
2260 A8 = ((SHRA+1)/4)^2
2270 A9 = ALPHA/(SIN(ALPHA))^2-COS(ALPHA)/SIN(ALPHA)
2280 A10 = COS(ALPHA)/SIN(ALPHA)
2290 A11 = 2*PI*SIGMAL
2300 '
2310 '     ------------------------------------------------------------
2320 '     Functions FNF1() thru FNF() model the processes which occur.
2330 '     ------------------------------------------------------------
2340 '
2350 DEF FNF1(P,V)   = (BRC*(P/1000)^BRI+PEC*V/C1)*2*CW/WT
2360 DEF FNF2(P,V)   = P*(1+A1*V^2)^(A2*A12)
2370 DEF FNF3(D)     = PHE1*(VTOT/(VTOT-D*APT))^SHRH
2380 DEF FNF4(P)     = THE1*(P/PHE1)^(1/A4)
2390 DEF FNF5(P,V,T) = P*(1+A5*V^2/T)^(A4*A12)
2400 DEF FNF6(V)     = FC1-V*FC2
2410 DEF FNF7(D,DS)  = PHE1*(VTOT/(VTOT-(D-PISTPR)*APT+(DS-PROJPR)*ALT))^SHRH
2420 DEF FNF8(VS)=1+A6*(VS/SS1)^2+(SHRA*VS/SS1)*SQR(1+A8*(VS/SS1)^2)
2430 '
```

```
2440  '     ------------------------------------------------
2450  '     :   Initial times and values are set.
2460  '     ------------------------------------------------
2470  '
2480  T=0 : T2=0 : T3=0 : TE=0 : TE2=0 : TPR=TIP
2490  FL1=1 : FL5=1
2500  K1=1 : K2=1 : GOSUB 5950
2510  PR(0,1) = PAV : NB(0,1) = PB : V = 0
2520  '
2530  '     ------------------------------------------------
2540  '     A 4th order Runge-Kutta scheme which provides the starting values
2550  '     to be used in Hammings method is utilized.
2560  '     ------------------------------------------------
2570  '
2580  FOR KK=1 TO 3
2590  FOR K=1 TO 4
2600  IF K=2 OR K=3 THEN KD=2 ELSE KD=1
2610  J=K-1
2620  P=PAV+U(J,1)/KD : N=PB+U(J,2)/KD
2630  U(K,1)=TI*((FNF1(P,V)*FP)/(VBR-(CW-N)/DP-CPG*N))
2640  U(K,2)=TI*FNF1(P,V)
2650  NEXT K
2660  PAV=PAV+(U(1,1)+2*U(2,1)+2*U(3,1)+U(4,1))/6
2670  PB =PB +(U(1,2)+2*U(2,2)+2*U(3,2)+U(4,2))/6
2680  PR(KK,1)=PAV : NB(KK,1)=PB.
2690  NB(KK,2)=FNF1(PAV,V)
2700  PR(KK,2)=(NB(KK,2)*FP)/(VBR-(CW-PB)/DP-CPG*PB)
2710  T=T+TI
2720  '
2730  IF ABS(T-TPR)-.0000001 > 0 THEN GOTO 2760
2740  TPR=TPR+TIP
2750  GOSUB 6020
2760  NEXT KK
2770  '
2780  '     ------------------------------------------------
2790  '     The variables to be used in Hammings method are initialized.
```

```
2800  '  ------------------------------------------------------------
2810  '
2820  T=4*TI
2830  P0=PR(0,1) :  P1=PR(1,1) :  P2=PR(2,1) :  P3=PR(3,1)
2840  PD1=PR(1,2) :  PD2=PR(2,2) :  PD3=PR(3,2)
2850  N0=NB(0,1) :  N1=NB(1,1) :  N2=NB(2,1) :  N3=NB(3,1)
2860  ND1=NB(1,2) :  ND2=NB(2,2) :  ND3=NB(3,2)
2870  Q1=0 :  Q2=0 :  Q3=0
2880  QD0=0 :  QD1=0 :  QD2=0 :  QD3=0
2890  QDD1=0 :  QDD2=0 :  QDD3=0
2900  S1=PROJP :  S2=S1  :  S3=S2
2910  SD0=0  :  SD1=0  :  SD2=0  :  SD3=0
2920  SDD1=0  :  SDD2=0  :  SDD3=0
2930  '
2940  P3P=P3  :  P3C=P3
2950  N3P=N3 :  N3C=N3
2960  QD3P=QD3 :  QD3C=QD3
2970  SD3P=SD3 :  SD3C=SD3
2980  FL4=0 :  FL2=0
2990  '
3000  '  ------------------------------------------------------------
3010  '  Point at which conditions are checked and flags are set.
3020  '  ------------------------------------------------------------
3030  '
3040  IF  PB>=CW THEN FL1=0 ELSE FL1=1
3050  IF  FL2=1 THEN GOTO 3070
3060  IF  PAV>SPP THEN FL2=1 ELSE  FL2=0
3070  IF  PISTP+LP>LPT THEN FL3=1 :  TE=TE+TI ELSE FL3=0
3080  IF  PISTP+LP>LPT+LP/2 THEN TE2=TE2+TI
3090  IF  FL4=1 THEN  T2=T2+TI :  GOTO 3110
3100  IF  PHE2<DFS THEN FL4=0 ELSE FL4=1  :  T2=T2+TI :  GOSUB 4690
3110  IF  PISTV<=0 AND FL3=1 THEN FL5=0 ELSE FL5=1
3120  IF  PROJP>=LLT THEN FL7=0 :  T3=T3+TI ELSE FL7=1
3130  IF  FL5=0 AND FL7=0 THEN GOSUB 6170 :  GOTO 5680
3140  '
3150  '  ------------------------------------------------------------
```

```
3160 '   Hammings method, predictor and modifier calculations are made.
3170 ' -------------------------------------------------------------------
3180 '
3190 IF FL5=0 THEN GOTO 3250
3200 P4P=P0+(2*PD3-PD2+2*PD1)*4*TI/3
3210 IF FL1=0 THEN GOTO 3230
3220 N4P=N0+(2*ND3-ND2+2*ND1)*4*TI/3
3230 IF FL2=0 THEN GOTO 3250
3240 QD4P=QD0+(2*QDD3-QDD2+2*QDD1)*4*TI/3
3250 IF FL4=0 THEN GOTO 3290
3260 IF FL7=0 THEN GOTO 3290
3270 SD4P=SD0+(2*SDD3-SDD2+2*SDD1)*4*TI/3
3280 '
3290 IF FL5=0 THEN GOTO 3360
3300 P4M=P4P-(P3P-P3C)*112/121
3310 IF FL1=0 THEN GOTO 3330
3320 N4M=N4P-(N3P-N3C)*112/121
3330 IF FL2=0 THEN GOTO 3360
3340 QD4M=QD4P-(QD3P-QD3C)*112/121
3350 Q4P=(9*Q3-Q1+3*TI*(QD4M+2*QD3-QD2))/8
3360 IF FL4=0 THEN GOTO 3460
3370 IF FL7=0 THEN GOTO 3460
3380 SD4M=SD4P-(SD3P-SD3C)*112/121
3390 S4P=(9*S3-S1+3*TI*(SD4M+2*SD3-SD2))/8
3400 '
3410 ' -------------------------------------------------------------------
3420 '   Functions are called to determine the modified values
3430 '   of higher order derivatives.
3440 ' -------------------------------------------------------------------
3450 '
3460 P=P4M : N=N4M : V=QD4M : D=Q4P : VS=SD4M : DS=S4P
3470 GOSUB 4240
3480 PD4M=DPDT : ND4M=DNDT : QDD4M=DVDT : SDD4M=DSDT
3490 '
3500 ' -------------------------------------------------------------------
3510 '   Hammings method, corrector and final values are determined.
```

1.106

```
3520  '  -------------------------------------------------------------------
3530  '  -
3540  IF FL5=0 THEN GOTO 3600
3550  P4C=(9*P3-P1+3*TI*(PD4M+2*PD3-PD2))/8
3560  IF FL1=0 THEN GOTO 3580
3570  N4C=(9*N3-N1+3*TI*(ND4M+2*ND3-ND2))/8
3580  IF FL2=0 THEN GOTO 3600
3590  QD4C=(9*QD3-QD1+3*TI*(QDD4M+2*QDD3-QDD2))/8
3600  IF FL4=0 THEN GOTO 3640
3610  IF FL7=0 THEN GOTO 3640
3620  SD4C=(9*SD3-SD1+3*TI*(SDD4M+2*SDD3-SDD2))/8
3630  '
3640  IF FL5=0 THEN GOTO 3710
3650  P4F=P4C+(P4P-P4C)*9/121
3660  IF FL1=0 THEN GOTO 3680
3670  N4F=N4C+(N4P-N4C)*9/121
3680  IF FL2=0 THEN GOTO 3710
3690  QD4F=QD4C+(QD4P-QD4C)*9/121
3700  Q4F=(9*Q3-Q1+3*TI*(QD4F+2*QD3-QD2))/8
3710  IF FL4=0 THEN GOTO 3810
3720  IF FL7=0 THEN GOTO 3810
3730  SD4F=SD4C+(SD4P-SD4C)*9/121
3740  S4F=(9*S3-S1+3*TI*(SD4F+2*SD3-SD2))/8
3750  '
3760  '  -------------------------------------------------------------------
3770  '  Functions are called to determine the final values
3780  '  of higher order derivatives.
3790  '  -------------------------------------------------------------------
3800  '
3810  P=P4F : N=N4F : V=QD4F : D=Q4F : VS=SD4F : DS=S4F
3820  GOSUB 4240
3830  PAV=P4F : PB=N4F : PISTP=Q4F : PISTV=QD4F : PISTA=DVDT
3840  '
3850  '  -------------------------------------------------------------------
3860  '  A check for printing and storing results is made.
3870  '  -------------------------------------------------------------------
```

1.107

```
3880 '
3890 IF FL4=0 THEN GOTO 3920
3900 PHES=ES1/ALT : PROJP=S4F : PROJV=SD4F : PROJA=DSDT
3910 IF K2=1 THEN GOSUB 6110 : TPR=T+TIP : GOTO 4020
3920 IF ABS(T-TPR)-.0000001 > 0 THEN GOTO 4020
3930 TPR=TPR+TIP
3940 IF FL4=0 THEN GOSUB 6020 : GOTO 4020
3950 GOSUB 6170
3960 '
3970 '----------------------------------------------------------
3980 '   The time step is incremented and variables are reassigned
3990 '   for the next step in the integration.
4000 '----------------------------------------------------------
4010 '
4020 T=T+TI
4030 PD1=PD2 : PD2=PD3 : PD3=DPDT
4040 P3P=P4P : P3C=P4C
4050 P0=P1 : P1=P2 : P2=P3 : P3=P4F
4060 ND1=ND2 : ND2=ND3 : ND3=DNDT
4070 N3P=N4P : N3C=N4C
4080 N0=N1 : N1=N2 : N2=N3 : N3=N4F
4090 QDD1=QDD2 : QDD2=QDD3 : QDD3=DVDT
4100 QD0=QD1 : QD1=QD2 : QD2=QD3 : QD3=QD4F
4110 QD3P=QD4P : QD3C=QD4C
4120 Q1=Q2 : Q2=Q3 : Q3=Q4F
4130 IF FL4=0 THEN GOTO 4180
4140 SDD1=SDD2 : SDD2=SDD3 : SDD3=DSDT
4150 SD0=SD1 : SD1=SD2 : SD2=SD3 : SD3=SD4F
4160 SD3P=SD4P : SD3C=SD4C
4170 S1=S2 : S2=S3 : S3=S4F
4180 GOTO 3040
4190 '
4200 '----------------------------------------------------------
4210 '   Routine which evaluates the governing equations.
4220 '----------------------------------------------------------
4230 '
```

```
4240 IF FL1=1 THEN DNDT=FNF1(P,V) ELSE DNDT=0
4250 IF FL5=0 THEN GOTO 4300
4260 IF FL7=1 THEN GOTO 4280
4270 IF ABS(T3-TI)-.0000001<0 THEN GOSUB 4620 ELSE GOSUB 4650
4280 IF V<0 THEN A12=-1 : ELSE A12=1
4290 IF FL3=0 THEN FR4=0 : APF=APT : VPF=V ELSE GOSUB 4910
4300 IF FL4=1 THEN GOTO 4410
4310 IF FL2=0 THEN GOTO 4380
4320 FR1=APT*FNF2(P,V)
4330 PHE2=FNF3(D)
4340 THE2=FNF4(PHE2)
4350 FR2=APF*FNF5(PHE2,VPF,THE2)
4360 FR3=FNF6(ABS(V))
4370 PHEAVG=(PHE2+FR2/APF)/2
4380 DVDT=GC*FL2*(FR1-FR2-FR3*A12-FR4)/MP
4390 DPDT=(DNDT*FP-A3*DVDT*V-P*V*APT)/(VBR+APT*D-(CW-N)*FL1/DP-CPG*N)
4400 RETURN
4410 IF FL7=0 THEN GOTO 4420 ELSE PHE2=FNF7(D,DS) : PHEAVG=PHE2
4420 THE2=FNF4(PHE2)
4430 IF FL5=0 THEN GOTO 4470
4440 FR1=APT*FNF2(P,V)
4450 FR2=APF*FNF5(PHE2,VPF,THE2)
4460 FR3=FNF6(ABS(V))
4470 IF FL7=0 THEN GOTO 4510
4480 FS1=ALT*PHE2*(1+A5*VS^2/THE2)^(-A4)
4490 FS2=PI*(FS1/ALT)*(DLT^2)*M*CF
4500 FS3=ALT*PLT*FNF8(VS)
4510 IF FL5=0 THEN GOTO 4540
4520 DVDT=GC*(FR1-FR2-FR3*A12-FR4)/MP
4530 DPDT=-V*APT*SHRP*PAV0*V0^SHRP*(V0+(D-PISTPR)*APT)^(-(SHRP+1))
4540 DSDT=GC*(FS1-FS2-FS3)/MS
4550 RETURN
4560 '
4570 ' ------------------------------------------
4580 ' Routine which evaluates the drop in helium pressure
4590 ' after the projectile leaves the launch tube.
```

```
4600 ' -------------------------------------
4610 '
4620 PHE1=PHEAVG
4630 THE1=THE2
4640 VLT=VTOT-(PISTP-PISTPR)*APT+LLT*ALT
4650 PHE2=PHE1*EXP(((-PROJV*ALT)/VLT)*T3)
4660 IF PHE2<PATM THEN PHE2=PATM
4670 PHEAVG=PHE2
4680 RETURN
4690 '
4700 ' -------------------------------------
4710 '   Routine which initializes values at the time of
4720 '   diaphragm failure.
4730 ' -------------------------------------
4740 '
4750 BEEP : PRINT : PRINT
4760 PRINT " ***   THE DIAPHRAGM HAS FAILED   ***"
4770 PRINT : PRINT
4780 '
4790 VTOT=VPT-PISTP*APT+VNOZ+VHPS+ALT*PROJP
4800 PHE1=PHEAVG*((VTOT-ALT*PROJP)/VTOT)^SHRH
4810 THE1=(PHE1*VTOT)/(MHE*GCH) : THE2=THE1
4820 PISTPR=PISTP : PROJPR=PROJP
4830 V0=VBR+PISTP*APT-CPG*CW
4840 PAV0=PAV
4850 RETURN
4860 '
4870 ' -------------------------------------
4880 '   Routine which determines the extrusion force on the piston.
4890 ' -------------------------------------
4900 '
4910 DX=D+LP-LPT
4920 IF DX<EXT1 THEN DXX=APEX-DX-APEX*(1-3*DX/APEX)^(1/3) : FL6=0
4930 IF DX>EXT1 THEN DXX=2*LNOZ/3+APEX/3-DX+(DPT/EDN)^2*(DX-APEX/3) : FL6=1
4940 EX=DX+DXX
4950 IF FL6=1 THEN APF=AHPS : ERAD=EDN/2 : EDIST=APEX-LNOZ : GOTO 4980
```

```
4960  ERAD=(DPT/2)*(APEX-EX)/APEX
4970  APF=PI*ERAD^2 : EDIST=APEX-EX
4980  R0=DPT/2 : R02=R0^2
4990  VPF=V*R02/(ERAD^2)
5000  WP1=A7*R02*V*LOG(R0/ERAD)
5010  WP2=A7*R02*V*A9/(2*SQR(3))
5020  WP3=A7*M*V*R02*A10*LOG(R0/ERAD)/SQR(3)
5030  WP4=PI*DPP*V*R02*(VPF^2-V^2)/(GC*2)
5040  IF FL6=1 THEN WP5=WP2 ELSE WP5=0
5050  WPT=WP1+WP2+WP3+WP4+WP5
5060  IF DX<LP/2 THEN WLT=0 : GOTO 5170
5070  DXL=DX-LP/2
5080  DXXL=APEX-DXL-APEX*(1-3*DXL/APEX)^(1/3)
5090  EXL=DXL+DXXL
5100  ERADL=R0*(APEX-EXL)/APEX
5110  VLF=V*R02/(ERADL^2)
5120  WL1=A11*R02*V*LOG(R0/ERADL)
5130  WL2=A11*R02*V*A9/(2*SQR(3))
5140  WL3=A11*ML*V*R02*A10*LOG(R0/ERADL)/SQR(3)
5150  WL4=DL*PI*V*R02*(VLF^2-V^2)/(2*GC)
5160  WLT=(WL1+WL2+WL3+WL4)*TE2/(APEX-EXL)
5170  FR4=WPT*TE/EDIST + WLT
5180  RETURN
5190  '
5200  '-----------------------------------
5210  '  Routine which displays the program heading.
5220  '-----------------------------------
5230  '
5240  LOCATE 5,1
5250  PRINT "      ***   THE FOLLOWING PROGRAM IS AN INTERACTIVE ROUTINE   ***"
5260  PRINT "            WHICH MODELS   THE FIRING  OF A   TWO-STAGE LIGHT"
5270  PRINT "            GAS  GUN  WITH A DEFORMABLE PISTON.   THE PROGRAM"
5280  PRINT "            ALLOWS THE USER TO PLOT THE CALCULATED RESULTS."
5290  PRINT "
5300  PPIX=75
5310  PPIY=35
```

```
5320 LINE  (.5*PPIX,3.5*PPIY)-(1.1*PPIX,3.9*PPIY),,B
5330 LINE  (1.1*PPIX,3.55*PPIY)-(4.1*PPIX,3.85*PPIY),,B
5340 PSET  (4.1*PPIX,3.55*PPIY)
5350 LINE  -(4.9*PPIX,3.65*PPIY)
5360 LINE  -(4.9*PPIX,3.75*PPIY)
5370 LINE  -(4.1*PPIX,3.85*PPIY)
5380 LINE  (4.9*PPIX,3.65*PPIY)-(8*PPIX,3.75*PPIY),,B
5390 LINE  (1.1*PPIX,3.55*PPIY)-(1.6*PPIX,3.85*PPIY),,BF
5400 LINE  (5.2*PPIX,3.65*PPIY)-(5.2*PPIX,3.75*PPIY)
5410 LINE  (5.3*PPIX,3.65*PPIY)-(5.6*PPIX,3.75*PPIY),,BF
5420 LINE  (0,0)-(639,224),,B
5430 LOCATE 24,2
5440 INPUT "Press <RETURN> to continue : ",U
5450 CLS
5460 RETURN
5470 '
5480 ' ------------------------------------------------
5490 '       Routine which reads in the shot parameters.
5500 ' ------------------------------------------------
5510 '
5520 PRINT : PRINT
5530 INPUT " THE CHARGE WEIGHT OF THE PROPELLANT (grams)? ",CW : PRINT
5540 INPUT " THE MASS OF THE PISTON (grams)? ",MP : PRINT
5550 INPUT " THE INITIAL HELIUM PRESSURE (psig)? ",PHEl : PRINT
5560 INPUT " THE STRESS AT WHICH THE DIAPHRAGM FAILS (psi)? ",DFS : PRINT
5570 INPUT " THE PROJECTILE/SABOT MASS (grams)? ",MS : PRINT
5580 INPUT " THE INITIAL PRESSURE IN THE LAUNCH TUBE (psig)? ",PLT : PRINT
5590 INPUT " THE AMBIENT TEMPERATURE (deg-F)? ",TA : PRINT
5600 INPUT " THE TIME INCREMENT FOR COMPUTATION (sec)? ",TI : PRINT
5610 INPUT " THE TIME INCREMENT FOR DISPLAYING THE RESULTS (sec)? ",TIP : PRINT
5620 RETURN
5630 '
5640 ' ------------------------------------------------
5650 '       Routine which summarizes the shot inputs and the results.
5660 ' ------------------------------------------------
5670 '
```

```
5680 PRINT
5690 PRINT " ----------------------------------- "
5700 PRINT " SHOT PARAMETERS AND RESULTS "
5710 PRINT " ----------------------------------- "
5720 PRINT " propellant =";CW*C3;"grams"
5730 PRINT " piston =";MP*C3;"grams"
5740 PRINT " helium =";R(1,6);"psig"
5750 PRINT " diaphragm =";DFS;"psi"
5760 PRINT " projectile =";MS*C3;"grams"
5770 PRINT " muzzle velocity =";PROJV/C1;
5780 PRINT USING " #####,";PROJV/C1;
5790 PRINT " ft/s"
5800 PRINT " extrusion dist. =";
5810 PRINT USING " ##.##";PISTP+LP+DXX-LPT;
5820 PRINT " in"
5830 PRINT " sabot max press =";MAXPS;
5840 PRINT USING " #######,";MAXPS;
5850 PRINT " psi"
5860 PRINT : BEEP
5870 IF ED-LNOZ>1 THEN PRINT "NOTE : Piston has extruded into the launch tube!"
5880 INPUT "Press <RETURN> to continue :",V
5890 GOTO 6560
5900 ' ---------------------------------------------
5910 ' Routine which displays the results.
5920 ' ---------------------------------------------
5930 '
5940 '
5950 CLS
5960 PRINT " TIME AVG PRESS PR BURNED PIST ACCEL. ";
5970 PRINT " PIST VEL. PIST POS" 
5980 PRINT " (sec) (psi) (grams) (ft/s^2) ";
5990 PRINT " (ft/s) (in)"
6000 PRINT " ---- ------- ------- -------- ";
6010 PRINT " ------- ------ "
6020 PRINT USING "#.###### ";T;
6030 PRINT USING "######,.## ";PAV-PATM;
```

```
6040 PRINT USING "####,.##   ";PB*C3;
6050 PRINT USING "+#######,.##   ";PISTA/C1;
6060 PRINT USING "+######,.##   ";PISTV/C1;
6070 PRINT USING "####,.##   ";PISTP
6080 GOSUB 6310
6090 RETURN
6100 ,
6110 PRINT "     TIME     PR PRESS     He PRESS    PIST POS ";
6120 PRINT "  PIST VEL.  PROJ POS   PROJ VEL."
6130 PRINT "  (sec)        (psi)      (psi)        (in)    ";
6140 PRINT "  (ft/s)       (in)      (ft/s)"
6150 PRINT "  ---      --------   --------   --------";
6160 PRINT "  --------   --------   --------"
6170 PRINT USING "#.######   ";T;
6180 PRINT USING "#######,.##   ";PAV-PATM;
6190 PRINT USING "#######,.##   ";PHEAVG-PATM;
6200 PRINT USING "####.##   ";PISTP+LP+DXX;
6210 PRINT USING "####.##   ";PISTV/C1;
6220 PRINT USING "####.##   ";PROJP;
6230 PRINT USING "#######,.##   ";PROJV/C1
6240 GOSUB 6310
6250 RETURN
6260 ,
6270 ' ------------------------------------------------
6280 '   Routine which stores the data for plotting.
6290 ' ------------------------------------------------
6300 '
6310 R(K1,0)=T : R(0,0)=K1
6320 IF FL5=0 THEN GOTO 6400
6330 R(K1,1)=PAV-PATM : R(0,1)=K1
6340 R(K1,3)=PISTP : R(0,3)=K1
6350 R(K1,4)=PISTV/C1 : R(0,4)=K1
6360 R(K1,5)=PISTA/C1 : R(0,5)=K1
6370 R(K1,12)=FR3+FR4 : R(0,12)=K1
6380 IF FL1=0 THEN GOTO 6400
6390 R(K1,2)=PB*C3 : R(0,2)=K1
```

1.114

```
6400   R(K1,6)=PHEAVG-PATM : R(0,6)=K1
6410   R(K1,7)=THE2-C2 : R(0,7)=K1
6420   IF FL4=0 THEN GOTO 6540
6430   IF FL7=0 THEN GOTO 6540
6440   R(K2,8)=PROJP : R(0,8)=K2
6450   R(K2,9)=PROJV/C1 : R(0,9)=K2
6460   R(K2,10)=PROJA/C1 : R(0,10)=K2
6470   R(K2,11)=PHES-PATM : R(0,11)=K2
6480   R(K2,13)=FS2 : R(0,13)=K2
6490   R(K2,15)=FS3/ALT-PATM : R(0,15)=K2
6500   R(K2,16) = FS1-FS2-FS3 : R(0,16)=K2
6510   R(K2,14)=T2 : R(0,14)=K2
6520   IF MAXPS<R(K2,11) THEN MAXPS=R(K2,11)
6530   K2=K2+1
6540   K1=K1+1
6550   RETURN
6560   '
6570   '  --------------------------------------
6580   '  Routine which plots the results of the computation.
6590   '  --------------------------------------
6600   '
6610   PRINT : PRINT
6620   PRINT "The calculations are completed, would you like to see the"
6630   INPUT "results plotted (YES or NO) ? . . . . . . . . . . ",X1
6640   IF X1="YES" THEN GOTO 6650 ELSE PRINT : PRINT : GOTO 8120
6650   CLS
6660   LINE (0,0)-(639,224), ,B : LOCATE 2,4
6670   PRINT "The following are the parameters which may be graphed :"
6680   LOCATE 4,2                   Set A                          Set B"
6690   PRINT "
6700   LOCATE 5,3
6710   PRINT "      (from time=0 to end)        (from diap. failure to end)"
6720   LOCATE 6,3
6730   PRINT "      ----------------------      ----------------------------"
6740   LOCATE 7,3
6750   PRINT "      1A - AVG PROP PRESS         1B - PROJ POSITION"
```

```
6760 LOCATE 8,3
6770 PRINT "    2A -  PROP BURNED                2B - PROJ VELOCITY"
6780 LOCATE 9,3
6790 PRINT "    3A -  PISTON POSITION            3B - PROJ ACCEL."
6800 LOCATE 10,3
6810 PRINT "    4A -  PISTON VELOCITY            4B - PRESS ON PROJ BASE"
6820 LOCATE 11,3
6830 PRINT "    5A -  PISTON ACCEL.              5B - FRICTION ON SABOT"
6840 LOCATE 12,3
6850 PRINT "    6A -  FRICTION ON PISTON         6B - PRESS ON PROJ FACE"
6860 LOCATE 13,3
6870 PRINT "    7A -  AVG He PRESS               7B - TOTAL FORCE ON PROJ"
6880 LOCATE 14,3
6890 PRINT "    8A -  AVG He TEMP                8B - TIME"
6900 LOCATE 15,3
6910 PRINT "    9A -  TIME"
6920 LOCATE 17,4
6930 PRINT "The parameters chosen for the X-Y axes must come from the same set."
6940 LOCATE 18,4
6950 PRINT "Enter the number/letter indicator for selection of the desired"
6960 LOCATE 19,4
6970 PRINT "parameter."
6980 LOCATE 22,4
6990 INPUT "INPUT THE CODE FOR THE PARAMETER DESIRED ON THE Y-AXIS : ",YA
7000 LOCATE 23,4
7010 INPUT "INPUT THE CODE FOR THE PARAMETER DESIRED ON THE X-AXIS : ",XA
7020 FOR I=1 TO 2
7030 IF I=1 THEN Z=YA ELSE Z=XA
7040 IF Z="1A" THEN II=R(0,1)  :  IPLOT(I)=1
7050 IF Z="2A" THEN II=R(0,2)  :  IPLOT(I)=2
7060 IF Z="3A" THEN II=R(0,3)  :  IPLOT(I)=3
7070 IF Z="4A" THEN II=R(0,4)  :  IPLOT(I)=4
7080 IF Z="5A" THEN II=R(0,5)  :  IPLOT(I)=5
7090 IF Z="6A" THEN II=R(0,12) :  IPLOT(I)=12
7100 IF Z="7A" THEN II=R(0,6)  :  IPLOT(I)=6
7110 IF Z="8A" THEN II=R(0,7)  :  IPLOT(I)=7
```

1.116

```
7120  IF  Z="9A"  THEN  II=R(0,0)   :  IPLOT(I)=0
7130  IF  Z="1B"  THEN  II=R(0,8)   :  IPLOT(I)=8
7140  IF  Z="2B"  THEN  II=R(0,9)   :  IPLOT(I)=9
7150  IF  Z="3B"  THEN  II=R(0,10)  :  IPLOT(I)=10
7160  IF  Z="4B"  THEN  II=R(0,11)  :  IPLOT(I)=11
7170  IF  Z="5B"  THEN  II=R(0,13)  :  IPLOT(I)=13
7180  IF  Z="6B"  THEN  II=R(0,15)  :  IPLOT(I)=15
7190  IF  Z="7B"  THEN  II=R(0,16)  :  IPLOT(I)=16
7200  IF  Z="8B"  THEN  II=R(0,14)  :  IPLOT(I)=14
7210  NEXT I
7220  KX=IPLOT(2)
7230  KY=IPLOT(1)
7240  II=R(0,KY)
7250  MAXY=R(1,KY)  :  MAXX=R(1,KX)
7260  FOR I = 2 TO II
7270  IF R(I,KY)>MAXY THEN MAXY=R(I,KY)
7280  IF R(I,KX)>MAXX THEN MAXX=R(I,KX)
7290  NEXT I
7300  MAXY = MAXY/E(KY)  :  MAXX = MAXX/E(KX)
7310  IF MAXY<=1 THEN INCY=.2
7320  IF MAXY>1 AND MAXY<=5 THEN INCY=.5
7330  IF MAXY>5 AND MAXY<=10 THEN INCY=1
7340  IF MAXY>10 AND MAXY<=20 THEN INCY=2
7350  IF MAXY>20 AND MAXY<=50 THEN INCY=5
7360  IF MAXY>50 AND MAXY<=100 THEN INCY=10
7370  IF MAXY>100 AND MAXY<=200 THEN INCY=20
7380  IF MAXY>200 THEN INCY=40
7390  IF MAXX<=1 THEN INCX=.2
7400  IF MAXX>1 AND MAXX<=5 THEN INCX=.5
7410  IF MAXX>5 AND MAXX<=10 THEN INCX=1
7420  IF MAXX>10 AND MAXX<=20 THEN INCX=2
7430  IF MAXX>20 AND MAXX<=50 THEN INCX=5
7440  IF MAXX>50 AND MAXX<=100 THEN INCX=10
7450  IF MAXX>100 AND MAXX<=200 THEN INCX=20
7460  IF MAXX>200 THEN INCX=40
7470  TY=INCY
```

```
7480 IF TY>MAXY THEN GOTO 7500
7490 TY=TY+INCY : GOTO 7480
7500 MAXY=TY
7510 TX=INCX
7520 IF TX>MAXX THEN 7540
7530 TX=TX+INCX : GOTO 7520
7540 MAXX=TX
7550 CLS
7560 LINE (0,0)-(639,224),,B
7570 LINE (135,175)-(135,10)
7580 LINE (135,175)-(600,175)
7590 DY = (175-10)/(MAXY/INCY)
7600 FOR I=10 TO 175 STEP DY
7610 PSET(135,I) : DRAW "R3"
7620 NEXT I
7630 DX = (600-135)/(MAXX/INCX)
7640 FOR I=135 TO 600 STEP DX
7650 PSET(I,175) : DRAW "U2"
7660 NEXT I
7670 J=0
7680 FOR I=175 TO 10 STEP -DY*2
7690 LOCATE I/9+1,135/9-3
7700 PRINT USING "###.#";INCY*J
7710 J=J+2
7720 NEXT I
7730 J=0
7740 FOR I=135 TO 600 STEP DX*2
7750 LOCATE 175/9+2,I/8-2
7760 PRINT USING "###.#";INCX*J
7770 J=J+2
7780 NEXT I
7790 E=(600-135)/2+135
7800 LOCATE 175/9+4,E/9
7810 DX=(LEN(XT(KX))+LEN(XU(KX)))/2
7820 LOCATE 175/9+4,E/8-DX
7830 PRINT XT(KX);" ";XU(KX)
```

```
7840 R=(175-10)/2+10 : E=6
7850 DY=(LEN(XT(KY)))/2
7860 R1 = R/9-DY
7870 IF R1<=1.5 THEN R1=2
7880 LOCATE R1,E
7890 FOR I=1 TO LEN(XT(KY))
7900 YT = MID$(XT(KY),I,1)
7910 PRINT YT
7920 LOCATE R1+I,E
7930 NEXT I
7940 DY = LEN(XU(KY))/2
7950 LOCATE R1+I,E-DY
7960 PRINT XU(KY)
7970 DY = (175-10)/MAXY
7980 DX = (600-135)/MAXX
7990 PSET (R(1,KX)*DX/F(KX)+135,175-R(1,KY)*DY/F(KY))
8000 FOR I=2 TO II
8010 CX=R(I,KX)*DX/F(KX)+135
8020 CY=175-R(I,KY)*DY/F(KY)
8030 LINE -(CX,CY)
8040 NEXT I
8050 LOCATE 24,2,0 : INPUT "      ",V
8060 CLS
8070 LINE (0,0)-(639,224), ,B : LOCATE 12,15,1
8080 INPUT "WOULD YOU LIKE TO MAKE ANOTHER PLOT  (YES or NO)? ",X1
8090 IF X1="YES" THEN GOTO 6650
8100 CLS
8110 LINE (0,0)-(639,224), ,B : LOCATE 12,14
8120 INPUT "WOULD YOU LIKE TO RUN THE PROGRAM AGAIN (YES or NO)? ",X1
8130 IF X1="YES" THEN CLS : CLEAR : GOTO 1060 ELSE CLS : END
```

1.119

```
1000 '---------------------------------------
1010 '- Program which creates the input file for the
1020 '- main program GASGUN.
1040 '---------------------------------------
1050 '
1060 OPEN "O",#1,"DATA.GUN"
1070 '
1080 '---------------------------------------
1090 '  The Gun Dimensions and Material Properties
1100 '---------------------------------------
1110 '
1120 PRINT#1, 23              ' Length of breech - (in)
1130 PRINT#1, 4.5             ' Diameter of breech - (in)
1140 PRINT#1, 233.75          ' Length of pump tube - (in)
1150 PRINT#1, 3               ' Diameter of pump tube - (in)
1160 PRINT#1, 6.85            ' Length of nozzle - (in)
1170 PRINT#1, 1.1811          ' Diameter at small end of restriction - (in)
1180 PRINT#1, 5.4             ' Length of reduced area in HPS - (in)
1190 PRINT#1, 120             ' Length of launch tube - (in)
1200 PRINT#1, 1.1811          ' Diameter of launch tube - (in)
1210 PRINT#1, 36.126          ' Volume of spit tube - (in^3)
1220 PRINT#1, 9.75            ' Length of piston - (in)
1230 PRINT#1, 8500            ' Yield strength of polypropylux
1240 PRINT#1, .34             ' Shear factor of piston material
1250 PRINT#1, .046965         ' Density of polypropylux
1260 PRINT#1, 30000!          ' Yield strength of lead
1270 PRINT#1, .75             ' Shear factor for lead
1280 PRINT#1, .411            ' Density of lead
1290 PRINT#1, .24             ' Coefficient of friction
1300 '
1310 '---------------------------------------
1320 '  Interior Ballistic Constants
1330 '---------------------------------------
1340 '
1350 PRINT#1, 4020000!        ' Impetus of propellant - (in*lbf/lbm)
```

```
1360 PRINT#1, 29.69          ' Covolume of propellant gas - (in^3/lbm)
1370 PRINT#1, 1.252          ' Specific heat ratio of propellant gas
1380 PRINT#1, .0603          ' Density of propellant - (lbm/in^3)
1390 PRINT#1, 1.5            ' Pressure gradient factor
1400 PRINT#1, .17            ' Heat loss factor
1410 PRINT#1, 3.3            ' Density Distribution Factor
1420 PRINT#1, .029           ' Web thickness of propellant - (in)
1430 PRINT#1, .372245356#    ' Burn rate coefficient
1440 PRINT#1, .84457612#     ' Burn rate index
1450 '
1460 ' ----------------------------------------
1470 '     Gas Constants of Helium and Air
1480 ' ----------------------------------------
1490 '
1500 PRINT#1, 1.659          ' Specific heat ratio of helium
1510 PRINT#1, 4635.96        ' Gas constant He - (in*lbf/lbm*R)
1520 PRINT#1, 1.4            ' Specific heat ratio of air
1530 PRINT#1, 640.08         ' Gas constant air - (in*lbf/lbm*R)
1540 '
1550 ' ----------------------------------------
1560 '     The Initial Values , (t=0)
1570 ' ----------------------------------------
1580 '
1590 PRINT#1, 500            ' IV of Pav - (lbf/in^2)
1600 PRINT#1, 0              ' IV of Nb (prop. burned)
1610 PRINT#1, 0              ' IV of piston acceleration
1620 PRINT#1, 0              ' IV of piston velocity
1630 PRINT#1, 0              ' IV of piston position - (in)
1640 PRINT#1, 2000           ' Start pressure of piston (lbf/in^2)
1650 PRINT#1, 0              ' IV of projectile acceleration
1660 PRINT#1, 0              ' IV of projectile velocity
1670 PRINT#1, 1              ' IV of projectile position - (in)
1680 '
1690 ' ----------------------------------------
1700 '     Conversion Factors and Constants
1710 ' ----------------------------------------
```

```
1720 '
1730 PRINT#1, 12                                        ' inches/foot
1740 PRINT#1, 460.67                                    ' deg-F to deg-R
1750 PRINT#1, 453.59237#                                ' lbm/gram
1760 PRINT#1, 3.141592654#                              ' PI
1770 PRINT#1, 14.7                                      ' Atmospheric pressure (psi)
1780 PRINT#1, 386.088                                   ' Gravitational Constant
1790 '
1800 ' -------------------
1810 '      Labels for Graphs
1820 ' -------------------
1830 '
1840 PRINT#1, "TIME" : PRINT#1, " (milli-sec)"
1850 PRINT#1, "AVG PROP PRESS" : PRINT#1, " (kpsi)"
1860 PRINT#1, "PROP BURNED" : PRINT#1, " (kg)"
1870 PRINT#1, "PISTON POSITION" : PRINT#1, " (inches)"
1880 PRINT#1, "PISTON VELOCITY" : PRINT#1, " (kft/s)"
1890 PRINT#1, "PISTON ACCEL" : PRINT#1, " (Mft/s^2)"
1900 PRINT#1, "AVG He PRESS" : PRINT#1, " (kpsi)"
1910 PRINT#1, "AVG He TEMP" : PRINT#1, " (kdeg-F)"
1920 PRINT#1, "PROJ POSITION" : PRINT#1, " (inches)"
1930 PRINT#1, "PROJ VELOCITY" : PRINT#1, " (kft/s)"
1940 PRINT#1, "PROJ ACCEL" : PRINT#1, " (Mft/s^2)"
1950 PRINT#1, "PRESS ON PROJ BASE" : PRINT#1, " (kpsi)"
1960 PRINT#1, "FRICTION ON PISTON" : PRINT#1, " (kips)"
1970 PRINT#1, "FRICTION ON SABOT" : PRINT#1, " (kips)"
1980 PRINT#1, "TIME" : PRINT#1, " (milli-sec)"
1990 PRINT#1, "PRESS ON PROJ FACE" : PRINT#1, " (kpsi)"
2000 PRINT#1, "TOTAL FORCE ON PROJ" : PRINT#1, " (kips)"
2010 PRINT#1,.001;1000;1000;1;1000;1000000;1000;1000;1;1000;1000000;1000;1000
2020 PRINT#1,1000;.001;1000;1000
2030 CLOSE#1
2040 END
```

PART 2:   Calculation of Fluid Properties
                           in the Pump Tube of a
                          Two-Stage Light Gas Gun

                                ABSTRACT

        An enhancement for a microprocessor-based program for performance
estimation of a two-stage light gas gun with deformable piston has been
developed. The procedure uses an explicit finite-difference algorithm for
the numerical solution of the gasdynamic equations in the pump tube region
between piston face and projectile base during the firing cycle of the gun.
A virial-type equation of state is used to model the real gas properties of
the light gas. An adaptive grid generation system which accounts for
moving end boundaries provides sufficient computational accuracy to permit
determination of longitudinal property gradients in the pump tube, thus
alleviating one of the shortcomings of the Patin model. To date the grid
generation and equation solution algorithms have been developed. The real
gas equation of state has not yet been included in the analysis, and the
entire routine has not yet been incorporated into the performance predic-
tion program for the gun.

OBJECTIVES

The primary objective of this research is to develop a computer program which will determine the gas dynamics for an internal flow field. The program will calculate fluid properties as a function of space and of time for a quasi-one-dimensional, compressible, and inviscid flow of a real gas. Gas property distributions will be derived for a flow field with moving boundaries and a change of area. All computations will be performed using a personal computer, namely the Zenith Z-100. The Zenith Z-100 was chosen because it was readily available and it would keep computational expenses at a minimum.

The main application for the computer program will be to determine gas property distributions in the second stage of a two-stage light-gas gun.

ANALYSIS AND METHOD OF SOLUTION

The flow may be considered as a quasi-one-dimensional flow of an inviscid and compressible fluid moving through a tube. The tube has a variable cross sectional area and the longitudinal boundaries move at different rates. The fluid will be treated as a real gas since high temperatures and pressures may exist in the tube. The results will be compared to results obtained by using ideal gas and uniform field assumptions.

The equations for the flow are the one-dimensional conservation equations for mass, momentum, and energy. The differential forms of the conservation equations are as follows:

CONSERVATION OF MASS

$$\frac{\partial \rho}{\partial t} + \frac{\partial(\rho u)}{\partial x} + \frac{1}{A}\frac{dA}{dx}(\rho u) = 0 \qquad (1)$$

CONSERVATION OF MOMENTUM

$$\frac{\partial(\rho u)}{\partial t} + \frac{\partial}{\partial x}(\rho u^2 + P) + \frac{1}{A}\frac{dA}{dx}(\rho u^2) = 0 \qquad (2)$$

CONSERVATION OF ENERGY

$$\frac{\partial e}{\partial t} + \frac{\partial}{\partial x}(ue + uP) + \frac{1}{A}\frac{dA}{dx}(ue + uP) = 0 \qquad (3)$$

The variables in the above equations are:

    ρ - the mass per unit volume

    u - the velocity in the axial direction

    t - time

X - the axial position

A - the cross sectional area of the tube

P - pressure

e - the total energy per unit volume

The total energy, e, can be expressed as:

$$e = \frac{P}{\gamma - 1} + \frac{1}{2} \rho u^2 = \rho C_v T + \frac{1}{2} \rho u^2 \qquad (4)$$

where

γ is the specific heat ratio, Cv is the specific heat at constant volume, and T is the temperature. An appropriate equation of state for the gas is the Harrison real gas equation which is a fourth order equation based on empirical coefficients. The Harrison model[1] is given by:

$$P = \rho R T \left[1 + B(T) \rho + C(T) \rho^2 + D(T) \rho^3 \right] \qquad (5)$$

where R is the gas constant and B(T), C(T), and D(T) are the empirical coefficients.

In order to obtain the property distribution in the gas, Equations (1) through (5) are used along with the positions of the two longitudinal boundaries. A moving grid must be established to move with the longitudinal boundaries, and numerical methods are used to integrate the conservation equations. The conservation equations are integrated using a finite-different method. The finite-difference representations for the partial differential equations are obtained using the MacCormack explicit two-level algorithm[2]. An explicit scheme uses past and present information to obtain future information. The two-level finite-difference method uses

1.126

a predictor step and then a corrector step. The predictor step employs a backward difference, and the corrector step uses a forward difference. The predictor and corrector equations are as follows:

CONSERVATION OF MASS

Predictor

$$\rho_j^{\overline{n+1}} = \rho_j^n - \Delta t \left(\frac{m_j^n - m_{j-1}^n}{\Delta x^-} + \frac{m_j^n}{A_j} \frac{dA}{dx_j} \right) \quad (6)$$

Corrector

$$\rho_j^{n+1} = \frac{1}{2} \left[\rho_j^n + \rho_j^{\overline{n+1}} - \Delta t \left(\frac{m_{j+1}^{\overline{n+1}} - m_j^{\overline{n+1}}}{\Delta x^+} + \frac{m_j^{\overline{n+1}}}{A_j} \frac{dA}{dx_j} \right) \right] \quad (7)$$

CONSERVATION OF MOMENTUM

Predictor

$$m_j^{\overline{n+1}} = m_j^n - \Delta t \left[\frac{\left(P + \frac{m^2}{\rho} \right)_j^n - \left(P + \frac{m^2}{\rho} \right)_{j-1}^n}{\Delta x^-} + \left(\frac{m^2}{\rho A} \right)_j^n \frac{dA}{dx_j} \right] \quad (8)$$

Corrector

$$m_j^{n+1} = \frac{1}{2} \left\{ m_j^n + m_j^{\overline{n+1}} - \Delta t \left[\frac{\left(P + \frac{m^2}{\rho} \right)_{j+1}^{\overline{n+1}} - \left(P + \frac{m^2}{\rho} \right)_j^{\overline{n+1}}}{\Delta x^+} + \left(\frac{m^2}{\rho A} \right)_j^{\overline{n+1}} \frac{dA}{dx_j} \right] \right\} \quad (9)$$

CONSERVATION OF ENERGY

Predictor

$$e_j^{\overline{n+1}} = e_j^n - \Delta t \left[\frac{\left(\frac{m}{\rho} (e + P) \right)_j^n - \left(\frac{m}{\rho} (e + P) \right)_{j-1}^n}{\Delta x^-} + \left(\frac{m(e + P)}{\rho A} \right)_j^n \frac{dA}{dx_j} \right] \quad (10)$$

Corrector

$$e_j^{n+1} = \frac{1}{2} \left[e_j^n + e_j^{\overline{n+1}} - \Delta t \left\{ \frac{\left(\frac{m}{\rho} (e + P) \right)_{j+1}^{\overline{n+1}} - \left(\frac{m}{\rho} (e + P) \right)_j^{\overline{n+1}}}{\Delta x^+} + \left(\frac{m(e + P)}{\rho A} \right)_j^{\overline{n+1}} \frac{dA}{dx_j} \right\} \right] \quad (11)$$

The variables in the above equations are:

      j - space index

      n - time index

m - ρu

Δt - time step

ΔX^+ - forward change in x

ΔX^- - backward change in x

To effect a solution, the predictor variables are determined. The corrector variables are then determined using the results obtained from the predictor calculations. Once the corrector values have been determined they may be combined with the equation of state to determine the gas properties at the corresponding position in the flow field. This is repeated for each grid point. When the time index is increased from "n" to "n+1", the spacial grid translates and changes in overall length due to the moving boundaries. The corrector values for time "n" must be determined for the new grid by interpolation. New predictor and corrector values are then determined for the new time, and the entire process is repeated for the desired number of time intervals.

1.128

GRID GENERATION

The grid is partitioned using the positions of the piston and the projectile as endpoints. The entire grid moves as the piston and projectile move. The length of the grid also changes since the velocity of the piston will be different from that of the projectile. As the grid moves, it must be adjusted so that a grid point coincides with both the beginning of the transition section and the end of the transition section. This divides the total grid into three zones with each zone having its own grid spacing.

The initial grid is set up by dividing the total length between the piston and projectile into the desired number of equal grid spaces. The uniform grid spacing is determined using the following equation:

$$GS = \frac{LT}{NG} = \frac{X4 - X1}{NG} \qquad (12)$$

where

GS - grid spacing

$X1$ - piston position

$X4$ - projectile position

LT - overall grid length

NG - number of grid points

The grid is subdivided into three sections so that a grid point will be located at the beginning and at the end of the transition section. The grid must be divided into three zones due to the sudden area changes at the beginning and at the end of the transition section. This is accomplished by moving the grid points near the ends of the transition section either left or right. The four cases that need to be considered are listed with Figure 3.

As an example of how the grid points are shifted and how the adjusted grid is then generated consider the second case (see Fig. 3). In case two grid point nine is shifted to the right so that it is in position A, which is the beginning of the transition section. Grid point thirteen is shifted to the left so that it is in position B, which is the end of the transition section. The overall grid is now divided into three zones. The first zone extends from the piston to position A. The second zone is the region between position A and position B. The third zone extends from position B to the projectile. A separate grid must be created for each of the three zones. The grid spacing for zone one is determined as follows:

$$GS1 = \frac{L1}{NG1} = \frac{X2 - X1}{NG1} \tag{13}$$

where

    $GS1$ - grid spacing in zone one

    $X1$ - piston position

    $X2$ - position of beginning of transition section

    $L1$ - length of zone one

    $NG1$ - number of grid points in zone one

    The number of grid points in zone one is found as follows:

$$NG1 = \text{Integer Portion of}\left(\frac{L1}{GS}\right) \tag{14}$$

where

    $L1$ - length of zone one

    GS - original grid spacing

    The grid spacing for zone three is determined next using the same method with the following equations:

1.130

$$GS3 = \frac{L3}{NG3} = \frac{X4 - X3}{NG3} \tag{15}$$

$$NG3 = \text{Integer}\left(\frac{L3}{GS}\right) \tag{16}$$

where

    $GS3$- grid spacing in zone three

    $X3$ - position of end of transition section

    $X4$ - projectile position

    $NG3$- number of grid points in zone three

    $L3$ - length of zone three

    GS - original grid spacing

The grid spacing for zone two is determined using the following
equations:

$$GS2 = \frac{L2}{NG2} = \frac{X3 - X2}{NG2} \tag{17}$$

$$NG2 = NG - NG1 - NG3 \tag{18}$$

where

    $GS2$- grid spacing for zone two

    $X2$ - position of beginning of transition section

    $X3$ - position of end of transition section

    $L2$ - length of zone two

    $NG2$- number of grid points in zone two

    NG - number of grid points in original grid

    $NG1$- number of grid points in zone one

    $NG3$- number of grid points in zone three

The modified grid is shown in Figure 4.

A similar procedure is used for each of the other cases listed with Figure 3. The equations for GS1, GS2, and GS3 are the same for all cases. The equations for NG1, NG2, and NG3 are different for each case. The equations for all four cases are listed below.

$$GS1 = \frac{L1}{NG1} \qquad \frac{X2 - X1}{NG1} \tag{19}$$

$$GS2 = \frac{L2}{NG2} \qquad \frac{X3 - X2}{NG2} \tag{20}$$

$$GS3 = \frac{L3}{NG3} \qquad \frac{X4 - X3}{NG3} \tag{21}$$

CASE 1

$$NG1 = \text{Integer}\left(\frac{L1}{GS}\right) \tag{22}$$

$$NG2 = NG - NG1 - NG3 \tag{23}$$

$$NG3 = \text{Integer}\left(\frac{L3}{GS}\right) + 1 \tag{24}$$

CASE 2

$$NG1 = \text{Integer}\left(\frac{L1}{GS}\right) \tag{25}$$

$$NG2 = NG - NG1 - NG3 \tag{26}$$

$$NG3 = \text{Integer}\left(\frac{L3}{GS}\right) \tag{27}$$

CASE 3

$$NG1 = \text{Integer}\left(\frac{L1}{GS}\right) + 1 \tag{28}$$

$$NG2 = NG - NG1 - NG3 \tag{29}$$

$$NG3 = \text{Integer}\left(\frac{L3}{GS}\right) \tag{30}$$

CASE 4

$$NG1 = \text{Integer}\left(\frac{L1}{GS}\right) + 1 \tag{31}$$

$$NG2 = NG - NG1 - NG3 \tag{32}$$

$$NG3 = \text{Integer}\left(\frac{L3}{GS}\right) + 1 \tag{33}$$

Once a grid is set up, the initial fluid properties are assigned to the grid points. At time equal to zero the fluid properties will be uniform throughout the entire flow field. The fluid velocity will also be equal to zero. The initial temperature and pressure of the fluid will also be known. The initial density can be determined using the equation of state (Equation 4) and iterating. Since the temperature is known the coefficients for Equation (5) can be obtained from a table of coefficients. The gas constant, R, is given as 4636.96 (in lbf/lbm R) for helium, which is used in the gas gun. An initial value for the fluid density is assumed to begin iterating. A good first guess would be the value obtained using ideal gas behavior where:

$$\rho = \frac{P}{RT} \tag{34}$$

The initial guess is plugged into Equation (5) and a pressure is calcuated. The actual pressure is known and the correct density is obtained when the

1.133

calculated pressure and the actual pressure match. If the calculated pressure is lower than the actual pressure, a larger value for density should be tried. Once a value for density has been determined, the energy may be calculated using Equation (4). Values for Cv will have to be obtained from an emperical equation for the specific heat at constant pressure, Cp, and an equation relating R, Cv, and Cp.

$$Cp = R(A = bT + cT^2 + dT^3 + eT^4) \qquad (35)$$

$$Cv = Cp - R \qquad (36)$$

The initial velocity of the fluid will be zero and therefore the initial momentum will be zero. The initial values for density, momentum, energy, pressure, and temperature are assigned to the initial grid points.

DETERMINING FLUID PROPERTIES AS BOUNDARIES MOVE

After all initial fluid properties have been determined and assigned to the grid coordinates, the time should be incremented by one timestep. This will cause the grid to move and the fluid properties to change. New values for the predictor and corrector equations have to be calculated for each of the new grid points.

In order to determine the new predictor and corrector values, the fluid properties from the old grid at time "n" must be related to the new grid at time "n+1". The fluid properties for the new grid are interpolated from the old grid. The interpolation equation is:

$$(*)_j^{n+1} = (*)_j^n - \frac{\left(X_j^n - X_j^{n+1}\right)\left((*)_j^n - (*)_{j+1}^n\right)}{\left(X_j^n - X_{j+1}^n\right)} \tag{37}$$

where

  $(*)$ - property value for given time and space index

  X - axial position of grid point

  n - time index

  j - space index

A problem arises when the last grid point of the new grid is reached. The interpolation equation requires that the old property value for position "j+1" be known to solve for a new value for position "j". When the end of the new grid becomes position "j", there is no value for the old position "j+1". To obtain a solution for the endpoint of the new grid, a value is determined by extrapolation using values from the new grid. The extrapolation equation is:

$$(*)_j^{n+1} = (*)_{j-1}^{n+1} + \frac{\left((*)_{j-1}^{n+1} - (*)_{j-2}^{n+1}\right)\left(X_j^{n+1} - X_{j-1}^{n+1}\right)}{\left(X_{j-1}^{n+1} - X_{j-2}^{n+1}\right)} \tag{38}$$

1.135

where

(*) - property value

X - axial position

j - space index

n - time index

Figure 5 shows how the grid is rezoned.

The new grid with fluid properties from time "n" has been constructed. The fluid properties for the current time, "n+1", are now determined using Equations (4) through (11) and Equations (35) and (36). The predictor equations are solved first, starting with the second grid point. The predictor values are determined for all grid points except the first point since the predictor equations rely on the values from the previous grid point. The predictor equations cannot be evaluated at the first point since there is not point preceding it. The predictor values for the first point are determined by extrapolation using the second and third points. The extrapolation equation is:

$$(*1) = (*2) + \frac{(*2 - *3)(X1 - X2)}{(X2 - X3)} \tag{39}$$

where

$(*1)$ - predictor value at point one

$(*2)$ - predictor value at point two

$(*3)$ - predictor value at point three

$X1$ - axial position of point one

$X2$ - axial position of point two

$X3$ - axial position of point three

The corrector values are now determined for all grid points except the

1.136

last point. The values for the last point cannot be determined using the corrector equations since they rely on the values of "j+1" which does not exist when the endpoint is at "j". The corrector values for the last grid point are determined by extrapolation using Equation (38) where "*" denotes the corrector values. The corrector values are the density, momentum, and energy of the fluid at the corresponding grid points.

The temperature and pressure of the fluid at each grid point can be calculated using the corrector values and Equation (4), (35), and (36). The velocity of the fluid at each point can be determined from the momentum equation since the density is known.

$$u = \frac{m}{\rho} \tag{40}$$

Using Equations (4), (35), and (36) simultaneously, the temperature may be calculated. An iterative process will be necessary since Cv is unknown. A value for the temperature is assumed and Equation (35) is solved to get a value for the specific heat at constant pressure, Cp. Equation (36) is then solved to get a value for Cv. The values for Cv and temperature are then used in Equation (4) to obtain an energy value. If the energy just calculated does not match the actual energy, a new temperature guess must be tried. Once the correct temperature has been determined, the equation of state (Equation 4) can be used to determine the pressure. After the temperatures and pressures have been calculated for each grid point, the time is incremented and a new grid is generated. The entire process is repeated for the new grid and all successive grid until the desired amount of time has elapsed.

STATUS OF PROJECT

Work has begun on a computer program which will calculate the fluid properties in the flow field. The program is being written in a modular format. Each portion of the program is being written as a separate module or subroutine.

The grid module generates a grid based on the positions of the two longitudinal flow boundaries and any abrupt area changes in the tube in which the gas is flowing. For the gas gun problem the moving boundaries are the piston and the projectile faces. The abrupt area changes occur at the beginning and ending of the transition section of the pump tube (see Figure 1). A grid point is required to line up with both, the beginning point and the ending point of the transition section, due to the abrupt area changes. This is accomplished by shifting grid points to make them line up with the desired points of the gas gun. The grid is then composed of three regions or zones. The grid is then composed of three regions or zones. The grid points are shifted in a manner which keeps the grid spacing as uniform as possible. At this time the grid module is complete except for the cases when the piston reaches the beginning of the transition section and during piston extraction.

The second module of the program calculates values for the predictor equations. This module calculates predictor values at all grid points except at the piston and projectile. A simple extrapolation routine needs to be added to obtain values at those points.

Some work has been done on the corrector module. It will calculate corrector values and it will be similar to the predictor module.

A separate routine will be written to evaluate the equation of state. Since the coefficients in the equation of state are determined empirically,

1.138

a table of coefficients will have to be included as part of the program.

There will also be a module which will calculate the flow properties and store them on a disk. A separate module for plotting the various fluid properties versus time and position will also be included.

A listing of the portion of the program completed to date is included in the appendix. Several grid generation examples are included with the program listing.

COMPLETION OF PROJECT

The proposal submitted to SCEEE preceding the award of this subcontract called for a deliverable in the form of a finite difference code for the flow field between the piston face and the projectile base. At the present time that code is not in production form. However, the code will be completed and delivered in compliance with the subcontract without further expenditure of the contract funds. This delivery will take place in May, 1986.

The following parts of the subject code have been completed.

1. Grid generation scheme which apportions computational space according to piston and projectile dynamics.

2. The predictor portion of the MacCormack two-level explicit finite difference code for the solution of the equations of fluid motion in the solution space. The corrector code is complete but not operational.

These routines are currently written to perform computations with a specified set of dynamics rather than interacting with the dynamics generation program. This approach was taken because it was felt that the detailed finite difference calculations might slow down the analysis program excessively, particularly with the real gas equations included in the analysis.

The following parts of the code have not yet been completed:

1. Coding and inclusion of the Harrison real gas model procedure into the simulation.

2. Incorporation of all modification in to the basic performance estimation program.

When the above tasks have been completed, the performance of the program will be determined. The effort here is not only to determine the

important effects of property gradients and a real gas model of the pump tube flow, but also to include these effects in the performance estimation program without compromising the rapid, on-site analysis and test design capabilities of the basic program. If the finite difference calculations consume excessive time, then another approximating procedure may be required. At any rate, a thorough study of these effects, not possible under the current contract time limitations, will be completed and submitted to the SCEEE as indicated above.

CONCLUSIONS

A microcomputer-based program for the rapid determination of two-stage light gas gun performance has been developed. Gun geometry, propellant, driving gas and piston and projectile characteristics can be coded into the program easily, making it adaptable to most gun configurations. The shot conditions are entered interactively, and the program output is normally routed to the screen for quick review. The program computes gas properties, piston motion and projectile motion during the firing cycle, thus permitting parametric studies for optimizing test design. A parallel set of subroutines has also been prepared to allow for assessment of real gas effects in the light gas and the determination of property variations in the second stage of the gun. These latter procedures have not yet been thoroughly tested to determine their utility in on-line calculations. A thorough study of these effects and a suitable procedure for incorporating them into the performance analysis program will be completed in May of 1986.

FIGURES

1.143
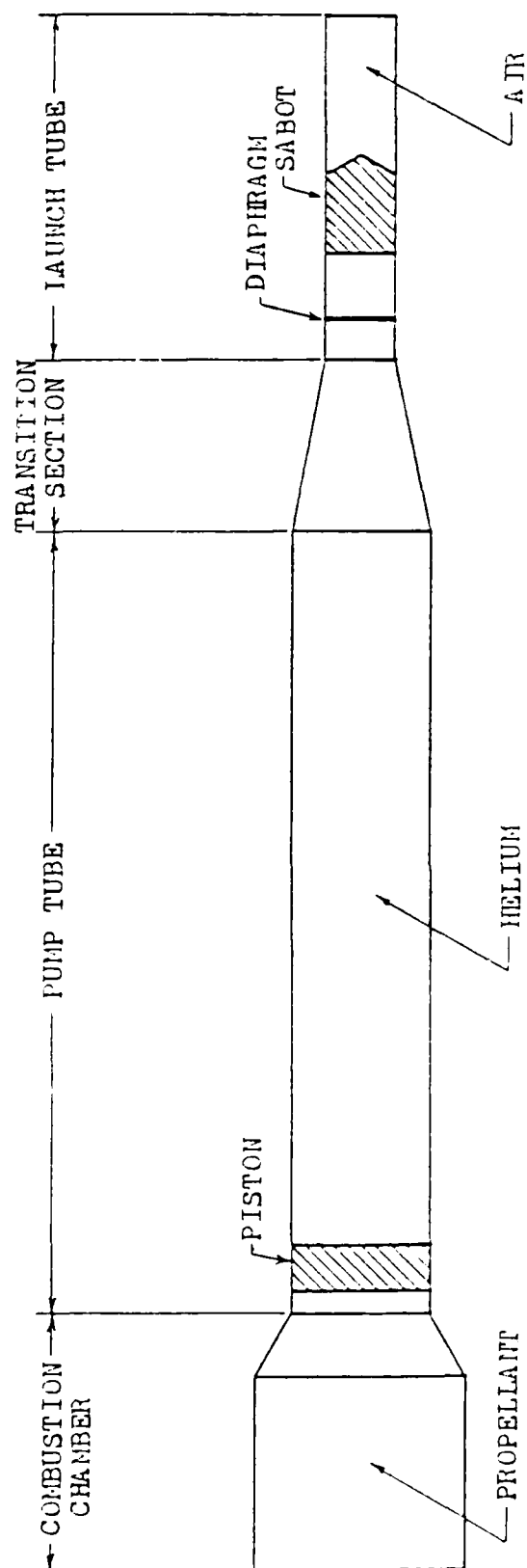
FIGURE 1. TYPICAL ARRANGEMENT OF TWO-STAGE LIGHT GAS GUN

1.144
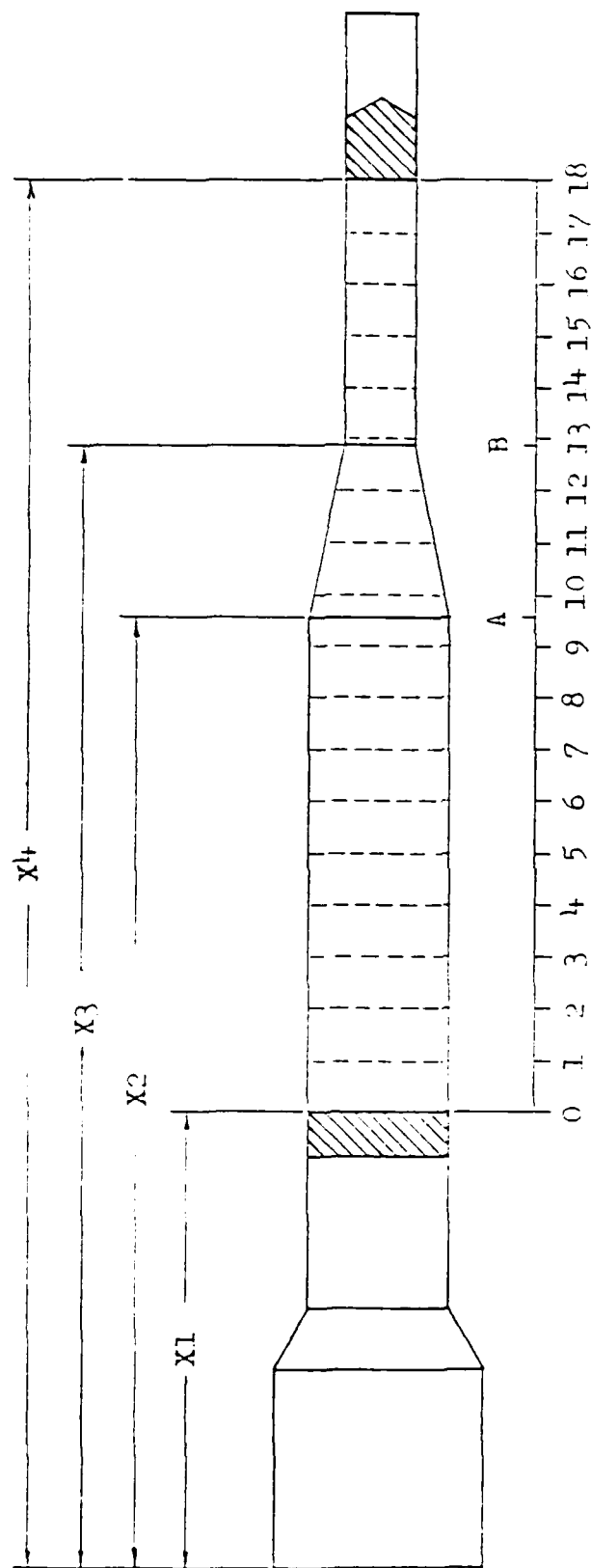
FIGURE 2. INITIAL GRID SPACING WITH NG = 18

1.145
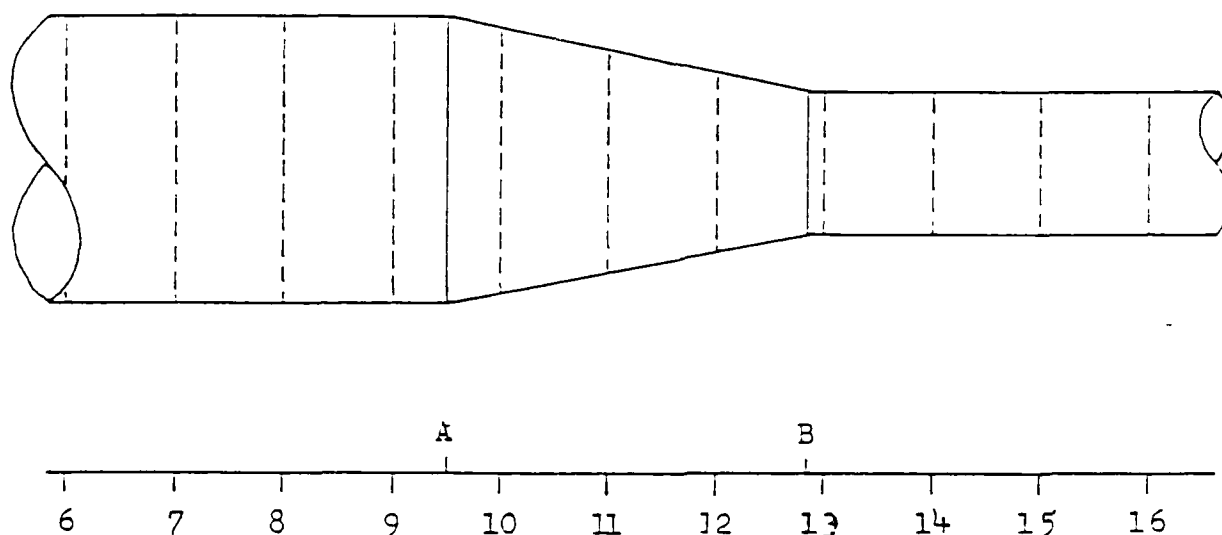
FIGURE 3. ENLARGED VIEW OF TRANSITION SECTION
WITH INITIAL GRID SPACING

CASE 1

Grid pt. 9 is shifted right to position A
Grid pt. 12 is shifted right to position B

CASE 2

Grid pt. 9 is shifted right to position A
Grid pt. 13 is shifted left to position B

CASE 3

Grid pt. 10 is shifted left to position A
Grid pt. 13 is shifted left to position B

CASE 4

Grid pt. 10 is shifted left to position A
Grid pt. 12 is shifted right to position B
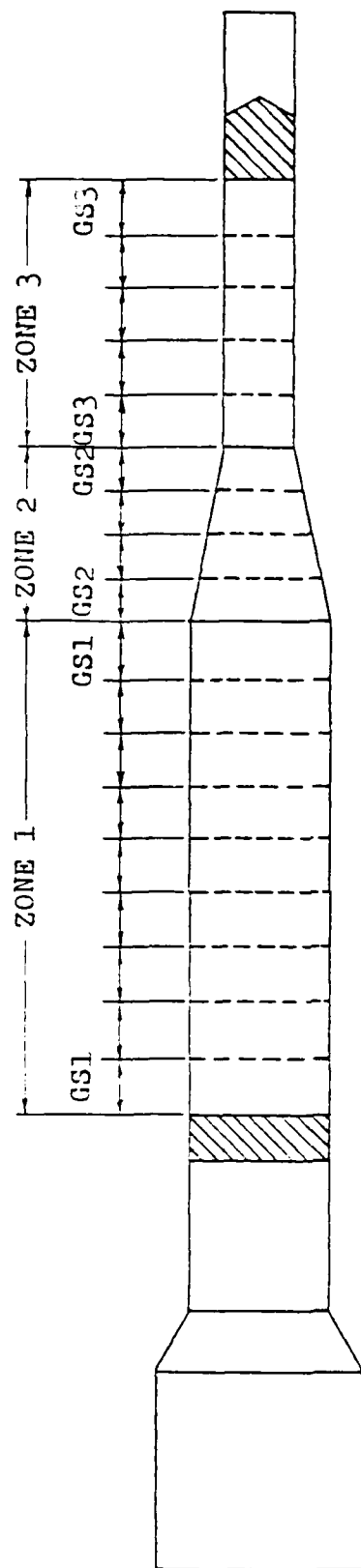
FIGURE 4. MODIFIED GRID WITH SHIFTED GRID POINTS

1.147
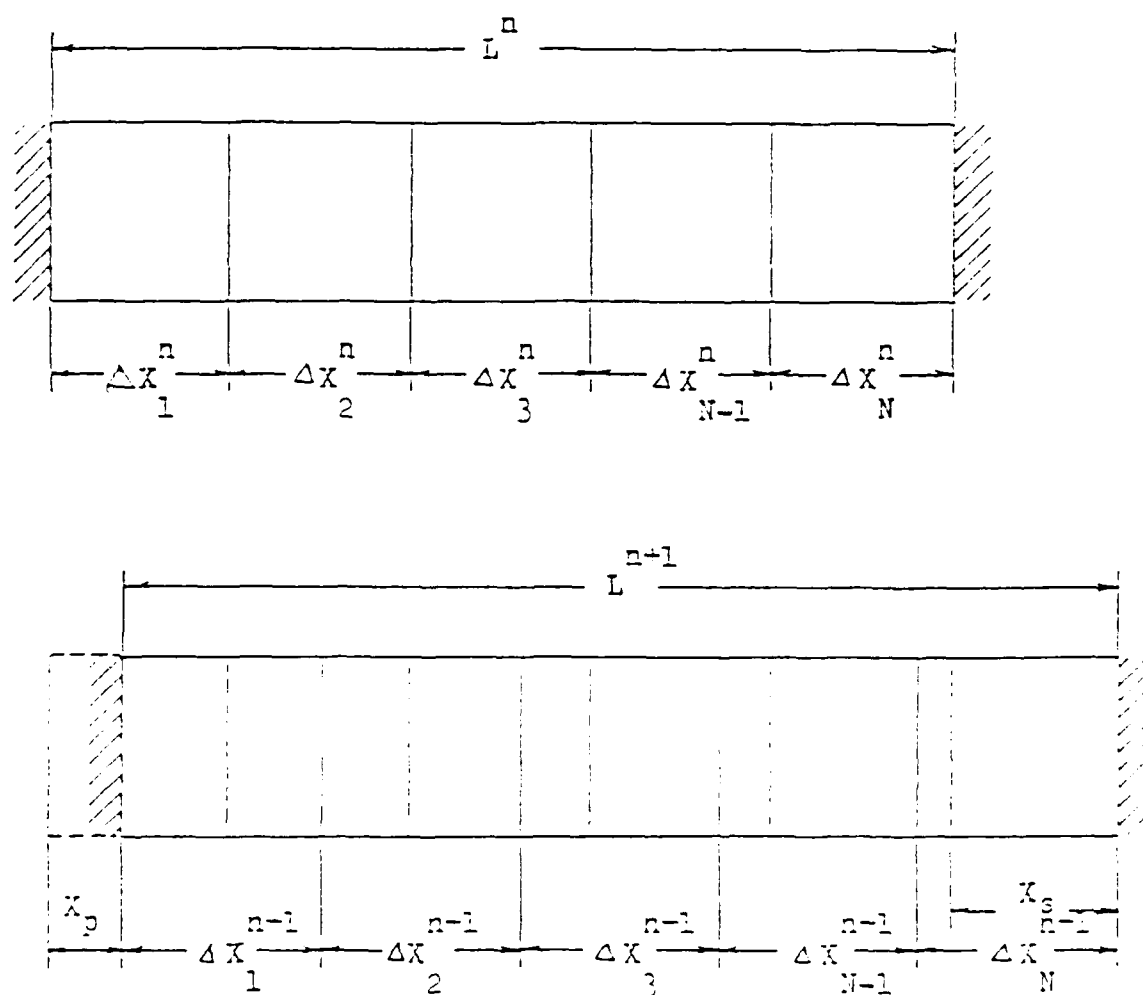
FIGURE 5. REZONING STRUCTURE FOR ONE-DIMENSIONAL GRID

REFERENCES

1. Harrison, E. H., "Intermolecular-Force Effects on the Thermodynamic Properties of Helium with Applications," AIAA Journal, October, 1964.

2. MacCormack, R. W., "The Effect of Viscosity in Hypervelocity Impact Cratering," AIAA Paper Number 69-354, May, 1969.

BIBLIOGRAPHY

1. Courter, R. W., "Development of an Explicit Finite Difference Code for Internal and External Compressible Flow Analysis," Martin Marietta Corporation Report Number MMC-82ESO-55179, Denver, CO, July, 1982.

2. Courter, R. W., "Internal Flow Studies of a Class of Ballistic Launchers," Final Report to AFOSR, F49620-82-C-0035, July, 1984.

3. Harrison, E. H., "Intermolecular-Force Effects on the Thermodynamic Properties of Helium with Applications," AIAA Journal, October, 1964.

4. Hornbeck, R. W., "Numerical Methods," Quantum Publishers, Inc., 1975.

5. MacCormack, R. W., "The Effect of Viscosity in Hypervelocity Impact Cratering," AIAA Paper Number 69-354, May, 1969.

6. Murty, H. S., and Gottlieb, J. J., "Analytical and Numerical Study of the Flow in a Shock Tube With an Area Change at the Diaphragm Section," University of Toronto Institute for Aerospace Studies Technical Note Number 255 CN ISSN 0082-5263, University of Toronto, May, 1984.

7. Patin, R. M., "A Mathematical Model of a Two-Stage Light Gas Gun With a Deformable Piston," Thesis, Louisiana State University, Baton Rouge, Louisiana, May, 1985.

8. Smith, G. D., "Numerical Solution of Partial Differential Equations: Finite Difference Methods", Clarendon Press, Oxford, 1978.

9. Van Wylen, G. J., and Sonntag, R. E., "Fundamentals of Classical Thermodynamics," John Wiley and Sons, 1978.

10. Zucrow, M. J., and Hoffman, J. D., "Gas Dynamics vol 1," John Wiley and Sons, 1976.

APPENDIX A

Appendix A contains a listing of the completed portion of a computer
program written in the computer language of BASIC which will calculate
fluid properties in the pump tube of a two-stage light gas gun. Several
grid generation examples are included with the program listing.

1.151

```basic
1000    DEFDBL A-Z
1100    DEFSNG I-K,M-N
1200    OPTION BASE 0
1300    DIM RHO(75,5),EM(75,5),ENER(75,5)
1400    DIM GR(4,3),EROR(4),XGRID(75,5),TEMP(75,5)
1500    DIM RHOP(75,5),EMF(75,5),ENERP(75,5),PMR(75,5),EFMR(75,5)
1600    DIM RHOP(75,5),EMF(75,5),ENERP(75,5),PMR(75,5),EFMR(75,5)
1600    DIM PR(75,5),R(75)
1700    PI=3.14159234#
1800    INPUT "CONTRACTION BEGINNING ,                  X2=",X2
1900    INPUT "CONTRACTION END ,                         X3=",X3
2000    INPUT "PUMP TUBE DIAMETER (INCHES) ,             D1=",D1
2100    INPUT "LAUNCH TUBE DIAMETER (INCHES) ,           D2=",D2
2200    INPUT "HELIUM PRESSURE (PSI) ,                 PRES=",PRES
2300    INPUT "TEMPERATURE OF HELIUM (DEG. F) ,       HTEMP=",HTEMP
2400    INPUT "SPECIFIC HEAT RATIO (GAMMA=1.659) ,    GAMMA=",GAMMA
2500    INPUT "SPECIFIC HEAT AT CONST. VOL. (CV=0.754) ,  CV=",CV
2600    INPUT "NUMBER OF GRID POINTS ? ,                 NG=",NG
2700    INPUT "TIME INCREMENT ,                          DT=",DT
2800    TEMPR=HTEMP+460!
2900    R1=D1/2! :R2=D2/2!
3000    REM    GAS CONSTANT FOR HELIUM (R) = 4635.96 (IN LBF/LBM degR)
3100    REM    RHEL = GAS CONST FOR HELIUM
3200    RHEL=4635.96
3300    DENS1=PRES/(RHEL*TEMPR)
3400    EMINIT=0!
3500    ENERIN=PRES/(GAMMA-1!)
3600    REM
3700    REM
3800    N=0
3900    TME=0!
4000    FOR I=0 TO NG
4100    RHO(I,N)=DENS1
4200    EM(I,N)=EMINIT
4300    ENER(I,N)=ENERIN
4400    TEMP(I,N)=TEMPR
4500    PR(I,N)=PRES
4600    PMR(I,N)=PRES+EMINIT^2/DENS1
4700    EPMR(I,N)=EMINIT/DENS1*(ENERIN+PRES)
4800    NEXT I
4900    REM
5000    INPUT "PISTON POSITION ,                        X1=",X1
```

1.152

```
5100 INPUT "PROJECTILE POSITION ,                          X4=",X4
5200 REM
5300 LT=X4-X1 : GLT=LT/NG
5400 FOR I=0 TO NG
5500 TX=GLT*I
5600 IF TX=X2 THEN MIKE1=1 : MI1=I
5700 IF TX=X3 THEN MIKE2=1 : MI2=I
5800 NEXT I
5900 REM FOLLOWING LINES ARE INCOMPLETE-------------******
6000 IF MIKE1=1 AND MIKE2=1 THEN GOTO
6100 IF MIKE1=1 THEN GOTO
6200 IF MIKE2=1 THEN GOTO
6300 REM ----------------------------------****
6400 L1=X2-X1 : WJ1=L1/GLT
6500 L2M=X3-X1 : WJ2=L2M/GLT
6600 L3=X4-X3 : WJ3=L3/GLT
6700 L2=X3-X2
6800 REM-------------------------------
6900 GR(1,1)=L1/INT(WJ1)
7000 GR(1,3)=L3/INT(WJ3+1)
7100 GR(1,2)=L2/(NG-INT(WJ1)-INT(WJ3+1))
7200 ER1=ABS((GR(1,1)-GR(1,2))/GR(1,2))
7300 ER2=ABS((GR(1,3)-GR(1,2))/GR(1,2))
7400 EROR(1)=SQR(ER1^2+ER2^2)
7500 REM-------------------------------
7600 GR(2,1)=L1/INT(WJ1+1)
7700 GR(2,3)=L3/INT(WJ3)
7800 GR(2,2)=L2/(NG-INT(WJ1+1)-INT(WJ3))
7900 ER3=ABS((GR(2,1)-GR(2,2))/GR(2,2))
8000 ER4=ABS((GR(2,3)-GR(2,2))/GR(2,2))
8100 EROR(2)=SQR(ER3^2+ER4^2)
8200 REM-------------------------------
8300 GR(3,1)=L1/INT(WJ1+1)
8400 GR(3,3)=L3/INT(WJ3+1)
8500 GR(3,2)=L2/(NG-INT(WJ1+1)-INT(WJ3+1))
8600 ER5=ABS((GR(3,1)-GR(3,2))/GR(3,2))
8700 ER6=ABS((GR(3,3)-GR(3,2))/GR(3,2))
8800 EROR(3)=SQR(ER5^2+ER6^2)
8900 REM-------------------------------
9000 GR(4,1)=L1/INT(WJ1)
```

```
9100    GR(4,3)=L3/INT(NN3)
9200    GR(4,2)=L2/((NG-INT(NN1)-INT(NN3))
9300    ER7=ABS((GR(4,1)-GR(4,2))/GR(4,2))
9400    ER8=ABS((GR(4,3)-GR(4,2))/GR(4,2))
9500    EROR(4)=SQR(ER7^2+ER8^2)
9600    REM-------------------------------
9700    SMALL=EROR(1)
9800    ISMALL=1
9900    FOR I = 2 TO 4
10000      IF EROR(I) > SMALL THEN GOTO 10300
10100      SMALL = EROR(I)
10200      ISMALL=I
10300   NEXT I
10400   REM-------------------------------
10500   NGL1=L1/GR(ISMALL,1)
10600   NGL2=L2/GR(ISMALL,2)
10700   NGL3=L3/GR(ISMALL,3)
10300   REM-------------------------------
10898   LPRINT"TOTAL GRID LENGTH = ";LT
10899   LPRINT " "
10900   LPRINT"LENGTH OF ZONE 1 = ";L1
10910   LPRINT"NO. OF GRID PTS. IN ZONE 1 = ";NGL1
10920   LPRINT"LENGTH OF GRID SPACES IN ZONE 1 = ";GR(ISMALL,1)
10930   LPRINT " "
10940   LPRINT"LENGTH OF ZONE 2 = ";L2
10950   LPRINT"NO. OF GRID PTS. IN ZONE 2 = ";NGL2
10960   LPRINT"LENGTH OF GRID SPACES IN ZONE 2 = ";GR(ISMALL,2)
10970   LPRINT " "
10980   LPRINT"LENGTH OF ZONE 3 = ";L3
10990   LPRINT"NO. OF GRID PTS. IN ZONE 3 = ";NGL3
11000   LPRINT"LENGTH OF GRID SPACES IN ZONE 3 = ";GR(ISMALL,3)
11010   LPRINT " "
11020   LPRINT"PISTON LOCATION       XP = ";X1
11030   LPRINT"PROJECTILE LOCATION   XPR = ";X4
11040   LPRINT"CONTRACTION BEGINNING XCB = ";X2
11050   LPRINT"CONTRACTION END       XCE = ";X3
11060   LPRINT " "
```

1.154

```
11200  FOR I=0 TO NG
11300  IF I > (NGL1+NGL2) THEN 11900
11400  IF I > NGL1 THEN 11700
11500  XGRID(I,N)=X1+GR(ISMALL,1)*I
11600  GOTO 12000
11700  XGRID(I,N)=XGRID(I-1,N)+GR(ISMALL,2)
11800  GOTO 12000
11900  XGRID(I,N)=XGRID(I-1,N)+GR(ISMALL,3)
12000  NEXT I
12100  FOR I = 0 TO NG
12200     LPRINT "XGRID";I;"=",XGRID(I,N)
12300  NEXT I
12400  GRS1=GR(ISMALL,1)
12500  GRS2=GR(ISMALL,2)
12600  GRS3=GR(ISMALL,3)
12700  REM
12800  FOR J=2 TO NG-1
12900  IF J > NGL1+NGL2 THEN 13600
13000  IF J < NGL1 THEN 14000
13100  DXN=GRS2
13200  RADIUS=((R2-R1)/(X3-X2))*(XGRID(J,N)-X2)+R1
13300  AREA=PI*RADIUS^2
13400  DAREA=2!*PI*RADIUS*(R2-R1)/(X3-X2)
13500  GOTO 14300
13600  DXN=GRS3
13650  RADIUS=R2
13700  AREA=PI*R2^2
13800  DAREA=0!
13900  GOTO 14300
14000  DXN=GRS1
14050  RADIUS=R1
14100  AREA=PI*R1^2
14200  DAREA=0!
14300  REM
14350  REM PRINT "AREA = ";AREA," RADIUS = ";RADIUS
14355  R(J)=RADIUS
14400  REM------------------------------------------------------
14500  RHOP(J,N+1)=RHO(J,N)-DT*((EM(J,N)-EM(J-1,N))/DXN+EM(J,N)*DAREA/AREA)
14600  PMR(J,N)=PR(J,N)+EM(J,N)^2/RHO(J,N)
14700  EMR(J,N)=EM(J,N)/RHO(J,N)*(ENER(J,N)+PR(J,N))
14800  EMP(J,N+1)=EM(J,N)-DT*((PMR(J,N)-PMR(J-1,N))/DXN-EM(J,N)^2/(RHO(J,N)*ARE
A)*DAREA)
14900  ENERP(J,N+1)=ENER(J,N)-DT*((EPMR(J,N)-EPMR(J-1,N))/DXN+EPIR(J,N)*DAREA/A
REM)
15000  NEXT J
```

```
TOTAL GRID LENGTH =   260

LENGTH OF ZONE 1 =   200
NO. OF GRID PTS. IN ZONE 1 =   24
LENGTH OF GRID SPACES IN ZONE 1 =   8.33333333333333

LENGTH OF ZONE 2 =   30
NO. OF GRID PTS. IN ZONE 2 =   3
LENGTH OF GRID SPACES IN ZONE 2 =   10

LENGTH OF ZONE 3 =   30
NO. OF GRID PTS. IN ZONE 3 =   3
LENGTH OF GRID SPACES IN ZONE 3 =   10

PISTON LOCATION            XP =    0
PROJECTILE LOCATION        XPR =   260
CONTRACTION BEGINNING      XCB =   200
CONTRACTION END            XCE =   230

XGRID 0 =         0
XGRID 1 =         8.33333333333333
XGRID 2 =         16.6666666666667
XGRID 3 =         25
XGRID 4 =         33.3333333333333
XGRID 5 =         41.6666666666667
XGRID 6 =         50
XGRID 7 =         58.3333333333333
XGRID 8 =         66.6666666666667
XGRID 9 =         75
XGRID 10 =        83.3333333333333
XGRID 11 =        91.6666666666667
XGRID 12 =        100
XGRID 13 =        108.333333333333
XGRID 14 =        116.666666666667
XGRID 15 =        125
XGRID 16 =        133.333333333333
XGRID 17 =        141.666666666667
XGRID 18 =        150
XGRID 19 =        158.333333333333
XGRID 20 =        166.666666666667
XGRID 21 =        175
XGRID 22 =        183.333333333333
XGRID 23 =        191.666666666667
XGRID 24 =        200
XGRID 25 =        210
XGRID 26 =        220
XGRID 27 =        230
XGRID 28 =        240
XGRID 29 =        250
XGRID 30 =        260
```

```
TOTAL GRID LENGTH =  265

LENGTH OF ZONE 1 =   155
NO. OF GRID PTS. IN ZONE 1 =  18
LENGTH OF GRID SPACES IN ZONE 1 =  8.61111111111111

LENGTH OF ZONE 2 =   30
NO. OF GRID PTS. IN ZONE 2 =  3
LENGTH OF GRID SPACES IN ZONE 2 =  10

LENGTH OF ZONE 3 =   80
NO. OF GRID PTS. IN ZONE 3 =  9
LENGTH OF GRID SPACES IN ZONE 3 =  8.88888888888899

PISTON LOCATION             XP =  45
PROJECTILE LOCATION        XPR =  310
CONTRACTION BEGINNING      XCB =  200
CONTRACTION END            XCE =  230

XGRID 0  =        45
XGRID 1  =        53.6111111111111
XGRID 2  =        62.2222222222222
XGRID 3  =        70.8333333333334
XGRID 4  =        79.4444444444445
XGRID 5  =        88.0555555555556
XGRID 6  =        96.6666666666667
XGRID 7  =        105.2777777777778
XGRID 8  =        113.8888888888889
XGRID 9  =        122.5
XGRID 10 =        131.1111111111111
XGRID 11 =        139.7222222222222
XGRID 12 =        148.3333333333333
XGRID 13 =        156.9444444444444
XGRID 14 =        165.5555555555556
XGRID 15 =        174.1666666666667
XGRID 16 =        182.7777777777778
XGRID 17 =        191.3888888888889
XGRID 18 =        200
XGRID 19 =        210
XGRID 20 =        220
XGRID 21 =        230
XGRID 22 =        238.8888888888889
XGRID 23 =        247.7777777777778
XGRID 24 =        256.6666666666667
XGRID 25 =        265.5555555555556
XGRID 26 =        274.4444444444444
XGRID 27 =        283.3333333333333
XGRID 28 =        292.2222222222222
XGRID 29 =        301.1111111111111
XGRID 30 =        310
```

```
TOTAL GRID LENGTH =  311

LENGTH OF ZONE 1 =  140
NO. OF GRID PTS. IN ZONE 1 =  13
LENGTH OF GRID SPACES IN ZONE 1 =  10.76923076923077

LENGTH OF ZONE 2 =  30
NO. OF GRID PTS. IN ZONE 2 =  3
LENGTH OF GRID SPACES IN ZONE 2 =  10

LENGTH OF ZONE 3 =  141
NO. OF GRID PTS. IN ZONE 3 =  14
LENGTH OF GRID SPACES IN ZONE 3 =  10.07142857142857

PISTON LOCATION            XP =  60
PROJECTILE LOCATION        XPR =  371
CONTRACTION BEGINNING      XCB =  200
CONTRACTION END            XCE =  230

XGRID 0 =        60
XGRID 1 =        70.76923076923077
XGRID 2 =        81.53846153846154
XGRID 3 =        92.30769230769231
XGRID 4 =        103.07692307692331
XGRID 5 =        113.8461538461538
XGRID 6 =        124.6153846153846
XGRID 7 =        135.3846153846154
XGRID 8 =        146.1538461538462
XGRID 9 =        156.9230769230769
XGRID 10 =       167.6923076923077
XGRID 11 =       178.4615384615385
XGRID 12 =       189.2307692307692
XGRID 13 =       200
XGRID 14 =       210
XGRID 15 =       220
XGRID 16 =       230
XGRID 17 =       240.0714285714286
XGRID 18 =       250.1428571428572
XGRID 19 =       260.2142857142857
XGRID 20 =       270.2857142857143
XGRID 21 =       280.3571428571429
XGRID 22 =       290.4285714285714
XGRID 23 =       300.5
XGRID 24 =       310.5714285714286
XGRID 25 =       320.6428571428571
XGRID 26 =       330.7142857142857
XGRID 27 =       340.7857142857143
XGRID 28 =       350.8571428571428
XGRID 29 =       360.9285714285714
XGRID 30 =       371
```

USAF-SCEEE

RESEARCH INITIATION IN SCIENCE AND ENGINEERING PROGRAM

Sponsored by the

AIR FORCE OFFICE OF SCIENTIFIC RESEARCH

Conducted by the

SOUTHEASTERN CENTER FOR ELECTRICAL ENGINEERING EDUCATION

FINAL TECHNICAL REPORT

A LOW-COST LOCAL-AREA NETWORK for DESKTOP COMPUTERS

Research Conducted by:	Myron A. Calhoun
Academic Rank:	Associate Professor
Department and University:	Computer Science Dept. Kansas State Unversity
Research Location:	Hanhattan, KS 66506
Report Date:	October 26, 1985
Contract No:	F49620-82-C-0035
Subcontract No:	84 RIP 02

A LOW-COST LOCAL-AREA NETWORK for DESKTOP COMPUTERS

by

Dr. Myron A. Calhoun

ABSTRACT

Users of local-area networks benefit from the simplified communication
which results between interconnected stations, including pooling of
information and sending electronic memos. Overall cost savings and
other benefits result from sharing expensive peripherals such as
printers and hard disk drives. Unfortunately, most commercial local-
area networks are not cheap, and the cost of interconnecting the work
stations often outweighs the expected benefits, especially when the
stations themselves are very INexpensive.

The goal of this project was to design a very low-cost local-area
network utilizing the Z-100, the Air Force "standard" desktop computer,
and to implement a working prototype.

The report describes the hardware and software design of one such low-
cost network. A USERS' MANUAL which describes the functioning of all
of the network commands is also included in the appendix. The software
itself has not yet been completely debugged, but work is progressing.

DESCRIPTION OF THE PROPOSED RESEARCH

RESEARCH OBJECTIVES

A "local-area network" (LAN) is an interconnection of two or more
computer systems or "work stations" controlled by a single organization
or group and located within a geographically-limited area. A LAN lets
its users share hardware and software; the intent may be to reduce
costs, to improve the accessability of unique peripherals, or merely to
provide simplified communication between the users.

The major advantages of networks include:

1) Reduced equipment costs resulting from snaring relatively expensive
   peripherals among many users:

   When several users all need hardcopy output capability, the normal
   solution furnishes each user with an inexpensive printer, because
   good printers are not cheap. Unfortunately, cheap printers are also
   usually slow and noisy, and their very numbers mean that considerable
   maintenance will be necessary. The LAN solution permits a more-
   expensive but faster, quieter, and easier-to-maintain printer to be
   shared among many users. Similarly, other high-cost peripherals such
   as hard disks and plotters may be shared.

2) File sharing:

   Suppose, for example, that several people in an accounting department
   must use a large accounting program. Maintenance of this program is
   an ongoing fact of life.   If each person has his/her own copy, every
   modification to the original program requires time-consuming updates
   to each copy. An even worse situation developes if non-identical
   versions of the supposedly common program exist; the very integrity
   of the accounting being performed is obviously in doubt. But if the
   users are connected by a LAN, a single copy of that program can be
   maintained on a central file and used by all.

3) Security and data integrity:

   Access to files may require password authorization. File "locking"
   software can prevent one person from reading from or writing to a
   file while another person is working on that same file. In addition,
   with all files stored on a shared disk, data backup procedures are
   much faster and are easier to implement. Legally, it might be

2.3

possible to purchase just ONE copy of little-used copyrighted software and store it in the central file; this single copy could be shared among the many stations, yet file locking can insure that no more than one station could use the software at any one time.

4) Electronic "mail" and other utilities:

The ability of network users to send and receive memos to and from each other without the hassle of addressing envelopes, leaving notes, etc., although seemingly such a minor convenience, oftentimes provides one of the most-appreciated functions of a network!

Potential disadvantages of using networks include:

1) File-locking may prohibit two or more individuals from working on parts of a file when the actual work is actually mutually exclusive, thus resulting in decreased work performance.

2) Copyright-protection violation: if file-locking is NOT implemented, a single copy of a copyrighted program may be utilized by more than one person at a time, thus violating the copyright.

3) Increased costs: Networks are not free. In addition to a cost per station which averages about $500, many commercial networks also require a centralized network controller which may cost several thousands of dollars. There is also the cost of installing cable (usually coaxial) between the stations.

Local area networks are a fairly recent development, an outgrowth of the micro-computer and office-automation revolutions of the late 1970's. During the last few years, various aspects of LAN's have been heavily studied. Performance evaluation has interested many researchers. The design of high-speed networks occupies many companies, but the design of lower-capability, slower-speed LAN's has been neglected until recently, perhaps because the rewards appear to be much smaller. The purpose of this project was to design a very low-cost local-area network utilizing the Z-100, the Air Force "standard" desktop computer, and to implement a working prototype.

The International Standards Organization (ISO) has published a widely-accepted model for open communications systems which differentiates between many necessary communication functions [1]. This model defines seven "layers" of abstraction, with each layer using the services of the layer below and providing services to the layer above. Including the physical transmisison media and the user's program, neither of which is part of the ISO model, the layering of the model is summarized briefly on the next page.

ISO LAYER	FUNCTION
User Program	Application program (not part of the ISO model)
7. Application	Provides all services directly comprenensible to application programs
6. Presentation	Restructures data to/from standardized format used within network
5. Session	Manages address translation and access security
4. Transport	Provides transparent, reliable data transfer from end station to end station
3. Network	Performs message routine for data transfer between non-adjacent stations
2. Data Link	Improves error rate for messages moved between adjacent stations
1. Physical	Encodes and physically transfers messages between adjacent stations
Media	Wires, cables, etc., that link nodes (not part of the ISO model)

This research effort has focused on:
A) determining which network configuration should be used,
B) developing and documenting a set of functional specifications for the network software,
C) writing and verifying the operation of the required software,
D) interconnecting a several-station prototype (using the Z-100's in one of the laboratories at Kansas State University), and
E) evaluating the implementation based on student use of the network.

Each of the above is described in following sections of this report.

A. NETWORK CONFIGURATION DETERMINATION

The first decision which had to be made was to choose the transmission medium. The most obvious possibilities and their major characteristics are shown in the following table:

TRANSMISSION MEDIUM	RELATIVE COST	MAXIMUM SPEED	INTERFACING REQUIRED
optical fiber	high	very high	a lot
coaxial cable	medium	high	a lot
twisted pair	low	low	none

It is not difficult to conclude, on the basis of cost and interfacing effort, that twisted pair (e.g. normal telephone wiring) would be the best transmission medium. Although the RS-232C standard (adopted in 1969) states that the maximum cable length between any two stations should be less than 50 feet, the author has personally transmitted such signals at 19,200 baud over 1200 feet of standard 4-wire telephone cable in an electrically-noisy environment with no errors and without using special line-drivers or receivers. A twisted-pair transmission medium should be perfectly acceptable for LAN workstations situated within the confines of a reasonably-sized building or in adjacent buildings, but part of the testing phase of this project will have to verify this decision.

The Z-100 desktop computer has two RS-232 ports capable of handling serial data at a maximum rate of 38,400 baud, or about 3,800 bytes per second. Although this rate may seem slow compared to that which would be possible using coaxial cable or optical fiber, it is not insignificant: at this rate, a double-spaced typewritten page requires less than half a second of transmission time!

At the outset, three low-cost network configurations seemed particularly promising, but two of them were easily discarded:

STAR: The Z-204-RD Multiport Input/Output Card, an accessory for the Zenith Z-100 desktop computer, provides one parallel and four serial I/O ports, of which the latter may be used to connect to the serial ports of other computers to implement a "star" configuration. Thus one Z-100 acting as a central controller could serve many work stations in a LAN. At a price of about $300 per Card, the distributed per-station interface hardware cost would be less than $100. Even including the cost of a dedicated network server (about $1,700), twelve stations would make the per-station hardware cost less than $250.

RING: Using one of the built-in serial ports and no additional
interface card, a "ring" configuration could interconnect a very
large number of Z-100's, with the major limitation being the network
response time (a request from one station plus the recipient's response
would have to make a complete circuit of the ring, being relayed by each
intervening station). The per-station hardware cost, however, is
essentially zero (exclusive of wire costs), and no particular station
has to be reserved for a central controller.

BUS: Again using one of the built-in serial ports and only a very
simple interface card, a diode-isolated "bus" configuration could
interconnect a smaller number of Z-100's, with the major limitation
being the driv-current lim........ .. ...-232 port and the load each
receiver puts on the net. The limits lead to a three-way trade-off of
distance, speed, and number of receivers: six devices separated by 20
feed communicating at 19,200 baud, or three devices two miles apart
running at 300 baud [2].

Unfortunately, without a more complicated hardware interface (which
would be costly), both the "ring" and the "bus" configurations require
every work-station in the network to be operating in order for the
network to be intact. Since desktop computers are often powered off or
are otherwise inoperable, it is apparent that neither a ring nor a bus
configuration will meet the requirements. Thus the "star" configuration
was chosen to implement level one of the ISO model.

B. FUNCTIONAL SOFTWARE SPECIFICATIONS

During the summer of 1984, the author designed and partially implemented
a Software Driver Package to provide a user-oriented interface between
BASIC programs and the Z-204 Multiport Input/Output Card [3]. A "User's
Guide" which described the use of the I/O card and the Driver Package
was also written [4]. A full implementation, including a small package
of programs demonstrating the bidirectional transmission of messages
between a five-computer "star" configuration, was later completed and
sent to the Computer Science Directorate (AD/KRSC) at Eglin Air Force
Base, Florida.

In essence, the Z-204 card provided the "Physical Link" (level 1), the
Software Driver Package provided the "Data Link" (level 2), and the
demonstration programs provided a simple "Network" (level 3) of the ISO
model.

Only a relatively small modification of this Software Driver Package was
required to adapt it for use as a low-level network interface callable
from assembly-language programs. (Assembly language is required because
BASIC and other high-level programming languages do not execute fast
enough to provide adequate network response.)

MS-DOS and Z-DOS, an earlier version of MS-DOS, are the most commonly used operating systems on the Z-100 desktop computer. UNIX, a very popular operating system on many larger computers, also has several derivatives (XENIX, etc.) used on desktop computers. Chosing from both UNIX and MS-DOS, a set of functions which would provide a minimal network operating environment was selected. To reduce conflict with program names already used by others, the names of these functions were prefixed with the word "NET". They are:

```
NETCD      - network change directory
NETCOPY    -    "     copy file
NETDEL     -    "     delete (erase) file
NETDIR     -    "     display directory
NETIN      -    "     user sign in
NETMAIL    -    "     send and receive mail
NETMD      -    "     make directory
NETOUT     -    "     user sign out
NETPASS    -    "     user password change
NETPATH    -    "     directory path for data files
NETPRINT   -    "     print file
NETRD      -    "     remove directory
NETREN     -    "     rename existing file
NETRUN     -    "     load and run program
NETWHO     -    "     user information lookup program
```

NETIN, NETMAIL, NETOUT, and NETPASS are patterned after the UNIX functions "login", "mail", "logout", and "passwd". NETWHO is derived from a combination of UNIX functions "who" and "finger". NETRUN is somewhat patterned after the MS-DOS function COMMAND.COM. Although all of the remaining functions closely mimic MS-DOS functions which have the same name (less the "NET" prefix), it should be noted that many MS-DOS concepts (redirection, pipes, filters, directories, etc.) and functions were themselves originally "borrowed" from UNIX!

Under "Research Objectives", four potential advantages of networks were listed. The functions chosen to implement this minimal network environment support these advantages as follows:

1) NETCD, NETCOPY, NETDEL, NETDIR, NETMD, NETPATH, NETRD, NETREN, and NETRUN support the sharing of a large (and relatively expensive) hard disk. NETPRINT suports the sharing of an expensive printer.

2) NETPATH and NETRUN directly support file sharing

3) NETIN, NETOUT, NETPASS, and NETRUN support security and data integrity.

4) NETMAIL and NETWHO support electronic "mail".

2.8

The specification of each of these functions is given in the USER'S
MANUAL which is included in this document as Appendix A. Functions
which are derived from MS-DOS functions are (intentionally) so similar
to their counterparts that their specification often refers the user to
the corresponding entry in the MS-DOS manual [5] for more complete
information.

C. WRITING AND VERIFYING SOFTWARE

Frankly, because the author "bit off more than he could chew" in the
time alloted for this project, the software has not yet been completed.
However, just as his 1984 SFRP project was not fully completed until
several months later, so too will this project be completed in the
months ahead. All of the equipment necessary to support continuation of
the project has been purchased (see Appendix B), much of the software
has been written, and the author is committed to finishing. Only more
time is necessary to see the project through to completion.

D. PROTOTYPE VERIFICATION

During the summer of 1985, a small prototype network consisting of one
Z-100 desktop computer acting as the network server and interfaced to
four more Z-100 computers with a Z-204 Card was configured in one of the
microlabs at Kansas State University. Using this hardware and initial
versions of the ISO level 2 "Data Link" software, simultaneous
bi-directional transmission of messages between the network server and
the four outlying workstations was demonstrated. However, none of the
user-oriented network functions NETMAIL, NETDIR, etc. were then
operational, so it can not be claimed that a meaningful prototype has
been verified. However, the fundamental concept of a "star" network
based on the Z-100 and using the Z-204 interface card was proven.

E. EVALUATION

Because a working network has not been completed, it has not been
possible to evaluate one in action. Thus this phase of the project
must necessarily be delayed.

It has recently come to the author's attention that it may be possible
to replace the NETCD, NETCOPY, NETDEL, NETDIR, NETMD, NETPATH, NETRD,
NETREN, and NETRUN functions with a device driver which behaves as if
the network is actually just a special kind of disk. Because of the
potential great simplification of the software, this possibility is
currently being given the utmost consideration. This will not affect
the functional descriptions which follow, but may make it possible to
use the built-in MS-DOS software to perform the functions.

TRADEMARKS

MS and XENIX are trademarks of Microsoft Corporation.
Z-DOS is a trademark of Zenith Data Systems Corporation.
UNIX is a trademark of The Bell Telephone Laboratories.
Intel is a trademark of Intel Corporation.

REFERENCES

1. "Hands-on network-design project gives insight into LAN features",
   Robert H. Cushman, EDN Magazine, 22 March 1984, pp. 219 ff.

2. "Ultra-Low-Cost Network for Personal Computers", Ken Clements and
   Dave Daugherty, BYTE magazine, October, 1981, pp. 50 ff.

3. "Software Drivers for the Z-204 Multiport Interface Card", Myron A.
   Calhoun, Final Report for 1984 USAF-SCEEE SFRP, Sept. 14, 1984.

4. "USER'S GUIDE to the Software Driver Package and the Z-204 Multiport
   Input/Output Card", Myron A. Calhoun, included in Final Report for
   1984 USAF-SCEEE SFRP, Sept. 14, 1984.

5. "Microsoft MS-DOS Version 2" manual, Zenith Data Systems Corporation,
   St. Joseph, Michigan 49085.

PERSONNEL

Myron A. Calhoun is an Associate Professor of Computer Science at Kansas
State University. He received an A.A. degree from Graceland College in
1961, a B.S. degree from the University of Kansas in 1963, an M.S.
degree from Colorado State University in 1964, and his Ph.D. degree from
Arizona State University in 1967, all in the field of electrical
engineering. Prior to joining KSU, he did some part-time teaching of
computer-oriented subjects in the California public school system and
worked for Bell Telephone Laboratories (NJ), E.G. & G., Inc. (NV), and
Fairchild Semiconductor Research and Development Laboratory (CA).
His professional interests center on the application of computers to the
needs of people, especially the physically handicapped. He is available
for consulting during the long, hot Kansas summers. In his spare time,
he enjoys such hobbies as amateur radio (W0PBV), beekeeping, farming,
and boating. He is a member of the IEEE and is active in the Amateur
Radio Emergency Service (ARES/RACES).

APPENDIX A.

USER'S MANUAL
----

for

A LOW-COST LOCAL-AREA NETWORK for DESKTOP COMPUTERS
----

by

Myron A. Calhoun, Ph.D.
Associate Professor
Computer Science Department
Kansas State University
Manhattan, KS 66506

26 October 1985

NAME
  NETIN - network sign in

ENTRY FORM
  NETIN [name] {Return}

DESCRIPTION
  The NETIN command is used when a user initially signs in, or it may be
  used at any time to change from one user to another.

  If NETIN is invoked without an argument, it asks for a user name and
  a password. If NETIN is invoked with an argument, it assumes the
  argument is a user name and continues by asking for a password.
  Echoing is turned off during the typing of the password so that it
  appears neither on the screen nor on any written record of the
  session.

  After a successful login, accounting files are updated, the user is
  informed of the existence of waiting mail, and the message of the day
  (if any) and the time s/he last logged in are displayed on the screen.

ERROR MESSAGES
  "Login incorrect": either the name or password (or both) is bad.

  "System going down": the net server has been told that the system is
                        about to be taken down (e.g., for maintenance).

  "Cannot open password file": consult a network guru.

NAME
  NETOUT - network sign out

ENTRY FORM
  NETOUT {Return}

DESCRIPTION
  The NETOUT command is used when a user wishes to sign off and there is
  not another user immediately wishing to sign in.

  NETOUT is invoked without an argument; accounting files are updated,
  the user is informed of the existence of any unread mail, and control
  is returned to COMMAND.COM.

ERROR MESSAGE
  None

NAME
    NETMAIL - network send and receive mail

ENTRY FORM
    NETMAIL [user(s)] [< filespec]

DESCRIPTION
    NETMAIL allows you to send messages and files to other users, whether
    or not those users are currently logged in. It also allows you to
    read, at your own convenience, messages which have been sent to you by
    other users.

    Sending mail. To send a message to one or more users, invoke NETMAIL
    with argument(s) giving the login name(s) of people to whom your mail
    should be sent (e.g. "NETMAIL name" or "NETMAIL name name ...."). You
    type in your message, followed by an EOF (control-Z). Alternatively,
    redirection may be used to send a copy of the contents of a specified
    file to the indicated people (e.g. "NETMAIL name < filespec" or
    "NETMAIL name name .... < filespec").

    Reading mail. If NETMAIL is invoked with no arguments, (eg. "NETMAIL")
    the header (first line) of each message waiting for you in the post
    office is displayed on the screen. The current message is initially
    the first message (numbered 1) and can be displayed in its entirety
    using the 't' (type) command. To examine other messages, you can use
    the commands 'n' (next), '+' and '-' to move forwards and backwards
    among the various messages, or you can indicate a specific message
    number after the 't' command.

    Replying to mail. You can initiate a response to the current message
    by using the 'r' (reply) command, which automatically directs your
    response back to the person from whom the message came. You then type
    in your message, followed by an EOF (control-Z).

    Saving copies of mail. After examining a message you can 's' (save)
    it, which causes a copy of the message to be written to a specified
    file in your current directory (e.g., "s filespec").

    Ending a mail processing session. You can end a NETMAIL session with
    the 'q' (quit) command, in which case messages that have not been
    examined remain in the post office for later perusal. Examined mail
    is removed from the post office and discarded, never to be seen again.
    If the NETMAIL session is ended with 'x' (exit), ALL messages are left
    in the post office for later (re)examination. A ^C break produces the
    same effect as 'x'.

SUMMARY
A command usually consists of one character and is typed on a line by
itself. The 't' command can take a message number as an argument; if
no message number is given, the next message forward is used. If
there are no messages forward of the current message, the search wraps
around to the first message.

-           Change to the previous message and display it.

+ or n   Change to the next message and display it.

?   Display a brief summary of these commands.

h   List the header (first lines) of all of the messages.

q   Quit the session, leaving all unreferenced messages in the
            post office and discarding all referenced messages. If
            new mail has arrived during the session, the message
            "You have new mail" is given.

r   Reply to the originator. This does not send your reply to
            other recipients of the original message.

s filespec Save the current message in the specified file.

t   Type the next or indicated message on the user's terminal.
            A message number can be given as an argument: 't 3' or
            't3' types message 3.

x   Exit the session, leaving all mail in the post office for
            later re-examination.

MESSAGES
  "You have new mail": This message is given upon exiting a session if
                        new mail has arrived during the session.

2.15

NAME
  NETCD - network change directory

ENTRY FORMS
  NETCD
  NETCD d:pathname   (same as MS-DOS resident CD)
  NETCD z:pathname

DESCRIPTION
  NETCD is an enhancement of the MS-DOS 2.0 resident CD (or CHDIR)
  command to support changing your current working directory on the
  shared Z: disk on the network server computer to a different path, or
  to display the path name for your current working directory. If NETCD
  is invoked without any parameters, the path name for your current
  working directory on the Z: disk is displayed. If NETCD is invoked
  and the parameter does not refer to the Z: disk, the request is
  forwarded directly to the resident CD (CHDIR) command processor, which
  will change your current working directory on one of the disks in your
  local computer to the indicated path as if NETCD had not been invoked.
  But if the parameter does refer to the Z: disk, NETCD changes your
  current working directory on the Z: disk to the indicated path.

  For additional information concerning CD (CHDIR), refer to the MS-DOS
  manual.

ERROR MESSAGES
  Same as those found in the description of the resident CHDIR (CD)
  command in the MS-DOS manual.

NAME
  NETCOPY - network copy file

ENTRY FORMS
  NETCOPY d:filespec d:filename   (same as MS-DOS resident COPY)
  NETCOPY z:filespec d:filename
  NETCOPY d:filespec z:filename
  NETCOPY z:filespec z:filename   (not implemented)

DESCRIPTION
  NETCOPY is an enhancement of the MS-DOS 2.0 resident COPY command to
  support file transfers to and from your file space on the shared Z:
  disk on the network server computer. If NETCOPY is invoked and
  neither the source filespec nor the destination filename refers to the
  Z: disk, the request is passed directly to the resident COPY command
  for completion. But if either the filespec or the filename refers to
  the Z: disk, NETCOPY copies your indicated source file to the
  specified destination. To reduce unnecessary proliferation of
  identical files on the shared Z: disk, NETCOPY does not support direct
  replication of files on the Z: disk, nor does it support concatenation
  of several files into one combined file.

  For additional information concerning COPY, refer to the MS-DOS
  manual.

ERROR MESSAGES
  "Replication not permitted": both the source filespec and the
                                destination filename refer to the shared
                                Z: disk

  Other error messages may be found in the description of the resident
                              COPY command in the MS-DOS manual.

NAME
  NETDEL - network delete (erase) file

ENTRY FORMS
  NETDEL d:filespec   (same as MS-DOS resident DEL)
  NETDEL z:filespec
  NETDEL z:filespec d:filespec

DESCRIPTION
  NETDEL is an enhancement of the MS-DOS 2.0 resident DEL (or ERASE)
  command to support deletion of one or more of your files from your
  portion of the shared Z: disk on the network server computer. If
  NETDEL is invoked and no filespec refers to the Z: disk, the request
  is passed directly to the resident ERASE command for execution. But
  for each filespec which does refer to the Z: disk, NETDEL erases the
  indicated file from your Z: disk directory space: disk; any remaining
  filespecs are then passed to the resident ERASE command.

  For additional information concerning DEL (ERASE), refer to the MS-DOS
  manual.

ERROR MESSAGES
  Same as those found in the description of the resident ERASE (DEL)
  command in the MS-DOS manual.

NAME
  NETDIR - network display directory

ENTRY FORMS
  NETDIR
  NETDIR d:pathname   (same as MS-DOS resident DIR)
  NETDIR z:pathname

DESCRIPTION
  NETDIR is an enhancement of the MS-DOS 2.0 resident DIR command to
  support displaying directory entries in your current or specified
  directory on the shared Z: disk on the network server computer. If
  NETDIR is invoked without any parameters, the directory for your
  current working directory on the Z: disk is displayed. If NETDIR is
  invoked with a parameter which does not refer to the Z: disk, the
  request is forwarded directly to the resident DIR command, which
  displays all or selected entries in the current or specified directory
  on your local computer as if NETDIR had not been invoked. But if the
  parameter does refer to the Z: disk, NETDIR displays all or selected
  entries in the specified directory on the Z: disk.

  For additional information concerning DIR, refer to the MS-DOS
  manual.

ERROR MESSAGES
  Same as those found in the description of the resident DIR command in
  the MS-DOS manual.

NAME
  NETMD - network make directory

ENTRY FORMS
  NETMD d:pathname   (same as MS-DOS resident MKDIR)
  NETMD z:pathname

DESCRIPTION
  NETMD is an enhancement of the MS-DOS 2.0 resident MD (or MKDIR)
  command to support the creation of new directories within your part of
  the shared Z: disk on the network server computer. If NETMD is
  invoked and the parameter does not refer to the Z: disk, the request
  is passed directly to the resident MKDIR command processor for
  processing. But if the parameter does refer to the Z: disk, NETMD
  creates the new directory within your portion of the shared Z: disk.

  For additional information concerning MD (MKDIR), refer to the MS-DOS
  manual.

ERROR MESSAGES
  Same as those found in the description of the resident MKDIR (MD)
  command in the MS-DOS manual.

NAME
  NETPATH - network directory search path for data files

ENTRY FORMS
  NETPATH   (similar to MS-DOS resident PATH)
  NETPATH pathlist   (similar to MS-DOS resident PATH)
  NETPATH +pathlist

DESCRIPTION
  The MS-DOS PATH command is used to specify directories to be searched
  in the event that a requested transient command is not found in the
  current working directory.

  NETPATH is an addition to the PATH command to support similar searches
  for data files, including, but not limited to, files which may be in
  your portion of the shared Z: disk on the network server computer. If
  NETPATH is invoked without a parameter, the current data file search
  path is displayed on the screen. If NETPATH is invoked with a
  parameter, the new pathlist replaces any previous data file pathlist,
  unless the parameter begins with a plus sign ("+"), in which case the
  new pathlist is appended to the end of the former pathlist (if any).

  For additional information concerning NETPATH, refer to the PATH
  command in the MS-DOS manual.

ERROR MESSAGES
  Same as those found in the description of the resident PATH command in
  the MS-DOS manual.

NAME
  NETPRINT - network print

ENTRY FORMS
  NETPRINT d:filespec   (same as MS-DOS resident PRINT)
  NETPRINT z:filespec

DESCRIPTION
  NETPRINT is an enhancement of the MS-DOS 2.0 resident PRINT command to
  invoke spooled ("Simultaneous Peripheral Operation On Line") or
  background printing of specified files while other MS-DOS commands are
  being processed or user-application programs are running in the
  foreground.

  If the parameter does not refer to the Z: disk, a copy of the
  specified file from one of the disks on your local computer is sent to
  the network print spooler on the network server and from thence to the
  network printer. If the parameter does refer to the Z: disk, the
  specified file from your portion of the shared Z: disk is printed on
  the network printer.

  For additional information concerning NETPRINT, refer to the PRINT
  command in the MS-DOS manual.

ERROR MESSAGES
  Same as those found in the description of the resident PRINT command
  in the MS-DOS manual.

NAME
  NETRD - network remove directory

ENTRY FORMS
  NETRD d:pathname   (same as MS-DOS resident RD)
  NETRD z:pathname

DESCRIPTION
  NETRD is an enhancement of the MS-DOS 2.0 resident RD (or RMDIR)
  command to support the removal of directories from your portion of the
  shared Z: disk on the network server computer. If NETRD is invoked
  and the parameter does not refer to the Z: disk, the request is passed
  directly to the resident RMDIR command processor for execution. But
  if the parameter does refer to the Z: disk, NETRD removes the
  indicated directory from your portion of the shared Z: disk.

  For additional information concerning RD (RMDIR), refer to the MS-DOS
  manual.

ERROR MESSAGES
  Same as those found in the description of the resident RMDIR (RD)
  command in the MS-DOS manual.

NAME
  NETREN - network rename an existing file

ENTRY FORMS
  NETREN d:filespec filename   (same as MS-DOS resident REN)
  NETREN z:filespec filename

DESCRIPTION
  NETREN is an enhancement of the MS-DOS 2.0 resident REN (or RENAME)
  command to support changing the name of one of your files in your
  portion of the shared Z: disk on the network server computer. If
  NETREN is invoked and the filespec does not refer to the Z: disk, the
  request is passed directly to the resident RENAME command processor
  for execution. If the filespec does refer to the Z: disk, NETREN
  changes the name of the indicated file in your portion of the Z: disk
  to the new filename.

  For additional information concerning REN (RENAME), refer to the
  MS-DOS manual.

ERROR MESSAGES
  Same as those found in the description of the resident RENAME (REN)
  command in the MS-DOS manual.

NAME
  NETRUN - network load and run a program

ENTRY FORM
  NETRUN d:programspec   (Equivalent to typing "programspec")
  NETRUN z:programspec

DESCRIPTION
  NETRUN is an ennancement of MS-DOS to support controlled execution of
  programs from the snared Z: disk on the network server computer. If
  the specified programspec does not reference the Z: disk, NETRUN
  forwards the request to execute the indicated program directly to
  COMMAND.COM for processing. If the programspec does reference the Z:
  disk, and if the indicated program is copyrighted, NETRUN cnecks to
  see if sufficient copies nave been purchased to satisfy the current
  number of requests for executable copies. If the number of currently
  active requests is less than the number of copies available, or if
  the requested program is not copyrighted, then NETRUN fetcnes the
  indicated program from your current directory or the root directory
  on the Z: disk, loads it into the memory of your local computer, and
  executes it.

ERROR MESSAGES
  "Program not found": The indicated program was not found in your
                        current directory nor in the root directory on
                        the snared Z: disk.

  "Program not available": All available copies of the indicated
                            program are currently in use; please try
                            again in a few minutes.

2.25

NAME
  NETPASS - network password change

ENTRY FORMS
  NETPASS

DESCRIPTION
  This command changes the password associated with the user name.

  The program prompts for the old password and then for the new one.
  You must supply both. The new password must be typed twice, to
  forestall mistakes.

  Passwords must be at least four characters long and cannot be longer
  than eight characters. Any shifted or unshifted printable characters
  may be included, but no control characters are allowed.

  Only the owner of a password may change the password; you must prove
  you know the old password.

ERROR MESSAGES
  "Too short": Passwords must be at least four characters long.

  "Too long": Passwords cannot be longer than eight characters.

NAME
    NETWHO - network user information lookup program

ENTRY FORM
    NETWHO [name(s)]

DESCRIPTION
    Invoked without an argument, NETWHO lists the login name, full name,
    login time, and office location and phone number (if they are known)
    for each user currently logged in.

    With an argument, NETWHO lists the above information for only the
    specified names. Login names as well as first and last human-oriented
    names of users are accepted.

ERROR MESSAGES
    None
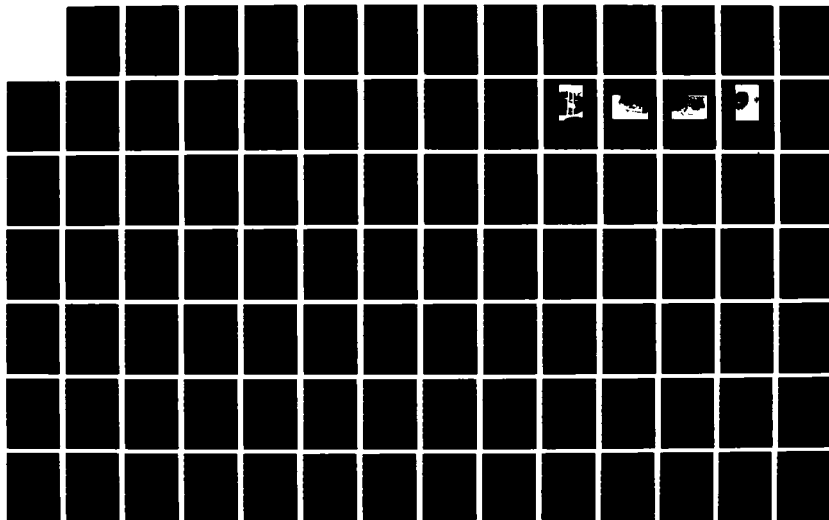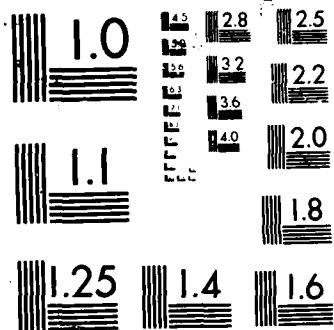
APPENDIX B.

Although complete "accounts, records, documents, and other evidence
showing and supporting all costs incurred under this Subcontract" have
been submitted routinely during the project, the following list shows
the items which were purchased using funds provided through the RISE
research grant. For simplicity, all amounts have been rounded to the
nearest dollar.

        Software
            74 MS-DOS Version 2 Operating System
           100 MS-DOS Version 2 Programmer's Utility Package
            98 MicroSoft FORTRAN 86, Version 3.3

        Hardware
           616 Four 8" DSDD floppy drives   [See note 1]
           419 Drive cabinets & power supplies
            84 Cables and cable adapters
            64 AC power strips and surge adapter
           212 Votrax Type'n Talk Synthesizer   [Note 2]

        Interface Cards for Z-100
           809 2 Megabyte RAM, RAM-Drive software [Note 1]
           269 Cromemco Model D + 7A I/O
            75 S-100 Extender board with probe
           178 MCPI ICB-10 Input/Output controller [Note 2]

        Miscellaneous supplies
           116 8087 co-processor chip
            24 NEC V20 (8088 microprocessor)   [Note 1]
            76 Intersil ICM7226A EV/kit
           111 74XX Integrated circuits
            50 Digital multitester
           ⁻25 D-25 gender changers (haven't arrived yet)

        Total = $3,400

Notes:
1. The RISE proposal equipment budget included the purchase of a hard
   disk subsystem. Unfortunately, hard disks are quite succeptible to
   damage when being moved, and the author's development system is often
   moved. To attain the equivalent mass storage, several 8" floppy
   disk drives were substituted; to gain the equivalent speed, an 8088
   microprocessor faster than the Intel version and a 2-megabyte RAM
   memory and ram-drive software were substituted.

2. Not included above is one item which was listed in the RISE proposal
   budget (the Z-204 Multiport Input/Output Card) but which was
   purchased by the KSU CS Department out of its own funds before the
   RISE proposal had been approved so that the author could complete his
   1984 SFRP project. Two items supporting use of the prototype network
   by a blind student were substituted.

DEVELOPMENT OF PREDICTION MODELS
FOR HUMAN TORQUE STRENGTH

Final Research Report on Subcontract
#84 RIP 03

Submitted to

Southeastern Center for Electrical
Engineering Education
St. Cloud, Florida

by

S. Deivanayagam, Ph.D., P.E.
Associate Professor of Industrial Engineering
The University of Texas at Arlington

August 1985

INTRODUCTION

Historically, in the design development of weapon systems, the maintainability and supportability considerations have had a low priority. At best, they are relegated to later stages of design analysis and evaluation (1). This practice, often has resulted in recognizing certain design "deficiencies" only late in the life cycle of the system. At that point in time, either the design modifications are performed at a considerable cost or no change is made in order to save the cost of design modifications. But the later practice leads to high costs associated with maintenance and support functions. It is estimated that approximately 35 percent of the total lifetime cost of military systems is spent for maintenance purposes (2).

> "We have had substantial growth in the cost to support our weapons and in the technical competence required to maintain them."
>
> - Richard D. DeLauer, Under Secretary of Defense (3).

Due to the fact that maintainability and supportability costs are significant, the United States Air Force is attempting to reduce such costs without any reduction in the readiness and effectiveness of the weapon system.

> "We want equipment which requires the least number of operators and which is easiest to support. We must avoid hardware too sophisticated that it cannot be properly maintained by our users."
>
> - Frank C. Carlucci, Deputy Secretary of Defense (4).

Maintainability must be considered as a characteristic of the system that evolves from the design and installation of the system. Quantitative measures of maintainability usually include one or more of such variables as the time, the effort, and the

cost required to repair the failed system. Reliability is generally considered as the numerical probability of failure-free operations of the system for a specified time duration under a set of given conditions. Inadequate consideration of maintainability of a system during its design development stage often results in inordinate amounts of time and effort requirement to accomplish even simple maintenance tasks. Once the design development has proceeded to a point, design changes for the sake of maintainability are often not considered. Thus, for the rest of the life of the system, the maintenance personnel may have to cope with the difficult to maintain system, spending hours instead of minutes. Difficulty in maintenance may be experienced in one or more of the following area:

1. Troubleshooting

2. Accessibility to part to be repaired/replaced

3. Strength requirements to perform the task

4. Environmental conditions

Much of the maintainability problems can be attributed to the failure of the designer to address these areas during the design development of the system. In fairness to the designer, it must be mentioned that this failure on the part of the designer is caused by the nonavailability of proper and useful information, tools, and techniques. Recognizing this major deficiency, the Air Force Human Resources Laboratory (AFHRL) and the Air Force Aerospace Medical Laboratory (AFAMRL) have initiated a program to develop a computer-aided design tool. This tool is conceived to be in

the form of a computerized biomechanical man model of a
maintenance technician. This model, called CREW CHIEF, when
fully developed, will provide the aircraft system designer
with a tool to input appropriate ergonomic information and
evaluate the design concepts from maintainability point of
view.

PRESENT RESEARCH

The CREW CHIEF model, among other other things, requires an
ergonomic database describing the maintenance technician's body
size and strength capabilities in order to properly simulate
those characteristics. In this context, a pilot study was
conducted during the summer of 1984 by the principal
investigator to collect certain torque strength data (5).
This research is aimed at developing predictive models for human
torque strength using the data collected in the previous study.

Objectives

The present investigation was undertaken for the following two
objectives.

1. To develop mathematical models that would be useful in
   predicting the torque strength of a maintenance technician
   while using a ratchet wrench under certain task
   conditions.

2. to develop a microcomputer based human torque
   measurement system at UTA similar to the one at the
   ergonomic laboratory of AFAMRL so that additional
   experimentation and data collection can be performed at
   UTA in support of the CREW CHIEF program.

3.4

The development of predictive models was based on regression modeling technique using the data collected during the pilot study at Wright-Patterson AFB. A complete description of the study is available in ref. 5. A brief description of the experimental conditions, the independent variables and their levels is given below.

A. Bolt Head Elevation - Stature Level and Knuckle Level

B. Bolt Head Orientation - Vertical, Facing, and Transverse

C. Wrench Position - 0, 90, 180, and 270 degrees positions of the handle.

D. Direction of Torque - Clockwise and counterclockwise

E. Anthropometric Variables - Thirty-six different variables as shown in Table I.

F. Subjects - 10 males and 10 females

The handtool used was a snap-on make 1/2" diameter drive 10" long ratchet wrench. The task point was represented by a 5/8" diameter bolt head welded firmly to a base so that the isometric torque can be measured. There were a total of 2160 data points, consisting of real time torque data for the four second duration of strength exertion.

Model Development

Approach

It was decided to use the average torque during 1 to 4 seconds as the dependent variable to be modeled. This measure was chosen over others (such as peak value) as it can be considered to represent the isometric strength of an individual for a brief sustained period of time. For modeling purposes, the statistical regression analysis technique was used. The stepwise

TABLE 1

ANTHROPOMETRIC MEASUREMENTS FOR TORQUE STRENGTH STUDY

MALE(N=10)			FEMALE(N=10)	
MEAN	SD	MEASUREMENT	MEAN	SD
166.97	42.60	Weight	127.77	14.33
178.09	6.20	Stature	165.20	3.70
146.33	5.34	Acromiale Ht	133.10	2.73
106.43	5.26	Iliac Crest Ht	100.39	2.47
92.46	4.54	Trochanterion Ht	86.03	2.12
77.92	4.15	Metacarpale III Ht	72.62	2.76
7.25	0.99	Lateral Mall. Ht	6.31	0.49
35.74	1.18	Shoulder-Elbow Lgth	31.51	1.01
33.50	1.39	Acromion-Radiale Lgth	29.02	1.22
28.07	1.72	Elbow-Wrist Lgth	25.72	1.11
25.62	1.55	Radiale-Stylion Lgth	23.72	0.64
39.90	2.05	Biacromial Br	37.21	1.15
23.85	3.31	Chest Depth	22.10	0.99
33.27	2.38	Bitrochanteric Br	32.96	2.11
26.93	1.62	Foot Length	24.05	1.16
115.60	10.72	Shoulder Circ	100.40	4.14
95.89	11.61	Chest Circ	87.93	3.39
32.50	4.72	Biceps Circ, Flexed	27.21	2.00
29.70	2.99	Forearm Circ, Flexed	25.44	1.30
17.21	1.46	Wrist Circ	15.23	0.32
19.53	0.93	Hand Lgth	17.44	0.69
8.74	0.50	Hand Br	7.49	0.39
94.78	3.71	Sitting Ht	88.83	4.02
62.35	2.71	Acromion Ht, Sitting	56.45	3.05
55.51	2.83	Knee Ht, Sitting	50.89	1.14
59.91	2.47	Buttock-Knee Lgth	56.86	2.11
35.94	3.58	Hip Breadth, Sitting	38.40	2.79
1.50	0.69	Subscapular Skinfold	1.18	0.37
1.17	0.60	Triceps Skinfold	1.35	0.49
0.61	0.31	Biceps Skinfold	0.75	0.38
1.95	0.63	Iliocristale Skf	1.35	0.36
108.40	20.92	Grip Strength, R1	68.50	7.43
109.30	25.04	Grip Strength, R2	66.00	9.70
106.10	26.59	Grip Strength, L1	64.00	8.89
104.00	24.27	Grip Strength, L2	59.50	12.54
179.10	6.61	Span	163.26	5.31
217.93	8.65	Vert Grip Reach	197.34	4.16

NOTE: Weight and grip strength in pounds.
All others in centimeters.

regression procedure available in the SAS statistical package was used on the IBM 4341 mainframe computer at the University of Texas at Arlington. In developing the models, the following two assumptions were implied.

(a) The regression between the dependent variable (i.e. torque strength) and the selected independent variables is only linear.

(b) There will be no interaction within the quantitative variables and within the indicator variables. However, interaction between the two sets of variables is considered.

The model development was performed in three sets of different complexities. The model Set I considered was the most detailed one. Model Set II was a subset of Model Set I in which only a few of the variables from Set I were included. Model Set III included the nonquantitative variables representing wrench positions and also the bench mark exertion values as independent variables.

Model Set I

Nine anthropometric measurements were selected and were run for multiple regression models individually for each bolt orientation, elevation, wrench position and replication. Such models were developed for males and females separately and then combined as a single group. The following anthropometric variables were used.

X_1 - weight of the subject in lbs.

X_2 - Height in cms.

X_3 - Knee Height Sitting in cms.

X_4 - Rt. Grip Strength in Kgms.

X_5 - Rt. Biceps Circumference, flexed, in cms.

X_6 - Rt. Forearm Circumference, flexed, in cms.

X_7 - Rt. Wrist Circumference, flexed, in cms.

X_8 - Span in cms.

X_9 - Vertical Grip Reach in cms.

The above anthropometric variables are generally thought to have most significant influence on the hand applied torque strength of an individual.

The summary of the results for Model Set I regression analysis is given in Tables II A through D. It can be seen that when males and females are considered separately the resulting models are generally better than when they are combined. The R^2 values for models when males and females are considered separately range about 0.9 while if the sexes are combined the R^2 values are around 0,8 or lower. The reason for this is the increased variability resulting due to combining the males and females.

This set of models can be considered as the most detailed set. There is a specific model for each task related condition of bolt orientation height, wrench portion, direction of torque and sex. These models are based on anthropometric variables only. The task related variables are not included in the model. Thus the user will have to select the correct model for prediction. From CREW CHIEF point of view, the utility of these models will be limited as the task conditions are not included as

3.8

Table IIA. Model Set I - Males and Females
Combined: Clockwise Torque

Vertical

Elevation	Wrench Postn.	Const.	X_1	X_2	X_3	X_4	X_5	X_6	X_7	X_8	X_9	R^2
Knuckle	0	33.08	-.03	-	-	.35	.38	-	-	-	-.25	0.88
	90	10.46	.25	-	-1.97	.55	3.44	-	-7.48	-.78	1.34	0.76
	180	26.30	-.33	-.82	-2.65	.58	2.32	2.69	-6.23	-1.37	2.30	0.89
	270	-23.23	-.18	-	-.51	.09	1.71	-	-	-1.36	1.30	0.73
Stature	0	-38.28	-	-.15	-	-	-	.60	-	-	.29	0.76
	90	48.36	-	.26	-1.96	.58	4.18	-5.36	-3.70	-1.10	1.26	0.84
	180	-11.88	-.08	.37	-.64	.31	-1.10	-	-	-.31	.65	0.90
	270	-145.23	-.16	.61	-1.27	-.17	-1.36	5.03	-	-	.33	0.73

Facing

Elevation	Wrench Postn.	Const.	X_1	X_2	X_3	X_4	X_5	X_6	X_7	X_8	X_9	R^2
Knuckle	0	-73.6	-.16	.27	-1.47	.07	-	3.68	.24	-.48	.59	0.83
	90	-66.7	-.19	-	-2.80	.44	2.75	.65	.71	-1.15	1.64	0.75
	180	-131.05	-.28	2.09	-3.10	.24	1.82	1.26	-	-	-.51	0.74
	270	24.18	-.15	-1.02	-	.35	1.69	2.14	-2.46	-.89	1.23	0.73
Stature	0	-36.62	-.10	-	-1.04	.21	-	-	3.08	.30	-	0.89
	90	7.39	-.19	-	-1.54	.67	3.39	-.55	-4.07	-.73	.94	0.86
	180	23.24	-.20	-.56	-1.13	.41	2.59	.97	-2.60	-.63	.97	0.72
	270	-171.22	-.31	-	-1.98	-.40	-2.37	9.84	3.11	-1.36	1.74	0.78

Transverse

Elevation	Wrench Postn.	Const.	X_1	X_2	X_3	X_4	X_5	X_6	X_7	X_8	X_9	R^2
Knuckle	0	-71.80	-.36	-	-2.05	.22	1.56	1.88	4.51	-.42	.70	0.80
	90	-54.68	-.22	-	-1.53	-	-1.46	8.85	-3.17	-1.39	1.39	0.66
	180	-131.16	-.18	-	-3.24	.19	-1.39	6.23	-	-.42	1.44	0.83
	270	-176.02	-.31	-	-4.15	-	2.19	4.50	-5.91	-1.20	2.88	0.75
Stature	0	49.37	.20	-.94	1.61	.05	-	-1.29	-2.24	.47	-	0.60
	90	-78.65	-.09	.38	-1.83	.30	2.20	-1.42	1.63	-	.39	0.87
	180	-36.08	-.08	-.25	-1.75	.34	1.52	-1.44	-	-.29	1.12	0.84
	270	18.22	-.19	-1.18	-1.40	.34	-	4.12	-	-.76	1.45	0.81

3.9

Table IIB. Model Set I - Males and Females
Combined: Counterclockwise Torque

Vertical

Elevation	Wrench Postn.	Const.	X_1	X_2	X_3	X_4	X_5	X_6	X_7	X_8	X_9	R^2
Knuckle	0	81.41	-.12	-.76	-.25	.43	1.43	.02	-	-.38	.65	0.81
	90	26.31	-	-	-2.01	.44	-	-	-	-.37	.67	0.61
	180	-44.78	.22	.42	-1.73	.33	1.30	1.93	-4.73	-.48	.79	0.85
	270	-17.78	-	.32	-1.25	.32	1.73	-	.25	-1.14	1.38	0.90
Stature	0	-45.22	-.15	-	-1.07	-	-	2.31	-	-.37	.64	0.70
	90	-37.46	.20	.36	-1.48	.38	1.15	1.47	-2.14	-.07	.87	0.91
	180	-16.99	-.07	.28	-.45	.23	1.08	-	-2.07	-.46	.40	0.80
	270	-54.72	-	-	-	-	-.49	2.89	-	-.23	.25	0.82

Facing

Elevation	Wrench Postn.	Const.	X_1	X_2	X_3	X_4	X_5	X_6	X_7	X_8	X_9	R^2
Knuckle	0	-134.86	-.39	-	-1.84	-	2.33	4.49	-	-.68	1.19	0.80
	90	-36.32	-.25	-	-3.83	.49	3.34	1.78	-6.54	-1.65	2.49	0.80
	180	-144.26	-.14	3.17	-2.45	.21	-	2.18	-4.41	-	-1.10	0.74
	270	-57.69	.09	.64	-	-	-1.93	8.70	-5.38	-1.44	.73	0.75
Stature	0	4.30	-.09	-.33	-.44	.24	1.02	-.67	2.84	-	.12	0.89
	90	-39.32	-.33	-.65	-2.52	.29	1.55	2.22	5.25	-.34	1.01	0.76
	180	-4.86	.051	-	-	.20	.65	-.59	-	-	-	0.71
	270	-236.19	-.45	1.48	-	-.17	1.71	4.75	-	-.46	-	0.66

Transverse

Elevation	Wrench Postn.	Const.	X_1	X_2	X_3	X_4	X_5	X_6	X_7	X_8	X_9	R^2
Knuckle	0	-28.39	-.37	-.57	-2.05	.32	3.48	2.45	-6.69	-.59	1.61	0.80
	90	-134.76	-.31	.36	-3.69	-	-1.13	5.51	2.50	-.70	1.46	0.79
	180	-47.05	-.30	1.41	-4.78	.51	-1.39	4.67	-	-	-	0.60
	270	-167.70	-.68	.52	-3.82	.30	4.47	6.42	-4.98	-1.00	1.74	0.80
Stature	0	-55.57	-.10	-.29	-1.08	.26	-	.75	-	-	.70	0.82
	90	9.01	.08	-	-2.29	.29	.55	-	3.51	-.24	.43	0.76
	180	45.16	-	-	-2.60	.63	2.23	-1.62	-	-	.29	0.79
	270	-68.05	-.25	1.10	-	.46	3.46	1.32	-4.16	-.85	-	0.81

3.10

Table IIC. Model Set 1 - Males: Clockwise
Torque - Selected Models

Vertical

Elevation	Wrench Posn.	Const.	X_1	X_2	X_3	X_4	X_5	X_6	X_7	X_8	X_9	R^2
Knuckle-C	90	161.05	-	-2.04	-3.84	.79	4.17	-	-19.22	-	2.65	0.76
Knuckle-CC	90	64.72	-.44	7.35	-	1.03	4.39	19.19	-47.19	-5.78	-1.06	6.89
Stature-C	0	47.56	-.07	-.30	.86	.20	1.08	-	.11	-.73	.26	.95

Facing

Elevation	Wrench Posn.	Const.	X_1	X_2	X_3	X_4	X_5	X_6	X_7	X_8	X_9	R^2
Knuckle-C	0	-60.40	-.18	2.47	.51	.14	1.34	8.79	-15.32	-1.79	-.38	0.92
Stature-C	180	19.29	.44	-8.60	-6.41	.13	1.54	-3.84	-8.87	4.78	5.40	0.98
Stature-CC	270	-331.54	-.74	13.39	6.64	.27	6.93	26.28	-60.74	6.43	-5.01	0.91

Transverse

Elevation	Wrench Posn.	Const.	X_1	X_2	X_3	X_4	X_5	X_6	X_7	X_8	X_9	R^2
Knuckle-CC	180	-126.40	.20	-6.07	-12.89	.37	-3.44	11.26	-24.33	3.42	6.76	0.94
Knuckle-CC	270	135.71	-.51	1.90	-3.61	.80	7.21	10.61	-31.23	-2.68	1.25	0.94
Stature-C	90	37.78	-	-	-	.50	4.76	-2.90	-6.67	-	-	0.91

3.11

Table IID. Model Set I - Females: Clockwise
Torque - Selected Models

Vertical

Elevation	Wrench Postn.	Const.	X_1	X_2	X_3	X_4	X_5	X_6	X_7	X_8	X_9	R^2
Knuckle-C	90	-397.26	-.16	-	-	-	2.01	1.99	5.75	-.67	1.86	0.87
Knuckle-CC	90	-367.99	-.23	-	-	.01	-.97	6.95	2.84	-1.021	2.00	0.94
Stature-C	0	-98.38	-	-	1.14	.34	1.06	-1.36	-4.48	-.88	1.25	0.79

Facing

Elevation	Wrench Postn.	Const.	X_1	X_2	X_3	X_4	X_5	X_6	X_7	X_8	X_9	R^2
Knuckle-C	0	-127.10	-	-	-	.72	1.77	-3.70	4.63	-.93	1.13	0.94
Stature-C	180	-96.49	.12	-.70	2.92	.85	1.22	.07	-14.85	-3.86	4.24	0.97
Stature-CC	270	22.59	.29	-.11	3.82	.91	4.06	-5.74	-15.08	-5.23	5.60	0.98

Transverse

Elevation	Wrench Postn.	Const.	X_1	X_2	X_3	X_4	X_5	X_6	X_7	X_8	X_9	R^2
Knuckle-CC	180	-747.70	-2.59	7.67	-16.31	-1.43	.09	16.33	45.46	7.76	-8.25	0.98
Knuckle-CC	270	-903.94	-1.41	2.05	-3.99	-	8.11	2.47	30.86	1.48	-	0.89
Stature-C	90	-232.41	.27	-.35	2.22	.76	1.88	-3.01	-7.36	-3.04	3.82	0.96

3.12

Table III. Model Set II - Selected Models Only
Regular Regression - Combined Males
and Females Clockwise Torque

Elevation	Wrench Postn.	Const.	X_1	X_3	X_4	X_5	X_6	X_9	R^2
				Vertical					
Knuckle	0	27.79	-.04	-.09	.33	.22	.36	-.21	0.88
	90	-44.02	-.33	-2.21	.45	3.26	-1.60	.76	0.71
	180	-79.84	-.38	-2.56	.44	2.94	-.39	.91	0.78
	270	-81.05	-.14	-.88	.03	1.77	-.29	.60	0.51
Stature	0	-39.84	-.01	-.24	.02	.13	.48	.24	0.76
	90	17.68	-.02	-2.06	.52	4.41	-7.23	.31	0.79
				Facing					
Knuckle	0	-17.17	-.13	-1.47	.04	-.06	3.36	.49	0.80
	270	-69.77	-.19	-.50	.23	1.82	1.43	.25	0.69

variables. Therefore, the models cannot predict strength values
at any new task condition. Also, the number of variables in the
models may be considered high. It will be useful from CREW CHIEF
point of view to have a limited number of models with as few
variables as possible. Therefore, the next set of models was
developed.

Model Set II

The results of Model Set I were analyzed for the most
contributing variables in order to reduce the number of terms.
The following considerations were taken into account to retain or
eliminate a variable.

1. The sequence of entry in step-wise regression.

2. The value of coefficient in relation to the value of the
    variable.

3. The occurrence of the variables in the set of models.

Based on the above, it was decided to drop height (X_2) and right
wrist circumference (X_7) from the model input variables. As this
will influence the coefficients for other variables and the
correlation coefficients regular regression models were developed
for combined male and female population for selected task
conditions. The results are shown in Table III. These models,
as the previous ones, also do not show any consistent pattern of
coefficients,. The R^2 values are lower as can be expected due to
the elimination of two variables. Thus, Model Set II also does
not show any great promise for CREW CHIEF purposes.

Model Set III

At this stage, it was thought worthwhile to include the bench mark torque strength values and the task condition variables such as bolt head elevation, wrench position, and direction of torque, and the bench mark torque strength values as independent variables in the regression model. Wrench position and direction of torque are not quantitative variables. Therefore, the following technique of indicator variables was adopted to represent the levels of those variables.

Wrench Position	Values for Indicator Variables
0 degrees	$X_3 = 1$, $X_4 = 0$, and $X_5 = 0$
90 degrees	$X_3 = 0$, $X_4 = 1$, and $X_5 = 0$
180 degrees	$X_3 = 0$, $X_4 = 0$, and $X_5 = 0$
270 degrees	$X_3 = 0$, $X_4 = 0$, and $X_5 = 0$

Further clockwise torquing condition was represented by $X_7 = 1$ and counterclockwise condition by $X_7 = 0$. The following two task conditions were considered as quantitative variables.

(i) Vertical bolt head at knuckle height with 90 degrees clockwise torque as variable G.

(ii) Transverse bolt head at stature height with 0 degrees counterclockwise torque as variable H.

The bolt head elevation in actual height was considered as a quantitative variable, K. The selected anthropometric variables were represented by A through F.

The resulting regression models can be considered as the generalized model as the various task conditions are included in the model. Initially attempts were made to include bolt head

3.15

orientation and sex in the model. However, the resulting models were very poor with R^2 values less than 0.5. Given below are the models with the corresponding R^2, M.S.E., and C_p values indicated. These models have quite acceptable values of the above criteria. The models for females seem to be slightly better than those for males. However, it must be cautioned here that the sample size is only 10 in each case. This means that while this approach looks promising, additional data on large sample and other task conditions will have to be collected before the models can be used with any confidence for prediction purposes. It is hoped that the planned series of experiments under the CREW CHIEF program will provide the necessary data for this purpose.

Generalized Regression Model for Males at Facing Bolt Head Orientation

Y = -109.6 + 1.27 (knee height) - 0.34 (grip strength)

  - 0.9 (Biceps Circumference) + 4.2 (Forearm Circumference)

  + 0.56 (Bench Mark) - 0.07 (Elev. Variable)

  - 2.0 (Knee Ht $*X_4$) - 1.4 (Knee Ht $*X_5$)

  + 4.1 (Biceps Circumference $*X_4$) + 1.5 (Forearm
       Circumference $*X_5$)

  -6.5 (Forearm Circumference $*X_4$) - 3.7 (Forearm
       Circumference $*X_5$)

R^2 = 0.716

MSE = 99.5

C_p = 6.50

Generalized Regression Model for Males
at Vertical Bolt Head Orientation

$Y = -127.9 - 0.15$ (Weight) $- 2.55$ (Knee Ht.)

$\qquad -0.18$ (Grip Strength) $- 1.11$ (Biceps Circumf.)

$\qquad +5.45$ (Forearm Circumf.) $+ 1.03$ (Vert. Grip Reach)

$\qquad +0.46$ (Bench Mark 1) $- 0.35$ (Bench Mark 2)
$\qquad\qquad -0.08$ (Elevation Variable)

$\qquad +73.19$ (1 for 90 degrees, 0 otherwise) $+ 123.5$ (1 for 180
$\qquad\qquad$ degrees, 0 otherwise)

$\qquad + 3.34$ (Biceps Circumf. $* X_4$) $+ 3.36$ (Knee Ht. $* X_5$)

$\qquad + 2.93$ (Biceps Circumf. $* X_5$)

$R^2 = 0.703$

$MSE = 73.73$

$C_p = 20.97$

Generalized Regression Model for Females
at Vertical Bolt Heat Orientation

$Y = 112.5 + 0.18$ (Weight) $- 0.55$ (Knee Ht.)

$\qquad + 0.08$ (Grip Strength) $- 1.4$ (Biceps Circumf)

$\qquad - 0.36$ (Vertical Grip Reach) $+ 0.28$ (Bench Mark 1 \

$\qquad + 0.39$ (Bench Mark 2) $- 0.06$ (Elev. Variable)

$R^2 = 0.792$

$MSE = 18.61$

$C_p = 10.65$

Generalized Regression Model for Males
at Transverse Bolt Head Orientation

Y = -30.84 - 0.08 (Weight)

+ 1.36 (Biceps Circumf.) + 1.49 (Forearm Circumf.)

+ 0.52 (Bench Mark 1) - 0.07 (Elev. Variable)

-1.0 (Biceps Circumf. * X_3) - 1.2 (Biceps Circumf. * X_5)

R^2 = 0.559

MSE = 166.54

C_p = 1.98

Generalized Regression Model for Females
at Transverse Bolt Head Orientation

Y = 231.6 + 0.25 (Weight) - 0.59 (Knee Ht.)

+0.36 (Grip Strength) - 2.39 (Biceps Circumf.)

- 0.82 (Forearm Circumf.) - 0.85 (Vertical Grip Reach)

+ 0.74 (Bench Mark 1) + 0.5 (Bench Mark 2) - 0.05 (Elev. Var)

+ 110 (1 for 180 degrees orientation, 0 otherwise)
        -44.1 (Forearm Circumf. * X_5)

-1.1 (Knee Ht. * X_5)

R^2 = 0.604

MSE = 59.65

C_p = 12.59

Generalized Regression Model for Females
at Facing Bolt Head Orientation

Y = 226.4 + 0.09 (Weight) - 1.6 (Biceps Circumf.)

- 1.0 (Vertical Grip Reach) + 0.58 (Bench Mark 1)

+ 0.62 (Bench Mark 2) - 2.49 (Biceps Circumf. * X_5)

R^2 = 0.692

MSE = 40.02

C_p = 27.7

Torque Strength Measurement System

The second objective of the present effort is to develop a system at UTA to measure the torque strength of individuals under simulated maintenance task conditions. It was desired that this system be identical to the one at the ergonomic laboratories of AFAMRL. This was highly encouraged by the AFAMRL personnel as it would be advantageous to U. S. Air Force to develop a research resource in this area at a university such as UTA. The needed financial resources were drawn from this research initiation grant and from the regular budgetary allocation of the Industrial Engineering Department at UTA. The AFAMRL has loaned several pieces of critical equipment through the University of Dayton Research Institute.

The development of the system involved several phases of activities such as design of hardware, purchasing of equipment, integration of the various units and calibration. All of these activities have been accomplished and the system is ready for conducting experiments.

Description of the System

The system consists of the following major components.

A. Torque testing hardware including a strain gage sensor and a rigid frame work.

B. Microcomputer based data acquisition system.

The torque dynamometer and the bridge amplifier have been loaned to UTA by AFAMRL. The "Unistrut" framework was designed and fabricated at UTA. The "Compaq" microcomputer, the printer and other accessories were bought under this grant and using

3.19

UTA's   matching funds.

The necessary software was developed by the University of
Dayton Research Institute under contract for U. S. Air Force.
This software has been loaned to UTA. Figures 1 through 3 show
various pieces of the system. Also shown in Figure 4 is a weight
lift test machine built as per U. S. Air Force Publication
AFAMRL-TR-80-0040 for subject screening and strength assessment
in future experimental studies. Figure 5 shows a sample printout
of the data relating to a torque measurement test.

The primary objective for developing this system is to
develop UTA's capability to provide the needed research support
in this area to U. S. Air Force. By successfully meeting this
objective, UTA has recently been asked to provide the research
support to experimentally collect the torque strength of
individuals under simulated maintenance task conditions as a
subcontractor under the CREW CHIEF program through the University
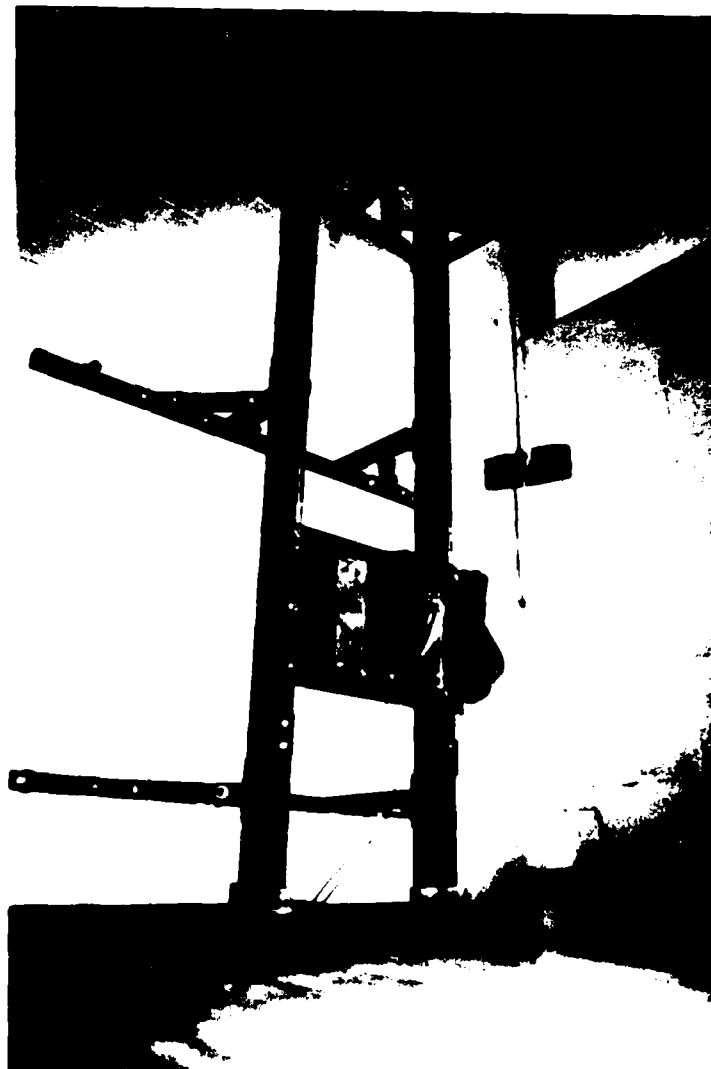of Dayton Research Institute.

Figure 1.   The Torque Dynamometer and the
Supporting Framework

Figure 2.   The Microcomputer Based Data
Acquisition System

Figure 3.   Showing a Trial Torque Exertion

Figure 4.   The Weight-Life Test Machine
            Built as per AFAMRL-TR-84-040

```
EXPERIMENT - TEST          SUBJECT   - 001        DATE - SAT 07/27/85
POSTURE    - STAND         HEIGHT    - K          BOLT ORI.  - F
WRENCH POS - 90            ARM       - R          EXTRA VAR. - 5


 TIME    TORQUE
(SEC)    (FT-LB)

0.000     10.1
0.100      9.7
0.200     15.1
0.300     26.2
0.400     40.1
0.500     52.8
0.600     65.0
0.700     77.6
0.800     88.2
0.900     96.4
1.000    101.8
1.100    107.5
1.200    109.6
1.300    111.2
1.400    110.8
1.500    111.5
1.600    111.7
1.700    111.5
1.800    111.5
1.900    111.1
2.000    111.6
2.100    110.9
2.200    110.4
2.300    110.1
2.400    107.8
2.500    107.0
2.600    106.5
2.700    105.6
2.800    108.1
2.900    108.3
3.000    109.0
3.100    108.9
3.200    107.1
3.300    104.9
3.400    102.7
3.500    102.0
3.600    102.1
3.700    102.2
3.800    103.5
3.900    103.5
4.000    102.5


START TIME - 03:15:48.72
MEAN VALUE FROM 1 TO 4 SEC =    107.5 FT-LB
PEAK VALUE FROM 0 TO 1 SEC =    101.8 FT-LB AND OCCUR AT    1.000 SEC
PEAK VALUE FROM 1 TO 4 SEC =    111.7 FT-LB AND OCCUR AT    1.600 SEC
RATIO ( PEAK 0 TO 1 ) / ( MEAN 1 TO 4 ) =   0.9469
TOTAL      0 VALUES FROM 1 TO 4 SEC OUTSIDE 10% OF THE MEAN [    96.7,   118.3]
```

Figure 5.   Sample Printout

REFERENCES

1. D. F. Spray, "Functional Requirements for a Computer
    Graphics Model of a Maintenance Technician", Masters Thesis,
    Air Force Institute of Technology, Dayton, Ohio, September
    1983.

2. J. W. McDaniel and W. B. Askern, "Computer Aided Design
    Models to Support Ergonomics", USAF Technical Report. (To be
    published)

3. R. D. DeLauer, "The FY 1984 Department of Defense, Program
    for Research, Development, and Acquisition. Statement to
    98th Congress, U. S. Government Printing Office, 1983.

4. F. C. Carlucci, "We Must Do It", Air Force Journal of
    Logistics, Winter 1982.

5. S. Deivanayagam, "An Experimental Investigation of Human
    Torque Strength", Final R⊢ ʼort to SCEE, September 20, 1984.

1984 USAF-SCEEE RESEARCH INITIATION GRANT PROGRAM

Sponsored by the

AIR FORCE OFFICE OF SCIENTIFIC RESEARCH

SOUTHEASTERN CENTER FOR ELECTRICAL ENGINEERING EDUCATION

FINAL TECHNICAL REPORT

THE ROLE OF ANTIOXIDANT NUTRIENTS IN PREVENTING HYPERBARIC
OXYGEN DAMAGE TO THE RETINA

Prepared by :   William L. Stone, Ph.D.

Academic Rank: Assistant Professor

Department and
    University: Department of Pediatrics and Biomedical Sciences
                       Meharry Medical College

Research Location: Meharry Medical College and
                   Brooks Air Force Base, School of Aerospace
                   Medicine, Division of Hyperbaric Medicine.

USAF Research: Col. Richard Henderson, M.D., current address is
                       Armed Forces Institute of Pathology
                       CPL-A, Washington, D.C., 20306-6000

Date: September 24, 1985

Contract No.   F49620-82-C-0035

ABSTRACT

Hyperbaric oxygen treatment was found to adversely affect the electrophysiological response of the retina to light in rats fed a basal diet deficient in both vitamin E and selenium (the B diet). Both vitamin E and selenium are micronutrients that play essential roles in preventing in vivo lipid peroxidation. After 4 weeks of hyperbaric oxygen treatment (3.0 ATA of 100 % oxygen, 1.5 hrs per day, 5 day/week) rats fed the B diet deficient in vitamin E and selenium showed decreased ($p < 0.005$) in a-wave amplitudes (83 ± 13 μV, N=8) and b-wave amplitudes (255 ± 30 μvolts) compared with a-wave amplitudes (151 ± 12 μV, N=17) and b-wave amplitudes (369 ± 29 μvolts) for rats fed an identical B diet but not treated with hyperbaric oxygen. Rats fed a basal diet supplemented with both vitamin E and selenium (the B+E+Se diet) or with vitamin E alone (the B+E diet) showed fairly constant a- and b- wave amplitudes that did not decrease after 4 weeks of hyperbaric oxygen treatment. Dietary antioxidants appear to provide protection from hyperbaric oxygen damage to the retina.

I. INTRODUCTION:

Hyperbaric oxygen therapy is currently being utilized at the School of Aerospace Medicine to enhance wound healing and to treat a variety of clincal disorders. These clinical disorders include radiation necrosis, gas gangrene, gas embolism, decompression sickness, osteomyelitis, carbon monoxide and acute cyanide poisoning. Hyperbaric oxygen therapy has also been used on an experimental basis to treat sickle cell crisis, hydrogen sulfide poisoning and carbon tetrachloride poisoning and to promote fracture healing.

The therapeutic benefits of long term hyperbaric oxygen treatment are potentially limited by the adverse clinical and pathological effects of high oxygen concentration upon the retina and the lung (1,2) and by adverse interactions with prooxidant drugs (3). Gable and Townsend (4) have observed pulmonary lesions in victims of fatal military aircraft accidents "possibly attributable to prolonged intermittent supplemental oxygen, stressing the potential hazard of oxygen toxicity for aviators". Oxygen toxicity to retinal and pulmonary tissues most likely involves free radical damage to biological membranes.

The retina is more sensitive to toxic and environmental disorders than most other tissues. The retina is particularly predisposed to the toxic effects of lipid peroxidation initiated by oxy-radicals. This is because the retina has: a) a very high content of polyunsaturated fatty acids (about 30% 22:6n3) which are very susceptible to lipid peroxidation (5); b) a very high consumption of oxygen, about seven times more per g of tissue than the brain; c) the presence of pigments (e.g. retinal) capable of inducing photosensitized oxidation reactions (6).

In some animal models hyperbaric oxygen causes severe retinal pathology and, in humans, causes loss of visual fields and visual definition (7). The ability of the retina to resist oxidative damage is very dependent upon the functioning of both enzymatic and chemical antioxidant mechanisms (8,9). Vitamin E and selenium are micronutrients that play a central role in physiological antioxidant mechanisms. Vitamin E effectively quenches free radicals generated by lipid peroxidation. Selenium is a cofactor for glutathione peroxidase which detoxifies lipid hydroperoxides. Dietary deficiency of vitamin E and/or selenium cause in vivo lipid peroxidation (10).

We have previously found that retinas from rats fed a standard Purina diet have significant levels of vitamin E and the selenoenzyme glutathione peroxidase. Retinal levels of vitamin E and glutathione peroxidase are decreased to very low levels by nutritional deficiency of vitamin E and selenium, respectively (9,11).

Rats fed a diet deficient in both vitamin E and selenium (the B diet) for 20 weeks or longer show retinal damage as indicated by decreased a- and b-wave electroretinogram (ERG) amplitudes (6). The retinal pigment epithelium of rats fed the B diet also show a large accumulation of lipofuscin pigment as well as major ultrastructural alterations (11,12). Lipofuscin pigment is thought to be a by-product

of in vivo lipid peroxidation. Recent in vitro studies of Armstrong, et al. (13), have shown that intravitrael injections of synthetic lipid hydroperoxides into rabbit eyes causes a marked decrease in the amplitude of the a-, b- and c-waves of the ERG.

II. OBJECTIVES OF RESEARCH EFFORT:
The research outlined in this preproposal is a direct continuation and follow-up of the pilot research project initiated at the USAF School of Aerospace Medicine (Brooks AFB) during the Summer of 1984. The objectives of the current research effort were to:

i) Investigate the toxic effects of long term hyperbaric oxygen on rats fed diets deficient in antioxidant nutrients. The toxicity of hyperbaric oxygen was measured by recording electroretinograms, weight, weight gain, and food consumption.

ii) Determine if short term hyperbaric oxygen treatment will cause retinal damage in rats previously fed an antioxidant deficient diet for 6 weeks.

iii) Investigate the possible protective effects of antioxidants nutrients on hyperbaric oxygen damage to the retina.

iv) Determine if hyperbaric oxygen treatment results in decreased levels of plasma vitamin E or plasma and glutathione peroxidase

III. EXPERIMENTAL DESIGN:
The project was divided into two phases. In phase I , weanling rats were fed the B or B+E+Se diets. After two weeks on this dietary regimen, HBO treatment was given to half the rats in each dietary group for five days a weeks for a total of four weeks. ERG measurements were made in all groups after two and four weeks of HBO treatment. During phase I, rats in B+HBO group were being depleted of vitamin E and selenium and continuously treated with HBO. It is reasonable, therefore, to ask whether any observed retinal damage in the phase I B+HBO rats actually required long term HBO treatment. An alternative hypothesis is that a critical level of vitamin E and glutathione peroxidase exits below which retinal damage will be produced even with short short term HBO treatment. This alternative hypothesis was tested in phase II of the project by treating rats fed the B diet for 6 weeks with a short term (3 days) treatment with HBO and then recording the ERG amplitudes. In this experiment the rats would already be depleted of vitamin E and selenium at the time of HBO treatment. The detailed methodology for phase I and phase II of the project are detailed below.

Animals and Diets
Male, 30 g, inbred Fischer-344 (CDF) rats from Charles River Breeding Laboratory were housed in suspended stainless steel, wire-bottomed cages and maintained at 25±2 C and 50% relative humidity. Lighting was on a 6:00 AM to 6:00 PM light period and a 6:00 PM to 6:00 AM dark

period.   Upon arrival at Brooks AFB the rats were fed a normal Purina
laboratory chow (Rodent Laboratory Chow 5001, Ralston Purina Co., St.
Louis, MO) and water ad libitum for one week while under quarantine.
The rats were then randomly divided into the two dietary groups.   One
group (24 rats) was fed a basal diet deficient in both vitamin E and
selenium (the B diet) and the other group (24 rats) was fed an
identical diet but supplemented with both these micronutients (the
B+E+Se diet).   The basal diet, although deficient in vitamin E and Se,
has adequate levels of all other nutrients as proposed by the National
Research Council for the Laboratory Rat (14).   The B+E+Se diet was
supplemented with 50 mg vitamin E per kg of diet (1.1 IU per mg of
DL-alpha-tocopherol) and 0.4 ppm Se (added as sodium selenite).

All dietary supplies were purchased from U.S. Biochemical Co,
Cleveland, OH.   Diets were frequently prepared in small batches by
slowly mixing the constituents to avoid heating, and stored at 2 C.
Glass and stainless steel feeders (Hazelton Systems, Aberdeen, MD)
were filled every 2 days and any uneaten food discarded to minimize
rancidity.   Rats in all the dietary groups were provided with
deionized water to which 3 ppm chromium (as $CrCl3$) was added.   Both
diet and drinking water were provided ad libitum. The composition of
the B diet is given in Table 1.

Phase I-Hyperbaric Oxygen Treatment
After being fed the B or B+E+Se diets for two weeks, eight rats in
each dietary group were exposed to 3.0 ATA of 100 % oxygen for 1.5
hr/day, five days per week on a Monday to Friday schedule.   The
hyperbaric chamber was installed in the animal care room and oxygen
was directly vented to the outside.   Eight rats in each dietary group
were not treated with HBO.   These nonHBO rats served as controls to
monitor retinal damage that might be due to antioxidant deficiency
alone.   The electroretinograms in the set of 32 phase I rats was
measured every two weeks.   When the rats in the B+HBO group showed
diminished ERG a- and b-wave amplitudes they were euthanized under
halothane anesthetic and tissue samples collected for furture
structural and biochemical studies.   The remaining rats in the phase I
study were also euthanized for future studies.

Phase II-Short term HBO Expossure.
Eight rats in each dietary group were not exposed to either HBO
treatment nor did they have ERGs recorded in phase-I of the
experiment.   These phase II rats were used for a "short-term" HBO
treatment experiment.   When the B+HBO rats showed ERG deterioration
(about 4 weeks of HBO treatment) then the 8 phase-II rats in each
dietary group were treated with HBO for 3 days and ERGs recorded.   If
ERGs in the phase-II B+HBO rats decreased as a result of this
short-term HBO treatment, it would indicate that dietary deficiencies
of vitamin E and Se are more important than 4 weeks of chronic HBO
expossure.   From our previous pilot experiment, we know that rats fed
the B diet for 6 weeks, and not placed in the HBO chamber, do not
suffer ERG amplitude decreases.

Electroretinograms
The electroretinograms (ERGs) were recorded in biweekly intervals.
ERG measurements were made using an aluminized mylar plastic positive

electrode placed on the cornea. This electrode effectively eliminates the possibility of corneal damage. The ground electrode was attached to the ear lobe and a negative pin electrode inserted under the scalp. We used a ganzfeld (whole field) flash, a Grass photostimulator and a Tektronic model 6512 recording oscilloscope with a 5A22N differential amplifier and a 5B10N time base amplifier. Animals were placed in a dark room for at least 1 hr before measuring ERGs. About 10 min before recording an ERG, each rat was anesthetized (IM injection) with 0.1 ml of ketamine (50 mg/ml). At least six a- and b-wave amplitude measurements were made for each eye in each rat.

Vitamin E and Glutathione Peroxidase Activities.
Four rats from each group were evaluated for plasma vitamin E, plasma glutathione peroxidase (GSHPX), and red blood cell GSHPX on a biweekly basis. GSHPX is a selenoenzyme and its activity in plasma and red blood cells (RBCs) is a good measure of selenium status. Blood was obtained from each rat after cutting (under methoxyfluorane anesthetization) off a small section from the end of the tail. This process is relatively untraumatic and can easily be done on the same rat on a biweekly basis. Blood was separated into plasma and washed RBCs. The plasma vitamin E and GSHPX assays on plasma and RBCs were done at Meharry Medical College by the P.I.

Statistics
Student's t-test and analysis of variance (ANOVA) were used to establish statistically significant differences (i.e. a $P < 0.05$) in the a- and b-wave ERG amplitudes of rats in the various dietary groups.

IV RESULTS:
Phase I-Effects of antioxidant nutrients and long term hyperbaric oxygen treatment on electroretinograms.
Table 2 shows the a- and b-wave amplitudes recorded for the B and B+E+Se groups either treated or not treated with HBO for 2 or 4 weeks. After 2 weeks, we found the ERG amplitudes to be very similar in both the B and B+E+Se dietary groups and unaffectd by HBO treatment. Two-way analysis of variance with unequal subsamples confirmed that the mean a-waves (or b-waves) were indistinguishable in the four treatment groups at week 2.

After 4 weeks of HBO treatment there was a marked decrease in the a-wave ($p < 0.005$) and b-wave ($p < 0.05$) ERG amplitudes of rats in the B+HBO group compared to rats in the B+nonHBO group. Rats supplemented with both vitamin E and Se showed no decreases in a- or b-wave ERG amplitudes after 4 weeks of HBO treatment. Furthermore, the ERG amplitudes of the B+E+Se group (both HBO and nonHBO) were similar at both 2 and 4 weeks after the start of HBO treatment.

Phase II- The effects of short term HBO on rats deficient in both vitamin E and Se.
In phase II, we examined the effects of a 3-day treatment with HBO (3.0 ATA of 100% oxygen for 1.5 hr/day) on six rats previously fed the B diet for eight weeks but not treated with HBO. A control group of four B rats were not treated with HBO. The a-wave amplitudes for this B+HBO group was 130+12 microvolts, which was very similar to that

4.6

observed for the control nonHBO B rats and similar to that previously
observed for B+E+Se rats (HBO or nonHBO). These data indicate that
prolonged HBO treatment, as well as vitamin E and selenium deficiency
are required for a decrease in a-wave amplitudes.

The b-wave amplitudes in the phase II B+HBO and B+nonHBO were 262 ± 61
and 273 ± 59 microvolts, respectively. The fact that the b-wave
amlitudes were similar indicates that short term HBO treatment did not
cause any decrease in retinal function. The b-wave amplitudes for the
B rats was , however, somewhat lower after 8 weeks of B diet than
after 6 weeks. This could indicate that prolonged antioxidant
deficiency can cause retinal damage independent of HBO treatment.

Plasma vitamin E and selenium-glutathione peroxidase levels
Table 3 provides the plasma vitamin E levels and the plasma
Se-glutathione peroxidase activities for rats in all treatment groups
at both 2 and 4 weeks after start of HBO. Rats fed the vitamin E and
Se deficient diet had significantly lower ($p < 0.005$) plasma vitamin E
and plasma glutathione peroxidase than rats fed the diet supplemented
with these micronutrients. This was true at both 2 and 4 weeks.

It is important to note that the levels of vitamin E and the the
activity of glutathione peroxidase were not influenced by 4 weeks of
hyperbaric oxygen treatment. This result is somewhat surprising. We
anticipated that hyperbaric oxygen would increase vitamin E
utilization and therefore increase vitamin E depletion in rats fed the
B diet and treated with HBO.

Weight, weight gain and food consumption.
The weights, weight gains and food consumption of rats in all dietary
groups at both 2 and 4 weeks of HBO treatment are given in Table 4.
These data indicate that neither diet or HBO treatment has any
significant effects on the weights, weight gains or food consumption
of rats in the experimental protocol. From our previous pilot
experiment, we know that rats fed the B diet and treated with HBO will
have a decreased weight gain compared to nonHBO B rats soon after 4
weeks of HBO treatment.

V RECOMMENDATIONS:
Dietary deficiences of both vitamin E and selenium were found to
adversely effect the electrophysiological response of the retina to
light in rats treated with hyperbaric oxygen for 4 weeks. Decreased
a-wave and b-wave ERG amplitudes as a result of hyperbaric oxygen
treatment were apparent only in rats deficient in both vitamin E and
selenium. Hafeman and Hoekstra (10) have shown that dietary
deficiency of both vitamin E and selenium is much more effective in
promoting in vivo lipid peroxidation than dietary deficeincy of either
vitamin E or selenium alone.

    Rats are generally considered a species very resistant to oxidative
damage. Rats have enzymatic antioxidant mechanisms that can be
induced in response to oxidative stress (8,9,15). The degree to which
a organism can induce these enzymatic antioxidant mechanisms may be an
important parameter in determining an organism's susceptibility to
oxygen toxicity. For example, glutathione-S-transferase activity in

the rat lung increases in response to hyperoxia (15). A number of
glutathione-S-transferase isozymes have a "nonselenium glutathione
peroxidase" activity that may protect against damaging in vivo lipid
peroxidation reactions. These potential enzymatic responses to HBO
treatment in rats must be characterized before the relevancy of our
results to humans can be understood.

Our results suggest that nutritional supplementation of patients with
antioxidant nutrients could diminish the oxygen toxicity problems
associated with HBO therapy. Hyperbaric oxygen therapy has been been
experimentally used in the treatment of sickle cell crisis episodes.
We and other investigators have found that sickle cell disease
patients have a profound deficiency of vitamin E. We would therefore
recommend that the vitamin E status of sickle cell patients be
carefully considered before any treatment with hyperbaric oxygen.
Precautions in using HBO therapy would also be indicated in any
disease states in which antioxidant mechanisms could be impaired.

Four animals in the B, B+HBO, B+E+Se and the B+E+Se+HBO groups were
euthanized at week 6 and samples of lung, liver, and retina tissue
were stored at -70 C for biochemical analyses. Four rats were also
perfused with Karnofsky's fixative. Retinal tissues were embedded in
Epon for future analyses by fluorescent microscopy, phase contrast
microscopy, and electron microscopy. We recommended follow-on
biochemical studies of lung, liver and retinal tissues and detailed
light/electron microscopy studies of retinal tissues, be pursued.

REFERENCES:

1) Clark JM, and Fisher AB, Oxygen toxicity and extension of tolerence in oxygen therapy. In: Davis, JC, and Hunt, TK, eds Hyperbaric Oxygen Therapy. Bethesda: Undersea Medical Society, 1979, :61-77.

2) Small, A, New perspectives on hyperoxic pulmonary toxicity-a review. Undersea Biomed Res 1984; 11;1-24.

3) Kappus, K, Sies, H, Toxic drug effects associated with oxygen metabolism: redox cycling and lipid peroxidation. Experientia 1981; 37; 1233-1241.

4) Gable, WD, Townsend, FM (1962) Aerospace Med. 33, 1344.

5) Farnsworth, CC, Stone, WL, and Dratz, EA. (1978) Biochim. Biophys. Acta, 552, 281-293.

6) Stone, WL, Katz, ML, Lurie, M, Marmor, MF and Dratz, EA (1979) Photochem. Photobiol., 29, 725-730.

7) Nichols, C.W. and Lambertson, C.J. (1969) New Engl. J. Med., 281, 25-30.

8) Stone, W.L. and Dratz, E.A. (1982) Exp. Eye Res., 35, 405-412.

9) Stone, WL, and Dratz, EA. Increased glutathione s-transferase activity in antioxidant-deficient rats. Biochim Biophys Acta 1980; 631; 503-506.

10) Hafeman, DG and Hoekstra, WG. Lipid peroxidaton in vivo during vitamin E and selenium deficiency in the rat as monitored by ethane evolution. J Nutr 1977; 107; 666-672.

11) Katz, ML, Stone, WL, and Dratz, EA. Fluorescent pigment

accumulation in retinal pigment epithelium of
antioxidant-deficient rats. Invest Ophthalmol 1978; 17;
1049-1058.

12) Katz, M.L., Parker, K.R., Handelman, G.J., Bramel, T.L.

13) Armstrong, D, Hiramitsu, T, Gutterridge, J, and
    Nilsson, SE. Studies on experimentally induced retinal
    degeneration. 1. Effects of lipid peroxides on
    electroretinographic activity in the albino rabbit.
    Exp Eye Res 1982; 35; 157-171.
    Dratz, E.A. (1982) Exp. Eye Res., 34, 339-369.

14) National Research Council Publication on Nutrient
    Requirements of Labvoratory Animals, No. 10, p 56,
    Washington, DC, Nat Acad Sci, 1978.

15) Jenkinson, SG, Lawrence, RA, Burk, RF and Gregory, PE,
    Non-selenium-dependent glutathione peroxidase activity
    in rat lung assGciated with lung
    glutathione s-transferase acitivity and effects of
    hyperoxia. Toxicol and Applied Pharmacol; 1983; 68;
    399-404

Table 1.   Composition of basal diet.

        Ingredient   g/100g

    Tourla yeast   36.00

    Sucrose   43.05

    Corn oil, tocopherol stripped   14.50

    Vitamin mix   1   2.20

    Mineral mix   Draper 2   4.00

    L-Methionine   0.25

----

1. The vitamin mixture provided: (in mg/100 g of diet)
ascorbic acid, 99; inositol, 11; choline chloride, 16.5;
p-aminobenzoic acid, 11; niacin, 9.9; riboflavin, 2.2;
pyridoxine-HCl, 2.2; thiamin HCl, 2.2; calcium pantothenate,
6.6; biotin, 0.05; folic acid, 0.2; vitamin B-12, 0.003. In
addition the vitamin mixture contains: (in units /100 g of
diet) vitamin A acetate, 1980; calciferol(D3), 220.2.

2. The salt mix provided (in mg/100 g of diet): $CaCO_3$, 654;
$CuSO_4.5H_2O$, 0.72; $Ca_3(PO_4)_2$, 1422; Ferric citrate.$3H_2O$, 64;
$MnSO_4.H_2O$, 5.5; potassium citrate.H_2O, 946; KI, 0.16;
K_2HPO_4, 309; NaCl, 432; $ZnCO_3$, 1.8; and $MgCO_3$, 164.

Table 2

The effects of hyperbaric oxygen (HBO) on a- and b-wave electroretinogram (ERG) amplitudes for rats fed diets either deficient or supplemented with vitamin E and selenium. Each entry is mean±SEM and the number of animals is indicated in parentheses.

time weeks	treatment	diet	a-wave	b-wave microvolts
2	HBO(8)	B	148±20	332±61
	nonHBO(8)	B	139±14	320±31
2	HBO(8)	B+E+Se	148±10	359±23
2	nonHBO(7)	B+E+Se	140±14	320±31
4	HBO(8)	B	83±13*	255±30**
4	nonHBO(17)	B	151±12	369±29
4	HBO(6)	B+E+Se	139±17	360±38
4	nonHBO(18)	B+E+Se	135±9	326±22

* $p < 0.005$ ** $p < 0.05$ vs. nonHBO

4.12

Table 3

Antioxidant levels (mean±SEM) in rats fed diets supplemented (B+E+Se) or deficient (B) in vitamin E and selenium and with or without hyperbaric oxygen (HBO) treatment.

time	treatment	vitamin E ug/ml of plasma	glutathione peroxidase milli e.u./ul of plasma
2	B+HBO	1.6±0.1*	4.0±0.2*
2	B	2.0±0.1*	4.2±0.6*
2	B+E+Se+HBO	5.5±0.6	11.0±1.0
2	B+E+Se	6.1±0.4	8.9±1.2
4	B+HBO	0.8±0.1*	2.2±1.0*
4	B	0.8±0.1*	2.1±0.5*
4	B+E+Se+HBO	5.0±0.8	8.2±1.4
	B+E+Se	4.3±0.5	9.8±2.8

1. Rats were on the indicated diets for 2 weeks longer than the time indicated in the table. Four rats were used in each table entry. Milli e.u. for glutathione peroxidase activity is nanomoles of NADPH oxidized per min.

* indicates a $p < 0.005$ vs. the B+E+Se groups.

Table 4

Weight (g), weight gain/day (g/day) and food consumption (g/day) for rats fed diets either deficient (B diet) or supplemented (B+E+Se) with vitamin E and selenium. Rats in both dietary groups were either treated (HBO) or not treated with hyperbaric oxygen (nonHBO).

treatment group	time on diets (weeks)			
	0	2	4	6
B(20)+nonHBO				
weight	94.2±0.2	131.0±1.8	168.2±6.8	186.0±10.7
wt.gain/day	–	2.6	2.7	1.3
food/day	–	–	11.1	11.4
B+HBO(8)				
weight	92.1±2.0	126.8±3.3	161.0±4.2	183.0±6.3
wt.gain/day	–	2.5	2.5	1.6
food/day	–	–	10.8	10.2
B+E+Se+nonHBO(20)				
weight	93.3±1.9	128.9±3.0	176.1±3.2	200.0±3.2
wt.gain/day	–	2.5	3.4	1.7
food/day	–	–	10.9	12.3
B+E+Se+HBO(9)				
weight	94.0±3.0	127.5±3.2	161.0±4.2	178.0±4.9
wt.gain/day	–	2.4	2.4	1.2
food/day	–	–	11.2	10.4

The number of rats is given in parentheses. Each data entry is mean±SEM

1984-1985 USAF-SCEEE RESEARCH INITIATION GRANT

Sponsored by the

AIR FORCE OFFICE OF SCIENTIFIC RESEARCH

and the

SOUTHEASTERN CENTER FOR ELECTRICAL ENGINEERING EDUCATION

Final Report

THE INFLUENCE OF MELTING AND REACTANT CONSUMPTION ON
TEMPERATURE TRANSIENTS IN SPHERICAL AND CYLINDRICAL
CHARGES OF EAK

by

John W. Sheldon
Physics Department
Florida International University
Miami, Florida 33199

USAF Research - Thomas G. Floyd

Contract No: F49620-82-C-0035

Starting date Oct. 1, 1984

Completion date Aug. 31, 1985

Acknowledgement

THE INFLUENCE OF MELTING AND REACTANT
CONSUMPTION ON TEMPERATURE TRANSIENTS IN SPHERICAL
AND CYLINDRICAL OF EAK

by

John W. Sheldon

ABSTRACT

Basic programs for the Tektronix 4052 desktop computer utilizing the SSI (semi-symmetric implicit) scheme are used to compute explosive induction time for heat generating first order chemical reactions in slabs, cylinders and spheres of EAK with and without considering reactant consumption. In numerical tests the SSI results compare well with the results of exact calculations, calculations using the explicit scheme and with other work employing less flexible methods.

I. Introduction

EAK (45.68% ethylenediamine dinitrate, 46.17% ammonium nitrate and 8.15% potassium nitrate, by wt.) is in the process of being classified as an insensitive high explosive (IHE). As a part of justifying the IHE classification the response of EAK to elevated environmental temperature must be evaluated.[1] Materials such as EAK that undergo exothermic chemical decomposition reactions can exhibit self-heating phenomena. At steady state the heat lost by conduction and or convection is just balanced by the heat generated; however above a certain critical external temperature more heat will be generated than can be removed by these means and the temperature will rise to ignition or explosion. All self-heating calculations in which the heat loss is assumed to be by conduction have only considered a single phase material.[2-8] Since EAK melts at 103.6°C it clearly undergoes a phase change as its temperature rises from ambient to critical.

Preliminary calculations of the influence of the melting process on transient temperature distributions in finite and infinite slab configurations were carried out by the author during the 1984 USAF-SCEEE Summer Faculty Research Program at Eglin AFB. Since that work the application of a symmetric semi-implicit (SSI) finite differences scheme to thermal conduction problems has been reported.[9] Since finite difference schemes allow much more flexibility than the previously used method   . the SSI computational scheme has been adopted in the work reported here.

In section II the SSI scheme is described for heat conduction problems with a generalized temperature dependent heat generation term. The procedures including the melting process and reactant consumption in the calculations are presented in Section III. The numerical results of test

cases are given in section IV where they are compared with exact calculations
and previous work. The SSI basic programs are presented in section V for slab,
cylindrical and spherical symmetry. Heat generation is by first order chemical
reaction, melting of the solid explosive during self-heating is included and a
version of each program is provided which includes reactant consumption. The
results for an EAK sphere of one cm radius are given in Section VI.

II. The SSI scheme

The heat conduction equation with internal heat generation is given by

$$\rho C(\partial u/\partial t) = \lambda \nabla^2 u + H(u) \tag{1}$$

where u is the temperature, λ the thermal conductivity, ρ the density, C the
heat capacity and H(u) the rate of heat generation. Writing (1) in the SSI
scheme of Livne and Glasner [9] for the cell (i).

$$\rho C V_i (u_i^{j+1} - u_i^j)/\Delta t = - \sum_k J_{ik} A_{ik} + H(u_i^j) V_i + q_i \tag{2}$$

where J_{ik} is the heat flux from cell (i) to (k), A_{ik} is the area bounding
the (i) and (k) cells, V_i is the volume of cell (i), u_i^{j+1} is its temperature
at the end of the time step Δt and u_i^j its temperature at the beginning of
the time step. The term q_i is added [9] to approximate energy conservation
at the interface between cell (i) and its neighbors. For one independent
spacial variable in plane, cylindrical or spherical symmetry,

$$J_{i,k} = - \lambda (u_k^j - u_i^{j+1}) \Delta x \tag{3}$$

and

$$q_i = (\lambda/2\Delta x) [(u_{i+1}^j + u_i^j - u_{i+1}^{j-1} - u_i^{j-1}) A_{i,i+1} + (u_{i-1}^j + u_i^j - u_{i-1}^{j-1} - u_i^{j-1}) A_{i,i-1} \tag{4}$$

where u_k^{j-1} is the temperature of the cell (k) at the time step prior to
that indicated by u_k^j. Defining the geometric factors

$$G_{i\pm} = A_{i,i\pm1} \Delta x/V_i$$

and the Fourier number

$$F = \lambda \Delta t/\rho C \Delta x^2$$

5.5

some algebra yields,

$$u_i^{j+1} = \frac{F(u_{i+1}^j G_{i+} + u_{i-1}^j G_{i-}) + h_i + Q_i + u_i^j}{1 + F(G_{i+} + G_{i-})} \tag{5}$$

where the thermal properties are considered constant,

$$h_i = (\Delta t / \rho C) H(u_i^j)$$

and

$$Q_i = (F/2) [u_{i+1}^j + u_i^j - u_{i+1}^{j-1} - u_i^{j-1}) G_{i+} + (u_{i-1}^j + u_i^j - u_{i-1}^{j-1} - u_i^{j-1}) G_{i-}].$$

III. A. The Melting Calculation

In order to include the effects of melting in the SSI calculations of the temperature distributions in self-heating explosives the following scheme [10] is used. First the temperature drop that would occur if the latent heat of fusion were abstracted from a finite difference cell of explosive is calculated. This is the "temperature worth" of the heat of fusion. When, during the application of the SSI scheme described in section II, a finite difference cell temperature is first predicted to exceed the melting temperature, the cell temperature is set equal to the melting temperature and the difference between the first predicted temperature and the melting temperature recorded. During subsequent iterations this adjustment procedure is continued until the cumulative total of adjustments equals the temperature worth of the heat of fusion. At that point the cell temperature is allowed to increase in the manner predicted by the SSI scheme.

III. B. Reactant Consumption

Boddington and co-workers [11,12] have studied the influence of reactant consumption on criticality and induction times. When reactant consumption is ignored thermal runaway can occur and infinite temperatures are reached in a finite time and non explosive reaction is characterized by a low stationary state of self-heating. When reactant consumption occurs each temperature time history evolves to a maximum temperature and then decays back to ambient. For the present case

5.6

of first order chemical reactions when reactant when reactant consumption is
considered the reactant concentration C(t) decreases exponetially with time
according to the expression

$$C(t) = C_o \exp(-kt)$$

where C_o is the initial reactant concentration.

IV. Numerical Tests of the SSI Scheme

A. Constant heat addition

The SSI scheme was tested for the case of constant heat addition in a slab
of RDX with half-thickness 1 cm. The physical properties of RDX are taken from ref.
[8]. No melting or reactant consumption effects are included. The initial
temperature of the slab was 300°K and the wall temperature was fixed at 300°K.
The heat generation term was calculated from the date in ref.[8] for a constant
temperature of 500°K. The temporal and spacial temperature distributions cal-
culated by the SSI method are shown in Fig. 1 for Fourier Numbers of 1.56 and
3.90. The exact solution for this constant heat addition problem given by
Carslaw and Jaeger [13] is also shown in Fig. 1 for comparison.

B. Heat Generation by First Order Chemical Reaction

The SSI difference scheme was also tested for heat generation by first order
chemical reaction. For this case

$$H(u) = \rho Q \, Z \exp(-E/Ru)$$

where Q is the heat of reaction, Z is the Arrhenius pre-exponential frequency
constant, E is the activation energy and R the gas constant. No melting or
reactant consumption effects are included. Eq. (5) was used to calculate the
temperature profiles in 2.54 cm thick slabs and 2.54 cm diameter spheres of RDX
beginning with the RDX uniformly at 300°K and the wall temperature U_w. The
calculation advanced by time steps until a temperature reached 5000°K at which
point an explosion was considered to have been initiated and the induction time,

t_i recorded. The results are shown in Fig. 2 where they are compared with the numerical calculation of Zinn and Mader [8]. An explicit finite difference scheme was also used to compute t_i over the limited range for which it was practical. These results are also displayed on Fig. 2.

Experience with the SSI scheme has shown that the time step is limited in practice by the nature of the heat generation term. While the time step must, of course, be small compared to the induction time, steps up to 50 times greater than allowed for the explicit scheme can give sufficient accuracy. The SSI results compare well with the results of exact calculations, calculations using the explicit scheme and with other work employing less flexible methods.

600

500

TEMPERATURE , K

400

300

	t, s	Δt, s	F
○	50	0.2	1.56
●	50	0.5	3.90
□	25	0.2	1.56
■	25	0.5	3.90

0   0.4   0.8   1.2

DISTANCE FROM CENTERLINE , CM
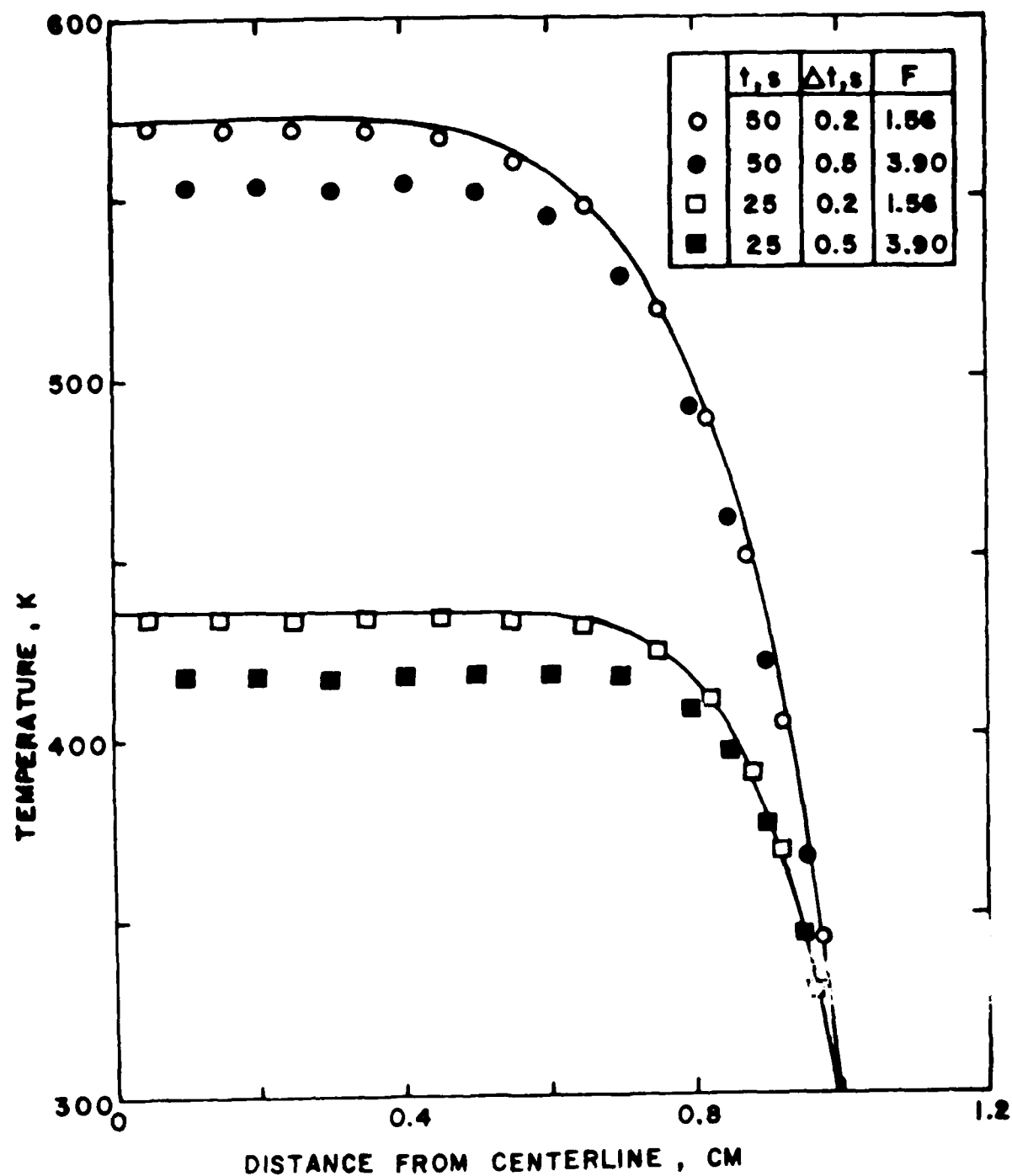
Figure IV. 1. Temperature profiles in a 1 cm half-thickness RDX slab with
constant heat generation. Curves are exact solutions, symbols
are present SSI scheme calculations.

5.9

Figure IV. 2. Induction time to explosion in 2.54 cm slabs and 2.54 cm diameter spheres of RDX. Curves are calculations of ref. 8, symbols are present calculations.

t_i , s

SLAB

SPHERE

$1000/u_w$, K^{-1}

Δt_i, s	F	SSI	EXPL.	SSI
		SLAB	SLAB	SPHERE
0.10	0.48	○	—	—
1.0	4.84	—	△	●
5.0	24.2	□	—	—

5.10
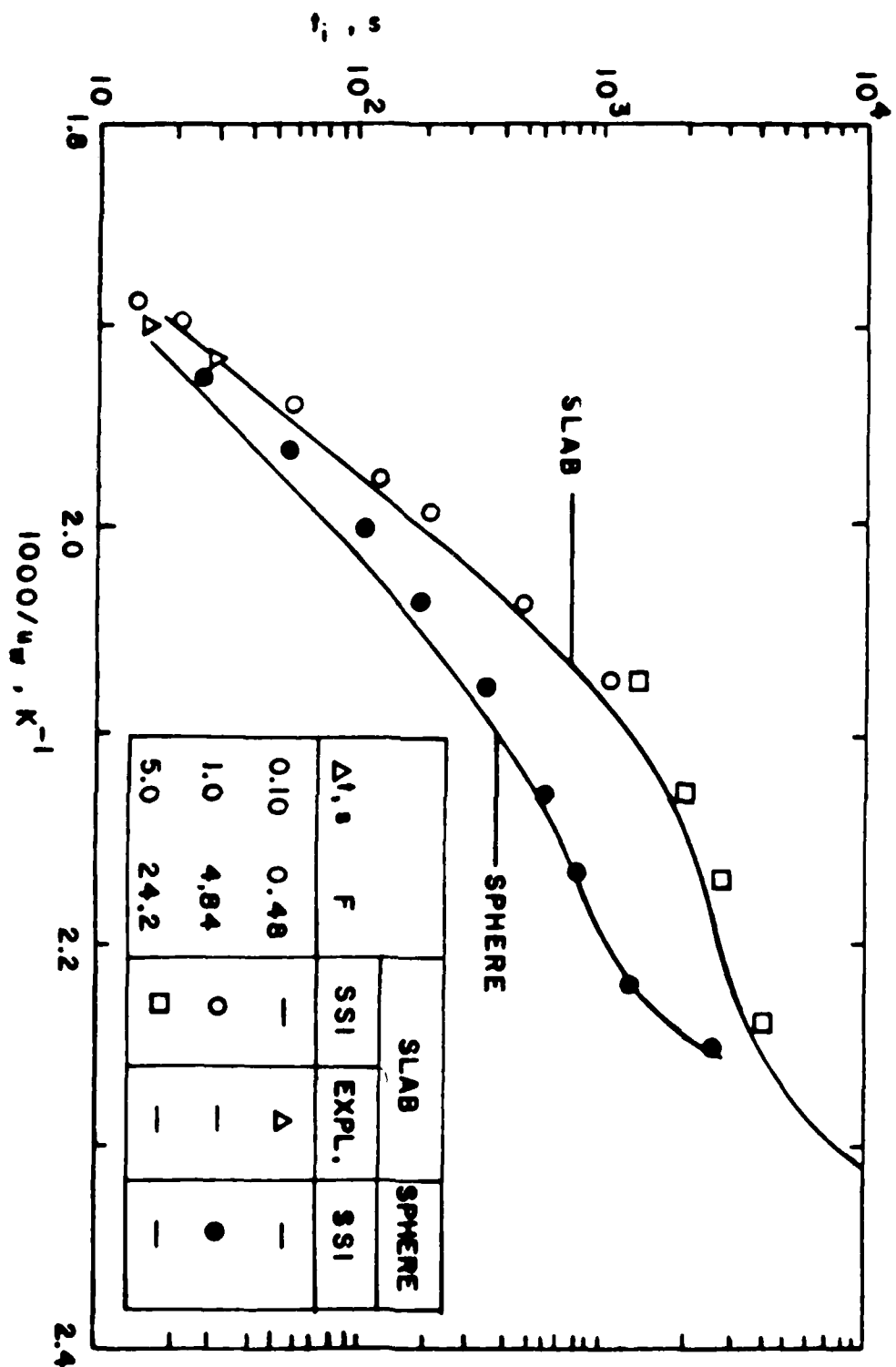
V. Program Listings

This section contains listings of six basic programs which run on the
Tektronix 4052 desktop computer. The physical properties of EAK as re-
ported in ref. 14 are used. Since the heat of fusion for EAK is not well
known, a value of 40 cal/gm is assumed. The listings are heavily remarked
so as to be self explanatory. Each program computes the induction time
to explosion as a function of wall temperature. An explosion is considered to
occur when a temperature in the calculated profile exceeds 5000°K. The
output prints the induction time, the wall temperature and the tempera-
ture profile one time step before explosion. Time steps of 0.1 s are
included below. Longer time steps can be used to shorten computation
time, but F, the Fourier number should not be much greater than 1.0 and
the time step should be small enough so that at least 50 steps are re-
quired.

```
100 REM FILE 1
110 REM******************* THERMAL INITIATION OF EXPLOSION ***********
120 REM****************** INFINITE SLAB SYMMETRY *****************
130 REM*********** SYMMETRIC SEMI-IMPLICIT SCHEME(SSI) ************
140 REM****************** EXPLOSIVE:EAK ******************
150 REM V1=INITIAL TEMP.,K.
160 V1=300
170 REM V2=MELTING TEMP.,K.
180 V2=376.6
190 REM V3=WALL TEMP.,K.
200 REM***  INITIAL WALL TEMP. SET  ***
210 V3=600
220 REM L=SLAB HALF-THICKNESS,CM.
230 L=1
240 REM A1=THERMAL DIFFUSIVITY,CM-CM/S.
250 A1=7.25E-4
260 REM H=HEAT OF FUSION,CAL/GM.
270 H=40
280 REM C=HEAT CAPACITY,CAL/GM-K.
290 C=0.46
300 REM E1=ACTIVATION ENERGY,CAL/MOL.
310 E1=47000
320 REM R=GAS CONSTANT,CAL/MOL-K.
330 R=1.987
340 REM Q=HEAT OF REACTION,CAL/GM.
350 Q=500
360 REM Z=PRE-EXP. RATE CONSTANT,1/S.
370 Z=2.89E+17
380 REM N=NO. SPACIAL STEPS
390 N=100
400 REM T1=TIME STEP,S.
410 T1=0.1
420 DIM U(N+1)
430 DIM U1(N+1)
440 DIM Q2(N+1)
450 DIM U4(N+1)
460 DIM U5(N+1)
470 FOR I=1 TO N+1
480    U(I)=0
490    U1(I)=0
500    Q2(I)=0
510    U4(I)=0
520 NEXT I
530 REM X1=SPACIAL STEP,CM.
540 X1=L/N
550 Q1=H/C
560 E=E1/R
570 A=T1*Q*Z/C


580 F=A1*T1/X1^2
590 FOR I=1 TO N+1
600    Q2(I)=Q1
610 NEXT I
620 T=0
630 FOR I=1 TO N
```

5.12

```
640      U(I)=V1
650 NEXT I
660 U(N+1)=V3
670 FOR I=1 TO N+1
680      U5(I)=U(I)
690 NEXT I
700 REM*********** FINITE DIFF. CALCULATION  *************************
710 FOR I=1 TO N
720      IF I=1 THEN 980
730      U1(I)=F*(U(I+1)+U(I-1))+U(I)
740      U1(I)=F*(U(I+1)+U(I-1)+2*U(I)-U5(I+1)-U5(I-1)-2*U5(I))/2+U1(I)
750      U1(I)=U1(I)/(1+2*F)
760      U1(I)=U1(I)+EXP(LOG(A)-E/U(I))/(1+2*F)
770      IF U1(I)>5000 THEN 1020
780      IF U(I)>V2 THEN 870
790      IF U1(I)<V2 THEN 870
800      U2=U1(I)-Q2(I)
810      IF U2<V2 THEN 850
820      U1(I)=U2
830      Q2(I)=0
840      GO TO 870
850      Q2(I)=Q2(I)-(U1(I)-V2)
860      U1(I)=V2
870      U4(I)=U1(I)
880 NEXT I
890 U4(1)=U1(1)
900 U4(N+1)=U(N+1)
910 FOR I=1 TO N+1
920      U5(I)=U(I)
930      U(I)=U4(I)
940 NEXT I
950 IF T=5000 THEN 1030
960 T=T+T1
970 GO TO 710
980 U1(I)=F*(U(I+1)+U(I))+U(I)
990 U1(I)=F*(U(I+1)+U(I)+2*U(I)-U5(I+1)-U5(I)-2*U5(I))/2+U1(I)
1000 GO TO 750
1010 REM******************** PRINT EXPLOSION DATA  ********************
1020 PRINT @41:V3,T
1030 FOR I=N+1 TO 1 STEP -1
1040      PRINT @41:U(I)
1050 NEXT I


1060 IF U(1)<310 THEN 1070
1070 IF T=5000 THEN 1110
1080 REM******************** SET NEW WALL TEMP.  ********************
1090 V3=V3-10
1100 GO TO 420
1110 END
```

```
100 REM TITLE 2
110 REM************* THERMAL INITIATION OF EXPLOSION **************
120 REM*********** CYLINDRICAL    SYMMETRY  ***************************R
130 REM*********** SYMMETRIC SEMI-IMPLICIT SCHEME(SSI) **************
140 REM************* EXPLOSIVE:EAK  **************
150 REM V1=INITIAL TEMP.,K
160 V1=300
170 REM V2=MELTING TEMP.,K
180 V2=376.6
190 REM V3=WALL TEMP.,K
200 REM***  INITIAL WALL TEMP. SET  *******
210 V3=600
220 REM L=RADIUS,CM.
230 L=1
240 REM A1=THERMAL DIFFUSIVITY,CM-CM/S.
250 A1=2.25E-4
260 REM H=HEAT OF FUSION,CAL/GM.
270 H=40
280 REM C=HEAT CAPACITY,CAL/GM-K.
290 C=0.46
300 REM E1=ACTIVATION ENERGY,CAL/MOL.
310 E1=47000
320 REM R=GAS CONSTANT,CAL/MOL -K.
330 R=1.987
340 REM Q=HEAT OF REACTION,CAL/GM.
350 Q=500
360 REM Z=PRE-EXP. RATE CONSTANT,1/S.
370 Z=2.89E+17
380 REM N=NO. SPACIAL STEPS.
390 N=100
400 REM T1=TIME STEP,S.
410 T1=0.1
420 DIM U(N+1)
430 DIM U1(N+1)
440 DIM Q2(N+1)
450 DIM U4(N+1)
460 DIM U5(N+1)
470 REM X1=SPACIAL STEP,CM.
480 X1=L/N
490 Q1=H/C
500 E=E1/R
510 A=T1*(Q*Z/C
520 F=A1*T1/X1^2
530 FOR I=1 TO N+1
540    Q2(I)=Q1
550 NEXT I
560 I=0
570 FOR I=1 TO N


580    U(I)=V1
590 NEXT I
600 U(N+1)=V3
610 U1(N+1)=V3
620 FOR I=1 TO N+1
```

```
650      US(I)=U(I)
660 NEXT I
650 REM********** FINITE DIFF. CALCULATION  ***********************
660 FOR I=1 TO N
670    IF I=1 THEN 960
680    G1=I/(I^2-(I-1)^2)
690    G2=(I-1)/(I^2-(I-1)^2)
700    U1(I)=2*F*(U(I+1)*G1+U(I-1)*G2)+U(I)
710    U1(I)=U1(I)+F*G1*(U(I+1)+U(I)-US(I+1)-US(I))
720    U1(I)=U1(I)+F*G2*(U(I-1)+U(I)-US(I-1)-US(I))
730    U1(I)=U1(I)/(1+2*F*(G1+G2))
740    U1(I)=U1(I)+EXP(LOG(A)-E/U(I))/(1+2*F*(G1+G2))
750    IF U1(I)>5000 THEN 1030
760    IF U(I)>V2 THEN 850
770    IF U1(I)<V2 THEN 850
780    U2=U1(I)-Q2(I)
790    IF U2<V2 THEN 830
800    U1(I)=U2
810    Q2(I)=0
820    GO TO 850
830    Q2(I)=Q2(I)-(U1(I)-V2)
840    U1(I)=V2
850    U4(I)=U1(I)
860 NEXT I
870 U4(1)=U1(1)
880 U4(N+1)=U(N+1)
890 FOR I=1 TO N+1
900    U5(I)=U(I)
910    U(I)=U4(I)
920 NEXT I
930 IF T=5000 THEN 1040
940 T=T+T1
950 GO TO 660
960 G1=I/(I^2-(I-1)^2)
970 G2=(I-1)/(I^2-(I-1)^2)
980 U1(I)=2*F*(U(I+1)*G1+U(I)*G2)+U(I)
990 U1(I)=U1(I)+F*G1*(U(I+1)+U(I)-US(I+1)-US(I))
1000 U1(I)=U1(I)+F*G2*(U(I)+U(I)-US(I)-US(I))
1010 GO TO 730
1020 REM**************** PRINT EXPLOSION DATA  ********************
1030 PRINT @41:V3,T
1040 FOR I=N+1 TO 1 STEP -1
1050    PRINT @41:U(I)



1060    IF U(I)<310 THEN 1080
1070 NEXT I
1080 IF T=5000 THEN 1120
1090 REM**************** SET NEW WALL TEMP. ********************
1100 V3=V3-10
1110 GO TO 420
1120 END
```

5.15

```
100 REM FILE 3
110 REM************** THERMAL INITIATION OF EXPLOSION **************
120 REM*****************SPHERICAL SYMMETRY *********************
130 REM*********** SYMMETRIC SEMI-IMPLICIT SCHEME(SSI) *************
140 REM*********** EXPLOSIVE:EAK ***************************
150 REM V1=INITIAL TEMP.,K
160 V1=300
170 REM V2=MELTING TEMP.,K
180 V2=376.6
190 REM V3=WALL TEMP.,K
200 REM*****  INITIAL WALL TEMP. SET  ******
210 V3=600
220 REM L=RADIUS,CM.
230 L=1
240 REM A1=THERMAL DIFFUSIVITY,CM-CM/S.
250 A1=7.25E-4
260 REM H=HEAT OF FUSION,CAL/GM.
270 H=40
280 REM C=HEAT CAPACITY,CAL/GM-K.
290 C=0.46
300 REM E1=ACTIVATION ENERGY,CAL/MOL.
310 E1=47000
320 REM R=GAS CONSTANT,CAL/MOL -K.
330 R=1.987
340 REM Q=HEAT OF REACTION,CAL/GM.
350 Q=500
360 REM Z=PRE-EXP. RATE CONSTANT,1/S.
370 Z=2.89E+17
380 REM N=NO. SPACIAL STEPS.
390 N=100
400 REM T1=TIME STEP,S.
410 T1=0.1
420 DIM U(N+1)
430 DIM U1(N+1)
440 DIM Q2(N+1)
450 DIM U4(N+1)
460 DIM U5(N+1)
470 REM X1=SPACIAL STEP,CM.
480 X1=L/N
490 Q1=H/C
500 E=E1/R
510 A=T1*Q*Z/C
520 F=A1*T1/X1^2
530 FOR I=1 TO N+1
540    Q2(I)=Q1
550 NEXT I
560 T=0
570 FOR I=1 TO N


580    U(I)=V1
590 NEXT I
600 U(N+1)=V3
610 U1(N+1)=V3
620 FOR I=1 TO N+1
```

```
630     U5(I)=U(I)
640 NEXT I
650 REM********  FINITE DIFF. CALCULATION  ***************************
660 FOR I=1 TO N
670     IF I=1 THEN 960
680     G1=I^2/(I^3-(I-1)^3)
690     G2=(I-1)^2/(I^3-(I-1)^3)
700     U1(I)=3*F*(U(I+1)*G1+U(I-1)*G2)+U(I)
710     U1(I)=U1(I)+1.5*F*G1*(U(I+1)+U(I)-U5(I+1)-U5(I))
720     U1(I)=U1(I)+1.5*F*G2*(U(I-1)+U(I)-U5(I-1)-U5(I))
730     U1(I)=U1(I)/(1+3*F*(G1+G2))
740     U1(I)=U1(I)+EXP(LOG(A)-E/U(I))/(1+3*F*(G1+G2))
750     IF U1(I)>5000 THEN 1030
760     IF U(I)>V2 THEN 850
770     IF U1(I)<V2 THEN 850
780     U2=U1(I)-Q2(I)
790     IF U2<V2 THEN 830
800     U1(I)=U2
810     Q2(I)=0
820     GO TO 850
830     Q2(I)=Q2(I)-(U1(I)-V2)
840     U1(I)=V2
850     U4(I)=U1(I)
860 NEXT I
870 U4(1)=U1(1)
880 U4(N+1)=U(N+1)
890 FOR I=1 TO N+1
900     U5(I)=U(I)
910     U(I)=U4(I)
920 NEXT I
930 IF T=5000 THEN 1040
940 T=T+T1
950 GO TO 660
960 G1=I^2/(I^3-(I-1)^3)
970 G2=(I-1)^2/(I^3-(I-1)^3)
980 U1(I)=3*F*(U(I+1)*G1+U(I)*G2)+U(I)
990 U1(I)=U1(I)+1.5*F*G1*(U(I+1)+U(I)-U5(I+1)-U5(I))
1000 U1(I)=U1(I)+1.5*F*G2*(U(I)+U(I)-U5(I)-U5(I))
1010 GO TO 730
1020 REM****************  PRINT EXPLOSION DATA  *******************
1030 PRINT #41:V3,T
1040 FOR I=N+1 TO 1 STEP -1
1050     PRINT #41:I,U(I)


1060     IF U(1)<310 THEN 1080
1070 NEXT I
1080 IF T=5000 THEN 1120
1090 REM****************  SET NEW WALL TEMP. *********************
1100 V3=V3-10
1110 GO TO 420
1120 END
```

5.17

```
100 REM FILE 4
110 REM****************** THERMAL INITIATION OF EXPLOSION ************
120 REM*********** WITH REACTANT CONSUMPTION  *******************
130 REM******************** INFINITE SLAB SYMMETRY ****************
140 REM*********** SYMMETRIC SEMI-IMPLICIT SCHEME(SSI)  ***********
150 REM********** EXPLOSIVE:EAK  *******************************
160 REM V1=INITIAL TEMP.,K.
170 V1=300
180 REM V2=MELTING TEMP.,K.
190 V2=376.6
200 REM V3=WALL TEMP.,K.
210 REM******* INITIAL WALL TEMP. SET  **********
220 V3=600
230 REM L=SLAB HALF-THICKNESS,CM.
240 L=1
250 REM A1=THERMAL DIFFUSIVITY,CM-CM/S.
260 A1=7.25E-4
270 REM H=HEAT OF FUSION,CAL/GM.
280 H=40
290 REM C=HEAT CAPACITY,CAL/GM-K.
300 C=0.46
310 REM E1=ACTIVATION ENERGY,CAL/MOL.
320 E1=47000
330 REM R=GAS CONSTANT,CAL/MOL-K.
340 R=1.987
350 REM Q=HEAT OF REACTION,CAL/GM.
360 Q=500
370 REM Z=PRE-EXP. RATE CONSTANT,1/S.
380 Z=2.89E+17
390 REM N=NO. SPACIAL STEPS
400 N=100
410 REM T1=TIME STEP,S.
420 T1=0.1
430 C1=1
440 DIM U(N+1)
450 DIM U1(N+1)
460 DIM Q2(N+1)
470 DIM U4(N+1)
480 DIM U5(N+1)
490 FOR I=1 TO N+1
500    U(I)=0
510    U1(I)=0
520    Q2(I)=0
530    U4(I)=0
540 NEXT I
550 REM X1=SPACIAL STEP,CM.
560 X1=L/N
570 Q1=H/C



580 E=E1/R
590 A=T1*Q*Z/C
600 F=A1*T1/X1^2
610 FOR I=1 TO N+1
620    Q2(I)=Q1
```

```
630 NEXT I
640 T=0
650 FOR I=1 TO N
660    U(I)=V1
670 NEXT I
680 U(N+1)=V3
690 FOR I=1 TO N+1
700    US(I)=U(I)
710 NEXT I
720 REM*********** FINITE DIFF. CALCULATION  ***********************
730 FOR I=1 TO N
740    IF I=1 THEN 1030
750    U1(I)=F*(U(I+1)+U(I-1))+U(I)
760    U1(I)=F*(U(I+1)+U(I-1)+2*U(I)-US(I+1)-US(I-1)-2*US(I))/2+U1(I)
770    U1(I)=U1(I)/(1+2*F)
780    K8=EXP(LOG(Z)-E/U(I))
790    K9=-T1*K8+LOG(A)-E/U(I)
800    IF K9<-15 THEN 820
810    U1(I)=U1(I)+C1*EXP(K9)/(1+2*F)
820    IF U1(I)>5000 THEN 1070
830    IF U(I)>V2 THEN 920
840    IF U1(I)<V2 THEN 920
850    U2=U1(I)-Q2(I)
860    IF U2<V2 THEN 900
870    U1(I)=U2
880    Q2(I)=0
890    GO TO 920
900    Q2(I)=Q2(I)-(U1(I)-V2)
910    U1(I)=V2
920    U4(I)=U1(I)
930 NEXT I
940 U4(1)=U1(1)
950 U4(N+1)=U(N+1)
960 FOR I=1 TO N+1
970    US(I)=U(I)
980    U(I)=U4(I)
990 NEXT I
1000 T=T+T1
1010 IF T=5000 THEN 1080
1020 GO TO 730
1030 U1(I)=F*(U(I+1)+U(I))+U(I)
1040 U1(I)=F*(U(I+1)+U(I)+2*U(I)-US(I+1)-US(I)-2*US(I))/2+U1(I)
1050 GO TO 770



1060 REM******************* PRINT EXPLOSION DATA  ********************
1070 PRINT @41:V3,T
1080 FOR I=N+1 TO J STEP -1
1090    PRINT @41:U(I)
1100    IF U(I)<310 THEN 1120
1110 NEXT I
1120 IF T=5000 THEN 1160
1130 REM****************** SET NEW WALL TEMP.  ********************
1140 V3=V3-10
1150 GO TO 440
1160 END
```

```
100 REM FILE 5
110 REM************* THERMAL INITIATION OF EXPLOSION ******************
120 REM************* WITH REACTANT CONSUMPTION ********************
130 REM********** CYLINDRICAL  SYMMETRY ******************************R
140 REM*********** SYMMETRIC SEMI-IMPLICIT SCHEME(SSI) **************
150 REM******** EXPLOSIVE:EAK ****************************
160 REM V1=INITIAL TEMP.,K
170 V1=300
180 REM V2=MELTING TEMP.,K
190 V2=376.6
200 REM V3=WALL TEMP.,K
210 V3=600  !  INITIAL WALL TEMP. SET
220 REM L=RADIUS,CM.
230 L=1
240 REM A1=THERMAL DIFFUSIVITY,CM-CM/S.
250 A1=7.25E-4
260 REM H=HEAT OF FUSION,CAL/GM.
270 H=40
280 REM C=HEAT CAPACITY,CAL/GM-K.
290 C=0.46
300 REM E1=ACTIVATION ENERGY,CAL/MOL.
310 E1=47000
320 REM R=GAS CONSTANT,CAL/MOL -K.
330 R=1.987
340 REM Q=HEAT OF REACTION,CAL/GM.
350 Q=500
360 REM Z=PRE-EXP. RATE CONSTANT,1/S.
370 Z=2.89E+17
380 REM N=NO. SPACIAL STEPS.
390 N=100
400 REM T1=TIME STEP,S.
410 T1=0.1
420 C1=1
430 DIM U(N+1)
440 DIM U1(N+1)
450 DIM U2(N+1)
460 DIM U4(N+1)
470 DIM U5(N+1)
480 REM X1=SPACIAL STEP,CM.
490 X1=L/N
500 Q1=H/C
510 E=E1/R
520 A=T1*Q*Z/C
530 F=A1*T1/X1^2
540 FOR I=1 TO N+1
550    Q2(I)=Q1
560 NEXT I
570 T=0


580 FOR I=1 TO N
590    U(I)=V1
600 NEXT I
610 U(N+1)=V3
620 U1(N+1)=V3
```

```
630 FOR I=1 TO N+1
640     U5(I)=U(I)
650 NEXT I
660 REM********* FINITE DIFF. CALCULATION *********************
670 FOR I=1 TO N
680     IF I=1 THEN 1000
690     G1=I/(I^2-(I-1)^2)
700     G2=(I-1)/(I^2-(I-1)^2)
710     U1(I)=2*F*(U(I+1)*G1+U(I-1)*G2)+U(I)
720     U1(I)=U1(I)+F*G1*(U(I+1)+U(I)-U5(I+1)-U5(I))
730     U1(I)=U1(I)+F*G2*(U(I-1)+U(I)-U5(I-1)-U5(I))
740     U1(I)=U1(I)/(1+2*F*(G1+G2))
750     K8=EXP(LOG(Z)-E/U(I))
760     K9=-T1*K8+LOG(A)-E/U(I)
770     IF K9<-15 THEN 790
780     U1(I)=U1(I)+C1*EXP(K9)/(1+2*F*(G1+G2))
790     IF U1(I)>5000 THEN 1070
800     IF U(I)>V2 THEN 890
810     IF U1(I)<V2 THEN 890
820     U2=U1(I)-Q2(I)
830     IF U2<V2 THEN 870
840     U1(I)=U2
850     Q2(I)=0
860     GO TO 890
870     Q2(I)=Q2(I)-(U1(I)-V2)
880     U1(I)=V2
890     U4(I)=U1(I)
900 NEXT I
910 U4(1)=U1(1)
920 U4(N+1)=U(N+1)
930 FOR I=1 TO N+1
940     U5(I)=U(I)
950     U(I)=U4(I)
960 NEXT I
970 T=T+T1
980 IF T=5000 THEN 1060
990 GO TO 670
1000 G1=I/(I^2-(I-1)^2)
1010 G2=(I-1)/(I^2-(I-1)^2)
1020 U1(I)=2*F*(U(I+1)*G1+U(I)*G2)+U(I)
1030 U1(I)=U1(I)+F*G1*(U(I+1)+U(I)-U5(I+1)-U5(I))
1040 U1(I)=U1(I)+F*G2*(U(I)+U(I)-U5(I)-U5(I))
1050 GO TO 740



1060 REM**************** PRINT EXPLOSION DATA ********************
1070 PRINT @41:V3,T
1080 FOR I=N+1 TO 1 STEP -1
1090     PRINT @41:U(I)
1100     IF U(I)<310 THEN 1120
1110 NEXT I
1120 IF T=5000 THEN 1160
1130 REM**************** SET NEW WALL TEMP. *********************
1140 V3=V3-10
1150 GO TO 430
1160 END
```

5.21

```
100 REM FILE 6
110 REM*************** THERMAL INITIATION OF EXPLOSION ****************
120 REM****************** WITH REACANT CONSUMPTION ****************
130 REM*****************SPHERICAL SYMMETRY ****************************
140 REM*********** SYMMETRIC SEMI-IMPLICIT SCHEME(SSI) ***************
150 REM************* EXPLOSIVE:EAK ****************************
160 REM V1=INITIAL TEMP.,K
170 V1=300
180 REM V2=MELTING TEMP.,K
190 V2=376.6
200 REM V3=WALL TEMP.,K
210 V3=600
220 REM L=RADIUS,CM.
230 L=1
240 REM A1=THERMAL DIFFUSIVITY,CM-CM/S.
250 A1=7.25E-4
260 REM H=HEAT OF FUSION,CAL/GM.
270 H=40
280 REM C=HEAT CAPACITY,CAL/GM-K.
290 C=0.46
300 REM E1=ACTIVATION ENERGY,CAL/MOL.
310 E1=47000
320 REM R=GAS CONSTANT,CAL/MOL -K.
330 R=1.987
340 REM Q=HEAT OF REACTION,CAL/GM.
350 Q=500
360 REM Z=PRE-EXP. RATE CONSTANT,1/S.
370 Z=2.89E+17
380 REM N=NO. SPACIAL STEPS.
390 N=100
400 REM T1=TIME STEP,S.
410 T1=0.1
420 C1=1
430 DIM U(N+1)
440 DIM U1(N+1)
450 DIM Q2(N+1)
460 DIM U4(N+1)
470 DIM U5(N+1)
480 REM X1=SPACIAL STEP,CM.
490 X1=L/N
500 Q1=H/C
510 E=E1/R
520 A=T1*Q*Z/C
530 F=A1*T1/X1^2
540 FOR I=1 TO N+1
550    Q2(I)=Q1
560 NEXT I
570 T=0


580 FOR I=1 TO N
590    U(I)=V1
600 NEXT I
610 U(N+1)=V3
620 U1(N+1)=V3
```

5.22

```
630 FOR I=1 TO N+1
640     U5(I)=U(I)
650 NEXT I
660 REM********* FINITE DIFF. CALCULATION **********************************
670 FOR I=1 TO N
680     IF I=1 THEN 1000
690     G1=I^2/(I^3-(I-1)^3)
700     G2=(I-1)^2/(I^3-(I-1)^3)
710     U1(I)=3*F*(U(I+1)*G1+U(I-1)*G2)+U(I)
720     U1(I)=U1(I)+1.5*F*G1*(U(I+1)+U(I)-U5(I+1)-U5(I))
730     U1(I)=U1(I)+1.5*F*G2*(U(I-1)+U(I)-U5(I-1)-U5(I))
740     U1(I)=U1(I)/(1+3*F*(G1+G2))
750     K8=EXP(LOG(Z)-E/U(I))
760     K9=-T1*K8+LOG(A)-E/U(I)
770     IF K9<-15 THEN 790
780     U1(I)=U1(I)+C1*EXP(K9)/(1+3*F*(G1+G2))
790     IF U1(I)>5000 THEN 1070
800     IF U(I)>V2 THEN 890
810     IF U1(I)<V2 THEN 890
820     U2=U1(I)-Q2(I)
830     IF U2<V2 THEN 870
840     U1(I)=U2
850     Q2(I)=0
860     GO TO 890
870     Q2(I)=Q2(I)-(U1(I)-V2)
880     U1(I)=V2
890     U4(I)=U1(I)
900 NEXT I
910 U4(1)=U1(1)
920 U4(N+1)=U(N+1)
930 FOR I=1 TO N+1
940     U5(I)=U(I)
950     U(I)=U4(I)
960 NEXT I
970 IF T=5000 THEN 1080
980 T=T+T1
990 GO TO 670
1000 G1=I^2/(I^3-(I-1)^3)
1010 G2=(I-1)^2/(I^3-(I-1)^3)
1020 U1(I)=3*F*(U(I+1)*G1+U(I)*G2)+U(I)
1030 U1(I)=U1(I)+1.5*F*G1*(U(I+1)+U(I)-U5(I+1)-U5(I))
1040 U1(I)=U1(I)+1.5*F*G2*(U(I)+U(I)-U5(I)-U5(I))
1050 GO TO 740



1060 REM**************** PRINT EXPLOSION DATA **********************
1070 PRINT @41:V3,T
1080 FOR I=N+1 TO 1 STEP -1
1090     PRINT @41:U(I)
1100     IF U(I)<310 THEN 1120
1110 NEXT I
1120 IF T=5000 THEN 1160
1130 REM**************** SET NEW WALL TEMP. **********************
1140 V3=V3-10
1150 GO TO 430
1160 END
```

VI. EAK Results

Typical results of induction time calculations obtained using the programs of the previous section are presented here. The effect of time step size on calculated induction times to explosion is shown in Figure VI-1. The accuracy of the calculation increases with decreasing step size and the choice of step size is a compromise between computing time and desired accuracy.

The induction times to explosion for EAK spheres of 1 cm radius are presented in Figure VI-2. The curve is smoothed through the indicated points which were calculated at 10°K steps in wall temperature. A time step size of 0.2 s was used. The critical temperature for this configuration of EAK is 464°K.

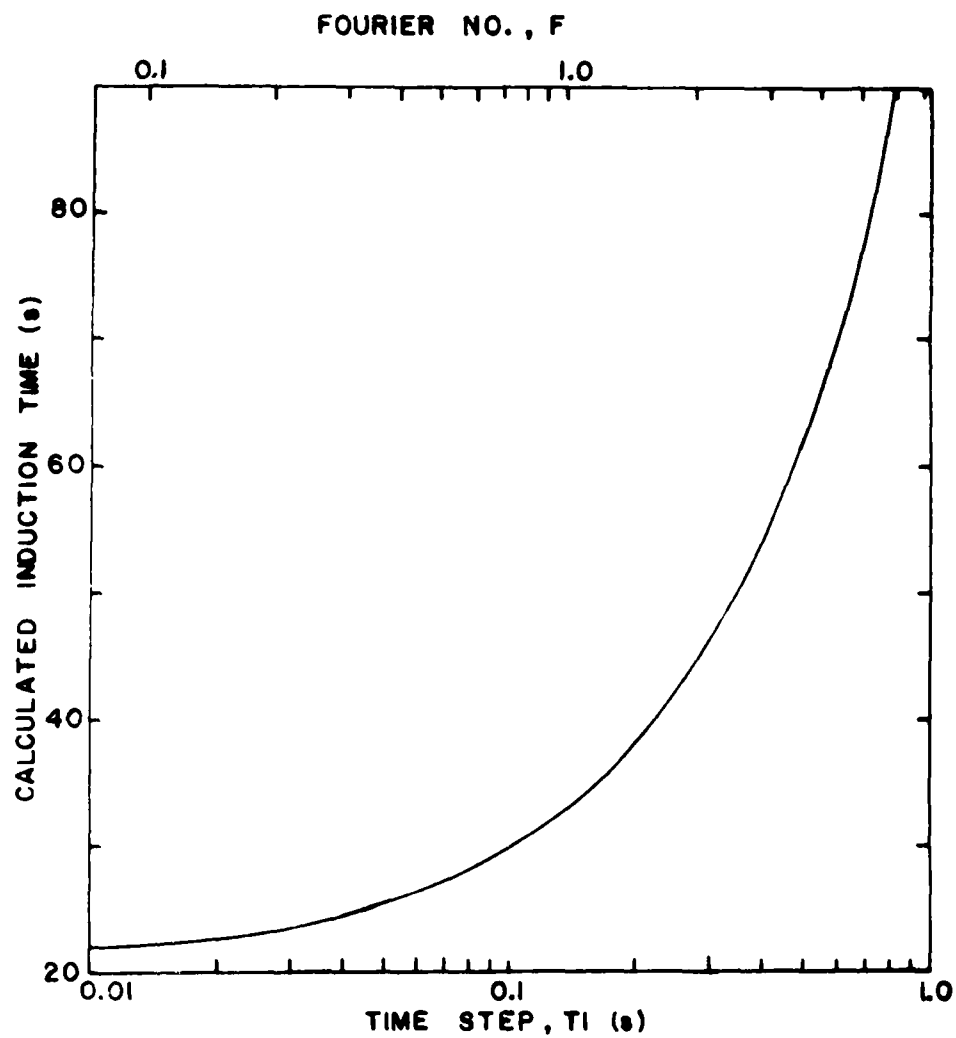Figure VI-1.   The effect of time step size on calculated induction
            time for EAK spheres of 1 cm radius and wall tempera-
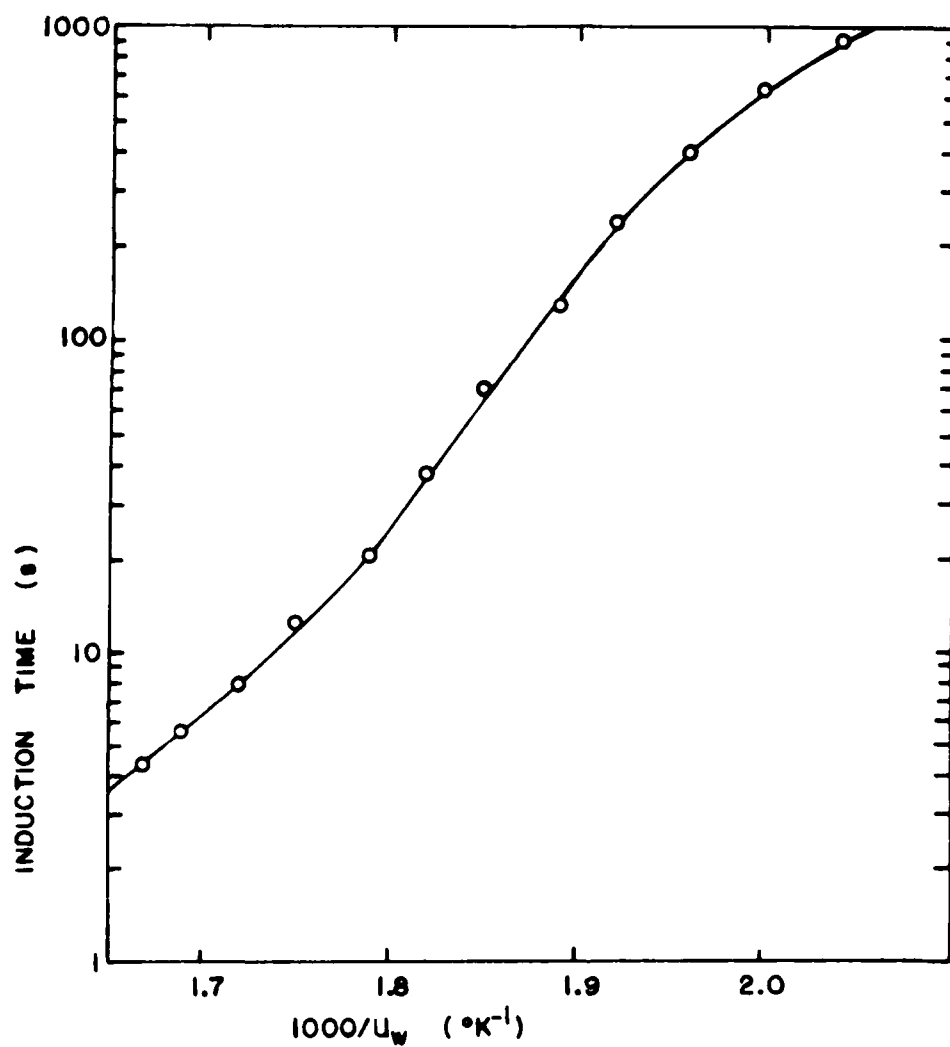   ture of 550°K.

Figure VI-2.   Induction time for an EAK sphere of 1 cm radius.   Cal-
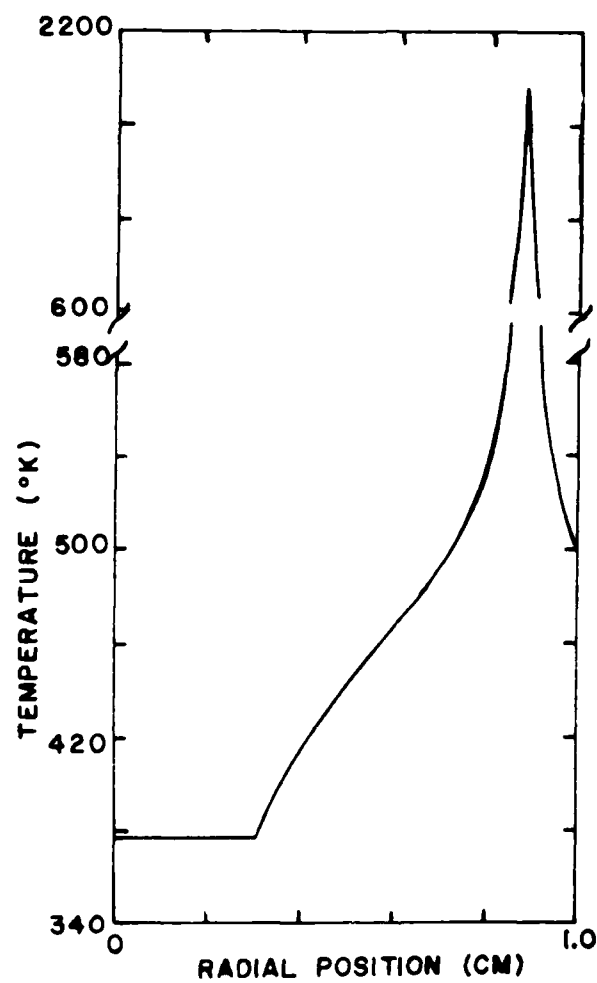   culations use a time step of 0.2 s.

5.26

Figure VI-3. Temperature profile in an EAK sphere of 1 cm radius

0.2 s prior to explosion. The wall temperature is

500°K.

5.27

The temperature profile in the 1 cm EAK sphere 0.2 s prior to explosion is shown in Figure VI-3 for a wall temperature of 500°K. The spacial step size is 0.01 cm. Note that in this example the explosive has completely melted prior to explosion.

VII. Conclusions

Basic programs for the Tektronix 4052 desktop computer utillizing the SSI (semi-symmetric implicit) scheme can be used to compute explosive induction time for heat generating first order chemical reactions in slabs, cylinders and spheres of EAK with and without considering reactant consumption. In numerical tests the SSI results compare well with the results of exact calculations, calculations using the explicit scheme and with other work employing less flexible methods. Experience with the EAK programs presented here indicates the time step should be chosen such that the Fourier number is not much greater than 1.0.

VIII. References

1. Safety and Performance Tests for Qualifications of Explosives, NAVORD OD 44811 Vol. 1, Jan 1972.

2. D.A. Frank-Kamenetzky, Acta Phyisicochimica U.R.S.S. 10, 365 (1939).

3. P.L. Chambre, J. Chem. Phys. 20, 1795 (1952).

4. A.R. Shouman, A.B. Donaldson and H.Y. Tsao, Combustion and Flame 23, 17, (1974).

5. A.R. Shouman and A.B. Donaldson, Combustion and Flame 29, 213 (1977).

6. W. Kordylewski, Combustion and Flame 34, 109 (1979).

7. T. Boddington, C. Feng and P. Gray, J. Chem. Soc. Faraday II, 79, 14-9 1983.

8. J. Zinn and C.L. Mader, J. Appl. Phys. 31, 323 (1960).

9. E. Livne and A. Glasner, J. Comp. Phys. 58 (1985), 59.

10. D.R. Croft and D.G. Lilley, Heat Transfer Calculations Using Finite Difference Equations, Applied Science Publishers Ltd, London (1977).

11. T. Boddington, P. Gray, W. Kordylewski and S.K. Scott, Proc. R. Soc. Lond. A390, 13 (1983).

12. T. Boddington, C.G. Feng and P. Gray, Proc. R. Soc. Lond. A391, 269 (1984).

13. H.S. Carslaw and J.C. Jaeger, Conduction of Heat in Solids, Claredon Press, (1959).

14. I. Akst, T.A. Crone, B.M. Dobratz, J.L. Janney, R.N. Rogers, J.A. Sanchez and A.P. Torres, EA Investigation FY 1982 Annual Report to the Air Force, Los Alamos progress report LA-9823-PR (1983).

USAF-SCEEE SUMMER FACULTY RESEARCH INITIATION PROGRAM

Sponsored by the

، IR FORCE OFFICE OF SCIENTIFIC RESEARCH

Conducted by the

SOUTHEASTERN CENTER FOR ELECTRICAL ENGINEERING EDUCATION

FINAL REPORT

GEOSTROPHIC ADJUSTMENT IN A THREE-DIMENSIONAL
MESOSCALE NUMERICAL MODEL OF THE ATMOSPHERE

Prepared by: Dr. Keith L. Seitter

Academic Rank: Assistant Professor

Department and
    University: Department of Earth Sciences
                    University of Lowell

Research Location: Air Force Geophysics Laboratory
                    Meteorology Division
                    Atmospheric Prediction Branch

Date: 1 October 1985

Contract Number: 84 RIP 06
                    under F49620-82-C-0035

ABSTRACT

This study investigates the geostrophic adjustment
process in meso-beta scale numerical models of the
atmosphere. A one-dimensional shallow water model is used
as well as a three-dimensional atmospheric model.
These models were coded with several different lateral
boundary condition formulations. Simulations were made with
these models using initial conditions whose mass and wind
fields were out of geostrophic balance in some way. It is
shown that for localized imbalances, whose scales are much
smaller than the Rossby radius of deformation, the
adjustment occurs rapidly, provided the model's lateral
boundary conditions allow removal of the waves generated
during the adjustment. In the simulations carried out in
this study, only a radiation-type lateral boundary condition
allowed the adjustment to progress naturally. Imbalances
in the large scale gradients imposed in the model
initialization adjust much more slowly than the local
imbalances, requiring more time than a typical meso-beta
forecast. These results suggest that the choice of lateral
boundary conditions are very important in meso-beta models
and that great care should be taken in the initialization
to remove as much of the large scale imbalance as possible.

I. Introduction

Numerical modeling of mesoscale processes in the
atmosphere has progressed rapidly in recent years with the
advent of faster, more powerful computers. A continuing
problem with these models, however, is in obtaining the
necessary mesoscale observations to use as input to the
model. In the absence of this data, most models use
smoothed fields obtained from interpolations of synoptic
observations or horizontally homogeneous fields derived from
a single sounding (Nickerson, 1979). In general, the wind
and mass fields initialized in this way will not satisfy
geostrophic (or gradient) balance and will undergo an
adjustment (known as geostrophic adjustment) during the
early stages of model integration. Useful predictive
information is available only after the adjustment is
complete, so an understanding of this process in the model
is important for its operational use.

This study is specifically concerned with modeling on
the meso-beta scale. On this scale, the model domain is
much smaller than a synoptic forecast model domain, but the
time and space scales are large enough to require inclusion
of the Coriolis effect. This leads to the possibility of
interior errors being caused by the geostrophic adjustment
of errors in the boundary values.

A complete discussion of geostrophically adjusted
boundary errors was presented by Anthes and Warner (1978).
We can think of the mean values of velocity and temperature

over the domain in terms of wavenumber zero flow. The
mean velocities in the domain are related geostrophically
only to gradients of the mass variables across the domain.
An error in one of the mass variables on the boundary will
imply a change in the large scale gradient and lead to
a change in the mean geostrophic velocity in the domain.
The mean geostrophic velocity error is proportional to the
boundary value error divided by the domain width. Thus,
the meso-beta scale model should be much more suseptable
to this type of error than a meso-alpha or synoptic
scale model.

Geostrophic adjustment in a limited area model is
intrinsically tied to the lateral boundary conditions used
in the model. The adjustment is accomplished by the
generation of atmospheric waves which propagate away from
the imbalance region to leave a balanced state behind. If
the model's boundary conditions do not allow these waves to
exit the domain, or do not absorb them in some manner, a
balanced state cannot be reached. This report will present
the results of geostrophic adjustment experiments in both a
one-dimensional shallow water model and a three-dimensional
hydrostatic atmospheric model. These models have been
formulated with a variety of lateral boundary conditions,
and it will be shown that the ability of the model to adjust
to an initial imbalance is determined almost completely by
the type of boundary condition used.

II. Objectives

The primary objective of this study is the investigation of factors which promote or inhibit natural geostrophic adjustment in a three-dimensional meso-beta model. A complete investigation would require many comparative simulations using a full three-dimensional model. In the early stages of this study, it became apparent that this approach would be prohibitively expensive. At that time, the research objectives were modified to introduce the development and use of a computationally efficient and inexpensive one-dimensional model. The following objectives were then set forth:

(1) Develop a one-dimensional shallow water model of the same scale as the three-dimensional model and which used the same numerical techniques.

(2) Code and debug the one-dimensional model with a variety of lateral boundary conditions.

(3) Run simulations with the one-dimensional model to investigate geostrophic adjustment on the meso-beta scale.

(4) Using guidance gained from the one-dimensional simulations, code a few of the lateral boundary conditions into the three-dimensional model and run geostrophic adjustment experiments.

(5) Investigate the lack of geostrophic adjustment reported by Brown and Ridge (1984) in their simulations using the three-dimensional model.

(6) Draw conclusions about the ability of the model to adjust to different types of imbalances and the time required for the adjustment.

III. The Models

a. The One-dimensional Model

The one-dimensional equations governing the velocities u and v and the depth η (see fig. 1) using the shallow water approximation on an f-plane can be written

$$\frac{\partial}{\partial t}(\eta u) + \frac{\partial}{\partial x}(u\eta u) - f(\eta v) = -\frac{1}{2}g\frac{\partial \eta^2}{\partial x} + \nu\frac{\partial^2}{\partial x^2}(\eta u) , \qquad (1)$$

$$\frac{\partial}{\partial t}(\eta v) + \frac{\partial}{\partial x}(u\eta v) + f(\eta u) = \nu\frac{\partial^2}{\partial x^2}(\eta v) , \qquad (2)$$

$$\frac{\partial \eta}{\partial t} + \frac{\partial}{\partial x}(\eta u) = 0 , \qquad (3)$$

where g is the acceleration of gravity, f is the Coriolis parameter, and ν is an eddy viscosity. The height-weighted velocities, ηu and ηv, are analogous to the pressure-weighted velocities used as prognostic variables in many meso-scale hydrostatic models (Anthes and Warner, 1978; Nickerson, 1979) and the continuity equation, (3), is analogous to the pressure tendency equation in a hydrostatic model. In fact, the set (1) through (3) is identical to the equation set which is obtained when a hydrostatic mesoscale model is collapsed to one-dimension along the x-axis.

We nondimensionalize the equations using the undisturbed height, H, as a scale. Thus, letting primes denote the nondimensional quantities, we have

$$\eta = H\eta' ,$$
$$u = \sqrt{gH}\, u' ,$$
$$v = \sqrt{gH}\, v' ,$$
$$t = H/\sqrt{gH}\, t' = \sqrt{H/g}\, t' , \qquad (4)$$

$$x = Hx' ,$$

$$f = \sqrt{gH} / Hf' = \sqrt{g/H}\, f' ,$$

$$\nu = H\sqrt{gH}\, K' .$$

Then the nondimensional equations are (dropping primes)

$$\frac{\partial}{\partial t}(\eta u) + \frac{\partial}{\partial x}(u\eta u) - f(\eta v) = -\frac{1}{2}\frac{\partial \eta^2}{\partial x} + K \frac{\partial^2}{\partial x^2}(\eta u) , \qquad (5)$$

$$\frac{\partial}{\partial t}(\eta v) + \frac{\partial}{\partial x}(\eta v) + f(\eta u) = K \frac{\partial^2}{\partial x^2}(\eta v) , \qquad (6)$$

$$\frac{\partial \eta}{\partial t} + \frac{\partial}{\partial x}(\eta u) = 0 . \qquad (7)$$

Note that K may now be regarded as an inverse Reynolds number.

The choice of a value for the nondimensional Coriolis parameter determines a relationship between the height scale and the implied latitude. Thus, if a latitude of interest is prescribed, a dimensional length scale must be implicitly chosen even in the nondimensional analysis. We chose to let $f = 10^{-4}\ s^{-1}$ (ϕ = 43 Lat), and choose a height scale H = 8 km (approximately the density scale height). This yeilds a gravity wave speed of $\sqrt{gH}$ = 280 m/s.

The equations are finite differenced on a staggered grid as shown in fig. 1. Time integration is accomplished with the leapfrog scheme with an Asselin filter (Asselin, 1972) to control timesplitting. The Asselin filter factor is set at 0.5 as suggested by Schlesinger et al. (1983) for the "lagged", weak diffusion used in the model. The normal model domain has 26 grid points for η. A larger domain with 50 grid points for η can also be run. The

nondimensional grid spacing is chosen to be $\Delta x = 2.5$ which corresponds to 20 km. This value, and the resulting domain size of 500 km is typical of meso-beta models and is identical to the three-dimensional model described below. It also assures that all waves resolved in the model satisfy the shallow water assumption on which the equations are based. With the parameter values chosen, a nondimensional time of 1.0 corresponds to 28.6 s. The timestep is chosen to be $\Delta t = 0.8$. This is about half the size required for linear stability (including the reduction required by the use of the Asselin filter), but is typical of the value required in a 2-D or 3-D model with the same Δx value. The inverse Reynolds number is set at $K = 7.813 \times 10^{-3}$ which corresponds to an eddy viscosity of 1.75×10^{4} m^2/s. The model has been coded with a variety of lateral boundary conditions.

b. The Three-Dimensional Model

The three-dimensional model is basically the model described in detail by Nickerson (1979), so only the general features of this model and the differences between it and the description given by Nickerson will be given here. The model is a primitive equation, hydrostatic model which is written in a modified sigma-coordinate system. The horizontal domain is 500 km X 500 km with a grid spacing of 20 km in both directions. In the vertical, the model uses 16 levels to cover the region from the surface to zero

pressure with the modified sigma-coordinate packing several
model layers in the surface boundary layer. The variables
are distributed on a staggered grid as described by Anthes
and Warner (1978).

Time integration is accomplished using the leapfrog
scheme with an Asselin filter. The time step is 20 s and
the filter factor is set at 0.5. The Coriolis parameter is
constant in the model and set at $f = 10^{-4}$ s^{-1}. The model
includes a lagged Fickian diffusion on all variables with
the eddy viscosity set at 2×10^4 m^2/s. No other
smoothing operator is used in the model. All of the moist
processes described by Nickerson (1979) have been removed
from the model in order to make it computationally more
efficient and because moist processes play little role in
the classical geostrophic adjustment problem. While the
model was designed to include complex terrain in a
straightforward manner, all of the experiments described
here were made with a flat horizontal terrain in the model.
This model was also coded with several different lateral
boundary conditions.

IV. Description of the Adjustment Experiments

The major concern of most lateral boundary condition
formulations is their ability to allow waves generated in
the domain to exit (or be absorbed) without reflection. If
this is accomplished, the lateral boundary will appear

transparent and allow the limited area model to better represent the unbounded region it is simulating. Another concern is the possibility of errors in the large scale gradients implied by the boundary values being geostrophically adjusted throughout the domain. On the meso-beta scale, temperatures and windspeeds must be specified with errors of less than about 1°C and 2 m/s, respectively, in order to give acceptable geostrophically adjusted interior errors (Anthes and Warner, 1978).

A major source of waves in the domain during a simulation is the geostrophic adjustment of imbalances between the dynamic fields. In general, at the start of the integration, the velocity and mass fields will not be in perfect gradient balance and gravity and Lamb waves will be generated during the adjustment process. These waves radiate away from the imbalance to leave behind a balanced state. If the lateral boundary conditions of a numerical model reflect some or all of the wave energy back into the interior, the reflected waves will unrealistically influence the simulated solution, interfering with the balance and prohibiting the adjustment process.

In this study, experiments were conducted with two different types of localized initial imbalances as initial conditions. Initial condition 1 is a perturbation in the height field and initial condition 2 is an imbalanced local wind. The scale of these imbalanced regions is smaller than the domain size of the model (500 km) and therefore

much smaller than the Rossby radius of deformation
(λ = C/f = 2.8 x 10^3 km). Theory predicts that the pressure
should adjust to the winds with the wind field remaining
essentially unchanged.

Each of these two initial conditions were run in the
large domain one-dimensional model in order to determine
their natural evolution during adjustment. For these
simulations, the model used a radiation lateral boundary
condition with the phasespeed set to the analytical value
of C = 1.0. This will be shown to be the least
reflective formulation.

The first imbalance (initial condition 1) is a
perturbation in height only with the velocities set to zero.
The initial height field and its evolution are shown in fig.
2. The perturbation is a height deficit of 0.3 %
(comparable to a pressure deficit of 3 mb) in the center of
the domain. Height excesses are located on either side of
the deficit so that the equalibrium height is η = 1.0. As
linear shallow water theory would predict, the evolution of
this disturbance is for two deficit waves to propagate in
opposite directions at the shallow water wavespeed, C = $\pm$1.0,
leaving a (trivially) balanced state behind. The Coriolis
effect plays little role in this adjustment as indicated by
a simulation with f = 0 (not shown) which yielded
essentially identical results. The primary velocities are
in the u component due to the height gradient. Small values
of v are accelerated geostrophically as the first half of

6.11

the wave passes a point. However, these are quickly diminished as the sign of the acceleration changes during the passage of the rest of the wave. Note that by t = 72, the wave is no longer present in the area covered by the small domain and the height field is level.

In the second adjustment experiment, the height field is initially specified as η = 1.0, but a limited jet is imposed in v with u initially zero. This is essentially the geostrophic adjustment problem studied by Cahn (1945) using a linear shallow water model. The t = 0 frame of fig. 3 shows the extent of the jet, which was set at v = 10 m/s (dimensionally). The remainder of the figure shows the evolution of the height field. As predicted by linear theory, the height field adjusts to the imbalance by producing a wave of excess which moves to the right and a wave of deficit which moves to the left. The resulting height field has a height gradient in geostrophic balance with the velocity in the region of the jet and a constant height in balance with the zero velocities away from the jet. Note that, unlike initial condition 1, the balanced state requires final boundary values to be different from their initial values. Also note that while the Coriolis effect plays little role in the evolution of initial condition 1, it is essential to the evolution shown in fig. 3. If f = 0, the v component is decoupled from the other variables in equations (1) through (3) and no adjustment would be necessary.

In the following sections, specific lateral boundary
condition formulations will be described and the results of
tests using these conditions in the one- and three-dimensional
models will be presented. All boundary conditions used in
the one-dimensional model were tested with both initial
conditions. In the figures which allow comparison of the
boundary conditions, the height field labeled "LD" is the
large domain's center 26 grid points and may be thought
of as the "exact" solution. The three-dimensional model
was only run with an initial condition similar to
initial condition 1. Each boundary condition formulation
will be denoted with a three letter descriptor (such as
FXD for fixed conditions) which is used in the
figures.

V. Lateral Boundary Condition Formulations

a. One-dimensional model formulations

1) Fixed boundary condition (FXD). This boundary
condition consists simply of specifying boundary values
initially and holding these values constant throughout
the integration. It may be written

$$\frac{\partial \phi}{\partial t} = 0 \quad , \tag{8}$$

where ϕ is any prognostic variable (η, u, or v in
the present model). This approach eliminates the
potential problem of geostrophically adjusted boundary

errors, provided the initial boundary values are correctly chosen. This boundary condition is not mathematically well-posed, however, in that it results in an overspecification of the problem. It also is purely reflective of waves generated in the domain's interior.

2) Combination of fixed and extrapolated (FEX). In order to allow the boundary to be more "open", while still controlling geostrophically adjusted errors, some mesoscale models use fixed conditions on some variables while extrapolating others (Anthes and Warner, 1978; Nickerson, 1979). The typical approach is to fix the pressure and thermodynamic variables and set the horizontal gradients of the velocities equal to zero (Anthes and Warner, 1978). Here, the formulation follows Nickerson (1979) with the height specified and the velocities extrapolated only when the flow is outward. That is

$$\frac{\partial \eta}{\partial t} = 0 \quad ,$$

$$\left\{ \begin{array}{ll} \frac{\partial u}{\partial x} = \frac{\partial v}{\partial x} = 0 & \text{for u outward} \\ \frac{\partial u}{\partial t} = \frac{\partial v}{\partial t} = 0 & \text{for u inward} \end{array} \right. \quad . \tag{9}$$

3) Zero-gradient condition (GRD). This condition extrapolates all variables on the boundary by specifying the horizontal gradient to be zero. This may be writtten

$$\frac{\partial \phi}{\partial x} = 0 \quad , \tag{10}$$

where $\phi = \eta$, u, or v. This condition is implemented
by setting the boundary value equal to the value one
grid point interior to the boundary at each timestep.

4) Sponge condition (SPG). This condition follows the
formulation of Perkey and Kreitzberg (1976). The
boundary values are specified and do not change in
time. However, the time tendencies at the gridpoints
are modified such that

$$\frac{\partial \phi}{\partial t} = W(I) \frac{\partial \phi}{\partial t} \quad , \tag{11a}$$

where

$$W(I) = \begin{cases} 0.0 & \text{for I = boundary grid points} \\ 0.4 & \text{for I = boundary-1 grid points} \\ 0.7 & \text{for I = boundary-2 grid points} \\ 0.9 & \text{for I = boundary-3 grid points} \\ 1.0 & \text{for all interior grid points} \end{cases} \tag{11b}$$

This type of boundary condition absorbs waves by
reducing their phase speed to zero as they approach the
boundary (Perkey and Kreitzberg, 1976). As the
phasespeed is reduced, the wavelength also becomes
smaller. This adds energy to $2\Delta x$ waves. Therefore, a
filter of some sort is required. A fourth-order
diffusion term is used in this study to remove this $2\Delta x$
energy.

5) Radiation condition (ORP). Radiation type lateral
boundary conditions are based on the Sommerfeld
radiation condition

$$\frac{\partial \phi}{\partial t} + C \frac{\partial \phi}{\partial x} = 0 \quad , \tag{12}$$

where ϕ is the variable of interest on the boundary
and C is the phasespeed of the outgoing wave.
C is required to satisfy the Courant-Friedrichs-Levy
(CFL) condition, and, if C is calculated to be
inward, it must be set equal to zero to prevent
spurious generation of waves. Thus, C must satisfy

$$C = \begin{cases} 0 & \text{for C inward} \\ C & \text{for } 0 < C < \Delta x/\Delta t \\ \Delta x/\Delta t & \text{for } C > \Delta x/\Delta t \end{cases} \qquad (13)$$

Note that for C = 0, (12) reduces to $\partial\phi/\partial t = 0$
for that timestep. The finite difference form
of the radiation condition used here follows
Orlanski (1976). C is calculated by inverting (12)
and evaluating $\partial\phi/\partial t$ and $\partial\phi/\partial x$ at the previous
timestep and one grid point interior to the boundary.
That is

$$C = -\frac{\partial\phi}{\partial t}\left[\frac{\partial\phi}{\partial x}\right]^{-1}, \qquad (14)$$

where

$$\frac{\partial\phi}{\partial t} = \frac{1}{2\Delta t}\left[\phi_{b-1}^{\tau} - \phi_{b-1}^{\tau-2}\right] \qquad (15)$$

and

$$\frac{\partial\phi}{\partial x} = \frac{1}{\Delta x}\left[\frac{1}{2}\left(\phi_{b-1}^{\tau} + \phi_{b-1}^{\tau-2}\right) - \phi_{b-2}^{\tau-1}\right]. \qquad (16)$$

In the above, ϕ_{b-i} is the ith grid point interior to
the boundary and the superscript denotes the timestep.
The term in parenthesis in (16) is used to prevent
timesplitting on the boundary point. The new boundary
value is then given by

$$\phi_b^{\tau+1} = \frac{[1 - C\Delta t / \Delta x]}{D} \phi_b^{\tau-1} + \frac{2C\Delta t / \Delta x}{D} \phi_{b-1}^{\tau} \quad , \quad (17)$$

where $D = 1 + C\Delta t / \Delta x$. For the shallow water system, the phase speed is known to be $C = 1.0$, so this known analytic value can be used in (17) to allow a nearly perfect radiation of waves. This will be denoted ORE.

b. Boundary Conditions for the Three-Dimensional Model

1) Combination of fixed and extrapolated (FEX). These conditions are the same as those used in the one-dimensional model.

2) Sponge condition (SPG). This also is implemented in essentially the same manner as in the one-dimensional model. However, since the three-dimensional model is coded to have only three adjacent x-z planes of gridpoints in core at any one time, a fourth-order diffusion could not be used. Instead, a second-order diffusion term was added which increased the diffusion in the sponge region to a value of 1×10^5 m^2/s.

3) Three-dimensional radiation condition (RKP). Most two- or three-dimensional models which use a radiation boundary condition implement this condition in the form used in the one-dimensional model along the coordinate normal to the boundary. Here we use the multi-dimensional radiation condition developed by Raymond and Kuo (1984) which can allow a fully three-dimensional form. This condition may be written

$$\frac{\partial \phi}{\partial t} + C_x \frac{\partial \phi}{\partial x} + C_y \frac{\partial \phi}{\partial y} + C_z \frac{\partial \phi}{\partial z} = 0 \quad . \tag{18}$$

Again, all C values are required to satisfy the CFL
condition and the phasespeed perpendicular to the
boundary is set to zero if it is calculated to
be inward. Relationships allowing the evaluation of
the C values are derived by inverting (18) and using
the orthoganality of the phasespeeds. For the case
where C_x is perpendicular to the boundary we have
(Raymond and Kuo, 1984)

$$C_x = \frac{\partial \phi}{\partial t} \left[\frac{\partial \phi}{\partial x} \right] / M \quad , \tag{19a}$$

$$C_y = \frac{\partial \phi}{\partial t} \left[\frac{\partial \phi}{\partial y} \right] / M \quad , \tag{19b}$$

$$C_z = \frac{\partial \phi}{\partial t} \left[\frac{\partial \phi}{\partial z} \right] / M \quad , \tag{19c}$$

where

$$M = \left(\frac{\partial \phi}{\partial x} \right)^2 + \left(\frac{\partial \phi}{\partial y} \right)^2 + \left(\frac{\partial \phi}{\partial z} \right)^2 \quad , \tag{20}$$

and

$$\frac{\partial \phi}{\partial t} = \left[\phi_{b-1,j,k}^{\tau+1} - \phi_{b-1,j,k}^{\tau-1} \right] / 2\Delta t \quad , \tag{21a}$$

$$\frac{\partial \phi}{\partial x} = \left[\tfrac{1}{2} \left(\phi_{b-1,j,k}^{\tau+1} + \phi_{b-1,j,k}^{\tau-1} \right) - \phi_{b-2,j,k}^{\tau} \right] / \Delta x \quad , \tag{21b}$$

$$\frac{\partial \phi}{\partial y} = \left(\phi_{b-1,j+1,k}^{\tau} - \phi_{b-1,j-1,k}^{\tau} \right) / 2\Delta x \quad , \tag{21c}$$

$$\frac{\partial \phi}{\partial z} = \left(\phi_{b-1,j,k-1}^{\tau} - \phi_{b-1,j,k+1}^{\tau} \right) / 2\Delta z \quad . \tag{21d}$$

In (21d), note that the vertical index, k, increases
downward and that in the sigma coordinate system Δz
is variable in space and time. The model calculates

the geopotential height, Φ, for each grid point,
so we let

$$2 \Delta z = \frac{1}{g} \left(\Phi_{b,j,k-1} - \Phi_{b,j,k+1} \right) . \qquad (22)$$

The boundary value is then updated using the calculated
phasespeeds in

$$\phi_{b,j,k}^{\tau+1} = \frac{[1 - c_x \Delta t / \Delta x]}{D} \phi_{b,j,k}^{\tau-1} + \frac{2 c_x \Delta t / \Delta x}{D} \phi_{b-1,j,k}^{\tau}$$
$$- c_y \frac{\Delta t}{\Delta x} \left[\phi_{b,j+1,k}^{\tau} - \phi_{b,j-1,k}^{\tau} \right] / D \qquad (23)$$
$$- c_z \frac{\Delta t}{\Delta z} \left[\phi_{b,j,k-1}^{\tau} - \phi_{b,j,k+1}^{\tau} \right] / D ,$$

where $D = 1 + C \Delta t / \Delta x$. Note that this condition
reduces to the one-dimensional radiation condition
when $C_y = C_z = 0$. In the results shown in this report,
a slight modification of the boundary condition was
used which set $C_z = 0$, so a two-dimensional condition
resulted. Simulations with variable C_z developed an
instability on the boundary early in the integration.
The source of this instability has not yet been
determined.

VI. Results for Small Scale Initial Imbalances

a. One-dimensional model results for initial conditions
    1 and 2

    Figures 4 and 5 show the height field in comparative
test results for initial condition 1 at the nondimensional

times t = 36 and t = 72, respectively. The height field
labeled LD is the center 26 grid points of the large domain
model and may be thought of as the solution resulting from
truly open lateral boundaries. All the conditions yield
similar results out to t = 36, but after that time the
simulations begin to differ markedly. It is clear that
the ability of the model to approach geostrophic
adjustment is strongly influenced by the lateral boundary
condition used.

The fixed and fixed/extrapolated (FXD and FEX)
conditions produced nearly identical results. This suggests
that extrapolation of only the velocities does not allow the
boundary to be more open to the outgoing wave.
Extrapolation of all the variables through the zero-gradient
condition (GRD) is not adequate either. This condition
appears to produce errors of comparable magnitude to FXD
and FEX (though of different phase). The sponge condition
fails to completely absorb the wave. This may be a
result of the small number of gridpoints in the model
(which is typical of the number of grid points in one
direction in a 3-D model). It may also be a result of the
relatively rapid phasespeed of the wave in this model.
Tests of the sponge condition reported by Perkey and
Kreitzberg (1976) which showed nearly completed absorption
involved internal gravity waves which required many
timesteps to traverse the width of the sponge. If the
sponge had completely absorbed the outgoing waves, it

would have allowed an acceptable balance to be reached in this case.

The radiation condition formulations (ORP and ORE) yield results superior to the other boundary conditions, allowing the adjustment to proceed almost exactly as in the large domain model (LD). The radiation condition with the exact phasespeed (ORE) was superior to ORP which calculates the phasespeed. Since the phasespeed is exact in ORE, the small errors apparent at $t = 72$ must be due to the finite differencing of the scheme. An important and very noticable point in the variable phasespeed formulation results (ORP) is that the height field has dropped below the equilibrium level of $\eta = 1.0$ at $t = 72$. This indicates that mass has been lost through the open boundaries as waves exited. This is a potentially serious problem which could adversely affect the performance of a more complicated atmospheric model. This is clearly related to the variable phasespeed since the exact phasespeed results do not exhibit a noticable change in mass.

A similar comparative display for initial condition 2 at times $t = 36$ and $t = 72$ is shown in figures 6 and 7. It is impossible for any of the boundary conditions which hold the boundary value fixed (FXD, FEX, SPG) to achieve the balanced final state. This leads to a very disturbed solution as the initial jet in the v component continually forces a height gradient but the reflection of the waves generated interferes with the height field adjustment. The

only acceptable balanced final state for these conditions is for the jet in v to be diminished to zero. Since the geostrophic adjustment on this scale is made by the height field, however, v is only diminished by the small viscosity in the model.

The zero-gradient condition (GRD) which is not constrained by fixed endpoint values appears initially to be allowing the adjustment to proceed with only small errors. At $t = 36$, the height gradient in the jet region is approximately correct. We can see also that the endpoints have adjusted in the right sense, although they are further from the equalibrium height than they should be. However, by $t = 72$, it is clear that this condition is not handling the adjustment properly.

Since the boundary values in the radiation condition are able to evolve in time, this formulation allows natural adjustment to take place. In this case, ORP performed nearly as well as ORE. This is a significant result since exact analytic phasespeeds are not available for a general atmospheric model. There was little evidence of a change in mass in the radiation condition experiments using initial condition 2.

b. Three-dimensional model results

The three-dimensional model was run with an initial condition similar to initial condition 1 used in the one-dimensional model. This initial condition was constructed

by starting the model at t = 0 with a horizontally
homogeneous atmosphere with no winds whose temperature
profile was given by the U.S. Standard Atmosphere. An
oblate ellipsoid temperature perturbation was added
gradually during the first 20 min of integration. This warm
bubble was 200 km in diameter and about 5 km thick, centered
at about 700 mb with a maximum temperature in the center of
about 3 C above the environment. This imposed temperature
perturbation produced the surface pressure perturbation
field shown in fig. 8. The central pressure deficit is
3.1 mb. An annular region of small pressure excess is
located around the central deficit so that the domain
average of pressure perturbation is zero. At t = 20 min the
temperature perturbation is artificially removed, leaving an
imbalance in pressure similar to the imbalance of initial
condition 1. After t = 20 min the model solution is allowed
to evolve naturally.

Before discussing the evolution of these simulations it
should be noted that this perturbation did not adjust
directly toward a balanced state of zero pressure
perturbation as in the one-dimensional model. Instead,
upward motion produced by the temperature excess during the
first 20 min initiated a bouyancy oscillation in the center
of the domain. This slightly damped oscillation should have
a frequency given by the Brunt-Vaisala frequency appropriate
for the Standard Atmsophere stability (~ 0.01 s^{-1}), giving a
period of approximately 10 min. The surface pressure

perturbation field should reflect this with an alternating pressure deficit and excess as the upward and downward motion cools and warms the column, respectively. It should also be noted that the initial perturbation was centered on grid point (12,12) which is one-half grid point southwest of the center of the domain. This small assymetry provided a convenient method of determining the extent of wave reflections off the boundaries because the interference pattern of any reflected waves will be noticably assymetric.

Figures 9, 10, and 11 show the surface pressure perturbation fields at t = 30 min for the model with FEX, SPG, and RKP lateral boundary conditions, respectively. As can be seen, the deficit wave is moving outward from the center of the domain very rapidly. Unlike the shallow water model, this model admits more than one type of wave. The rapidly propagating wave evident in the figures is the Lamb wave which has a phasespeed of approximately 300 m/s. The model equations also permit slower moving internal gravity waves. At t = 30 min, all three model results appear quite similar with the deficit wave just reaching the boundary. The ability of the radiation condition (RKP) to allow outward transmission of the wave is evident even at this early time. The fixed/extrapolated condition (FEX) will cause total reflection of this wave and the sponge condition (SPG) will reflect that portion of the wave not absorbed, similar to the one-dimensional model results.

Figures 12, 13, and 14 show the surface pressure

perturbation fields at t = 60 min for FEX, SPG, RKP, respectively. Striking differences are apparent at this time. The differences in the evolution leading up to this time are actually much larger than would be implied by these figures alone. Analysis of the FEX simulation showed that the field depicted in fig. 12 is almost totally a result of the contructive and destructive interference of the reflected deficit wave and the internal gravity wave. This reflection can be easily traced in frames plotted for times between t = 30 and t = 60 min (not shown), indicating that the solution at this time has little bearing with reality. The "sloshing" of this model solution continues with only minor damping for the entire 3 hr of the integration. Thus, use of the FEX condition prohibits an evolution toward a natural balanced state.

The sponge condition did absorb a significant portion of the energy of the initial wave, but allowed some reflection as well. The reflection of the initial wave was especially noticable in the corner regions at t = 40 min (not shown). Analysis indicates that the pressure pattern shown in fig. 13 is at least partly physical, but clearly influenced by the reflected portion of the waves. The phasespeed of waves within the sponge region is modified (Perkey and Kreitzberg, 1976), so the interference patterns created in this simulation by the wave reflection are considerably different than for FEX. Since energy of the reflected waves is partly absorbed whenever the waves enter

the sponge region, this condition eventually removes the nonphysical portion of the solution. This simulation produced a reasonably balanced state after about 2 hr of integration. (Note, however, that nonlinear interactions with the reflected waves can alter the physical solution in the early stages of integration and therefore cast doubts on the later results.)

The radiation condition simulation (RKP) was the only one which allowed rapid removal of the imbalance. Even this condition resulted in a small amount of reflection, though, which is evident by the assymetry in fig. 14. At times beyond about t = 50 min, the central bouyancy oscillation was clearly evident in this simulation and had a period very close to what theory would predict. This result indicates that the radiation condition allowed the model to adjust naturally and correctly to the imbalance. There was a problem with this simulation, however, in that an instability developed on the boundary after t = 120 min which grew rapidly and destroyed the solution. The source of this instability has not been isolated, but it has some of the characteristics of a time-splitting instability. If this is a time-splitting instability, it should be possible to remove it by casting the radiation condition in an upstream difference form as suggested by Miller and Thorpe (1981). While the one-dimensional simulations suggested a potential problem with a change of mass in the domain during integration, no evidence of this was found in the three-dimensional simulation.
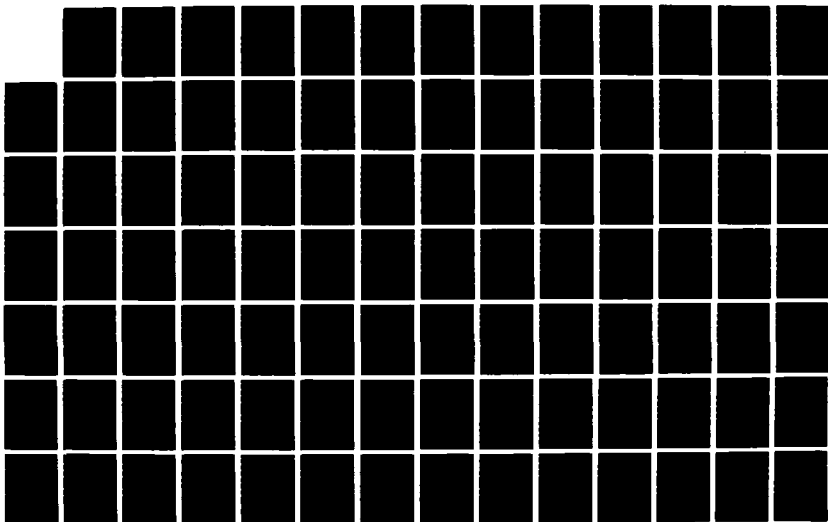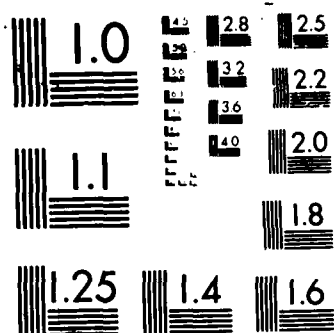
VII. Adjustment to Large Scale Imbalances

The results for initial conditions 1 and 2 described above involve geostrophic adjustment of imbalances on scales smaller than the Rossby radius of deformation. In these cases, the height field adjusts to the winds. The model's response to imbalances in the large scale ("wavenumber zero") fields yields results of importance to both model initialization and lateral boundary condition formulation. Even though the model domain is smaller than the radius of deformation, a constant gradient of height which is out of balance with a constant wind will be treated by the model as an infinitely large disturbance. In this case, theory predicts that the winds should adjust to the pressure.

One experiment involved initializing the one-dimensional model with a constant height gradient which would be in geostrophic balance with a v velocity of 2 m/s. The initial v component was set to zero, however, so the fields were out of balance. The adjustment process in this case is fairly clear from a consideration of equations (1) through (3). The height gradient accelerates a u velocity (from (1)) which in turn accelerates a v velocity (from (2)). As v becomes larger and approaches geostrophic balance with the height gradient, the acceleration of u is diminished (through the Coriolis term in (1)) and eventually u is decelerated to zero leaving only the geostrophically balanced v component and height gradient. Simulations with the one-dimensional

model show this adjustment process to be an order of
magnitude slower than the adjustment of a localized
disturbance. By the nondimensional time t = 240, the v
component had been accelerated to a dimensional value of
only 0.44 m/s.

In a different experiment, the same height gradient was
imposed but the v component was initialized at 1 m/s. Thus,
v was half the value required to be in geostrophic balance.
This experiment was carried out to verify that the previous
results were not influenced by the initial choice of v = 0,
which prohibits any immediate nonlinear interaction by the
advective terms. The v component in this experiment was
accelerated to a value of 1.22 m/s by the nondimensional
time t = 240. The smaller acceleration in the same time
compared to the previous results follows from the adjustment
process discussion in the preceding paragraph, where the time
rate of change of v decreases as v approaches geostrophic
balance.

For comparison, a third experiment was made with the
height initially at η = 1.0 and a uniform value of v = 2 m/s
specified. Again, the velocity should adjust to the height
field for this wave number zero imbalance, so the v
component should be decelerated to zero. By the
nondimensional time t = 240 in this simulation, the v
velocity was decreased to 1.55 m/s while the height field
remained virtually unchanged (the maximum change in η was
1.9×10^{-6} at t = 240).

The results of these simulations can be used to explain the lack of geostrophic adjustment in the three-dimensional model simulations by Brown and Ridge (1984). They initialized the full, moist three-dimensional model with horizontally homogeneous wind fields which were not in geostrophic balance with the topographically induced height gradients. After 6 hr of simulation, the upper atmospheric winds had turned to flow primarily down the height gradient rather than parallel to the height contours as required in geostrophic (or gradient) balance. Brown and Ridge (1984) attributed this result to an undetermined model coding error. This result, however, is completely consistent with geostrophic adjustment of a large scale imbalance. The initial accelerations are down gradient before being turned geostrophically to contour-parallel flow. For example, in the one-dimensional model results of the first experiment described in this section, the u velocity at t = 240 had been accelerated to u = -1.24 m/s while the v component was only v = 0.44 m/s. Since the height gradient was in the x-direction, this flow was also primarily down the height gradient.

The results of these one-dimensional model experiments and the problems encountered by Brown and Ridge (1984) indicate that it is very important for the large scale gradients to be very close to balance in an atmospheric model's initialization. The local imbalances due to topography or higher resolution data present in the

initialization will balance quickly provided an appropriate lateral boundary condition is used. Imbalances in the large scale gradients, however, will adjust in a time scale comparable to the inertial period (~17 hours).

These results also indicate that the concern of Anthes and Warner (1978) about geostrophically adjusted boundary value errors is not warranted in meso-beta models, which typically make forecasts for periods much shorter than one day. However, it may still be important for larger scale models which forecast for a day or more. The adjustment process is sufficiently slow that errors produced by the boundary conditions will require several hours to significantly affect the mean geostrophic flow in the interior. In chosing lateral boundary conditions for meso-beta models, then, emphasis should be placed on the ability of the condition to deal with waves generated in the interior of the domain by natural processes or by the geostrophic adjustment of initial local imbalances.

VIII. Conclusions

This study has investigated the geostrophic adjustment process in meso-beta scale models of the atmosphere. In simulations with both one- and three-dimensional models it was demonstrated that the ability of the model to reach a balanced state is intrinsically tied to the lateral boundary conditions used in the model. Of the boundary conditions

used in this study, the radiation condition allowed the most

natural adjustment. Also, the radiation condition

was the only condition which allowed correct adjustment

of imbalances requiring modification of the boundary values.

Imbalances in the initial large scale gradients were

found to require times on the order of the inertial period

to adjust. This result explains the lack of adjustment

found by Brown and Ridge (1984) in their three-dimensional

simulations since these integrations were for a period much

smaller than the inertial period. In general, on the meso-

beta scale, local imbalances will adjust on time scales of

about one hour while large scale imbalances require on the

order of one day. These results point to the necessity of a

good initialization which produces at least a near balance

in the large scale gradients.

IX. Recommendations

The results of this study lead to a series of

recommendations which should be incorporated into the

operational version of the three-dimensional model.

> (1) The model should use some sort of radiation
>   lateral boundary condition to allow waves
>   generated by the adjustment of local imbalances
>   to exit the domain.

> (2) A more sophisticated method of initialization
>   should be developed which results in the large
>   scale gradients being brought into near geostrophic
>   balance. If sufficient data is available, this may
>   be accomplished by some form of objective analysis
>   which uses geostrophic constraints. If the model
>   is initialized with a single sounding, a scheme

must be developed which uses geostrophic and thermal relations to specify the initial gradients. Of course, if the model is nested in a larger domain model, the gradients specified by the larger model will be in near balance and provide acceptable initial fields.

(3) Small scale imbalances due to topographic effects and higher resolution surface data will always be present in the initialization. An "adjustment period" will be required at the beginning of any operational forecast to allow the removal of these imbalances before any useful predictive information is available. The results of this study show that in a 500 km domain, the adjustment of local imbalances should occur in less than one hour. Thus, a 40-60 min adjustment period should be considered part of the initialization and be carried out prior to the start of the operational forecast.

(4) Although not directly addressed in this study, the waves produced in the initial adjustment could affect initialized cloud and moisture fields. This might leave the cloud, moisture, and possibly precipitation fields with inappropriate values at the end of the adjustment period before the actual forecast begins. Thus, it might be desirable to re-initialize these fields after the adjustment period. Alternatively, the adjustment period could be carried out with these fields held fixed in time. This latter choice would probably prohibit a truly natural adjusment, but should yield a more balanced state at the end of the period.

6.32

Acknowledgments

References

Anthes, R.A., and T.T. Warner, 1978: Development of hydrodynamic
    models suitable for air pollution and other mesometeorological
    studies. Mon. Wea. Rev., 106, 1045-1078.

Asselin, 1972: Frequency filter for time integration. Mon. Wea.
    Rev., 100, 487-490.

Brown, H.A., and D.V. Ridge, 1984: Baseline tests of a
    mesoscale numerical cloud/precipitation model. AFGL
    Tech. Memo.

Cahn, A., 1945: An investigation of the free oscillations of a
    simple current system. J. Met., 2, 113-119.

Miller, M., and Thorpe, A., 1981: Radiation conditions for the
    lateral boundaries of limited-area numerical models. Quart.
    J. R. Met. Soc., 107, 615-628.

Nickerson, E.C., 1979: On the simulation of airflow and clouds
    over mountainous terrain. Beit. Atmos. Phys., 52, 161-177.

Orlanski, I., 1976: A simple boundary condition of unbounded
    hyperbolic flows. J. Comp. Phys., 21, 251-269.

Perkey, D.J., and C.W. Kreitzberg, 1976: A time-dependant lateral
    boundary scheme for limited-area primitive equation models.
    Mon. Wea. Rev., 104, 744-755.

Raymond, W.H., and H.-L. Kuo, 1984: A radiation boundary condition
    for multi-dimensional flow. Quart. J. R. Met. Soc., 110,
    535-551.

Schlesinger, R.E., L.W. Uccellini, and D.R. Johnson, 1983: The
    effects of the Asselin time filter on numerical solutions to
    the linearized shallow water wave equations. Mon. Wea. Rev.,
    455-467.

Figure 1. Schematic diagram of the shallow water model domain showing the staggered grid.
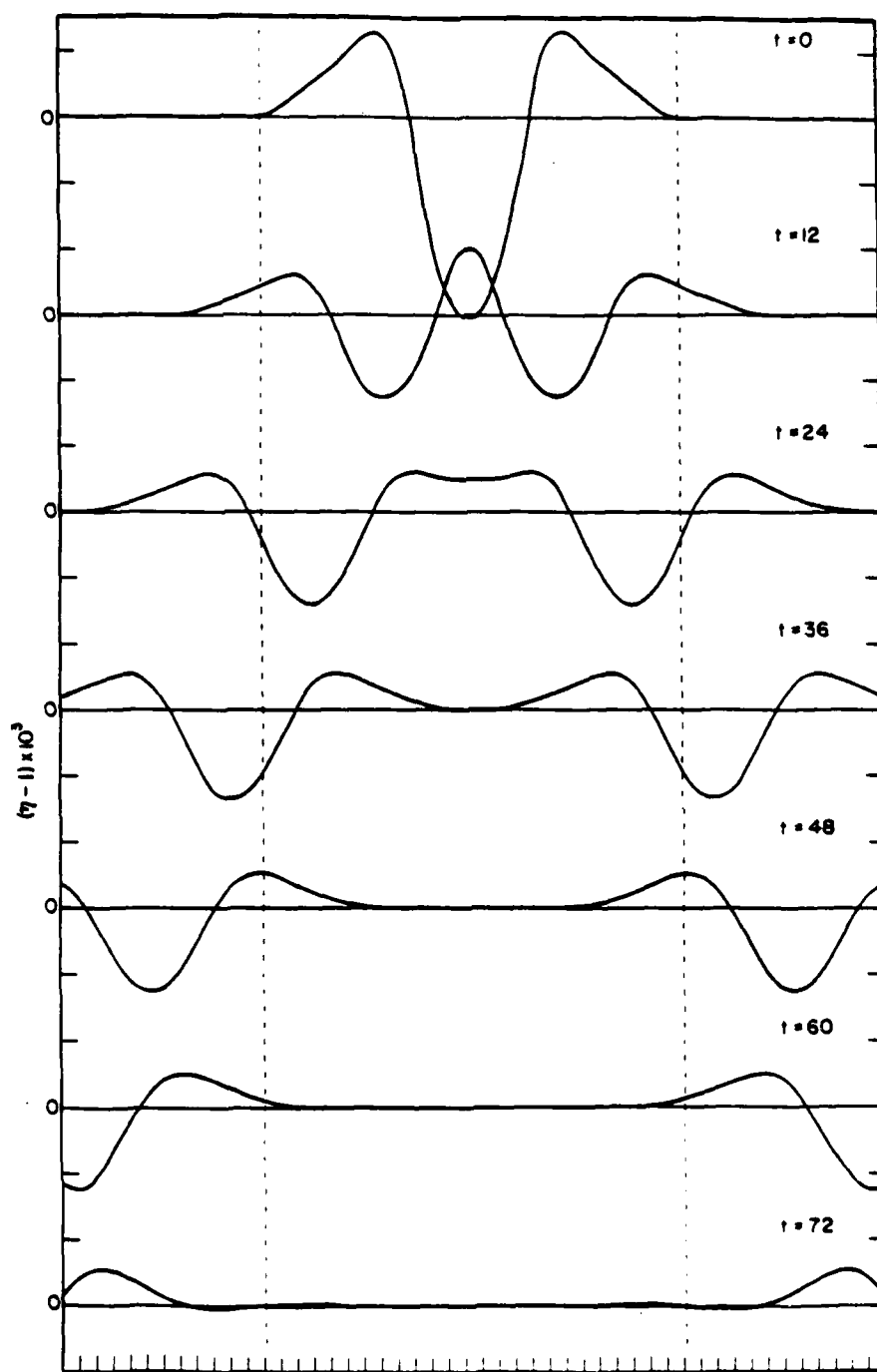
Figure 2. Evolution of initial condition 1 in the large domain
model. Tick marks along the bottom show the location of
grid points, and the dashed lines indicate the location of
endpoints in the 26 gridpoint model.

6.36
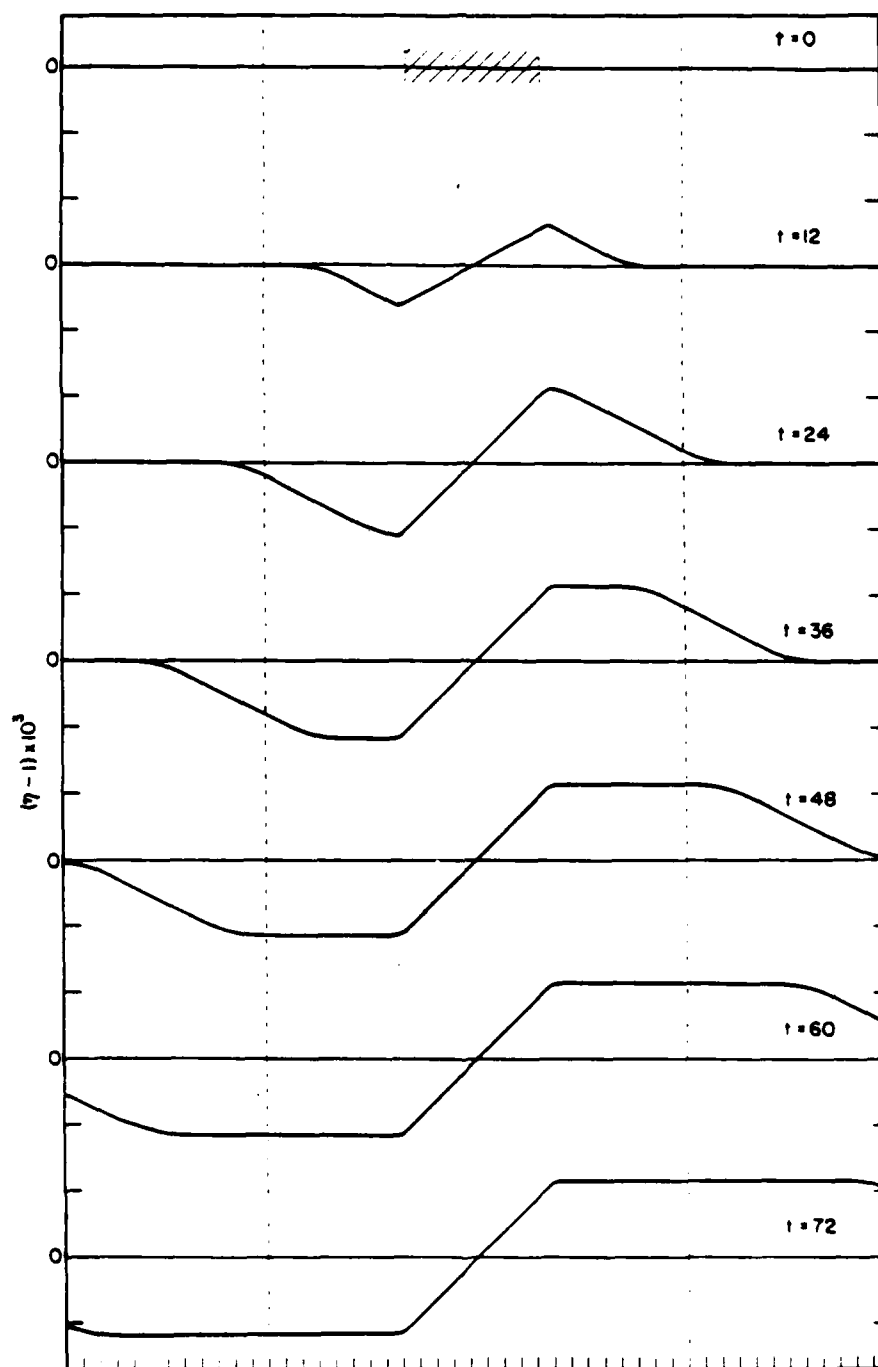
Figure 3. As fig. 2 for initial condition 2. Hatched region
shows the extent of the initially specified v-component jet.
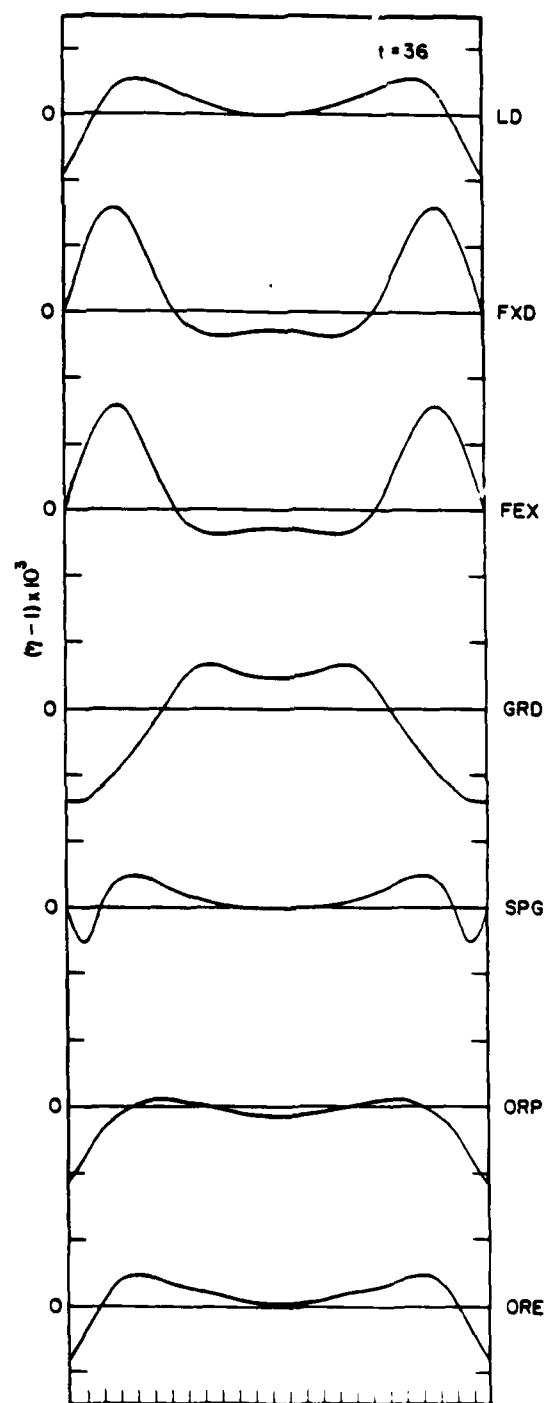
Figure 4. Comparison of the height field at t = 36 using the
indicated boundary conditions in the 26 gridpoint model
with initial condition 1.
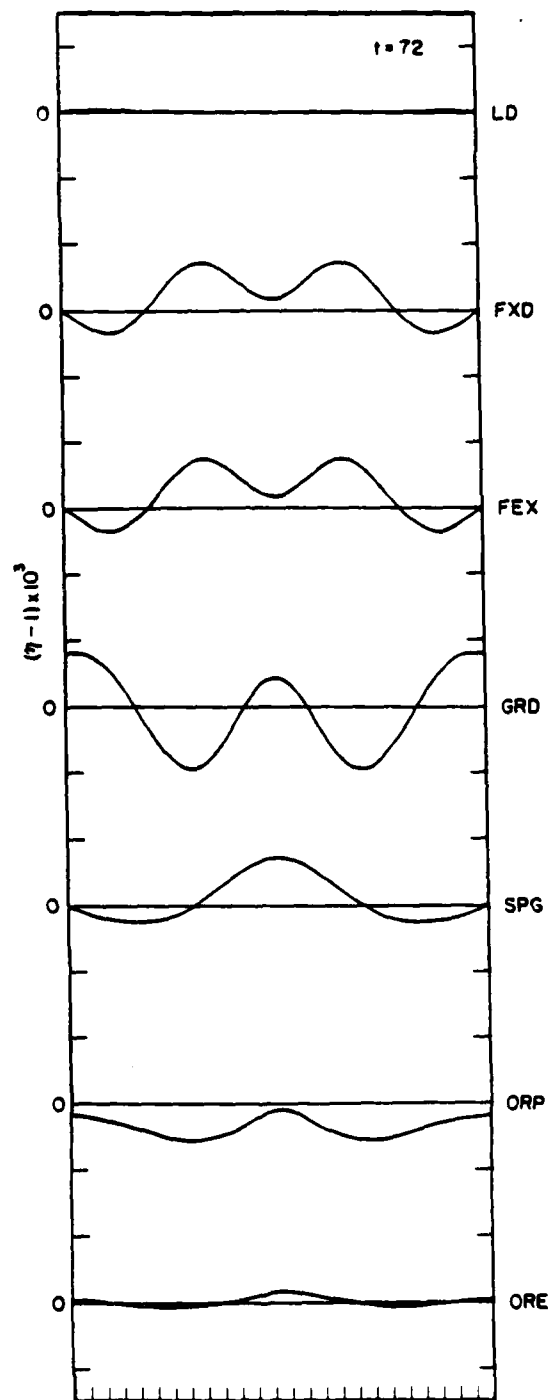
Figure 5.   As fig. 4 at t = 72.
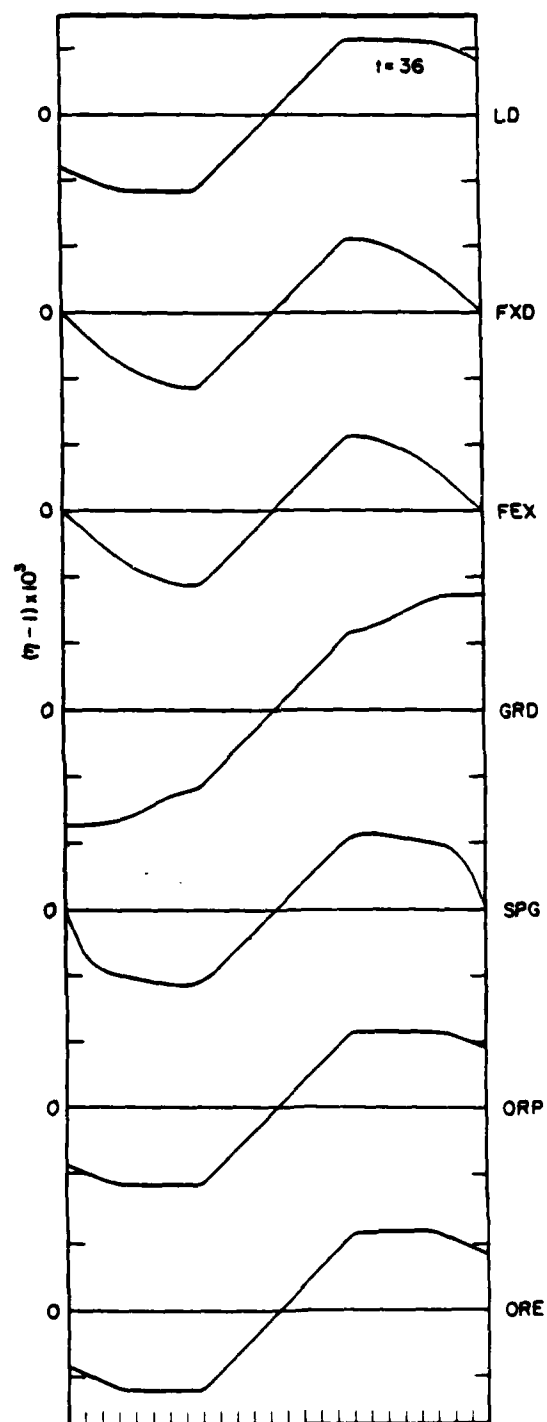
Figure 6.   As fig. 4 for initial condition 2.

6.40
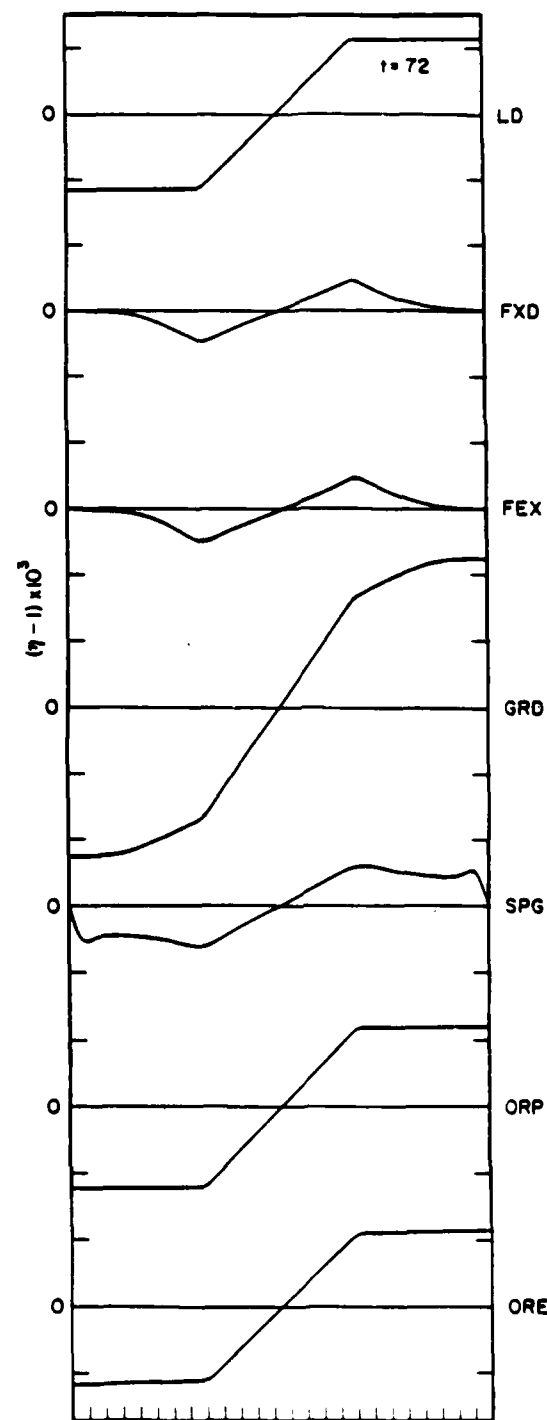
Figure 7.   As fig. 4 at t = 72 for initial condition 2.
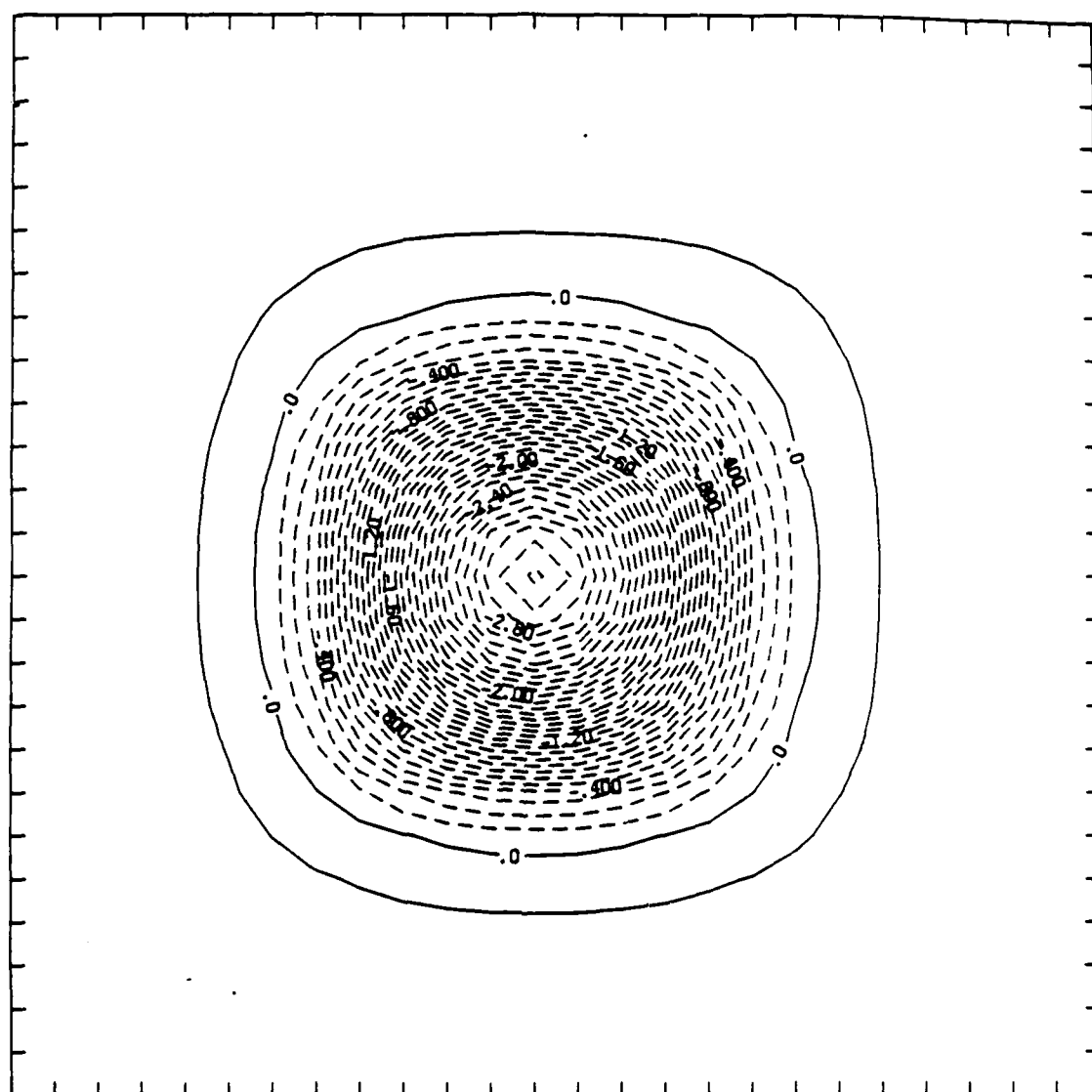
Figure 8. Surface pressure perturbation field at t = 20 min in the three-dimensional model. Contour interval is 0.1 mb with negative contours being dashed. Tick marks indicate the location of grid points.
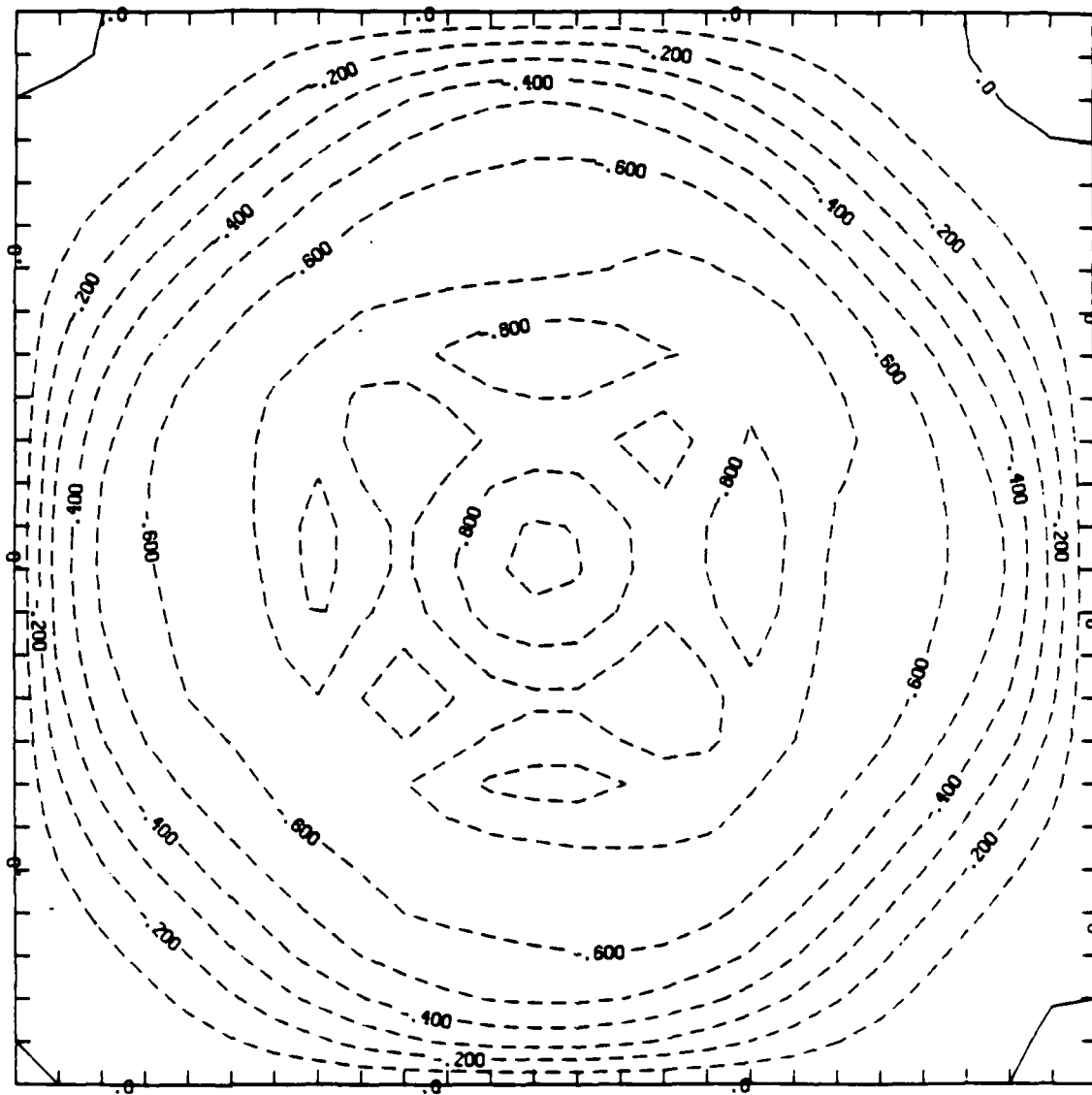
Figure 9. Surface pressure perturbation field at t = 30 min
for three-dimensional model with FEX.
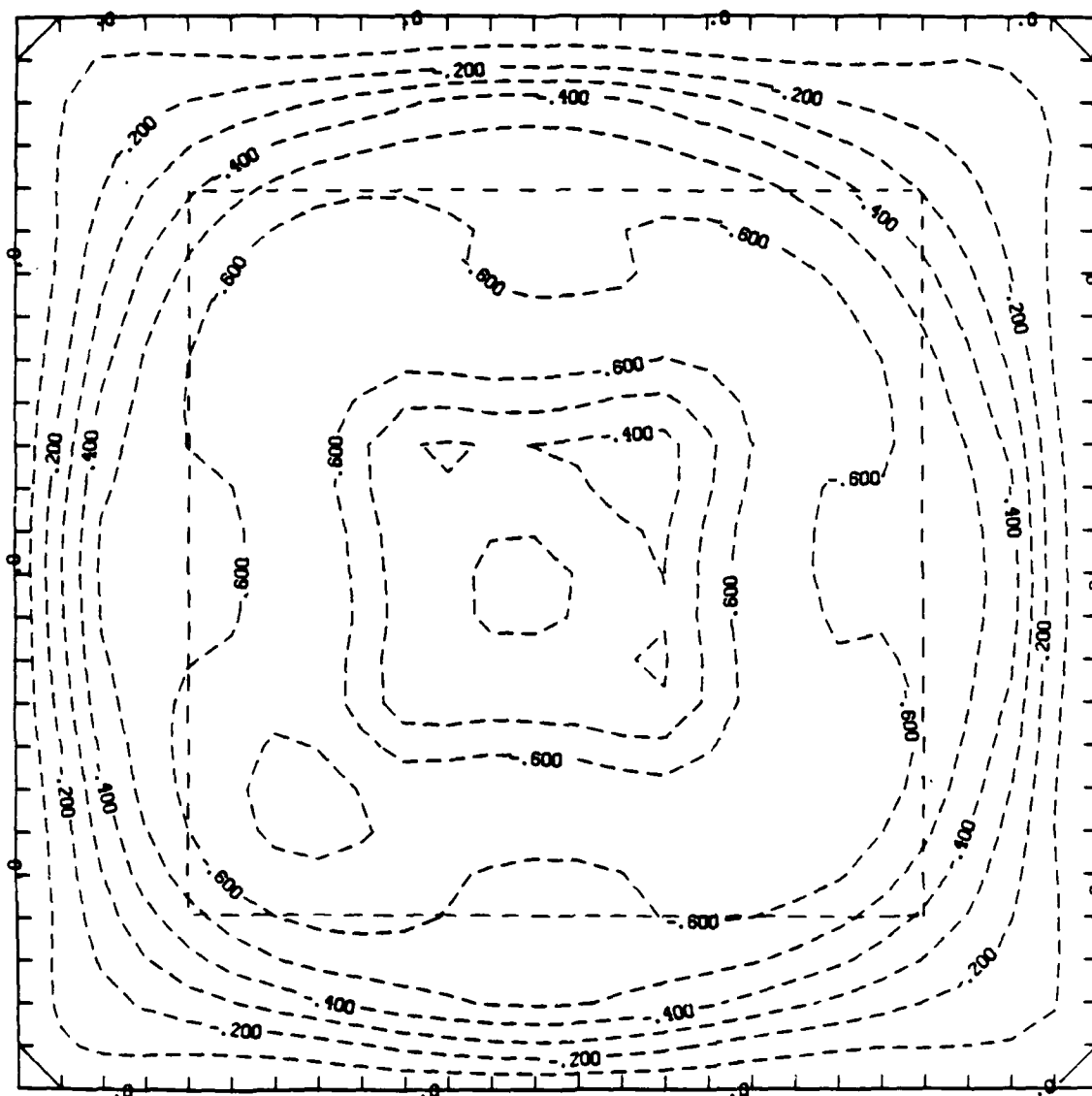
Figure 10. Surface pressure perturbation field at t = 30 min
for three-dimensional model with SPG. The sponge region
lies between the outer boundary and the dashed interior
square.
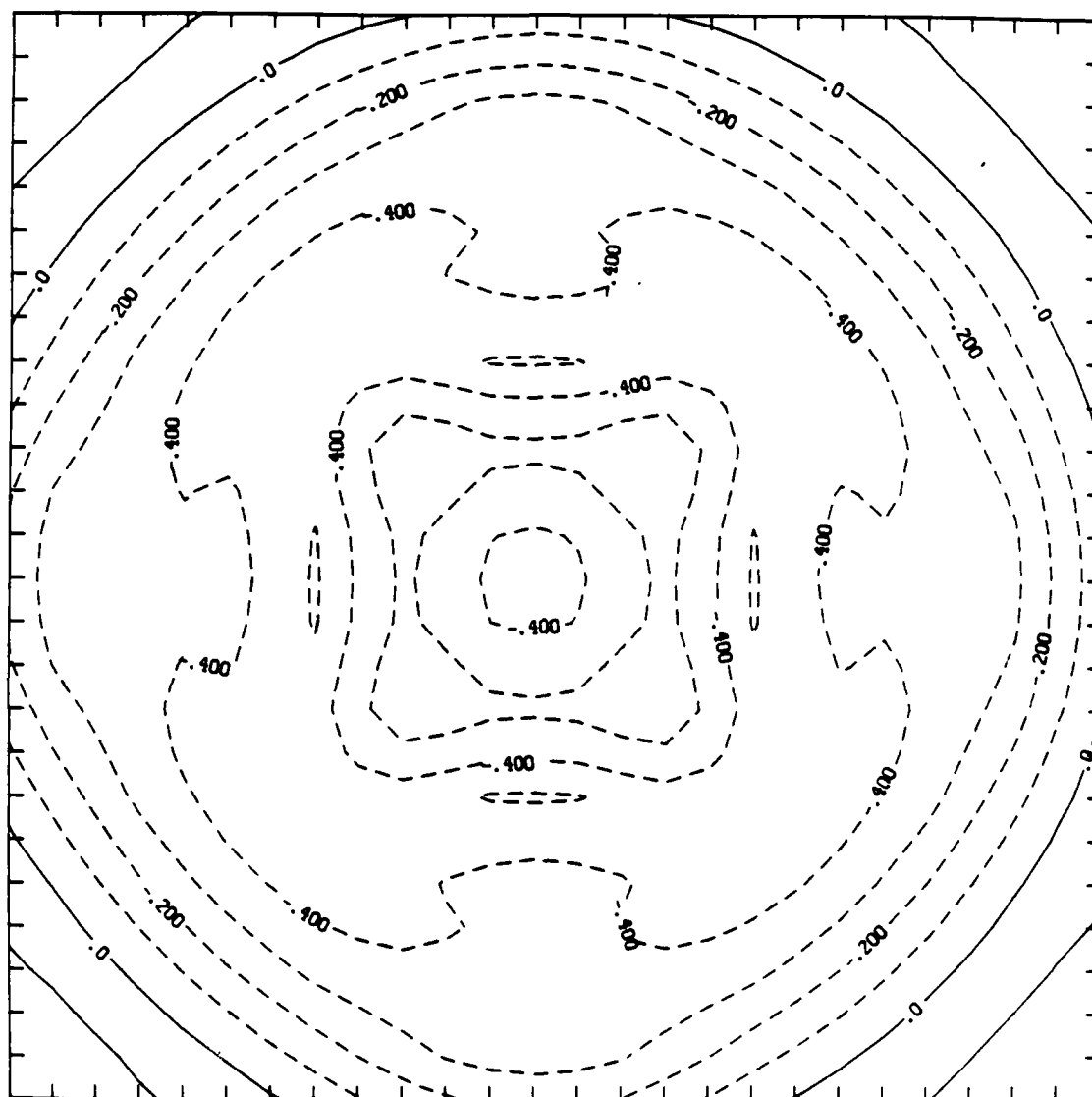
Figure 11.   Surface pressure perturbation field at t = 30 min
        for three-dimensional model with RKP.
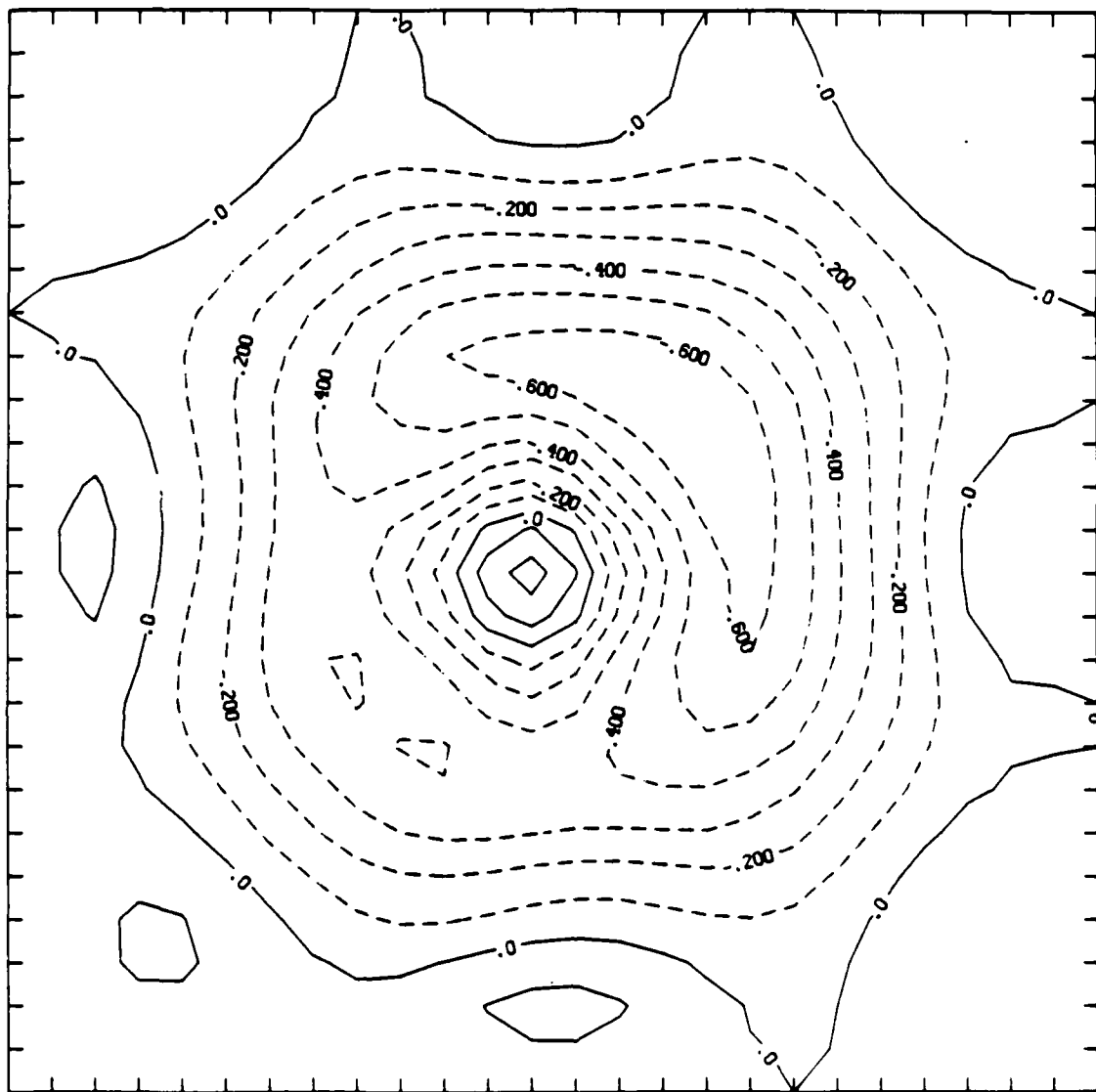
Figure 12.   As fig. 9 at t = 60 min (FEX).
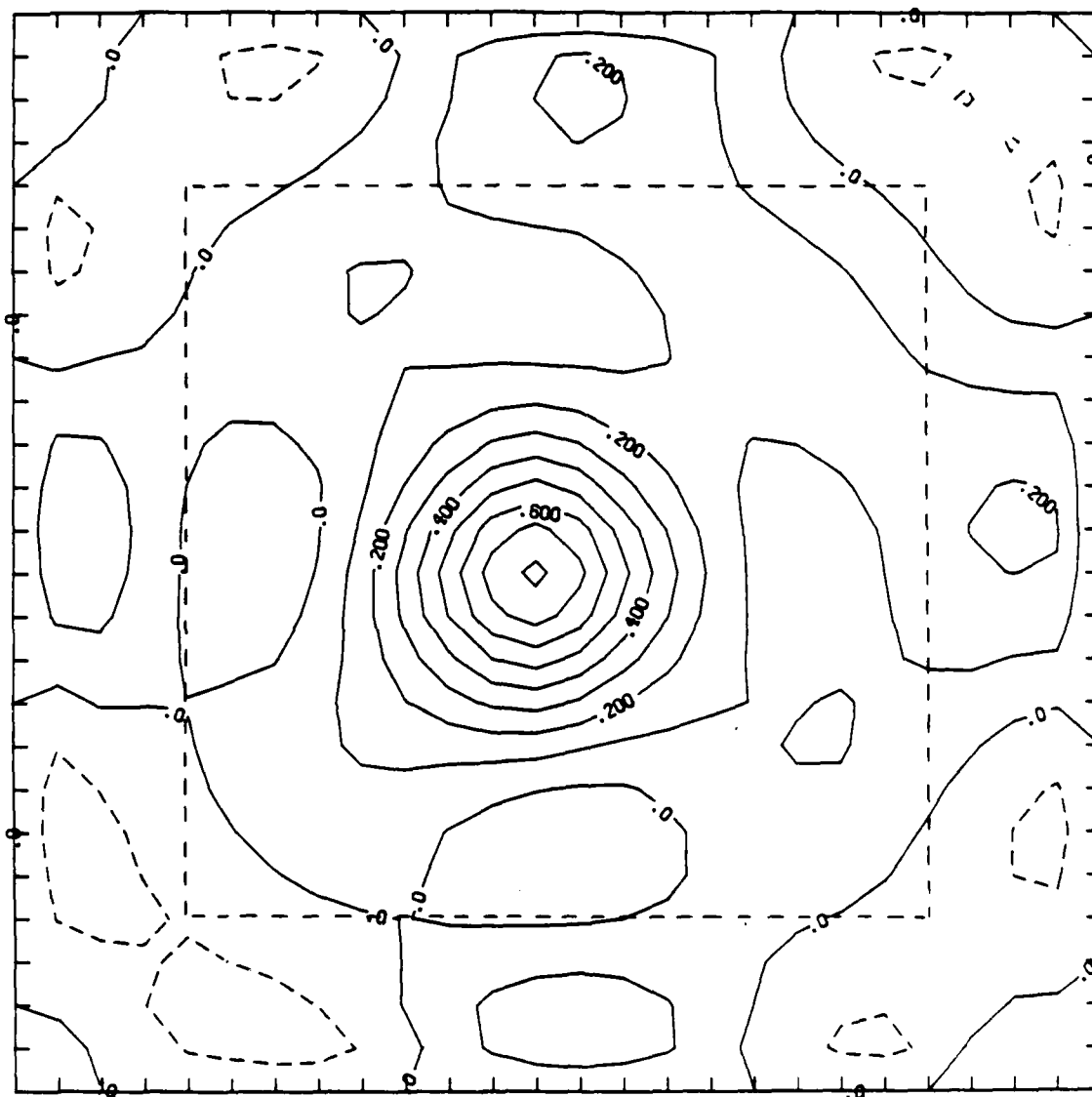
Figure 13.   As fig. 10 at t = 60 min (SPG).
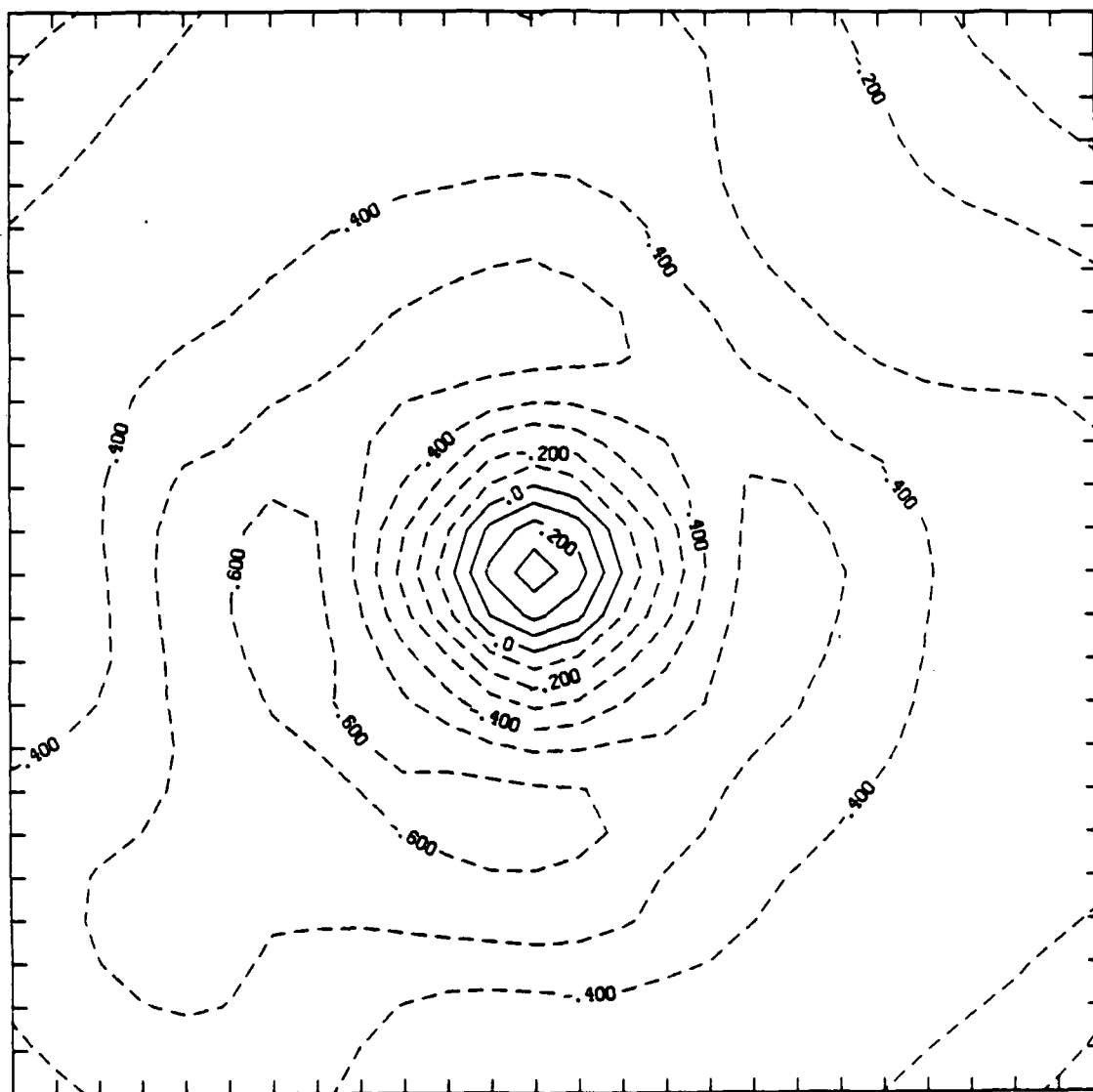
Figure 14.   As fig. 11 at t = 60 min (RKP).

1985 USAF-SCEEE RESEARCH INITIATION PROGRAM

Sponsored by the

AIR FORCE OFFICE OF SCIENTIFIC RESEARCH

Conducted by the

SOUTHEASTERN CENTER FOR ELECTRICAL ENGINEERING EDUCATION

FINAL REPORT

EFFECTS OF TEMPERATURE AND REACTANT SOLVATION UPON

THE RATES OF GAS-PHASE ION-MOLECULE REACTIONS

Prepared by:	Peter M. Hierl
Academic Rank:	Professor
Department and University:	Department of Chemistry University of Kansas
Research Location:	Air Force Geophysics Laboratory (LID) Hanscom Air Force Base, Massachusetts
Inclusive Dates:	05/16/85 to 11/31/85
Award Number:	84 RIP 08 -- F49620-82-C-0035

I. RESEARCH OBJECTIVES

The objective of this research project was to determine the effects
of temperature and reactant solvation upon both the rates and the
product branching ratios for the gas-phase reactions of selectively
solvated anions such as $OH^-(H_2O)_n$ (where $n = 0$, 1, 2 or 3) with
neutral molecules such as acetonitrile, the hydrogen halides, the
methyl halides, and others. These reactions include proton transfer,
nucleophilic displacement (methyl cation transfer), and solvent
switching. These studies were motivated by the recognition that
solvated ions play an important role in the chemistry of the lower
ionosphere,[1] where their reactions significantly affect the
atmospheric composition subsequent to natural and artificial
perturbations such as aurora, nuclear detonation, and missle reentry.

More specifically, this project had the following objectives:

(1) The _processing_ of a large amount of kinetic data collected at
the Air Force Geophysics Laboratory, where the author spent ten weeks
as an AFOSR Summer Faculty Research Program participant during the
summer of 1984.

(2) The _analysis_ of the processed data to determine the effects of
reactant solvation, temperature, and reaction exothermicity upon the
rate constants and product branching ratios for the reactions studied.

(3) The _interpretation_ of these results, including comparison of
the experimentally measured rate constants (and their temperature
dependences) with the predictions of current theoretical models.

(4) The _publication_ in scientific journals of the results obtained
in this study.

8.2

II. STATUS OF THE RESEARCH

A. Processing of Kinetic Data

During the ten-week period spent at the Air Force Geophysics Laboratory in the summer of 1984, the author used the AFGL Selected Ion Flow Tube[2] to obtain kinetic data on the reactions of selectively solvated anions with a number of neutral molecules over the temperature range 200-500K. Although a variety of reactions were studied, particular emphasis was given to the following two types of reactions because of their importance in both gas-phase and solution ion chemistry.

(1) Proton transfer (acid-base) reactions between hydrated OH^- and various proton donors (HA), including acetonitrile and the hydrogen halides,

$$OH^-(H_2O)_n + HA \longrightarrow A^-(H_2O)_m + (n+1-m)H_2O \qquad (1)$$
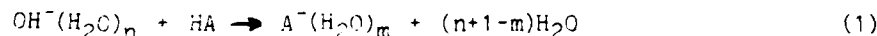
where n = 0, 1, 2 or 3, and A = CH_2CN, F, Cl, Br, or I.

(2) Nucleophilic displacement (methyl cation transfer) reactions between hydrated OH^- and the methyl halides, CH_3Y,

$$OH^-(H_2O)_n + CH_3Y \longrightarrow Y^-(H_2O)_m + CH_3OH + (n-m)H_2O \qquad (2)$$
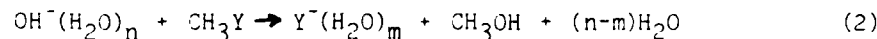
where Y = F, Cl, Br or I.

For most of these reactions, data were obtained at several (i.e., 3-7) different temperatures in the range 200-500K. At each temperature a number N (typically, N = 3-7) replicate runs were performed. In each run, reactant and product ion intensities were measured as functions of the concentration of the neutral reactant in the flow tube, these concentrations being stepped through 8-10 values per run.

To process these data, the ion intensitites observed for a given reaction at a given temperature in the N replicate runs were first combined and plotted vs. the concentration of the neutral reactant, thereby producing a graphical representation of the ionic intensity profiles for the given reaction.

Next, a reaction mechanism was assumed and appropriate differential equations written to describe the rates of disappearance of the reactant ion and formation of the product ions. Integration of these rate equations then yielded equations for the intensities of each of the ionic species as functions of the concentration of the neutral reactant.

Finally, a computer program was written which optimized the fit of these integrated rate equations to the observed ionic intensity profiles, thereby giving rate constants for reactant consumption and product formation for each reaction at each temperature.

B. Data Analysis

1. Reactant Solvation

The effect of reactant anion solvation upon the rate constant $k_n(T)$ for a particular reaction at a given temperature T was investigated by plotting $k_n(T)$ vs. n for the reaction of interest. Figure 1, for example, illustrates the effect of reactant solvation upon the room temperature rate constants for the proton transfer reactions of OH^- with the hydrogen halides. Three features are apparent. First, the reactions of unsolvated OH^- with HX are all very fast, having rate constants in the range $(1-3)\times10^{-9}$ cc/molec-s at 298K. Second, for reaction with a given anion, minor differences in rate constants are observed for the various hydrogen halides, with the order of

reactivity being HF > HCl > HBr > HI. Third, the rate constant for the reaction of a given hydrogen halides decreases slightly as the number of water molecules clustered to the reactant anion is increased from zero to three.

The nucleophilic displacement reactions of CH_3X with $OH^-(H_2O)_n$, however, exhibit quite different behavior with increaed reactant solvation (see Figure 2). CH_3Cl, CH_3Br, and CH_3I react very rapidly with the unsolvated OH^- anion, the room temperature rate constant all being about 2×10^{-9} cc/molec-s. (CH_3F reacts immeasurably slowly, with a rate constant $< 10^{-12}$ cc/molec-s, and will not be included in the subsequent discussion.) The addition of a single solvent molecule to the OH^- reactant anion reduces these rate constants by a factor of 2-5, and the addition of a second solvent molecule to the reactant anion further reduces them by an additional factor of 10-100, the reaction with methyl chloride being most affected by reactant solvation and that with methyl iodide the least. The addition of a third solvent molecule o the reactant anion effectively quenches all three reactions, reducing their rate constants below the detectable limit of 10^{-12} cc/molec-s.

The product distributions for these two types of reactions also show different dependences upon reactant anion solvation. For the nucleophilic displacement reactions, the unsolvated halide anion X^- is the major product in all cases, irrespective of the extent to which the reactant anion is solvated. This indicates that water molecules are not transferred efficiently from the OH^- reactant to the X^- product; consequently, increasing reactant solvation, which stabilizes the reactants and thus decreases the exothermicity for production of

8.5

the unsolvated product anion, ultimately quenches reaction. Conversely, solvent transfer appears to be facile in the proton transfer reactions; in all cases the dominant reaction channel was found to be that for which a sufficient number of water molecules were transferred to the product anion that the process remained exothermic.

2. Temperature Dependence

Both types of reaction, regardless of the extent of reactant solvation, were found to exhibit negative temperature dependences, the rate constant decreasing with increasing temperature. This behavior was more marked for the nucleophilic displacement reactions than for the proton transfer reactions. Among the nucleophilic displacement reactions, that of CH_3Cl is most strongly affected by temperature and that of CH_3I the least. These findings are discussed in more detail below.

C. Data Interpretation

In an attempt to understand the effects described above of solvation and temperature upon the rate constants, the measured reaction rate constant have been compared with calculated rate constants for collisions of ions with polar molecules. Four theoretical models have been employed to calculate these collision rate constants: (1) the AADO theory of Bowers and co-workers,[3] (2) the parameterized trajectory method of Su and Chesnavich,[4] (3) the statistical approach of Ridge,[5] and (4) the ACCSA approach of Clary.[6] Over the temperature range studied here (200-500K), the collision rate constants predicted by these four approaches differed by no more than 20% and usually by less than 10%.

8.6

The measured rate constants for the proton transfer reactions of the unsolvated OH⁻ anion with HX are plotted vs. temperature over the range 200-500K in Figure 3. Also shown are the collision rate constants calculated for each of these reactions on the basis of AADO theory (broken lines). The close agreement between the measured rate constants and the calculated collsion rate constants reveals that these reactions occur with essentialy unit efficiency over the temperature range studied, and that the slight negative temperature dependence shown by these proton transfer reactions is caused by a decreasing contribution to the collision rate from the ion-dipole term with increasing temperature.

Similar plots (not shown) for the proton transfer reactions of the solvated hydroxide anions with the hydrogen halides show similarly good agreement between the measured reaction constants and the calculated collision rate constants. This indicates that the proton tranfser reactions between $OH^-(H_2O)_n$ and HX always occur with unit efficiency (i.e., at the collision rate), regardless of the temperature or the degree of reaction solvation. The slight variations observed in the reaction rates with changes in temperature, solvation, and the identity of the halide can, therefore, be be attributed solely to the variations these changes cause in the collision rates.

The nucleophilic displacement reactions of CH_3X with $OH^-(H_2O)_n$, however, exhibit quite different behavior. In the reaction of methyl chloride with the hydroxide anion, for example, the measured reaction rate constant is considerably less than the calculated collision rate constant at all temperatures studied, with the disparity being

8.7

greatest at the higher temperatures. Thus, the displacement reaction between OH^- and CH_3Cl does not occur on every collision, and the relatively strong negative temperature dependence shown by this reaction is seen to be caused by a decrease in both the collision rate constant and the reaction efficiency with increasing temperature.

This behavior is summarized for the reactions of OH^- with the various methyl halides in Figure 4, where the reaction efficiency (i.e., the ratio of the measured reaction rate constant to the calculated collision rate constant) is plotted vs. temperature. The reaction efficiency is seen to decrease with increasing temperature for all three reactions studied, this effect being most pronounced in the case of the least exothermic reaction (i.e., that of methyl chloride).

As shown in Figure 5, the addition of a single solvent molecule to the reactant hydroxide anion further reduces the reaction efficiency, which again exhibits a negative temperature dependence. Again, the efficiency of the least exothermic reaction, that of methyl chloride, is the most strongly affected by increases in reactant solvation and in temperature.

These findings are consistent with the predictions of the "double-minimum model" developed by Brauman and co-workers.[7] The essential features of this model are as follows (see Figure 6): the reactants form an adduct at the collision rate, k_1. This adduct may then either reform the reactants with a rate constant k_{-1}, or pass over the central barrier with the rate constant k_2 to form the product adduct. For such exothermic reactions as those studied here, the overwhelming majority of these product adducts will then go on to form the separated products, so that the observed rate constant k is given by

8.8

$$k = k_1 k_2 / (k_{-1} + k_2).$$

Since k_1 is just the collision rate constant, the reaction efficiency equals the ratio $k_2/(k_{-1} + k_2)$. That is, the reaction efficiency is simply the fraction of reaction adducts that surmount the central barrier to form the product adducts and will therefore be determined by the relative magnitudes of k_{-1} and k_2.

If the reactants possess appreciable energy ΔE in excess of that required to surmount the central barrier, k_2 will be larger than k_{-1}, and the reaction efficiency will approach unity. This appears to be the situation in the proton transfer reactions, which would be expected to have relatively low central barriers. Although the nucleophilic displacement reactions would be expected to have higher barriers, the reactions of the unsolvated hydroxide ion with the methyl halides are so exothermic that ΔE will again be large and the reaction efficiency will approach unity. Solvation of the reactant anion, however, will lower the energy of the reactants more than that of the transition state, reducing the excess energy ΔE available for surmounting the central barrier and thereby decreasing k_2 and the reaction efficiency. This effect will be most pronounced for the least exothermic reactions because they intrinsically possess the least excess energy ΔE.

Entropic considerations, on the other hand, favor k_{-1} over k_2, and thus tend to reduce the reaction efficiency. This effect increases in importance with increasing temperature and thus explains the negative temperature dependence exhibited by the nucleophilic displacement reactions. Because the reaction efficiency is determined by the relative magnitude of k_{-1} with respect to k_2, the greatest dependence

8.9

upon temperature will be shown by those reactions for which the excess energy ΔE and hence the rate constant k_2 are small; that is, the least exothermic nucleophilic displacement reactions would be expected to exhibit the largest decrease in reaction efficiency with increasing temperature, whereas the efficiency of the proton transfer reactions would be relatively insensitive to temperature changes.

D. Publications

The results obtained in this study are being disseminated via three mechanisms: articles published in scientific journals, lectures presented at scientific conferences, and "in-house" reports submitted to AFGL. The current status of these activities is given below.

1. Publications: At this time four manuscripts have been prepared for submission to scientific journals. These manuscripts have been forwarded to Dr. John F. Paulson at AFGL for final approval before submission for publication.

a. "Translational Energy Dependence of Cross Sections for Reactions of $OH^-(H_2O)_n$ with CH_3Cl and CH_3Br," P. M. Hierl, M. J. Henchman, and J. F. Paulson (to be submitted to J. Chem. Phys.).

b. "Rate Constant and Product Distributions as Functions of Temperature for the Reaction of $OH^-(H_2O)$ with CH_3CN," P. M. Hierl, A. F. Ahrens, M. J. Henchman, and J. F. Paulson (to be submitted to J. Am. Chem. Soc.).

c "Proton Transfer as a Function of Hydration Number and Temperature: Rate Constants and Product Distributions for $OH^-(H_2O)_{0,1,2,3}$ + HF from 200-500K," P. M. Hierl, A. F. Ahrens, M. Henchman, A. A. Viggiano, and J. F. Paulson (to be sumitted to J. Am. Chem. Soc.).

8.10

d. "Nucleophilic Displacement as a Function of Hydration Number and
Temperature: Rate Constants and Product Distributions for
$OD^-(D_2O)_{0,1,2,3}$ + CH_3Cl from 200-500K," P. M. Hierl, A. F.
Ahrens, M. Henchman, A. A. Viggiano, and J. F. Paulson (to be
submitted to J. Am. Chem. Soc.).

Single copies of each of these manuscripts accompany this report.
In addition to the manuscripts listed above, four other manuscripts
reporting the findings of this study are in preparation.

2. Lectures:

a. "Effects of Temperature and Reactant Solvation upon the Rates
of Ion-Molecule Reactions," P. M. Hierl, A. F. Ahrens, M. J.
Henchman, A. A. Viggiano, and J. F. Paulson, contributed paper
presented at the 33rd Annual Conference on Mass Spectrometry
and Allied Topics, San Diego, CA, May 30, 1985.

b. "How Does Solvation Affect Reactivity?", P. M. Hierl, M. J.
Henchman, A. A. Viggiano, A. F. Ahrens, and J. F. Paulson,
invited paper presented by M. J. Henchman at the International
Conference on Chemical Kinetics, NBS, Gaithersburg, MD, June
17-19, 1985.

c. "Nucleophilic Displacement in the Gas Phase as a Function of
Temperature, Translational Energy, and Solvation Number," M.
Henchman, P. M. Hierl, and J.F. Paulson, invited paper
presented by M. J. Henchman at the National ACS Meeting,
Chicago, IL, Sept. 1985.

d. "Reactivity of Ionic Clusters as a Function of Temperature and
Cluster Size," P. M. Hierl, A. F. Ahrens, M. Henchman, A. A.

Viggiano, and J. F. Paulson, presented by M. Henchman at the Gordon Conference on Metallic Clusters, Aug. 1985.

e. "Reactivity as a Function of Solvation Number," M. J. Henchman, P. M. Hierl, and J. F. Paulson, to be presented at the National ACS Meeting, New York, NY, April, 1986.

3. Reports: A report evaluating current theories for calculating ion-polar molecule collision rate constants as functions of temperature has been submitted to Drs. M. J. Henchman and J. F. Paulson, AFGL.

REFERENCES

1. See, for example, F. C. Fehsenfeld and D. L. Albritton, in Atmospheric Water Vapor, edited by A. Deepak, T. D. Wilkerson, and L. H. Ruhnke, Academic Press, New York (1980), pp. 587-597.

2. A. A. Viggiano and J. F. Paulson, J. Chem. Phys. 79, 2241 (1983); T. M. Miller, R. E. Wetterskog, and J. F. Paulson, J. Chem. Phys. 80, 4922 (1984).

3. T. Su, E. C. F. Su, and M. T. Bowers, J. Chem. Phys. 69, 2245 (1978).

4. T. Su and W. J. Chesnavich, J. Chem. Phys. 76, 5183 (1982).

5. D. P. Ridge, "Ion Polar Molecule Capture Collision Rates: A Three Dimensional Statistical Approach," July 1984 (unpublished results).

6. D. C. Clary, Molec. Phys. 53, 3 (1984); ibid. 54, 605 (1985).

7. W. N. Olmsted and J. I. Brauman, J. Am. Chem. Soc. 99, 4219 (1977).

FIGURE CAPTIONS

Figure 1. Rate constant k at 298K vs. extent of reactant anion
solvation n for the proton transfer reactions of $OH^-(H_2O)_n$
with the hydrogen halides. The lines connecting the data
points have no significance other than serving as guides
to the eye.

Figure 2. Rate constant k at 298K vs. extent of reactant anion
solvation n for the nucleophilic displacement reactions of
$OH^-(H_2O)_n$ with the methyl halides. The lines
connecting the data points have no significance other than
serving as guides to the eye.

Figure 3. Rate constant k vs. temperature T for the proton transfer
reactions of OH^- with the hydrogen halides HF, HCl, and
HBr. The data points represent the measured reaction rate
constants and the broken lines show the collision rate
constants calculated on the basis of AADO theory for the
corresponding pair of reactants.

Figure 4. Reaction efficiency vs. temperature T for the nucleophilic
displacement reactions of OH^- with the methyl halides
CH_3Cl, CH_3Br, and CH_3I. The data points represent the
ratios of the measured reaction rate constant k to the cor-
responding collision rate constant k_T calculated on the basis
of AADO theory at the same temperature. The broken lines
have no significance other than serving as guides to the eye.

Figure 5. Same as Figure 4, but for the nucleophilic displacement reactions of $OH^- \cdot H_2O$ with the methyl halides CH_3Cl, CH_3Br, and CH_3I.

Figure 6. Schematic representation of the double-minimum model. See text for a discussion of the essential features of the model.
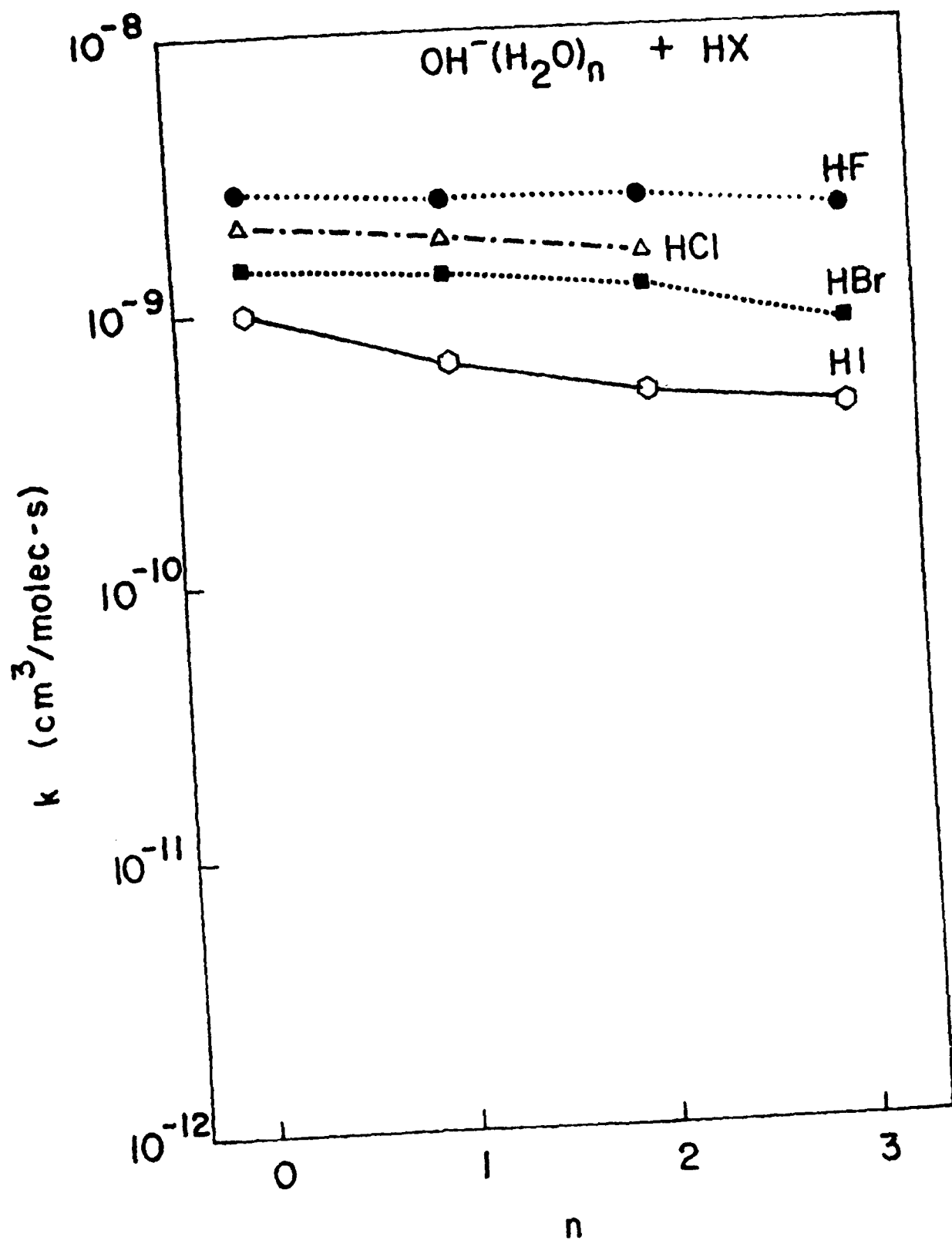
Figure 1. 8.16
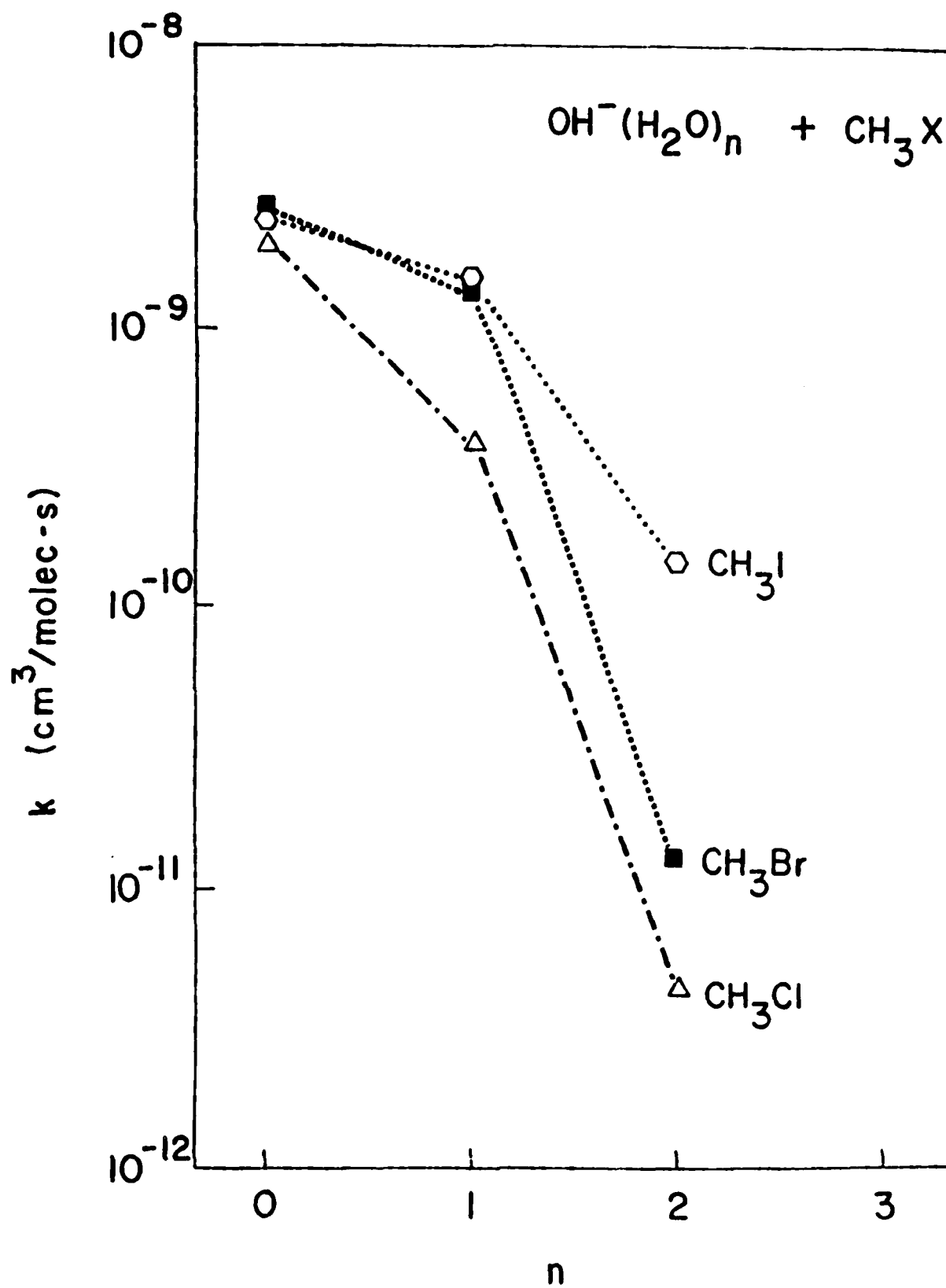
Figure 2   8.17
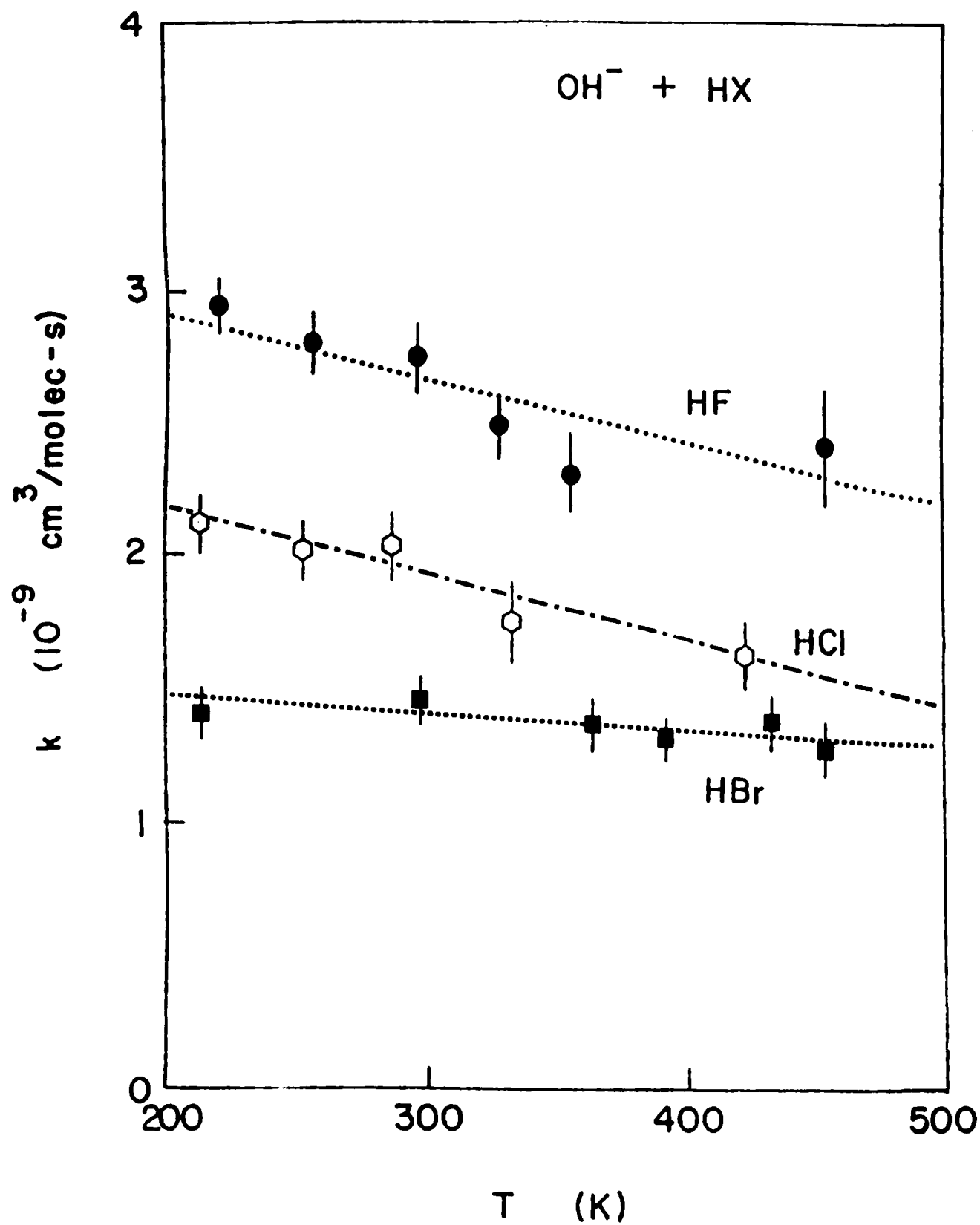
Figure 3. 8.18
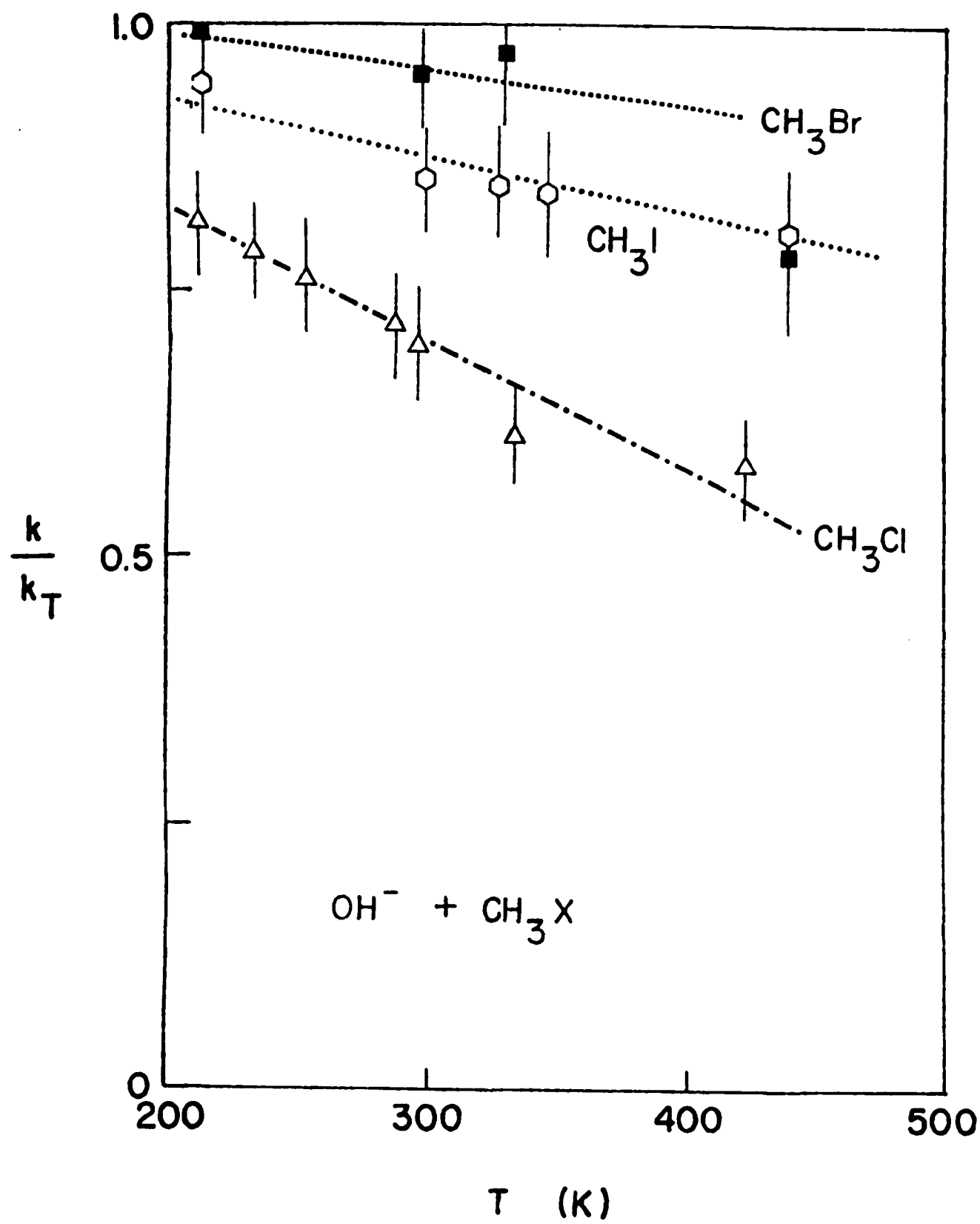
Figure 4   8.19

Figure 5   8.20

$$A^- + B \xrightleftharpoons[k_{-1}]{k_1} A^- \cdot B \xrightleftharpoons[k_{-2}]{k_2} C^- \cdot D \xrightleftharpoons[k_{-3}]{k_3} C^- + D$$
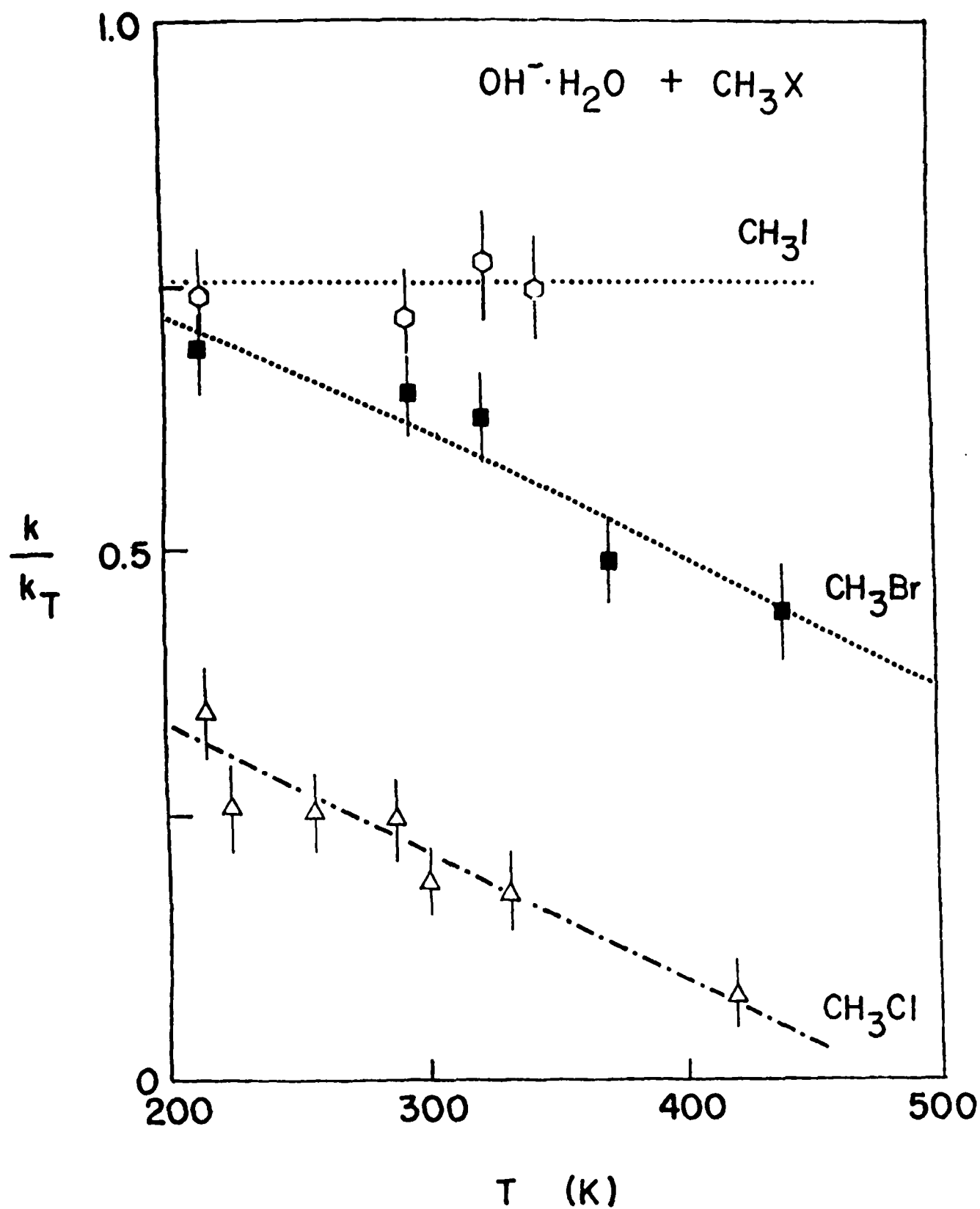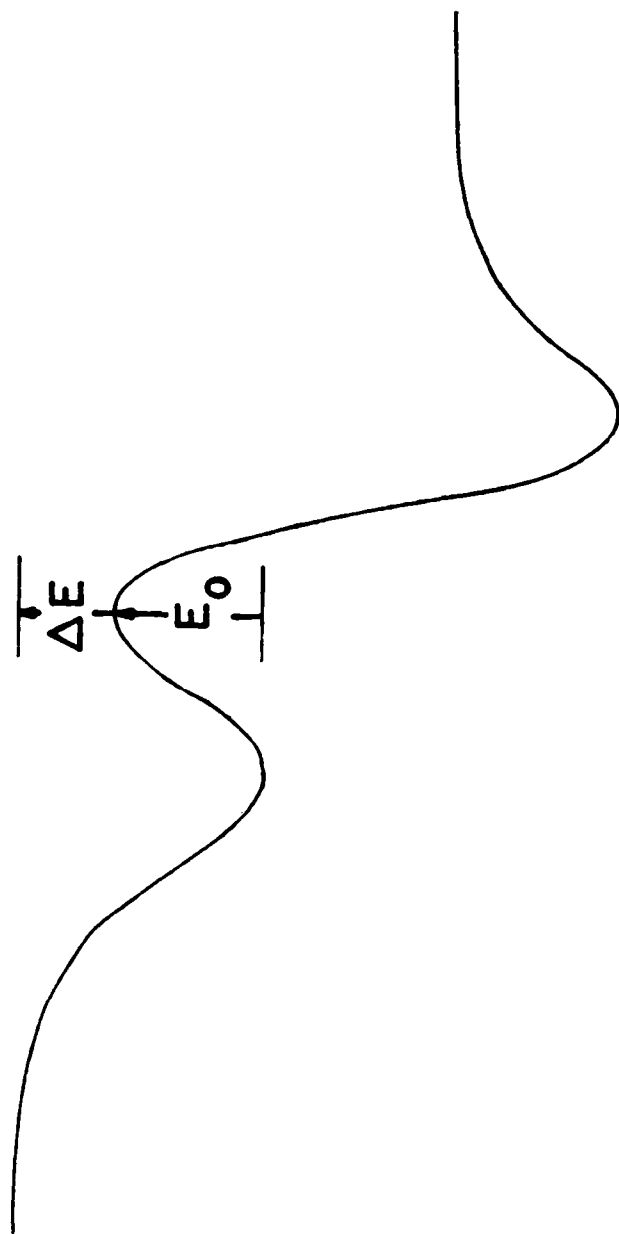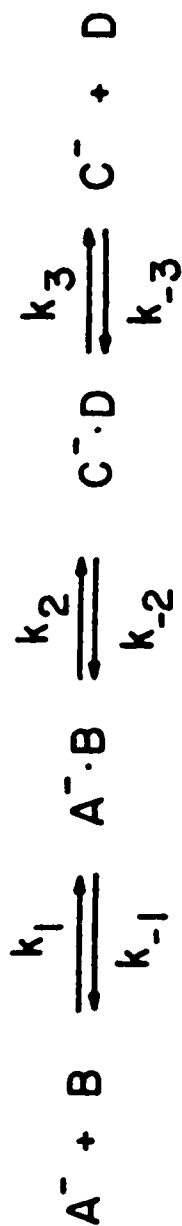
$$k = \frac{k_1 k_2 k_3}{k_{-1}(k_{-2} + k_3) + k_2 k_3} \qquad \text{if } k_3 >> k_{-2}$$

$$\cong \frac{k_2}{k_1} \frac{k_1}{k_{-1} + k_2}$$

Figure 6

8.21

EFFECTS OF NUCLEAR RADIATION ON THE OPTICAL
CHARACTERISTICS OF LASER COMPONENTS

FINAL REPORT
Subcontract No. 84 RIP 09

prepared by

Dr. Hermann J. Donnert
Professor of Nuclear Engineering

submitted to

Southeastern Center for Electrical Engineering Education
and
Air Force Office of Scientific Research

by

Kansas State University
Department of Nuclear Engineering
Ward Hall
Manhattan, Kansas 66506-7039

EFFECTS OF NUCLEAR RADIATION ON THE OPTICAL CHARACTERISTICS OF LASER COMPONENTS

ABSTRACT

In view of requirements stemming from projects under the auspices of the Strategic Defense Initiative, work has been initiated to explore the effects of nuclear radiation on the optical characteristics of laser components. Pre-irradiation tests have been conducted and samples have also been exposed to the fast-neutron environment in the beam stop of the Los Alamos Meson Physics Facility and to energetic electrons in the beam of EG&G's LINAC. Computer codes for analysis of experimental data have been developed, tested, and used to obtain preliminary results. Further experiments of relevance are in various stages of planning.

PREAMBLE

Work supported by AFOSR-SCEE Subcontract No. 84 RIP 09 has been continued under the auspices of the 1985 AFOSR-UES SFRP and GSSSP and is currently being carried on under AFOSR-UES Subcontract No. S-760-OMG-008. Therefore, the contents of this document should be viewed as an interim report with significant efforts and results yet to come in the future.

I. INTRODUCTION:

Determination of nuclear-radiation effects on the optical characteristics of laser components, such as mirrors and windows, has recently become a matter of vital interest with the scope of several projects under the auspices of the Strategic Defense Initiative (SDI). Such knowledge, at least of a phenomenological nature, is of utmost and urgent importance for the design of laser systems for anti-missile defense applications. In the long run, basic understanding of response kinetics and the concomitant ability to formulate theoretical models will be essential to harden these systems and reduce their vulnerability to hostile actions.

Based on the common knowledge of solid-state physics, energy deposition from absorption of nuclear radiation changes the microstructure of the crystal lattice and the distribution of the electrons and holes in quantum - mechanically available energy states; to complicate matters, inevitable impurities and dislocation defects are generally of profound importance. Such changes impact a variety of physical properties of the solid material, such as electrical conductivity and optical absorbance. Thus, the essential question to be answered is not whether germane effects will actually occur, but as to what their magnitude and the associated practical significance for the military systems design might be.

Except fo efforts by the author and his graduate students at FJSRL[1,2,3,4,5,6] and by researchers at Sandia National Laboratory (SNL)[7,8], virtually no significant research to explore this vital problem area had been reported. Published observations of nuclear-irradiation effects on the performance of fiber optics[9], although in themselves certainly interesting, are of exceedingly limited value in addressing the laser-component problem because the vagaries in solid-state behavior and the lack of a sound

9.4

theoretical understanding preclude any quantitatively credible scientific inference. Also, some very preliminary and limited information for dielectric coatings relating to cosmic radiation encountered by space vehicles, having been published lately[10], is of very little relevance for SDI system applications. Simply speaking, the state-of-the-art is on square one.

To conduct the investigation reported here requires diversified expertise in several scientific disciplines: radiation physics and nuclear radiation effects, solid-state physics, plasma physics, laser physics, and optics. All these necessary ingredients are within the author's repertoire of extensive research experience.

II. OBJECTIVES OF THE RESEARCH EFFORT:

The objectives of the research effort is the exploration of nuclear-irradiation effects on the laser-damage threshold of laser components to be used in military application of laser systems with strong emphasis on problems relevant to the Strategic Defense Initiative (SDI). Short-range goals are directed toward satisfying some immediate high-priority SDI requirements in a timely manner. Long range goals entail the development of theoretical models and basic understanding of the relationship between observed macrophenomena (reflectivity, absorbance, etc.) and microphenomena at the atomic and electronic scale of solid-state physics.

III. NEUTRON IRRADIATION EFFECTS

Mirrors (multiple dielectric coatings of ZrO_2 and SiO_2 on Si substrate) designed for optimum reflectivity at the I-laser wavelength $\lambda = 1.315$ μm, were exposed to fast neutrons in the beam stop of the Los Alamos Meson Physics Facility (LAMPF). The pristine-sample reflectivity $R_o = 0.99 \pm 0.01$ was reduced to $R = 0.71 \pm 0.08$ for samples subjected to a fast-neutron

fluence[11] of about 1.5×10^{22} neutrons/m^2. Further samples will be exposed to lesser fluence levels after the current modification project of the LAMPF beam-stop facility is completed. Detailed results are documented in reports by Ferrel.[12,13]

IV. EFFECTS OF ELECTRON-BEAM IRRADIATION

Mirrors (multiple dielectric coatings of Al_2O_3 and SiO_2 on fused silica substrate) designed for optimum reflectivity at the KrF-laser wavelength $\lambda = 248$ nm as well as metal-coated mirrors (200 nm Al layer on fused-silica substrate and layers of 90 nm Cu plus 200 nm Ag on fused-silica substrate) were irradiated with intense energetic-electron pulses in the beam of the electron LINAC operated by EG&G Energy Measurements, Inc. The coatings were subjected under the following nominal conditions:[14] (a) pulse duration $\tau = 20$ nm, dose rate $\dot{D} = 2.5$ krad/ns, dose $D = 50$ krad; (b) pulse duration $\tau = 20$ ns, dose rate $\dot{D} = 3.5$ krad/ns, dose $D = 70$ krad; (c) pulse duration $\tau = 45$ ns, dose rate $\dot{D} = 2.8$ krad/ns, dose $D = 126$ krad; (d) pulse duration $\tau = 200$ ns, dose rate $\dot{D} = 0.1$ krad/ns, dose $D = 20$ krad; and (e) pulse duration $\tau = 500$ ns, dose rate $\dot{D} = 0.1$ krad/ns, dose $D = 50$ krad. Reflectivity of the samples was observed during and immediately following the electron-beam pulse. Reflectivity and absorption of the samples were also measured two weeks after irradiation. Comparison of the results with values for the pristine samples reveals that the effects are very small. It should be noted that these electron irradiations give, at least qualitatively, an indication of gamma-radiation damage effects that might be anticipated. Preliminary results are documented in reports by G.W. Scronce[15] and K. A. Stroh,[16] as well as a paper presented at the 1985 Topical Meeting on High-Power-Laser Optical Components.[17]

ACKNOWLEDGEMENTS

9.7

REFERENCES

1. M.A. Ferrel, FJSRL and KSU, private communication.

2. G.W. Scronce, FJSRL and KSU, private communication.

3. K.A. Strong, FJSRL and KSU, private communication.

4. M.A. Ferrel, Final Report, 1984 USAF-SCEEE GSSSP.

5. H.J. Donnert, Final Report, 1984 USAF-SCEEE SFRP.

6. H.J. Donnert, M.A. Ferrel, and K.D. Zook, "Effects of Neutron Irradiation on the Optical Properties of Laser Mirrors," Proceedings of Topical Meeting on High-Power-Laser Optical Components, DARPA, October 18 & 19, 1984.

7. P.J. Brannon and R.A. Hamil, SNL, private communication.

8. P.J. Brannon and R.W. Morris, "Nuclear Radiation Induced Absorption in Optical Materials," SNL Report SAND84-2437, 1985.

9. D. Boucher, ed., "Optical Fibers in Adverse Environments," SPIE Report, Volume 404, 1983.

10. L.B. Fogdall, S.S. Cannaday, and T.M. Donovan, "Radiation Stability of Dielectric Coatings for HF Laser Optics," Proceedings of the High Power Laser Optical Components Meeting, 19-20 November 1981, Report AFWAL-TR-84-4152, 1984.

11. R.D. Brown, LANL, private communication.

12. M.A. Ferrel, Final Report, 1985 USAF-UES GSSSP.

13. M.A. Ferrel, "The Effects of Radiation on the Optical Characteristics of (SiO_2 + ZrO_2 Coated, Si Substrate) Mirrors, M.S. Thesis, Kansas State University, 1986.

14. P.A. Zagarino, EG&G, private communication.

15. G.W. Scronce, Final Report, 1985 USAF-UES GSSSP.

16. K.A. Stroh, Final Report, 1985 USAF-UES GSSSP.

17. H.J. Donnert, M.A. Ferrel, G.W. Scronce, and K.A. Stroh, "Radiation Effects on Reflecting Surfaces," Proceedings of the Topical Meeting on High-Power-Laser Optical Components, SDIO, October 31 & November 1, 1985.

1984 USAF-SCEEE RESEARCH INITIATION PROGRAM

Sponsored by the

AIR FORCE OFFICE OF SCIENTIFIC RESEARCH

Conducted by the

SOUTHEASTERN CENTER FOR ELECTRICAL ENGINEERING EDUCATION

FINAL REPORT

A REVIEW OF CL1PUTER SIMULATIONS FOR
AIR CRAFTDSURFACE DYNAMICS

Prepared by: Geroge R. Doyle, Jr.

A REVIEW OF COMPUTER SIMULATIONS

FOR AIRCRAFT-SURFACE DYNAMICS

by

George R. Doyle, Jr.

ABSTRACT

In recent years the United States Air Force, aerospace
companies, and universities have developed simulation techniques
to predict aircraft dynamics during ground operations, specifi-
cally taxiing over unpaved or repaired runways. These techniques
are used to determine: the strength of the airframe and landing
gears; the ability of the pilot to function in a vibratory
environment; and if sufficient thrust is available to overcome
soil drag, reach liftoff velocity, and takeoff in the available
distance. The purposes of this report are to: first, review the
computer simulations that have been developed for the prediction
of aircraft response to austere airfield surface conditions;
second, to comment on simulation techniques that could be
improved in accuracy or running time; and third, to recommend
future efforts that would improve the simulations.

I. Introduction

During the design of an aircraft heavy emphasis is placed on
flight-induced motions and loads. However, ground based
operations produce an environment that can generate significant
aircraft dynamics that could be uncomfortable to passengers, or

damaging to the cargo. In addition, high vertical accelerations in the cockpit represent a potential disorientation problem for the pilot, which may cause landing or take off accidents. Perhaps more important the aircraft structure can be subjected to large local deformations leading to stress failure, or the gears could experience loads beyond their design limits. For normal commerical aircraft and airports, ground loads (except for landing impact) should be of secondary concern. But aircrafts such as crop dusters and small private planes, which often operate from unimproved fields, experience a harsh environment during ground operations. Perhaps of greatest importance is the growing need of military aircraft to be operational from austere airfields.

Most current United States Air Force (USAF) aircraft operate on rigid, smooth, paved Main Operating Base (MOB) surfaces. In all the recent wars that the United States has been involved in, it enjoyed air superiority, and its airbases were generally well protected and operational under normal procedures. Future conflicts may, however, be fought from MOB that are vulnerable to enemy attack, and MOB surface damage or MOB denial are anticipated. Therefore, the Air Force is placing greater emphasis on aircraft-surface operations, particularly on repaired bomb damage MOB surfaces, soil and other emergency surfaces.

One effort to meet this challenge, which is presently underway in the United States is to define the rough surface capabilities of mainline fighters and cargo planes. The USAF is establishing these capabilities, through a program called HAVE BOUNCE[1] under which:

  ·Simulations are prepared for each aircraft on bomb damage
   repaired (BDR) runways.
  ·Aircraft component weaknesses are identified through
   simulation.
  ·Simulations are validated with test data.
  ·Operational limitations are developed.

   The HAVE BOUNCE program is scheduled to be completed in 1985.

A second related ongoing effort is the Soil Airfield Fighter Environment (SAFE) Program. The objectives of SAFE are to improve and validate existing techniques for predicting aircraft operations on soil, and to adapt these techniques for predictions on Alternate Launch and Recovery Surfaces (ALRS).

II. Objectives

In the past five to ten years a substantial number of computer simulations have been developed to predict aircraft-surface interaction. Many of these programs have been written by personnel in the USAF or have been contracted to various organizations by the USAF. Others have been developed by aircraft companies to meet their own needs, or by individuals at universities, or in foreign countries (most notably in NATO countries).

The objectives of this study were to review the literature concerning aircraft-surface dynamic simulation techniques: 1) to establish a historical view of the improvement in the state-of-the-art, 2) to recognize the individuals and organizations which have played a prominent roll in advancing the state-of-the-art, 3) to develop a knowledge base of physical phenomena that have been simulated, 4) to identify mathematical techniques that have been used, 5) to classify the simulations according to their general purpose, complexity, and accuracy, and 6) to suggest areas in which simulation techniques could be improved, and tests could be run to validate the simulations.

This report contains a brief summary of the computer programs that have been written to predict the dynamic displacements and forces resulting from nonflight aircraft operations. The capabilities of each program along with their limitations and numerical techniques are cited.

III Simulations

A literature search and review on aircraft-surface dynamics was conducted by Cox, et.al.[2] in 1977-78. They gave a general discussion of input characteristics for simulations, the types

of modeling techniques used, the outputs of the models, solution techniques, and the relation of automobile and rail dynamics to aircraft dynamics. Only five aircraft-surface simulation codes were mentioned. Drevet[3] developed a simulation on an analog computer to investigate aircraft takeoff. Wignot, et.al.[4] included airframe flexible degrees of freedom in a digital program to study dynamic loads during taxiing. Boozer and Butterworth[5] used a flexible aircraft with nonlinear landing gear and tire stiffnesses to study the dynamic response of a C-141A taxiing on a rough runway. A follow-on computer code by Gerardi and Lohwasser[6] increased the complexity of the gear model, but attempted to keep the simulation as simple and as versatile as possible so that any aircraft could be simulated at a reasonable cost. The previous two programs predicted the aircraft dynamics and strut forces. Kilner's[7] simulation predicted aircraft component loads in an attempt to establish acceptable BDR techniques. It is important to note that all of the above aircraft-surface programs were for pitch plane dynamics only, and that no attempt was made to model the soil as a viscoelastic element. The authors[2] also made the point that the pilot was not included in the simulations (open-loop).

Many of the aircraft-surface computer codes have been written in the past five to ten years to satisfy the HAVE BOUNCE or SAFE programs, but many computer codes, in addition to those reviewed by Cox, et. al.[2] existed prior to these major programs.

In 1962 Silsby[8] used a simple linear model to determine the power spectrum acceleration response of a rigid frame supersonic transport due to the power spectrum of runway unevenness. The aircraft had two degrees of freedom: pitch and bounce; and the undercarriages each had a vertical degree of freedom. All damping and stiffness characteristics of each strut were linear and identical. Silsby's results were strongly and inconsistently influenced by speed; but he did conclude that the acceleration response at the cockpit of a supersonic transport would be worse than that of a subsonic transport.

Tung, et.al.[9] developed a ten degree of freedom digital simulation to investigate supersonic aircraft vibrations when traversing runway intersections and other unevennesses. The model included rigid body bounce and pitch of the airframe and bounce of two landing gears, six flexural modes of a free-free airframe, and nonlinear damping and stiffness characteristics, with friction, in the struts. The equations were numerically integrated to determine the vertical acceleration of the pilot. The results indicated that supersonic aircraft, with a long slender fuselage, produce significantly higher cockpit accelerations then subsonic aircraft, and that the flexural modes greatly increased the cockpit acceleration.

Ortasse[10] suggested a different approach in constructing a deterministic runway profile with the same spectral content as several representative measured profiles. Although he discussed the importance of airframe roll and asymmetric modes, his model was pitch plane only with rigid body pitch and bounce and four symmetric flexible modes. Undercarriage nonlinearities were discussed, as were aerodynamics and structural damping. His theoretical results showed good agreement with measured data at low taxi speeds, but inaccuracy increased with speed.

Bolton, et.al.[11] developed digital and hybrid computer simulations for both deterministic and random runway input to predict undercarriage and airframe loads on the Boeing 747. Their deterministic model was three-dimensional and included the nonlinearities of the oleopneumatic* struts. Runway inputs were 1-cosine waves. The input for the random analysis was P.S.D.'s for commerical runway profiles. All loads were below the design load levels.

*Oleopneumatic implies a nonlinear force-stroke relation involving a polytropic process of compressing a gas, and a nonlinear force-stroke velocity relation involving the forcing of a hydraulic fluid through an orifice.

In 1968 Richmond, et. al.[12] developed an analog model for taxiing, and digital models for landing and takeoff, specifically to analyze a Boeing 367-80 on substandard runways. The model included three airframe rigid body modes (vertical, pitch, and roll), and three symmetric and two asymmetric airframe flexible modes. The landing gear degrees of freedom included vertical stroke and fore-aft spring back for each of three gears, and truck pitch for the two main gears—a total of sixteen degrees of freedom. The gears were oleopneumatic; the tires were non-linear springs with a point-contact follower; the soil was a nonlinear, rate sensitive spring; and the runway obstacle was modeled by 1-cosine dips or bumps.

Sharp[13] used the same test results as Richmond[12] on the Boeing 367-80 to verify a one degree of freedom simulation for C-141 and C-5 takeoffs on clay or sand airfields. Although Sharp's wheel/soil interaction was very detailed, none of the strut characteristics were included. Much of the wheel/soil interaction model was based on empirical data. Sharp used a fourth order Runge-Kutta with a variable time step for numerical integration.

Furnish and Anders[14] developed a three-demensional model of a flexible aircraft: bounce, longitudial, pitch, roll, yaw, and up to ten coupled flexible modes. The emphasis in this model was the gear, which included: polytropic air compression, velocity squared damping, variable orifice shape, snubber orifice damping, and strut friction with breakout and lockup. This model was verified by mounting an A-37B aircraft on hydraulic actuators and simulating a 1-cosine bump.

A statistical approach was used by Kirk and Perry[15,16] in which they only considered the vertical degrees of freedom of the airframe, wheel, and the first symmetric wing bending mode. The strut stiffness and damping were linearized, and the input was defined as the vertical spectral density of the runway. Transfer function techniques were used to predict RMS displacements and forces. An extension to the statistical model was made by Kirk[17] when he added the pitch rigid body mode, but he removed the

flexible mode used in his first model. Furthermore, to simplify
the analysis, he uncoupled the heave and pitch motions by
assuming that the mass/stiffness relationships of the nose and
main struts were identical. Comparsion to experimental data from
the Boeing 707 differed by 18 percent at the center of gravity
and 10 percent at the cockpit.

In his doctoral thesis Hsueh[18,19] developed time and
frequency domain simulations of the pitch plane dynamics of a
flexible aircraft during ground operations. Rigid body degrees
of freedom included fuselage bounce and pitch, and nose and main
gear bounce. Symmetic flexible modes for a free-free airframe
were also included. The tires were represented by linear
springs, and the landing gear mechanism by a parallel combination
of a nonlinear spring, a nonlinear dashpot, and a Coulomb
friction device, Aerodynamic lift was included. Numerical
integration was performed by a finite difference method.
Comparisons of the variance in vertical accelerations at the
cockpit and center of gravity, and main and nose landing gear
tire forces were made for a Boeing 707 airplane with rigid body
modes only and with the flexural modes included. The flexural
modes decreased the tire forces and the center of gravity
acceleration, but generally increased the cockpit acceleration.

A master's thesis by Corsetti[20] simulated a C-130 aircraft
with active hydraulic controllers in the struts. The analysis
was stochastic; and the performance criterion was to reduce wing
fatigue damage. Three separate models were developed with the
most complex including airframe bounce, pitch, and roll along
with wing flexibility represented by an additional spring/mass/
damper arrangement. Results showed that wing fatigue damage
would be reduced by optimizing the active controllers in the
struts.

Lynch, Dueweke, and Young[21] developed a general six degree
of freedom simulation for a rigid airframe with up to five
landing gears. The program could simulate control and performance
during glide slope, flare, landing, or takeoff, all under
conditions of winds, braking or strut or engine failure. It also

10.8

modeled ground effects, engine reversal, drag chute, carrier takeoff, inclined runways, runway perturbations, landing gear loads, and control systems. The integration technique used was a fourth order Runge-Kutta with variable step size leading to a long solution time.

Mitchell[22] developed a two-dimensional model to study the cockpit acceleration of the Concorde during taxiing. His model included the bounce and pitch rigid body modes plus the first eight symmetric modes of the airframe. The struts were modeled with nonlinear stiffness, damping, friction and stiction. Aerodynamics were included. Mitchell concluded that taxi performance could be improved by significant reductions in the stiffnesses of the struts.

Whitehead[23] presented a thesis in which he developed a two-dimensional hybrid simulation of an aircraft taxiing over deterministic runway profiles. The model assumed two rigid body (bounce and pitch) and five symmetic flexible modes for the airframe, and one bounce mode each for both the nose and main undercarriages. The gears contained nonlinear stiffness, damping, friction and stiction, and the tires were assumed to have linear stiffness and damping with point-contact. Aerodynamic lift and moment were included. Whitehead proposed an optimization technique based on ride comfort and structural fatigue to determine the undercarriage parameters. The simulation time histories were compared to Mitchell's[22] results for the Concorde for validation.

A complex three-dimensional model of aircraft dynamics on a runway was developed by Reynolds[24]. The model included symmetric and asymmetric flexible airframe modes, all the nonlinearities for any number of undercarriages, and ground effect aerodynamics. A Runge-Kutta Merson numerical integration technique was used to obtain solutions. The main results of the study was that the model was impractical because of long comuter times.

In 1975, Crenshaw[25] developed a series of five computer programs to investigate soil/wheel interaction and aircraft response during landing, taxiing, takeoff, and turning. The

first program predicted the number of passes by an aircraft over a soil before a certain rut depth was produced. The rut depth formula was based on empirical results developed by Waterways Experiment Station (WES)[26], and was only good for low-speed operation. The second program computed vertical wheel load during landing impact on a yielding surface, and the rut depth due to the vertical load and spin-up load. In this dynamic simulation the ground model was a primary soil spring in series with a secondary soil spring and viscous damper in parallel. Wheel slip and soil hardening effects were included. The airframe had two degrees of freedom (bounce and pitch) and was acted upon by aerodynamic lift and strut forces. The struts were modeled as single degree of freedom oleopneumatic elements with no bearing friction. The tires' load-deflection characteristics were nonlinear. Because of the high frequency of the unsprung mass, a fourth order Runge-Kutta integration was used. The third computer code included landing impact and runout with cyclic braking.

The fourth program developed by Crenshaw[25] simulated taxi and takeoff in the pitch plane for an aircraft with up to five landing gears. At the beginning of taxiing, static balance was achieved by iteration. Aerodynamic lift and drag, but not moment, were included, as well as thrust as a function of velocity. The same soil and landing gear models used for landing were used for the taxi and takeoff simulations, but the numerical integration technique used was a Taylor series rather than Runge-Kutta. The fifth program simulated turning, using the landing gear and soil models developed for the landing and takeoff programs. After a short taxi time the nose gear was rotated such that the wheel had both a free rolling and a skidding component. To accommodate the turning effect, two additional airframe degrees of freedom were assumed for a total of four: bounce, pitch, lateral, and yaw. Taylor series integration was also used in the turning simulation.

Durham and Murphy[27] used the U.S. Army's vehicle dynamics model to predict the pitch plane response of a C-12A on substandard

runways. Four rigid body degrees of freedom were used: body bounce and pitch, and nose and main gear bounce. The nonlinear stiffness and damping characteristics of the struts were modeled; and the tires were assumed to be clusters of radial springs.

An aircraft simulation by Gerardi and Lohwasser[6] was a pitch plane analysis of aircraft response during a takeoff roll over a runway, approximated by a third order polynomial at elevations specified every two feet. The degrees of freedom included: horizontal, pitch and vertical, and fifteen flexible modes for the airframe; and the nose and main gears' strokes. The struts were nonlinear oleopneumatic (friction neglected), but the tires were linear point-contact springs. The equations of motion were integrated using a three term Taylor series. In 1977 a roll degree of freedom was added Gerardi[28], along with 15 asymmetric airframe flexible modes, and asymmetric runway profiles.

A digital program was developed by Kilner[29] to specifically simulate the dynamics of the F-4C and F-111 aircraft taxiing over BDR runways. Somm, et.al.[30] used a modification of the program to analyze the T-43A, KC-135, and YC-14. The model simulated the bounce and pitch modes of the airframe, and the bounce of the nose and main wheels along with symmetric flexible modes (eight for the F-4C and fifteen for the F-111). Aerodynamic lift and pitching were applied, and used to calculate loads on the fuselage and wings. Strut forces included pneumatic springs, hydraulic damping, stops, and friction. Wheel drag loads were also calculated. A dynamic programing language (MIMIC) was used with FORTRAN subroutines added for initial conditions and I/O variables. A Runge-Kutta technique with automatic time step adjustment integrated the equations of motion. The simulation predictions were used to establish aircraft component failure criteria.

The general capabilities of a digital simulation used at McDonnel-Douglas is summarized by Burkhart and Wilson[31]. This time domain simulation assumed four rigid and up to ten symmetric, flexible body degrees of freedom for the airframe. Strut oleopneumatic and friction forces were modeled for up to

five flexible landing gears—each with six degrees of freedom. Thrust, braking and control surfaces could be varied based on taxiing or landing simulations. Aerodynamics and ground friction were also modeled. BDR runway profiles were simulated by ramps and constant curvature arcs. A predictor-corrector technique with a constant time step was used to numerically integrate the equations of motion. Numerous computer runs indicated potential structural problems in operating the F-4C and F-4E on BDR runways.

The "EASY" computer program is basically an analytical tool which was originally developed by Boeing to model control systems. As such, the program has many capabilities, e.g. root locus, eigenproblem, stability, etc. The code consists of modules which must be assembled in the model generation part of the program. The model is then analyzed based on the desires of the user. In 1979, "EASY" was expanded to EASY-ACLS (Air Cushion Landing System).[32] Aircraft equations of motion, various air cushion devices, and arresting gear capability were added. The model generator could select up to six rigid body degrees of freedom, thrust variations, and wind gusts. The program could simulate landing, takeoff, taxiing, and flight. Integration techniques available were Runge-Kutta (fixed or variable step), Adams/Bashforth/Moulton predictor-corrector, Euler, Heun, and Gear.

A second revision to "EASY" was made in 1980 when Warren and Kilner added an Advanced Brake Control System.[33] This new version of the program was developed to simulate aircraft-surface response during adverse weather conditions. The program included pilot input in the form of control surfaces, throttle, and brakes. Each strut had four degrees of freedom: stroke, fore-aft, lateral, and steering. The tire characteristics were nonlinear properties of displacement. The ground profile (different for each wheel) could be sinusoidal or random.

A different approach to rigid body aircraft simulation was taken by Gajewski[34] when he developed the total simulation model (bounce, pitch and roll) based on modal equations. Knowing natural frequencies, damping ratios and mode shapes, he integrated the equations of motion using the Newmark or Wilson θ method. Symmetric or asymmetric surface roughness on a rigid runway was used to excite the aircraft. The strut and tire stiffnesses were combined in series, and the wheel masses ignored.

Dawson and Larkins[35] developed a pitch plane dynamic simulation for the F-4E traversing runway irregularities including AM-2 mats. The airframe had three rigid body modes— forward, bounce, and pitch, and fifteen flexible modes for the wing, fuselage, and pylons. Each nose and main gear had a vertical mode, and the struts were oleopneumatic with rebound snubbing and friction. The tire was modeled as either a nonlinear spring with point-contact or a pneumatic membrane that enveloped surface irregularities. Thrust and aerodynamic lift, drag, and pitching moment acted at the aircraft's center of gravity, and were used to calculate loads on the wings and fuselage. This model had an unusual feature that would simulate the effect of tail scrape. An iteration process was used to balance the aircraft for initial steady state conditions, and a Runge-Kutta numerical integration with variable time steps solved the equations of motion.

A Master's thesis by eight graduate students at the Air Force Institue of Technology resulted in a three-dimensional simulation of an aircraft operating over a BDR runway[36]. The primary purpose of the simulation was to investigate one active and three passive alternatives to the current F-16 shock strut. The airframe was modeled with five rigid degrees of freedom (bounce, pitch, longitudinal, lateral, and roll), and up to twenty symmetric flexible modes. Each strut had a vertical degree of freedom and was modeled as a nonlinear spring and damper in parallel. The tire was modeled as a nonlinear spring having point-contact with the surface. The surface was assumed

to be rigid with roughness elevation modeled by algebraic or trigonometric expressions. The Adam's predictor-corrector was used to integrate the equations of motion.

A seven degree of freedom model by Ottens and Nederveen[37] was part of the Netherland's contribution to NATO's investigation of aircraft response induced by runway bumps or repairs. The model included the bounce, longitudinal, and pitch motion of the airframe, and the vertical and longitudinal motion of the nose and main gears. Landing struts were represented by oleopneumatic sliding members and a linear torsional spring. Tire stiffness was a function of deflection, and point-contact was assumed at the tire/surface interface.

Work done in Czechoslovakia by Kropac, et.al.[38] produced a frequency domain computer program that predicted the vertical vibrations of an aircraft excited by runway unevenness and propulsion forces. The results were interpreted as comfort criteria for the crew and passengers, and for structural safety. The model included five degrees of freedom: sprung mass, unspring mass, flexible body sprung mass, passenger or cargo mass, and the mass of a propulsion device. Linear elastic and damping elements were used to connect the different masses, and the tire was represented by a linear spring.

Much of England's contribution to NATO's investigation of military aircraft response on damage and repaired runways was summarized by Payne, et.al.[39,40] While their stated goal was to use relatively simple general-purpose computer programs, many important details were considered. The models contained both rigid and flexible modes for the fuselage; polytropic gas spring, velocity-squared damping, and friction/stiction in the gears; tire models; undercarriage details; and even parachute deployment. A Kutta-Merson variable step integration resulted in a significant savings in computer time compared to a fixed step. Several aircraft were modeled (Concorde, C-130, VC-10, Jaguar, etc.), and excellent correlation with measured data for low speeds was made.

An initial examination of the suitability of hand-held

programmable calculators to predict aircraft response was made by Taylor, et.at.[41] Both a TI-59 and a HP-41C were used. In particular the TI-59 was used to integrate the bounce degree of freedom of an aircraft traversing a runway repair mat. Stiffness and damping forces were linear, and a Runge-Kutta numerical integration was used. Lack of memory limited the analysis to one degree of freedom, but the gear load response correlated well with Gajewski's[34] model which also ignored wheel mass.

Cook[42] developed a computer simulation that was simple in terms of only three degrees of freedom, but complex in the tire/soil interaction. The program simulated a single rigid landing gear supporting an effective aircraft mass. The degrees of freedom were bounce, longitudinal, and wheel spin. Surface roughness was approximated by a fourth order polynomial, while soil flexibility was modeled as a nonlinear spring and damper in series. The tire was modeled as radial springs whose force dependency on displacement was quadratic. An iteration procedure was used to determine the forces in the tire and soil at each time step. Integration was performed by a Taylor series. The program could predict tire sinkage for a static aircraft, and then axle start-up loads due to thrust buildup and subsequent motion.

Due to the need for a short takeoff capability, the U.S. Navy has investigated ramp-assisted takeoff.[43] The model included bounce, pitch, and longitudinal for the airframe, and stroke for the nose and main gears. The struts were oleopneumatic, and the tires were nonlinear point-contact followers with rolling friction. Detailed aerodynamics, controlled by pilot input to control surfaces, and thrust as a function of velocity, throttle setting, and air temperature were modeled. The ramp was either circular or user-supplied. The fourth order Runge-Kutta technique was used to integrate the equations of motion. An wasteful feature of this simulation was that it integrated the lateral, yaw, and roll equations of motion even though there were no motions in those directions.

A third major modification by Skinner[44] was made to the Gerardi's simulations[6,28]. The new program was a modularization of the old ones for the purpose of making it more flexible to model any aircraft. The new program used a Newton-Raphson iteration to balance the aircraft and produce initial conditions. In addition to the Taylor series integration technique, the program could also use the Adams-Moulton predictor-corrector with a Runge-Kutta starter. Skinner's modifications included new capabilities such as simulating landing impact, a variety of landing gear geometries, and braking and aerodynamic devices such as a tailhook or drag chute.

A one-dimensional simulation of an aircraft under the actions of weight, aerodynamic lift and drag, soil drag, and thrust was developed by Phillips, et. al.[45] Although this model had only one degree of freedom (longitudinal), it did contain Cook's tire/soil model[42], which was a tire with quadratic radial springs and a damper and spring in series for the soil. The program predicted sinkage and drag during takeoff or landing on soil. It used a fourth order Runge-Kutta numerical integration with a variable time step.

Levy[45] summarized work that had been done at Fairchild Republic Company to analyze the pitch plane dynamics of the A-10 aircraft traversing both deterministic and stochastic runways or soil. The main emphasis was to study six conceptual landing gears and their effect on gear/wheel loads, ground loads, tire deflection and rut depth. The soil was modeled with a linear spring in series with a combined parallel linear spring and velocity damper. The tire was represented by "n" radial springs with quartic and cubic force-displacement functions, based on the University of Dayton model.[42] Articulated and active landing gears and anti-skid brakes were modeled. The degrees of freedom included rigid body airframe longitudinal, vertical, and pitch; wing bending and torsion; fuselage bending; stores lateral and pitch; and vertical, horizontal, and pitching of struts. Time domain studies were done with a second order Taylor series numerical integration. One interesting study was made to

determine when the multi-element tire model would yield significantly different results than a single-point tire model. Multi-element tires gave higher loads, especially for small-scale irregularities at low to moderate taxi speeds.

Crenshaw and Hollenbeck[47] developed a three-dimensional model to investigate a F-4C fighter taxiing over a surface of varying strength. In particular this simulation included turning in soil. The airframe had six, while each wheel had one, rigid body degrees of freedom. In addition, each strut had a flexible bending mode which effected the gear load, but did not effect the airframe dynamics. The strut suspensions were oleopneumatic. The tire was modeled by a point-contact follower or a distributed contact (radial springs)[42]. The soil was modeled in the vertical direction as a spring in series with a spring and damper in parallel. In the longitudinal direction a free rolling wheel with rolling drag, and in the side direction an element that included bulldozing drag and wheel skid was assumed. Due to both soil and tire flexibility, an iteration was necessary to determine soil deflection; the Method of False Position was used. The equations of motion were integrated using a fourth order Runge-Kutta, but the program has undergone modification to an Adam's predictor-corrector[48].

Cook used his previously developed[42], detailed tire/soil interaction model, and expanded it to a complete three-dimensional aircraft model[49]. The airframe had six rigid body degrees of freedom. Each of three wheels had a spin degree of freedom which included braking and slip effects; and each strut was modeled as oleopneumatic with sliding friction. The tires were modeled with quadratic radial springs, the soil with a spring and damper in series, and the surface profile with a fourth order polynomial. Pitch plane aerodynamics and thrust through the center of gravity were included. The program could be used in three modes of operation: takeoff; landing; and stop, sink, and start up. Numerical integration was performed by a Taylor series.

A more complete simulation by Taylor, et. al.[41,50] was

developed to run on an Apple II computer. The model included the
rigid body bounce, pitch, and roll degrees of freedom of the
fuselage, the bounce degree of freedom of up to five wheels, and
up to five symmetric airframe flexible modes. Gear
characteristics were represented by oleopneumatic elements, and
the tires were linear point-contact springs. Five numerical
integration techniques were available: 4th-order Runge-Kutta,
Houbolt's, Central Differences, Taylor Series, and Newmark. The
model could be used to simulate either three or five post aircraft
traversing single or double runway repair mats. This model
originally developed for an Apple II computer was made
operational on a VAX and used to investigate the response of the
F-16 to ramp inputs.

As part of the HAVE BOUNCE program, Crenshaw and Owen[51]
modified and improved existing simulations to predict C-130
aircraft dynamic response and loads when traversing AM-2 mats.
Although the program contained the airframe roll degree of
freedom, only bounce and pitch motions were simulated over
symmetric obstacles. The first eight flexible modes due to wing
bending and torsion were also used. The strut models contained the
oleopneumatic nonlinearities plus bearing friction, while the
tires were point-contact, nonlinear spring wih linear damping.
Each wheel axle had a vertical degree of freedom. Control inputs
for elevator deflection, thrust, and braking were provided.
Aerodynamic lift and moment as functions of ground speed and
aircraft altitude were a major development in the simulation. The
computer simulations were compared to test data, and the program
was modified, resulting in reasonable accuracy in peak load
predictions. The equations of motion were numerically integrated
using a fourth order Runge-Kutta.

Also as part of the HAVE BOUNCE program, Justice[52] developed
an aircraft-surface simulation for the C-141B cargo plane. The
model included four rigid body degrees of freedom for the
airframe (vertical, longitudinal, pitch, and roll) and fifteen
airframe flexible modes. The three struts were oleopneumatic
with sliding friction. Each strut also had a spring-back degree

of freedom. The tires were represented by nonlinear springs, and interacted with the ground as point-contacts. Runway roughness simulated AM-2 mat configurations by using ramps and flats or 1-cosine bumps. Pitch plane aerodynamics and thrust as a function of velocity were included. The simulation was capable of landing impact, landing and takeoff runout and taxiing. The equations of motion were numerically integrated using the Runge-Kutta Gil technique. This basic computer simulation was also used by Kent, Justice, and Vennel[53] to simulate the C-5A for the HAVE BOUNCE program.

A project recently completed by Northrop[54] was to develop a computer simulation to combine airframe structural modeling with the latest advances in tire, soil and landing gear modeling. This program was an extension of TAXIG[44] and generally applicable to any military aircraft regardless of landing gear type. Because the program was written in modules, the user can select different components to solve a particular problem, or can write his own module. The airframe had six rigid body degrees of freedom and up to fifteen flexible modes. Each gear had four degrees of freedom: three translations and one in rotation. For a multiple wheel truck, each wheel had an angular degree of freedom, which could include soil drag, rolling friction, and slip forces. The basic tire model was either a nonlinear spring with hysteretic damping or a multispring model[42]. When the wheel was yawed, cornering forces were calculated. The landing gears were oleopneumatic with friction, spin-up/spring-back, and stiction. For the soil Crenshaw's model[47] was modified. Several runway surface models were available that would allow for random elevations, various spacing of bomb damage repairs, and different forcing profiles on each wheel. Aerodynamic forces and moments due to fixed geometry and control surfaces, plus general thrust capabilities were available. Integration techniques included either a fourth order Adams-Moulton predictor-corrector, with a variable time step or a Taylor series. Simulations involved landing, takeoff, taxiing, and turning.

IV. Observations

In a comparison of the simulation techniques reviewed, it would be easy to identify some models as being more accurate for a wider variety of conditions than other models. On the other hand, some models were developed to predict special phenomena, or to simply look at relative tradeoffs. In these cases a detailed model can not be justified. However, there are several comments that can be made which apply to the general area of aircraft-surface simulation.

First, few of the simulations reviewed used a frequency domain approach in which the outputs were RMS values of vertical force or displacement. Most simulations were directed at predicting the dynamic response due to discrete events, or in the case of operations on soil, the actual peak forces generated. This emphasis leads one to believe that the general thinking was that failure to successfully launch or retrieve an aircraft depends on avoiding a catastrophic occurrance, e.g. a landing gear failure due to a single BDR. Although catastrophic events must be avoided, high cycle fatigue may also cause a landing gear failure or a structural failure of the airframe. High cycle fatigue may be due to as few as a couple dozen takeoffs and landings on an unpaved runway.

Second, several simulations considered the effect of asymmetric perturbations on the main gears. This required the introduction of extra degrees of freedom for the second main gear and also for the airframe. In most cases an airframe roll degree of freedom was added, but not a lateral degree of freedom. This constrains the aircraft to roll about its long-itudinal axis rather than translating laterally and rolling simultaneously. Although it might be argued that the effect is negligible, its significance would surely depend on the specific aircraft and the magnitude and phasing of the runway perturbations. None of the above reports attempted to justify the absence of an airframe lateral degree of freedom when the roll degree of freedom was included.

Third, many of the simulations used a point-contact at the tire/surface interface, and a few of the simulations assumed that the tire stiffness was linear. Although tire properties are not as easily specified as metallic properties, they are available, and the radial stiffness is nonlinear. Any time domain simulation attempting to predict the dynamic response due to perturbations in which the tire undergoes more than a small deflection, should model the tire stiffness as a nonlinear spring. The relative merits of using a point follower are less obvious. If the slope of the perturbation is gradual and its wavelength is long compared to the tire's footprint, a point follower is probably adequate. However, for steep, short perturbations and soil, the enveloping effect of the tire may be significant in determining the maximum forces developed.

Another phenomena associated with the tire/surface interface is the loss of runway contact of the tire due to a sharp drop off in runway elevation. Although several of the models could handle the event because they simulated actual takeoff and landing, it was not clear whether or not some of the models, which might simulate landing or takeoff runout or high speed taxiing, would allow the tire spring to expand beyond the undeformed tire radius (tension).

The last observation is in regard to the numerical integration techniques used. While fourth order Runge-Kutta was the most common, several other techniques were used, e.g., Adams predictor-corrector, Hamming predictor-corrector, Taylor series, etc. The EASY, TAXIG and Northrop simulations gave the user a choice of several techniques. Some codes used a simple Taylor series technique because the number of calculations was large, but the frequencies were low. Runge-Kutta techniques were reserved for high frequency oscillations. None of the documentation actually attempted to establish criteria for which technique should be used.

V. Conclusions

A review of dynamic simulations of aircraft-surface opera-

tions revealed a wide variety of computer programs that predicted gear loads, structural response, and soil behavior when the aircraft traversed BDR runways, or manuevered on soil. The simulation codes ranged from linear, single degree of freedom models to nonlinear three-dimensional models with flexible airframe modes. Except for a few programs, the simulations involved numerical integration and sometimes an iteration. Many of the codes had been partially validated by test data or comparison to other codes.

Based on the programs reviewed, there seemed to be less effort to consider frequency domain analysis in an attempt to predict high cycle fatique than to use time domain analysis to predict catastrophic failure, especially in the past ten years. Although some simulations included a detailed tire model, most used a point-contact to model the tire/ground interface. Lastly, several numerical integration techniques were used. Numerical instability and long running times were cited as problems by more than one author.

VI. Recommendations

Although there have been many worthwhile developments of dynamic simulations for aircraft-surface operations, there are several areas where future efforts could improve or add to present techniques. The following suggestions are given:

- Develop frequency domain simulations to determine high cycle effects.
- Improve the tire model to more accurately model the traversing of short wavelength obstacles or dips
- Determine the accuracy of using a point-contact follower for the tire/ground interface.
- Determine which numerical integration technique gives the most accurate and efficient results.
- Determine the effect of neglecting the lateral degree of freedom when an airframe roll degree of freedom is included to simulate asymmetric obstacles.

10.22

•Investigate the effect of wheel/runway loss of contact when
negotiating obstacles.

•Develop small scale and full scale testing techniques to verify
existing and future models. Some of the full scale tests could
be accomplished using only the tire or tire and strut, e.g.
better tire models or loss of contact when negotiating
obstacles.

Acknowledgements

REFERENCES

1 Gerardi, A.G., Minnetyan, L., "Status of Computer Simulations
   of USAF Aircraft and an Alternate Simulation Technique,"
   Conference Procedings No. 326, Aircraft Dynamic Response to
   Damaged and Repaired Runways, AGARD, August, 1982.

2 Cox, J.J., Jr., Henghold, W.M., Russell, J.J., "A Literature
   Search and Review of the Dynamics of Aircraft-Surface
   Interaction," CEEDO-TR-78-39, Tyndall, AFB, FL, June 1979.

3 Drevet, J., "Influence of Runway Roughness on the Dynamic
   Behavior of Aircraft at Take-off," European Space Agency
   Technical Translation-329, October, 1976.

4 Wignot, J.E., et.al., "The Development of Dynamic Taxi Design
   Procedures," FAA-DS-68-11, Aircraft Development Service,
   Washington, D.C., June, 1968.

5 Boozer, D.E., Jr., Butterworth, C.K., "C-141A Computer Code
   for Runway Roughness Studies, Volume I: Program Development,
   Volume II: Program Documentation," AFWL-TR-70-71, Kirtland
   AFB, NM, August, 1970.

6 Gerardi, A.G., Lohwasser, A.K., "Computer Program for the
   Prediction of Aircraft Response to Runway Roughness, Volume
   I: Program Development, Volume II: User's Manual," AFWL-TR-
   73-109, Kirtland AFB, NM, September, 1973.

7 Kilner, J.R., "Roughness Criteria for Bomb Damage Repair of
   Airfield Pavements," CEEDO-TR-77-50, Tyndall AFB, FL,
   September, 1977.

8 Silsby, N.S., "An Analytical Study of Effects of Some
   Airplane and Landing Gear Factors on the Response to Runway
   Roughness with Application to Supersonic Transports," NASA
   TN-1492, 1962.

9 Tung, C.C., Penzien, J., Horonjeff, R., "The Effect of Runway
   Unevenness on the Dynamic Response of Supersonic Transports,"
   NASA CR-119, 1964.

10 Ortasse, R., "Evaluation of a Method to Determine Airplane
   Taxi Loads Using a Generated Random Profile," AIAA Paper No.
   66-469, 1966.

11 Bolton, B.A., Trippett, R.J., Rogers, J.T., "Landing and Taxi
   Dynamic Loads Analysis of the Boeing Model 747 Airplane,"
   AIAA Paper No. 68-310, 1968.

12 Richmond, L.D., Brueske, N.W., De Bord, K.J., "Aircraft
   Dynamic Loads from Substandard Landing Sites," AFFDL-TR-67-
   145, 1968.

13 Sharp, A.L., "Computer Programs for the Prediction of
    Aircraft Take-off Performance on Clay and Sand Airfields,"
    AFFDL-TR-68-115, WPAFB, Ohio, April, 1969.

14 Furnish, J.F., Anders, D.E., "Analytical Simulation of
    Landing Gear Dynamics for Aircraft Design and Analysis," SAE
    710401, 1971.

15 Kirk, C.L., Perry, P.J., "Analysis of Taxiing Induced
    Vibrations in Aircraft by the P.S.D. Method," The
    Aeronautical Journal, Vol. 75, March, 1971.

16 Kirk, C.L., "The Random Heave-Pitch Response of Aircraft to
    Runway Roughness," The Aeronautical Journal, Vol. 75, July,
    1971.

17 Kirk, C.L., "Analysis of Taxiing Induced Vibrations in Air-
    craft by the Power Spectral Density Method," AFFDL-TR-72-74,
    Cranfield Inst. of Tech. (England), Jan., 1973.

· 18 Hsueh, T.M., "Stochastic Dynamic Response of Airplanes to
    Runway Unevenness," Doctoral thesis presented to the
    University of California, at Berkeley, California in 1971.

19 Hsueh, T.M., Penzien, J., "Dynamic Response of Airplanes in
    Ground Operations," Transportation Engineering Journal,
    August, 1974.

20 Corsetti, C.D., "A Study of the Practicality of Active
    Vibration Isolation Applied to Aircraft during the Taxi
    Conditions," United States Air Force Institute of Technology
    Thesis, GGC/EE/71-6, Wright Patterson AFB, Ohio.

21 Lynch, U.H., Dueweke, J.J., and Young, F.O., "Takeoff and
    Landing Analysis (TOLA) Computer Program," AFFDL-TR-71-115,
    WPAFB, Ohio, Feb., 1972.

22 Mitchell, C.G.B., "Some Measured and Calculated Effects of
    Runway Unevenness on a Supersonic Transport Aircraft,"
    Symposium of Non-linear Dynamics, Loughborough University of
    Technology, Paper C-2, March, 1972.

23 Whitehead, M.R., "The Optimisation of Aeroplane Undercarriages
    Using an Hybrid Computing Facility," Loughborough University
    of Technology, TT7414, December, 1974.

24 Reynolds, J., Thesis to Loughborough University of Tech-
    nology, 1975.

25 Crenshaw, B.M., "Development of an Analytical Technique to
   Predict Aircraft Landing Gear/Soil Interation," AFFDL-TR-74-115,
   Lockheed-Georgia, Jan., 1975.

26 Turnage, G.W., Green, A.J. Jr., "Performance of Soils Under
    Tire Loads, Report 4, Analysis of Tests in Sand from
    September, 1962 through November 1963," U.S. Army Waterways
    Experiment Station, Vicksburg, Mississippi, Feb., 1966.

27 Durham, G.N., Murphy, N.R., Jr., "Preliminary Evaluation of
    the Ability of the C-12A Aircraft to Operate Safely on
    Substandard Airstrips," WES-MP-M-76-18, Oct., 1976.

28 Gerardi, A.G., "Digital Simulation of Flexible Aircraft
    Response to Symmetrical and Asymmetrical Runway Roughness,"
    AFFDL-TR-77-37, WPAFB, Ohio, Aug., 1977.

29 Kilner, J.R., "Roughness Criteria for Bomb Damage Repair of
    Airfield Pavements," CEEDO-TR-77-50, Boeing Commercial Air-
    plane Company, October, 1977.

30 Somm, P.T., Straub, H.H., Kilner, J.R., "Adaptive Landing
    Gear for Improved Taxi Performance," AFFDL-TR-77-119, The
    Boeing Aerospace Company, October, 1977.

31 Burkhart, T.H., Wilson, E.G. Jr., "F-4 Response to Ground
    Induced Loads," CEEDO-TR-79-04, McDonnell Aircraft Company,
    June, 1979.

32 Wahi, M.K., et.al., "EASY-ACLS Dynamic Analysis," AFFDL-TR-
    79-3105, Boeing Military Airplane Development, Seattle, WA,
    Sept., 1979.

33 Warren, S.M., Kilner, J.R., "Advanced Brake Control System,"
    AFWAL-TR-80-3082, Boeing Military Airplane Development,
    Seattle, WA, Aug., 1980.

34 Gajewski, R.R., "Modal Analysis for Aircraft Response to
    Runway Surface Roughness," ESL-TR-80-32, Tyndall AFB, June 1980.

35 Dawson, K.L., Larkins,C.D., "Validation of Software for the
    Simulation of the F-4E Dynamic Response to Surface
    Roughness," ESL-TR-80-23, Boeing Military Airplane Company,
    April, 1980.

36 Cocchiarella, C.M., et.al., "Investigation of F-16 Landing
    Gear Alternatives for Operation on Repaired Bomb Damaged
    Runways," AFIT/GSE-80D, Master Thesis, Dec., 1980.

37 Ottens, H.H., Nederveen, A., "Description of a Model for Taxi
    Response Calculations of the NF-5A Aircraft," NLR-TR-81103C,
    1981.

38 Kropac, O., Spinc,J., Prochazka, M., "The Oscillation and
    Vibration of Aircraft during Ground Operations," Zpravodaj
    VZLU, Nr. 5(149), 1981, Czechoslovakia, translated by
    SCITRAN, FTD-ID(RS)T-0524-84, May, 1984.

39   Payne, B.W., Dudman, A.E., Morris, B.R., Hockenhull, M.,
     "Development of a Cost Effective Approach to Modeling
     Aircraft Response to Repaired Runways," Conference
     Proceedings No. 326, Aircraft Dynamic Response to Damaged and
     Repaired Runways, AGARD, August, 1982.

40   Payne, B.W., Dudman, A.E., Morris, B.R., "U.K. Approach to
     Aircraft Dynamic Response on Damaged and Repaired Runways,"
     AGARD Report No. 685, Aircraft Dynamic Response to Damaged
     Runways, March, 1980.

41   Taylor, R.F., McMahon, T.A., Miller, K.L., "Application of
     Small-Scale Computing Systems to Prediction of Aircraft
     Dynamic Response," AFWAL-TR-83-3014, University of Dayton
     Research Institute, March, 1983.

42   Cook, R.F., "Prediction of Aircraft Tire Sinkage and Startup,
     Takeoff, and Landing Impact Axle Loads on Rough Soil Sur-
     faces," AFWAL-TR-83-3061, University of Dayton Research
     Institute, June, 1983.

43   Clark, J.W., Jr., "CTOL Ski Jump Dynamic Analysis Model and
     Computer Program," NADC-83035-60, Naval Air Systems Command,
     June , 1983.

44   Skinner, M., et.al., "TAXIG-Modified TAXI Computer Program,"
     ESL-TR-83-32, BDM Corporation, McLean, VA, August, 1983.

45   Phillips, N.S., et.al., "Aircraft Operation on Soil
     Surfaces—Computer Routine Revisions and Improvements," ESL-
     TR-82-29, University of Dayton, August, 1983.

46   Levy, R.S., "Rough/Soft Field Landing Gear for an A-10
     Aircraft," AFWAL-TR-83-3035, Fairchild Republic Co., September,
     1983.

47   Crenshaw, B.M., Hollenbeck, W.W., "F-4C Soil Airfield Fighter
     Environment (SAFE)," AFWAL-TR-83-   , Lockheed-Georgia,
     Oct., 1983.

48   Oral Communications with Crenshaw, B.M., Lockheed-Georgia,
     July, 1984.

49   Cook, R.F., "Computer Program for Predicting Aircraft Ground
     Loads During Start-up, Take-off, and Landing on Rough Soil
     Surfaces," ESL-TR-83-   , University of Dayton Research
     Institute, Nov., 1983.

50   Taylor, R.F., "Response of the F-16 Aircraft to Ramps Using
     the PADRAS Code," UDR-TM-83-21, University of Dayton Research
     Institute, November, 1983.

51 Crenshaw, B.M., Owen, M.M., "C-130 Response to Bomb Damage-Repaired Runways," ESL-TR-82-23, Lockheed-Georgia, December, 1983.

52 Justice, R.S., "C-141 Response to Repaired Bomb-Damaged Runways," ESL-TR-81-52, Lockheed-Georgia, March, 1984.

53 Kent, J.W., Justice, R.S., Vennel, W.W., "C-5A Response to Repaired Bomb-Damaged Runways," ESL-TR-83-71, Lockheed-Georgia, July, 1983.

54 Pi, W.S., Yamane, J.R., Smith, M.J.C., "Dynamic Response of Aircraft on Rough Standard/Nonstandard Airfields," Contract F33615-82-C-3216, Northrop, April, 1985.

APPENDIX

SUMMARY FORMS: AIRCRAFT-SURFACE DYNAMICS SIMULATIONS

The following forms contain a more complete description of
the aircraft-surface dynamic simulations than given in the body
of this report. In many cases the details were incomplete
because the source of the information was lacking in those areas.
As often as possible, the actual reference was paraphrased; and
many of the comments concerning limitations and validations were
based on statements made by the original developers of the
simulations.

Program Name (Acronym): TAXI

Descriptive Title:

    Computer Program for the Prediction of Aircraft Response to Runway
Roughness

Brief Description (Capabilities):

    Pitch-plane analysis of a general aircraft response to runway profiles.
Different aircraft geometries can be input to obtain specific aircraft's
responses at the pilot station, c.g. and tail section. Program showed good
correlation to measured data.

Key Words (Categories):

    aircraft dynamic response, runway roughness, pavement smoothness,
    aircraft/pavement interaction, aircraft vertical accelerations

Author(s):   Name(s): A. G. Gerardi, and A. K. Lohwasser

                            Organization: Air Force Flight Dynamics Laboratory

                            Address: Wright-Patterson AFB, Ohio 45433

Date Written: September 1973

Program Language: FORTRAN

Software Operations: Computer(s): CDC 6600

                        Mode (batch, interactive): Batch

                        Pre- or Post-Processors: Calcomp plotting

Documentation Adequacy:

Theory:

Presented in Reference 1, outlines major areas.

User's Manual:

Flow charts and program listings, variable definitions, sample input
and output contained in Reference 1.

Other (sample problems, etc.):

Provided five examples of measured vs simulated for different
aircraft on various runways.

Model: Theoretical (number and types of equations, concepts modeled):

1) Fuselage: 3-DOF rigid body with pitch, vertical and horizontal, plus
    up to 15 flexible modes.
2) Landing Gear: Sum of tire forces and weight of unsprung mass equals
    the strut force.
    Strut bogie was modeled as a single wheel and tire. One nose gear
    and multiple main gears can be modeled.
3) Struts: Conventional or articulated and/or double acting type
    (oleopneumatic).
4) Tires: Point-contact; linear spring constant.
5) Runway: Elevations at 2-foot increments were used to fit a 3rd-order
    polynomial of surface elevation. Three elevations and the slope of
    the previous increment were used to find the constants in the
    trinomial.

Numerical Techniques (integration, iteration, interpolation, etc.):

Taylor series used for numerical integration.

Validation:

Compared experimental results with theoretical. Showed good correlation
for five different aircraft.

Input Data:

Aircraft geometries, weight, initial velocity and thrust, rotation speed, aerodynamic coefficients; main and nose gear parameters, number of struts, piston areas and other strut parameters, main and nose gear tire spring constants, integration step size, plot options, mode shapes and frequencies for the flexible body and the runway profile magnetic tape.

Output Data:

1) Time history Calcomp plot of c.g. and pilot station vertical accelerations and the runway profile traversed by the nose gear.
2) Prints main and nose gear strut strokes, strut forces, tail accelerations, pilot station and c.g. accelerations, speed, distance and time.

Limitations (assumptions, inaccuracies, peculiar problems, etc.):

Pitch-plane analysis only.
Point-contact tire model only.

Recommendations (suggested improvements):

References:

1.   Gerardi, A. G. and Lohwasser, A. K., "Computer Program for the Prediction of Aircraft Response to Runway Roughness, Vol. I, Program Development; Vol. II, User's Manual," AFWAL-TR-73-109, Ki tland AFB, NM, Sept. 1973.

Program Name (Acronym):

Descriptive Title:

   Stochastic analysis of supersonic transports on runways.

Brief Description (Capabilities):

   Based upon a stochastic analysis of aircraft dynamics on runways, it was
   concluded that acceleration responses of supersonic transports would be
   worse than subsonic transports at the cockpit.

Key Words (Categories):

   Stochastic analysis, taxiing, supersonic transport dynamics

Author(s):   Name(s): N. S. Silsby

                           Organization:

                           Address:

Date Written: 1962

Program Language:

Software Operations: Computer(s): Hybrid

                           Mode (batch, interactive):

                           Pre- or Post-Processors:

Documentation Adequacy:

    Theory:

    Model description in Reference 1.

    User's Manual:

    Other (sample problems, etc.):

Model: Teoretical (number and types of equations, concepts modeled):

1.   Rigid airframe: vertical and pitch.
2.   Under carriage: vertical.
3.   All struts had linear damping and stiffness characteristics and were identical.
4.   Tires had linear stiffness and no damping.
5.   No aerodynamics.
6.   Linear model-stochastic analysis.

    Numerical Techniques (integration, iteration, interpolation, etc.):

Validation:

Input Data:

1. Power spectrum of runway unevenness.
2. Aircraft geometry and inertias.

Output Data:

1. Power spectrum of acceleration at various points along longitudinal axis.

Limitations (assumptions, inaccuracies, peculiar problems, etc.):

Recommendations (suggested improvements):

References:

1. Silsby, N. S., "An Analytical Study of Effects of Some Airplane and Landing Gear Factors on the Response to Runway Roughness with Applications to Supersonic Transports," NASA, TN-1492, 1962.

Program Name (Acronym):

Descriptive Title;

    Dynamic response of aircraft due to runway profiles at intersections and due to uneven settlement.

Brief Description (Capabilities):

    A pitch plane nonlinear digital simulation of the flexible and rigid vibrational modes of a supersonic aircraft determined that cockpit acceleration was significantly greater than for subsonic transports, and when flexural modes were included.

Key Words (Categories):

    Aircraft runway dynamics, taxiing, runway, intersection, supersonic transport digital simulation.

Author(s):   Name(s): C. C. Tung, J. Penizen, R. Horonjeff

                            Organization:

                            Address:

Date Written: 1964

Program Language:

Software Operations: Computer(s):

                            digital

                            Mode (batch, interactive):

                            Pre- or Post-Processors:

Documentation Adequacy:

Theory:

Description in Reference 1.

User's Manual:

Other (sample problems, etc.):

Comparison of Boeing 707 and 733-94 (supersonic design) cockpit acceleration is given in Reference 1.

Model: Theoretical (number and types of equations, concepts modeled):

1. Airframe rigid: bounce and pitch.
2. Airframe flexible: six modes of free-free airframe.
3. Landing gears (2): vertical.
4. Statistical technique was discussed, but concentration of effort was in deterministic analysis.
5. Nonlinear stiffness and damping plus friction in struts.

Numerical Techniques (integration, iteration, interpolation, etc.):

Validation:

Input Data:

Runway profiles.

Output Data:

Vertical acceleration at pilots location.

Limitations (assumptions, inaccuracies, peculiar problems, etc.):

Recommendations (suggested improvements):

References:

1. Tung, C. C., Penzien, J. , Horonjeff, R., "The Effect of Runway Unevenness on the Dynamic Response of Supersonic Transports," NASA, CR-119, 1964.

Program Name (Acronym):

Descriptive Title:

    Airplane taxi loads due to a generated random runway profile.

Brief Description (Capabilities):

    A digital time domain computer simulation predicted airframe pitch plane
response traversing a deterministic runway having many spectral components.

Key Words (Categories):

    Taxiing, digital simulation, aircraft runway dynamics, random runway
profile

Author(s):   Name(s): R. Ortasse

                                   Organization:

                                   Address:

Date Written: 1966

Program Language:

Software Operations: Computer(s):

                                   Mode (batch, interactive):

                                   Pre- or Post-Processors:

Documentation Adequacy:

Theory:

Brief discussion in Reference 1.

User's Manual:

Other (sample problems, etc.):

Model: Theoretical (number and types of equations, concepts modeled):

1. Two rigid body modes: bounce and pitch.
2. Four symmetric flexible modes of airframe.
3. Anti-symmetric modes and nonlinear struts are discussed but do not appear to be in the model.
4. A theoretical deterministic runway profile was generated having the same spectral content as a number of measured random profiles.

Numerical Techniques (integration, iteration, interpolation, etc.):

Validation:

Good comparison between predicted and measured data at low taxi speeds with inaccuracy increasing with speed.

Input Data:

Output Data:

Limitations (assumptions, inaccuracies, peculiar problems, etc.):

Recommendations (suggested improvements):

References:

1. Ortasse, R., "Evaluation of a Method to Determine Airplane Taxi Loads
    Using a Generated Random Profile," AIAA Paper No. 66-469, 1966.

Program Name (Acronym):

Descriptive Title:

    Runway dynamic load analysis on Boeing 747 landing gears and airframe

Brief Description (Capabilities):

    Discrete and random runway inputs were simulated to show that the loads on the Boeing 747 were less than 75% of design load levels during taxiing on commercial runway profiles.

Key Words (Categories):

Author(s):   Name(s): B. A. Bolton, R. J. Trippett, J. T. Rogers

                               Organization: Boeing Company

                               Address:

Date Written: 1968

Program Language:

Software Operations: Computer(s):

                               digital and hybrid

                               Mode (batch, interactive):

                               Pre- or Post-Processors:

Documentation Adequacy:

Theory:

User's Manual:

Other (sample problems, etc.):

Model: Theroretical (number and types of equations, conepts modeled):

Three-dimensional model.

Nonlinear oleopneumatic struts with friction.

Runway inputs were 1-cosine bumps.

Numerical Techniques (integration, iteration, interpolation, etc.):

Both numerical integration and P.S.D. techniques were used.

Validation:

Input Data:

Output Data:

Limitations (assumptions, inaccuracies, peculiar problems, etc.):

Recommendations (suggested improvements):

References:

1.   Bolton, B. A., Trippett, R. J., Rogers, J. T., "Landing and Taxi Dynamic
      Loads Analysis of the Boeing Model 747 Airplane," AIAA Paper No. 68-310,
      1968.
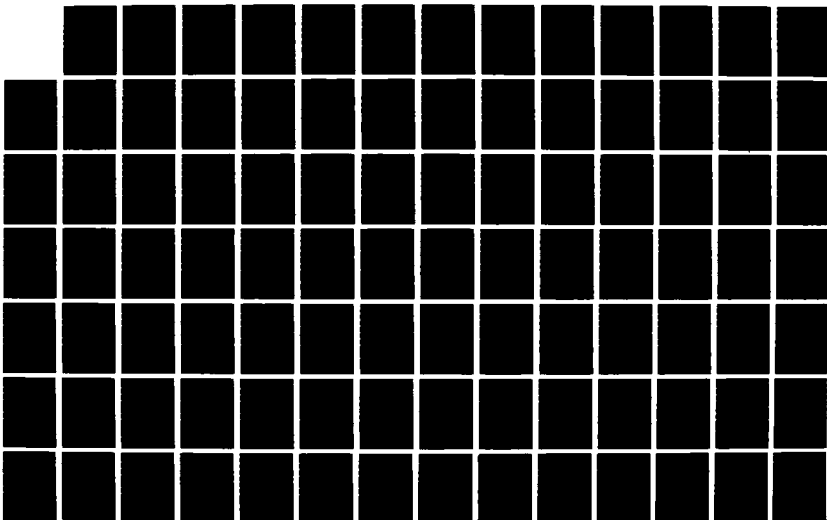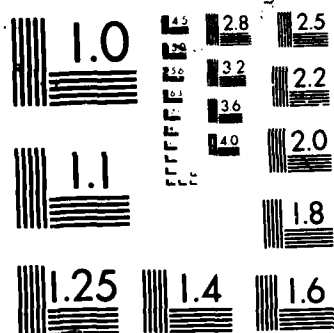
Program Name (Acronym):

Descriptive Title:

   Aircraft dynamics during taxiing, take-off and landing on soils or over
discrete obstacles.

Brief Description (Capabilities):

   Mathematical simulations were developed to predict the dynamic response
of a Boeing 367-80 on substandard runways during landing, take-off and
taxiing. Flexible aircraft modes, soil and 1-cosine bumps were modeled.
Tires were high floatation (low pressure).

Key Words (Categories):

   computer simulation, taxiing, landing, take-off, rough runways, soils,
   obstacles, sinkage

Author(s):   Name(s): L. D. Richmond, N. W. Brueske,
                                        K. S. DeBord

                              Organization: Boeing Company

                              Address: Renton, Washington

Date Written: 1968

Program Language:

Software Operations: Computer(s): Analog for taxi analysis
                                        digital for landing and take-off analysis

                          Mode (batch, interactive):

                          Pre- or Post-Processors:

Documentation Adequacy:

Theory:

Summary of theory in Reference 1.

User's Manual:

Other (sample problems, etc.):

Model: Theoretical (number and types of equations, concepts modeled):

1) Rigid body: Aircraft vertical, pitch and roll.
2) Flexible: 3 symmetric and 2 asymmetric aircraft modes.
3) Landing gear: vertical and fore-aft bending for each of 3 gears and truck pitch for 2 main gears.
4) Oleopneumatic gears.
5) Tire - nonlinear spring.
6) Soil - nonlinear, rate sensitive spring.
7) Obstacle - 1-cosine dips and bumps.

Numerical Techniques (integration, iteration, interpolation, etc.):

Validation:

Input Data:

1) Aircraft inertias and geometry.
2) Pneumatic gear properties.
3) Runway profile.
4) Tire properties.
5) Soil characteristics.
6) Runway PSD.

Output Data:

1) Time history of dynamics of c.g., pilot and tail of aircraft.
2) RMS values of dynamics.
3) Soil sinkage.
4) Probability of exceedance.

Limitations (assumptions, inaccuracies, peculiar problems, etc.)

Roll but no lateral motion.

Recommendations (suggested improvements):

References:

1. Richmond, L. D., et al., "Aircraft Dynamic Loads from Substandard Landing Sites," AFFDL-TR-67-145, Vol. 1, Part 5, 1968.

Program Name (Acronym):   TAKEOFF (Also SOLDG and SOLDG2)

Descriptive Title:

   Take-off performance on clay and sand airfields.

Brief Description (Capabilities):

   A prediction technique for determining wheel sinkage, gear drag and take-off speed on clay and sand airfields.

Key Words (Categories):

   wheel/soil interaction, aircraft take-off, sinkage

Author(s):   Name(s): Alfred L. Sharp

                         Organization: Flight Dynamics Lab

                         Address: WPAFB, Ohio

Date Written: April 1969

Program Language: FORTRAN 4

Software Operatioins: Computer(s):

                         Mode (batch, interactive): Batch

                         Pre- or Post-Processors:

Documentation Adequacy:

Theory:

Details of wheel/soil interaction discussed in References 1 and 2.

User's Manual:

Listing given in Reference 1. Variables defined in listing.

Other (sample problems, etc.):

Sample input/output given in Reference 1 for Boeing 367-80, C-141, C5.

Model: Theoretical (number and types of equations, concepts modeled):

1) Wheel/soil interaction (Drag) is based on empirical data.
2) One rigid body DOF-longitudinal.
3) 3 models
   a) SOLDG - assumes constant taxi speed, no lift or drag
   b) SOLDG2 - assumes constant taxi speed
   c) TAKEOFF - complete 1-DOF simulation.

Numerical Techniques (integration, iteration, interpolation, etc.):

Runge-Kutta integration (4th order with variable step size).

Validation:

Good agreement with Boeing 367-80 test data.

<u>Input Data</u>:

1) Aircraft weight and geometry.
2) Thrust vs velocity.
3) Tire geometry and characteristics.
4) Soil properties.

<u>Output Data</u>:

Time history of aircraft's longitudinal motion, drag and sinkage on nose and main gears.

<u>Limitations (assumptions, inaccuracies, peculiar problems, etc.)</u>:

<u>Recommendations (suggested improvements)</u>:

<u>References</u>:

1. Sharp, A. L., "Computer Programs for the Prediction of Aircraft Take-off Performance on Clay and Sand Airfields," AFFDL-TR-68-115, WPAFB, April 1969.
2. Richmond, L. D., Bruske, N. W., and DeBord, K. J., "Aircraft Dynamic Loads from Substandard Landing Sites," AFFDL-TR-67-145, 1968.

Program Name (Acronym):

Descriptive Title:

Analytical simulation of landing gear dynamics traversing a bump.

Brief Descriptive (Capabilities):

A 3-dimensional model was developed to analyze landing gears while taxiing over discrete runway bumps.

Key Words (Categories):

Landing gear, hydraulic systems, taxiing, aircraft simulation

Author(s):   Name(s): J. F. Furnish and D. E. Anders

                    Organization: Military and Twin Div.
                                       Cessna Aircraft Co.

                    Address: Wichita, Kansas

Date Written: 1971

Program Language: DSL (Digital Simulation Language)

Software Operations: Computer(s):

                        Mode (batch interactive):

                        Pre- or Post-Processors:

Documentation Adequacy:

    Theory: Summarized in Reference 1.

    User's Manual:

    Other (sample problems, etc.):

Model: Theoretical (number and types of equations, concepts modeled):

1) Rigid body 5 DOF: bounce, longitudinal, pitch, roll, and yaw.
2) Flexible model: with up to 10 coupled vibration modes.
3) Gear included: polytropic air compression, velocity squared damping, variable orifices shape, snubber orifice damping and strut friction with breakout and lockup.

    Numerical Techniques (integration, iteration, interpolation, etc.):

Validation:

    Model was verified by mounting an A-37B aircraft on hydraulic actuators and simulating a (1-cos) bump. Correlation between test and predictions were good.

Input Data:

Output Data:

    1) Aircraft dynamics.
    2) Gear dynamics and loads.

Limitations (assumptions, inaccuracies, peculiar problems, etc.):

    Roll DOF with no lateral DOF.

Recommendations (suggested improved):

References:

1.   Furnish, J. F. and Anders, D. E., "Analytical Simulation of Landing Gear
       Dynamics for Aircraft Design and Analysis," SAE 710401, 1971.

Program Name (Acronym):

Descriptive Title:

    Rigid body, pitch plane, random analysis of aircraft taxiing.

Brief Description (Capabilities):

    P.S.D. analysis of rigid body aircraft taxiing. Pitch and heave degrees
of freedom are uncoupled.

Key Words (Categories):

    Dynamic simulation, random analysis, taxiing

Author(s):   Name(s): C. L. Kirk

                      Organization:

                      Address:

Date Written: 1971

Program Language:

Software Operations: Computer(s):

                      Mode (batch, interactive):

                      Pre- or Post-Processors:

Documentation Adequacy:

    Theory:

        Brief description in Reference 1.

    User's Manual:

    Other (sample problems, etc.):

Model: Theoretical (number and types of equations, concepts modeled):

1.   2 rigid body degrees of freedom - pitch and heave.
2.   Pitch and heave motions were uncoupled by assuming that the
     mass/stiffness relationships of the nose and main struts were identical.
3.   All stiffness and damping elements were linearized for P.S.D. analysis.

    Numerical Techniques (integration, iteration, interpolation, etc.):

Validation:

    Comparison of theoretical and experimental results from a Boeing 707 at
the center of gravity and cockpit were good.

Input Data:

Output Data:

Limitations (assumptions, inaccuracies, peculiar problems, etc.):

Recommendations (suggested improvements):

References:

1. Kirk, C. L., "The Random Heave-Pitch Response of Aircraft to Runway
    Roughness," The Aeronautical Journal, Vol. 75, July 1971.

Program Name (Acronym): RMS Solution

Descriptive Title:

RMS response of a taxiing aircraft by PSD method.

Brief Description (Capabilities):

Simulation predicts the statistics of the dynamic response of an aircraft excited by a rough runway defined by a PSD.

Key Words (Categories):

Power Spectral Density (PSD), aircraft taxiing, runway roughness.

Author(s): Name(s): C. L. Kirk

Organization: Cranfield Institute of Technology

Address: Cranfield, Bedford, England

Date Written: January 1973

Program Language: FORTRAN 4

Software Operations: Computer(s): ICL 1905

Mode (batch, interactive):

Pre- or Post-Processors:

Documentation Adequacy:

Theory:

Given in Reference 1.

User's Manual:

Listing of code and flowchart in Reference 1.

Other (sample problems, etc.):

Sample input/output in Reference 1.

Model: Theoretical (number and types of equations, concepts modeled):

1) 3 linear degrees of freedom: airframe and wheel vertical and first symmetric wing bending.
2) Velocity squared damper in strut is linearized by assuming an equivalent viscous damper with equal energy dissipation.
3) Runway is represented as a PSD.

Numerical Techniques (integration, iteration, interpolation, etc.):

Calculate transfer functions and find PSD of vehicle motion as a function of PSD of runway.

Validation:

Input Data:

1) PSD of runway.
2) Aircraft and main wheel mass.
3) Strut linear stiffness and damping.

Output Data:

1) RMS displacements, velocities and accelerations of aircraft c.g., wheel, and strut.
2) RMS force in strut.
3) PSD of dynamic variables.

Limitations (assumptions, inaccuracies, peculiar problem, etc.):

No nose gear.
No pitch degree of freedom on aircraft.

Recommendation (suggested improvements):

References:

1. Kirk, C. L., "Analysis of Taxiing Induced Vibrations in Aircraft by the Power Spectral Density Method," AFFDL-TR-72-74, Jan. 1973.
2. Kirk, C. L. and Perry, P. J., "Analysis of Taxiing Induced Vibrations in Aircraft by the PSD Method," The Aeronautical Journal, Vol. 75, March 1971.

Program Name (Acronym): SANS

Descriptive Title:

Time and frequency domain simulation of pitch plane dynamics of flexible airplanes in ground operations.

Brief Description (Capabilities):

Computer programs were developed to predict dynamics and loads of a flexible aircraft in the pitch plane. Excitation was discrete runway unevenness or a spectral density of the runway.

Key Words (Categories):

aircraft ground operations, flexible aircraft modes, time domain simulation, runway spectral density, frequency domain simulation

Author(s):   Name(s): T. Hsueh and J. Penzien

                              Organization: Division of Structural Engineering and
                                             Mechanics
                                             University of California

                              Address: Berkeley, California

Date Written: 1974

Program Language: FORTRAN IV

Software Operations: Computer(s): CDC

                          Mode (batch, interactive):

                          Pre- or Post-Processors:

Documentation Adequacy:

Theory:

General description of the model is given in Reference 1. Details in Reference 2.

User's Manual:

Details in Reference 2.

Other (sample problems, etc.):

A Boeing 707 was simulated in both the time and frequency domains at 100 fps runway taxiing.

Model: Theoretical (number and types of equations, concepts modeled):

Four rigid body degrees of freedom - fuselage bounce and ptich, nose and main gear bounce.
Finite number of symmetric flexible modes of a free-free airframe.
Tires are represented by linear springs.
Landing gear mechanism is a parallel combination of a nonlinear spring, a nonlinear dashpot, and a Coulomb friction device.
Aerodynamic lift is included.

Numerical Techniques (integration, iteration, interpolation, etc.):

Finite difference method for numerical integration.

Validation:

Input Data:

Runway spectral density.

Output Data:

Time history of vertical accelerations and tire forces in time domain.
Variance of vertical accelerations and tire forces in frequency domain.

Limitations (assumptions, inaccuracies, peculiar problems, etc.):
.

Recommendations (suugested improvements):

Reference:

1. Hsueh, T. M. and Penzien J., "Dynamic Response of Airplanes in Ground
    Operations," Tarnsportations Engineering Journal, August 1974.
2. Hsueh, T. M., "Stochastic Dynamic Resoonse of Airplanes to Runway
    Unevenness," Doctoral thesis presented to the University of California,
    at Berkeley, California in 1971.

Program Name (Acronym):

Descriptive Title:

Active control in the undercarriage system to reduce wing fatigue due to runway induced vibrations during taxiing.

Brief Description (Capabilities):

A stochastic three-dimensional analysis of the C-130 with an active hydraulic controller in the strut was used to assess fatigue damage in the wing during taxiing.

Key Words (Categories):

Stochastic analysis, taxiing, aircraft dynamics, fatigue, C-130

Author(s):   Name(s): C. D. Corsetti

                       Organization: Air Force Institute of Technology

                       Address: Wright-Patterson AFB, Ohio

Date Written: 1971

Program Language:

Software Operations: Computer(s):

                        Mode (batch, interactive):

                        Pre- or Post-Processors:

Documentation Adequacy:

Theory:

Description in Reference 1.

User's Manual:

Other (sample problems, etc.):

Results showed that wing fatigue damage could be reduced by optimizing the active controller in the struts.

Model: Theoretical (number and types of equations, concepts modeled):

1. Rigid body airframe: bounce, pitch and roll.
2. Wing flexibility was simulated by an additional spring/mass/damper system.

Numerical Techniques (integration, iteration, interpolation, etc.):

Stochastic analysis.

Validation:

Input Data:

Output Data:

Limitations (assumptions, inaccuracies, peculiar problems, etc.):

Recommendations (suggested improvements):

References:

1. Corsetti, C. D., "A Study of the Practicality of Active Vibration
    Isolation Applied to Aircraft during the Taxi Conditions," United States
    Air Force Institute of Technology Thesis, GGC/EE/71-6, Wright-Patterson
    AFB.

Program Name (Acronym): TOLA (FATOLA includes flexible body modes)

Descriptive Title:

   Take-off and Landing Analysis Program

Brief Description (Capabilities):

   Program capabilities include: control and performance during glide
slope, flare, landing or take-off roll, all under conditions of winds, braking
or strut or engine failure. It also models ground effects, engine reversal,
drag chute, carrier take-off, inclined runways, runway perturbations, landing
gear loads, and control systems.

Key Words (Categories):

   Take-off, landing, ground effects, aircraft dynamics, landing gears,
   computer simulation, aircraft control

Author(s):   Name(s): V. H. Lynch, J. J. Dueweke and F. O. Young

                           Organization: Flight Dynamics Lab

                           Address: Wright-Patterson AFB, Ohio

Date Written: February 1972

Program Language: FORTRAN 4

Software Operations: Computer(s): IBM, CDC

                           Mode (batch, interactive): Batch

                           Pre- or Post-Processors: Calcomp plotting.

Documentation Adequacy:

Theory:

Very well-documented in Part 2 of Reference 1.

User's Manual:

Defines subroutines and presents flowcharts for each in Part 4. No
program lisitng given; however, the flowcharts are very detailed.

Other (sample problems, etc.):

Sample problems and selected output can be found in Part 1.

Model: Theoretical (number and types of equations, concepts modeled):

.
1) Six degrees of freedom on general rigid airframe (longitudinal,
   lateral, vertical, pitch, roll, yaw).
2) Up to five independent landing gear struts (5 DOF).
3) Tire forces depend on the vertical deflection and the coefficient of
   friction between ground and tire (which is dependent on "percent
   skid").
4) Gear bounce can be simulated.
5) Auto pilot with lag time is modeled:
   - a)   senses errors in trajectory
   - b)   defines maneuver to correct errors
   - c)   specifies magnitudes of control variables to
     achieve maneuver.

Numerical Techniques (integration, iteration, interpolation, etc.):

Runge-Kutta variable step-size integration techniques.

Validation:

Compared well with test results.

Input Data:

1) Inertia, geometric, aerodynamic, and thrust characteristics of aircraft.
2) Oleopneumatic strut and tire characteristics.
3) Control system variables.

Output Data:

1) Dynamic response of aircraft and landing gears.
2) Information on maneuver logic and autopilot.

Limitations (assumptions, inaccuracies, peculiar problems, etc.):

1) Computational time may be large due to variable step-size integration.
2) Will not predict accurate drag forces over rough terrain.

Recommendations (suggested improvements):

.

References:

1. Lynch, U. H., Dueweke, J. J. and Young, F. O., "Take-off and Landing Analysis (TOLA) Computer Program, Part I - Capabilities of the Take-off and Landing Analysis Computer Program, Feb. 1972; Part II - Problem Formulation, May 1974; Part III - Users Manual, April 1974; Part IV - Programmer's Manual," Jan. 1975, AFFDL-TR-71-155, Air Force Flight Dynamic Laboratory, Wright-Patterson AFB.

Program Name (Acronym):

Descriptive Title:

    Taxi vibrations in supersonic aircraft.

Brief Description (Capabilities):

    A two-dimensional model of the Concorde prototype was used to predict cockpit accelerations during taxiing.

Key Words (Categories):

    dynamic simulation, taxiing, Concorde

Author(s):   Name(s): C. G. B. Mitchell

                               Organization: Loughborough University of Technology

                               Address:

Date Written: 1970

Progrm Language:

Software Operations: Computer(s):

                               Mode (batch, interactive):

                               Pre- or Post-Processors:

10.70

Documentation Adequacy:

Theory:

Discussed in Reference 1.

User's Manual:

Other (sample problems, etc.):

Results indicate that stiffness of struts should be lowered to lower cockpit accelerations.

Model: Theoretical (number and types of equations, concepts modeled):

1. Rigid body airframe: bounce, pitch
2. Flexible airframe: first eight symmetric modes
3. Nonlinear stiffness, damping, friction and stiction in struts.
4. Aerodynamics applied to airframe.

Numerical Techniques (integration, iteration, interpolation, etc.);

Validation:

Fair correlation with Concorde test data.

Input Data:

Output Data:

Limitations (assumptions, inaccuracies, peculiar problems, etc.):

Recommendations (suggested improvements):

References:

1. Mitchell, C. G. B., "A Theoretical Analysis of Undercarriage Loads and Taxi Vib..tion on a Supersonic Transport Aircraft with Experimental Comparison and an Assessment of Modifications to Reduce Ground Loads," Unpublished Ministry of Technology Report, Loughborough University of Technology, 1970.
2. Mitchell, C. G. B., "Some Measured and Calculated Effects of Runway Unevenness on a Supersonic Transport Aircraft," Symposium of Nonlinear Dynamics, Loughborough University of Technology, Paper C-2, March 1972.

Program Name (Acronym):

Descriptive Title:

    Optimization of aircraft undercarriage for comfort and safety due to runway excitation.

Brief Description (Categories):

    Aircraft/runway dynamics, hybrid simulation, taxiing, flexible airframe, Concorde.

Author(s):   Name(s): M. R. Whitehead

                            Organization: Department of Transport Technology

                            Address: Loughborough University of Technology

Date Written: 1974

Program Language: April and Autocode

Software Operations: Computer(s): Hybrid

                            Digital: Ferranti Argus model 108 with 8K storage
                            Analog: SC60 and EAL TR48 each with 60 op. amps.

                            Mode (batch, interactive):

                            Pre- or Post-Processors:

                            Runway data tapes were produced on an I.C.L. 1904A
                            digital computer

<u>Documentation Adequacy</u>:

    <u>Theory</u>:

        Derivation for two-dimensional model given in Reference 1.

    <u>User's Manual</u>:

    <u>Other (sample problems, etc.)</u>:

<u>Model</u>: Theoretical (number and types of equations, concepts modeled):

1.   Rigid airframe: bounce and pitch.
2.   Flexible airframe: first five symmetric modes of free-free structure.
3.   Undercarriages: bounce of nose and main.
4.   Nonlinear stiffness, damping, friction and stiction in gears.
5.   Aerodynamic lift and drag.
6.   Inputs were measured profiles of existing runways.
7.   Tires were represented by a linear spring and damper having point contact.
8.   Rosenbrock optimization was used to determine under carriage parameters.

    <u>Numerical Techniques (integration, iteration, interpolation, etc.)</u>:

    Analog integration.

<u>Validation</u>:

1.   Predicted natural frequencies compared well with measured response.
2.   Taxi simulation on runways were correlated with an independent computer simulation.

Input Data:

Output Data:

Limitations (assumptions, inaccuracies, peculiar problems, etc.):

    .

Recommendations (suggested improvements):

References:

1. Whitehead, M. R., "The Optimization of Aeroplane Undercarriages Using
    Hybrid Computer Facilities," Department of Transport Technology,
    Loughborough University of Technology, TT7414, December 1974.

Program Name (Acronym):

Descriptive Title:

   Three-dimensional simulaton of runway induced vibrations of aircrafts.

Brief Description (Capabilities):

   A three-dimensional simulation of aircraft dynamics including flexible modes, nonlinear struts, aerodynamics, and several undercarriages predicts aircraft performance on runways.

Key Words (Categories):

   dynamic simulation, taxi, aircraft/ground vibrations, flexible aircraft

Author(s):   Name(s): J. Reynolds

                        Organization: Loughborough University of Technology

                        Address:

Date Written: 1975

Program Language:

Software Operations: Computer(s):

                        Mode (batch, interactive):

                        Pre- or Post-Processors:

10.76

Documentation Adequacy:

    Theory:

        Reference 1

    User's Manual:

    Other (sample problems, etc.):

Model: Theoretical (number and types of equations, concepts modeled):

1. Three-dimensional model of airframe and undercarriage system.
2. All the nonlinearities in the shock absorbers.
3. Any number of undercarriages.
4. Symmetric and antisymmetric flexibility of the airframe.
5. Nonlinear aerodynamics including ground effects.

    Numerical Techniques (integration, iteration, interpolaiton, etc.):

    Runge-Kutta-Merson numerical integration.

Validation:

Input Data:

Output Data:

Limitations (assumptions, inaccuracies, peculiar problems, etc.):

    Solution time proved to be impractical.

    .

Recommendations (suggested improvements):

References:

1.   Reynolds, J., Thesis to Loughborough University of Technology, 1975.

Program Name (Acronym):

Descriptive Title:

   Use of the Army's ground vehicle model to simulate an aircraft on a rough runway.

Brief Description (Capabilities):

   Pitch plane dynamics of the C-12A traversing discrete obstacles was predicted with a model developed to describe the dynamics of land vehicles.

Key Words (Categories):

   C-12A aircraft, taxiing, dynamic model

Author(s)   Names(s): G. N. Durham, N. R. Murphy, Jr.

                     Organization: U. S. Army Engineer Waterways Experiment Station

                     Address: Vicksburg, Mississippi 39180

Date Written: 1976

Program Language: Fortran

Software Operations: Computer(s):

                      Mode (batch, interactive):

                      Pre or Post-Processors:

Documentation Adequacy:

Theory:

Details in Reference 2.

User's Manual:

Details in Reference 2.

Other (sample problems, etc.):

Model: Theoretical (number and types of equations, concepts modeled):

1. Four rigid degrees of freedom: body bounce and pitch, nose and main gear
    bounce.

2. Struts: nonlinear stiffness and damping with hysteresis.

3. Tires: radial spring cluster

4. No aerodynamics

Numerical Techniques (integration, iteration, interpolation, etc.):

Validation:

Input Data:

1. Mass and pitch inertia
2. Gear masses
3. Damping and stiffness characteristics of gears
4. Aircraft/gear geometry.

Output Data:

Limitations (assumptions, inaccuracies, peculiar problems, etc.):

Recommendations (suggested improvements):

References:

1. Durham, G. N., Murphy, N. R., Jr., "Preliminary Evaluation of the Ability of the C-12A Aircraft to Operate Safely on Substandard Airstrips," WES-MP-M-76-18, October 1976.

2. Murphy, N. R., Alvin, R. B., "AMC-74 Vehicle Dyunamics Module," Technical Report M-76-1, U. S. Army, WES, January 1976.

Program Name (Acronym): TAX2

Descriptive Title:

   Dynamic response of a flexible aircraft during taxiing or take-off from asymmetrical runway profiles.

Brief Description (Capabilities):

   TAX2 simulates the dynamic response of a flexible aircraft during constant speed taxi or during take-off on rough runways. Runway elevations at each wheel are the forcing functions.

Key Words (Categories):

   Aircraft taxi, aircraft take-off, runway surface, flexible aircraft.

Author(s):   Name(s): Tony G. Gerardi

                        Organization: Air Force Flight Dynamics Laboratory

                        Address: Wright-Patterson AFB, Ohio 45433

Date Written: August 1977

Program Language: FORTRAN

Software Operations: Computer(s): CDC

                        Mode (batch, interactive): Batch

                        Pre- or Post-Processors:
                        Calcomp plotting
                        Runway profile read from a tape.

Documentation Adequacy:

Theory:

Mathematical model is detailed in Reference 1 and is summarized in Reference 2.

User's Manual:

Input data defined in Reference 2 and on computer listing output data and computer listing given in Reference 2.

Other (sample problems, etc.):

Boeing 727, AMST and C9-A taxiing on rough runway or traversing 1-cos dip, or take-off from a rough runway with and without flexible wings, and with and without roll are simulated and compared.

Model: Theoretical (number and types of equations, concepts modeled):

1) Aircraft rigid body DOF: Longitudinal, vertical, pitch, roll.
2) Aircraft flexible DOF: Up to 30 modes of vibration.
3) Landing Gear DOF: axial for each wheel-pneumatic spring/hydraulic damper.
4) Tire is modeled as a point contact with linear stiffness.
5) Runway profiles (independent) for each wheel are defined at two-foot increments.

Numerical Techniques (integration, iteration, interpolation, etc.):

1) Numerical integration: 3-term Taylor series for displacement, 2-terms for velocity.
2) Surface profile is made continuous by fitting a 3rd-order polynomial through three elevations and the slope at the end of the previous profile segment.

Validation:

Limited comparison to test data was satisfactory.

10.83

Input Data:

    1) Aircraft weight, inertias, geometry, thrust and aerodynamics.
    2) Gear weights, hydraulic and pneumatic characteristics.
    3) Tire stiffness.
    4) Flexible body mode shapes, generalized mass, modal frequency.
    5) Runway elevation.

Output Data:

    1) Landing gear deflections, runway elevations at gears.
    2) Aircraft pitch and roll displacements and accelerations.
    3) Aircraft longitudinal position and velocity.
    4) Aircraft c.g. and pilot's vertical acceleration.

Limitation (assumptions, inaccuracies, peculiar problems, etc.):

    1) Strut bearing friction force is neglected.
    2) Lateral degree of freedom is neglected, eliminating high center or
       low center roll.

Recommendations (suggested improvements):

    1) Add lateral DOF.
    2) Taylor series integration should be replaced by a better technique.
    3) Add strut bearing friction.

References:

1.   Gerardi, A. G. and Lohwasser, A. K., "Computer Program for the Prediciton
     of Aircraft Response to Runway Roughness," AFWL-TR-73-109, Vols. I and
     II, Kirtland AFB, NM, Sept. 1973.
2.   Gerardi, A. G., "Digital Simulation of Flexible Aircraft Response to
     Symmetrical and Asymmetrical Runway Roughness," AFFDL-TR-77-37, Wright-
     Patterson AFB, Ohio, Aug. 1977.

Program Name (Acronym):

Descriptive Title:

Dynamic simulation of F-4C and F-111 traversing bomb damage repaired runways.

Brief Description (Capabilities):

A digital program simulates the rigid and flexible modes of vibration of F-4C and F-111 aircraft taxiing over BDR runways.

Key Words (Categories):

Aircraft dynamic simulation, bomb damage repair, surface simulations, taxi, aircraft loads criteria.

Author(s):   Name(s): J. R. Kilner

                       Organization: Boeing Commercial Airplane Company

                       Address: P. O. Box 3707
                                 Seattle, Washington 98124

Date Written: October 1977

Program Language:

MIMIC dynamic programming language with FORTRAN subroutines to calculate initial conditions, and I/O variables.

Software Operations: Computer(s):

                          Mode (batch, interactive):

                          Pre- or Post-Processors:

<u>Documentation Adequacy</u>:

    <u>Theory</u>:

        Discussed in Reference 1.

    <u>User's Manual</u>:

    <u>Other (sample problems, etc.)</u>:

        Sample output data.
        Landing gears of the T-43A, and YC-14 were analyzed - Reference 2.

<u>Model</u>: <u>Theoretical (number and types of equations, concepts modeled)</u>:

1. Rigid Body: vertical and pitch of airframe, vertical of nose and main wheel axles.
2. Flexible airframe: eight symmetric modes for F-4C, 15 for F-111.
3. Aerodynamic lift and pitching moment is applied to the aircraft c. g.
4. Steady-state distributed aerodynamic loads are used to calculate loads on the wing and fuselage.
5. Strut forces include: pneumatic spring, hydraulic damping, stops and friction.
6. Wheel drag loads.
7. Landing gear linkage kinematics.

    <u>Numerical Techniques (integration, iteration, interpolation, etc.)</u>:

    Runge-Kutta integration with automatic time step adjustment.

<u>Validation</u>:

Input Data:

1. Terrain geometry
2. Aircraft inertia and geometry
3. Gear and tire characteristics

Output Data:

1. Shears and moments in fuselage, wing, tail and pylon
2. Vertical accelerations
3. Gear loads
4. Tire deflections

Limitations (assumptions, inaccuracies, peculiar problems, etc.):

Recommendations (suggested improvements):

References:

1. Kilner, S. R., "Roughness Criteria for Bomb Damage Repair of Airfield Pavements," CEEDO-TR-77-50, October 1977.
2. Somm, P. T.; Straub, H. H.; Kilner, J, R., " Adaptive Landing Gear for Improved Taxi Performance," AFFDL-TR-77-119.

Program Name (Acronym):

Descriptive Title:

    McDonnell-Douglas Landing and Taxi Loads Computer Program

Brief Description (Capabilities):

    Time history solution to determine landing gear and airframe loads during taxi and/or landing over runway obstacles.

Key Words (Categories):

   • Aircraft-ground dynamics, digital simulation, ground induced loads, external stores response, taxi loads, landing gear loads, flexible aircraft response

Author(s):   Name(s): T. H. Burkhart, E. G. Wilson, Jr.

                          Organization: McDonnell Aircraft Company

                          Address: P. O. Box 516
                                           St. Louis, MO   63166

Date Written: 1978

Program Language:

Software Operations: Computer(s):

                             Mode (batch, interactive):

                             Pre- or Post-Processors:

Documentation Adequacy:

Theory:

Brief description given in Reference 1.

User's Manual:

Other (sample problems, etc.):

Many time histories of loads are shown in Reference 1, some showing potential structural problems in operating the F-4C and F-4E on BDR runways.

Model: Theoretical (number and types of equations, concepts modeled):

1. Four rigid body degrees of freedom (vertical, fore-aft, pitch, roll).
2. Ten flexible aircraft modes based upon a free-free vibration in pitch plane.
3. Strut hydro-pneumatic and friction forces.
4. Aircraft aerodynamics.
5. Ground friction.
6. Thrust and control surfaces are balanced for proper landing configuration.
7. For taxi problems, thrust, control surfaces, and braking can be varied.
8. Up to five flexible landing gears with six degrees of freedom.
9. Bomb damage repair runway profiles were simulated by ramps and constant curvature arcs.

Numerical Techniques (integration, iteration, interpolation, etc.):

Predictor corrector with a constant time step.

Validation:

Acceleration response measured during taxi tests of a RF-4C correlated well with prediction of peak acceleration and frequency, but correlation was poor in damping.

Input Data:

Output Data:

   1. Time history of loads, displacements, velocities and accelerations.
   2. Tables of maximum and minimum accelerations at c.g. and pilot
      location, gear loads, and wing loads.

Limitations (assumptions, inaccuracies, peculiar problems, etc.):

   Airframe roll with no lateral degree of freedom.

Recommendations (suggested improvements):

References:

1. Burkhart, T. H. and Wilson, E. G., Jr., "F-₄ Response to Ground Induced
    Loads," CEEDO-TR-79-04, June 1979.

Program Name (Acronym): EASY-ACLS

Environmental Analysis Control System-Air Cushion Landing System

Descriptive Title:

Dynamic simulation of aircraft with Air Cushion Landing System (ACLS) using a general purpose computer program.

Brief Description (Capabilities):

EASY-ACLS simulates the dynamic response of aircraft with a variety of Air Cushion Landing System components which include aircraft flight model components, wind, engine and air flow components, inelastic-trunk and cushion, air bag skid and arresting gear model components.

Key Words (Categories):

Air Cushion Landing Systems, aircraft dynamics, arresting systems, air bag, aircraft take-off, aircraft landing, eigenproblem, stability, transfer functions, root locus, optimal control.

Aauthor(s):   Name(s): M. K. Wahi, G. S. Duleba, J. R. Kilner, and
                              P. R. Perkins

                     Organization: Boeing Military Airplane Development

                     Address: Boeing Aerospace Company
                              P. O. Box 3999
                              Seattle, WA 98124

Date Written: September 1979

Program Language: FORTRAN

Software Operations: Computer(s): CDC

                        Mode (batch, interactive): Batch

                        Pre- or Post-Processors:

1) EASY Model Generation program is a pre-compiler program which processes model description instructions to formulate the specific model.

2) Plotting of output variables.

Documentation Adequacy:

Theory:

Details given in Reference 1, Vol. I.

User's Manual:

Reference 1, User's Manual
Reference 1, Vol. II - Computer Program

Other (sample problems, etc.):

Flight, drop landing, take-off, air bag, arresting, taxiing simulations
of JINDIVIK RPV, XC-8A, and YC-14 aircraft in Reference 1, Vol. III.

Model: Theoretical (number and types of equations, concepts modeled):

1) Aircraft rigid body: 6-DOF, or 4-DOF, or 3-DOF longitudinal, or
   3-DOF lateral or 2-DOF longitudinal.
2) Engine thrust and control thrusters.
3) Wind gust.
4) Trunk and air bag models.
5) Arrestor.
6) 3-D aerodynamics.

Numerical Techniques (integration, iteration, interpolation, etc.):

Integration using: Runge-Kutta (fixed or variable step);
Adams/Bashforth/Moulton predictor-corrector, Euler, Heuns, Gear.

Validation:

1) Some good correlation with XC-8A flight simulator; Reference 1, Vol.
   III.
2) Some good and some poor correlation with XC-8A flight test data;
   Reference 1, Vol. III.

Input Data:

Before running a simulation, the user must specify the system components necesary to solve his problem. EASY will connect the components and produce a schematic that illustrates the model, input data required, and output quantities provided.

Output Data:

Limitations (assumptions, inaccuracies, peculiar problems, etc.):

1) Air cushion system unstable during take-off of XC-8A; Reference 1, Vol. III.

2) XC-8A taxiing simulation indicates a trim angle different than test data; Reference 1, Vol. III.

Recommendations (suggested improvements):

Simulation needs validation because of instability in the air cushion system, because of improper trim angle, and because of poor correlation with test data.

References:

1) Wahi, M. K., et al., "EASY-ACLS DYNAMIC ANALYSIS, Vols. I, II, III, User's Manual," AFFDL-TR-79-3105, Boeing Military Airplane Development, Seattle, Washington 98124, September 1979.

Program Name (Acronym): EASY/ABCS

Descriptive Title:

Dynamic analysis of aircraft with Advanced Brake Control System (ABCS) using a general purpose computer program.

Brief Description (Capabilities):

EASY/ABCS controls the rudder, steering and braking systems to make maximum use of ground and aerodynamic reactions to maintain control during adverse weather conditions.

Key Words (Categories):

brake control system, anti-skid system, runway veer-off, taxiing, landing, take-off, adverse weather

Author(s):   Name(s): S. M. Warren and J. R. Kilner

                        Organization: Avanced Airplane Branch
                                       Boeing Military Airplane Co.

                        Address: Seattle, WA 98124

Date Written: August 1980

Program Language: FORTRAN

Software Operations: Computer(s): CDC

                        Mode (batch, interactive): Batch

                        Pre- or Post-Processors: Same as EASY-ACLS

10.94

Documentation Adequacy:

    <u>Theory</u>:

        Reference 1

    <u>User's Manual</u>:

        Reference 1, Vol. II

    <u>Other (sample problems, etc.)</u>:

        F4E simulated in Ref. 1, Vol. I

<u>Model</u>: <u>Theoretical (number and types of equation, concepts modeled)</u>:

    1) Rigid body aircraft - nonlinear, 6 DOF.
    2) 3-D aerodynamics.
    3) Landing gear: 4 DOF - stroke, fore-aft, lateral, steering.
    4) Tire: includes lateral, longitudinal, vertical, spin, braking and
        slip as nonlinear functions of the applied forces.
    5) Ground profile: 1-cosine, or random entered in tabular form; all
        wheels can see different profiles.
    6) Pilot inputs: throttle, stabilator and brake.

<u>Numerical Techniques (integration, iteration, interpolation, etc.)</u>:

    see EASY-ACLS

<u>Validation</u>:

Input Data:

Output Data:

Limitations (assumptions, inaccuracies, peculiar problems, etc.):

Recommendations (suggested improvements):

References:

1. Warren, S. M. and Kilner, J. R., "Advanced Brake Control System, Vol. I, Vol. II," AFWAL-TR-80-3082, Boeing Military Airplane Company, Seattle, WA 98124, August 1980.

Program Name (Acronym):

Descriptive Title:

   Dynamic response of aircraft taxiing over spalls.

Brief Description (Capabilities):

   One and three DOF modal equations of motion.

Key Words (Categories):

   Taxiing, modal analysis, runway roughness, aircraft response.

Author(s):   Name(s):   R. R. Gajewski

                    Organization: Department of Engneering Mechanics
                                       United States Air Force Academy

                    Address: Colorado   80840

Date Written: June 1980

Program Language: CAL (computer analysis language)

Software Operations: Computer(s):

                        Mode (batch, interactive):

                        Pre- or Post-Processors:

Documentation Adequacy:

Theory:

Given in Reference 1.

User's Manual:

Other (sample problems, etc.):

Model: Theoretical (number and types of equations, concepts modeled):

1) Rigid body 3 DOF - bounce, pitch and roll.
2) Surface is modeled as straight line segments on a flat runway.
3) Surface spalls may be asymmetric.
4) Rigid body 1 DOF - bounce.
5) Strut and tire stiffness combined in series.

Numerical Techniques (integration, iteration, interpolation, etc.):

1) Newmark or Wilson $\ominus$ numerical integration.
2) Modal analysis - superposition.

Validation:

Good correlation with TAXI in gear loads traversing a spall with 3 DOF model.

Input Data:

Natural frequencies, damping ratios and mode shapes for 3 DOF from test data.

Output Data:

3 DOF dynamics and gear loads.

Limitations (assumptions, inaccuracies, peculiar problems, etc.):

1) Roll DOF, but no lateral.
2) Linear vibrations.
3) Wheel mass ignored.
4) Natural frequencies, damping ratios and mode shapes must be known from test data or other computer programs.

Recommendations (suggested improvements):

.

References:

1. Gajewski, R. R., "Modal Analysis for Aircraft Response to Runway Surface Roughness," ESL-TR-80-32, Tyndall AFB, June 1980.

Program Name (Acronym):   BOUNCE

Descriptive Title:

   Pitch plane dynamics of F-4E aircraft traversing runway irregularities.

Brief Description (Capabilities) :

   The F-4E was modeled with both rigid and flexible degrees-of-freedom in
the pitch plane to predict its response due to surface irregularities.
Aerodynamics, thrust, oleopneumatic struts and a nonlinear or pneumatic tire
were included.

Key Words (Categories):

   Aircraft/ground dynamics, bomb damage runway, pneumatic tire, taxiing,
flexible aircraft.

Author(s):   Name(s): K. L.Dawson, C. D. Larkins,

                           Organization: Boeing Military Airplane Company

                           Address: Seattle, Washington 98124

Date Written: April 1980

Program Language: MIMIC dynamic programming language and FORTRAN 4
subroutines

Software Operations: Computer(s): CDC

                       Mode (batch, interactive):

                       Pre- or Post-Processors:

                       Calcomp plots of time histories

Documentation Adequacy:

Theory:

Condensed version of equations and model description given in Volume 2, Reference 1.

User's Manual:

Other (sample problems, etc.):

Sample input data for F-4E

Model: Theoretical (number and types of equations, concepts modeled):

1. Aircraft rigid body: forward, bounce and pitch.
2. Aircraft flexible: first fifteen free-free modes for wing, fuselage, and pylons.
3. Nose and main gears vertical.
4. Aerodynamic lift, drag, and pitching moment at center of gravity.
5. Distributed aerodynamic loads on wings and fuselage.
6. Forward acceleration was a function of drag and thrust.
7. Struts were dual-stage pneumatic springs, hydraulic damping, rebound snubbing, and cylinder friction.
8. Tire models: a) nonlinear stiffness with point contact, b) a tire that envelopes surface irregularities.
9. Surface irregularities include AM-2 mats, cables, spalls, and curbs.
10. Tail scrape.

Numerical Techniques (integration, iteration, interpolation, etc.):

Iteration process was used to find the initial steady-state conditions. Runge-Kutta numerical integration with variable time step.

Validation:

Validations of the simulation and penumatic tire behavior in Volume 1, Reference 1.

Input Data:

       Aircraft and landing gear characteristics
       Aerodynamics and thrust
       Runway elevation
       Tire characteristics
       Pneumatic, hydraulic, friction and snubbing characteristics.

Output Data:

       Time histories of dynamics and loads.

Limitations (assumptions, inaccuracies, peculiar problems, etc.):

Recommendations (suggested improvements):

References:

1.   Dawson, K. L., Larkins, C. D., "Validation of Software for the Simulation of the F-4E Dynamic Response to Surface Roughness, Volume I: Test Versus Analysis Correlation, Volume II: Appendicies," ESL-TR-80-23, Boeing Military Airplane Company, April 1980.

Program Name (Acronym): RUNWAY

Descriptive Title:

    Simulation of aircraft dynamics and landing gear loads during operation over a repaired bomb damaged runway.

Brief Description (Capabilities):

    Surface profiles of repaired bomb craters are forcing functions on the tire and strut of the F-16 during take-off or landing operations. Alternative landing gear concepts are investigated.

.

Key Words (Categories):

    Aircraft landing or take-off, aircraft landing gear loads, bomb repaired runways, aircraft dynamic simulation.

Author(s):   Name(s):   C. M. Cocchiarella, et al.

                             Organization: Air Force Institute of Technology

                             Address: Graduate Systems Engineering
                                                  Wright-Patterson AFB, Ohio

Date Written: December 1980

Program Language: FORTRAN IV

Software Operations: Computer(s): CDC

                                 Mode (batch, interactive): Both batch and interactive

                                 Pre- or Post-Processors: Two files must be generated for input. Up to three files are used for output. Graphics program to plot 55 output variables (up to 3 per ordinate) versus time available.

Documentation Adequacy:

   Theory:

      Detailed explanations, especially of the landing gear models, given
      in Reference 1.

   User's Manual:

      Flow chart, input/output variables defined, subroutines described and
      computer listing given in Reference 1.

   Other (sample problems, etc.):

      Sample input and output given for both batch and interactive modes.
      COMMON BLOCK variables and control parameters are defined in comment
      statements in main program and each subroutine.

Model: Theoretical (number and types of equations, concepts modeled):

1) . Rigid aircraft DOF: Longitudinal, lateral, vertical, pitch, roll.
2)   Flexible aircraft DOF: 20 modes of deflection - symmetric about the
     fuselage centerline.
3)   Strut DOF: Vertical for nose and 2 main gears.
4)   Thrust and aerodynamics, including ground effects, are modeled.
5)   Rigid runway profile is modeled as an elevation based on aircraft
     position, and algebraic and trigonometric equations depending on crater
     size, upheaval, sag, etc.
6)   The strut is modeled as a nonlinear spring and nonlinear damper in
     parallel (active or passive).
7)   The tire is modeled as a nonlinear spring-point contact with surface.

   Numerical Techniques (integration, iteration, interpolation, etc.):

      Adam's predictor-corrector is used to integrate equations of motion.

Validation

      Comparison to the Edwards AFB test of a F-16 taxiing over an AM-2 mat:
   Nose gear load prediction was fair; main gear loads predictions were good
   except for a high frequency oscillation superimposed on parts of the load
   oscillation-looks like numerical instability; C.G. and gear attachment motions
   compared very well with the program.

Input Data:

1) Description of runway roughness: bomb crater width, upheaval width, sag in AM-2 mat, distances between mats, etc.
2) Aircraft and landing gears inertias.
3) Aircraft/landing gears geometry.

Output Data:

1) Runway surface elevation at gears, and C.G.
2) Displacement, velocity and acceleration of DOF.
3) Forces and moments at landing gears.

Limitations (assumptions, inaccuracies, peculiar problems, etc.):

If the aircraft flexible modes are included, both main gears must encounter similar surface profiles at the same time because all flexible modes were assumed to be symmetric.

Rigid body variables (DOF) and first derivations are contained in one array, S-dimensioned 16.

Recommendations (suggested improvements):

References:

1. Cocchiarella, C. M., et al., "Investigation of F-16 Landing Gear Alternatives for Operation on Repaired Bomb Damaged Runways," AFIT/GSE-80D, Master Thesis, December 1980.

Program Name (Acronym):

Descriptive Title:

   Pitch plane dynamics of aircraft taxiing over rigid obstacles.

Brief Description (Capabilities):

   A simple pitch plane model simulates the motion of the aircraft and landing gear loads induced by runway bumps or repairs.

Key Words (Categories):

   Aircraft Simulation, taxi, gear loads

Author(s):   Name(s):   H. H. Ottens, and A. Nederveen

                    Organization: National Aerospace Laboratory NLR

                    Address: Amsterdam, Netherlands

Date Written: 1981

Program Language: FORTRAN

Software Operations: Computer(s):

                        Mode (batch, interactive):

                        Pre- or Post-Processors):

<u>Documentation Adequacy</u>:

    <u>Theory</u>:

        Summary in Reference 1.
        Full description is given in Reference 2.

    <u>User's Manual</u>:

    <u>Other (sample problems, etc.)</u>;

<u>Model</u>: <u>Theoretical (number and types of equation, concepts modeled)</u>:

    1) 7 DOF: Vertical, longitudinal and pitch of rigid aircraft. Vertical
        and longitudinal of nose and one main gear.
    2) Landing struts are represented by linear torsional springs and an
        oleopneumatic sliding member.
    3) Tire stiffness is a function of tire pressure and deflection.
    4) Point contact for wheels.

    <u>Numerical Techniques (integration, iteration, interpolation, etc.)</u>:

<u>Validation</u>:

    Compression of nose gear, aircraft pitch angle, and aircraft vertical
acceleration predictions over a rigid bump compared well to test date.

Input Data:

1) Aircraft inertias and geometry.
2) Landing strut characteristics.
3) Tire characteristics.
4) Obstacle characteristics.

Output Data:

1) Aircraft response dynamics.
2) Strut loads.

Limitations (assumptions, inaccuracies, peculiar problems, etc.):

Recommendations (suggested improvements):

.

References:

1. Ottens, H. H., "Predicted and Measured Landing Gear Loads for the
    NF-5 Aircraft Taxiing Over a Bumpy Runway," presented at 54th
    Meeting, AGARD Structures and Materials Panel, 4-9 April 1982.
2. Ottens, H. H. and Nederveen, A., "Description of a Model for Taxi
    Response Calculations of the NF-5A Aircraft," NLR-TR-81103C, 1981.

Program Name (Acronym):

Descriptive Title:

    Frequency analysis of vertical vibrations of aircraft during ground
operations.

Brief Description (Capabilities):

    A frequency domain digital computer program simulates the vertical
vibrations of an aircraft excited by runway unevenness and propulsive
forces. The results is interpreted as comfort criteria for crew and
passengers, and for structural safety.

Key Words (Categories):

    aircraft simulation, ground operation, spectral density, vertical
    vibrations

Author(s):   Name(s): O. Kropac, J. Spinc, and M. Prochazka

                        Organization:

                        Address:

Date Written: 1981

Program Language:

Software Operations: Computer(s):

                        Mode (batch, interactive):

                        Pre- or Post-Processors:

Documentation Adequacy:

Theory:

Equations of motion are discussed and presented in Reference 1.
General discussion of author's experiences is presented.

User's Manual:

Other (sample problems, etc.):

Several figures showing input and output spectral densities are
given.

Model: Theoretical (number and types of equations, concepts modeled):

Five vertical degrees of freedom: unsprung mass; rigid body sprung mass;
flexible body sprung mass, passenger or cargo mass; mass of propulsive
device.
Linear elastic and damping elements.
Excitation is both the spectral density of the runway's unevenness and
the spectral density of the forces of vibration due to the propulsive
device.

Numerical Techniques (integration, iteration, interpolation, etc.):

Frequency domain solutions were obtained for passenger/crew accelerations
and aircraft's vertical deflections through spectral density
calculations.

Validation:

Analytical results have been verified by experimental data according to
Reference 1.

Input Data:

       Inertia components of aircraft, cargo, crew, and propulsive device.
       Linear stiffness and damping elements.
       Spectral densities of runway unevenness and propulsive forces.

Output Data:

       Maximum acceleration of cargo and crew (comfort).

Limitations (assumptions, inaccuracies, peculiar problems, etc.):

Recommendations (suggested improvements):

References:

1.   Kropac, O., Spinc, J. and Prochazka, M., "The Oscillation and Vibration of Aircraft During Ground Operations," Translation from Czechoslovakia, FTD-ID(RS)T-0524-84, May 24, 1984.

Program Name (Acronym):

Descriptive Title:

An overview of U.K.'s approach to aircraft dynamic response on damaged and repaired runways.

Brief Description (Capabilities):

Emphasis is placed on a relatively simple general purpose computer program to predict aircraft operations on damaged and repaired runways.

Key Words (Categories):

Aircraft dynamic response, repaired runways, taxiing, dynamic simulation.

Author(s):   Name(s): B. W. Payne, A. E. Dudman, B. R. Morris,
                                        and M. Hockenhull

                              Organization: British Aerospace Aircraft Group
                                             Weybridge-Bristol Divison

                              Address: Brooklands Road
                                        Weybridge
                                        Surrey KT13 OSF U.K.

Date Written: 1982

Program Language:

Software Operations: Computer(s): Mini-computer system

                              Mode (batch, interactive):

                              interactive

                              Pre- or Post-Processors:

                              Animation and plotting of time histories
                              envelopes of maximum and minimum values.

Documentation Adequacy:

    Theory:

    User's Manual:

    Other (sample problems, etc.):

    Comparison of results from a detailed model to a simplified model were good.

Model: Theoretical (number and types of equations, concepts modeled:

Several aircraft have been modeled: Concorde, C-130, VC10, Jaguar, etc. The actual model depended upon the aircraft, but the following concepts have been used.

1.   Rigid body and flexible fuselage.
2.   Polytropic gas spring, velocity-squared damping, and friction/stiction in gears.
3.   Tire models.
4.   Parachute deployment.
5.   Undercarriage details.

    Numerical Techniques (integration, iteration, interpolation, etc.):

    Kutta-Merson variable step integration resulted in a significant savings in computer time compared to a fixed step.

Validation:

    Excellent correlation of predicted gear loads with measured data for low speeds over planks (Reference 2).

Input Data:

Output Data:

Limitations (assumptions, inaccuracies, peculiar problems, etc.):

Space limitations because of mini-computers.

Recommendations (suggested improvements):

References:

1. Payne, B. W., Dudman, A. E., Morris, B. R., Hockenhull, M., "Development of a Cost Effective Approach to Modeling Aircraft Response to Repaired Runways," AGARD Conference Proceedings No. 326, August 1982.

2. Payne, B. W., Dudman, A. E., Morris, B. R., Ormerod, M., Brain C., "U.K. Approach to Aircraft Dynamic Response on Damaged and Repaired Runways," AGARD Report No. 685, March 1980.

Program Name (Acronym):

Descriptive Title:

   Bounce response of an aircraft using a hand-held calculator.

Brief Description (Capabilities):

   A TI-59 hand-held calculator is used to integrate the bounce degree-of-freedom of an aircraft traversing a runway repair mat.

Key Words (Categories):

   Aircraft response, runway repair mats, hand-held calculators.

Author(s):   Name(s): R. F. Taylor, T. A. McMahon,
                              K. L. Miller

                     Organization: University of Dayton Research
                                   Institute

                     Address: 300 College Park
                              Dayton, Ohio 45469

Date Written: November 1982

Program Language: Algebraic Operating System

Software Operation: Computer(s): TI-59 Progammable Calculator
                                  HP-41C Programmable Calculator

                     Mode (batch, interactive): interactive

                     Pre- or Post-Processors:

                     Attached to a printer, low-quality plots were
                     available

Documentation Adequacy:

Theory:

Equation of motion, mat profile, system characteristics are given in Reference 1.

User's Manual:

Vol. II

Other (sample problems, etc.):

Sample input and response to a half MAT is presented in Reference 1.

Model: Theoretical (number and types of equations, concepts modeled):

Bounce degree-of-freedom.
A single repair mat configuration with 4 slope changes.
Stiffness and damping are linear.

Numerical Techniques (integration, iteration, interpolation, etc.):

Runge-Kutta numerical integration.

Validation:

Main gear load response correlated well with Gajewski's model analysis model which also ignored wheel masses.

Input Data:

Vehicle mass
Landing gear stiffness and damping coefficient
Runway profile
Forward velocity

Output Data:

Force in main gear strut

Limitations (assumptions, inaccuracies, peculiar problems, etc.):

Lack of memory limited the analysis to one degree-of-freedom with a
single mat disturbance.

Effect of nose gear encountering obstacle and inducing a response is
ignored.

Recommendations (suggested improvements):

References:

1. Taylor, R. F., et al., "Application of Small-Scale Computing Systems to
    Prediction of Aircraft Dynamic Response, Vol. 1 - Theory and Application,
    Vol. 2 - User's Manual," AFWAL-TR-83-3014, March 1983.

Program Name (Acronym): ROUGH

Descriptive Title:

    Prediction of Aircraft Tire Sinkage and Start-up, Take-off and Landing Impact Axle Loads on Rough Soil Surfaces.

Brief Description (Capabilities):

    Simulates a single F-4C main landing gear. Uses an effective mass in place of the aircraft. Provides gear axle loads, tire sinkage and start-up axle loads for soil operations. Also gives take-off and landing impact axle loads for operation on smooth or rough surfaces.

Key Words (Categories):

        tire sinkage, landing impact, take-off, aircraft dynamics, ground operations, rough runway

Author(s):   Name(s):   Robert F. Cook

            Organization: University of Dayton Research Institute

            Address: 300 College Park Avenue
                           Dayton, Ohio 45469

Date Written: June 1983

Program Language: FORTRAN

Software Operations: Computer(s): CDC

                        Mode (batch, interactive): Batch

                        Pre- or Post-Processors: none

Documentation Adequacy:

Theory:

Documents modifications made to computer program of Reference 2. No other theory is shown or explained from that reference. Reference 1 summarizes theory.

User's Manual:

Gives program listing, flow chart, separate input and program variable listings, sample input and output, in Reference (1).

Other (sample problems, etc.):

Model: Theoretical (number and types of equations. concepts modeled):

1) 3-Degrees of freedom: translational, wheel spin-up, vertical motion.
2) Surface roughness is expressed as a fourth-order polynomial.
3) Tire model is quadratic radial springs.
4) Soil model is a spring and damper in series - both are a function of wheel velocity and tire footprint length.
5) Tire sinkage for a static aircraft and axle loads experienced at start-up are predicted.
6) No strut flexibility.

Numerical Techniques (integration, iteration, interpolation, etc.):

1) Integrates equations of motion using truncated Taylor series.
2) Iteration at each time step to determine tire/soil interface force.

Validation: Compared computed (DRAG/Fvert vs Rut/Diam) against the same ratios obtained from F-4E ground tests at McClellan AFB.[2] Computed results fell within a wide range of experimentally obtained results.

Input Data:

Thirteen lines of input data required for each mode, which include soil parameters (profile heights, strengths, etc.) and tire data (spring constants, section heights . . .).

Output Data:

Echos aircraft parameters and soil constants. Prints a table consisting of x-coordinates, vertical and drag forces, depth of rut, displacement and engine thrust.

Limitations (assumptions, inaccuracies, peculiar problems, etc.):

There is an error in the development of the equations for vertical and drag forces, with the omission of a $1/\sin\theta$ in the second-order term of the tire force/deflection equations. This results in a negligible error in the final calculations of $F_{vertical}$ and F_{drag} (approx. 1/2 of 1% for a worst case).

Recommednations (suggested improvements):

Include $1/\sin\theta$ in the tire force/deflection equations.

References:

1. Cook, R. F., "Prediction of Aircraft Tire Sinkage and Start-up, Take-Off and Landing Impact Axle Loads on Rough Soil Surfaces," AFWAL-TR-83-3061, Univ. of Dayton Research Institute, June 1983.

2. Cook, R. F., "Tire Model for Computing Axle Loads and Displacements from Short Wavelength Obstacles," UDR-TR-81-40, Univ. of Dayton, March 1981.

Program Name (Acroynym): JUMP

Descriptive Title:

Ramp-assisted (Ski Jump) take-off for conventional take-off and landing aircraft.

Brief Description (Capabilities):

The computer simulation predicts the aircraft trajectory through take-off roll, through the ramp, and during free flight.

Key Words (Categories):

Ski jump, aircraft simulation, take-off, pilot control

Author(s):   Name(s): Clark, J. W., Jr.

                              Organization: Naval Air Development Center

                              Address: Warminister, PA 18974

Date Written: June 1983

Program Language: FORTRAN 4

Software Operations: Computer(s): CDC

                              Mode (batch, interactive: Batch

                              Pre- or Post-Processors:
                              Off-line plotting of trajectory output.
                              Data file must be generated to read input
                              values.

Documentation Adequacy:

Theory:

Details outlined in Reference (1).

User's Manual:

Reference (1) defines input/output, gives a listing and defines the
use of each subroutine.

Other (sample problems, etc.):

Reference (1) gives a sample problem of a F-14A Ski-Jump take-off
along with plotted results.

Model: Theoretical (number and types of equations, concepts modeled):

1) Three rigid body DOF: longitudinal, vertical and pitch.
2) One DOF each for nose and main gears unidirectional stroke.
3) Struts include nonlinear spring and damping forces (oleopneumatic).
4) Tires include nonlinear, undamped spring force in the normal
   direction and rolling friction in tangential direction.
5) Aerodynamics is a function of angle of attack, horizontal stabilizer,
   wing flap deflections, and a ground effect.
6) Thrust is a function of aircraft velocity, throttle setting, and air
   temperature.
7) Pilot input determines control surface response.
8) Ramp: circular or user supplied.

Numerical Techniques (integration, iteration, interpolation, etc.):

1) Integration: 4th-order Runge-Kutta.
2) Uses a finite difference derivative estimation method to compute the
   aircraft stability and control derivatives.

Validation:

Good correlation of landing gear response, aircraft controllability and
take-off performance for T-2C, F-14A and F/A-18 shown in Reference (2).

Input Data:

1) Aircraft inertia, geometry, aerodynamics and thrust characteristics.
2) Gear/tire characteristics.
3) Pilot control parameters.

Output Data:

1) List of input variable values.
2) Time history of 65 trajectory parameters including aircraft dynamics,
    strut loads, aerodynamics, thrust, and pilot input.
3) 28 trajectory parameters are read to a tape for later plotting.
4) A summary of maximum/minimum values are outputted at the end of the
    run.

Limitations (assumptions, inaccuracies, peculiar problems, etc.):

1) Program integrates the lateral, roll, and yaw degrees of freedom
    unnecessarily.
2) Program jumps in and out of integration subroutine five times for
    each first-order differential equation to be integrated.

Recommendations (suggested improvements):

1) Eliminate extra degrees-of-freedom to reduce costs.
2) Simplify numerical integration routine.

References:

1. Clark, J. W., Jr., "CTOL Ski Jump Dynamic Analysis Model and Computer
    Program," NADC-83035-60, Naval Air Systems Command, June 1, 1983.
2. Clark, J. W., Jr. and Walters, M. M., "CTOL Ski Jump Analysis,
    Simulation, and Flight Test Results: T-2C and F-14A Aircraft," NADC
    Report (in preparation).

Program Name (Acronym): TAXIG

Descriptive Title:

Dynamic Response of a Flexible Aircraft Over Irregular Rigid Surfaces.

Brief Description (capabilities):

TAXIG simulates the dynamic response of a flexible aircraft operating on a rough runway. Its capabilities include irregular surface elevations, aerodynamics, thrust, thrust reverse, braking, drag chute, tailhook, hydraulic, pneumatic and friction forces in the nose and two main gear struts, landing impact.

Key Words (Categories):

Aircraft taxi, surface roughness, flexible aircraft, dynamic simulation, oleopneumatic struts, landing.

Author(s):   Name(s): Skinner, M., et al.

                              Organization: BDM Corporation

                              Address: 7915 Jones Branch Drive
                                        McLean, Virginia 22102

Date Written: August 1983

Program Language: FORTRAN 5

Software Operations: Computer(s): CDC, VAX

                              Mode (batch, interactive): Batch

                              Pre- or Post-Processors:
                              data is written to a file for later plotting

Documentation Adequacy:

Theory: Outline of theoretical developments given in Reference (1),
Volume I.

User's Manual: Variable definitions, input/output sample in Reference
(1), Volume I, Program Listing in Reference 1, Volume II.

Other (sample problems, etc.):

Model: Theoretical (number and types of equations, concepts modeled):

1) Aircraft Rigid Body DOF: Longitudinal, vertical, pitch, roll.
2) Aircraft Flexible DOF: Up to 15 bending modes for fuselage, up to 20
   lumped masses for wing bending and torsion.
3) Landing Gear DOF: axial for nose, main right and main left
   (polytropic pneumatic spring, friction, hydraulic damper).
4) Tires: Point contact.

Numerical Techniques (integration, iteration, interpolation, etc.):

Program is structured, making it easy to remove, replace or amend one
subroutine at a time. Newton-Raphson iteration method is used to balance
aircraft to find initial conditions. Integration is performed by a
three-term Taylor series or Adams-Moulton predictor-corrector, with a
fourth order Runge-Kutta starter. Linear interpolation between input
data points define the surface profile.

Validation:

Comparison of nose and main gear loads to test data and other
simulations showed reasonable correlation, Reference (1).

Input Data:

    1) Inertias and physical dimensions of aircraft.
    2) Surface profile for each gear.
    3) Thrust, braking, aerodynamic, strut characteristics.
    4) Modal masses, deflection coefficients, damping, and frequencies for flexible modes.

Output Data:

    1) Time history of aircraft dynamics and gear loads.
    2) Time at which maximum values are obtained.

Limitations (assumptions, inaccuracies, peculiar problems, etc.):

Lateral displacement is not allowed, eliminating "high-center" or "low center" roll. All dynamic variables and their derivatives are stored in array HD, dimensioned 88, pitch and roll angles and derivatives are small.

Recommendations (suggested improvements):

    1) Add lateral DOF.
    2) Eliminate Taylor-series integration technique.

References:

1.   Skinner, M., et al., "TAXIG - Modified TAXI Computer Program - Vols. I and II," ESL-TR-83-32, BDM Corporation, McLean, Virginia, August 1983.

Program Name (Acronym): TURNG

Descriptive Title:

   Prediction of aircraft landing gear loads during turning operation.

Brief Description (Capabilities):

   This program predicts the side and drag forces on the landing gear of an
aircraft during turning operations. It includes the effect of nose gear
steering angle, main gear brake-slip and thrust.

Key Words (Categories):

   Aircraft turning, tire/soil interaction, tire forces, sinkage, braking,
tire rut.

Author(s):   Name(s): Phillips, N. S. and Saliba, J. A.

                        Organization: University of Dayton
                                           Research Institute

                        Address: 300 College Park Avenue
                                      Dayton, Ohio 45469

Date Written: August 1983

Program Language: FORTRAN

Software Operations: Computer(s): CDC

                        Mode (batch, interactive): Batch

                        Pre- or Post-Processors: none

Documentation Adequacy:

Theory:

Basic equations outlined.

User's Manual:

Flow chart, program listing, variable definitions, and sample input/output given.

Other (sample problems, etc.):

Sample input/output for a F-4E simulation of turning.

Model: Theoretical (number and types of equations, concepts modeled):

The sums of the transverse forces and moments including inertia, at the center of gravity, are set equal to zero and the wheel forces and instantaneous center of turn are calculated. Each wheel drag is calculated as a function of braking, turn angle, and coefficient of friction or percent slip; wheel side forces are calculated as functions of turn angle, vertical tire deflection and coefficient of friction.

Numerical Techniques (integration, iteration, interpolation, etc.):

The Newton-Raphson iteration technique is used to find the instantaneous center of turn. Divergence due to large changes in the variables was prevented by limiting those changes to 50 percent.

Validation: none

Input Data:

1) Aircraft: moment of inertia, weight, velocity and distance from c.g. to gears.
2) Tires: number per axle, dimensions, percent deflection.
3) Engine: location w/r to aircraft centerline, and thrust.
4) Normalized nose wheel steering angle and braked slip angle in equal time increments. Maximum steering angle and percent slip and time increment.
5) Soil type and cone index.

Output Data:

1) Trajectory coordinates of aircraft c.g.
2) Thrust required to maintain speed.
3) Turn and steering angle on each wheel.
4) Drag and side forces, and turning torque on each wheel.
5) Sinkage and rut depth for each wheel.
6) Instantaneous radius of curvature.

Limitations (assumptions, inaccuracies, peculiar problems, etc.):

Recommendations (suggested improvements):

A better theoretical manual is needed, especially on soil/tire interaction.

Reference:

1. Phillips, N. S. and Saliba, J. A., "Aircraft Operation on Soil Surfaces-Computer Routine Revisions and Improvements, Vol. II - Computer Routine User's Manual," University of Dayton Research Institute, Dayton, Ohio, 1983.

Program Name (Acronym): LANDG

Descriptive Title:

   Aircraft response during take-off and landing on soil surfaces.

Brief Description (Capabilities):

   This program calculates the response of an aircraft in a three-point
attitude as it accelerates or decelerates under the actions of weight, lift,
aerodynamic and soil drag, and thrust.

Key Words (Categories):

   Aircraft take-off, aircraft landing, tire/soil interaction, sinkage.

Author(s):   Name(s): Phillips, N. S., Cook, R. F. and Saliba, J. A.

                    Organization: University of Dayton Research Institute

                         Address: 300 College Park Avenue
                                   Dayton, Ohio 45469

Date Written: August 1983

Program Language: FORTRAN

Software Operations: Computer(s): CDC

                        Mode (batch, interactive): Batch

                        Pre- or Post-Processors: none

Documentation Adequacy:

Theory:

Well-documented.

User's Manual:

Flow charts, program listing, variable definitions and sample input/output given.

Other (sample problems, etc.):

Sample input and output given for a simulation of an F-4E aircraft.

Model: Theoretical (number and types of equations, concepts modeled):

1) Longitudinal motion of aircraft during landing or take-off, including thrust, aerodynamic forces, and wheel sinkage and drag.
2) Tire: radial quadratic springs.
3) Soil: damper and spring in series.

Numerical Techniques (integration, iteration, interpolation, etc.):

A fourth-order Runge-Kutta numerical integration technique for first-order differential equations was used. Variable step size with a check on accuracy was incorporated into the routine.

Validation:

Input Data:

      1) Aircraft weight, thrust, gear spacing, wing reference area.

      2) Lift and drag coefficients.

      3) Tire dimensions, deflections and spacing.

      4) Soil type, cone index, density and shape.

Output Data:

      1) \ircraft accelerations, velocity and distance.

      2) Gear drag.

      3) Tire sinkage.

Limitations (assumptions, inaccuracies, peculiar problems, etc.):

The variable step size (check for numerical accuracy) should make the program very time consuming.

Recommendations (suggested improvements):

Replace the present numerical integration routine with one that is less time consuming.

References:

1. Phillips, N. S., Cook, R. F. and Saliba, J. A., "Aircraft Operation on Soil Surfaces-Computer Routine Revisions and Improvement Vol. II - Computer Routine User's Manual," University of Dayton Research Institute, Dayton, Ohio, August 1983.

Program Name (Acronym):

Descriptive Title:

   Pitch plane dynamics of the A-10 aircraft with various landing gear
configurations traversing deterministic or stochastic runways or soil.

Brief Description (Capabilities):

   A digital computer program was developed to study six conceptual landing
gears for the A-10 negotiating runway obstacles and soil. The gears employed
high floatation tires, and passive adaptive and active control systems.
Multi- and single-point tires were used as well as anti-skid braking.

Key Words (Categories):

   landing gear, wheel/soil interaction, aircraft ground dynamics, multi-
   point tires, stochastic runways, active control landing gear, articulated
   landing gear

Author(s):   Name(s): Robert S. Levy

                            Organization: Fairchild Republic Company

                            Address: Farmingdale, NY 11735

Date Written: September 1983

Program Language: FORTRAN

Software Operations: Computer(s): IBM, CDC

                           Mode (batch, interactive): Batch

                           Pre- or Post-Processors: Plotting

Documentation Adequacy

Theory:

Some details of mathematical model, especially the gears, are given in Reference 1, Vol. II. Theoretical results are presented in Reference 1, Vol. II.

User's Manual:

Other (sample problems, etc.)

A study was made to determine when the multi-element tire model would yield significantly different results than a single point tire model. Multi-element tire gave higher loads, especially, for small-scale irregularities at low to moderate taxi speeds.

Model: Theoretical (number and types of equations, concepts modeled):

1) Soil was modeled with a linear spring in series with a combined parallel linear spring and velocity damper.
2) Stochastic runway profile was represented by a spectral density function.
3) Tire was represented by "n" radial springs with a quartic-force displacement function.
4) Articulated landing gears were modeled by cantilever gear equivalents.
5) Active landing gear and anti-skid brake were modeled.
6) Rigid body airframe longitudinal, vertical, and pitch; wing bending and torsion; fuselage bending; stores lateral and pitch; vertical, horizontal, and pitching of strut.

Numerical Techniques (integration, iteration, interpolation, etc.):

Second-order numerical integration with Taylor series.

Validation:

10.134

Program Name (Acronym): LATAX

Descriptive Title:

Dynamic simulation of a C-130 traversing AM-2 mats.

Brief Description (Capabilities):

The program predicts loads and dynamics of a C-130 traversing AM-2 mats at constant speed, braking or accelerating. Nonlinear strut characteristics and aerodynamics are included. The program has been used extensively for pitch plane analyses.

Key Words (Categories):

Landing gear loads, taxiing, bomb damage repair, C-130 aircraft dynamics, AM-2 mats, HAVE BOUNCE

Author(s):   Name(s): B. M. Crenshaw, M. M. Owen

                            Organization: Lockheed-Georgia Company

                            Address: Marietta, Georgia 30063

Date Written: December 1983

Program Language: FORTRAN 4

Software Operations: Computer(s): CDC, Sigma VI

                            Mode (batch, interactive): batch

                            Pre- or Post-Processors:

                            MIDAS graphics package available for plotting

Documentation Adequacy:

Theory:

Main equations used in simulation were given in Volume 1 of Reference 1.

User's Manual:

1. Source listing with variable map in Volume 1, Reference 1.
2. Flowcharts, variable definitions, program instructions, and input/output data formats in Volume 2, Reference 1.

Other (sample problems, etc.):

Many comparisons of computer simulation and test results in Reference 1.

Model: Theoretical (number and types of equations, concepts modeled):

1. Aircraft rigid body: bounce, pitch, and roll (roll not utilized because all input loads were symmetric).
2. Aircraft flexible: eight lowest modes due to wing bending and torsion.
3. Aerodynamic lift and moment as a function of ground speed.
4. Wheel-axle: vertical acceleration.
5. Oleopneumatic characteristics for struts plus bearing friction.
6. Control inputs for elevator, throttle and brake.
7. Up to three laterally spaced, asymmetric bomb damage repair profiles.
8. Point contact for tires with nonlinear stiffnesses and linear damping.

Numerical Techniques (integration, iteration, interpolation, etc):

1. Numerical integration by fourth-order Runge-Kutta.
2. Iterative solution to balance aircraft at begining of simulation.

Validation:

Computer results were compared to C-130 test data, and the simulation was modified to increase its accuracy.
Comparisons of predicted and test results were reasonable.

Input Data:

1. Aircraft inertias and geometry
2. Runway repair profiles
3. Tire nonlinear characteristics
4. Aerodynamic coefficients
5. Thrust and braking profiles
6. Oleopneumatic strut characteristics.

Output Data:

Tire histories of aircraft dynamics, wing shear, bending and torsion moments.
Maximum and minimum values for gear and wing loads and accelerations.
Data files generated for later plotting.

Limitations (assumptions, inaccuracies, peculiar problems, etc.):

Roll degree-of-freedom with no lateral degree-of-freedom.

Recommendations (suggested improvements):

References:

1. Crenshaw, B. M., Owen, M. M., "C-130 Response to Bomb Damage-Repaired Runways: Volume 1: Test Program and Simulation Validation; Volume 2: Computer Program," ESL-TR-82-23, Dec. 1983.

Program Name (Acronym):   LNDTAX2

Descriptive Title:

 C-141 Response to Repaired Bomb-Damaged Runways

Brief Description (Capabilities):

 LNDTAX2 is a digital computer simulation for the dynamic response of the C-141B during taxiing, takeoff and landing roll, and landing impact. The response is forced by runway roughness due to repair configurations or 1-cosine bumps.

Key Words (Categories):

 HAVE BOUNCE, aircraft-surface interaction, runway roughness, landing gears, taxi, landing, takeoff, C-141B dynamic response, rapid runway repair.

Author(s):   Name(s): R. S. Justice

       Organization: Lockheed-Georgia Company

       Address: 86 South Cobb Drive
              Marietta, Georgia

Date Written: March 1984

Program Language:

 ANSI FORTRAN 4

Software Operations: Computer(s): CDC

       Mode (batch, interactive):

         batch

       Pre- or Post-Processors:

       Results are written to a permanent file for the MIDAS
       Graphics Package or other plotting routines.

Documentation Adequacy:

Theory:

Some details given in Reference 1, Volume I

User's Manual:

Excellent details given in Reference 1, Volume II

Other (sample problems, etc.):

Sample input/output given in Reference 1, Volume II

Model: Theoretical (number and types of equations, concepts modeled):

1. Rigid body: vertical, longitudinal, pitch, and roll
2. Flexible: 15 aircraft modes
3. Landing gears(3): nonlinear oleopneumatic struts, friction, metering pins, brakes, springback
4. Tires: point-contact, nonlinear tire spring, spin-up
5. Aerodynamics: lift, drag, pitching moment, spoiler and elevator variation
6. Runway roughness: AM-2 mat configurations using ramps and flats or 1-cosine bumps
7. Thrust: table lookup vs velocity

Numerical Techniques (integration, iteration, interpolation, etc.):

1. Numerical integration by 4th order Runge-Kutta-Gill
2. Aircraft is balanced by computing gear forces and iterating on vertical and pitch degrees of freedom
3. Newton-Raphson iteration used to find tire force for static balance

Validation:

Fair to good correlation with test data shown in reference 1.

Input Data:

1. Aircraft modal data is on a tape
2. Repair profile and runway survey data is on a tape
3. Oleopneumatic and tire characteristics
4. Aircraft inertias, thrust, aerodynamics, geometry
5. Spin-up/spring-back characteristics for tire/strut

Output Data:

1. Input data including repair profile, aircraft modal data
2. Aircraft static balance results
3. Time history of aircraft position, velocity and accelerations; tire and strut loads
4. Summary of peak loads
5. Time history plot tape and MIDAS plot tape generated

Limitations (assumptions, inaccuracies, peculiar problems, etc.):

1. No lateral degree of freedom
2. Integration scheme is confusing

Recommendations (suggested improvements):

Simplify Runge-Kutta integration subroutine.

References:

1. Justice, R. S., "C-141 Response to Repaired Bomb-Damaged Runways, Volume I: Computer Simulation Development and Validation, Volume II: Computer Simulation User's Manual, Volume III: Aircraft Limitations and Operational Procedures," ESL-TR-81-52, Lockheed, Georgia, March 1984.

Program Name (Acronym): NORTAX

Descriptive Title:

   Dynamic Response of Aircraft on Rough Standard/Nonstandard Airfields

Brief Description (Capabilities):

   Program objective: to combine airframe structural modeling with the
latest advances in tire, soil and landing gear modeling into a generally
applicable analytical prediction technique capable of providing rapid
assessment of the structural capability of military aircraft, regardless of
landing gear type or arrangement, to perform ground operations on rough
repaired or unpaved surfaces.

Key Words (Categories)

   landing, taxi, turning, braking, takeoff, landing gear, runway profile,
soil models, tire models

Author(s):   Name(s): Pi, W. S.; Yamane, J. R.; Smith, M. J. C.

                    Organization: Northrop Corporation

                    Address: Aircraft Division
                              One Northrop Avenue
                              Hawthorne, California 90250

Date Written: April 1985

Program Language: FORTRAN

Software Operations: Computer(s): IBM, CDC, VAX

                            Mode (batch, interactive): batch, interactive

                            Pre- or Post-Processors:

                            1. Output is saved on a file for later plotting.
                            2. Can interface with an aircraft loads program,
                            FLEXLODS
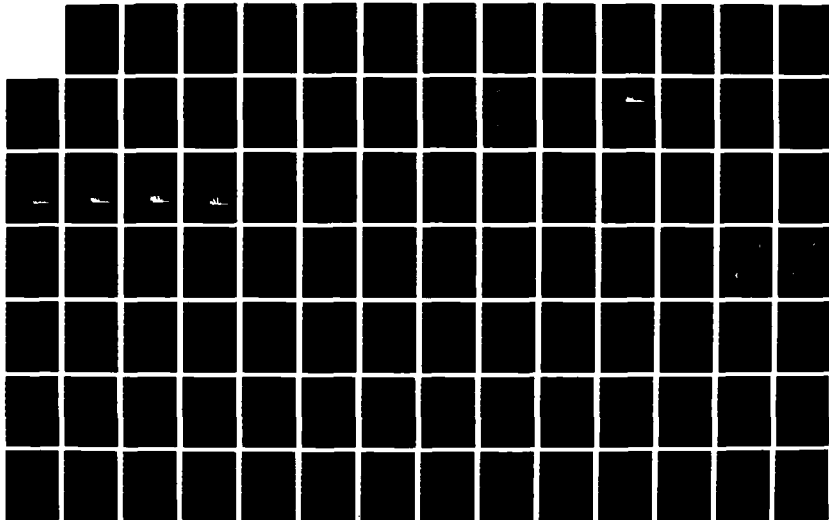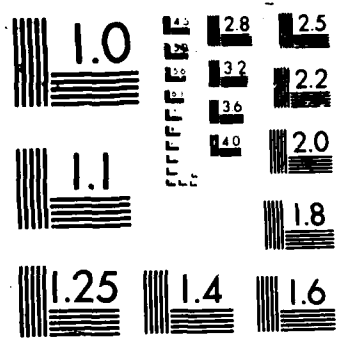
Documentation Adequacy:

Theory:

Detailed in Reference 1.

User's Manual:

Detailed in Reference 1.

Other (sample problems, etc.):

Sample input for C-141B, C-130, F-18, F-16, F-4E.
Sample output for C-141B.

Model: Theoretical (number and types of equations, concepts modeled):

1) Airframe: 6 DOF rigid body; up to 15 flexible symmetric and antisymmetric DOF.
2) Landing Gear: Up to 5 gears (tricycle, 4-post, 5-post, flexible or rigid cantilever, articulated, fully levered); 3 translational and one gear axle rotation DOF, plus pitch of bogie; Forces include: hydraulic damping, pneumatic force, friction, stiction, rebound damping, spin-up/spring-back, snubbing.
3) Tire: Normal, drag, and side loads; point contact or multispring model, damping and hysteresis, dynamic load-deflection characteristics.
4) Tire/Soil: A modification of Cranshaw's model-Lockheed, AFWAL-TR-74-115, Jan. 1975.
5) Surface: Separate random elevations for each strut on rigid or yielding surfaces.
6) Turning: Nose gear steering, asymmetric thrust, or rudder deflection.
7) Antiskid breaking, engine thrust, drag chute, tail hook, cross winds, aerodynamics.

Numerical Techniques (integration, iteration, interpolation, etc.):

1. Second-order Taylor series - fixed time step.
2. Fourth-order Adams-Moulton predictor-corrector with a Runge-Kutta starter variable time step.
3. Fourth-order Adams-Moulton predictor only - fixed time step.

Validation:

Simulated peak gear loads correlated well with test results on C-141B and F-4E, although simulated gear strokes were somewhat less.

Input Data:

Modular components must be selected or developed by user to solve a particular problem.

Aircraft types available for simulation are:
1. Fighter (F-111, F-16, F-4, F-15, F-5, F-18)
2. Cargo - four engine turboprop
3. Cargo - four engine turbojet (C-141 with pylon-hung engines)
4. Tanker (KC-10 configuration with centerline main gear).

Many landing gear configurations are defined.

Output Data:

Time histories of: 6 - DOF displacements of aircraft c.g., angle of attack and sideslip angle, forward speed and vertical acceleration, strut axial forces, landing gear loads transmitted to airframe, accelerations at specific locations on fuselage, wing, store and engine pylon, wind shear loads, bending and torsional moments, soil rut depths.

Plot max-min vertical accelerations and strut axial forces as a function of initial speed.

Variables associated with these extremes: instantaneous c.g. location and attitude, c. g. vertical acceleration, strut axial forces, instantaneous ground elevation under tires.

Limitations (assumptions, inaccuracies, peculiar problems, etc.):

Recommendations (suggested improvements):

References:

1. Pi, W. S., Yamane, J. R., Smith, M. J. C., "Dynamic Response of Aircraft on Rough Standard/Nonstandard Airfields, Part I. Theoretical Manual of the Generic Aircraft Ground Operation Simulation Code NORTAX; Part II. User's Manual of the Generic Aircraft Ground Operation Simulation Code NORTAX;" Contract F33615-82-C-3216, Northrop, April, 1985.

1984 USAF-SCEEE RESEARCH INITIATION PROGRAM

FINAL TECHNICAL REPORT

COMPUTATION OF TRANSONIC PROJECTILE AERODYNAMICS

Prepared By

Chen-Chi Hsu

Department of Engineering Sciences

University of Florida

Gainesville, Florida 32611

August 15, 1985

I. INTRODUCTION

Computational Fluid Dynamics is making an increasingly major impact on the design process of aerodynamic devices and flight vehicles. Recently a thin-layer Navier-Stokes code has been developed for high speed compressible fluid flow problems [1]. This code can provide unsteady or steady inviscid and viscous flow solutions; for the viscous case, one can further specify either a laminar flow or a turbulent flow. The turbulence closure model programmed in the code is a two-layer algebraic eddy viscosity model [2]. The Navier-Stokes code also has been simplified for axisymmetric flows to improve the computational effectiveness [3]. The application of the thin-layer Navier-Stokes code to transonic projectile aerodynamic problems has been investigated by the U. S. Army Ballistic Research Laboratory and acceptable accurate solutions had been obtained for a projectile with sting at zero angle of attack when a good adaptive grid system was provided [4].

Under the USAF Summer Faculty Research Program sponsored AFOSR, the principal investigator had spent the summer of 1984 with the Aerodynamic Branch of the Air Force Armament Laboratory at Eglin Air Force Base. The main objective of the summer research was to assess the accuracy of the thin-layer Navier-Stokes approximation coupled with the algebraic turbulence closure model as well as the implication of the solution algorithm. The Navier-Stokes code and a grid generation code obtained from Ballistic Research Laboratory were installed and investigated in detail for their application implication and effectiveness to the computation of transonic projectile aerodynamics. The result of the summer research conducted at Eglin AFB showed that the thin-layer Navier-Stokes code can provide satisfactory results for transonic

11.2

projectile problems if a good adaptive grid network is used in the computation; moreover, it also called for further assessment on the accuracy of the turbulence closure model for shock-boundary layer interaction regions [5].

II. OBJECTIVE

The main objective of this research is to further advance the application of Computational Fluid Dynamics in the analysis of transonic projectile aerodynamics. As stated in the research proposal for the RISE program the following studies were proposed for investigation:

1. Continue the summer research effort on assessing the algebraic turbulence model programmed in the Navier-Stokes code;

2. Assess a 3-D thin-layer Navier-Stokes code and its solution algorithm for transonic projectile aerodynamic problem;

3. Develop an adaptive grid generation technique based on constrained variational principles.

A major part of the research effort has been spent on completing the development of an adaptive grid generation technique for the computation of transonic projectile aerodynamics; consequently, the proposed studies, Item 1 and 2 cannot be completed.

III. RESULT AND DISCUSSION

The transonic flow past a secant-ogive-cylinder-boattail projectile with sting is considered in this study. The projectile model used has a 3-caliber secant-ogive part followed by a 2-caliber cylinder and 1-caliber 7-degree boattail which is further extended for about 1.7 calibers to meet a horizontal sting. The model is chosen for the study because accurate surface pressure measurements, Cp, are available for assessing the accuracy of numerical

11.3

results [6]. Critical features of the transonic projectile aerodynamics are the high pressure gradients caused by imbedded shock waves at the discontinuity of surface curvature, that is, at the ogive-cylinder and cylinder-boattail junctions. Therefore, the use of a properly adaptive grid system in the Navier-Stokes code is crucial to the accuracy and convergence of the solution algorithm.

As a continuation of the summer research effort a fixed 90 x 40 hyperbolic grid is used for the viscous transonic flow past the projectile at zero angle of attack. The integration process of the Navier-Stokes code was carried out to a maximum number of time steps N = 2800, 2400, 2800 and 2800, respectively, for four flow cases M_∞ = 0.91, 0.94, 0.96 and 0.98 considered. Figure 1 shows a few Cp-distributions computed at different times for M_∞ = 0.91. We observe that the agreement between the computed result and the measured data is excellent on the ogive and boattail portions and is acceptable on the cylinder portion of the projectile. A brief examination of the results obtained for the other three cases show the same. Therefore, one can conclude that the turbulence closure model programed in the thin-layer Navier-Stokes code can provide an acceptably accurate pressure field for the transonic flow problems.

For the computation of transonic flow past a projectile at an angle of attack we have obtained a vectorized 3-D thin-layer Navier-Stokes code from the U.S. Army Ballistic Research Laboratory. The largest grid system allowable in the code is of the size 80 x 21 x 24, which is apparently limited by the capacity of the supercomputer CRAY 1S. As a trial run we have considered an inviscid transonic flow past the projectile model at an angle of attack = 2°. A fixed hyperbolic grid system of the size 78 x 21 x 24 is used and the integration process of the Navier-Stokes code has been proceeded for

11.4
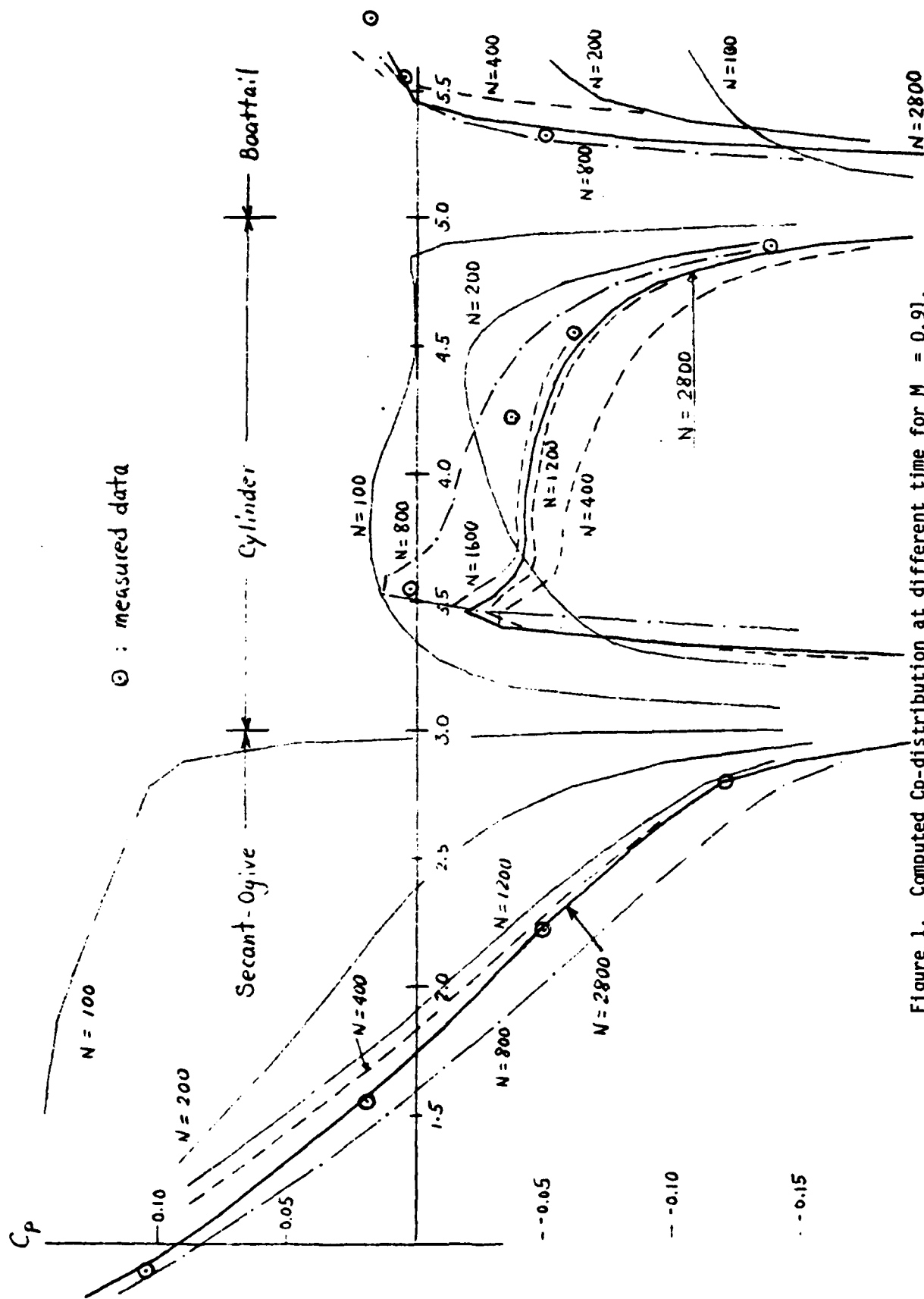
Figure 1. Computed Cp-distribution at different time for $M_\infty = 0.91$.

11.5

1200 time steps. A close examination of the computed Cp-distributions shows that the Navier-Stokes code is functioning properly and that a better adaptive grid system is needed for accurate solutions.

The development of an adaptive grid generation technique mainly based on constrained variational principles for the computation of inviscid transonic projectile aerodynamics has been successfully completed. The preliminary results of this work have been accepted and were presented at an open forum session of AIAA 7th Computational Fluid Dynamics Conference held in Cincinnati, Ohio, on July 15 - 17, 1985. The detail of the work accomplished is documented in the attached manuscript which has just been written and submitted to Journal of Computational Physics for possible publication.

REFERENCES

1. Pulliam, T. H. and Steger, J. L., "Implicit Finite-Difference Simulations of Three-Dimensional Compressible Flow," AIAA Journal, Vol. 18, Feb. 1980.

2. Baldwin, B. S. and Lomax, H., "Thin Layer Approximation and Algebraic Model for Separated Turbulent Flows, "Paper 78-257 presented at AIAA 16th Aerospace Sciences Meeting, Huntsville, Alabama, Jan. 1978.

3. Nietubicz, C. J., Pulliam, T. H. and Steger, J. L., "Numerical Solution of the Azimuthal-Invariant Thin-Layer Navier-Stokes Equations," Paper 79-0010 presented at 17th Aerospace Sciences Meeting, New Orleans, LA, Jan. 1979.

4. Nietubicz, C. J., "Navier-Stokes Computations for Conventional and Hollow Projectile Shapes at Transonic Velocities," AIAA-81-1262, 14th Fluid and Plasma Dynamics Conference, Palo Alto, CA, June 1981.

5. Hsu, C. C., "On a Thin-Layer Navier-Stokes Code and Transonic Projectile Aerodynamics," Final Report, 1984 USAF-SCEEE Summer Faculty Research Program, August 1984.

6. Kayerr, L. D. and Whiton, F., "Surface Pressure Measurements on a Boattailed Projectile Shape at Transonic Speeds," ARBRL-MR-03161, ADA 113520, U. S. Army Ballistic Research Laboratory, March 1982.

ATTACHMENT

11.7

An Adaptive Grid Generation Technique Based On Variational
Principles For Transonic Projectile Aerodynamics Computation

Chen-Chi Hsu and Chyuan-Gen Tu
Department of Engineering Sciences
University of Florida
Gainesville, FL 32611

Abstract

An adaptive grid generation technique mainly based on constrained
variational principles has been developed and coupled to a thin-layer Navier-
Stokes code for the computation of inviscid transonic projectile aero-
dynamics. In this technique the variational principles have been modified
with the assumption that the Lagrange's multipliers are variables but their
variation is zero; furthermore, a clustering technique has been implemented.
The numerical results obtained for three flow cases, $M_\infty = 0.91$. 0.96 and 1.10,
show that the technique developed indeed can provide, without any experimenta-
tion on boundary grid positioning, good grid systems for accurate computation
of the transonic projectile aerodynamics. The distribution of surface
pressure coefficient computed is in excellent agreement with measured data.

Introduction

An accurate prediciton of the aerodynamic drag force is essential to a better design of aerodynamic devices and flight vehicles. Recently a thin-layer Navier-Stokes code has been developed for high speed compressible fluid flow problems [1]. This code can provide acceptably accurate solutions for unsteady or steady inviscid and viscous flow problems if a good grid system is provided; for the viscous case, one can further specify either a laminar flow or a turbulent flow. The turbulence closure model programmed in the code is a two-layer algebraic eddy viscosity model [2]. The Navier-stokes code also has been simplified for axisymmetric flows to improve the computational effective-ness [3].

The application of the thin-layer Navier-Stokes code to transonic projectile aerodynamic problems has been investigated by the U. S. Army Ballistic Research Laboratory. The grid network used in the computation is an axisymmetric grid system formed by a sequence of planar grids around the axis of a projectile. The planar grid is obtained from a grid generation code named GRIDGEN [4]. This code can provide either an elliptic or a hyperbolic grid which is then modified with an exponential clustering along the grid lines normal to the streamwise direction to give sufficient grid resolution for the viscous region. Hence, a good adaptive grid can be obtained for transonic flows past a projectile with sting at zero angle of attack if the the boundary grid points are properly chosen. For a secant-ogive-cylinder-boattail (SOCBT) projectile with sting (i.e. no base flow) at zero angle of attack and Mach number $M_\infty = 0.91$, 0.94, 0.96, 0.98 and 1.10, the computed surface pressure coefficient C_p over secant-ogive portion and the boattail portion of the projectiles agrees rather well with the measured data; however, the agreement on the cylinder portion (between the shocks), which may be

11.9

acceptable, is not very satisfactory for some cases considered [5,6]. As reported in reference [7] a good adaptive planar grid for accurate solutions can be obtained from GRIDGEN only after considerable experimentation with boudary grid positioning. For the projectile model at 2° angle of attack and $M_\infty = 0.91$ the C_p-distribution computed from a CRAY 1S computer agrees qualitatively with the measured data but quantitatively the agreement over the cylinder and boattail portions is not satisfactory at all [7]. It is believed that the main cause for the unsatisfactory results can be attributed to the use of a grid system which is not properly adaptive to the solution.

A good grid system for fluid dynamics computations can be justified from the smoothness of grids, the orthogonality of grids, and the grid resolution adaptive to the solution in the physical space. It had been reported that rapid changes of the grid size and highly skewed grids can result in undesirable errors [8]. It is also well known in the approximation that the choice of high grid resolution in regions where the solution gradient is very large is essential to the accuracy of the numerical result. In fact an improper grid resolution in high gradient regions can be detrimental to the solution accuracy as well as to the convergence process of a solution algorithm. There have been a number of adaptive grid generation methods proposed and reported in symposium [8], workshop [9] and conference [10]. The method based on a constrained variational principle, proposed by Brackbill at the symposium, is rather general and seems to be a very promising approach for complex fluid problems in which shock waves, flame fronts, and viscous layers may cause extremely thin high-gradient regions of unknown location and orientation, since the governing differential equations for an adaptive grid system are derived from minimizing a general variational functional which consists of functionals for measuring the smoothness of grids, the

11.10

orthogonality of grids, and the grid resolution adaptive to a chosen control function. In fact Saltzman has investigated the application of an adaptive grid generation technique based on the variational principle to a two-dimensional inviscid supersonic flow past a step in a wind tunnel [11]. In his study, the adaptive gridding in the domain was controlled by the computed pressure gradient while the boundary grids were determined by extrapolation from internal grids out normally to the straight boundary. The unsteady solutions computed for the formation and propagation of shock waves were striking; they showed that the adaptive mesh generator moves the computation grid with shock fronts and consequently enhances significantly the desirable resolution of the finite-difference scheme for the accuracy.

The objective of this study is to explore further the application of variational principles for generating a good adaptive grid to the computation of transonic projectile aerodynamics. Numerical experiments have been carried out to assess the implication and difficulty of the grid generation method and, consequently, an adaptive grid generation technique mainly based on constrained variational principles has been developed and coupled to a thin-layer Navier-Stokes code for SOCBT projectile aerodynamics computations.

Variational Principles for Grid Generation

With a boundary conforming transformation an irregular two-dimensional domain Ω in the physical space, xy-plane, can be mapped into a rectangular domain Ω ' in the computational space, $\xi\eta$-plane; consequently, a square grid network in the computational space can be constructed for solving boundary value problems. The ξ and η coordinates then become the curvilinear coordinates for Ω in the physical space and constant ξ-lines and η-lines form a grid system in Ω. It is known that the coordinate transformation yields the

11.11

metrics relations

$$\xi_x = \frac{y_\eta}{J} , \quad \xi_y = -\frac{x_\eta}{J} , \quad \eta_x = -\frac{y_\xi}{J} , \quad \eta_y = \frac{x_\xi}{J} \tag{1}$$

in which J is the Jacobian of the transformation given by

$$J = x_\xi y_\eta - x_\eta y_\xi \tag{2}$$

If one chooses $\Delta\xi = \Delta\eta = 1.0$ in the computational space, then the Jacobian J represents the grid size in the physical space.

The smoothness of a grid network in the physical space can be measured by the integral

$$I_s = \int_\Omega [(\nabla\xi)^2 + (\nabla\eta)^2]dxdy \tag{3}$$

An extremization of this integral with prescribed boundary conditions will result in the Laplace equation; hence, a unique solution exists for the grid network. Moreover, the orthogonality of grids can be measured by the integral

$$I_o = \int_\Omega (\nabla\xi\cdot\nabla\eta)^2 J^3 dxdy \tag{4}$$

while the grid resolution adaptive to a control function $w(x,y)$ can be represented by

$$I_\nu = \int_\Omega wJ \ dxdy \tag{5}$$

We note that the term J^3 in Eq. (4) does emphasize the orthogonality for large grid and the choice of the cubic power is for the simplification of the resulting governing equations. Therefore, a good grid network in the physical space can be measured by the smoothness functional subject to the subsidiary conditions, the orthogonality functional and the grid resolution functional; consequently, a constrained variational principle for the grid generations is to minimize the functional

$$I = I_s + \overline{\lambda}_o I_o + \overline{\lambda}_\nu I_\nu \tag{6}$$

in which $\overline{\lambda}_o$ and $\overline{\lambda}_\nu$ are Lagrange's multipliers.

The introduction of undetermined Lagrange's multipliers requires prescribed values for the subsidiary conditions, Eq. (4) and Eq. (5). Since a

11.12

proper choice of these values for a good grid system is very difficult to make, if not impossible, it is more effective in practice to select values for the Lagrange's multipliers. Let L_p and L_c be respectively the characteristic length in the physical domain and the computational $\xi\eta$-plane. Also, denote W as a referenced quantity for the control function $w(x,y)$ in Eq. (5). We then observe that the integrand of the functionals I_s, I_o and I_v has the dimension of $(L_c/L_p)^2$, $(L_p/L_c)^2$ and $W(L_p/L_c)^2$. Therefore, if the Lagrange's multipliers are defined as

$$\overline{\lambda}_o = \frac{\lambda_o}{\tilde{\lambda}_o} \equiv \lambda_o \left(\frac{L_c}{L_p}\right)^4 \quad , \quad \overline{\lambda}_\nu = \frac{\lambda_\nu}{\tilde{\lambda}_\nu} \equiv \lambda_\nu \frac{1}{W} \left(\frac{L_c}{L_p}\right)^4 \tag{7}$$

then each term on the right hand side of Eq. (6) has the same order of magnitude provided λ_o and λ_ν are of $O(1)$. The relative importance of the three functionals for grid generation can be identified from the value chosen for λ_o and λ_ν.

For adaptive boundary gridding, one-dimensional variational principle can be employed. The functional consisting of a smoothness functional and a grid resolution functional can be written as

$$I_B = I_{BS} + \overline{\lambda}_{B\nu} I_{B\nu} \equiv \int_B \xi_s^2 \, ds + \overline{\lambda}_{B\nu} \int_B w_B(s) s_\xi \, ds \tag{8}$$

Similarly, the Lagrange's multiplier is defined as

$$\overline{\lambda}_{B\nu} = \frac{\lambda_{B\nu}}{\tilde{\lambda}_{B\nu}} \equiv \lambda_{B\nu} \frac{1}{W_B} \left(\frac{L_{BC}}{L_{BP}}\right)^3 \tag{9}$$

where L_{BP}, L_{BC} and W_B are characteristic quantities.

Governing Equations for Grid Generation

If a physical problem is to be solved in the transformed rectangular domain, the metrics of transformation must be provided. It implies that a curvilinear grid network in the physical domain must be generated; consequently, the dependent variables and the independent variables of the functionals have to be interchanged. Accordingly, applying the relation $dxdy = Jd\xi d\eta$ and the metrics relations Eq. (1), the general functional for grid, Eq. (6) becomes

$$I = \int_{\Omega} \frac{1}{J} [x_{\xi}^2 + x_{\eta}^2 + y_{\xi}^2 + y_{\eta}^2] d\xi d\eta + \overline{\lambda}_o \int_{\Omega} [x_{\xi} x_{\eta} + y_{\xi} y_{\eta}] d\xi d\eta \tag{10}$$
$$+ \overline{\lambda}_v \int_{\Omega} w(x,y) J^2 d_{\xi} d_{\eta}$$

in which the Jacobian J is defined in Eq. (2). Hence the governing equations for grid generation are the Euler equations for extremizing the functional I, provided $x(\xi,\eta)$ and $y(\xi,\eta)$ are prescribed on the boundary. They are the following two quasilinear elliptic differential equations

$$a_1 x_{\xi\xi} + a_2 x_{\xi\eta} + a_3 x_{\eta\eta} + b_1 y_{\xi\xi} + b_2 y_{\xi\eta} + b_3 y_{\eta\eta} + \frac{1}{2} \overline{\lambda}_v w_x J^2 = 0$$
$$b_1 x_{\xi\xi} + b_2 x_{\xi\eta} + b_3 x_{\eta\eta} + c_1 y_{\xi\xi} + c_2 y_{\xi\eta} + c_3 y_{\eta\eta}' + \frac{1}{2} \overline{\lambda}_v w_y J^2 = 0 \tag{11}$$

Here the coefficients a_i, b_i and c_i for $i = 1$, 2 and 3 are given by

$$a_i = a_{si} + \overline{\lambda}_o a_{oi} + \overline{\lambda}_v w(x,y) a_{vi}$$
$$b_i = b_{si} + \overline{\lambda}_o b_{oi} + \overline{\lambda}_v w(x,y) b_{vi}$$
$$c_i = c_{si} + \overline{\lambda}_o c_{oi} + \lambda_v w(x,y) c_{vi}$$

in which

$$a_{s1} = \alpha A, \quad a_{s2} = -2 \beta A, \quad a_{s3} = \gamma A$$
$$b_{s1} = -\alpha B, \quad b_{s2} = 2 \beta B, \quad b_{s3} = -\gamma B$$
$$c_{s1} = \alpha C, \quad c_{s2} = -2 \beta C, \quad c_{s3} = \gamma C$$

11.14

$$A = y_\xi^2 + y_\eta^2, \qquad B = x_\xi y_\xi + x_\eta y_\eta, \qquad C = x_\xi^2 + x_\eta^2$$

$$\alpha = \frac{1}{J^3}(x_\eta^2 + y_\eta^2), \qquad \beta = \frac{1}{J^3}(x_\xi x_\eta + y_\xi y_\eta), \qquad \gamma = \frac{1}{J^3}(x_\xi^2 + y_\xi^2)$$

$$a_{o1} = x_\eta^2, \qquad a_{o2} = 2(2\,x_\xi x_\eta + y_\xi y_\eta), \qquad a_{o3} = x_\xi^2$$

$$b_{o1} = x_\eta y_\eta, \qquad b_{o2} = x_\xi y_\eta + x_\eta y_\xi, \qquad b_{o3} = x_\xi y_\xi$$

$$c_{o1} = y_\eta^2, \qquad c_{o2} = 2(x_\xi x_\eta + 2\,y_\xi y_\eta), \qquad c_{o2} = y_\xi^2$$

$$a_{\nu 1} = y_\eta^2, \qquad a_{\nu 2} = -\,2\,y_\xi y_\eta, \qquad a_{\nu 3} = y_\xi^2$$

$$b_{\nu 1} = -\,x_\eta y_\eta, \qquad b_{\nu 2} = x_\xi y_\eta + x_\eta y_\xi, \qquad b_{\nu 3} = -\,x_\xi y_\xi$$

$$c_{\nu 1} = x_\eta^2, \qquad c_{\nu 2} = -\,2\,x_\xi x_\eta, \qquad c_{\nu 3} = x_\xi^2$$

Similarly the governing differential equation for adaptive boundary gridding can be derived from Eq. (8). One finds

$$[1 + \overline{\lambda}_{B\nu}\, w_B(s)\, s_\xi^3]\, s_{\xi\xi} + \frac{1}{2}\,\overline{\lambda}_{B\nu}\,\frac{dw_B}{ds}\, s_\xi^5 = 0 \qquad (12)$$

in which s is the distance measured along the boundary.

Numerical Experiments and Results

Transonic inviscid flows past a SOCBT projectile with sting at zero angle of attack have been considered for the study. This projectile model has a 3-caliber secant-ogive part followed by a 2-caliber cylinder and 1-caliber 7-degree boattail which is further extended for another 1.77 calibers to meet a horizontal sting. There are surface pressure measurements available for assessing the accuracy of numerical results [6]. The physical domain of the problem considered has about 4 projectile-lengths from nose, 5 projectile-lengths from the cylinder, and 3 projectile-lengths downstream of the base. The transonic aerodynamics problem is solved by an axisymmetric thin-layer Navier-Stokes code obtained from the U. S. Army Ballistic Research Laboratory. In this code the transformed thin-layer Navier-Stokes equations are

11.15

solved by the Beam and Warming scheme in which a second order implicit dissipation term and a fourth order explicit dissipation term haave been added for controlling the numerical stability. The code has an option for solving inviscid flow problems and a steady solution is resulted from a converged solution of the unsteady problem. It is mentioned in passing that a planar grid must be generated and provided to the code for the aerodynamics computation.

All planar grid networks generated and used in this study consist of 70 x 35 grid points with 70 points along the surface of projectile model; hence, the range of (ξ, η) in the computational space is from $(1,1)$ to $(70,35)$. Moreover, resulting from experience, we have fixed the distribution of boundary points along the projectile model as follows: 23 points on the ogive, 22 points on the cylinder, 17 points on the boattail, and 8 points on the sting. For grid generation, governing partial differential equations, Eq. (11), are approximated by second order central difference schemes and the resulting nonlinear algebraic equations are solved by the Newton-Raphson iterative method supplemented with overrelaxation. The boundary conditions for $x(\xi, \eta)$ and $y(\xi, \eta)$ at the projectile surface $\eta = 1$ and at the outer boundary $\eta = 35$ are predetermined by Eq. (12) for grid resolution; however, the conditions at the side boundaries, $\xi = 1$ and $\xi = 70$, are obtained and updated by extrapolation from inner grids at the end of each iteration. We note that the extrapolation technique for determining boundary grids on projectile surface can be detrimental because of the complex geometry.

The generation of a good adaptive grid based on the variational principle depends on a proper choice of the control function $w(x,y)$ in Eq. (5) for grid resolution as well as suitable choices of the Lagrange's multipliers $\bar{\lambda}_o$ and $\bar{\lambda}_v$ defined in Eq. (7), provided good adaptive boundary grids are prescribed. In

11.16

this study we have chosen the control function

$$w(x,y) = |P_x| + |P_y| \qquad\qquad (13)$$

in which P_x and P_y are components of the computed pressure gradient. A converged solution of the projectile problem at Mach number = 0.96 has been used to investigate the relative importance of the multipliers on the grid resolution functional I_ν, with $\overline{\lambda}_o = 1$ and $\overline{\lambda}_\nu$ varies from 0 to 10, the variance of I_ν over the mean of I_o changes from 9.0 to 7.8. It implies that different choices of the multipliers will have rather minimum effect on grid resolution adaptive to the control function. Hence, we have assumed for the following study that

$$\lambda_o = \lambda_\nu = \lambda \qquad\qquad (14)$$

Note that λ_o and λ_ν are related to the corresponding multiplier by Eq. (7).

For assessing the application of the adaptive grid generation technique, we have considered the projectile aerodynamics problem at $M_\infty = 0.91$. The characteristic lengths L_p and L_c used in Eq. (7) are the global ones similar to those used by Saltzman while λ is set to 4.0. The initial grid provided to the thin-layer Navier-Stokes code is a smooth one. The computed surface pressure coefficient C_p after 50 time steps, i.e., NT = 50, is shown in Figure 1(a); measured data for steady solution, ◇ , are also plotted for reference. A new grid adaptive to the computed result at NT = 50 is then generated for the continuation of the solution code. Figure 1(b) shows the grid network near the projectile. The thin-layer code is restarted for another 150 time steps, i.e. NT = 200, and the computed pressure coefficient is shown in Figure 1(c). Apparently the solution is not converging correctly, which can be attributed to the poor grid used in the computation. A new grid adaptive to the computed result at NT = 200 is again generated for the restart of the solution process. As shown in Figure 2, the result obtained at

11.17

(a) Surface pressure calculated at NT = 50

(b) Grid network near body surface at NT = 50

(c) Surface pressure calculated at NT = 200
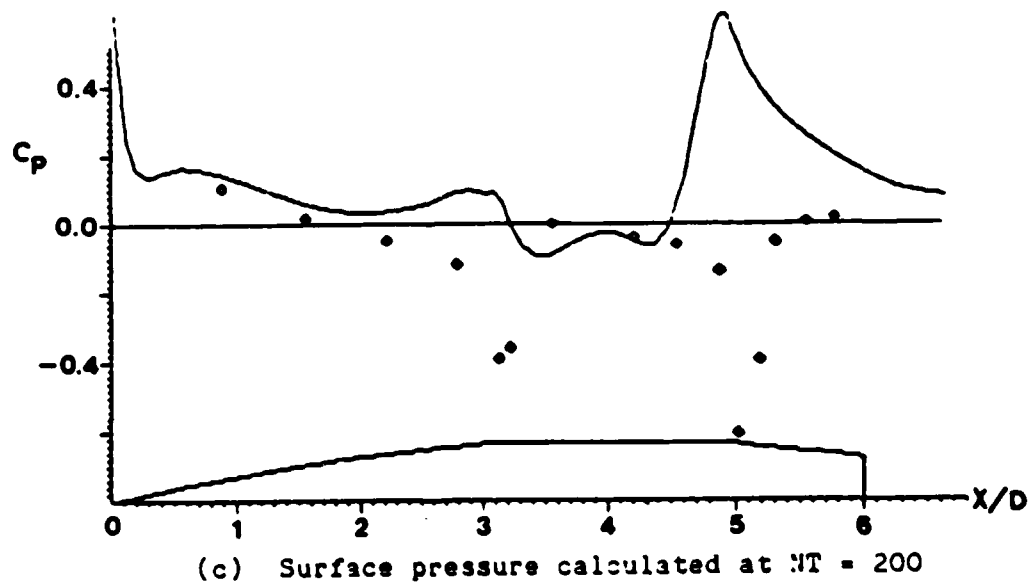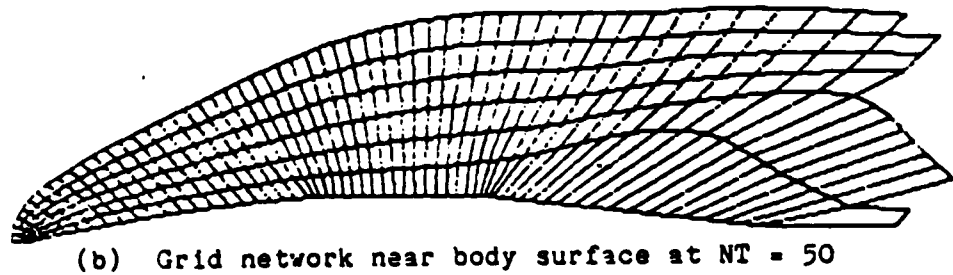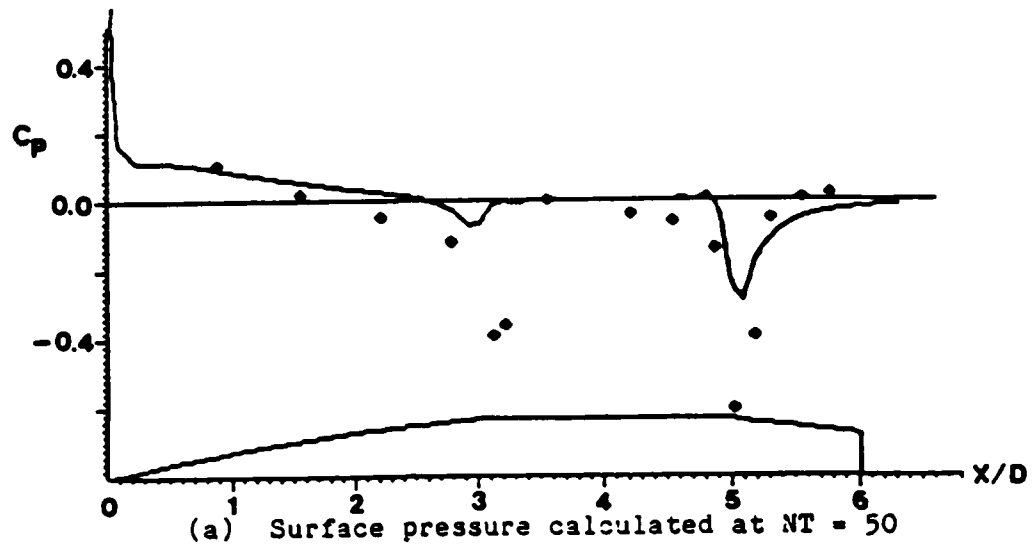
Figure 1. Surface pressure and adaptive grid; $M_\infty = 0.91$.

11.18
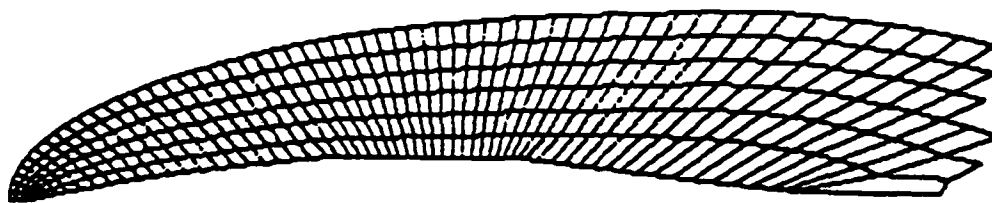
(a) Grid network generated at NT = 200
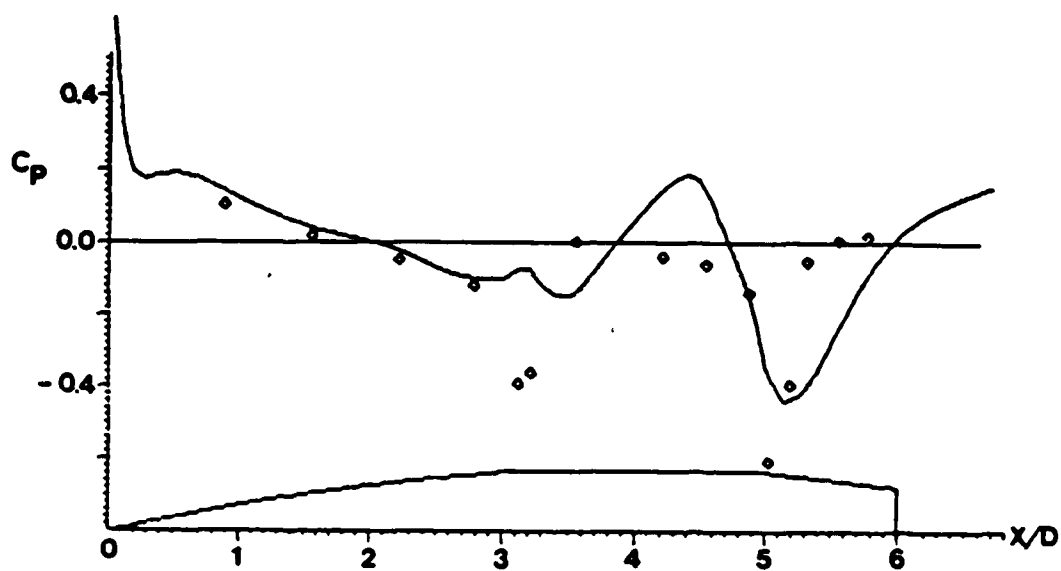
(b) Surface pressure at NT = 350
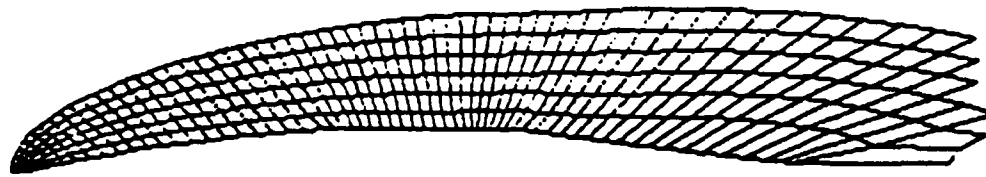
(c) Grid network generated at NT = 350

Figure 2. Surface pressure and adaptive grid; M_∞ = 0.91.

NT = 350 does not seem to be properly converging either, even though the grid used looks better than the one used previously; moreover, we note that the updated adaptive grid at NT = 350 is very similar to that at NT = 200. The continuation of the solution algorithm with the updated grid has failed within the next 150 time steps.

A close examination of the planar grids generated clearly indicates that the grid characteristics right next to the projectile are rather poor, particularly the grid resolution is not sufficient. It implies that the effect of boundary geometry to a good grid generation has to be investigated and considered in the control function. In this study, however, the difficulty is overcome by applying an exponential clustering along η-lines with the smallest spacing equal to 0.01 at the projectile. An adaptive grid with the clustering generated at NT = 350 is shown in Figure 3(a). With this new grid the thin-layer code provides a converging solution at NT = 500 as evidenced from the result shown in Figure 3(c). The process has been repeated and the distribution of C_p computed at NT = 650 indeed shows better agreement with the measured data.

The adaptive gridding with exponential clustering is next tested on the projectile problem at M_∞ = 0.96. The first adaptive grid is again generated at NT = 50, but subsequent new grids are generated at every 200 time steps interval. The solution process proceeded smoothly without any difficulty and provided acceptably accurate pressure distribution at NT = 850. For assessing the grid generation technique, however, the integration process was carried out further to NT = 1650. Figure 4 shows the agreement between computed C_p at NT = 1650 and measured data; however, appreciable differences observed on the cylinder and its junction with boattail still call for better grid resolutions in those regions.
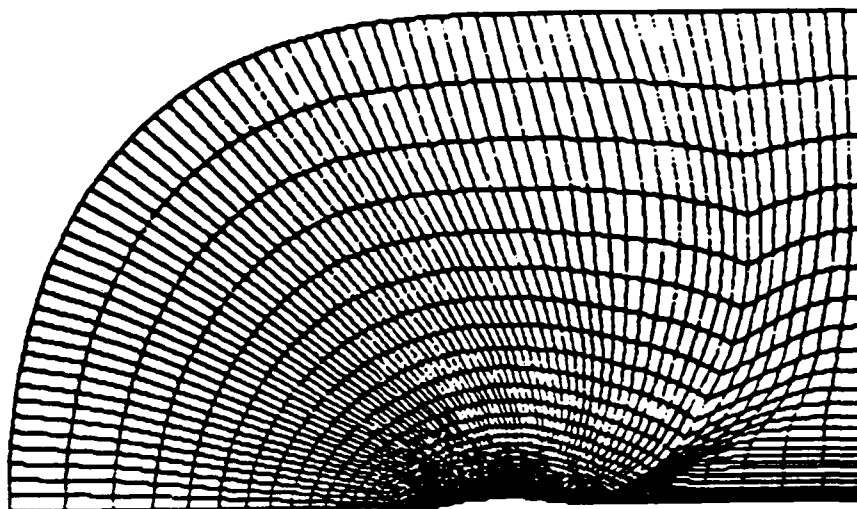
(a) Grid network with clustering (ΔS = 0.01) at NT = 350

(b) Expanded view of grids near the body surface
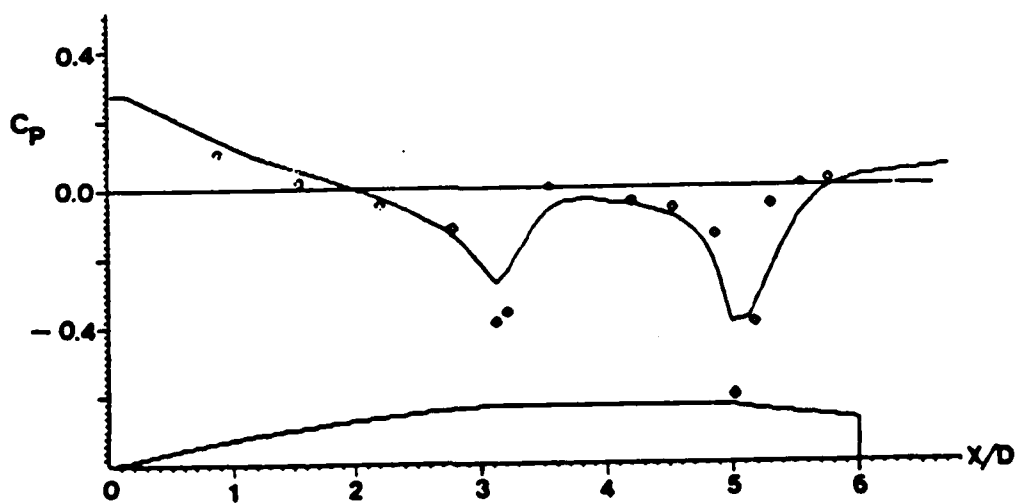
(c) Surface pressure calculated on the above grids at NT = 500

Figure 3. Adaptive grid with clustering and computed surface pressure.

11.21
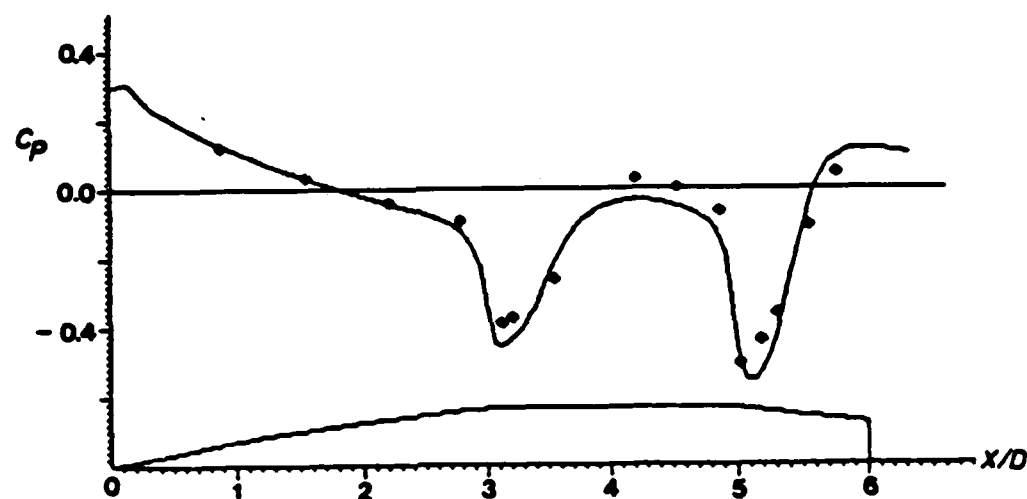
Figure 4. Surface pressure computed at NT = 1650 with adaptive gridding based on constant Lagrange's multipliers; M_∞ = 0.96.

The choice of the control function $w(x,y)$ for better grid resolutions is not a trivial one; it requires extensive parametric study and numerical experimentation. For instance, we have used a stronger control function equal to the square of the pressure gradient and experienced overflow in the process of grid generation. However, the expression for the general functional, Eq. (6), shows that the grid resolution can be enhanced by choosing a larger value for the multiplier $\bar{\lambda}_\nu$, that is, a large λ_ν defined in Eq. (7). Unfortunately, the use of an extremely large λ_ν can be detrimental to the grid generation. Moreover, a good adaptive grid should have not only good adaptive grid resolutions but also good orthogonality and smoothness characteristics. Therefore, the value for the parameter $\lambda_\nu = \lambda_o \equiv \lambda$ has to be in the order of magnitude one or 10 at most. For the projectile problem considered, the use of a large λ and global characteristic lengths for the multipliers has not resulted in a better adaptive grid. We observe that the grid resolution functional I_ν of Eq. (5) can be considered as a limiting case of the general functional; consequently, the variational principle of I_ν will give a grid best adaptive to the chosen control function $w(x,y)$. Apparently, the control function used in this study does not provide sufficient grid resolutions for the transonic flow problems.

The variational principle of the general functional I, Eq. (6) indicates that the effect of grid resolution functional can be enhanced locally if variable Lagrange's multiplier $\bar{\lambda}_\nu$ is used. Departing from the classical variational principle by assuming the variation of the Lagrange's multipliers $\bar{\lambda}_o$ and $\bar{\lambda}_\nu$ zero, the variation of I equal to zero will result in exactly the same Euler equations, Eq. (11), for grid generation. Now the variable $\bar{\lambda}_o$ and $\bar{\lambda}_\nu$ defined in Eq. (7) must be selected. In order to realize the relative weight of each term in Eq. (6) we have fixed the parameters λ_o

11.23

and λ_v and assumed the relation Eq. (14) in grid generation; accordingly, the referenced quantities L_c, L_p, and W are considered variables. In the following study we have chosen the local grid spacings as well as local values of the control function for the referenced quantities; hence, L_c of the computational space is equal to one. Equation (7) indicates that grid resolutions will be further enchanced locally in the region of small grids (i.e. small L_p), even though the weight of grid resolution term in Eq. (6) remains the same. In the process of grid generation, the nonlinear governing equations, Eq. (11), are solved by an iterative method; hence, the referenced quantities L_p and W are updated at the end of each iteration. Similarly, Eq. (12) for adaptive boundary gridding is solved with L_{BP} and W_B, defined in Eq. (9), taken as the local quantities.

The adaptive grid generation technique based on the modified variational principles and a clustering strategy is first investigated on the projectile problem at $M_\infty = 1.10$. An adaptive grid generation code developed has been coupled to the thin-layer Navier-Stokes code with a strategy of adaptive gridding fixed as follows: the first adaptive grid is generated at NT = 50 with $\lambda = 0.5$ and subsequently a new grid is generated and used at 150 time steps interval with $\lambda = 1.0$, 5.0, 7.5 and 10.0 at NT = 650 for enhancing the weight of grid resolution term. Figures 5-8 show the sequence of results computed to NT = 500. We observe that the solution algorithm is converging very smoothly and highly accurate results have been obtained at NT = 500; moreover, the adaptive grids generated exhibit clearly the development of the pressure field and shock waves. Exactly the same solution process has been applied without any difficulty to the projectile problem at $M_\infty = 0.91$ and 0.96. The surface pressure coefficient computed at NT = 650 and 800 for

11.24

SURFACE PRESSURE CALCULATED AT NT= 50
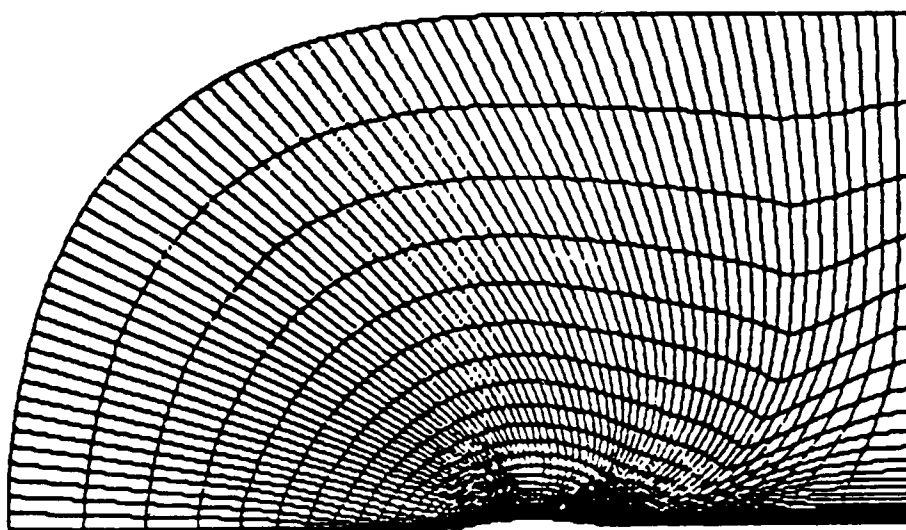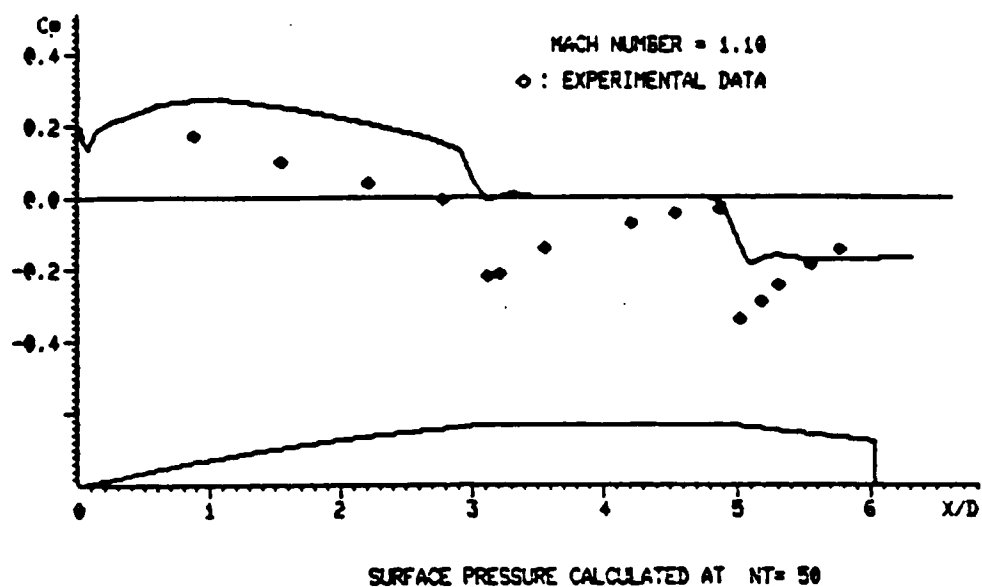
GRID NETWORK GENERATED AT NT= 50

Figure 5. Surface pressure and adaptive grid based on variable $\overline{\lambda}_0$ and $\overline{\lambda}_v$ at NT = 50.

11.25
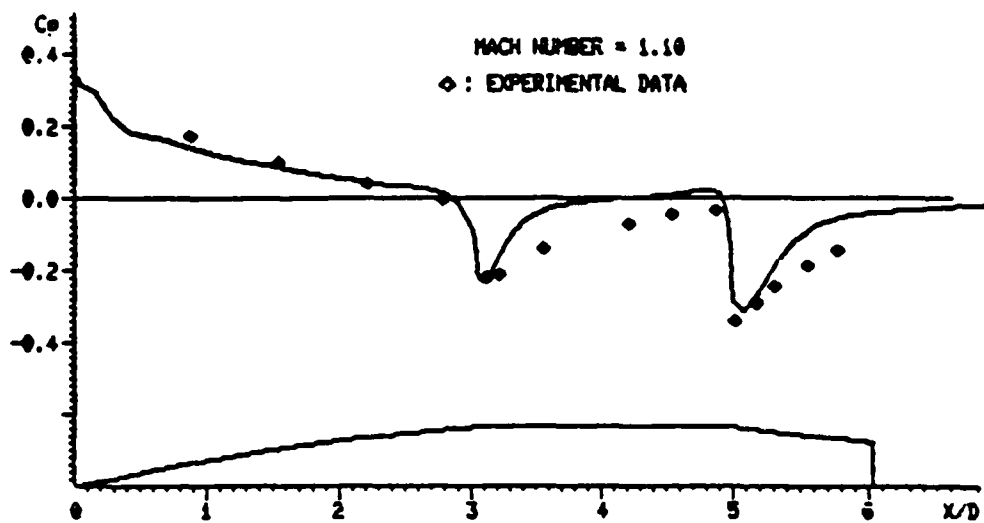
SURFACE PRESSURE CALCULATED AT NT= 200
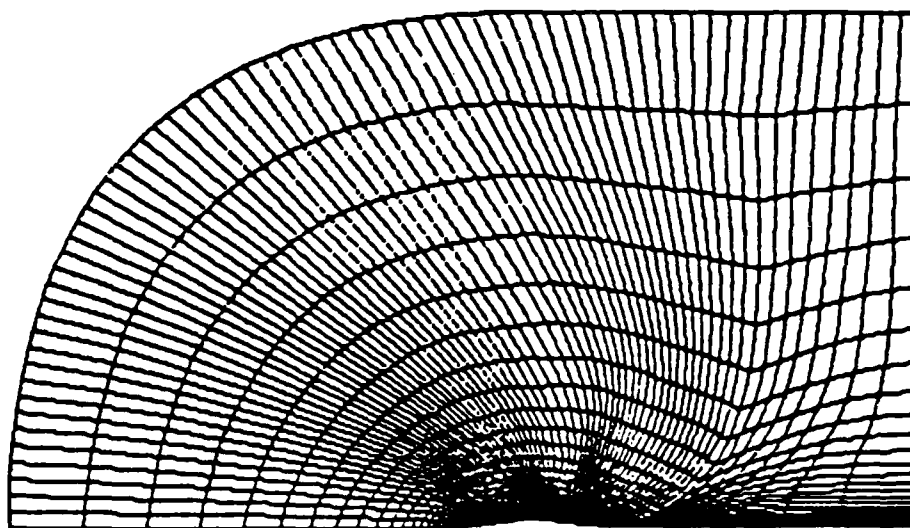
GRID NETWORK GENERATED AT NT= 200

Figure 6. Surface pressure and adaptive grid generated at NT = 200.

11.26

SURFACE PRESSURE CALCULATED AT NT= 350
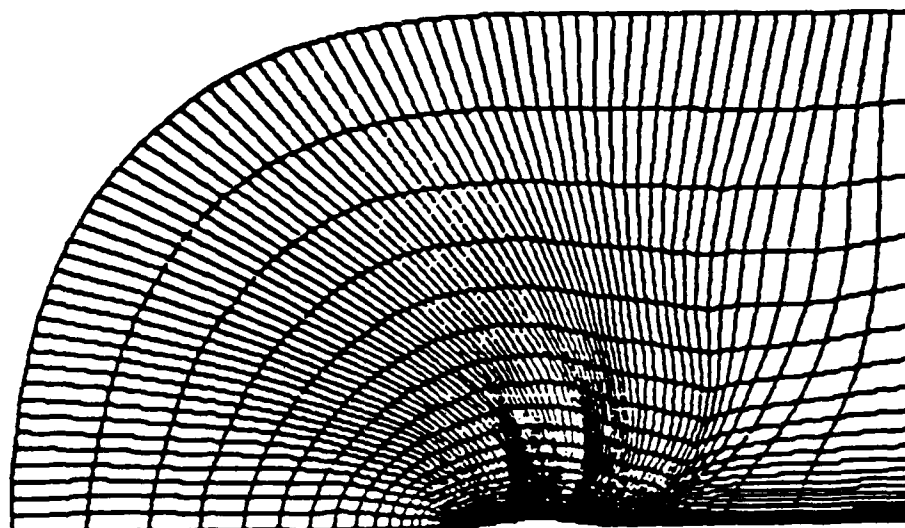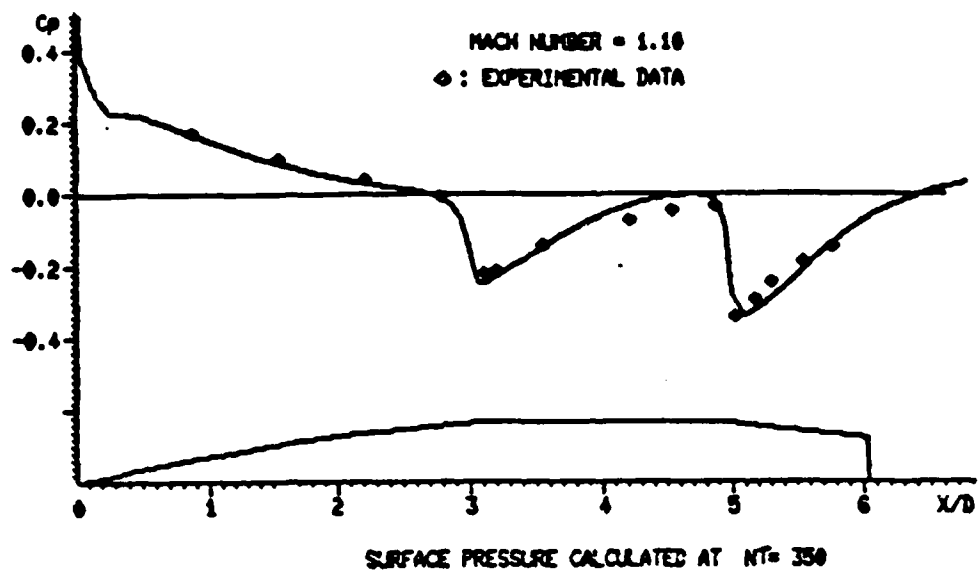
GRID NETWORK GENERATED AT NT= 350

Figure 7. Surface pressure and adaptive grid generated at NT = 350.

11.27
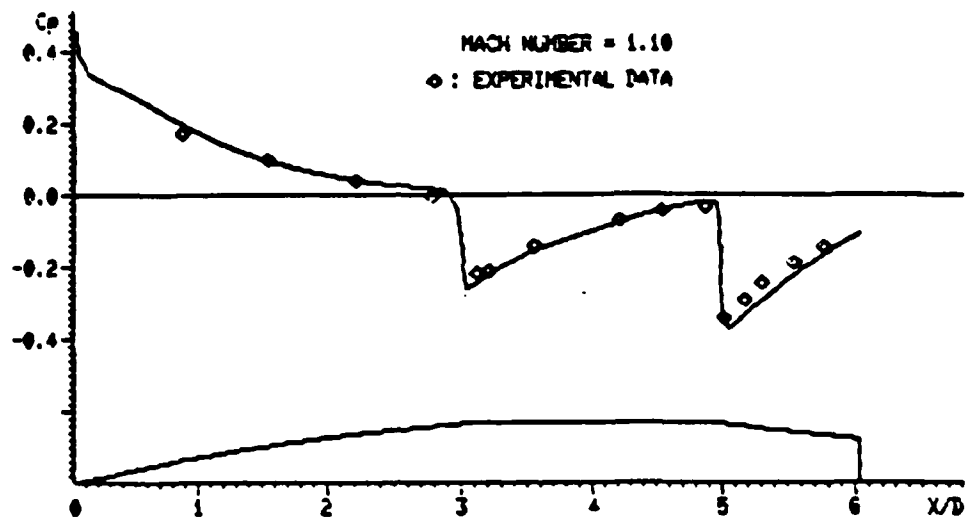
SURFACE PRESSURE CALCULATED AT NT= 500
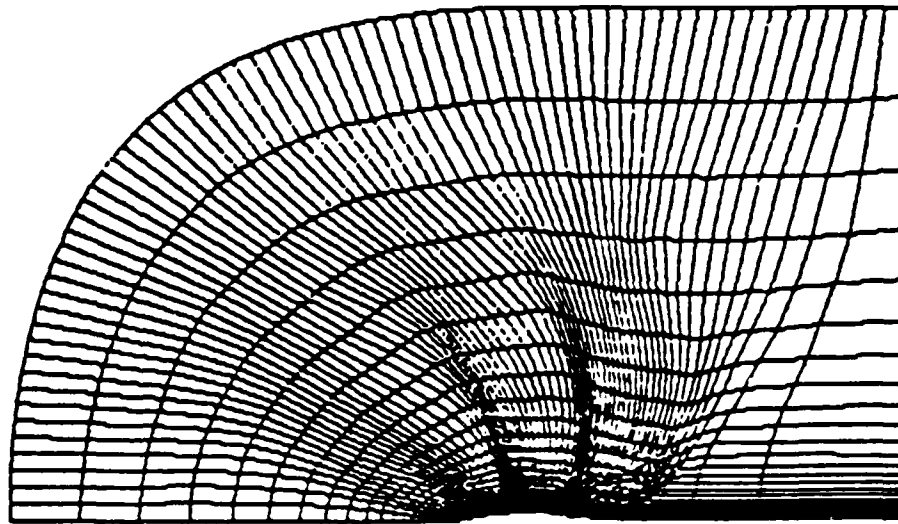
GRID NETWORK GENERATED AT NT= 500

Figure 8. Surface pressure and adaptive grid generated at NT - 500.

$M_\infty = 0.91$ and 0.96, respectively, and that of $M_\infty = 1.10$ are shown in Figure 9 with corresponding measured data plotted for comparison.

The adaptive grid generation technique developed indeed can provide, without any experimentation on boundary grid positioning, good grid systems for accurate computations of the transonic projectile aerodynamics. It is mentioned in passing that good adaptive inner grids and conforming adaptive boundary grids are often essential to the accuracy of the solution while good adaptive boundary grids only can be detrimental to the solution algorithm; moreover, a good grid adaptive to a converged solution may not be a proper one for use in solving unsteady problem.
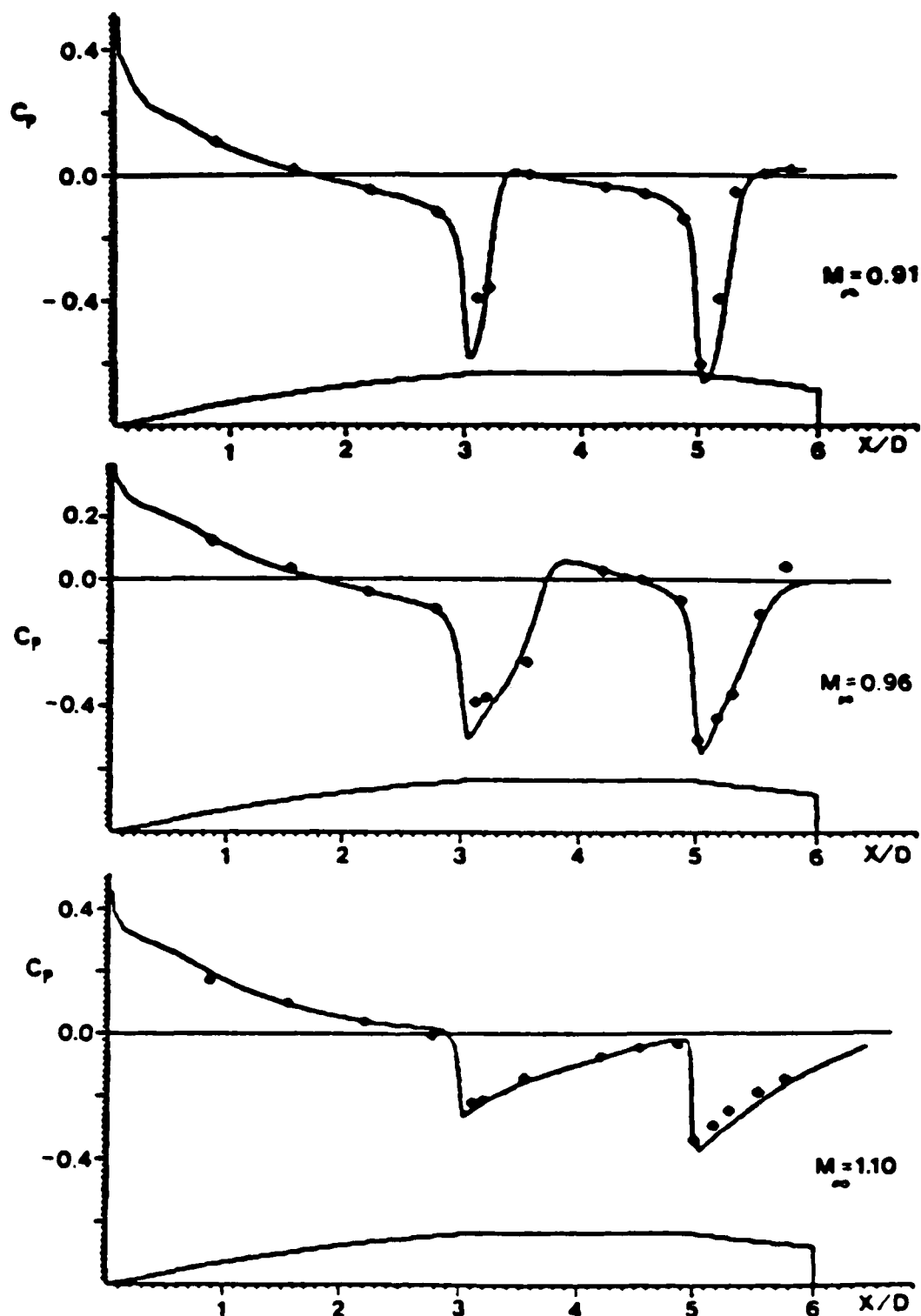
Figure 9. Converged surface pressure based on adaptive grid
generation technique developed.

11.30

References

1. Pulliam, T. H. and Steger, J. L., "Implicit Finite-Difference Simulations of Three-Dimensional Compressible Flow," AIAA Journal, Vol. 18, Feb. 1980.

2. Baldwin, B. S. and Lomax, H., "Thin-Layer Approximation and Algebraic Model for Separated Turbulent Flows," Paper 78-257, AIAA 16th Aerospace Sciences Meeting, Jan. 1978.

3. Nietubicz, C. J., Pulliam, T. H. and Steger, J. L., "Numerical Solution of the Azimuthal-Invariant Thin-Layer Navier-Stokes Equations," Paper 79-0010, AIAA 17th Aerospace Sciences Meeting, Jan. 1979.

4. Steger, J. L., Nietubicz, C. J. and Heavey, K. R., "A General Curvilinear Grid Generation Program for Projectile Configurations," ARBRL-MR-03142, U. S. Army Ballistic Research Laboratory, Oct. 1981.

5. Nietubicz, C. J., "Navier-Stokes Computations for Conventional and Hollow Projectile Shapes at Transonic Velocities," AIAA-81-1262, AIAA 14th Fluid and Plasma Dynamics Conference, June 1981.

6. Kayser, L. D. and Whiton, F., "Surface Pressure Measurements on a Boattailed Projectile Shape at Transonic Speeds," ARBRL-MR-03161, ADA 113520, U. S. Army Ballistic Research Laboratory, March 1982.

7. Sturek, W. B., "Opportunities for Application of Adaptive Grids in Computational Aerodynamics," in Proc. Adaptive Computational Methods for Partial Differential Equations, edited by I. Babuska et al, SIAM, 1983.

8. Numerical Grid Generation, edited by J. F. Thompson, Norht-Holland, 1982.

9. Adaptive Computational Methods for Partial Differential Equations, edited by I. Babuska, J. Chandra and J. E. Flaherty, SIAM 1983.

10. AIAA Computational Fluid Dynamic Conference - A Collection of Technical Papers, July 1983.

11. Saltzman, J., "A Variational Method for Generating Multidimensional Grids," Ph.D. Thesis, New York University, 1981.

1984 USAF - SCEEE RESEARCH INITIATION PROGRAM

FINAL TECHNICAL REPORT

DEVELOPMENT OF AN ADAPTIVE GRID GENERATION TECHNIQUE

FOR TRANSONIC PROJECTILE BASE FLOW PROBLEMS

prepared by

Christopher W. Reed and Chen-Chi Hsu
Department of Engineering Sciences
University of Florida
Gainesville, FL   32611

June   , 1985

DEVELOPMENT OF AN ADAPTIVE GRID GENERATION TECHNIQUE

FOR TRANSONIC PROJECTILE BASE FLOW PROBLEMS

by

Christopher W. Reed and Chen-Chi Hsu

ABSTRACT

An existing thin-layer Navier-Stokes code for the computation of
axisymmetric transonic flow past a projectile with sting has been studied and
consequently modified for the projectile base flow problem. The solution
obtained for a transonic flow over a sphere indicates that the modifications
made to the boundary conditions in the thin-layer code are correct and hence
the code should be applicable to other projectile base flow problems if a
proper grid is provided.

Preliminary results obtained from investigating the adaptive grid
generation technique for the sphere problem indicate that the method based on
constrained variational principles is indeed effective in the general domain;
however, additional analyses and experiments are required for proper choices
of the parameters and the control function so that high grid resolutions can
be achieved for the viscous sublayer region. Moreover, two methods of
adapting the boundary grid points have been developed and the testing results
show that both methods provide good conformity between the boundary grids and
the domain grids.

A continuation of the research project is being supported by a 1985 USAF-
UEC GSSP program.

INTRODUCTION

An accurate prediction of the aerodynamic drag force is essential to a
better design of aerodynamic devices and flight vehicles. Of specific
interest to the Air Force Armament Laboratory at Eglin AFB is an accurate
prediction of the aerodynamic drag force acting on stores which are to be
released from under aircraft traveling at transonic speeds. These forces
influence the stability of the stores and consequently the safety of the
aircraft. It is known that an accurate computation of the aerodynamic force
is difficult and involved; consequently an effective numerical algorithm for
predicting the forces is yet to be developed. The aerodynamic force in
general can be divided into three components from the physical as well as the
computational view; they are the pressure drag, viscous drag and base drag
with relative magnitudes for a standard store shape at transonic speeds of
20%, 30% and 50%, respectively.

Recently, a thin-layer Navier-Stokes code has been developed at NASA Ames
Research Center for three dimensional compressible fluid flow problems [1].
It has been shown that this code can give acceptably accurate solutions for a
number of high speed compressible flow problems provided a good grid is
used. The application of the thin-layer Navier-Stokes code to a specific
axisymmetric transonic projectile flow problem has been investigated by the
Aerodynamics Research Branch of the U.S. Army Ballistic Research Laboratory.
A secant-ogive-cylinder-boattail (SOCBT) projectile has been modified to
eliminate the computational difficulties associated with the base flow by
attaching a sting. For the axisymmetric case, the computed surface pressure
coefficient Cp agrees well with experimental data indicating that the code can
successfully compute both the pressure and viscous drag.

12.3

When the base region is to be included in the solution, however, the transonic flow problem becomes increasingly complex. Both a shock and separated flow are expected at the sharp corner of the base and for supersonic flows an additional shock is expected in the wake region.

The problem now becomes one of generating a good grid that will adequately resolve the large gradients associated with the flow, therefore the main objective of this program is to develop a theoretically sound adaptive grid generation technique for use with the thin-layer Navier-Stokes code to solve the complete transonic projectile flow problem. It should also be pointed out that the large number of grid points required for an accurate flow simulation is often limited by the capacity of existing super-computing systems; hence the development of an effective adaptive grid generation technique becomes essential for complex transonic projectile flow problems.

The necessary research and development to solve the complete transonic projectile flow problem can be organized into three parts.

(1) Modify the existing thin-layer Navier-Stokes code to include the base region.

(2) Develop an effective adaptive grid generation technique capable of generating a good grid for the base flow problem.

(3) Couple the adaptive grid generation scheme with the thin layer Navier-Stokes code to solve the axisymmetric transonic projectile flow problem and extend the solution method to three dimensions.

Part (1) has been completed and partial results obtained for Part (2) are presented in this report. Subsequent research to complete part (2) and begin part (3) is being supported through a 1985 USAF-UEC GSSSP program.

12.4

The Thin Layer Approximation

The complete set of governing equations for three dimensional compress-
ible flow problems includes the three momentum equations, the equation of
continuity, the energy equation, and an equation of state. However, in many
flows, such as high Reynolds number flow over projectiles, the velocity gradi-
ents along the projectile surface are small compared to the velocity gradients
normal to the surface in the boundary layer. The viscous terms in the govern-
ing equations containing these gradients can therefore be neglected without
introducing appreciable error. This 'thin layer' approximation to the Navier-
Stokes equations has considerable computational advantages. The elimination
of many viscous terms reduces substantially the size of the governing equa-
tions. These equations are still capable, however, of calculating separated
and reversed flows since many of the terms neglected in the boundary layer
equations are retained in the thin layer approximation. Also, larger grid
spacing can be used in directions along the body surface reducing both the
computer storage requirements and necessary CPU time to obtain a converged
solution.

Coordinate Transformation

It is general practice when applying computational techniques to
calculate flows over arbitrary shapes to use a boundary fitted curvilinear
coordinate system. Although the complexity of the governing equations
increases when transformed into the new coordinate system this approach does
have many advantages from a computational standpoint. By applying a general
transformation

12.5

$$\xi = \xi(x,y,z,t)$$
$$\eta = \eta(x,y,z,t)$$
$$\zeta = \zeta(x,y,z,t)$$
$$\tau = t$$

curved and unequally spaced coordinates in the physical domain are mapped into equally spaced rectilinear coordinates in the computational domain as is shown in Figure 1. Treatment of the boundary conditions is also simplified as the coordinate lines coincide with the boundaries on the edge of the domain. Furthermore, application of the thin-layer approximation can be accomplished simply by dropping the viscous derivatives parallel to the body surface (i.e. the η and ξ directions). However, the most important advantage in terms of providing a good grid is that the grid points can be adaptively clustered in the physical domain to adequately resolve the flow field gradients.

The Thin Layer Code

A thin-layer code has been developed at NASA Ames by Steger et al. [1] which solves the governing equations resulting from the thin layer approximation using an implicit approximate fractorization scheme developed by Beam and Warming [2]. The code has available a number of options to stipulate the assumed flow conditions. It can provide either unsteady or steady inviscid or viscous flow with the option of specifying either laminar or turbulent flow for the viscous case. The turbulent closure model is an extension of Cebeci's two layer eddy viscosity model which avoids the determination of the match point [3]. A simplified version of the Thin layer code has also been developed for the effective computation of axisymmetric transonic projectile problems [4]. The governing equations for the axisymmetric flow problem can be written in conservation law form as follows:

$$\frac{\partial \hat{q}}{\partial L} + \frac{\partial \hat{E}}{\partial \xi} + \frac{\partial \hat{G}}{\partial \zeta} + \hat{H} = Re^{-1} \frac{\partial \hat{S}}{\partial \zeta}$$

where $\hat{q}$ the vector of dependent variables and $\hat{E}$, $\hat{G}$, $\hat{H}$, and $\hat{S}$ are as follows:

$$\hat{q} = J^{-1} \left\{ \begin{array}{c} \rho \\ \rho u \\ \rho v \\ \rho w \\ e \end{array} \right\} \qquad\qquad \hat{E} = J^{-1} \left\{ \begin{array}{c} \rho U \\ \rho u U + \xi_x p \\ \rho v U + \xi_y p \\ \rho w U + \xi_z p \\ (e + p)U - \xi_t p \end{array} \right\}$$

$$\hat{G} = J^{-1} \left\{ \begin{array}{c} \rho W \\ \rho u W + \zeta_x p \\ \rho v W + \zeta_y p \\ \rho w W + \zeta_z p \\ (e + p)W - \zeta_t p \end{array} \right\} \qquad\qquad \hat{H} = J^{-1} \left\{ \begin{array}{c} 0 \\ 0 \\ \rho V \; [R_\zeta (U - \xi_t) + R_\zeta (W - \zeta_t)] \\ -\rho V R \; (V - \eta_t) - p/R \\ 0 \end{array} \right\}$$

$$S = J^{-1} \left\{ \begin{array}{l} \mu \, (\zeta_x^2 + \zeta_y^2 + \zeta_z^2) u_\zeta + \mu/3 \, (\zeta_x u_\zeta + \zeta_y v_\zeta + \zeta_z w_\zeta) \zeta_x \\ \mu \, (\zeta_x^2 + \zeta_y^2 + \zeta_z^2) v_\zeta + \mu/3 \, (\zeta_x u_\zeta + \zeta_y v_\zeta + \zeta_z w_\zeta) \zeta_y \\ \mu \, (\zeta_x^2 + \zeta_y^2 + \zeta_z^2) w_\zeta + \mu/3 \, (\zeta_x u_\zeta + \zeta_y v_\zeta + \zeta_z w_\zeta) \zeta_z \\ (\zeta_x^2 + \zeta_y^2 + \zeta_z^2) [0.5 \mu (u^2 + v^2 + w^2)_\zeta + \mu Pr^{-1} (\gamma - 1)^{-1} (a^2)_\zeta] \\ \quad + \mu/3 (\zeta_x u + \zeta_y v + \zeta_z w) \, (\zeta_x u_\zeta + \zeta_y v_\zeta + \zeta_z w_\zeta) \end{array} \right\}$$

The contravarient velocities U, V. W corresponding to the streamwise
coordinates, the circumferential coordinate η and the radial coordinate
ζ respectively are:

12.7

$$U = \xi_t + \xi_x u + \xi_y v + \xi_z w$$

$$V = \eta_t + \eta_x u + \eta_y v + \eta_z w$$

$$W = \zeta_t + \zeta_x u + \zeta_y v + \zeta_z w$$

The pressure is related through an equation of state

$$p = (\gamma - 1)[e - 0.5\zeta(u^2 + v^2 + w^2)]$$

The details of the derivation of these equations can be found in References [5] and [6]. Note that there are only two spatial derivations remaining, ξ and ζ, thus only a two dimensional grid will be required.

Modifications

The Aerodynamics Research Branch of the U. S. Army Ballistic Research Laboratory has applied the axisymmetric version of the thin Layer code successfully to determine the flow over a SOCBT projectile shape with a sting for a variety of Mach numbers in the transonic regime. These results are reported in Reference [4].

This thin layer code, however, applies boundary conditions corresponding to the simplified projectile flow problem in which a sting is attached to eliminate the base flow region. Thus, the code must be modified to apply the proper boundary conditions for the complete projectile problem which includes base flow.

The original code used by the Army, assumed a flow domain of the form shown in Figure 2 and the boundary conditions were applied to each segment of the domain as follows: Free stream values were assumed on the outerboundary BC. Along the downstream boundary CD it was necessary to use a first order extrapolation for all flow variables to supress high frequency oscillations

that would occur if the pressure was specified [6]. Along the upstream symmetry axis BA the conditions of symmetry are imposed:

$$\frac{\partial u}{\partial z} = 0$$

$$w = 0$$

$$\frac{\partial e}{\partial z} = 0$$

On the solid surface, line AED which includes both the projectile surface and the sting, the no-slip condition was enforced for viscous flow:

$$U = V = W = 0$$

and the other flow variables were set equal to those at the neighboring grid point.

In order to adapt the thin layer code for application to the base flow problem a new flow domain was assumed (Figure 3) and the boundary conditions were applied as follows. Identical boundary conditions are used on the outer boundary BC, the projectile surface AE, and the upstream axis of symmetry BA as were used as corresponding boundaries in the original code. As before, the flow variables are extrapolated to the downstream boundary CD but along ζ coordinates rather than ξ coordinates. The boundary ED now becomes an axis of symmetry similar to those used on the upstream symmetry axis were applied to this axis.

Results

In order to test the modifications made to the thin-layer code, the code was used to solve transonic flow over a sphere. The flow over a sphere serves as a good test case; it has a qualitatively similar flow field to that of a base flow problem in that there is separation and reversed flow, but does not

12.9

contain a sharp corner which creates difficulties in the grid generation. The grid used for the investigation which contains 60 points in the streamwise direction and 40 points in the radial direction is shown in Figure 4. A Mach number of 0.96 and a Reynolds number, based on the radius of 700,000 were used. These values correspond to typical values used in previous studies on transonic projectile aerodynamics. The results of the test shown in the form of a pressure coefficient plot along the surface and a streamline plot are shown in Figures 5a and 5b. Although there is no experimental data available for comparison, these results are believed to be qualitatively correct and it is assumed that these modifications will be satisfactory in applying the thin-layer code to the axisymmetric full transonic projectile aerodynamics problem.

Part 2 - ADAPTIVE GRID GENERATION

Mathematical Formulation

The general purpose of an adaptive grid generation scheme is to enhance the three properties of a good grid, smoothness, orthogonality and mesh refinement in regions where the flow variables have large gradients. Each of these characteristics has been shown to increase the stability and accuracy of numerical algorithms. The adaptive grid generation scheme used here, originally developed by Brackbill and Saltzman [7], is based on a variational principle. Each of the three characteristics can be represented by a functional and for a two dimensional grid, the three functionals I_s, I_o and I_w for smoothness orthogonality and adaptivity appear as follows:

$$I_s = \int (\nabla \xi^2 + \nabla \zeta^2) \, dxdy$$

$$I_o = \int (\nabla \xi \cdot \nabla \zeta) \, J^3 \, dxdy$$

$$I_w = \int w(x,y) \, J \, dxdy$$

In minimizing I_s by applying the Euler-Lagrange equations, Laplace's equations which are known to have a smoothing effect, are recovered. In the function I_o, the dot product:

$$\nabla \xi \cdot \nabla \zeta$$

represents the orthogonality of the ξ and ζ grid coordinates. By minimizing this functional the coordinates are forced to be orthogonal. The term J^3 is the Jacobian of the transformation cubed. It represents the grid spacing and its presence emphasizes orthogonality in regions of large grid cells. In the third functional, I_w, $w(x,y)$ is a weighting function which is to be prescribed. When minimizing I_w, the Jacobian J and consequently the grid spacing

12.11

will be small when $w(x,y)$ is large. If $w(x,y)$ was chosen as the pressure gradient, for instance, the minimization of I_w would cluster points in the vicinity of a shock, and thus I_w can be considered as representing adaptivity.

These three functionals can be combined into a total functional

$$I = I_s + \bar{\lambda}_o I_o + \bar{\lambda}_w I_w$$

where $\bar{\lambda}_o$ and $\bar{\lambda}_w$ are prescribed parameters that weight the importance of orthogonality and adaptivity to smoothness according to their perceived importance. In order to obtain a grid, the dependent and independent variables are first interchanged so that the solution can be obtained on the computational grid. Application of the Euler-Lagrange equations to the transformed functional:

$$I' = \int \frac{1}{J}(\nabla x^2 + \nabla z^2) d\xi d\zeta + \bar{\lambda}_o \int (x_\xi x_\zeta + z_\xi z_\zeta)^2 d\xi d\zeta + \bar{\lambda}_w \int w J^2 \, d\xi d\zeta$$

results in a set of elliptic partial differential equations which can be solved by a Newton-Raphson iterative technique. The solution in the form

$$x(\xi,\zeta) \quad y(\xi,\zeta)$$

defines a set of discrete points in the physical plane for integer values of ξ and ζ which constitute the grid. Details of this approach can be found in Reference [8]. However, there are two important considerations that must be addressed before this method will be successful. First, the relative magnitude of the three functionals must be determined through dimensional analysis to ensure that the parameters λ_o and λ_w will accurately reflect the perceived importance of each functional. Also, since the grid generation equations are elliptic, the boundary points must be prescribed. Successful application of the adaptive grid generation scheme requires consistency

12.12

between grid points along the boundary and in the domain; thus it is also necessary to develop adaptive techniques for the boundary.

Dimensional Analysis

In order to normalize the three functionals I_s, I_o, and I_w a dimensional analysis is applied. Let L be a physical length scale, L' be a computational length scale and $\overline{W}$ is a measure of the weight function. Using these scales the three functionals have the following orders of magnitudes:

$$I_s \sim (L')^2$$
$$I_o \sim L^4/L'^2$$
$$I_w \sim \overline{W} \frac{L^4}{L'^2}$$

The total functional I, can be rewritten as

$$I = I_\zeta + \frac{\lambda_o}{\lambda_o'} I_o + \frac{\lambda_w}{\lambda_w'} I_w$$

where λ_o' and λ_w' are determined to normalize the functionals I_o and I_w. According to the determined order of mangnitude for the functionals, the following choices

$$\lambda_o' \sim \left(\frac{L}{L'}\right)^4 \qquad \lambda_w' = \overline{w}\left(\frac{L}{L'}\right)^4$$

will accomplish the normalization. Currently the choices for the scales L, L' and $\overline{w}$ are as follows:

$$L = \sqrt{A}$$
$$L' = \sqrt{J_m \cdot K_m}$$
$$\overline{w} = \frac{1}{A} \int w\,dA$$

12.13

where A is the area of the physical domain, J_m is the number of grid points in the ξ direction and K_m the number in the ζ direction.

Boundary Adaptation

Two methods of adapting the boundary to obtain consistency with the domain have been developed. The first method is a one dimensional version of the variational principle. Let s be a measure of the physical arc length along the boundary and ξ be the coordinate coinciding with the boundary. Then a one dimensional version of I_s can be written as

$$I_s = \int_{S_o}^{S_F} (\xi_s)^2 \, ds$$

Let W(s) be the corresponding weight function along the boundary. Then I_w becomes:

$$I_w = \int W(s) \, S_\xi \, ds$$

where S_ξ is the Jacobian of the transformation. These two functionals can be combined and the variables interchanged to yield the total functional in the computational domain:

$$I = \int (S_\xi)^{-1} d\xi + \frac{\lambda_w}{\lambda_w'} \int W \cdot S_\xi^2 \, d\xi$$

A similar dimensional analysis shows that λ_w' should be:

$$\lambda_w' = \overline{W} \left(\frac{L}{L'}\right)^3$$

The scales L, L' and $\overline{W}$ for the one dimensional problem are defined as

$$L = S_{max}$$
$$L' = J_{max}$$
$$\overline{W} = \frac{1}{S_{max}} \int W \, ds$$

12.14

This boundary adaptive method has been implemented in the adaptive grid generation scheme to adapt the grid points along the body surface.

A second boundary adaptive technique has also been employed. This method is based on an extrapolation of the grid spacing from the domain onto the boundary. Let $S_D(\xi)$ represent the arc length distribution of the grid points along a coordinate adjacent to the boundary. The normalized distributions $\overline{S}_D$ can be obtained as:

$$\overline{S_D} = \frac{S_D(\xi)}{(S_D)_{max}}$$

where $(S_D)_{max}$ is the total length of the boundary. Let $S_B(\xi)$ be the arc length distribution along the boundary. After each iteration of the solution algorithm for the domain, the position of the boundary points can be updated to correspond to those of the domain with a zero order extrapolation:

$$S_B(\xi) = \overline{S_D}(\xi) \cdot (S_B)_{max}$$

Thus as the points in the domain move to satisfy the governing equations, the boundary points will continuously move to be consistent. This boundary adaptive technique also has been implemented in the grid generation scheme to adapt the points along the two axisymmetric boundaries. At this point, no boundary adaptive technique is employed along the outer or downstream boundary.

Results

As a test case to develop and analyze the adaptive grid generation scheme, the scheme was applied to a radial grid with 40 points in the circumferential ξ direction and 25 points in the radial ζ direction. There are two parameters λ_o and λ_w and one function $w(x,y)$ that must be given. In practice,

the weight function $w(x,y)$ will be some function of the pressure and velocity gradients that develop as part of the solution to the transonic flow problem. For purposes of this study, however, an artificial pressure distribution of the form

$$p = f(\xi, \zeta)$$

is applied to an initial 40 by 25 radial grid shown in Figure 6. The weighting function is calculated as:

$$w = |\nabla p| + |\nabla(|\nabla p|)|$$

The primary purpose of this analysis is to check the effectiveness of the adaptive grid generation and to determine the consistency between the adapted boundary grid points and the domain. Three separate cases were run each with a different pressure distribution.

The pressure distribution for the first case was chosen as

$$p = \exp\left[-\frac{1}{9} (\xi - 20)^2 \right]$$

which constitutes a spike centered on the $\xi = 20$ coordinate and consequently the weighting function w should be large in that region. The resulting adaptive grid, obtained with $\lambda_o = 2$ and $\lambda_w = 4$ is shown in Figure 7a and it is apparent the coordinates are clustering toward the region of large w. The enlarged view of the grid near the sphere (Figure 7b) reveals the good degree of consistency between the domain and the boundary obtained using the one dimensional variational approach along the sphere surface.

In order to analyze the second boundary adaptive method which was used along the axis of symmetry the following pressure distribution was applied:

$$p = \exp\left[-\frac{1}{9} (\xi - 20)^2 \right] + \exp\left[-\frac{1}{4} (\zeta - 17)^2 \right]$$

Use of this pressure distribution is expected to cluster the circumferential lines near the $\zeta = 17$ coordinate as well as near $\zeta = 20$. The results for $\lambda_o = 2$ and $\lambda_w = 4$ are shown in Figure 8. The good degree of consistency obtained between the domain and boundary using the extrapolating boundary adaptive technique is readily apparent along the two symmetry axes.

The third and final adaptive grid was generated using the pressure distribution

$$p = \exp \left[-\frac{1}{9} (\zeta - 20)^2 \right] + \exp \left[-\frac{1}{3} (\zeta - 1) \right]$$

which was expected to cluster the grid near the sphere surface as well as near the $\zeta = 20$ coordinate. The resulting grid obtained using $\lambda_o = 2$ and $\lambda_w = 4$ is shown in Figure 9. In a comparison with the grid of Figure 7a, it appears that the grid is clustering towards the sphere, but not to a large degree. A careful examination of the selected pressure distribution shows that the contribution of the second term to the magnitude of the weight function is not very overwhelming near the sphere surface. Note also that the clustering of the coordinates towards the $\zeta = 20$ line is not as strong in Figure 9 as it is in Figure 7a even though the same values were used for λ_o and λ_w.

The results of numerical experiments conducted have shown that both boundary adaptive techniques implemented can provide a grid with good degree of consistency between the boundary and domain at least for the circular boundary geometry considered. Moreover, the results indicate that it will be necessary to analyze the relative characteristics of terms constituting the weight function so that one term, the pressure gradient for instance, will not swamp the effect of other terms such as velocity gradient. It is clear that the adaptive grid generation scheme has potential for effectively generating a good grid; however, for a specific problem, more detailed analysis and

experimentation must be carried out to determine the effects of the parameters λ_o and λ_w as well as the choice of grid resolution control function for generating a good adaptive grid.

REFERENCES

1. Pulliam, T. H. and Steger, J. L., (1980), "Implicit Finite-Difference Simulations of Three Dimensional Compressible Flow", AIAA Journal, Vol. 18, No. 2.

2. Warming, R. F., and Beam, R., (1978), "On the Construction and Application of Implicit Factored Schemes for Conservation Laws", SIAM-AMS Proceedings, Vol. 2.

3. Baldwin, B. S., and Lomerx, H., (1978), "Thin Layer Approximation and Algebraic Model for Separated Turbulent Flows", AJAA 78-257, Presented at AIAA 16th Aerospace Sciences Meeting, Huntsville, AL.

4. Nietubicz, C. J., Pulliam, T. H. and Steger, J. L., (1979), "Numerical Solution of the Azimuthal-Invariant Thin Layer Navier-Stokes Equations", Paper 79-0010 presented at 17th Aerospace Sciences Meeting, New Orleans, LA.

5. Nietubicz, C. J., (1982), "Navier-Stokes Computations for Conventional and Hollow Projectile Shapes at Frarsonic Velocities", ARBRL-MR-03184, U. S. Army Ballistic Research Laboratory, Aberdeen Proving Ground, MD.

6. Sahu, J., Niebuticz, C. J. and Steger, J. L., (1983), "Numerical Computation of Base Flow for a Projectile at Transonic Speeds", ARBRL-TR-02495, U. S. Army Ballistic Research Laboratory, Aberdeen Proving Ground, MD.

7. Saltzman, J.and Brickbill, J. U., (1982) "Application and Generalization of Variational Methods for Generating Adaptive Meshes", in Numerical Grid Generation, J. F. Thompson (editior), North-Holland, NY, pp. 865-884.

8. Tu, C. G., (1985), "Development of an Adaptive Grid Generation Code for Projectile Aerodynamics Computation", Ph.d. Dissertation, University of Florida, Dept. of Engineering Sciences, Gainesville, FL.

FIGURE 2   PREVIOUS FLOW DOMAIN

FIGURE 3   NEW FLOW DOMAIN
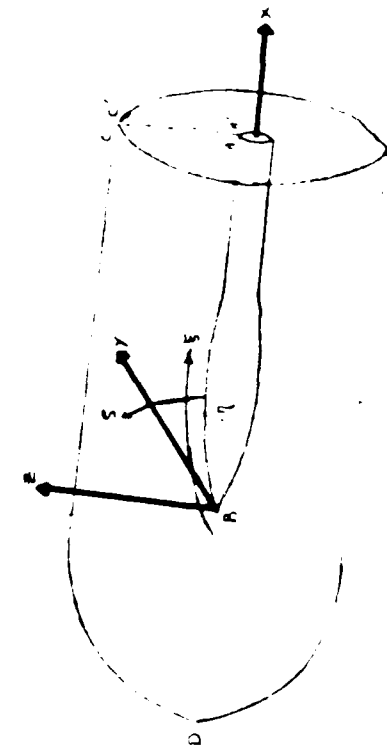
PHYSICAL DOMAIN
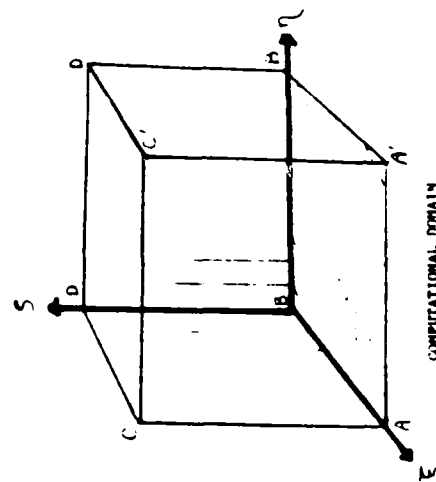
COMPUTATIONAL DOMAIN

FIGURE 1   COORDINATE TRANSFORMATION

12.19
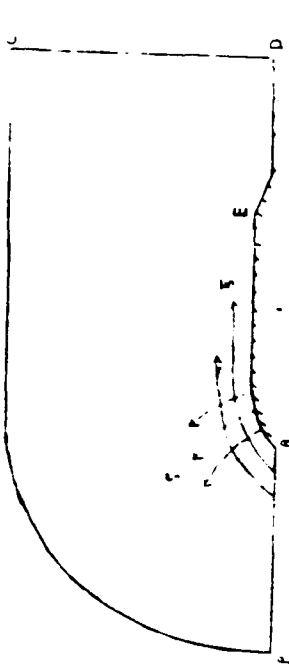
FIGURE 5b STREAMLINES
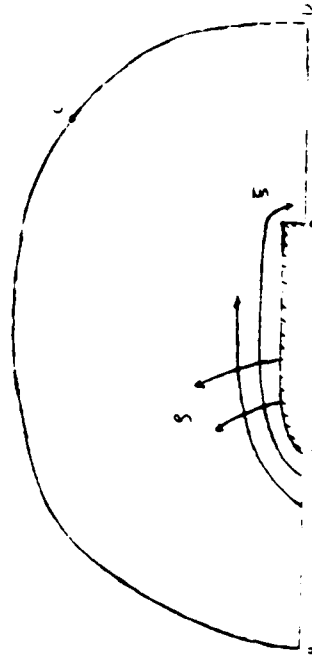
FIGURE 6 INITIAL 40 x 75 RADIAL GRID
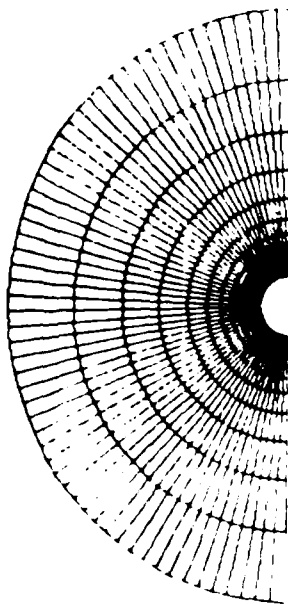
FIGURE 4 60 x 40 RADIAL GRID
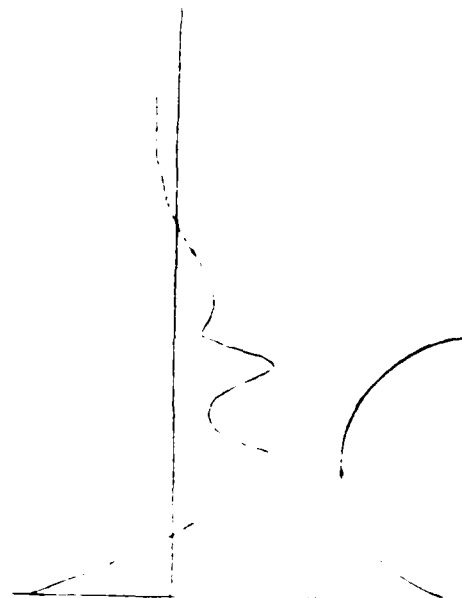
FIGURE 5a Cp ALONG THE SURFACE
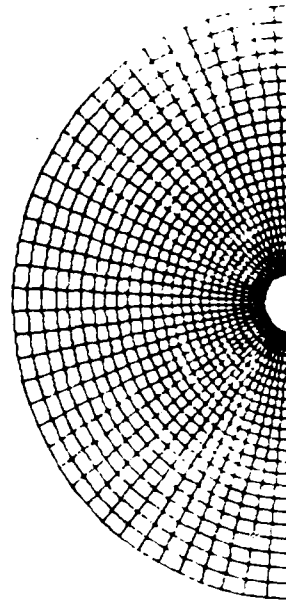
FIGURE 4   ADAPTIVE GRID #2

FIGURE 3   ADAPTIVE GRID #1
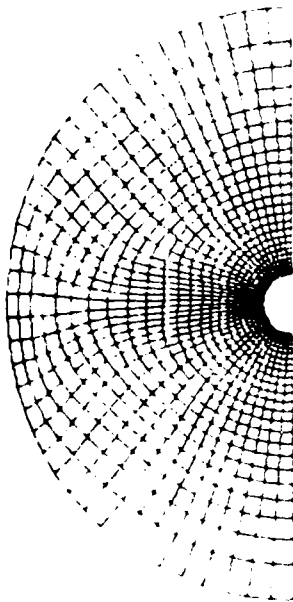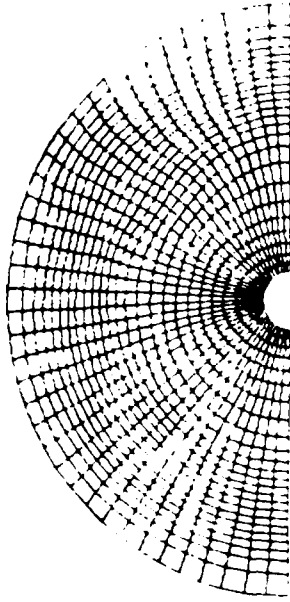
FIGURE 2a   ADAPTIVE GRID #1
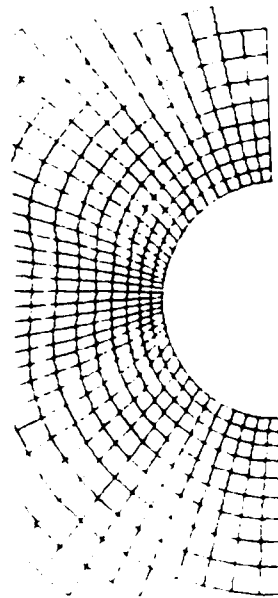
FIGURE 2b   ENLARGED VIEW NEAR SPHERE
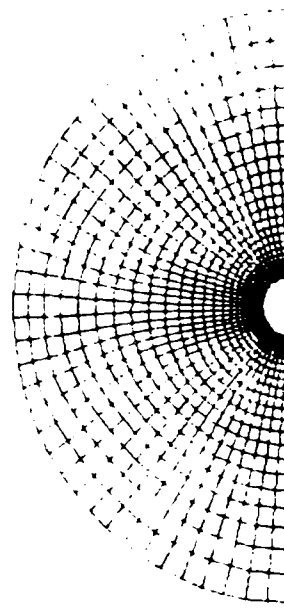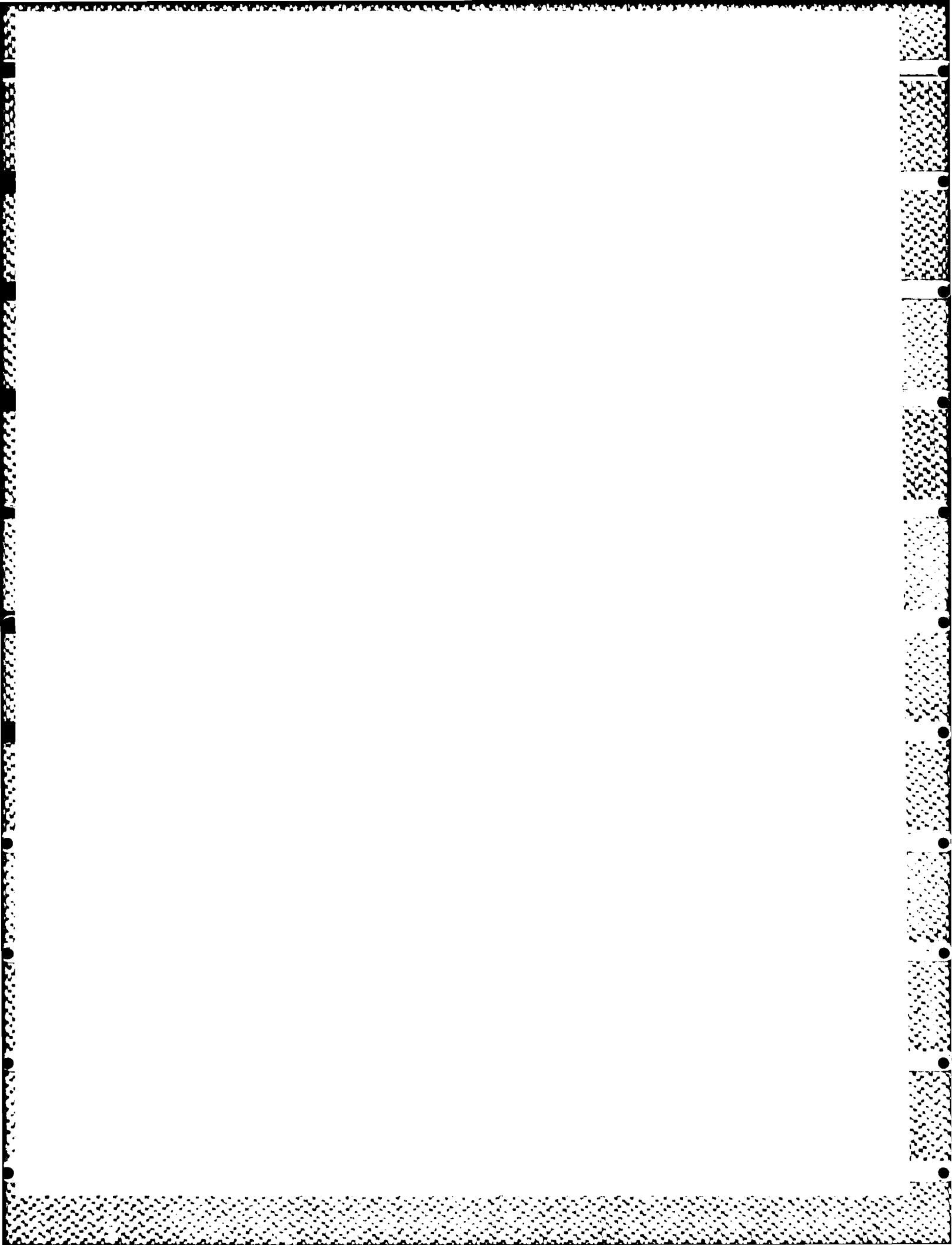
USE OF BAYESIAN DECISION THEORY IN ASSESSING
THE POTABILITY OF GROUND WATER BASED DRINKING WATER SUPPLIES

by

Stephan J. Nix
Assistant Professor

and

Jeffrey Schenck
Graduate Assistant

Department of Civil Engineering
Syracuse University
Syracuse, New York   13210

Submitted to

I.   INTRODUCTION

There is ample evidence to conclude that ground water is becoming increas-
ingly vulnerable to contamination by various chemical elements and compounds
(Hess et al., 1983). Ground water, long considered pristine and not particu-
larly susceptible to manmade pollution, has become the primary source of drinking
water for approximately half of the American population. Skeptics may take
solace in recent reports that only 1 to 2 percent of the useable ground water
in the United States is contaminated (Pye and Patrick, 1983; Lehr, 1982; USEPA,
1980b). Taken out of context this can be a misleading statement. When one
considers that man's activities, a primary source of pollution, are usually
located in the general vicinity of his sources of ground water and that these
estimates did not account for all pollution sources, it becomes quite clear
that the threat is much more substantial.

In a recent study, a survey of 1583 drinking water supplies that failed
to meet Environmental Protection Agency (EPA) regulations for inorganics revealed
that a large majority cited ground water as their source (Hess et al., 1983;
Clifford et al., 1983). The inorganic chemicals that appeared most commonly
in these supplies were chloride, nitrate, selenium, barium and arsenic. While
these are generally produced by natural processes, industrial and agricultural
sources may also be responsible. Also appearing were metals such as lead,
cadmium, chromium, mercury, and silver--usually indicators of manmade contamina-
tion. A recent paper by Hess et al. (1983) reports that more than 700 organic
compounds have been identified in ground water based drinking water supplies
in the U.S. Certain trihalomethanes appeared in as much as 70 percent of the
supplies and some chlorinated hydrocarbon solvents appeared in approximately
one out of four. While the appearance of trihalomethanes can often be traced

to chlorination (for disinfection), the presence of other oganics is probably
due to contamination of the ground water source.

Exacerbating this problem is the fact that many chemicals (especially
organic chemicals) have not been tested for their possible deleterious effects
on public health. In addition, analytical procedures have not been developed
to detect many organic compounds. Adding a further complication is the pollution
transport characteristics of ground water. The movement of ground water is
generally very slow and, thus, many trouble spots remain to be discovered.
It seems that the contamination of ground water based drinking water supplies
is a problem with no readily identifiable bounds, but it is almost certainly
significant and widespread.

The U.S. Air Force, because of its mission, has long been involved in
operations that generate considerable amounts of hazardous wastes and, thus,
the potential for contamination is present at many installations. Preliminary
data collected from monitoring wells at several Air Force installations indicate
that some ground water contamination is occurring as a result of past disposal
practices or accidents. These data were collected as part of the Installation
Restoration Program (IRP). This program is charged with identifying, quantifying
and controlling the problems associated with inactive hazardous material disposal
sites and past accidental spills (Dept. of Defense, 1981). A list of the detec-
ted contaminants is shown in Table 1. The effect on the drinking water supplies
at these installations is unclear at this time. However, there is sufficient
concern for Air Force officials to question the present and future quality
of drinking water supplies taken from ground water sources at all Air Force
installations, especially with regard to organic compounds.

Table 1.   Ground Water Contaminants Detected at IRP Sites.

Benzene	Ethylbenzene
Bis(2-chloroethyl) ether	Methylene Chloride
Bis(2-ethylhexyl) phthalate	Naphthalene
	N-Nitrosodimethylamine
Carbon Tetrachloride	N-nitrosodiphenylamine
Chlorobenzene	
Chloroform	1,1,2,2-Tetrachloroethane
Chloroethane	Tetrachloroethylene
	Toluene
1,2-Dichlorobenzene	1,2-Trans-dichloroethylene
1,3-Dichlorobenzene	1,2,4-Trichlorobenzene
1,4-Dichlorobenzene	
1,1-Dichloroethane	1,1,1-Trichloroethane
1,2-Dichloroethane	Trichloroethylene
1,1-Dichloroethylene	Trichlorofluoromethane
1,2-Dichloropropane	
2,4-Dimethylphenol	Xylenes
Di-n-butyl phthalate	Vinyl Chloride
2,6-Dinitrotoluene	

Air Force officials have also been concerned with the ability of the current drinking water surveillance program, as delineated in Air force Regulation 161-44 (Dept. of the Air Force, 1981), to effectively detect contamination by organic compounds. AFR 161-44 essentially monitors supplies for the contaminants contained in the EPA Interim Primary Regulations for Drinking Water and those contained in secondary regulations (see Table 2) once every three years. The list of regulated inorganic chemicals is not exhaustive but probably contains most of the major concern. The list of organic chemicals, however, contains some of the compounds detected thus far at several Air Force installations but it is lacking when one considers the hundreds that have been found in supplies around the U.S. Considering the apparent scope of the problem, it appears that AFR 161-44 is inadequate.

The principal investigator's brief tenure at the USAF Occupational and Environmental Health Laboratory (USAF OEHL), Brooks AFB, Texas for the SCEEE Summer Faculty Research Program was, in part, devoted to developing a methodology for assessing the potability of ground water based drinking water supplies at Air Force installations around the world. Only contamination by organic compounds was considered since their presence and the apparent inadequacy of AFR 161-44 to detect them were the major concerns of Air Force officials. The procedure is a rather simple, conservative decision making process that, as was noted in the associated report (Nix, 1984), should be modified as more information becomes available. The simplified nature of the methodology was dictated by the short time available for its development and the need of the Air Force for a procedure that would not consume large amounts of resources and time. The objective of this study is to solidify and enhance the decision making process used in this methodology by structuring the process within the

Table 2. USEPA Interim Primary and Secondary Regulations for
Drinking Water (USEPA, 1981; USEPA, 1980a)

PRIMARY			SECONDARY		
CONTAMINANT OR PARAMETER	MAXIMUM LEVEL		CONTAMINANT OR PARAMETER	MAXIMUM LEVEL	
Inorganic Chemicals			Chloride	250	mg/L
			Color	15 color units	
Arsenic	0.05	mg/L	Copper	1	mg/L
Barium	1.0	mg/L	Corrosivity	Noncorrosive	
Cadmium	0.010	mg/L	Foaming Agents	0.5	mg/L
Chromium	0.05	mg/L	Hydrogen Sulfide	0.05	mg/L
Lead	0.05	mg/L	Iron	0.3	mg/L
Mercury	0.002	mg/L	Manganese	0.05	mg/L
Nitrate (as N)	10	mg/L	Odor	3 Threshold Odor Number	
Selenium	0.01	mg/L			
Silver	0.05	mg/L	pH	6.5 - 8.5	
Fluoride	1.4-2.4	mg/L	Sulfate	250	mg/L
			TDS	500	mg/L
Organic Chemicals*			Zinc	5	mg/L
Endrin	0.0002	mg/L			
Lindane	0.004	mg/L			
Methoxychlor	0.1	mg/L			
Toxaphene	0.005	mg/L			
2,4-D	0.1	mg/L			
2,4,5-TP Silvex	0.01	mg/L			
Total Trihalomethanes	0.1	mg/L			
Turbidity	1 TU - 5 TU				
Coliform Bacteria	1/100 mL (mean)				
Radiological					
Radium 226 and 228	(5pCi/L)				
Gross Beta	4 mrem/year (50 pCi/L)				
Gross Alpha	(15 pCi/L)				

*Additional organic chemicals
proposed for inclusion:

Benzene
Chlorobenzene
Dichlorobenzene(s)
Trichlorobenzene(s)
1,1-dichloroethylene
cis-1,2-dichloroethylene
trans-1,2-dichloroethylene
Trichloroethylene
Tetrachloroethylene
Carbon Tetrachloride
1,1,1-Trichloroethane
1,2-Dichloroethane
Vinyl Chloride
Methylene Chloride

Notes:
mg/L = milligrams per liter
TU = turbidity units
mL = milliliters
pCi/L = picocuries per liter
mrem = millirems

framework provided by Bayesian decision theory. While the theoretical aspects of this management science discipline are not difficut to grasp, its application requires careful attention to the numerical assignments made to various facets of the decision making problem.

The assessment of drinking water quality certainly involves a measure of decision making since limited resources must be allocated effectively in order to correctly evaluate the potability of a large number of supplies. Not considered in this study is the decision making process involved in determining the fate of an individual supply. The true value of this work is the guidance it may provide for the improvement of AFR 161-44 in its ability to detect contamination by organic compounds and its cost-effectiveness. Additionally, the information provided here will be useful in formalizing and improving the decision making processes involved in other, similar Air Force activities within the area of environmental monitoring.

II. OBJECTIVES

The objectives of the study is to structure the monitoring and assessment of ground water based drinking water supplies at Air Force installations as a Bayesian decision process. Bayesian decision theory is a tool by which the decision making process can be identified, compartmentalized, and, in the end, better understood. The U.S. Air Force currently conducts a fairly extensive drinking water monitoring program that may be improved and made more cost effective if approached as a decision process involving experimentation, evaluation, and the assessment of risk. This study will outline an approach for using Bayesian decision theory in the development of this perspective. The focus of the effort is on the detection of organic compounds as these probably repre-

14.7

sent the most compelling challenge to the potability of ground water based

drinking water supplies.

III. REVIEW OF PRELIMINARY EFFORT

The principal investigator, while at the USAF OEHL under the aegis of
the Summer Faculty Research Program, was given the task of formulating a proce-
dure for assessing the potability of ground water based drinking water supplies
with regard to organic chemicals. This was and remains an important task.
Thousands of people at dozens of installations and an array of vital missions
are affected by the suitability of drinking water supplies. This task as part
of a larger set of concerns put forth by Air Force officials. More specifically,
the following questions were posed:

(1) Which Air Force installations rely directly on ground water sources,
     or vendors using ground water, for drinking water?

(2) Which of these installations are known or alleged to have reason
     to be concerned about the quality of their drinking water supplies
     with respect to contamination by organic compounds?

(3) Which water quality parameters and constituents are most commonly
     associated with contamination by organic compounds?

(4) Do present sampling schemes and analytical procedures detect and
     identify organic contaminants?

(5) If the answer to the last question is negative, what analyses should
     be performed to ensure that ground water sources are not contaminated
     and that future threats can be rapidly identified?

A survey has been conducted by the Air Force Engineering Services Center
(AFESC) to determine which Air Force installations are relying on ground water

14.8

sources, thus answering question 1 and providing a wealth of related information (see Nix, 1984). The focus of the earlier effort was the development of a methodology to answer question 2. As mentioned earlier, the methodology developed during the short summer research period is a rather simple, conservative procedure that should probably be enhanced. The effort in this study was directed toward improving the methodology and providing a vehicle for answering questions 3, 4 and 5.

The procedure developed during this effort is a chronological sequence designed to be applied to each installation using ground water. The priority in which the various installations are studied is not addressed. The procedure can be summarized by the sequence of steps given below and is shown in Figure 1. A more detailed description may be found in an earlier report (Nix, 1984).

Step 1a) Determine the potential for the drinking water supply to be contaminated by any nearby waste discharge or disposal sites or other sources of pollution. The analyst is asked to consider three basic questions in order to make this determination: (a) Are there waste discharge or disposal sites containing organic materials that could contaminate the ground water source? (b) Is there a possible hydrologic and/or hydraulic connection between the identified waste sites and the drinking water supply? (c) Is there a history of water quality standards and/or criteria violations or illnesses associated with contamination by organic compounds that have not been explained by localized accidental spills with short impact times? Some guidance is provided in order to answer these questions, but considerable weight is placed on the judgement and localized knowledge of the analyst. Given the answers, the analyst can state "yes", there is potential for contamin-
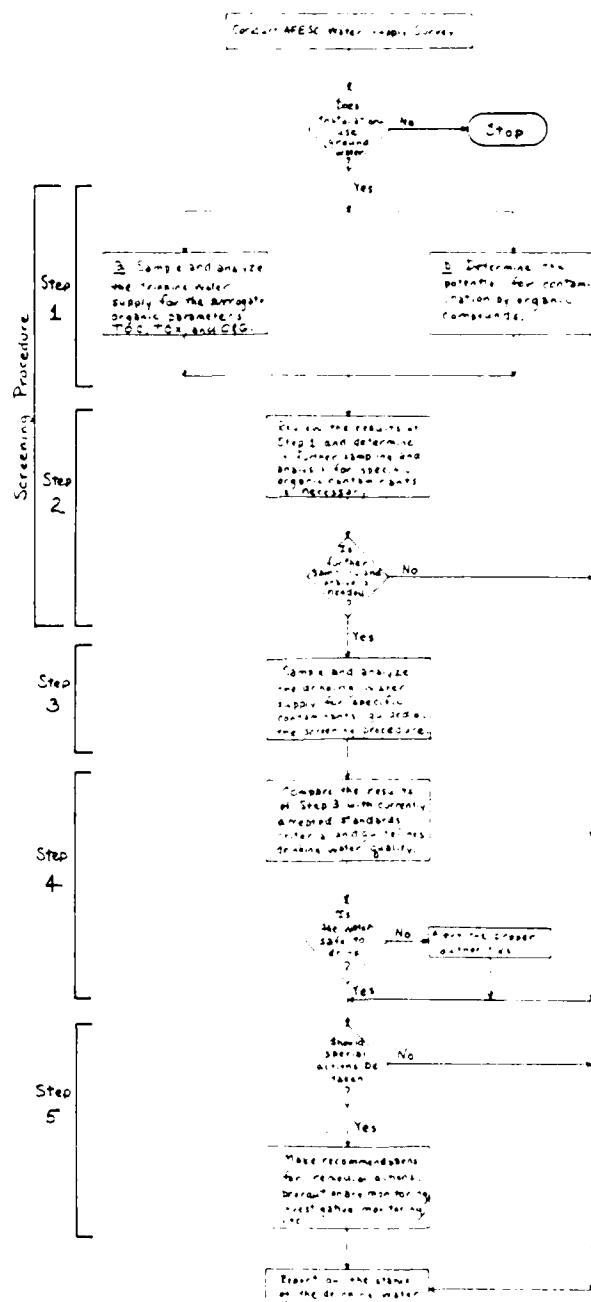
Figure 1. Preliminary Methodology to Assess the Potability of
Ground Water Based Drinking Water Supplies (Nix, 1984).

14.10

ation of the drinking water supply, or "no", there is none. This

simple response (although it is not implied that the determination

is easy) is used in a simple decision matrix, along with other informa-

tion, to determine if further sampling and analysis of the supply

is warranted. Positive responses to questions (a) and (b) indicate

that, "yes", there is a potential problem. A positive response to

question (c), even if not accompanied by responses to (a) and (b),

will also indicate a potential problem. Much of the information

used in this evaluation will be provided by the AFESC survey mentioned

earlier.

Step 1b) Sample and analyze the finished or treated water supply (i.e., that

which is presented to the consumer) for a small set of "indicative"

or "surrogate" water quality parameters that portend the presence

of various groups of organic compounds. Following the lead of other

related programs, it was proposed that those parameters should be

total organic carbon (TOC), total organic halogen (TOX), and oil

and grease (O&G). These parameters are listed in Table 3 along with

their analytical methods and detection limits. The parameter TOC

is useful for detecting general organic contamination. TOX is parti-

cularly useful because it detects an important class of compounds,

namely organic halogens, and because of its relatively low detection

limit. Oil and grease measurements are useful because of obvious

dependence the Air Force has on a number of petroleum products and

its low detection limit. A sampling and analysis scheme that includes

these parameters provides additional information, at a very low cost,

for use in determining the need for more detailed and costly schemes.

14.11

Table 3. Indicator Organic Parameters (Dept. of the Air Force, 1984).

Surrogate Parameter	Analytical Method	Detection Limit
Total Organic Carbon (TOC)....	EPA Method 415.1 (USEPA, 1979b)	1000 µg/L
Total Organic Halogens (TOX)..	EPA Method 9020 (USEPA, 1982)	5 µg/L
Oil and Grease (O&G)..........	EPA Method 413.2 (USEPA, 1979b)	100 µg/L

Note: µg/L = micrograms per liter

Since the detection limits given in Table 3 are relatively high when
compared to the levels of individual compounds known to cause health
problems (see Table 4), these limits given were suggested as food
"flags" for indicating the possible presence of organic contaminants.
It was also suggested that all available data collected under AFR
161-44 be consulted for possible indications.

Step 2) Review the results of Step 1 (parts a and b) and determine if detailed
sampling and analysis for specific contaminants is warranted. The
decision matrix is shown in Table 5. An important feature to note
is that the focus of any detailed sampling and analysis scheme is
guided by the knowledge of what types of contaminants may be expected
given the indications provided by Step 1. Prompted by an overriding
concern for public health, the decision is conservatively determined.
There is only one situation in which no further action is required.
The apparent presence of contamination and/or the potential threat
of contamination triggers more detailed sampling and analysis.

Step 3) If the results of Step 2 demand it, sample and analyze the finished
drinking water supply for specific contaminants. Again, the actual
scheme should be a function of the signals provided by Step 1.

Step 4) Compare the results of Step 3 with established standards, criteria,
and guidelines (see Tables 2 and 4) and assess the potability of
the finished drinking water supply. This involves the identification
of the offending contaminants and alerting installation officials
if a problem is found. Not addressed in this methodology is the
validity of the various standards, criteria, and guidelines. Its
purpose is to evaluate the supply in light of current wisdom.

14.13

Table 4. Water Quality Criteria for the More Common Toxic Organic Compounds (from Pettyjohn and Hounslow, 1983).

Name	PDWS (1,5)	T-O (2,5)	Toxic (3,5)	Cancer (4,5)
Non Aromatic Chains				
Hydrocarbons with or without O and/or N functional group				
Acrolein				
Acrylonitrile			320 µg/L	
N Nitroso Dimethylamine				0.0014 µg/L
N Nitroso Diethylamine				1.4 ng/L
N Nitroso Di N Butylamine				8.4 ng/L
N Nitroso Diphenylamine				4900 ng/L
N Nitrosopyrrolidine				160 ng/L
Single-Ring Aromatics				
Benzene				0.66 µg/L
Toluene			14.3 mg/L	
Ethyl Benzene			1.4 mg/L	
Phenol		0.3 mg/L	3.5 mg/L	
2,4 Dimethylphenol		400 µg/L		
2,4 Dinitrophenol			70 µg/L	
2,4-Dinitro-O-Cresol			13.4 µg/L	
Nitrobenzene			19.8 mg/L	
2,4 Dinitrotoluene		30 µg/L		0.11 µg/L
Dimethyl Phthalate			313 mg/L	
Diethyl Phthalate			350 mg/L	
Dibutyl Phthalate			34 mg/L	
Di 2 Ethyl Hexyl Phthalate			15 mg/L	
Polycyclic Aromatics				
Acenaphthylene		20 µg/L		
Fluoranthene			42 µg/L	0.17 ng/L
Pyrene			42 µg/L	42 ng/L
1,2 Diphenyl Hydrazine				
Organohalogen Compounds				
Neo Aromatics				
Methane Derivatives				
Halomethane				0.19 µg/L
Chloroform		100 µg/L		0.19 µg/L
Carbon Tetrachloride				0.4 µg/L
Ethane Derivatives				
Chloroethene (Vinyl Chloride)				2.0 µg/L
1,2 Dichloroethane				0.94 µg/L
Pentachloroethane		18.4 mg/L		0.33 µg/L
1,1,1 Trichloroethane				0.6 µg/L
1,1,2 Trichloroethane				0.6 µg/L
Trichloroethylene				0.17 µg/L
1,1,2,2 Tetrachloroethane				1.9 µg/L
Tetrachloroethylene				1.9 µg/L
Hexachloroethane				
Propane Derivatives				
Dichloropropane/Dichloropropene				
Butane Derivatives			87 µg/L	0.45 µg/L
Hexachlorobutadiene				

Name	PDWS (1,5)	T-O (2,5)	Toxic (3,5)	Cancer (4,5)
Pentane Derivatives				
Hexachlorocyclopentadiene			10.7 µg/L	
Hexachlorocyclohexane				
Alpha HCH				9.2 ng/L
Beta HCH				16.3 ng/L
Gamma HCH (Lindane)	4 µg/L			18.6 ng/L
Technical HCH				12.3 ng/L
Complex Cyclic Compounds				
Aldrin				0.0074 ng/L
Dieldrin				0.71 ng/L
Chlordane				0.46 ng/L
Heptachlor				0.28 ng/L
Isophorone			5.2 mg/L	
Endosulfan			7.4 µg/L	
Endrin	1 µg/L			
Toxaphene	5 µg/L			0.71 ng/L
Ether Derivatives				
Bis (Chloromethyl) Ether				0.0000 ng/L
Bis (2 Chloroethyl) Ether			24.7 µg/L	0.03 ng/L
Bis (2 Chloroethyl) Ether				0.03 ng/L
Bis (2 Chloroisopropyl) Ether				
Single-Ring Aromatics				
Monochlorobenzene				
Dichlorobenzenes		20 µg/L	448 µg/L	
1,2,4,5 Tetrachlorobenzene			403 µg/L	0.72 ng/L
Hexachlorobenzene			14 µg/L	
Pentachlorobenzene			74 µg/L	
Single-Ring Aromatics				
Monochlorophenol				
2,4 Dichlorophenol			0.12 µg/L	
2,4,5 Trichlorophenol				
2,4,6 Trichlorophenol			0.5 µg/L	
3,4 Dichlorophenol			0.2 µg/L	
2,4,5 Trichlorophenol			0.3 µg/L	
2,4,6 Trichlorophenol			1.0 µg/L	1.2 µg/L
2 Methyl 4 Chlorophenol			2.6 mg/L	
2 Methyl 4 Chlorophenol			1800 µg/L	
3 Methyl 4 Chlorophenol			3000 µg/L	
3 Methyl 6 Chlorophenol			20 µg/L	
Pentachlorophenol			30 µg/L	
2,4 D		100 µg/L	101 mg/L	
2,4,5 T		10 µg/L		
Polycyclic Aromatics				
3,3 Dichlorobenzidine				0.001 µg/L
Polychlorinated Biphenyls		0.1 mg/L		0.79 ng/L
DDT and Metabolites				0.24 ng/L
Methoxychlor				

Notes:
1. "EPA National Interim Drinking Water Regulations 40 CFR 141 July 1 1981 (USEPA, 1981)
2. "Organoleptic concentration, taste and odor
3. "Toxic concentration
4. "Increase in cancer risk over lifetime of one in one million.
   This does not represent risk assessment judgement on an "acceptable risk level
5. "Source: Modified after 45 FR 79318, November 28 1980"
   mg/L = milligrams/liter
   µg/L = micrograms/liter
   ng/L = nanograms/liter

(USEPA, 1980c)

14.14

Table 5. Screening Procedure Action Table.

| Case | Screening Tests (Step 1) | | Action |
	Contamination Potential	Surrogate Parameters[1]	
1	Potential Indicated	Detection Level Exceeded	Sample and analyze specific organic contaminants.[2]
2	Potential Indicated	No Detection	Review and possibly repeat Step 1. If original results are reproduced sample and analyze for specific contaminants.[2] If results change, take the appropriate action.
3	No Potential	Detection Level Exceeded	
4	No Potential	No Detection	No further action required.

Notes:

1. Any surrogate parameter exceeding a detection limit will trigger some sort of action (see note 2).

2. The sampling and analysis for specific contaminants is guided by the results of Step 1. In other words, a certain group of contaminnats may be expected given the information gained in assessing contamination potential and the presence of certain surrogate parameters.

14.15

Step 5) Review the results of Steps 3 and 4 and recommend any further action. If a potability problem was found, remedial action may be needed. Possible actions might include treatment of the supply, closure of the supply, control of the contamination source, or using alternative supplies. The appropriate action will be determined by the severity of the problem, the consequences of the action, and, of course cost. However, before any remedial action is recommended, a monitoring program should be used to pinpoint the cause of the problem. If no potability problem was found in Steps 3 and 4 but the results of Steps 1 and 2 suggested a potential problem it would certainly be prudent to initiate a precautionary monitoring program. This would be even more apropos if detectable but "safe" levels of various contaminants were present.

The methodology outlined above seems to be a reasonable approach for assessing ground water based drinking supplies at Air Force facilties around the globe. The procedure itself is rather simple, but it relies heavily on the judgement and experience of those carrying it out and the encapsulated techniques (e.g., chemical analyses) may be fairly involved. However, it seems obvious that a firmer foundation is necessary in the long run.

IV. CONTAMINATION DEFINED

An effective methodology needs a working definition of contamination. To contaminate means, by most dictionaries, "to make impure by contact or mixture." The classical environmental definition says that a contaminant is any material out of place in the environment. These are good general definitions but they beg the question of how impure must a medium such as ground water

become before the beneficial uses are impaired. Perhaps a contaminant should be defined as a material that causes the most beneficial use of the resource to be impaired. However, this just transfers the problem to other questions. What is the "most beneficial use"? What does "impaired" mean?

One might say that contamination is indicated when statutory limits are exceeded. This may satisfy the legal requirements but what if the regulations do not reflect the latest scientific knowledge? This is a particularly acute problem when one considers the rate at which new scientific literature is appearing on the subject of organic compounds and their impact on the environment and public welfare. Abandoning this definition, it could be said that contamination is indicated when natural or background levels are exceeded. What if the background levels already exceed recognized environmental and health thresholds? What if there is not enough information to establish these levels?

This issue defies simple resolution. However, a working definition is needed for any assessment methodology to be meaningful. Let's change the attack slightly and ask the question: "Is the water safe to drink?" Given this perspective and a sense of practicality, the following definition is proposed. A drinking water supply is contaminated when currently established and accepted public health guidelines are exceeded. These guidelines include regulatory standards, criteria, and recommendations put forth by respected scientific organizations.

Determining the safety or potability of a drinking water supply is not an easy task. If it is necessary to consider closing the supply, there are many economic, political, public relations, military preparedness, and public health issues that must be addressed. Of course, public health is paramount; but in marginal cases, other factors will play roles of varying importance depending upon the individual situation.

V. CONTAMINATION OF GROUND WATER

Sources of Contamination

Ground water quality can be affected by many different sources of contamination. These contaminant sources can be natural or anthropogenic in origin and may or may not be a concern with regard to drinking water supplies and human health. Contamination can originate from sources above or below ground and above or below the water table. The sources at or below the water table have a direct and immediate affect on ground water quality. Figure 2 summarizes the possible sources.

The ground water may become contaminated from natural recharge by surface waters if these waters are in fact themselves polluted. A common case is that where municipal or industrial waste is disposed of in a stream or river and pumping of nearby wells causes the polluted waters to be drawn into the well. The spreading of solid or liquid wastes, such as manure or municipal sewage sludges can result in ground water pollution. These waste materials are spread directly on the land surface and water soluble substances may leach out and flow to the water table. Another concern in colder climates is the use and storage of road deicing salts. These salts can dissolve and flow directly to the aquifier or may take an intermediate step by first polluting surface waters which recharge the aquifer. Dumps and landfills are another source of pollutant for ground water, their leachate is generally highly mineralized and can contain a wide variety of chemical and biological substances. In agricultural areas chemical fertilizers and pesticides may be a problem. Pesticides may contain highly mobile toxic substances. Fertilizers contain high concentrations of ammonia which degrades in part to nitrate. Accidental spills of hazar-

14.18
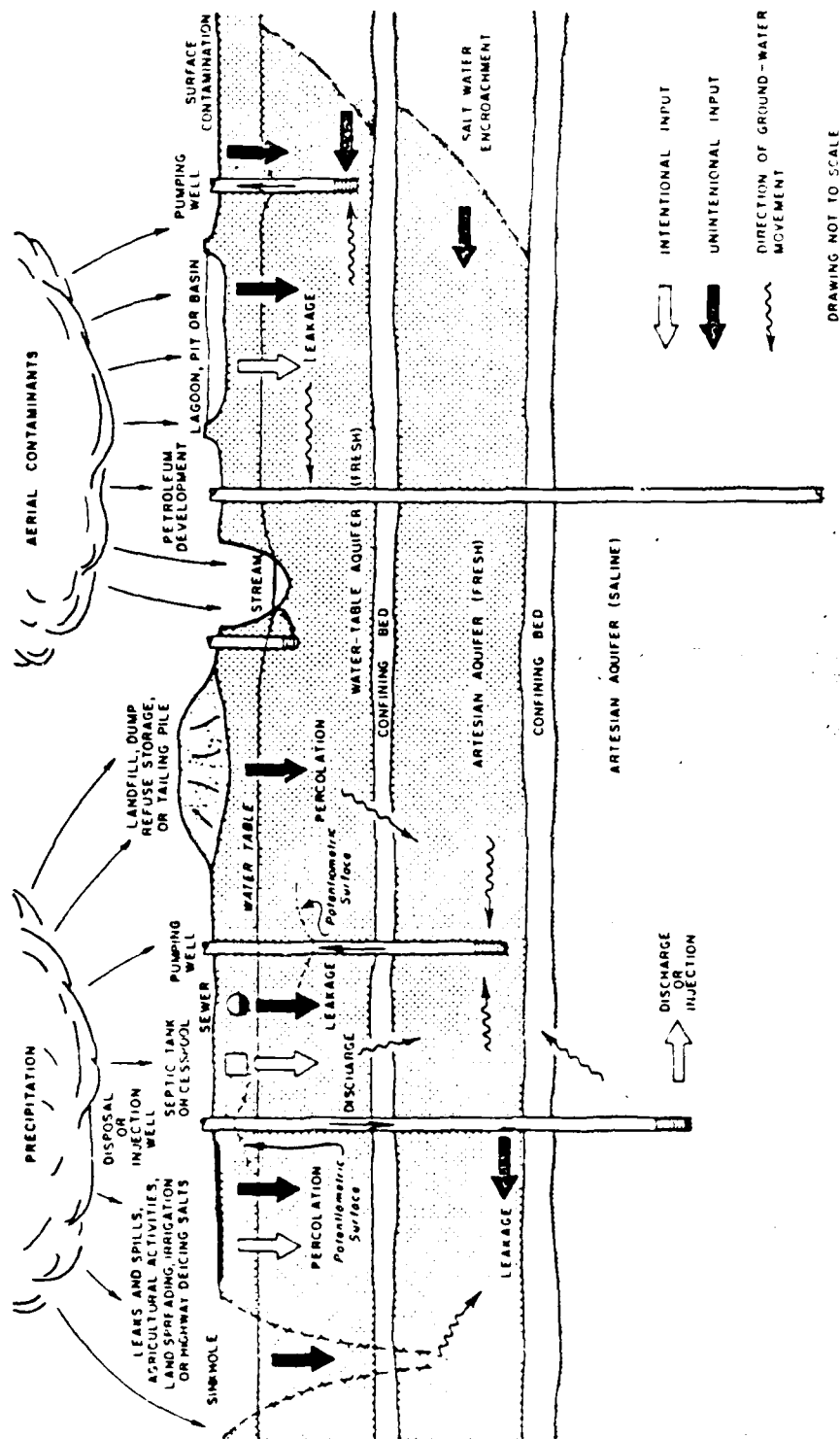
Figure 2. Routes for Ground Water Contamination (from Miller et al., 1977).

14.19

dous materials during use, storage or transport may result in ground water pollution. Other sources of ground water contamination originating at or above the ground surface might include stockyards or even particulates which have settled out of the air. In short almost any substance which could pollute the environment above the ground may have potential to pollute ground water.

Pollutant sources that exist in or under the ground are generally associated with the storage and transport of hazardous materials or treatment and disposal of wastes. Septic tanks are probably one of the most abundant possible sources of ground water contaminants and can cause problems if their density across an area is sufficiently high. Cesspools and privies may present similar problems. Holding ponds and lagoons for the storage or treatment of municipal or industrial wastes may leak into the subsurface if improperly designed or maintained. Leakage from underground storage tanks and pipelines may contribute to ground water polltuion. Common problems of this type are leakage from old and deteriorated gasoline storage tanks and municipal sewage systems. Metal storage tanks and pipelines which hold corrosive materials are exceptionally susceptible to leakage. The controlled or uncontrolled disposal of wastes in excavations can lead to problems like those of surface dumps. Leachate will flow into subsurface waters if precautions are not taken to prevent precipitation from flowing through the wastes. If an excavation is of sufficient depth to be at or below the water table at some point in time the ground water itself may transport the pollutants.

Some potential contaminant sources may have a direct connection to an aquifer. A simple case of this is a drainage canal dug to the depth of a shallow aquifer. Wells may also be used for drainage or artificial recharge of aquifers, or disposal of wastes. Abandoned or test wells may also transmit water from

14.20

the surface or from other aquifers if they are improperly sealed or cased.
In all of these cases the contamination potential is great if the quality of
the inflowing water is low.

It can be seen that the types of pollutant sources takes on many different
forms. This great diversity makes a close inspection of the area surrounding
a water supply well a must. The historic records of the area should also be
checked for potential sources that may now be hidden.

Factors Affecting Contamination Potential

The movement of groundwater is driven, like the flow of all water, by
the force of gravity. Surface waters flow into ground water systems from re-
charge areas and may remain in the ground water system for a long period of
time before returning to the surface from ground water discharge areas. These
recharge waters, as was previously mentioned, may present a source of ground
water contamination. There are many factors that determine whether a contaminant
source will or will not influence the quality of ground water based drinking
water supplies, but they may be placed in three major categories: dilution,
degradation, and direction of movement of the contaminant. These effects are
in turn determined by properties of the supply aquifer, the well, and the con-
taminants themselves.

The supply aquifer may have a natural defense against the influx of lower
quality ground water. Aquifers which have sufficient depth, sorption capacities,
impermeable flow barriers or a combination of these attributes may be able
to maintain good quality drinking water supplies against some or all forms
of contamination. Depth to the aquifer is one of the most important factors
to be considered when trying to determine if contamination is likely, because

14.21

it is directly related to the time it will take a contaminant to reach the

aquifer. As a contaminant moves through the unsaturated zone above the aquifer

it is subject to different physical, chemical and biological reactions which

serve to degrade and dilute the contaminant. Larger suspended particles may

be filtered out by the porous materials, clays and organic materials may dilute

by sorption of chemical compounds, and microbiological degradation may occur.

These same processes go on within the saturated zone below the water table.

When the contaminant plume reaches the water table, flow is generally horizontal

with direction determined by the hydraulic gradient. The hydraulic gradient

is also directly related to the velocity of the ground water, and is therefore

of great significance when attempting to predict when and if a contaminant

source will endanger the use of a drinking water supply well. The other para-

meter which is directly related to ground water velocity is the hydraulic conduc-

tivity of the aquifer material. Hydraulic conductivity is a function of the

fractional volume of voids to total volume of soil (porosity), and the size

and space distribution of these voids throughout the soil matrix. For example,

the flow of water through a well graded sand and a fractured limestone with

the same porosity and hydraulic gradient will not occur at the same rate.

The flow paths through the sand are small and tortuous and therefore longer

than the relatively straight and large pathways provided by a fracture system.

This difference gives the sand a lower hydraulic conductivity than that of

the fractured rock with the same porosity. Dispersion of a contaminant is

caused by two processes; molecular diffusion, important at very low velocities,

and hydrodynamic mixing, which is dominant at higher velocities. Mixing will

be more extensive in porous media with relatively long flow paths. Dispersion

occurs both longitudinally and transversely to the direction of flow. Aquifers

14.22

which are confined or overlain with a relatively impermeable strata will have
an added measure of protection from the inflow of contaminated waters. Confined
aquifers can bring in contaminated water if their recharge sources, which may
be a great distance from the area of interest, are polluted. Transport of
the contaminants from the polluted source may take a long period of time and
may result in contamination of a water supply which was thought to be at low
risk.

A pumping well can greatly affect the hydraulic gradient of the water
table in the area immediately surrounding the well. This effect, referred
to as drawdown, will create a cone of depression in the water table around
the well. The extent and depth of the cone of depression at any given time
is a function of the pumping rate and the aquifer properties of transmissivity
(or transmissibility) and storativity (or storage coefficient). The storativity
and pumping rate are directly related to the cone's size and depth while the
transmissivity has an inverse relationship. The drawdown cone can cause con-
taminated waters to flow into the well. It is therefore important to be able
to estimate the extent and hydraulic gradient of the cone. The most obvious
and important factor in determining a wells contamination potential is its
location relative to potential contaminant sources. The first concern is whether
the well is up or down gradient from the source(s) and if the distance is suffi-
cient to prevent or keep contamination at an acceptable level. The construction
of a well may also be important if the casing and seals on the well are not
properly installed. Contaminants may possibly flow along the well opening
and into the well or aquifer during a flood period or accidental spill. A
proper set of records (well logs) on the construction, use, and abandonment
of wells are invaluable in the assessment of contamination potential.

The chemical make-up of a contaminant will determine if it can persist
in its subsurface environment. The primary factor is the potential contaminants
initial concentration upon release. Another important consideration is the
density of the contaminant. A contaminant with a much higher or lower density
than water will tend not to mix well within the subsurface water column. Less
dense contaminants tend to collect on top of the water table and float in a
thin layer. Contaminants of greater density tend to collect on the bottom
of the aquifer and may become stagnated. In both these cases the depth of
a well screen may determine whether the contaminants are pumped into the well.

There are many chemical reactions which may take place to degrade a con-
taminant. Particularly important is the contaminant's affinity for adsorption
on the surface of the porous media. This is mostly a function of surface area
and organic content. A contaminant's capacity for sorption is affected by
its hydrophobility or aversion for dissolving in water, which is indicated
by the contaminant's octanol or water partition coefficient. Contaminants
with relatively large water partition coefficients tend to be adsorped or move
into the air. Hydrophobility and the fraction of organic carbon in the soil
matrix are the most significant factors in determining a contaminant's retarda-
tion in the soil (Roberts et al., 1982). Retardation factors, the ratio of
the groundwaters velocity to that of the contaminant's, generally range from
one to ten for some common groundwater pollutants in sand and gravel aquifers.
Therefore contaminants will move at a rate from ten to one hundred percent
of the groundwaters velocity in an aquifer of that type (Mackay et al., 1985).

Chemical reactions may also significantly influence the fate of contamin-
ants. The two most important reactions are oxidation and hydrolysis. It is
not know if empirical methods now used to determine rate constants for these

processes are applicable for reactions in groundwater. It is however thought that biological degradation reactions occur at a faster rate relative to oxidation and hydrolysis (Mackay et al., 1985).

Biological reaction rates are dependent on many different factors concerning microorganisms and their environment. Microorganisms grow on the surface of the soil particles and feed upon nutrients in the flowing groundwater (Mackay et al., 1985). Contaminants may act as food for microorganisms if they are at proper concentration levels and have a chemical composition which they can utilize. The contaminant's potential for utilization by microbes is affected by its chemical structure, toxicity, and the subsurface environment (aerobic or anaerobic). The concentration levels must be high enough to sustain the microorganisms, but there must also be low amounts of toxic constituents. The microorganisms may require a period of time to acclimate themselves to a contaminant before making use of it. Microbes can generally only use the soluble portion of a contaminant and can more easily utilize nonaromatic and unsaturated organic compounds. The microbial transformation of some contaminants may result in conversion to intermediate products which are incapable of being further transformed and/or more noxious than the original contaminant. Due to the vast number of factors which control biological and chemical reactions and the large degree of uncertainty surrounding the estimation of those factors it should be assumed that contaminants will endure for an indefinite period of time unless specific evidence is found to dispute this argument (Mackay et al.,1985).

The quantitative and temporal distribution of precipitation may affect a site's contamination potential. The relatively small amount of precipitation received in arid zones will usually produce a water table which is at a greater

depth and flatter than those characteristic of humid zones, which tend to be
closer to the land surface and more closely mimic the shape of the topography.
A contaminant which persists at a source may be periodically leached out by
intermittent rainfall. This process can result in small contaminant plumes
separated by clean water. These disjunct pulses may result in periods of high
quality water followed by low quality water being drawn from a supply well.
A similar situation may occur in humid areas where the water table has seasonal
fluctuations and rises to come in contact with a contaminant source.

VI.   ASSESSMENT OF CONTAMINATION POTENTIAL

The evaluation of a site's likelihood for contamination of a water supply
is, as can be seen from the previous section, a difficult task involving the
analysis of many complex and interrelated components. These components determine
contaminant behavior, but it is very difficult to determine the temporal and
spatial distributions of a contaminant due to the extensive nature of the para-
meters used to characterize the contributing factors. In an ideal situation,
a full hydrogeologic and chemical analysis would be performed, but this is
often not a viable economic possibility. It is therefore necessary to attempt
to determine, through a less extensive investigation, where contamination of
supply wells will most likely occur. Several relatively simple methods for
assessing an area's potential for contamination have been developed, each re-
quiring different types and quantities of data input. Three of these methods
are discussed in some detail below.

One system for evaluation of contamination potential for waste disposal
sites has been developed by LeGrand (1964). This system characterizes the
probable effect of five environmental factors on a contaminant source. These

five factors are: depth to the water table, distance from the source to point of use, the hydrualic gradient of the water table, the permeability of the aquifer, and its sorption capacity. These five factors can be measured or estimated on-site and evaluation is based on weighted values relative to their significance. The system was developed for unconfined aquifers and works best on relatively deep homogeneous soils. The method is not suitable for situations involving mixed wastes, such as those from dumps and landfills, or if the critical problem is slowly attenuated chemical waste. The five environmental factors are given point values determined by rating scales. An additional factor of depth to a parent material or bedrock strata may be added were applicable. The five (or six) values are added up to give a total point value. A "high" point value signifies a "low" contamination potential. What is an acceptable point value or contamination potential must be determined by the decision maker. LeGrand suggests a point value of zero to six as indicating high contamination potential and value above sixteen as very low potential sites and a values above sixteen as very low potential for contamination by normal sewage. A higher point value is desirable for most chemical wastes as they will often attenuate more slowly than sewage and be a greater health risk to possible receptors.

Another system, or model, which uses different weights for contamination factors of varying significance is the "Hazard Assessment Rating Methodology" developed for the U.S. Department of Defense and the U.S. Air Force (CH2M-Hill, 1983). This model is divided into three categories; receptors, waste characteristics and pathways. Each group is given a rating score. The average of the scores is then modified by a weight determined by the "waste management practice." The receptors category score is determined by summing the products

of the individual factor scores and their respective weighting constants. The pathways category rating procedure is designed around three possible routes of contaminant migration; surface water, flood water and ground water. For the purposes of this study only the groundwater migration score should be considered. This score is compared to a rating based on evidence of contamination migration. If direct evidence of contaminant migration is substantiated a maximum score of 100 points is assigned. A score of 80 points is given for indirect evidence. The pathways score is assigned the highest of the contamination evidence's or potential route's scores. The third category, waste characteristics, is scored in three parts. The first portion assigns a score from a waste characteristic matrix with three subfactors; waste quantity, hazard rating, and information confidence level. The subscore determined from the matrix is then multiplied by a "waste persistence factor" which serves to lower the score for contaminants which endure for relatively short periods of time. The total waste characteristics score is calculated by modifying the score from the first two sections with a "physical state multiplier". This multiplier ranges from one, for liquid wastes, to one-half for solid wastes. The final hazard assessment rating is found by application of the "waste management practices factor", which ranges from one, for sites with no containment, to one-tenth for well-contained and managed sites. This hazard assessment model is designed for sites with enough hazardous waste present to offer a potential for contamination and also potential for these wastes to migrate. The model has evolved from one developed for the EPA by modifying it to represent hazards found on Air Force installation.

A simple and rapid graphical approach to predicting a leachate plume's movement and respective concentrations has been developed by Kent et al. (1985).

14.28

The "nomograph for plume center-line concentration" is a one-dimensional model which can approximate one of the following variables if two are held constant; travel time, distance, or concentration at a point directly down gradient from a contamination source. This model requires inputs of aquifer thickness and porosity, velocity of groundwater flow, transverse and longitudinal dispersion rates, the retardation factor, volumetric flow rates, and the initial source contaminant concentration. Scale factors for use in the nomograph are then calculated as ratios with the primary variables distance, time and mass flow rate from the source. These factors are assumed to remain constant spatially and temporally. The nomograph is designed to model conservative chemical constituents taking into account dilution, dispersive mixing, and retardation.

The three preliminary assessment techniques reviewed above all scrutinize the same basic interrelated attributes to determine potential groundwater contamination at a site. These attributes are (1) time a contaminant has been in the groundwater system, (2) the distance a contaminant has or will move, and (3) the concentration at the space and time of interest. The LeGrand and Air Force hazard assessment methods attempt to qualify the three characteristics with a single scale or index number while the nomograph method makes an effort to quantify them and give a representation of the contaminant plume.

VII. CONFIRMATION OF CONTAMINATION

Indicator Parameters

The measurement of gross chemical parameters can give an indication of the extent and type of contamination a drinking water supply may have. Changes in the levels of total organic halogens (TOX), total organic carbon (TOC), pH, and specific conductance may indicate the presence of contaminants. The presence of any TOX concentrations should be of concern due to the lack of

possible natural sources. The levels of these indicator parameters should
not only be looked at quantitatively to assure levels below maximum permitted
levels, but also to detect any changes in the levels which can not be explained
by seasonal or other cyclic deviations. TOX measures the levels of organic
halogens, a group including many common groundwater pollutants such as trichloro-
ethylene or TCE. The levels of TOX and TOC may be compared with each other
to help determine what may or may not be a contaminant. Those levels should
also be compared with later, more detailed chemical analyses to measure their
efficiency. The measure of pH and specific conductance levels gives the acidity
or alkalinity and concentration of ionic constituents in the water respectively.
The pH measurements give an indication of an acidic or corrosive contamination,
while the specific conductance indicates the contamination of any ionic substance
including metals, chloride, acids and bases, etc. Another valuable indicator
parameter is the concentration of oil and grease. This level will indicate
the contamination of a water supply by a nondegraded petroleum product. The
observation of all these indicator parameters can give a good indication of
a change in the quality of a drinking water supply.

Detection of Specific Organic Contaminants

The indicator parameters discussed above are designed to measure fairly
large concentrations of organic matter. They are capable of identifying trends
in water quality and indicating the presence of groups of contaminants. However,
they are not capable of identifying trace levels of specific organic compounds
on the order of 1 μg/L or less. A cursory look at Table 4 reveals a number
of suspected carcinogenic levels at values much lower than 1 μg/L. There are
many publications dealing with specific sampling procedures and analytical

techniques and the reader is referred to them for more details (USEPA, 1979a; APHA, 1981, USEPA, 1979b; ASTM, 1983). The general protocol for detecting trace organic contaminants is shown in Figure 3. This protocol involves three steps (Tchobanoglous and Schroeder, 1985): isolation, resolution, and detection. The first step concentrates the trace contaminants in the sample. The second separates the contaminants into individual components. The last step quantifies the concentration of the individual contaminants. These procedures are, of course, more expensive than those for determining the indicator parameters. However, as analytical techniques improve the costs will decline. A set of indicator parameters (TOC, TOX, pH, and specific conductance) is fairly inexpensive--less than $100 in 1983 dollars (Barcelona et al., 1983). A full-scale interpretive analysis (organic and inorganic) may cost as much as $1400 in 1983 dollars (Barcelona et al., 1983). Undoubtedly, these costs will decline as the analytical techniques improve. But, there is no doubt that quantifying trace organics comes with a cost and it may be that the cost is not always justified.

VIII. ASSESSMENT METHODOLOGY

Bayesian Decision Theory

Bayesian decision theory is a form of systems analysis which structures a decision process into a simple analytical procedure for choosing and evaluating alternatives (Benjamin and Cornell, 1980; Davis et al., 1972). This method of analysis allows for inclusion of uncertainty with respect to the parameters affecting the different decision alternatives. There is also provision for the updating or improvement of the decision maker's selection of an alternative as new and better information becomes available. A "good" decision can be considered one which results in the maximum expected utility for the decision
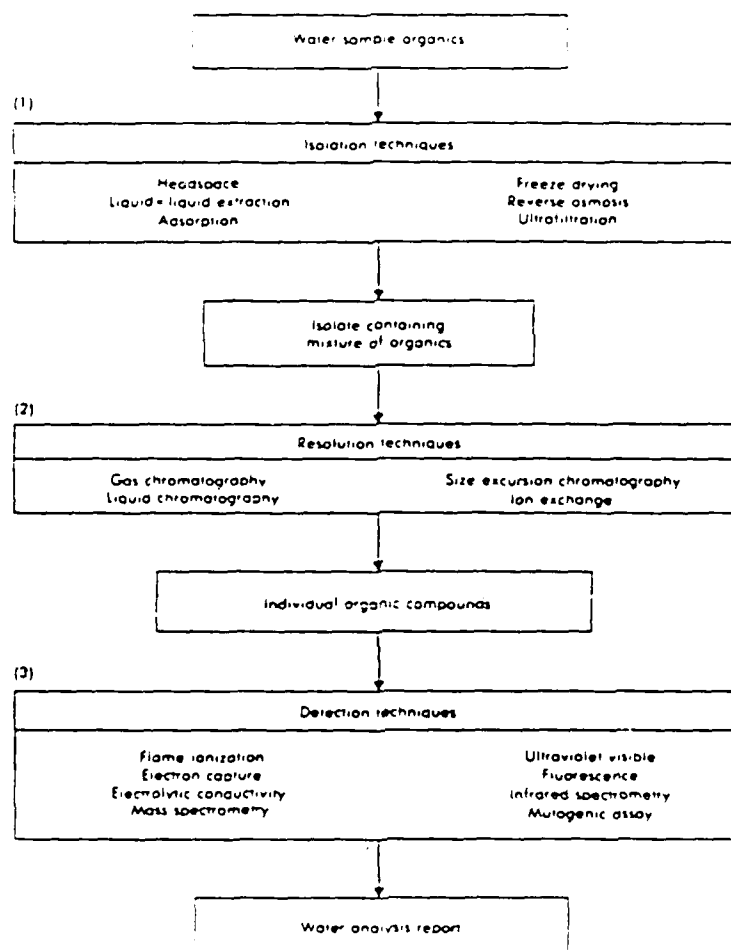
Figure 3. Protocol for the Determination of Trace Organics Using
Instrumental Methods (from Trussell and Trussell, 1980,
and Tchobanoglous and Schroeder, 1985).

14.32

maker's on the basis of the available information. Utility is a term used to describe the value or usefulness of the specific possible consequences of a decision process. The theory and assessment of utilities will be discussed later. The steps employed in a Bayesian decision analysis can be outlined as follows (Davis et al., 1972):

(I)   Define the decision and its viable alternatives.

(II) Determine the utilities for the possible outcomes of the decision process.

    (a) Select state and decision variables.

    (b) Assess uncertainties of variables.

(III) Make a sensitivity analysis to determine any dominated alternatives or outcomes which may be elminated.

(IV)   Make the decision.

    (a) Determine the expected utilities for each alternative.

    (b) Choose the alternative with the maximum expected utlity.

(V)   Analyze uncertainties.

    (a) Determine expected changes in utility due to uncertainty.

    (b) Evaluate information.

        (1) Determine the expected increase in utility due to further information.

        (2) Gain additional information if warranted, and repeat analysis.

This method of analysis enables the decision maker to combine the treatment of risk due to uncertainty and the value of information which may be used to reduce that risk. The level of risk is a function of a combination of random and uncontrollable factors and by the insufficient knowledge of some part(s)

of the system. There are three major catagories of risk associated with ground water contamination; socioeconomic risks, risks to human health, and risks to the environment. Through the use of the Bayesian decision process the changes which may occur to the amount and types of risk encountered at a site can be incorporated into a new assessment. A change in the level of risk may be attributed to a variety of factors. The advent of new or better information, such as alterations in management techniques, changes in population densities, or improvement of chemical analyses. These factors can result in a modification of uncertainty, the perceived risk, and ultimately the decision chosen. The value of additional data to a decision maker can be considered as the expected increase in the utility (due to a reduction in uncertainty) minus the utility of the cost of obtaining the information. Generally, information can be considered to have value (utility) only if it can cause a possible change in the final decision. The uncertainty of an outcome is inherent in the assessment of that outcome's utility. In other words, the possibility of further costs or damages from making the wrong decision are built into the process. This is especially relevant to ground water contamination where an improper decision could have extensive adverse effects on the environment and human health.

A general decision problem can be summarized as a set of experiments, a set of observations or information gained from those experiments, a set of actions based on that information, and finally a set of the states of nature (the environment) and their consequences (which are a result of the action taken). The decision tree is a representation of these linked events showing all the possible combinations that may occur throughout a decision process. The basic construction of a decision tree is very simple. A fork or node represents a selection which must be made by the decision maker or will be determined

14.34

by the state of nature. The branches from a node indicate the possible choices to be selected or determined. A typical decision tree is shown in Figure 4. The tree is employed by assigning utilities to each of the potential outcomes and probabilities to all possible experimental results and states of nature. The decision maker must then move down the decision tree, from utilities to experiments to determine which chain of decision will result in the greatest expected utility.

The subjective assessment of probabilities for the decision tree is aided by use of Bayes' Theorem (Benjamin and Cornell, 1970):

$$P(\theta_j/Z_i) = \frac{P(Z_i/\theta_j) \cdot P(\theta_j)}{P(Z_i)}$$

$$\text{and} \quad P(Z_i) = \sum_{k=1}^{n} P(Z_i/\theta_k) \cdot P(\theta_k)$$

with Z_i = the prediction from experiment i, and θ_j = the j state of nature. The unconditional probability of the j state of nature, $P(\theta_j)$, is known as the prior probability of θ_j, so-called because it is determined before any experimental information is evaluated. It logically follows that the conditional probability $P(\theta_j/Z_i)$ is referred to as the posterior probability. When experiments are done in series the posterior probability of the previous experiment will become the prior probability of the following experiment. The use of Bayes' Theorem to determine the posterior probability allows the decision maker to include a measure of their confidence for the experiment to predict the actual state of nature. This is done by assessing the conditional probability of experimental outcome Z_i, $P(Z_i/\theta_j)$.

The assessment of probabilities is one of two crucial ingredients to the decision problem. The other is the evaluation of the decision maker's utility for various outcomes. The numerical values associated with various levels of utilities is based on an arbitrary scale and the subsequent quantification of the decision maker's relative preference for different outcomes (Hammond, 1967; Benjamin and Cornell, 1970). Determining these numerical values can be demonstrated by the following example. Assume that a decision maker is given the choice between making an "insurance" payment of say $10,000,000 and a "lottery" in which he will either suffer no losses or a substantial loss of $50,000,000. The decision maker must ask himself what probability of no loss will cause him to be indifferent between the "sure thing" (i.e., the cost of insurance) or the lottery. This probability is called the crossover or indifference point. Let's assume this particular decision maker requires a probability of 0.90 or 90% that he would suffer no loss to be indifferent between the lottery and insurance. This means that if the probability were greater than 90% she would select the lottery (i.e., not pay the insurance); if it were less she would pay the insurance. More importantly, if we had arbitrarily assigned utilities to the best outcome (no loss) and the worst outcome ($50,000,000 loss), a utility could be assigned to the $10,000,000 cost of insurance. In other words, the utility of the decision maker for a loss of $10,000,000 could be identified. This is done by assuming that if she is indifferent between the "sure thing" and the lottery at the 90% probability level, then her utility for each must be equal. If the arbitrary utilities assigned to the best and worst lottery outcomes are 100 and 0, respectively, the expected utility of the lottery is 0.90 (100) + 0.10 (0) or 90. Thus, the utility of a loss of $10,000,000 is also 90.

If the lottery question was posed to the decision maker for several levels of insurance cost, a utility curve could be identified. Such curves show the utility associated with a range of outcomes which can, in turn, be used to assign utilities to the outcomes on a decision tree. Typical utility curves for three types of decision makers are shown in Figure 5. The risk averter has a decreasing marginal utility as the outcome improves. He enjoys the better outcomes but is not comfortable taking risks to achieve them. The risk lover or gambler also enjoys improving outcomes but he will risk much to achieve them, i.e., his marginal utility increases as the outcome improves. The risk-neutral decision maker is the rare individual who is neither risk averse or risk loving. His marginal utility is constant and the relationship between outcome and utility is linear.

The utility curve is a synopsis of the psyche of the decision maker. Within it are captured his or her assessment of risk, tangible and intangible costs and damages, and the value of information. Along with subjective probabilities associated with the experimental results and the states of nature, the decision tree can indicate the path of action that will maximize expected utility.

Proposed Approach

The Air Force has a large number of drinking water supplies based on ground water. The costs of detection for organic contaminants is substantial (but changing). Thus, it seems prudent to avoid detailed sampling and analysis if there is little likelihood of contamination. Essentially, the analyst (i.e., the decision maker) has three levels of attack to determine the possibility and extent of contamination:

● Decision point
X "Chance" point

| Experiment E | Outcome Z | Action A | State Θ | Value U |
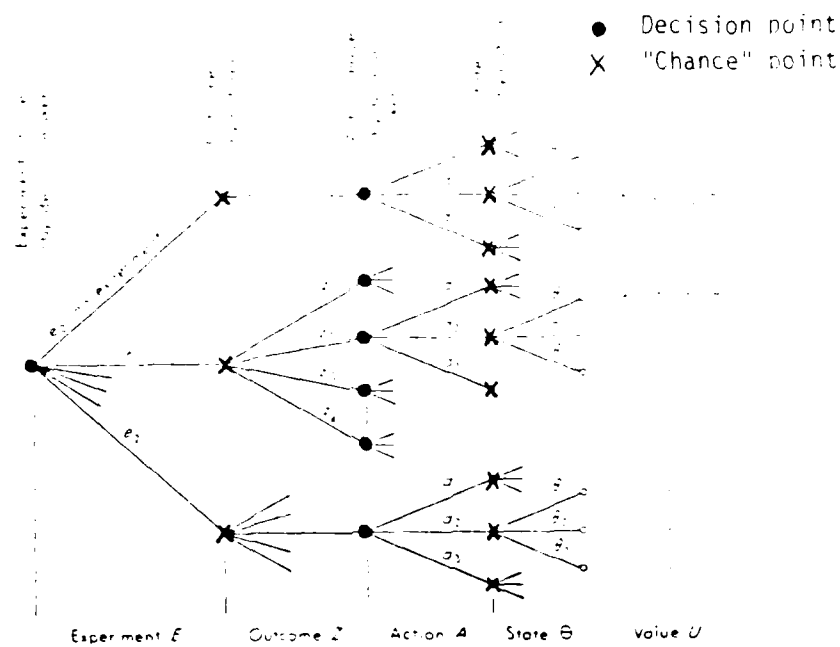
Figure 4. Generalized Decision Tree (from Benjamin and
          Cornell, 1970).

least   Outcome   most
preferred   preferred
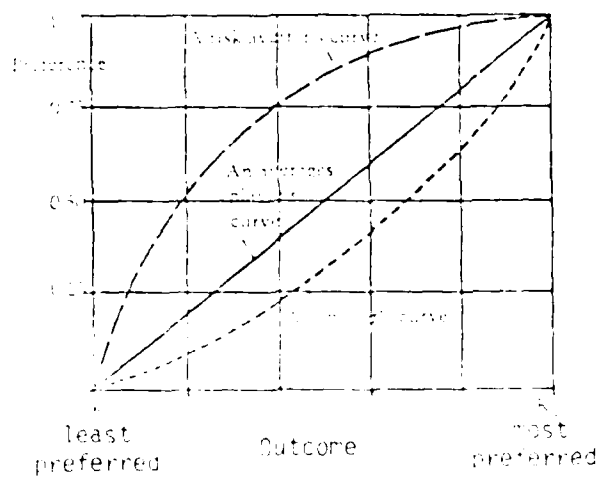
Figure 5. Commonly Observed Utility Curves (from
           Hammond, 1967).

1) preliminary site investigation

2) indicator parameters (i.e., TOC, TOX, pH, O&G, etc.), and

3) detection of specific organic contaminants.

The first level is nothing more than a good characterization of the site--something that should already be known and well established. A water supply located a long distance upgradient from any contamination source obviously has a low risk of contamination. Conversely, a supply located several hundred meters downgradient from a hazardous waste site most certainly demands close scrutiny. Sampling and analyzing for the gross indicator parameters is an inexpensive step that yields additional information and reduces uncertainty. However, without the site investigation the results of this step will be much less meaningful. The third step could be taken without the first two. While this will determine which contaminants are present, this information will come at quite a cost! The first two steps will not only give some indication of the need for such a measure, but they will also allow the analyst to tailor the program to what he expects to see. It appears unavoidable to conclude that a logical, structured approach to this assessment problem could improve the cost-effectiveness of the Air Force's ongoing efforts to monitor the drinking water supplies at its many installations. In other words, it is possible to construct truly useful monitoring programs that avoid unnecessary costs.

The problem of assessing the potability (with respect to organic compounds) of ground water based drinking water supplies can be formulated as a decision-making problem. The process is a series of experiments and decisions that is amenable to the decision tree shown in Figure 6. The tree appears complex, but it is actually quite simple. The first decision involves the analysis for contamination potential. Note that the decision to not analyze the conta-
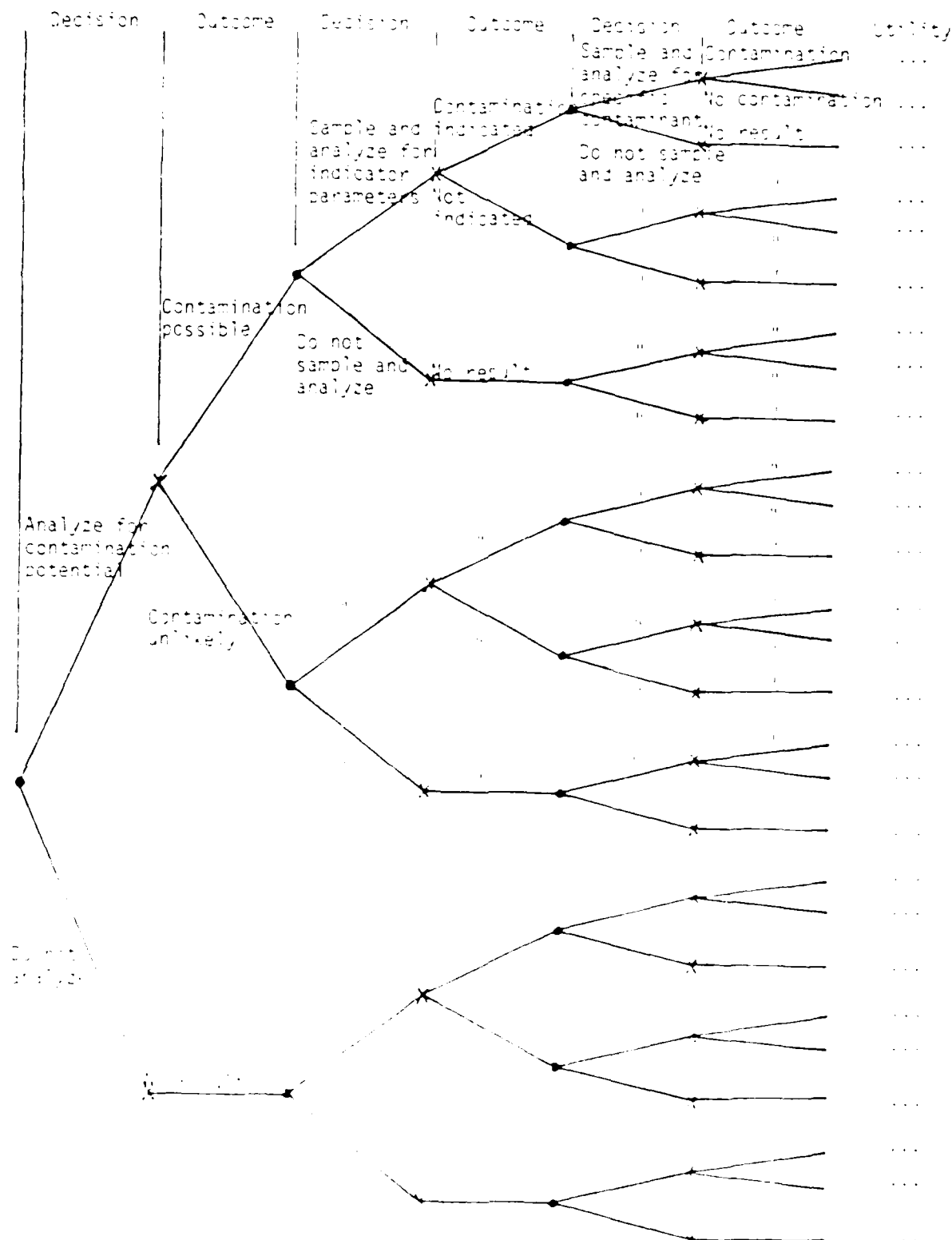
14.37

Decision | Outcome | Decision | Outcome | Decision | Outcome | Utility

Sample and analyze for . . . . contaminant . . . .

No contamination . . . .

Contamination indicated

No result

Sample and analyze for indicator parameters

Do not sample and analyze

Not indicated

Contamination possible

Do not sample and analyze

No result

Analyze for contamination potential

Contamination unlikely

Do not analyze

mination potential does not preclude the later possibility of sampling for the indicator parameters or specific contaminants. The second decision involves sampling and analyzing for the various indicator parameters. Once again, the decision not to do so does not preclude the possibility of testing for specific contaminants. The third decision involves the detection of specific contaminants.

The decision tree is easy to formulate; the difficulty comes with estimating the probability associated with each experimental result and the utility at the end of each path. The concepts behind these two cornerstones of a useful decision tree were discussed earlier. With the probabilities and utilities established, the decision maker selects the route that maximizes expected util. Expected utility is calculated at the "chance" nodes (see Figure 2) from right to left. The largest expected value determines the action made at the node and the expected value associated with the node.

IX. CONCLUSIONS AND RECOMMENDATIONS

The methodology outlined above suggests a logical approach to the potability of ground water based drinking water supplies with organic compounds. The U.S. Air Force has a large number at its installations around the world. The suggested the potential to reduce the costs of monitoring these tial process to assess potability. The concepts can help to redesign the Air Force's approach by promoting the use of available data potential and gross indicator parameters logical decision process should are sampled and analyzed
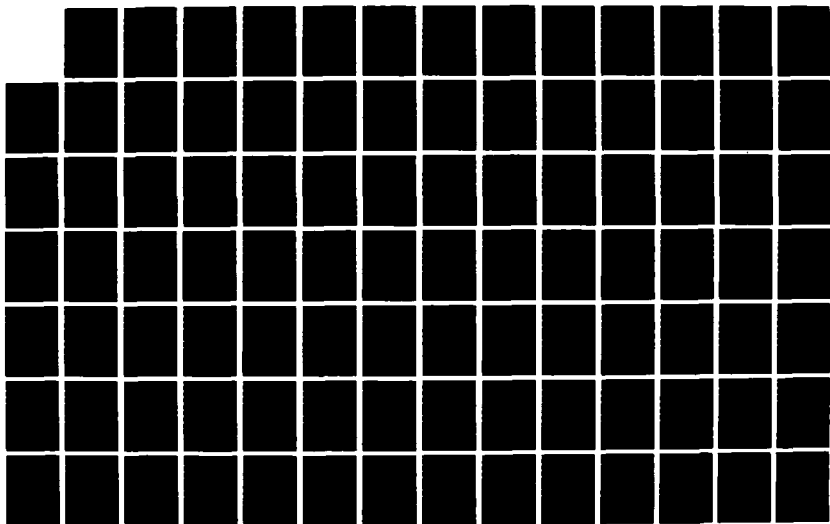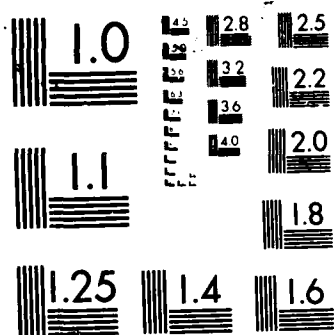
Problems encountered during the course of this project prevented the development of firm guidelines for establishing the probabilities and utility values needed to drive the decision making process. The probabilities can probably be established by studying the data base currently being developed by the Occupational and Evnironmental Health Laboratory (OEHL). These data involve site characteristics, many of the indicator parameters cited earlier, and the results of various sampling and analysis protocols for organic contaminants. The establishment of utilities for various outcomes requires the responsible decision maker to estimate his or her own utility function. Future study could develop some "typical" curves by interviewing decision makers (within the Air Force) responsible for environmental monitoring.

X. ACKNOWLEDGEMENTS

XI. REFERENCES

American Public Health Association, Standard Methods for the Examination of
    Water and Wastewater, 15th edition, APHA, Washington, D.C., 1981.

American Society for Testing and Materials, "Water and Environmental Technology",
    Section 11, 1983 Annual Book of ASTM Standards, ASTM, Philadelphia, Pennsylvania,
    1983.

Barcelona, M.J., Gibb, J.P., and Miller, R.A., "A Guide to the Selection of
    Materials for Monitoring Well Construction and Ground-Water Sampling,"
    ISWS Contract Report 327, Illinois State Water Survey, Champaign, Illinois,
    August, 1983.

Benjamin, J.R. and Cornell, C.A. Probability, Statistics, and Decision for
    Civil Engineers, McGraw-Hill, New York, 1970.

CH2M-Hill, Inc., "Hazardous Assessment Rating Methodlogy," 1983.

Clifford, D., Sorg, T., and Frank, P., "Survey of Inorganic Contaminants" Control
    of Inorganic Contaminants Seminar, AWWA, June 1983.

Davis, D.R., C.C. Kisiel, and L. Duckstein, "Bayesian Decision Theory Applied
    to Design in Hydrology," Water Resources Research, Vol. 8, No. 1, February,
    1972.

Department of the Air Force, "Management of the Drinking Water Surveillance
    Program," Air Force Regulation (AFR) 161-44, May 29, 1979, amended July
    22, 1980, August 5, 1981.

Department of the Air Force, "Installation Restoration Program: Phase II Management
    Concept," presented at the Air Force Bioenvironmental Engineering Symposium,
    May 1984.

Department of Defense, "DoD Installation Restoration Program," Defense Environmental
    Quality Program Policy memorandum (DEQPPM) 81-5, December 11, 1981.

Hammond, J.S., "Better Decisions with. Preference Theory," Harvard Business
    Review, November-December, 1967, pp. 123-141.

Hess, A.P., Dyksen, J.E., and Dunn, H.J., "Groundwater Contamination: Challenge
    of the 80's," Water Technology, Vol. 6, No. 7, September, 1983, pp. 40-46.

Kent, D.C. et al., "Analytical Methods for the Prediction of Leachate Plume
    Migation," Ground Water Monitoring Review, Vol. 5, No. 2, Spring 1985,
    pp. 44-60.

LeGrand, H.E., "System for Evaluation of Contamination Potential of Some Waste
    Disposal Sites," Journal of the American Water Works Association, Vol.
    56, No. 8, August, 1964, pp. 959-974.

Lehr, J.H., "How Much Ground Water Have We Really Polluted?" Ground Water Monitoring
    Review, Vol. 2, No. 1, Winter, 1982, pp. 4-5.

Mackay, D.M., P . Roberts, and J.A. Cherry, "Transport of Organic Contaminants
    in Groundwater," Environmental Science and Technology, Vol. 19, No. 5,
    May 1985, pp. 384-392.

Miller, J.C., Hackenberry, P.S., and DeLuca, F.A., "Ground Water Pollution Problems in the Southeastern United States," EPA-600/3-77-012, USEPA, Ada, Oklahoma, January, 1977.

Nix, S.J., "Assessing the Quality of Ground Water Based Drinking Water Supplies," Contract No. F49620-82-C-0035, SCEEE/AFOSR, July, 1984.

Pettyjohn, W.A. and Hounslow, A.W., "Organic Compounds and Ground-Water Pollution," Ground Water Monitoring Review, Vol. 3, No. 4, Fall, 1983, pp. 41-47.

Pye, V.I. and Patrick, R., "Ground Water Contamination in the United States," Science, Vol. 221, February 19, 1983, pp. 713-718.

Roberts, P.V. et al., "Movement of Organic Contaminants in Groundwater: Implications for Water Supply," Journal of the American Water Works Association, Vol. 74, No. 8, August, 1982, pp. 408-413.

Tchobanoglous, G. and E.D. Schroeder, Water Quality: Characteristics, Modeling, Modification, Addison-Wesley, Reading, Massachusetts, 1985.

Trussell, R.R. and A.R. Trussell, "Evaluation and Treatment of Synthetic Organics in Drinking Water," Journal of the American Waste Works Association, Vol. 72, No. 8, August 1980, p. 458.

U.S. Environmental Protection Agency, "Handbook for Analytical Quality Control in Water and Wastewater Laboratories," EPA 600/4-79-19, USEPA, Cincinnati, Ohio, 1979a.

U.S. Environmental Protection Agency, "Methods for Chemical Analysis of Water and Wastes," EPA-600/4-79-020, USEPA, Cincinnati, Ohio, March 1979b.

U.S. Environmental Protection Agency, "National Secondary Drinking Water Regulations," 1980a.

U.S. Environmental Protection Agency, "Planning Workshops to Develop Recommendations for Ground Water Protection Strategy: Appendices," EPA/ODW-2, USEPA, Washington, D.C., 1980b.

U.S. Environmental Protection Agency, "Water Quality Criteria Documents: Availability," 45 FR 79318, USEPA, Washington, D.C., November 28, 1980c.

U.S. Environmental Protection Agency, "National Interim Primary Drinking Water Regulations," 40 CFR 141, USEPA, Washington, D.C., July, 1981.

U.S. Environmental Protection Agency, "Test for the Evaluation of Solid Waste, Physical-Chemical Methods," EPA Report SW-846, USEPA, Washington, D.C., July, 1982.

MINI-GRANT

FINAL REPORT

"Design of a Digital EW Passive Receiver"

Author:	William S. McCormick
University:	Wright State University, Dayton, Ohio
Department:	Electrical Systems Department
Sponsoring Agency:	AFOSR - 85 - 045

(I)   Introduction

The frequency estimation of enemy radar pulses is of vital and obvious importance to the U.S. Air Force.[1] The passive EW receiver that performs this function is currently configured in either the Channelized Receiver (CR)   mode or the Instantaneous Frequency Measurement (IFM) mode.   The channelized receiver configuration is essentially a contiguous filter bank that has problems in the short pulse situation and is physically bulky.   The IFM configuration estimates frequency by measuring at a given sampling time the differential phase, $\omega_i \tau$, accumulated by passing the signal pulse through a known time delay, τ; Figure 1 illustrates.   The IFM receiver is a broadband receiver that handles the short pulse case well but can not estimate frequency in the multiple signal case. As originally configured, the IFM receiver[2] is primarily an analog device with dedicated time delays, amplifiers, mixers, and comparators. Given the constraints of the current receivers, it was possible at the end of the summer of 1984 to define the optimum digital receiver.   Such a receiver would realize the time delays by discrete sampling, would have the multiple signal capability of the CR receiver, and would possess the broadband and short pulse width capability of the IFM receiver.

Early attempts at digitizing the receiver design concentrated on the IFM configuration since it was more adaptable to the digital approach and was broadband in nature.   A fairly straightforward all-digital realization of the IFM receiver is defined and discussed in Section II. The sensitivity of this receiver to S/N, timing jitter, finite sampling

width, and quantization effects were analyzed and simulated. Although feasible, the all-digital IFM receiver is only a single frequency device that can not function in the multiple signal environment. Multiple frequency estimation requires some technique of spectral estimation. Modern discrete spectral estimation can be classified as either non-parametric or parametric in nature. Non-parametric linear techniques include the traditional fast fourier transform (FFT), the fast Walsh transform, and the recently developed number theoretic transform. In general, these non-parametric methods suffer from poor short pulse frequency resolution and from a high computational requirement. In contrast, by assuming a general waveform class, the parametric spectral estimation methods offer good short pulse frequency resolution but suffer from a generally higher noise sensitivity. Typical parametric methods include autoregressive modeling, the Pisarenko decomposition, and the classical Prony method. Although these highly similar methods differ in detail, they invariably include a computationally demanding matrix inversion and/or eigenanalysis in addition to a polynomial equation root finding step. Because of the sampling rate and computational requirements of the transform methods, a primary emphasis was placed in this report on the Prony method. A review of the Prony technique and a two frequency illustrative example are presented in section III.

Because of the noise sensitivity of the multiple frequency Prony, the subject of a Prony noise preprocessor is of great operational significance. The two noise preprocessors considered in this report are the all digital least squares approach of Hildebrand[7] and the

traditional IFM configuration wherein the in-phase, $z_{A_i} \cos(\omega_i r)$, and quadrature, $z_{A_i} \sin(\omega_i r)$ components, are presented at video bandwidths. Both configurations are analyzed and discussed in section IV along with some new multiplication free noise smoothing approaches.

The actual mechanism of the Prony noise sensitivity is analyzed in section V. Matrix condition numbers are derived and plotted for the two and three frequency case and the polynomial root noise sensitivity problem is discussed. An interesting multi-level Prony approach is also presented which has attractive noise supression properties. The multi-level approach, which is actually required because of current limitations in high speed A/D converters, introduces an ambiguity that can be resolved using the novel scheme presented in section VI.

The effects of signal limiting on the Prony algorithm is also discussed in section VII and two additional digital frequency estimation schemes are presented in the final section VIII.

(II) <u>All-Digital IFM Single Frequency Estimates</u>

An early attempt was made to use a standard differentiating approach as shown in Figure (1). Simulation indicated that the derivative operation greatly amplified the quantization noise and prevented successful operation. Various noise smoothing derivative-based methods involving central differences have been proposed but have not as yet been simulated.

In order to eliminate the amplifier, mixers, time delays, of the traditional IFM receiver, it was proposed to process sampled complex

data, y_{t_1}, y_{t_2}, y_{t_3},...,y_{t_i},...., as follows: let $A = y_i$, $B = y_{i+1}$ where $t_{i+1} - t_i = \tau$;

i.e.,

$$A = c_1\, e^{j\omega t_i} = |A|\underline{/A}$$

$$B = c_1\, e^{j\omega(t_{i+1})} = c_1\, e^{j\omega(t_i + \tau)} = |B|\underline{/B} \tag{1}$$

where c_1 is the complex magnitude of the sine wave. Rewriting B as $c_1 e^{j\omega t_i} \cdot e^{j\omega\tau}$, we can solve for $(j\omega)$ as

$$(j\omega) = \frac{1}{\tau} \ln\left[\frac{B}{A}\right] = \frac{1}{\tau} \ln\left[\left|\frac{B}{A}\right|\right] + j\theta/\tau \tag{2}$$

or

$$\omega = \frac{\theta}{\tau} \quad \text{where } \theta = \underline{/B} - \underline{/A}. \tag{3}$$

Using standard sensitivity analysis, the per unit effect of sampling time jitter can be shown to be:

$$\left[\frac{\sigma_\omega}{\omega}\right] = \frac{1}{\sqrt{2}}\left[\frac{\sigma_t}{\tau}\right] \tag{4}$$

where σ_t is the time jitter and τ is the nominal time delay. For a 1GHz signal and a τ of 5 nanosecs., a 0.1 % accuracy requires a sampling jitter of less than 10 pico seconds which is quite a severe requirement. As a way of circumventing this problem, the synchronized sampler of Figure (2) was proposed which reintroduces delay lines but allows for simultaneous sampling without jitter.

Quantization noise along with broadband noise was included in the simulation with an indicated S/N threshold of 20 db. Referring to equation (3), the frequency estimator is basically a phase demodulator with a phase noise variance twice that of the average complex sample.

Referring to Stremler[3] the threshold for pure phase demodulation in 14 db which with the added 6 db gives a threshold in close agreement with the simulation. The maximum liklihood noise preprocessor for the single frequency all-digital IFM receiver is the running sum, S_k, given as

$$S_k = \frac{1}{k} \sum_{i=1}^{k} R_i \quad \text{where } R_i = y_{i+1} / y_i \qquad (5)$$

Successful operation $\left[\frac{\sigma_\omega}{\omega} < 0.001 \right]$ has been realized at S/N ratios as low as 0 db for 1 μsec pulses using this preprocessor.

An interesting result was observed when the effect of finite sample width was simulated. Although preliminary analysis (incorrect) indicated a sensitivity, actual simulation results indicated no sensitivity whatsoever. The explanation for this effect is simply that the single frequency IFM receiver is actually a special case of the Prony algorithm which is not sensitive to sampling pusle width as will be demonstrated in section (V).

(III) Discussion of the Classical Prony Method

Because of its computational directness, the multiple frequency parametric estimator of choice is the classical Prony method. In the excellent review article of S.M. Kay[4], the equivalence of the Prony method to the auto-regressive maximum entropy, and linear prediction methods is established. The outstanding quality of the parametric methods is the excellent frequency resolution obtainable over short observation intervals. As with all the parametric methods, the Prony method is however quite noise sensitive and must be preceeded by a noise preprocessor.

In equation form, N uniformly sampled, complex samples for M unknown
frequencies of unknown power can be witten as follows:

$$y_o = c_1 \qquad + c_2 \qquad\qquad + c_3 \qquad\qquad +\ldots+ c_L$$

$$y_1 = c_1 e^{j\omega_1 \tau} \qquad + c_2 e^{j\omega_2 \tau} \qquad + c_3 e^{j\omega_3 \tau} \qquad +\ldots+ c_L e^{j\omega_L \tau}$$

$$y_2 = c_1 e^{j2\omega_1 \tau} \qquad + c_2 e^{j2\omega_2 \tau} \qquad + c_3 e^{j2\omega_3 \tau} \qquad +\ldots+ c_L e^{j2\omega_L \tau}$$
$$\bullet \qquad\qquad\qquad\qquad \bullet \qquad\qquad\qquad\qquad\qquad (6)$$
$$\bullet \qquad\qquad\qquad\qquad \bullet$$
$$\bullet \qquad\qquad\qquad\qquad \bullet$$

$$y_{N-1} = c_1 e^{j(N-1)\omega_1 \tau} + c_2 e^{j(N-1)\omega_2 \tau} + c_3 e^{j(N-1)\omega_3 \tau} +\ldots+ c_4 e^{j(N-1)\omega_L \tau}.$$

Since there are 2 M unknowns, N equals 2M in the usual Prony formulation.
As stated, the system of equations in (6) is a simultaneous set of non
linear algebraic equations which can be made explicit in expression 7
when $\mu_1 = e^{j\omega_1 \tau}$

$$y_o = c_1 \qquad + c_2 \qquad + c_3 \qquad + \ldots + c_M$$

$$y_1 = c_1 \mu_1 \qquad + c_2 \mu_2 \qquad + c_3 \mu_3 \qquad + \ldots + c_M \mu_M$$

$$y_2 = c_1 \mu_1^2 \qquad + c_2 \mu_2^2 \qquad + c_3 \mu_3^2 \qquad + \ldots + c_M \mu_M^2$$
$$\bullet \qquad\qquad\qquad\qquad\qquad\qquad\qquad\qquad (7)$$
$$\bullet$$
$$\bullet$$

$$y_{2M-1} = c_1 \mu_1^{2M-1} + c_2 \mu_2^{2M-1} + c_3 \mu_3^{2M-1} + \ldots + c_M \mu_M^{2M-1}$$

Because of the uniform sampling and the resulting polynomial structure, the solution of (7) can be realized by the Prony algorithm which is a two stage algorithm involving the solution of a set of linear equations followed by a polynomial root finding step as indicated in Figure (3).

As an illustration of the algorithm, the two frequency case will be presented. This example is especially relevant since the two frequence case is the only case treated in the simulation.

Let us assume that the unknown frequencies, $\mu_1\mu_2$, are roots of the quadratic equation, $\mu^2 - \alpha_1\mu - \alpha_2 = 0$. Given the following observation equations,

$$(1) \quad y_0 = c_1 + c_2$$
$$(2) \quad y_1 = c_1\mu_1 + c_2\mu_2$$
$$(3) \quad y_2 = c_1\mu_1^2 + c_2\mu_2^2 \qquad (8)$$
$$(4) \quad y_3 = c_1\mu_1^3 + c_2\mu_2^3$$

we first multiply equation #1 by α_2, equation #2 by α_1, equation #3 by -1 to yield

$$\alpha_2 y_0 = c_1\alpha_2 + c_2\alpha_2$$
$$\alpha_1 y_1 = c_1\alpha_1\mu_1 + c_2\alpha_1\mu_2 \qquad (9)$$
$$- y_2 = - c_1\mu_1^2 - c_2\mu_2^2$$

Adding the above equations, we arrive at

$$\alpha_2 y_0 + \alpha_1 y_1 - y_2 = c_1[\alpha_2 + \alpha_1\mu_1 - \mu_1^2] + c_2[\alpha_2 + \alpha_1\mu_2 - \mu_2^2] = 0 + 0 = 0 \quad (10)$$

or

$$y_2 = \alpha_1 y_1 + \alpha_2 y_0 \qquad (11)$$

In the second step, we multiply equations 2 thru 4 by α_2, α_1, -1 to yield as in step #1 a new equation given as

15.8

$$y_3 = \alpha_1 y_2 + \alpha_2 y_1 \qquad (12)$$

which when combined with (11) can be written in matrix form as

$$\begin{bmatrix} y_1 & y_0 \\ y_2 & y_1 \end{bmatrix} \begin{bmatrix} \alpha_1 \\ \alpha_2 \end{bmatrix} = \begin{bmatrix} y_2 \\ y_3 \end{bmatrix} = \begin{bmatrix} A \end{bmatrix} \begin{bmatrix} \alpha_1 \\ \alpha_2 \end{bmatrix} \qquad (13)$$

which yields solutions for α_1, α_2 which immediately give the two frequencies as

$$\mu_1, \mu_2 = \frac{\alpha_1 \pm \sqrt{\alpha_1^2 + 4\,\alpha_2}}{2} \qquad (14)$$

where

$$\omega_i = \left[\frac{1}{j\tau}\right] \ell n \, (\mu_i) \qquad (15)$$

Using the Prony method, we can then estimate two seperate frequencies from four complex samples. The resolution of the estimates is determined strictly from the S/N ratio which is to be contrasted to the Fourier Transform whose resolution is determined by the reciprocal of the total sampling aperture which then restricts a one megahertz FFT system to pulse widths greater than one microsecond. The Prony algorithm is highly sensitive to noise however since the matrix A of (13) is ill-conditioned (rows are highly correlated). The polynomial root finding step may also be quite sensitive to noise as discussed in the next section.

(IV)   Noise Sensitivity of the Prony Algorithm

The noise sensitivity of the Prony algorithm can be considered on a stage by stage basis as illustrated in Figure (3). Considering the effect of noise on the first stage, equation (13) can be rewritten, with additive white gaussian noise, $\bar{n}$, as follows:

$$\begin{bmatrix} y_2 \\ y_3 \end{bmatrix} + \begin{bmatrix} n_2 \\ n_3 \end{bmatrix} = \left\{ [A] + \begin{bmatrix} n_1 & n_0 \\ n_2 & n_1 \end{bmatrix} \right\} \begin{bmatrix} \alpha_1 \\ \alpha_2 \end{bmatrix} \qquad (16)$$

;the solution $\begin{bmatrix} \alpha_1 \\ \alpha_2 \end{bmatrix}$ can then be written as

$$\begin{bmatrix} \alpha_1 \\ \alpha_2 \end{bmatrix} = \left\{ [A] + \begin{bmatrix} n_1 & n_0 \\ n_2 & n_1 \end{bmatrix} \right\}^{-1} \cdot \left\{ \begin{bmatrix} y_2 \\ y_3 \end{bmatrix} + \begin{bmatrix} n_2 \\ n_3 \end{bmatrix} \right\} \qquad (17)$$

For reasonable S/N ratios, the major noise perturbation, $\begin{bmatrix} \Delta\alpha_1 \\ \Delta\alpha_2 \end{bmatrix}$, on the

(α_1, α_2) roots can be approximated by

$$\begin{bmatrix} \Delta\alpha_1 \\ \Delta\alpha_2 \end{bmatrix} \approx [A]^{-1} \cdot \begin{bmatrix} n_2 \\ n_3 \end{bmatrix}; \qquad (18)$$

i.e., $[A]^{-1}$ constitutes a noise gain matrix. One reasonable condition number for the [A] matrix is simply the modulus of the value of the determinant. Other condition numbers involving eigenvalues could be defined but the determinant modulus is as useful as any other. Evaluating the determinant of [A] for the two frequency case yields

$$\left| |A| \right| = y_1^2 - y_0 y_2 = 2c_1 c_2 \, e^{j(\omega_1 + \omega_2)\tau} - c_1 c_2 \, e^{j2\omega_1\tau} - c_1 c_2 e^{j2\omega_2\tau} \quad (19)$$

which reduces to

$$\left| |A| \right| = c_1 c_2 e^{j2\omega_1\tau} \left\{ 2e^{j\Delta\omega\tau} - 1 - e^{j2\Delta\omega\tau} \right\} \qquad (20)$$

where

$$\Delta\omega = \omega_2 - \omega_1.$$

For small $(\Delta\omega\tau)$, $\left| |A| \right|$ can be approximated by

$$\left| |A| \right| \approx |c_1||c_2| \left\{ (\Delta\omega\tau)^2 \right\} \qquad (21)$$

which indicates that noise sensitivity is most severe when $(\Delta\omega\tau)$ is ≈ 0 which is reasonable since this implies that too little differential phase, $(\Delta\omega\tau)$, has accumulated to distinguish the two signals from noise.

The determinant modulus, $\left|\,|A|\,\right|$, has also been evaluated for the three frequency case with the general expression given as

$$\left|\,|A|\,\right| = y_2{}^3 - 2y_1y_2y_3 - y_0y_2y_4 + y_1^2y_4 + y_0y_3{}^2 \tag{22}$$

with a small $(\Delta\omega\tau)$ approximation of

$$\left|\,|A|\,\right| \approx (13.5) \; \left|[c_1+c_2+c_3]\right|^2 \left\{c_2(\Delta\omega_2\tau)^2 + c_3(\Delta\omega_3\tau)^2\right\} \tag{23}$$

where

$$\Delta\omega_2 = \omega_2 - \omega_1$$
$$\Delta\omega_3 = \omega_3 - \omega_1.$$

Expressions (21) and (23) can be extended to any arbitrary number of frequencies. Expression (19) and (22) were computer evaluated in Figure (4) and (5) over a range of $(\Delta\omega\tau)$ for the two and three frequency case. The periodic nature of the condition number with $(\Delta\omega\tau)$ is evident in the figures. In the two frequency case, a $(\Delta\omega\tau)$ of around 0.5 appears to be a reasonable sensitivity threshold. In the three frequency case, the maximum noise sensitivity occurs when both $(\Delta\omega_2\tau)$ and $(\Delta\omega_3\tau)$ are close to zero but improves when either but not necessarily both $(\Delta\omega\tau)$ increases in value. This kind of noise sensitivity analysis illustrates the same type of tradeoff as the Cramer Rao bound but it is more direct to derive and offers more physical insight.

Referring again to Figure the noise sensitivity of the root finding stage can be considered in terms of the general polynomial equation, $P(x) = \alpha_o x^n + \cdots + \alpha_n = 0$, where a noise error in α_i, $\Delta\alpha_i$, produces a perturbation in the jth root ζ_j, $\Delta\zeta_j$, given by[5]

$$\Delta \ell_j = \Delta \alpha_i \left\{ \frac{\alpha_i \ell_j n-i}{p'(\ell_j)} \right\} \begin{array}{l} 1 \leq i \leq 2 \\ 1 \leq j \leq 2 \end{array} . \tag{24}$$

For the Prony two frequency case, $p(x) = x^2 - \alpha_1 x - \alpha_2 = 0$ has the root sensitivities given below for $n = 2$:

$$\Delta \ell_1 = \Delta \alpha_1 \left\{ \frac{\alpha_1 \ell_1}{2 \ell_1 - \alpha_1} \right\} \qquad \Delta \ell_2 = \Delta \alpha_1 \left\{ \frac{\alpha_1 \ell_2}{2 \ell_2 - \alpha_1} \right\}$$

$$\tag{25}$$

$$\Delta \ell_1 = \Delta \alpha_2 \left\{ \frac{\alpha_2}{2 \ell_1 - \alpha_1} \right\} \qquad \Delta \ell_2 = \Delta \alpha_2 \left\{ \frac{\alpha_2}{2 \ell_2 - \alpha_1} \right\} .$$

The maximum sensitivity occurs when $2 \ell_j - \alpha_1 = 0$ which corresponds to the zero discriminant or multiple root case. For the case where $2 \ell_j - \alpha_1 \neq 0$, equations (25) suggest that it may be possible for one root to be noise sensitive while the other is not due to the relative phasing of $\Delta \alpha_1$, $\Delta \alpha_2$, ℓ_1, ℓ_2, α_1, α_2. This situation has been observed frequently in the simulation.

In general, it is not always clear how to distinguish the noise effects of the linear stage from the root finding stage of the Prony algorithm since they both have their greatest sensitivity at the same operating condition, ($\Delta \omega \tau = 0$). Reflecting on the dynamics of the situation, it would seem that a strong noise effect in the linear stage would increase the apparent ($\Delta \omega \tau$) into the root finding stage and reduce its noise sensitivity whereas a weak noise effect in the linear stage would preserve the low ($\Delta \omega \tau$) and result in the most sensitive situation in the root finding stage. The overall effect is the same high noise sensitivity although the two mechanisms are different.

15.12

(V)   <u>Noise Preprocessing for the Prony Algorithm</u>

Without a noise preprocessor, the unprotected Prony algorithm has a S/N threshold of around 55 db. for ($\omega\tau$) products as high as 1.25. Simulations have indicated thresholds as high as 67 db. for lower ($\omega\tau$) products. Such high thresholds demand a noise preprocessor for practical application.   It should be mentioned that a postprocessor would not provide adequate noise smoothing since it occurs after the nonlinear Prony estimator. The following three sections present various approaches to noise preprocessing. The first section deals with some multiplication free methods for smoothing the oversampled set of the [α] equations given in expression (13).   The second section treats the analog IFM preprocessor which presents noise smoothed complex sampled values, $e^{j m \omega_i \tau}$, to the Prony algorithm and the third section considers the least squares smoothing of the [α] equation.

A.   <u>Analog, Multiplication Free Smoothing Methods</u>

For the oversampled case, expression (13) can be written as

$$y_1\alpha_1 + y_0\alpha_2 = y_2$$
$$y_2\alpha_1 + y_1\alpha_2 = y_3$$
$$\bullet$$
$$\bullet \qquad\qquad\qquad (26)$$
$$\bullet$$
$$y_{m-1}\alpha_1 + y_{m-2}\alpha_2 = y_m$$

where (M+1) is the number of samples. In the noise free case, the same (α_1, α_2) would satisfy all M equations and any sum of

15.13

equations would yield an equation with same (α_1, α_2) solution. It was therefore proposed to smooth the noisy $\{y_i\}$ values by analog adding M/2 equations in two subgroups to produce two smoothed equations in α_1 and α_2. Noise smoothing of this type lowers the noise variance by a factor of (2/M). Unfortunately, it also attenuates the signal since the processing is equivalent to passing the $\{y_i\}$ values through a filter with an impulse response equal to $\{\mu(t) - \mu[t - \frac{M}{2}\tau]\}$ where τ is the sampling period. The first null bandwidth of such a filter is $2/(M\tau)$ which would represent a significant attenuation over a frequency range of $(1/\tau)$ hertz. In general, the output S/N for this smoothing approach can be expressed as

$$ (S/N)_{Out} = (S/N)_{In} \left\{ \frac{M}{2} \right\} \text{sinc}^2 \left[\pi M f \tau \right] \qquad (27) $$

where f is the frequency of the sine wave.

The method was simulated with very little S/N improvement observed as is in fact suggested by (27).

A similar kind of noise smoothing is achieved with the sampling pulse width itself. Incorporating sampling pulse width, T_s, into the Prony expression (6), we get for M = 2, N = 4,

$$0 = c_1 \left\{ \frac{e^{j\omega_1 T_s} - 1}{j\omega_1} \right\} + c_2 \left\{ \frac{e^{j\omega_2 T_s} - 1}{j\omega_2} \right\}$$

$$y_1 = c_1 \left\{ \frac{e^{j\omega_1 T_s} - 1}{j\omega_1} \right\} e^{j\omega_1 T} + c_2 \left\{ \frac{e^{j\omega_2 T_s} - 1}{j\omega_2} \right\} e^{j\omega_2 \tau} \qquad (28)$$

$$y_2 = c_1 \left\{ \frac{e^{j\omega_1 T_s} - 1}{j\omega_1} \right\} e^{j\omega_1 (2\tau)} + c_2 \left\{ \frac{e^{j\omega_2 T_s} - 1}{j\omega_2} \right\} e^{j\omega_2 (2\tau)}$$

$$y_2 = c_1 \left\{ \frac{e^{j\omega_1 T_s} - 1}{j\omega_1} \right\} e^{j\omega_1 (3\tau)} + c_2 \left\{ \frac{e^{j\omega_2 T_s} - 1}{j\omega_2} \right\} e^{j\omega_2 (3\tau)}$$

which merely changes the values of the coefficients and does not affect the ω_1, ω_2 solutions. This has been verified by simulation. Unfortunately, the method also attenuates the signal as before.

B. **Analog IFM Processor**

The traditional IFM system has been a single frequency estimator that forms a frequency estimate from a ($\cos \omega \tau$, $\sin \omega \tau$) sample smoothed to video bandwidths. Figures 6 and 7 give two schematic illustrations of the IFM receiver. For the single frequency case, delayed and non-delayed in phase and quadrature channels as formed to produce terms like

$$A_1 = A \cos (\omega t - \omega \tau) - A \sin (\omega t) \qquad (29)$$

which, when squared by nonlinear diode action, becomes

$$A_1^2 = A^2 \cos^2(\omega t - \omega \tau) - 2A^2 \cos(\omega t - \omega \tau)\sin(\omega t) + A^2 \sin^2(\omega t) \qquad (30)$$

which, after low pass filtering to video bandwidths, reduce to

$$A_2 = A^2 - A^2 \sin \omega \tau. \qquad (31)$$

As suggested by Tufts[6], the IFM processor can also serve as a noise preprocessor for the multiple frequency Prony algorithm. For the general N-frequency signal case with arbitrary relative time delays, τ_n^d, and phase modulations, $\phi_n(t)$, the corresponding expression for A_1, becomes for a general delay of τ;

$$A_1 = -\sum_{n=1}^{N} An \sin\left[\omega_n(t-\tau_n^d) + \phi_n(t - \tau_n^d)\right]$$

$$+ \sum_{n=1}^{N} An \cos\left[\omega_n(t-\tau_n^d) - \omega_n\tau + \phi_n(t-t_n^d-\tau)\right] \qquad (32)$$

which leads to filtered expression for A_2 given by

$$A_2 = \sum_{i=1}^{N}\sum_{j=1}^{N} A_iA_j \sin\left[(\omega_j-\omega_i)t + \omega_j\tau_j^d-\omega_i\tau_i^d+\omega_j\tau \right.$$

$$\left. +\phi_j(t-\tau_j^d)-\phi_i(t-\tau_i^d-\tau)\right] . \qquad (33)$$

In expression (33), the i=j case produces the desired term given as follows for the zero phase modulation case:

$$\sum_{i=1}^{N} A_i^2 \sin(\omega_i\tau). \qquad (34)$$

Unfortunately, expression (33) also indicates difference or "beat" frequency terms, $(\omega_j-\omega_i)$, that can be passed by the low pass filter especially for the $\Delta f \approx 0$ case. The resulting error in the Prony algorithm is the result of the IFM processing itself and is not related to the sensitivity of the Prony method. The problem of the "beat" frequency term has been verified in a simulation of the IFM.

The presence of phase modulation reduces equation (34) to

$$\sum_{i=1}^{N} A_i^2 \sin[\omega_i \tau + \phi_i(t-\tau_i^d) - \phi_i(t-\tau_i^d-\tau)] \qquad (35)$$

which for small τ can be approximated by

$$\sum_{i=1}^{N} A_i^2 \sin[\omega_i \tau + (\tau) \dot{\phi}_i(t-\tau_i^d)] \qquad (36)$$

which results in a time varying phase modulation which completely masks the constant $(\omega_i \tau)$ phase term and defeats the Prony algorithm.

C. Least Squares Smoothing

As suggested by Hildebrand[7] the oversampled [α] equations of (26) can be solved for the (α_1, α_2) pair that minimizes the least squares error over the smoothing time. The normal equations[8] are are written as follows;

$$R_{01} = \bar{\alpha}_1 R_{11} + \bar{\alpha}_2 R_{21}$$
$$R_{02} = \bar{\alpha}_1 R_{12} + \bar{\alpha}_2 R_{22} \qquad (37)$$

where the autocorrelation functions, R_{ij}, are given as follows with T equaling the sampling period and τ equaling the Prony delay:

$$R_{01} = \sum_{i=1}^{N} y(nT) \; y^*(nT+r)$$

$$R_{11} = \sum_{i=1}^{N} y(nT+r) \; y^*(nT+r)$$

$$R_{21} = \sum_{i=1}^{N} y(nT+r) \; y^*(nT) \qquad\qquad (38)$$

$$R_{02} = \sum_{i=1}^{N} y(nT) \; y^*(nT+2r)$$

$$R_{12} = \sum_{i=1}^{N} y(nT+r) \; y^*(nT+2r)$$

$$R_{22} = \sum_{i=1}^{N} y(nT+2r) \; y^*(nT+2r)$$

and the minimum mean square error is given by

$$R_{00} - \bar{a}_1 R_{01} - \bar{a}_2 R_{02}. \qquad\qquad (39)$$

The optimum $\bar{a}_1$, $\bar{a}_2$ of (37) are then passed to the root finding stage where the estimated frequencies are calculated.

(VI.) <u>Operational Configuration</u>

In all Prony configurations, a complex sample must be sampled and quantized at four uniform time intervals, r, $2r$, $3r$, and $4r$, in order to represent the complex samples

$$y_i = c_1 \; e^{j(ir)\omega_1} + c_2 \; e^{j(ir)\omega_2} \quad (i = 1,2,3,4). \qquad\qquad (40)$$

Because sub-microsecond processing times are required, it is not possible to digitize to the 11 bit accuracy needed to measure to one

MHZ accuracy over a 2GHZ range. The common approach to achieving the 11 bit accuracy is to utilize multiple Prony's where the fundamental $\{r_i\}$ delays are related (for 4 levels) by $r_4 > r_3 > r_2 > r_1$ and the bit levels for the four stages are related by $b_1 \leq b_2 \leq b_3 \leq b_4$ with $b_1 + b_2 + b_3 + b_4 \geq 11$. The first r_1 level covers the entire frequency range $(1/r_1 > 2000)$ and the bit level, b_1, is chosen to be low in order to resist the effects of noise. Assuming a successful first Prony stage, the r_2 of the second stage should be chosen so that $1/r_2 \geq \dfrac{1}{(2^{b_1} r_1)}$ which then allows the second stage to resolve the known $\dfrac{1}{(2^{b_1} r_1)}$ interval into 2^{b_2} equal subintervals which is then equivalent to a resolution of $b_1 + b_2$ bits. This process can be continued as illustrated in Fig. (8) with $b_1 = 1$, $b_2 = 2$, and $r_3 = 2^{(b_1 + b_2)} r_1$. The third and final stage displays the frequencies to a resolution of 5 bits or $(1/2^5)$ of the original $1/r_2$ interval. Starting at the second stage, an ambiquity problem presents itself since the second stage must present its output modulo $1/r_2$ over the entire defining $1/r_1$ interval. In general, there is no way the Prony algorithm can distinguish a group of frequencies defined as $(f + n/r)$ for $n = 1,2,3, \cdots$ since a sine wave is modulo 2π. For any arbitrary frequency, f, the Prony output will always be the remainder term after dividing f by $1/r$. Referring again to the $f_1 = 20$, $f_2 = 60$ example of Figure (8), the ambiguity problem is apparent with a choice required between $(\bar{A}, \underline{B})$ and $(\underline{A}, \bar{B})$. It is further observed that $(\bar{A}, \underline{A})$, $(\bar{B}, \underline{B})$ are not viable candidates since they are generated as modulo $1/r_2$ frequencies and are recognized as such. (They can also be identified on the basis of equal amplitudes

where the Prony equations of (8) are solved for amplitude following the determination of frequency.) Because the ambiguity problem increases geometrically with additional stages, it is essential to resolve the ambiguity problem at each stage as it develops. Consequently, there will be only two preferred frequencies passed from one stage to the next. The actual ambiguity resolution algorithm is discussed in the next section.

(VII) Ambiguity Resolution Algorithm

In order to resolve the ambiguity, it is necessary to distinguish the true frequency pair (f_1, f_2) from the false frequency pair. The essential distinguishing characteristic of the false or reflected frequencies is their modulo $1/r$ representation given as

$$\hat{f}_1 + i/r$$
$$\left\{ \begin{matrix} i = = 1, \pm 2, \cdots \\ j = = 1, \pm 2, \cdots \end{matrix} \right\} \qquad (41)$$
$$\hat{f}_2 + j/r$$

where the carrot superscript, $\hat{\ }$, represents a quantized estimate. The resolution algorithm must somehow distinguish between the true case $(n=m=0)$ and the false case $(n \neq 0, m \neq 0)$. In order to test for the $n \neq 0$, $m \neq 0$ condition, some reference or comparison must be established. The algorithm forms this comparison by generating frequency estimates from a Prony with a r^B close in value to the original r^A. By a proper choice of r^A, r^B and the quantization levels, N^A, N^B, it can be assured that the true frequency pair will be closer in the r^A, r^B Prony's than any false or reflected pair. The notation for this discussion represents the r values as r_i^A and r_i^B where i refers to the ith level or stage of the Prony, A refers to the primary Prony of level i, and B

refers to the reference Prony of level i required to resolve the ambiguity generated at level i. In a sense, the proposed scheme appears to be a "boot strap" kind of arrangement but it does provide a solution to the ambiguity problem provided r_i^A, r_i^B, N_i^A, N_i^B are chosen properly. After the ambiguity is resolved at each stage and a best estimate frequency pair is chosen, intervals or "delimiting spans" are formed symmetrically about the two frequencies. The two intervals or spans will then define the acceptable candidate frequency pair vectors, $(f_1, f_2)_{i+1}^{A \text{ and } B}$, that will be tested in the next level i+1 with the ambiguity algorithm. The forming of the span intervals at level i effectively restricts the acceptable frequency range of level (i+1) to within at least $(1/r_{i+1})$ of the best previous estimate thereby maintaining a constant dimensionality as the frequency resolution improves with each new level. An updated estimate of the frequency pair is generated by the ambiguity algorithm as you proceed through the levels in a manner similar to that of a binary tree or successive approximation arrangement. Figure (9) illustrates a quantized second level with r = 30 n.s., N = 4, and delimiter spans from 0 to 33 MHZ for the low frequency (f_1 = 20 MHZ) and 66 MHZ to 100 MHZ for the higher frequency (f_2 = 80 MHZ). The setting of the delimiter span intervals results in a tradeoff between allowing enough range to include the correct frequency pairs and limiting the number of candidate frequency pairs that the ambiguity algorithm must resolve. In general, the delimiter span should be large enough to cover the remaining uncertainty in f_1 and f_2 and wide enough to allow for a gradual noise degradation in the Prony's.

The key step in ambiguity resolution is to compare each acceptable frequency pair vector from r_i^A with each acceptable frequency pair vector from r_i^B and to then choose as the best (f_1, f_2) estimate that pair vector from r_i^B which has the minimum euclidian distance from all acceptable pair vectors in r_i^A. That is, we form the scaler F given by

$$F_n = |(\hat{f}_1, \hat{f}_2)^A - (\hat{f}_1, \hat{f}_2)^B| \qquad (42)$$

where n ranges over all candidate pairings between r^A and r^B as defined by the delimiter. The best estimate is taken as that quantized frequency pair, $(\hat{f}_1, \hat{f}_2)^B$, that gives the minimum F. In equation (42), the $\hat{f}_1^A$ and $\hat{f}_1^B$ always belong to the same delimiter although in the false or reflected case either f_1^A of f_1^B would be a reflection of the other frequency, f_2, and would be identified as such by the ambiguity algorithm. These statements can be extended to the n-frequency case where there are now n delimiter spans with $\hat{f}_i^A$, $\hat{f}_i^B$ belonging to the same delimiter. In the general n frequency case, there are at least $(n!)^2$ values of F_n generated since n! is the minimum number of candidate pair vectors associated with both A and B, Prony's. With wider span intervals, the number of F_n generated will be greater. The ambiguity resolution algorithm works because the difference in $|i/r^A - j/r^B|$ associated with false frequencies, exceeds any possible difference due to quantization errors in the true estimates. Assuming a worst case situation, the greatest difference possible on a per frequency basis between a true frequency in r^A and a true frequency in r^B is the sum of their maximum quantization errors given by

$$\left\{ \frac{1}{2N^A r^A} + \frac{1}{2N^B r^B} \right\} . \qquad (43)$$

15.22

In order for the algorithm to suceed, the value of (43) must always be less than

$$\left|\frac{i}{\tau^A} - \frac{j}{\tau^B}\right| - \left\{\frac{1}{2N^A\tau^A} + \frac{1}{2N^B\tau^B}\right\} \qquad (44)$$

which assumes that the maximum quantization errors add destructively for the false frequencies which then results in the criterion

$$\left\{\frac{1}{N^A\tau^A} + \frac{1}{N^B\tau^B}\right\} \leq \left|\frac{i}{\tau^A} - \frac{j}{\tau^B}\right|; \quad \begin{array}{c} 1 \leq i \leq \tau/\tau^A \\ 1 \leq j \leq \tau/\tau^B \end{array} \quad \cdot \qquad (45)$$

Expression (45) refers to a comparison between false frequencies (A and B) in a span interval which can be shown to yield the lowest value of F of all comparisons involving at least one reflected component. The important quantity, $\left|\frac{i}{\tau^A} - \frac{j}{\tau^B}\right|$, is non-zero everywhere except at those integer values of $\bar{i}$, $\bar{j}$ where

$$\frac{\bar{j}}{\bar{i}} = \frac{\tau^B}{\tau^A} = R. \qquad (46)$$

The minimum non-zero value of $\left|\frac{i}{\tau^A} - \frac{j}{\tau^B}\right|$ will occur at $(\bar{i}-1)$, $(\bar{j}-1)$ where $\bar{i}$, $\bar{j}$ are the integers specified in (46). The delay ratio, $R = \tau^B/\tau^A$, can be written (commensurate delay lines) as the rational number $R = n/m$ where either n or m is a prime integer. If $\tau/\tau^A < n$, $\tau/\tau^B < m$, we can then write

$$i < \tau/\tau^A < n$$

and

$$j < \tau/\tau^B < m \qquad (47)$$

which implies from (47) that no $\bar{i}$, $\bar{j}$ can exist. The constraint (47) is actually too severe. The only real requirement is that $n >$ number of $(1/\tau^A)$ in span interval and $m >$ number of $(1/\tau^B)$ in span interval. For

15.23

typical span intervals, n need only be greater than 3 and m need only be greater than 2 which will lead from (47) to the condition $R < 3/2$. Under this constraint on R, there will be no $|\frac{i}{\tau^A} - \frac{j}{\tau^B}| = 0$ case within the delimiter spans other than the $\bar{i} = \bar{j} = 0$ true frequency case. The minimum possible value of $|\frac{i}{\tau^A} - \frac{j}{\tau^B}|$ under these conditions will be in the state (m-1, n-1) so that

$$\left| \frac{i}{\tau^A} - \frac{j}{\tau^B} \right| \geq \left| \frac{(m-1)}{\tau^A} - \frac{(n-1)}{\tau^B} \right| = \left| \left(\frac{m}{\tau^A} - \frac{n}{\tau^B} \right) + \left(\frac{1}{\tau^A} - \frac{1}{\tau^B} \right) \right|$$

$$= \left| 0 + \left(\frac{1}{\tau^A} - \frac{1}{\tau^B} \right) \right|$$

or

$$\left| \frac{i}{\tau^A} - \frac{j}{\tau^B} \right| \geq \left| \frac{1}{\tau^A} - \frac{1}{\tau^B} \right|. \tag{48}$$

Expression (48) leads from (45) to the final criterion given as

$$\frac{1}{N^A \tau^A} \left\{ 1 + \frac{1}{2^k R} \right\} \leq \frac{1}{\tau^A} \left| 1 - \frac{1}{R} \right| \tag{49}$$

where $N^B/N^A = 2^k$ $(k=0,1,2,\cdots)$.

Expression (49) leads directly to the following constraint on N^A,

$$N^A \geq \frac{\left\{ 1 + \frac{1}{2^k R} \right\}}{\left\{ 1 - 1/R \right\}}. \tag{50}$$

In the second level of the four level simulation (section VIII), R was set to 1.333, k equaled 1, and the required condition on N^A becomes

$$N^A \geq 5.5 \tag{51}$$

which was satisfied for the third and fourth levels and for the second level the great majority of the time. The validity of criterion (50) was confirmed in many runs. The worst case potential problem in the second level was only encountered for one frequency pair and it was

15.24

resolved simply by raising k from 1 to 2. The problem could be completely resolved by raising the bit level of the second level to 3; ie. N^A to 8. As long as criterion (53) is met, the ambiguity problem can be completley solved provided the Prony algorithms are accurate to within their quantization noise interval, $\frac{1}{2N\tau}$. If the Prony's are not accurate, the method will fail (as will any other method) since the entire foundation has been undermined. The criterion of equation (50) applies as stated only to the two frequency case. In the three frequency case, for example, the generation of F_n involves the comparison of two different reflected frequencies in a given delimiter which is a situation that did not arise in the two frequency case. One consequence of this fact is that expression (44) has a new term, ΔF, which is the difference between the two reflected frequencies and which enters expression (44) as $|\frac{1}{\tau^A} + \Delta F - \frac{j}{\tau^B}|$. How this affects ambiguity resolution remains to be determined.

Although the ambiguity resoltuion algorithm requires additonal computation, the computational demands are not as great as the Prony algorithm itself and much of the work can be done in parallel. For the four level case, seven Prony algorithms must be accurate for a successful estimate of multiple frequenices. Although this requirement sounds quite severe when compared to a single level (impossible in hardware) Prony, the requirement on a given Prony is less severe since the quanitzation noise interval is greater. In terms of noise suppression, the multi-level Prony seems to offer some of the same advantages as observed in bit stream regeneration in a repeater PCM

amplifier chain. This quantitative claim has not however been proven
analytically.

(VIII) <u>Computer Simulation</u>

Using the multiple pulse, filter-limiter-filter simulation program
developed under AFOSR/SCEEE support[1] in the summer of 1984, the
multi-level Prony algorithm was simulated along with the ambiguity
resolution algorithm and the IFM and least squares preprocessor. Using
a primary first level r of 5 n.s., the total frequency interval of
interest is 200 MHZ with an 11 bit resolution requirement representing
100 KHZ. Only the two frequency case will be considered in the
simulation although the method should be extendable to any arbitrary
number of frequencies.

The primary simulation program dealt with a four level Prony with
bit levels of quantization per level given by $b_1=1$, $b_2=2$, $b_3=2$, $b_4=6$.
The r_i^A, T_i^B, N_i^A, N_i^B, and R_i choosen are listed in the following table
(I):

Level Number	r_i^A	r_i^B	R_i	N_i^A	N_i^B
1	5.0 n.s.	N/A	N/A	2	N/A
2	15 n.s.	20 ns.	1.333	4	8
3	35.0 n.s.	45.0n.s.	1.29	4	8
4	145.0 n.s.	195 .s.	1.34	32	64

Table (I)

As observed from the R_i, N_i^A values, the criterion for ambiguity
resoltuion is met with the minimum F always yielding the correct
frequency pair. After some initial problems, the derivation of

criterion (50) motivated the parameter choice that solved the ambiguity problem. No false ambiguity indications were ever observed when the condition $0 < R_i < 1.5$ and $N_A^A \geq 4$ were observed. Except for the start-up first level, the delimiter spans were chosen 50% greater than the $1/\tau$ interval of the next Prony level (see discussion). The span or intervals were not found to be a sensitive parameter.

Tables II thru V list some typical output with the last two columns representing the effective bit level of resolution for that particular f_1, f_2. Tables II and III list a comparative study of the least squares and IFM preprocessor for a one microsecond pulse with the video bandwidth of the IFM processor set at one megahertz. A nominal S/N ratio of 20 db was choosen as the point of comparison. The threshold estimate in the least squares case is also included. The least square results are quite impressive with 11 bit resolution retained down to a threshold as low as 15 db without ambiguity.

The noise suppression properties of the multi-level Prony are illustrated by a comparison with the 11 bit single level Prony of Table IV. As expected, the single level resolution is quite sensitive to the noise sensitivity level as expressed by the $(\Delta\omega\tau)$ value. The multi-level Prony does not exhibit this dramatic noise sensitivity. A two level least square Prony is also included in Table V which shows good results although the A/D converters are operating at their upper bit limit. In general, the noise suppresion properties (which are not claimed to be dramatic) of the multi-level Prony exist because the quantization error interval is less in the multi-level case which then

15.27

permits a true track of the frequency pair within the delimiter spans until the last Prony level where the frequenices are finally estimated. A detailed analysis of this effect has not been completed.

Simulation has further shown that a "chirp" or quadratic phase modulation defeats the Prony with either noise preprocessor.

S/N (db)	f_1 TRUE	f_2 TRUE	f_1 MEASURED	f_2 MEASURED	bits f_1	bits f_1
37	47	111	45.8333	112.5000	7.42	7.05
37	7	18	6.9444	18.0555	11.81	11.81
20	5	92	3.9663	94.5913	7.59	6.27
20	19	123	18.9503	128.4050	11.97	5.21
20	20	60	20.8333	59.7220	7.90	9.49
37	70	82	(Lost In First Stage)			
29	5	87	3.9663	89.3830	7.60	6.39
20	17	29	18.0555	29.1666	7.56	10.22

TABLE (II): IFM PROCESSING
FOUR LEVEL PRONY
$b_1=1$, $b=2$, $b_3=2$, $b_4=6$

S/N (db)	f_1 TRUE	f_2 TRUE	f_1 MEASURED	f_2 MEASURED	bits f_1	bits f_1	Threshold (S/N
20	47	111	46.9952	111.0180	15.35	13.44	15db
20	7	18	6.8510	18.2292	10.39	9.77	15
20	5	92	6.2099	92.1074	7.36	10.86	15
20	19	123	18.8702	123.1970	10.58	9.98	10
20	20	60	20.1522	59.8157	10.35	10.08	15
20	15	75	15.1041	74.8798	11.00	10.70	15
20	70	82	69.9118	82.0112	11.00	14.00	15
20	5	87	5.0080	88.9023	11.00	8.57	15
20	17	29	16.9471	29.0464	11.88	12.07	11

TABLE (III): LEAST SQUARES PROCESSING
FOUR LEVEL PRONY
$b_1=1$, $b_2=2$, $b_4=6$.

S/N (db)	f_1 TRUE	f_2 TRUE	f_1 MEASURED	f_2 MEASURED	bits f_1	bits f_1	$(\Delta\omega T)$
20	47	111	47.0163	111.1570	13.58	10.32	2.01
20	7	18	8.7696	25.7193	6.82	4.70	0.346
20	5	92	4.9316	92.1196	11.51	10.71	2.73
20	19	123	18.9939	122.9690	15.00	12.60	3.27
20	20	60	19.8727	60.8792	10.62	7.83	1.26
20	70	82	71.1300	86.0900	7.46	6.02	0.377
20	5	87	4.9316	87.1406	11.51	10.47	2.57
20	17	29	18.7009	34.8130	6.87	5.10	0.377

TABLE (IV): LEAST SQUARES PROCESSING
SINGLE LEVEL PRONY
(b=11 or N =2048

S/N (db)	f_1 TRUE	f_2 TRUE	f_1 MEASURED	f_2 MEASURED	bits f_1	bits f_1
20	47	111	47.2653	111.3280	9.56	9.25
20	7	18	6.6406	18.1466	9.12	10.42
20	5	92	5.0781	91.7970	11.32	9.94
20	19	123	19.1410	123.0500	10.47	11.97
20	20	60	19.9220	59.7660	11.32	9.73
20	70	82	69.9220	82.4220	11.32	8.88
20	5	87	5.0781	87.1090	11.32	10.84
20	17	29	16.7970	29.2970	9.94	9.39

TABLE (V): LEAST SQUARES PROCESSING
TWO LEVEL PRONY: (N_1=32; N_2=64; b_1=5, b_2=6)

(IX)   <u>**Effect of Limiting on the Prony Algorithm**</u>

A limiter is included in the signal processing chain as a way of increasing the usable dynamic range. Since a limiter distorts the signal, it would be expected to have an effect on the Prony algorithm.

An analysis approach based on the analytic signal representation is proposed where the instantaneous output of the zero memory limiter is $f(E)$ where

$$E = \left[(P_1+P_2)^2 + (q_1+q_2)^2\right]^{1/2} \tag{52}$$

is the envelope of the sum of the two signals and (P_1,q_1), (P_2,q_2) are the analytic representation of the two signals. Representing the effect of the limiter as equivalent additive noise, (n_p,n_q), we can write the following equation:

$$\left\{(P_1+P_2),(q_1+q_2)\right\} + \left\{n_p, n_q\right\}$$
$$= \left\{ \frac{f\left[\sqrt{(P_1P_2)^2+(q_1+q_2)^2}\,\right]}{\sqrt{(P_1+P_2)^2+(q_1+q_2)^2}} \cdot \left[(P_1+P_2),(q_1+q_2)\right]\right\} \tag{53}$$

or

$$n_p = \left[\left[\frac{f(E)}{E} - 1\right](P_1+P_2)\right]$$

and

$$n_q = \left[\left[\frac{f(E)}{E} - 1\right](q_1+q_2)\right] . \tag{54}$$

The $\left[\frac{f(E)}{E}\right]$ ratio can be represented statistically as a describing function or statistical gain constant, K, which sets the effective $(S/N)_L$ ratio for noise free limiter operation as

$$\left[\frac{S}{N}\right]_L = \frac{1}{1-K} \quad (0 \leq K \leq 1) \tag{55}$$

15.31

A computer simulation was run to investigate the effects of hard limiting on the Prony. The same dependence on $(\Delta \omega \tau)$ was observed as with additive noise. For example, the two frequencies were lost at $(\Delta \omega \tau) = 0.3$ but were observed when τ was doubled to give $(\Delta \omega \tau) = 0.8$. This would tend to support the additive noise assumption. More analysis needs to be done on this topic.

(X) Other Digital Estimation Algorithm

A. Instantaneous Frequency Estimation

Given the availability of (I,Q) processing the prospect of directly measuring the instantaneous frequency has been considered as a way of estimating frequency. For the two frequency case, the analytic signal representation for the sum is given by

$$\left[A_1 + A_2 \cos(\Delta \omega_1 t) \right] = p(\text{in-phase}) \tag{56}$$

and

$$\left[A_2 \sin(\Delta \omega_1 t) \right] = q(\text{quadrature})$$

where $\Delta \omega_1 = \omega_2 - \omega_1$ and A_1, A_2 are the respective signal magnitudes. From the expression for instantaneous frequency, f_{INS}, [1]

$$f_{INS} = \frac{1}{2\pi} \left\{ \frac{p\dot{q} - q\dot{p}}{p^2 q^2} \right\} , \tag{57}$$

expression (56) yields the two frequency, f_{INS}, given by

$$f_{INS} = \frac{1}{2\pi} \left\{ \frac{(\Delta \omega_1) A_1 A_2 \cos(\Delta \omega_1 t) + \Delta \omega_1 A_2^2}{A_1^2 + A_2^2 + 2 A_1 A_2 \cos(\Delta \omega_1 t)} \right\} \tag{58}$$

For the $A_2 \ll A_1$ small signal case, expression (58) can be approximated as

$$f_{INS} \approx \frac{1}{2\pi} \left[\Delta \omega_1 \left[\frac{A_2}{A_1} \right]^2 + (\Delta \omega_1) \left[\frac{A_2}{A_1} \right] \cos(\Delta \omega_1 t) \right] \tag{59}$$

The instantaneous frequency is defined relative to the f_1 reference frequency. The phasor diagram of Figure (10a) illustrates the $A_1 \gg A_2$ case and suggests a smooth f_{INS} variation at the beat frequency $\Delta\omega$. Figure (11) illustrates a f_{INS} for a relative time delay of 50 n.s., $A_1 = 1$, $A_2 = 0.3$, $f_1 = -20$ MHZ, and $\Delta f_1 = -20$ MHZ. From expression (59), a predicted $2(\Delta f_1)\left[\dfrac{0.1}{1.0}\right] = 12$ MHZ peak-to-peak variation about -21.8 MHZ at the 20 MHZ beat frequency is predicted; Figure (11) confirms the prediction.

For the case $A_2 \approx A_1$ where $A_2 = A_2 + \bar{\Delta}A$, expression (58) can be rewritten as

$$f_{INS} = \frac{(\Delta\omega_1)}{4\pi} \left\{ \frac{(1+\overline{\dfrac{\bar{\Delta}A}{A_1}}) + \cos(\Delta\omega_1 t)}{(1+\cos(\Delta\omega_1 t))} + \frac{1}{([\dfrac{\bar{\Delta}A}{A_1}]^2 / (1+\dfrac{\bar{\Delta}A}{A_1}))} \right\} ; \qquad (60)$$

the rapid f_{INS} (t) variation in this case is suggested by the phasor diagram of Figure (10)b. For the $A_1 = 1.0$, $A_2 = 0.7$ case, expression (60) predicts a variation from -28 MHZ to 24 MHZ which is roughly verified in Figure (12). It is not clear why the positive beat frequency peaks are not at constant amplitude. It is speculated that it may be the result of a phasing problem. In the equal amplitude case ($\Delta\bar{A}=0$), expression (60) indicates a constant absolute -30 MHZ which is more or less suggested by Figure (13).

No great claims are made for this method. The above analysis serves only to establish some kind of model on which to base an estimate of f_1, f_2, A_1, A_2. No mention has even been made

15.33

concerning how to generate f_{INS} originally. Much more work needs to be done on this method.

B.   <u>The Fast Hadamard Transform</u>

Because the Hadamard transform has a fast algorithm and requires only additions instead of multiplication, it was considered as a frequency estimator. A one microsecond, 20 MHZ pulse was transformed using the algorithm of M. Kunt[10] and is given in Figure (14). It is displayed in sequence or mega zero crossing per second with a dominant 20 MZS appearing but with additional spurius spikes as well.

The computation demand for digital processing would be $[(N/2)\log_2 N]T_A$ where T_A is the fastest practical addition time. Assuming of T_A of one nanosecond, a one microsecond pulse requires about 1.73 μsec. to compute which is around twice real time. An all analog addition processor would operate at real time but would be a very complex circuit indeed. This whole approach merits added investigation.

(XI)   <u>Summary and Future Topics of Investigation</u>

The major accomplishments of the minigrant research are the following:

1.   A complete sensitivity analysis of the single frequency IFM detector was completed. The IFM and least squares noise preprocessors were simulated and added to the original simulation. An analysis of the effect of hard limiting on the Prony was made using analytical signal representation. Some new algorithms were also presented using the Hadamard transform and the instantaneous

15.34

frequency response.

2. The ambiguity problem associated with the multi-level, multi-frequency Prony was solved completely. The peculiar noise suppression properties of the multi-level were explained and demonstrated.

The following topics are promising areas for future investigation:

1. The ambituity resolution algorithm should be extended to n frequenices.

2. The multi-level Prony algorithm should incorporate some adaptive features to enhance its noise suppression capability. Specifically, it was observed in the simulation that a noise sensitive polymial root would lie near the origin of the complex plane while a noise insensitive root would lie near the unit circle. This phenomena, which was explained by S. Kay[11], could serve as an adaptive feature for the $\Delta f \approx 0$ case if the noisy root was set equal to the low noise root. Various simulation runs have indicated that such an intervention would keep the true root values within the delimiter spans and allow a lower Δf or improved frequency resolution.

3. Some attempt should be made to extend the Prony method to phase modulated signals. At present, the algorithm is totally defeated by phase modulation when smoothing is performed over the entire pulse width.

4. The simultaneous pulse problem should be considered in the context of the least squares processor. Perhaps, there is a way of recursively generating (α_1, α_2) to identify the number of frequencies present from the behavior of the α coefficients themselves.

REFERENCES

1. McCormick, W.S., "The Use of the Instantaneous Frequency Transient in the Design and Optimization of the Channelized Receiver and Instantaneous Frequency Measurement (IFM) Versions of the Passive EW Receiver", AFOSR/SCEEE Final Report, Contract No. 549620-82-0035, August 17, 1984.

2. Tsui, J.B., Microwave Receivers and Related Components, Avionics Lab, Air Force Wright Aeronautical Laboratories, PB84-108711, 1983.

3. F.G. Stremler, Introduction to Communication Systems, page 333, Addison Wesley, 1982.

4. Kay, S.M., "Spectrum Analysis - A Modern Perspective", Proc. of the IEEE, Vol. 69, No. 11, pp. 1380 to 14191, November, 1981.

5. J. Stoer, Introduction to Numerical Analysis, page 289, Springer-Verlag, 1980.

6. Tufts, D., Private Communication; Saunders Corp., 1985.

7. Hildebrand, Introduction to Numerical Analysis, pp. 378-380, McGraw Hill, 1956.

8. Papoulis, A., Probability, Random Variables, and Stochastic Processes, page 390, McGraw Hill, 1965.

9. Davenport, W.B. and Root, W.L., An Introduction to the Theory of Random Signals and Noise, page 256, McGraw Hill, 1958.

10. Kunt, M., "On Computation of the Hadamard Transform and the R. Transform in Ordered Form", IEEE Transaction on Computer, page 1120, September, 1975.

11. Kay, S.M., "The Effects of Noise on the Autoreggressove Spectral Estimator", IEEE Trans. ASSP, Vol. ASSP-27, No. 5, pp 475-485, October, 1979.

IBM/06/12/4/85

15.38
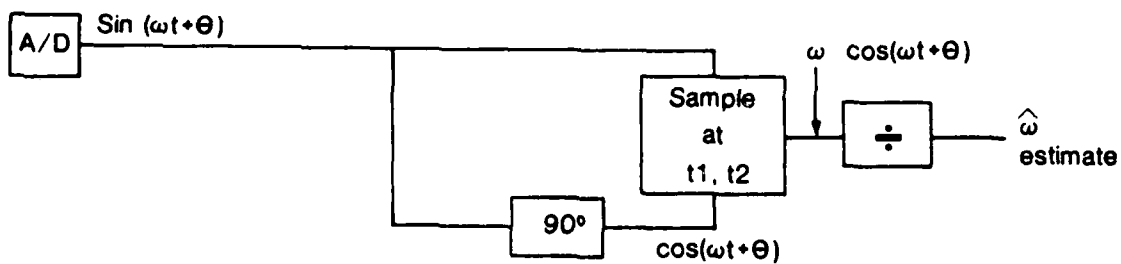
Figure 1: Differentiator
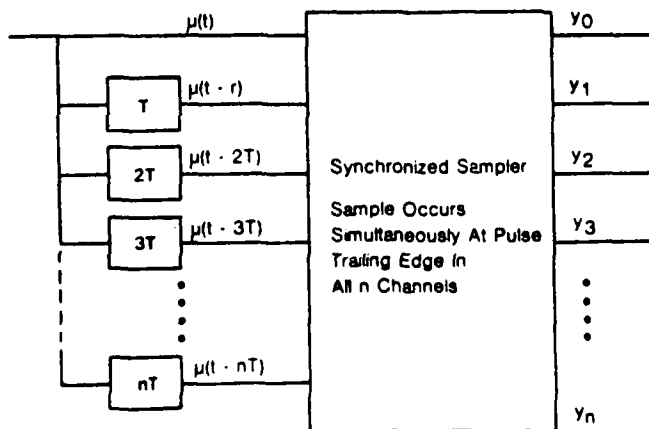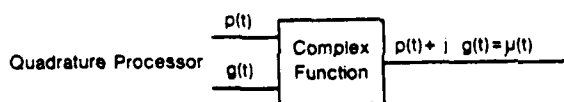
Figure 2: Synchronized Sampler
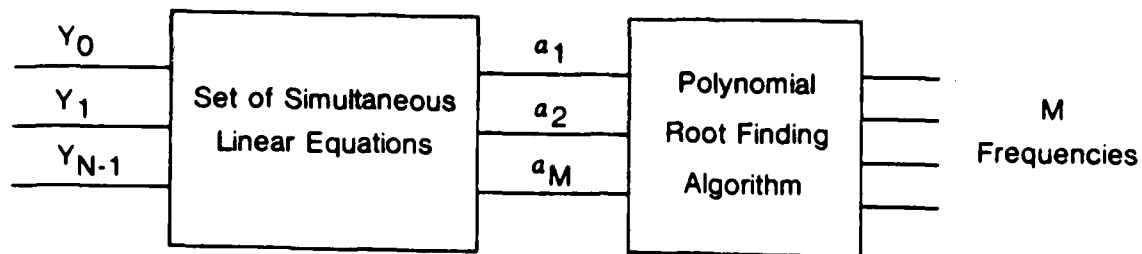
Figure 3: Prony Algorithm
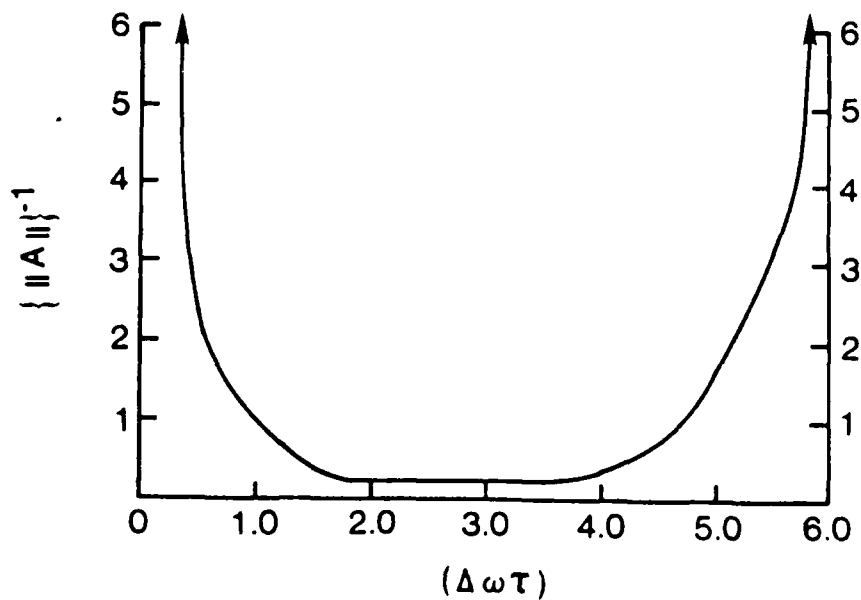
Figure 4: Condition Number For Two Frequency Core
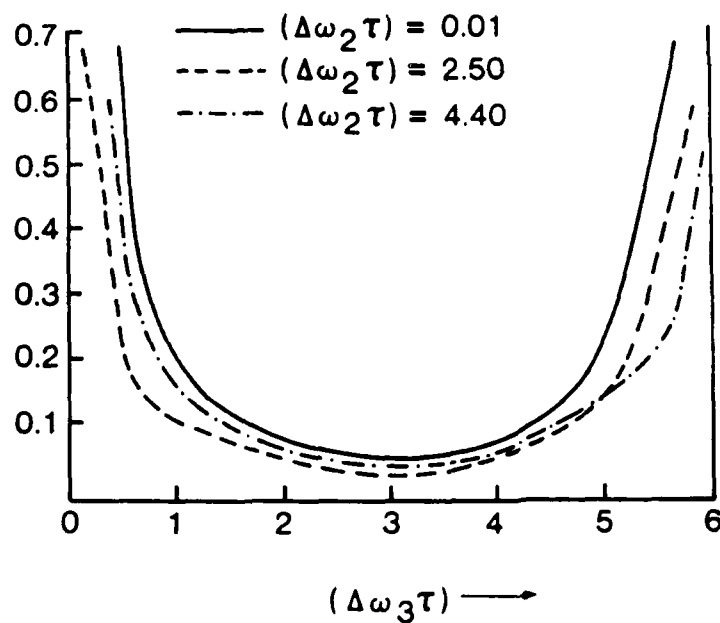
Figure 5: Condition Number For Three Frequency Core
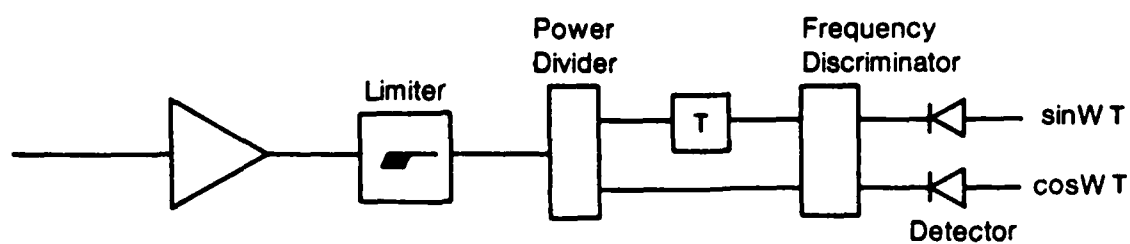
Figure 6: IFM Receiver Schematic

Phase
Discriminator

sin(wt +Θ−WT)

T

sin(wt +Θ)

A_1 A_2

B_1 B_2

C_1 C_2

D_1 D_2

Differencial Amplifiers

1   E

2   E
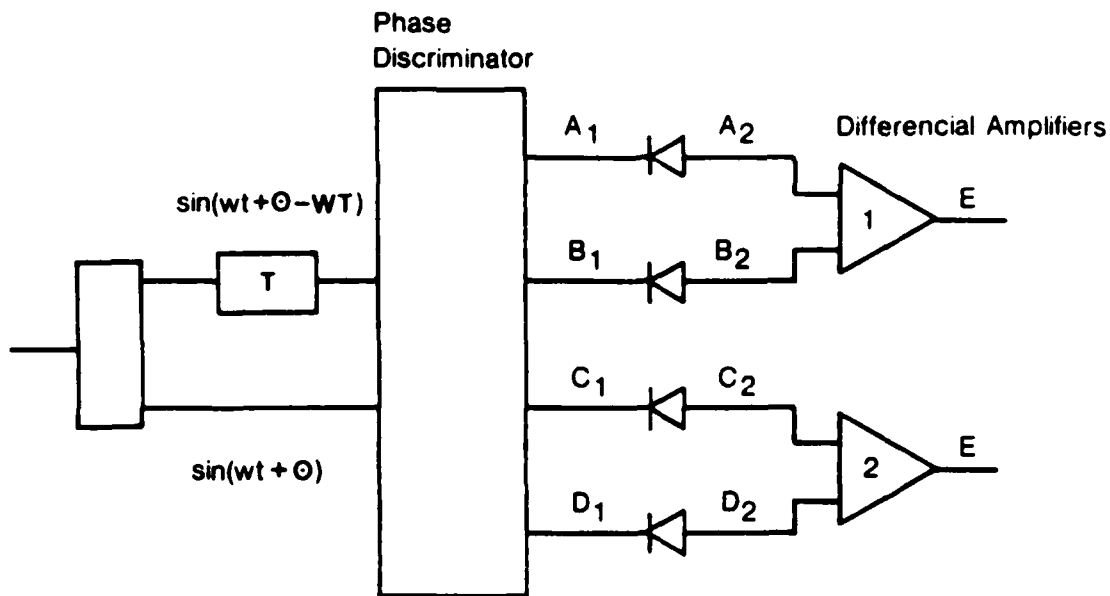
Figure 7: Detailed Schematic of IFM Phase Discriminator.

$T_3 = 8\tau_1$

16π
14π
12π
10π
8π
6π
4π
2π
0

100
$b_3 = 2$
50
etc
0

$T_2 = 2\tau_1$

4π
2π

100
$b_2 = 2$
$\bar{A}$ $\underline{B}$
50
A $\bar{B}$
0

τ_1

2π

100
$b_1 = 1$
50
0

$f_1 = 20$; $f_2 = 60$
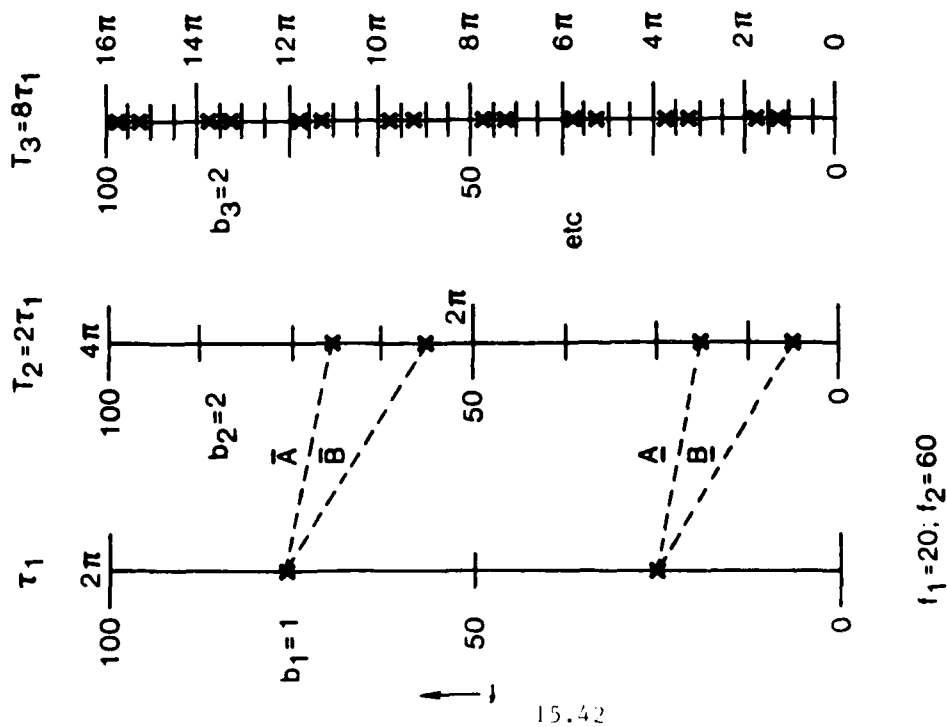
Question: $(\bar{A}, \underline{B})$ or $(A, \bar{B})$?

Figure 8: Illustration of Multi-Level Ambiguity

15.42

f1=20   f2=80

Unquantized First Level

$\tau_1 = .01$ μsec

| 0 | 20 | 50 | 80 | 100 (MHz) |

f_1 π f_2 2π

Quantized Second Level

$\tau_2 = .03$ μsec

| | 2π | 2π | 4π | 4π | 6π | 6π | |
| f_2 | f_1 | 2π | f_2 | f_1 | 4π | f_2 | f_1 | 6π |

| 0 | 14.57 | 19.46 | 33 | 47.6 | 52.79 | 66 | 81.23 | 86.17 | 100 (MHz) |

Delim Span   Delim Span
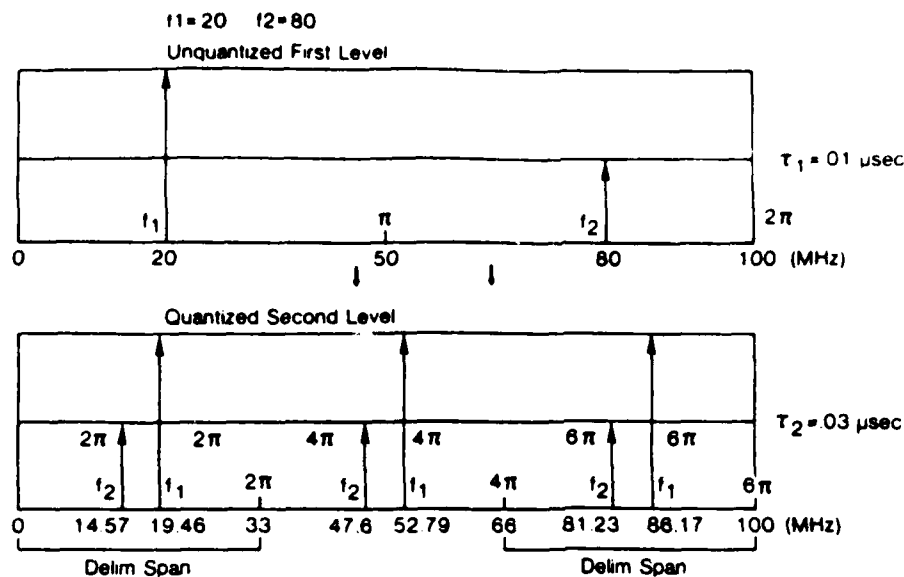
1. Order of f_1, f_2 in τ_1 is permuted in τ_2
2. Only one frequency pair in each delimiter Question: $f_2{}^{2\pi}$ and $f_1{}^{6\pi}$ or $f_1{}^{2\pi}$ and $f_2{}^{6\pi}$?

Figure 9. Illustration of Ambiguity Problem and Delimiter Interval or Span

(a) $A_2 \ll A_1$

(b) $A_1 = A_2$

A_2

A_1
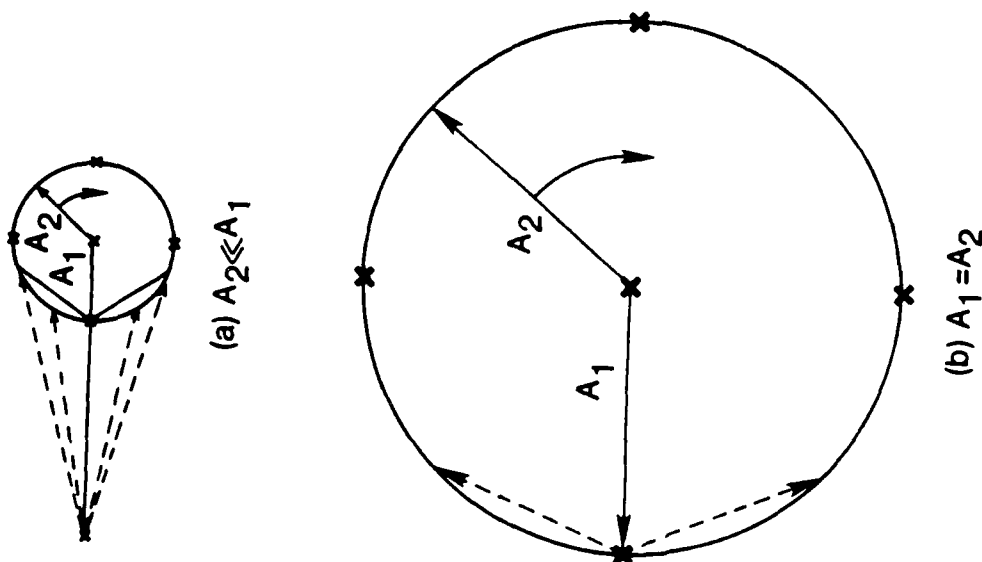
Figure 10: Phasor Diagram

15.43
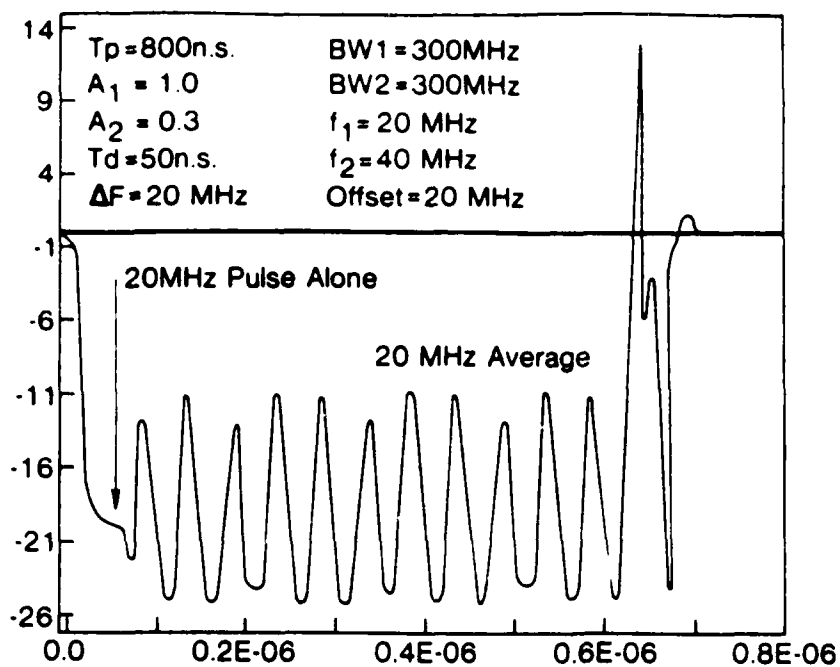
Figure 11: Instantaneous Frequency for A1 = 1.0, Ag = 0.3 Case
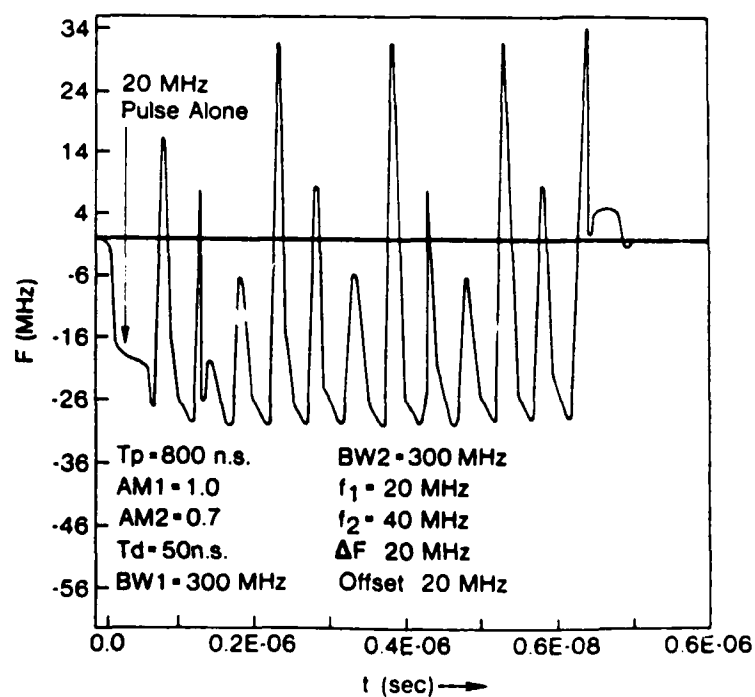
Figure 12: Instantaneous Frequency Two Signals Without a Limiter

15.44
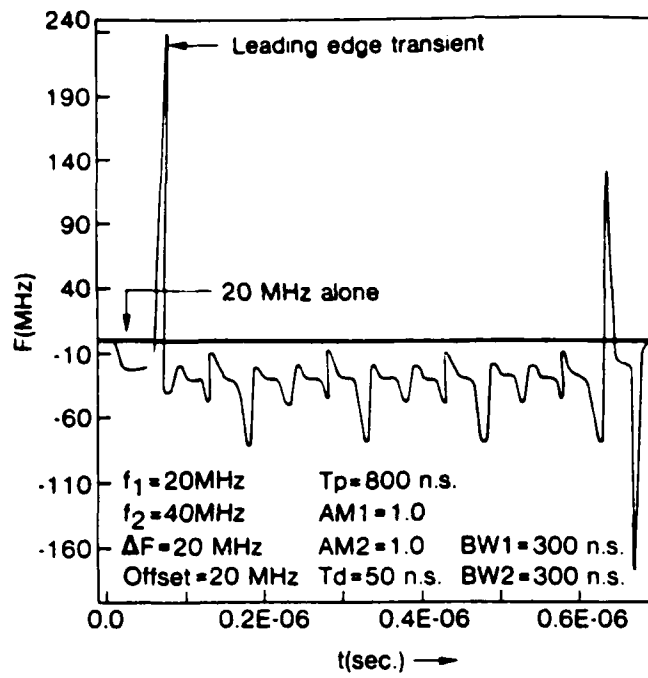
Figure 13: Instantaneous Frequency for Equal Amplitude Case

Parameters shown in figure:

$f_1 = 20$ MHz Tp = 800 n.s.
$f_2 = 40$ MHz AM1 = 1.0
$\Delta F = 20$ MHz AM2 = 1.0 BW1 = 300 n.s.
Offset = 20 MHz Td = 50 n.s. BW2 = 300 n.s.

Single Frequency
f = 20 MHz
Fast Hadamard Transform
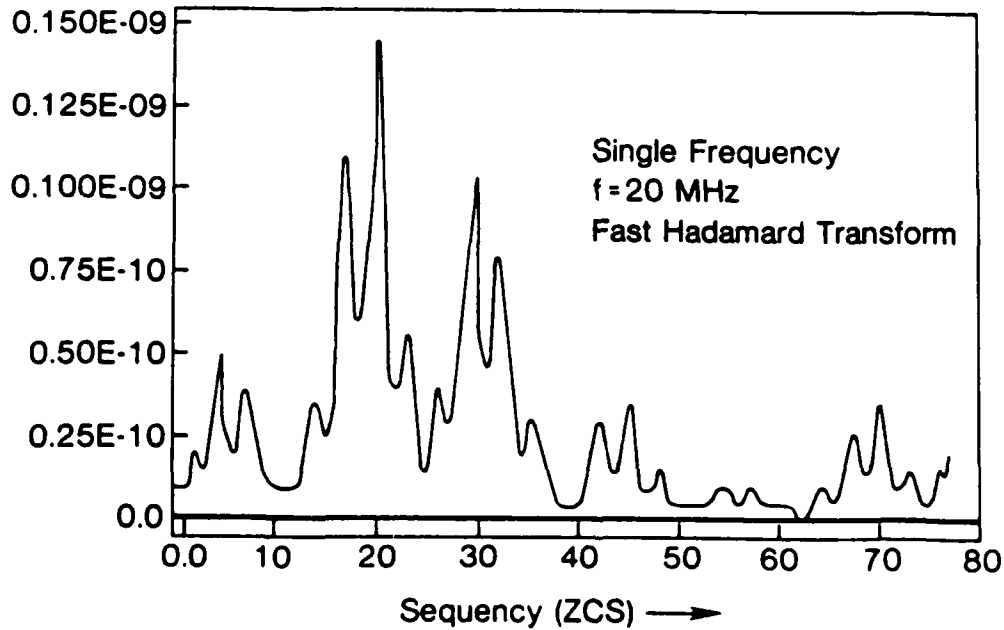
Figure 14: Fast Hadamard Transform for One Microsecond Pulse.

15.45

1985 USAF-SCEEE RESEARCH INITIATION PROGRAM

Sponsored by the

AIR FORCE OFFICE OF SCIENTIFIC RESEARCH

conducted by the

SOUTHEASTERN CENTER FOR ELECTRICAL ENGINEERING EDUCATION

and

GANNON UNIVERSITY

FINAL REPORT

DUAL CHANNEL FFT SYSTEM ANALYSIS FACILITY

FOR EVALUATING

INTEGRATED COMMUNICATION SYSTEMS

Prepared by: Paul B. Griesacker, Ph.D.

Academic Rank: Professor

Department and   Department of Physics
  University: Gannon University

Research Location: Gannon University
                      University Square
                      Erie, Pennsylvania   16541

                            and

                      Air Force Wright Aeronautical Laboratory
                      Systems Avionics Division, Information
                      Transmission Branch, AFWAL/AAAI

USAF Research: Mrs. Diane E. Summers and
                      Lt. Michael Gray

Date: 15 October 1985

Contract Number: F49620-82-C-0035

Subcontract Number: 89 RIP 16

I. INTRODUCTION

A solution to the problem of consolidating the many varied
communication, navigation and identification (CNI) systems, is the
Integrated Communication, Navigation and Identification Avionics
(ICNIA) system (1). It is apparent that ICNIA will be a complicated
system (Figure 1) and the hardware will include new technologies.
The evaluation of such a complicated and interrelated set of
subsystems will be a monumental task especially for testing
performance in hostile atmospheres containing noise, fade, jam,
multipath, etc., all in real time.

An answer to the ICNIA test and evaluation question is the
Integrated Electromagnetic System Simulator (IESS) (2). IESS is
designed to run software driven real time CNI scenarios with computer
stored and analyzed results as shown in Figure 2. IESS itself must
be evaluated as an adequate test facility for ICNIA. It will be
necessary to begin the evaluation process early on in the schedule,
since the new technology hardware may pose some problems related to
conventional evaluation techniques. Cross-talk between different
services may prove to be a complication since they share a common
data buss.

A systematic approach to the evaluation process is necessary to
keep the effort manageable and consistent. It will be useful to have
a diagnostic capability in addition to the evaluation capability.
The Linear systems approach is such a method. A linear time
invariant system can be characterized (3, 4, 5, 6) by studying the
output of the system relative to specific inputs, and great conveni-
ence is introduced if this is done in the frequency domain (7). Even
if a system is not completely linear, much information can be gained
by finding the gain and phase shift at frequencies of interest. This

BASELINE CNI SIGNAL SERVICE	ICNIA AIM SIGNAL GENERATED?	NUMBER OF REQUIRED TEST SIGNALS	NUMBER OF SIGNALS GENERATED BY AIM	(XMIT BAND)	COMMENTS
JTIDS	YES	2	2	L	ICNIA AIM provides functions of two (2) JTIDS terminals. Software and includes interleaved processing and scheduling of pulsed waveforms. Also supports simulation of multiple range delays via rescheduling of pulses
EJS	YES	1	1	L	ICNIA will provide functions of future Air Force AJ UHF communications
PLRS	YES	1	1	L	Software modified in ICNIA AIM to emulate Master Unit's control of PLRS user units and synchronization of PLRS net.
HAVE QUICK	YES	1	1	L	ICNIA provides functions of HAVE QUICK
SINCGARS	YES	1	1	L	ICNIA provides functions of SINCGARS
GPS	NO	4	0	L	Modification of ICNIA AIM to meet simulation requirement is not practical o Much new hardware would be required to generate a GPS signals o Without SHyS, extensive software would have to be redeveloped
TACAN	NO	1	0	L	TACAN simulation requirements are best achieved using off-the-shelf, supportable, and cost effective test equipment
MARK XII IFF	YES	1	1	L	ICNIA provides functions of MARK XII IFF
ILS/MLS	NO	1	0	L	ILS/MLS simulation requirements are best achieved using off-the-shelf, supportable, cost effective test equipment.
TCAS	YES	1	1	L	ICNIA provides functions of TCAS
MARK XV IFF	YES	1	1	L	ICNIA provides functions of MARK XV IFF
AFSATCOM	YES	1	1	L	Software modification in ICNIA AIM maps up-link and down-link modulation formats to allow back-to-back AFSATCOM terminal communication without relay satellite.
HF, VHF, and UHF	YES	3	0	L	ICNIA provides functions of HF, VHF, and UHF voice communications.
ADM	NO	1	0	L	ADM simulation requirements are best achieved using off-the-shelf, supportable, cost effective test equipment.

FIGURE 1.   A LISTING OF THE CNI SERVICES CONTAINED IN ICNIA

16.3

FIGURE 2. THE CONCEPTUAL IESS ARCHITECTURE

also is most conveniently done in the frequency domain. Furthermore, the input/output comparison can be applied to the complete system, i.e. compare the input of the transmitter to the output of the receiver; or it can be applied to one of the subsystems, i.e. one of the amplifiers. Even individual components can be examined in this manner.

This generalized approach to the evaluation of CNI systems, though simplistic in its perspective allows for a systematic analysis of the overall performance of the entire system by isolating the diverse functions of the subsystems or modules for closer scrutiny.

Some traditional methods of CNI system evaluations include measurements usually performed in EMI and Susceptibility analysis (8, 9). These will not be discussed in this report but they should be considered as an important part of any evaluation approach.

II. BASIS OF THIS RESEARCH

In Tables I and II are listed some basic functions and sequences found to be useful in digital signal processing. The first few: $x_i(k)$, $y_i(k)$ and sometimes $h_i(k)$ are usually the only ones measured. The others are calculated from them. For a given record i, the $x_i(k)$ are digital samples of the continuous $x(t)$ at sample times $\triangle t$ apart. The record length is $T = \triangle t \cdot NS$, where T is the length (time duration) of the record of NS discrete samples. NR is the number of different records recorded for taking averages.

An efficient method for evaluating the Discrete Fourier Transform (DFT) is called the Fast Fourier Transform (6,8,9). Figure 3 is a block diagram of a simple single-shot dual channel Fast Fourier Transform (FFT) analyzer. Starting with one record of $x(t)$ and $y(t)$, the analyzer will yield the Autosprecta $S_{xxi}(m)$ and $S_{yyi}(m)$, Cross-spectra $S_{yxi}(m)$, $S_{xyi}(m)$, and the Frequency Response Sequence $H_i(m)$, in the frequency domain. Then, after an Inverse Fast Fourier Transform (IFFT), it will yield the Auto-correlations $R_{xxi}(n)$, $R_{yyi}(n)$, Cross-correlations $R_{xyi}(n)$, $R_{yxi}(n)$ and Impulse Response Sequence $h_i(k)$ of the system under test. This is enough information to complete most system analysis studies (10, 11) excepting where noise is present or where there are nonlinearities in the system. Nonlinearities must be handled on a case by case basis, but the noise problem can be solved in many situations by averaging techniques. Table II and Figure 4 show how averaging can yield better estimates of the Auto-spectral and Cross-spectral Distribution Sequences $S_{xx}(m)$, $S_{yy}(m)$, $S_{xy}(m)$, and $S_{yx}(m)$ along with three different estimates of the Frequency Response Sequence $H_1(m)$, $H_2(m)$ and $H_a(m)$.

16.7

TABLE 1

(1) $x_i(k); \ 0 \le k \le NS-1$

The ith record or sequence of discrete samples for the input signal $x(t)$.

(2) $y_i(k) = \displaystyle\sum_{n=-\infty}^{+\infty} x_i(n) \, h_i(k-n)$

The ith record or sequence of discrete samples for the corresponding output signal $y(t)$.

(3) $h_i(k); \ 0 \le k \le NS-1$

The ith record or sequence of discrete samples for the Unit Impulse Response $h(t)$.

(4) $R_{xyi}(n) = \dfrac{1}{NS} \displaystyle\sum_{k=0}^{NS-|n|-1} x_i(k) \, x_i(k+n)$

The ith record of the discrete samples for the Autocorrelation sequence of the input signal.

(5) $R_{yyi}(n) = \dfrac{1}{NS} \displaystyle\sum_{k=0}^{NS-|n|-1} y_i(k) \, y_i(k+n)$

The ith record of the discrete samples for the Autocorrelation sequence of the corresponding output signal.

(6) $R_{xyi}(n) = \dfrac{1}{NS} \displaystyle\sum_{k=0}^{NS-|n|-1} x_i(k) \, y_i(k+n)$

The ith record of the discrete samples for the Cross-correlation sequence of the input and output signals.

(7) $X_i(m) = \dfrac{1}{NS} \displaystyle\sum_{k=0}^{NS-1} x_i(k) e^{-j\frac{2\pi}{NS} mk}$

The Discrete Fourier Transform (DFT) of the ith record of the input sequence $x_i(k)$.

(8) $Y_i(m) = \dfrac{1}{NS} \displaystyle\sum_{k=0}^{NS-1} y_i(k) e^{-j\frac{2\pi}{NS} mk}$

The Discrete Fourier Transform (DFT) of the ith record of the corresponding output sequence $y_i(k)$.

(9) $H_i(m) = \dfrac{1}{NS} \displaystyle\sum_{k=0}^{NS-1} h_i(k)^{-j\frac{2\pi}{NS} mk}$

The Discrete Fourier Transform (DFT) of the ith record of the Impulse Response Sequence $h_i(k)$.

(10) $S_{xxi}(m) = X_i(m) \, X_i(m)$
$= DFT \, [R_{xxi}(n)]$

The ith record of the discrete values for the Auto-spectra of the input sequence $x_i(k)$.

(11) $S_{yyi}(m) = Y_i^*(m) \, Y_i(m)$
$= DFT \, [R_{yyi}(n)]$

The ith record of the discrete values for the Auto-spectra of the corresponding output sequence $y_i(k)$.

(12) $S_{xyi}(m) = X_i^*(m) \, Y_i(m)$
$= DFT \, [R_{xyi}(n)]$

The ith record of the discrete values for the Cross-spectra of the input and output sequences $x_i(k)$ and $y_i(k)$.

TABLE II

(13) $\overline{S_{xx}}(m) = \frac{1}{NR} \sum_{i=1}^{NR} X_i^*(m) \, X_i(m)$

The sequence of expected values for the Autospectrum of x(t) averaged over NR records.

(14) $\overline{S_{yy}}(m) = \frac{1}{NR} \sum_{i=1}^{NR} Y_i^*(m) \, Y_i(m)$

The sequence of expected values for the Autospectrum of y(t) averaged over NR records.

(15) $\overline{S_{xy}}(m) = \frac{1}{NR} \sum_{i=1}^{NR} X_i^*(m) \, Y_i(m)$

The sequence of expected values for the Cross-spectrum of x(t) and y(t) averaged over NR records.

(16) $H_1(m) = \overline{S_{xy}}(m) / \overline{S_{xx}}(m)$

An estimate of the Frequency Response Sequence based on the Autospectrum of x(t) and the Cross-spectra.

(17) $H_2(m) = \overline{S_{yy}}(m) / \overline{S_{yx}}(m)$

An estimate of the Frequency Response Sequence based on the Autospectrum of y(t) and the Cross-spectra.

(18) $|H_a(m)|^2 = \overline{S_{yy}}(m) / \overline{S_{xx}}(m)$

An estimate of the magnitude of the Frequency Response Sequence based on the Auto-spectra of both x(t) and y(t).

(19) $\chi^2(m) = \overline{S_{xy}}(m) \, \overline{S_{yx}}(m) / \overline{S_{xx}}(m) \, \overline{S_{yy}}(m)$
$= H_1(m) / H_2(m)$

An estimate of the Coherence Sequence, a measure of the linear correlation of the output y(t) with the input x(t).

(20) $COP(m) = \chi^2(m) \cdot \overline{S_{yy}}(m)$

An estimate of the Coherent Output Power, a measure of the amount of the output power that is linearly correlated with the input x(t). It must be used with caution.

(21) $NCP(m) = (1 - \chi^2(m)) \cdot \overline{S_{yy}}(m)$

An estimate of the Non Coherent Power Sequence, a measure of output power not linearly correlated with the input x(t), Like the COP the NCP must be used with caution.

(22) $SNR(m) = \chi^2(m) / 1 - \chi^2(m)$

An estimate of the Signal to Noise Ratio Sequence. Like the NCP and the COP, the SNR must be used with caution.

$S_{xxi}(m)$

$R_{xxi}(n)$

$S_{yxi}(m)$

$R_{yxi}(n)$

$H_i(m)$

$h_i(k)$

$S_{xyi}(m)$

$R_{yyi}(n)$

$S_{yyi}(m)$

IFFT

IFFT

IFFT

IFFT

$X_i^*(m)\ X_i(m)$

$Y_i^*(m)\ X_i(m)$

$X_i^*(m)\ Y_i(m)$

$Y_i^*(m)\ Y_i(m)$

X

X

X

X

$X_i^*(m)$

$Y_i^*(m)$

CONJ.

CONJ.

$X_i(m)$

$X_i(m)$

$X_i(m)$

$H_i(m) = Y_i(m) / X_i(m)$

$Y_i(m)$

$Y_i(m)$

$Y_i(m)$

FFT

$x_i(k)$

A/D

$x(t)$
System Input

System Output
$y(t)$

A/D

$y_i(k)$

FFT
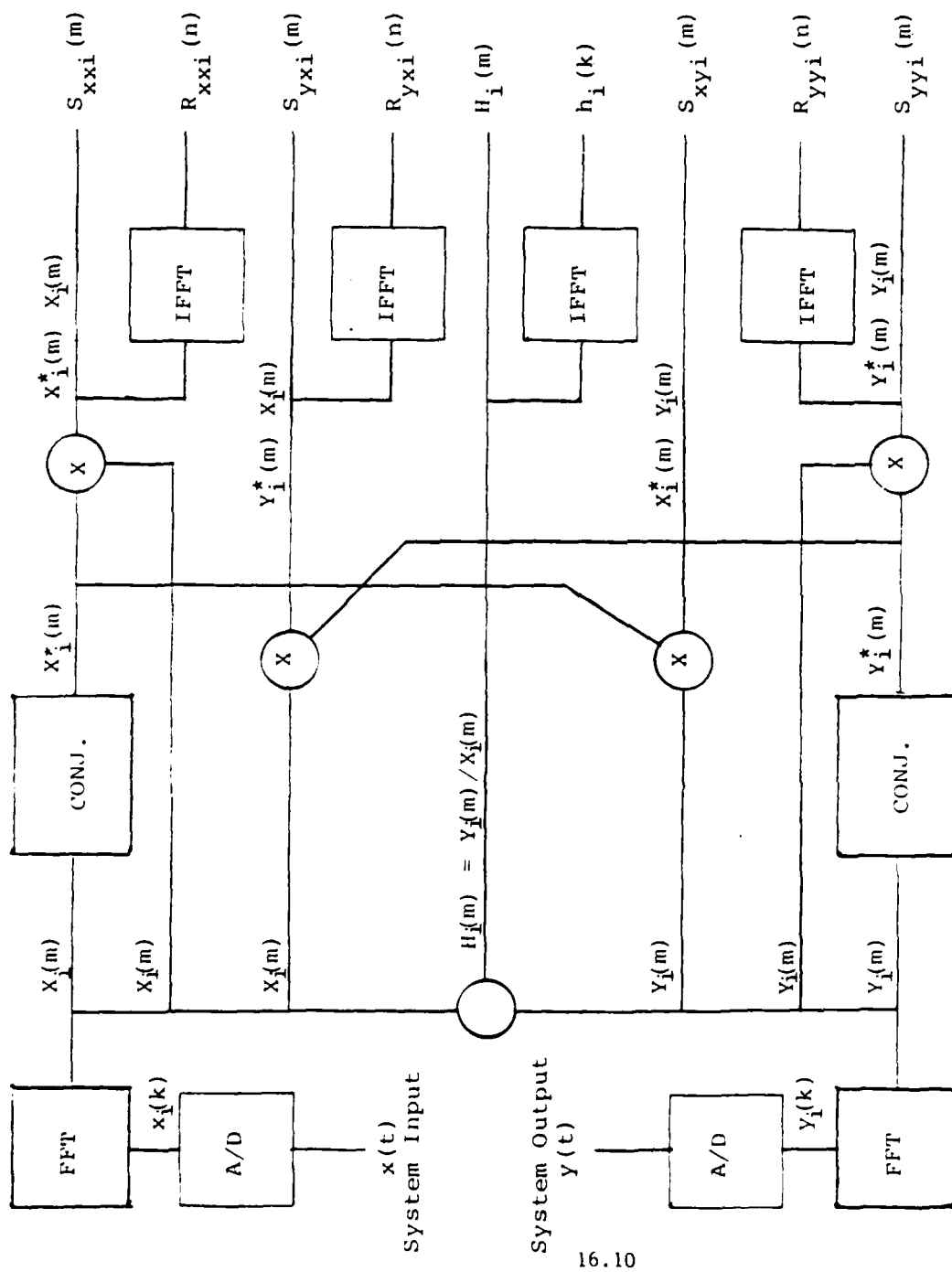
16.10

FIGURE 3. BLOCK DIAGRAM OF A SINGLE-SHOT DUAL CHANNEL FFT SYSTEM ANALYZER

$|H_a(m)|^2$

$COP(m)$

$\div$

$\overline{H(m)}$

$H_1(m)$

$\gamma^2(m)$

$\div$

$H_2(m)$

$\div$

$\div$

AVE. $\overline{S_{xx}(m)}$

AVE. $\overline{S_{yx}(m)}$

AVE.

AVE. $\overline{S_{xy}(m)}$

AVE. $\overline{S_{yy}(m)}$

$\times$ $S_{xxi}(m)$

$S_{yxi}(m)$

$S_{xyi}(m)$

$S_{yyi}(m)$ $\times$

$X_i^*(m)$

$Y_i^*(m)$

$\times$

$\times$

CONV.

CONV.

$X_i(m)$

$X_i(m)$

$X_i(m)$

$H_i(m) = Y_i(m)/X_i(m)$

$Y_i(m)$

$Y_i(m)$

$Y_i(m)$

$\div$

FFT

$x_i(k)$

A/D

$x(t)$
System Input

System Output
$y(t)$

A/D

$y_i(k)$

FFT

16.11
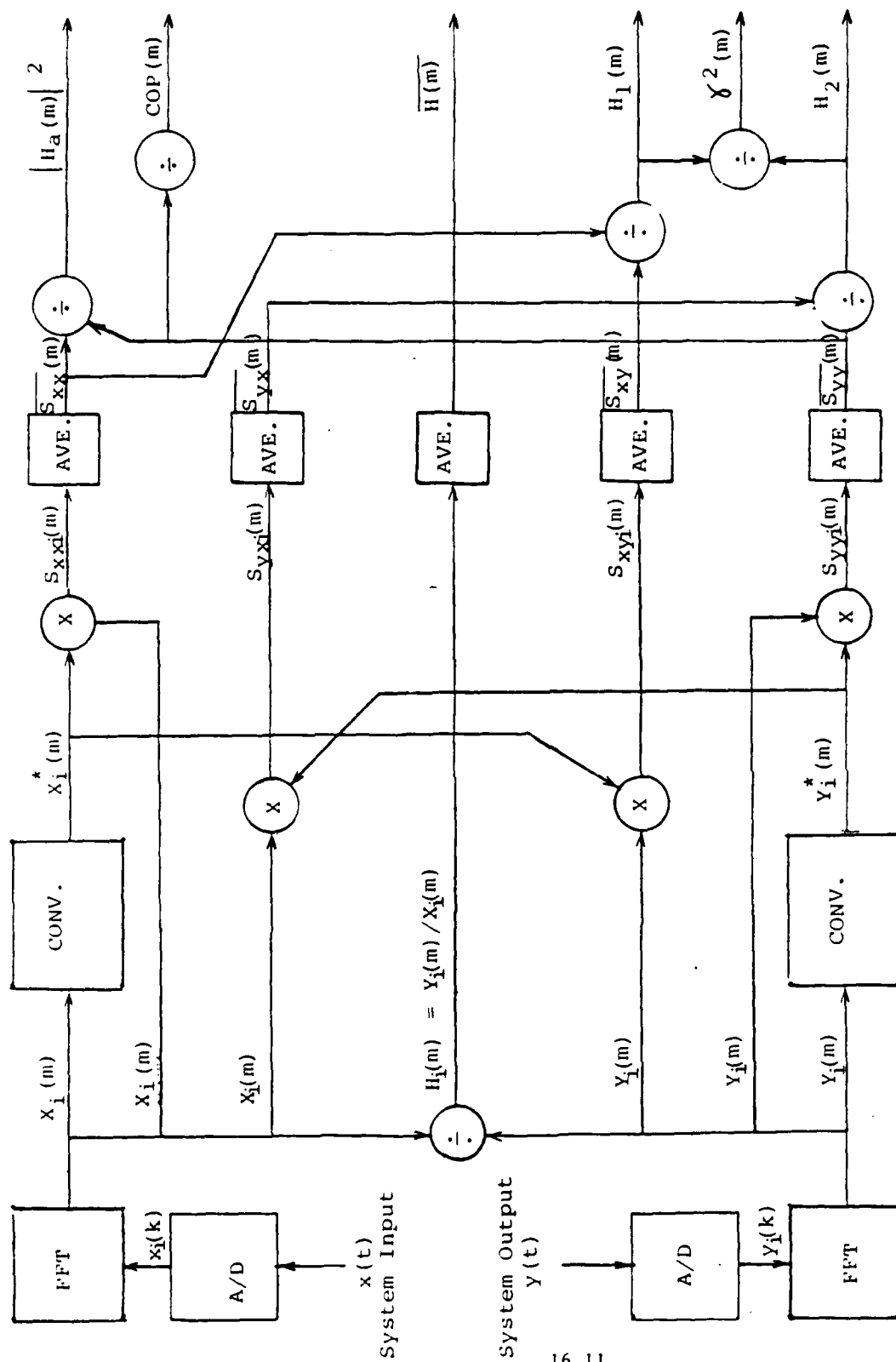
FIGURE 4. BLOCK DIAGRAM OF A DUAL CHANNEL FFT ANALYZER WITH AVERAGING CAPABILITY
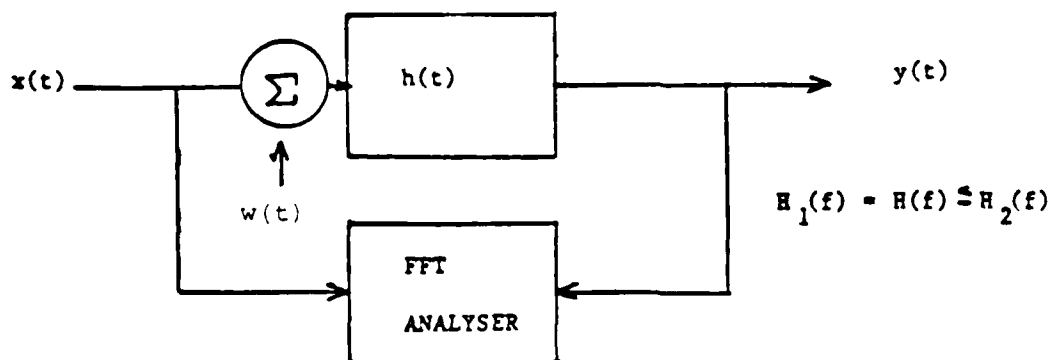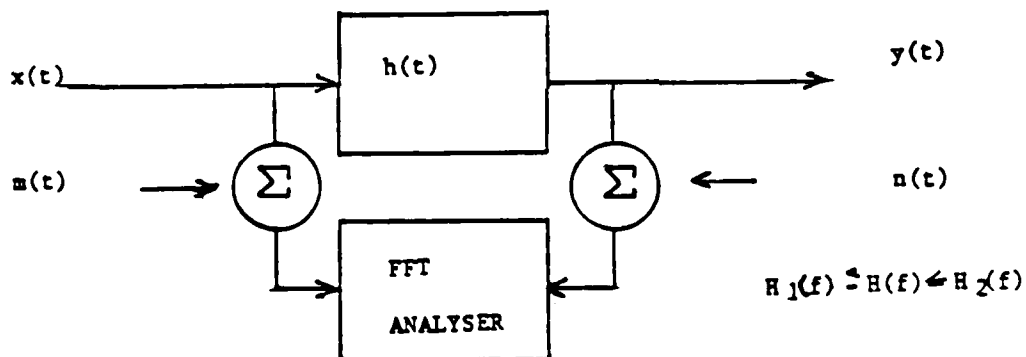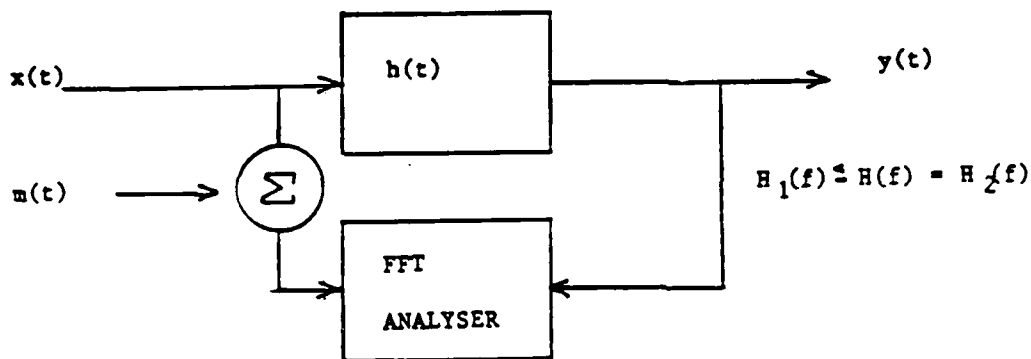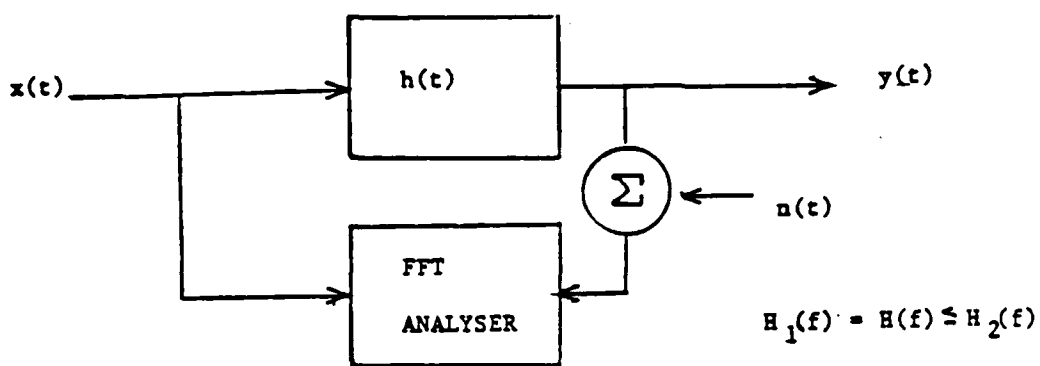
FIGURE 5.   EFFECTS OF NOISE IN DUAL CHANNEL FFT SYSTEM ANALYSIS

16.12

These three estimates of the Frequency Response Sequence can be shown by analytical methods (5, 16) to give somewhat different results depending on the source of noise. Figure 5 gives a summary of these results (10, 12, 13, 14). In Figure 5 n(t) is noise introduced at the output side of the system and w(t) is noise introduced at the input of the system, while m(t) is noise introduced at the analyzer input transducer on the input side of the system.

Furthermore, if the system is perfectly linear and time invariant, then

$$H_1(m) = H_2(m) \tag{23}$$

and

$$|H_1(m)| = |H_2(m)| = |H_a(m)| \tag{24}$$

If these equalities are not satisfied, the system is either not linear or time invariant or there is noise present. Some knowledge of the source of the noise and the information in Figure 5 allows one to select the most effective estimate of the Frequency Response Sequence for that application. From Table II and Figure 4, one can see that the Coherence, Coherent Output Power and Noncoherent Output Power are also available when the circumstances of the measurement indicate that their estimates are reliable (10, 12, 13). If a plotting capability is available, graphs of real and imaginary parts of the Frequency Response Sequence can be made or the magnitude and phase may be plotted. Bode, Nyquist and Nichols plots can also be easily made, even Cepstrum analysis can be done.

The dual channel FFT analyzer is a versatile system analysis tool (15) and the choice of outputs is largely dependent on the generality of the original design and the choices dictated by the application and the user.

Single channel analyzers (Spectrum Analyzers) are used to study

the Autospectrum (Power Spectrum) of a signal. Though several other functions are available with dual channel analysis compared to single channel analysis, the one major benefit of dual channel approach is the availability of the Cross Spectrum between the two signals. The Frequency Response Functions, Coherence, Cross Correlations, Coherent Output Power, etc....are all calculated from the four spectra, namely the two Autospectra and the two Cross Spectra as shown in Table II.

Transfer function measurements are conventionally done by using a network analyzer. Problems occur however when there is noise or multiple inputs to a system. The dual channel FFT analysis can help resolve some of these problems. For instance, when it is desired to know how much a given input signal influences the observed output the traditional approach has relied on determining the Cross-correlation Function between the suspected source and the output. The Coherence will also reveal these causality relations, but it has an additional advantage over the Cross-correlation Function. The Cross-correlation is a function of time, and its maximum value corresponds to the time delay (propagation time, or phase advance) between the suspected source and the observed output. However, the Coherence is a function of frequency, and its maximum values occur at the frequencies where the greatest transfer of energy is taking place. The filters and traps used to suppress interference (noise, cross-talk, etc.) depend on the frequency distribution of that interference. Thus, the co-herence not only can estimate the degree of causality but is useful in choosing the best means of solving the interference problem (19, 20).

III.   THE DUAL CHANNEL FACILITY AT GANNON

The version of a dual channel FFT analysis system written for
the PRIME 750 computer at Gannon University is based on the FFT
algorithms, programmed by Bergland and Dolan at Bell Laboratories and
documented in a Digital Signal Processing Publication by the IEEE
Press (16).

This program (see Appendix A) assumes that there are two files
stored on the disk, each containing a digitized signal. The signals
may be either real or complex. They may be either analytically
generated signals or actual data recorded in the laboratory and then
stored on the disk in digital form. The first line of each file is
expected to contain three integers in FORMAT (3 (3X, I10)). The
three integers are respectively the number of data samples (NS) per
experimental record, the number of experimental records (NR) and the
number of comment lines (NC) immediately following the first line
(this number may be zero). The limitation on these integers are as
follows: NS must be a power of 2 and $4 \leq NS \leq 2048$, $1 \leq NR$ and
$0 \leq NC$. There is no upper limit on NR because the calculations based
on each record are summed until all records are read then an average
is taken as in Equations 13, 14 and 15 of Table II. The next few
(NC) lines of the file are comments for the user's benefit but ig-
nored by the program. They may be used for file identification or
they may not be present (NC = 0). The next line of each file con-
tains the FORMAT to be used in reading the data samples that follow,
one data sample per line. This format of the data samples is typi-
cally (2 (3X, E15.7)). The FORMAT of this line itself is (A40). The
next line of the file contains a 'record header' which is present at
the beginning of each record. The 'record headers' are treated by
the program as comment lines and are for the users' benefit only.

Suggested contents for the 'record headers' are something along the line of: record M out of NR records, with suggested FORMAT (2 (3X, I10)).

The number of data samples per experimental record (NS) must be a power of two. Each data sample consists of two values (magnitude and phase) which is the polar form of a complex number. Positive real numbers have a phase of zero and negative real numbers have positive magnitude but phase of $\pm \pi$ (plus or minus PI). The program assumes that the first data file corresponds to $x_i(k)$ of Equation 1 in Table I and the second file corresponds to $y_i(k)$ of Equation 2 in Table I.

Given two filenames, the program reads each file from disk and calculates all the sequences listed in Table II. The user is then presented (as shown in Appendix B) a menu, listing the sequences resulting from the calculations described in Tables I and II. The user is asked to choose a sequence and then given the option to plot a graph of that sequence and/or write a file to disk for that sequence. When these options are completed, the menu is returned and the user may choose another sequence or end the session by entering 'Q'. A typical session, showing prompts and menus, is presented in Appendix B.

The plotting of the output sequences is accomplished by using DISSPLA, a graphic software package from Integrated Software Systems Corp. (ISSCO) which enables the user to do graphics on a line printer.

IV.   THE DUAL CHANNEL FACILITY AT AFWAL

The version of a dual channel FFT analysis system written for the HARRIS computer and AP120B array processor at AFWAL is quite similar to the program described above, excepting for some minor differences in the prompts and the fact that all input files are expected to be real valued sequences. The FFT algorithms and other calculations are based on the signal analysis and the mathematics software packages for the AP120B. Also, the plotting of output files is done on the Tecktronix graphics terminal in the CSEL laboratory at AFWAL. Since hard copies are available at the Tecktronix terminal, no provision for plotting on the line printer at AFWAL is planned at this time. A listing of a recent version of this program is shown in Appendix C. An excellent job of programming was done on this version of the AFWAL dual channel system by Lt. M. Gray of AAAI-4, as can be seen from the listing in Appendix C.

V. STANDARDIZED TEST DATA FILES

While the dual channel FFT analysis programs were being written at Gannon and at AFWAL, some characteristic input signals with known outputs were created and stored on disk to facilitate debugging and system tests and checks. These test signals have been archived on disk both at Gannon and at AFWAL. To simplify the identification of archived signals, a glossary of signals, filenames and data formats has been compiled and a listing is presented in Appendix D. An examination of Appendix D will show that the listing is self explanatory.

VI. DATA LINK

Since parallel efforts to program and test dual channel FFT
analysis systems were going on simultaneously at AFWAL and Gannon, a
method for transferring large files was initiated. Gannon's PRIME
computer had a 300 baud telephone modem port which recently has been
upgraded to 1200 baud. At Gannon a User File Directory number was
assigned to AFWAL and attempts were made to transfer files at 300
baud. This was found to be too slow and tied up the long distance
lines for inordinate periods of time.

The current method of data transfer is by using an Apple II and
telephone modem to copy files from the PRIME 750 onto diskettes in
APPLE CP/M TEXTFILE format. These diskettes are mailed to AFWAL
where an Apple II network is used to send the files to the DEC 10 and
from there to the HARRIS computer. Even though the 1200 baud tele-
phone link using an Apple IIc is available for possible future use,
the mailing of diskettes seems to be more efficient and adequate for
all transfers up to this time.

It should be pointed out that when the data transfer is made by
mailing a diskette, the format of the data written on the diskette
must be compatable with the operating system of the computer that
reads the diskette. When telephone modems are used to transfer data,
the restrictions on the operating systems of the two computers
involved are not as stringent and telephone modem link is ordinarily
easier to accomplish.

X file: T160   Y file: T168
Auto Spectrum of Y Input - Syy
RESONANCE AT NORMALIZED FREQUENCY 23

10/06/85
17:41:12

Frequency In x (DELTA.f)

FIGURE 7.   AUTOSPECTRUM OF TEST SIGNAL. T168.

X file: T160   Y file: T168
Auto Spectrum of Y Input - Sxx
RESONANCE AT NORMALIZED FREQUENCY 23

10/06/85
17:39:16

Frequency In x (DELTA.f)

FIGURE 6.   AUTOSPECTRUM OF TEST SIGNAL. T160.

16.20

VII.   THE FREQUENCY RESPONSE FUNCTION

The one most significant difference of the dual channel analysis approach from the single channel approach is the calculation of the Cross-spectra (Equation 15 of Table II). Since the Cross-spectra involve averaging the products of two different functions over many records at each frequency, the amount of coherence between these two different signals will effect the resulting average. Two different signals with spectral components at a given frequency that are not in phase with each other from record to record will average to a relatively small value of their Cross-spectrum at that frequency. Also if either one of the signals has no spectral component at a given frequency the Cross-spectra at that frequency will have negligable value excepting of course for the contribution of noise.

The Autospectra (Equation 13 and 14 of Table II) involve averaging the products of a function with its own complex conjugate over many records at each frequency. Therefore, the operands in these products will remain coherent with eacn other from record to record, excepting of course random signals and noise. Cross-spectra would then be expected to have more frequency components with small values of spectral energy than the corresponding Autospectra. It can be expected then, that ratios of these spectra will be sensitive to division by very small numbers, particularly when the Cross-spectra are in the denominator of the ratio. This circumstance will be aggravated by insufficient averaging over too few records and by nonlinearities.

The estimates of the Frequency Response Function (FRF) given by dual channel FFT analysis are defined in Equations 16, 17 and 18 of Table II. It can be seen that these estimators are based on ratios of the Cross-spectra and the Autospectra at each frequency. H1 and

X file: B   Y file: F
Transfer Function - H1
INPUT 10% URN -- OUTPUT 10% URN ; 100 RECORDS

09/29/85
21:46:36

FIGURE 9.   FREQUENCY RESPONSE FUNCTION FOR X FILE = T160, Y FILE = T168.

X file: T160   Y file: T168
Cross Spectrum - Sxy
RESONANCE AT NORMALIZED FREQUENCY 23

10/06/85
17:43:08

FIGURE 8.   CROSS SPECTRUM OF TEST SIGNAL T160 AND TEST SIGNAL T168.

16.22

HA are ratios with an Autospectrum in the denominator, whereas H2 is defined with a Cross-spectrum in the denominator. H2 then will be expected to be sensitive to the number of records to be averaged and to nonlinearities. These expectations were verified in this investigation.

It can be shown analytically (4, 5, 17) that H1, H2 and HA will only give the same estimate for the FRF if the system is completely linear and there is no noise present. If however noise is present, H1, H2 and HA will give different estimates for the FRF depending on the way that noise is introduced into the experimental design. The results of this analysis are presented in Figure 5. An attempt to verify these results was done using the dual channel FFT analysis facility at Gannon and described in Section III.

For this investigation, a simple 128 sample 8 cycle AC square wave with amplitude +/- 0.5 was created (T160) See Figure 6. This test signal was transformed to the Fourier domain where it was multiplied by a FRF with a resonance at the normalized frequency of 23. This product in the Fourier domain was then inverse-transformed to the time domain (T168). T160 was considered to be the input $x(t)$ to a time invariant linear system and T168 was considered to be the output $y(t)$ of this system showing the effects of the resonance as in Figure 7. The Cross-spectrum of T160 and T168 is shown in Figure 8.

A series of problems were run using T160 as the input $x(t)$ and T168 as the output $y(t)$. Uniform random noise was added to the input and to the output signals in varying amounts and different numbers of records were used in the averaging. The amplitude of the additive noise was specified as a fraction of the maximum signal amplitude. Typical noise amplitudes used in this investigation were 1%, 10% and 20%. The results using 20% additive noise were similar to those

16.23

x file: T160.10N, Y file: T168.0N   10/06/85
Transfer Function - H2   18:38:00
INPUT + 10% URN OUTPUT NO NOISE : 300 RECORDS

FIGURE 11. FREQUENCY RESPONSE FUNCTION ESTIMATED
            BY H2 WITH NO NOISE IN THE OUTPUT
            CHANNEL.

x file: T160.10N, Y file: T168.1N   10/06/85
Transfer Function - H2   17:23:08
INPUT + 10% URN OUTPUT + 1% URN : 300 RECORDS

FIGURE 10. FREQUENCY RESPONSE FUNCTION ESTIMATED BY H2
            WITH NOISE IN THE OUTPUT CHANNEL.

16.24

using 10%, excepting more records were required in the averaging to get equivalent results. Test problems were run with 10% noise on the input and 1% noise on the output and 1% noise on the input and 10% noise on the output. Problems were also run with 1% noise on both the input and output plus problems with 10% noise on both input and output.

Some overall conclusions can be drawn from the results of these test problems. H1 seemed to be the overall most reliable estimator of the FRF, but it tended to be noisy when there was relatively high noise added to the output. H1 seems to be relatively insensitive to noise added to the output as long as the noise on the output signal was not greater than the noise on the input signal. See Figure 9. H2 tended to be quite sensitive to noise on the output signal. Only 1% noise on the output signal yielded over-estimates of the FRF even when averages were taken up to 300 records as in Figure 10. However when there was no noise on the output signal, H2 seemed to be relatively insensitive to the amount of noise on the input signal as shown in Figure 11. HA was less sensitive to noise on the output signal than H2 but did not seem to be as reliable an estimator of the FRF as H1. The phase of both H1 and H2 in these tests seemed to be quite sensitive to small amounts of noise as can be seen in Figure 12.

These test problems may not have been realistic enough to test the dual channel FFT analysis approach under all possible circumstances, but the results herein are not inconsistent with a recent investigation using actual measured data (16).

X file: T160.IN , Y file: T164.IN   10/04/85
Auto Spectrum of Y input - Syy   05:04:12
COHERENT AND INCOHERENT SIGNALS ON OUTPUT

FIGURE 13. THE AUTOSPECTRUM OF T164 SHOWING FREQUENCY COMPONENTS AT NORMALIZED FREQUENCIES OF 16 AND 32. ALSO THE ADDITIONAL ENERGY IN THE FIRST AND SECOND HARMONICS IS EVIDENT.
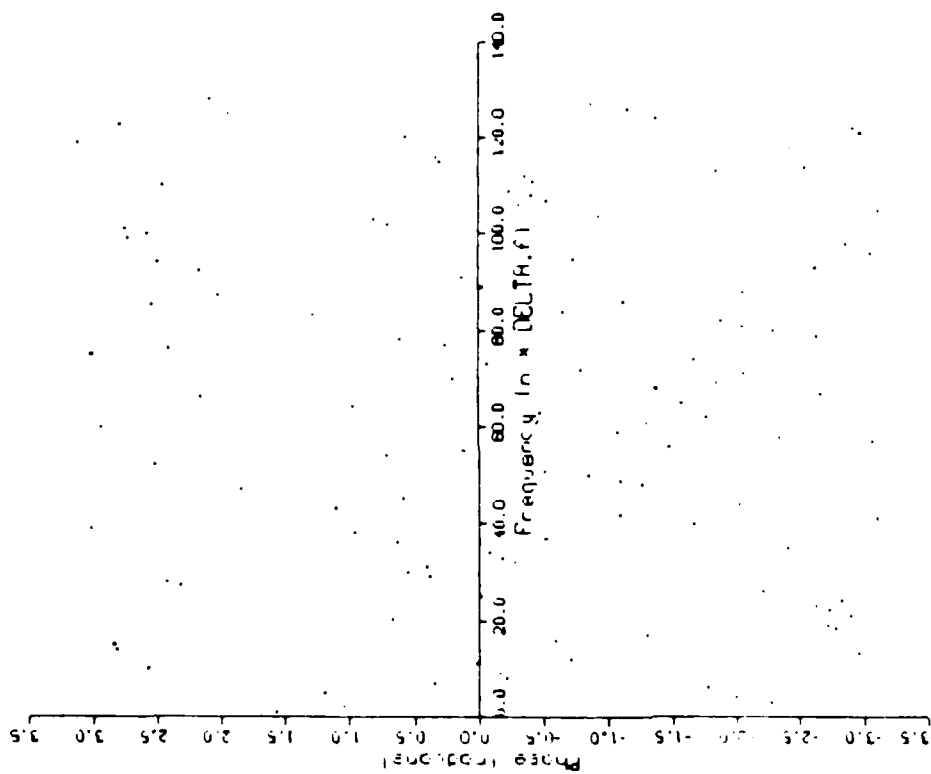
X file: T160.10N, Y file: T168.IN   10/06/85
Transfer Function - H1   17:22:08
INPUT : 10% URN OUTPUT : 1% URN : 300 RECORDS

FIGURE 12. PHASE OF THE FREQUENCY RESPONSE FUNCTION SHOWING THE RANDOMNESS OF THE PHASE WHEN THERE IS NOISE ON THE SIGNALS.

16.26

VIII. COHERENCE AND OUTPUT POWER

The Coherence (COH) (Equation 19, Table II) is a ratio which on
a scale from 0 to 1 measures the degree of linear relationship
between the input x(t) and the output y(t) at each frequency. All
the properties of the Correlation Coefficient of basic statistics
apply to the Coherence (4, 5, 17). The numerator of the Coherence is
the product of the two Cross-spectra. The Coherence will then be
zero at a frequency where either of the Cross-spectra are zero.
Coherence less than unity can be due to several causes: uncorrelated
noise in the input x(t) and/or output y(t), non-linearity of the
system under test, leakage (resolution bias error) and uncompensated
system delays. For the current investigation leakage and delays are
not considered to be important.

The Coherent Output Power (COP) (Equation 20, Table II) is
simply the Autospectrum of the output signal y(t) multiplied by the
Coherence at each frequency. It gives an estimate of the fraction of
the output power that is linearly related to the input at that
frequency. The Non-coherent Output Power (NCP) (Equation 21, Table
II) is a measure of the rest of the output power. That is the output
power due to uncorrelated noise and/or non-linearities at each
frequency. A graph of the Non-coherent Output Power is often helpful
in understanding a graph of the Coherent Output Power.

To demonstrate the ability of these three functions COH, COP and
NCP to identify correlated and uncorrelated components of a signal
two test signals were generated, one (T160) a simple AC square wave
with harmonics at normalized frequencies of 8, 24, 40 and 56 (Figure
6). Another signal (T162) was created by adding four pure sinusoids
to T160 with normalized frequencies of 8, 16, 24 and 32. A third
signal (T163) was produced by adding pure sinusoids to T160 with

X file: T160.IN , Y file: T164.IN
Coherent Output Power - COP
COHERENT AND INCOHERENT SIGNALS ON OUTPUT

10/04/85
05:23:44

FIGURE 15. THE COHERENT OUTPUT POWER FOR T160 AND T164 SHOWING LESS ENERGY AT NORMALIZED FREQUENCIES OF 8 AND 24 THAN THE AUTO-SPECTRUM OF THE OUTPUT IN FIGURE 13.

X file: T160.IN , Y file: T164.IN
Coherence Function - COH
COHERENT AND INCOHERENT SIGNALS ON OUTPUT

10/04/85
05:26:44

FIGURE 14. THE COHERENCE FOR T160 AND T164 SHOWING EITHER NOISE OR NONLINEARITIES AT NOR-MALIZED FREQUENCIES OF 8 AND 24. NOTHING ABOVE BACKGROUND NOISE IS SEEN AT FRE-QUENCIES OF 16 AND 32.

16.28

normalized frequencies at 8, 16, 24 and 32 but for T163 the sinusoids
at normalized frequencies of 8 and 16 were one half cycle out of
phase with the corresponding sinusoids in T162. To be realistic 40
records of T160 were created with 1% uniform random noise (URN) added
to each record. Also 20 records each of T162 and T163 were generated
with 1% URN added to each record. Then the 20 records of T162 were
combined with those of T163 into one file yielding a file 40 records
long (T164). The Autospectrum of T164 is presented in Figure 13.

These two 40 record signals were analyzed by the dual channel
analysis facility at Gannon, with T160 used as the system input x(t)
and T164 used as the system output y(t). The resulting Coherence is
shown in Figure 14. It can be seen that the Coherence is reduced at
normalized frequencies of 8 and 24. Also the Coherence is negligable
at normalized frequencies of 16 and 32 because the cross spectra are
zero since there is no input power at those frequencies. The
Coherence of normalized frequency 8 is less than that at 24 because
half of the sinusoids at frequency 8 were out of phase with the
others whereas all the sinusoids at frequency 24 had the same phase
relative to the input harmonic at 24. The Coherent Output Power
(Figure 15) shows that only the second harmonic at normalized
frequency 24 shows more power than it had in the input (Figure 6).
All the other added signals and noise were either uncorrelated with
the input or random.

Figure 5 shows the Non-coherent Output Power and indicates
similar information as the Coherence at frequencies of 8 and 24, but
the Non-coherent Output Power at frequencies of 16 and 32 were
neither indicated in the Coherence (Figure 14) nor in the Coherent
Output Power (Figure 15). The sinusoids with normalized frequencies
of 16 and 34 are identified in the Non Coherent Power (Figure 16)

HARRIS
COMPUTER

AP120B

CLOCK

A/D

A/D

UUT

x(t)

y(t)

FIGURE 17. A HARDWARE CONFIGURATION FOR A NEAR REAL TIME DUAL CHANNEL FFT ANALYZER ASSUMING USE OF THE GP10P FOR THE AP120B TO FACILITATE MAXIMUM DATA TRANSFER RATES.

X file: T160.IN , Y file: T164.IN   10/04/85
Non-Coherent Power - NCP   05:32:48
COHERENT AND INCOHERENT SIGNALS ON OUTPUT

Frequency in x (DELTA.f)

Magnitude

0.00 20.0 40.0 60.0 80.0 100.0 120.0 140.0

0.16
0.14
0.12
0.10
0.08
0.06
0.04
0.02
0.00

FIGURE 16. THE NON-COHERENT OUTPUT POWER SHOWING OUTPUT POWER INCOHERENT WITH THE INPUT AT NORMALIZED FREQUENCIES OF 8, 16, 24 AND 32.

16.30

because they are not random like noise, but they are not identified
in the Coherence since they are of the nature of nonlinearities in
the system under test. That is, the sinusoids at normalized frequency
32 are coherent with each other from record to record (unlike random
signals) but there is no component of the input signal for them to be
linearly correlated with at normalized frequency 32. The sinusoids
at normalized frequency 16 are not completely coherent with each
other from record to record so their output power will not be at a
maximum like those at frequency 32.

IX. HARDWARE RECOMMENDATIONS

For the CNI services in ICNIA, the high frequency services have RF transmissions ranging from 30 Mhz (SINGCARS) to 1215 Mhz (JTIDS). At this time the maximum digitizing rate for Analog to Digital (A/D) converters is 200 million samples per second (MSPS). The Nyquist criterion to prevent aliasing demands that a signal be sampled at a rate of at least 2 samples per cycle (SPC) at the signal's highest frequency. This criteria only prevents aliasing, but reliable reproduction of the signal may require as many as 20 SPC at the highest frequency of the signal's spectrum. It is readily seen that at 200 MSPS, 10 Mhz is the highest frequency that can be sampled at 200 SPC. It might be pointed out, however, that the bandwidth of the JTIDS baseband signal (information band) should not exceed 8 Mhz. Then 8 Mhz can be assumed to be the maximum frequency to be expected in the base band for any of the ICNIA family of CNI services. The 200 Mhz A/D then may be adequate for studying all ICNIA signals, at least in baseband.

If ICNIA has a universal IF of 24 Mhz for all CNI services, the 200 Mhz A/D would yield approximately 8 SPC and may be useful for some limited analysis of all ICNIA signals, on the 24 Mhz IF.

If the signals under study can be sent repetitively, there is another option available. For instance, the LeCroy 9400 dual Digital Storage Oscilliscope with an analog bandwidth of 125 Mhz uses a 100 MSPS A/D to achieve an effective 5 gigasample per second (GSPS) sampling rate by random interleaved sampling for repetitive signals. At a rate of 5 GSPS a sample density of 20 SPC could be achieved for frequencies up to 250 Mhz. This effective sampling rate for repetitive signals would be adequate for all the ICNIA services in the 24 Mhz IF. Even this alternative will not adequately sample the

ICNIA signals above 250 Mhz and therefore would not necessarily be useful for many of the ICNIA services in the RF.

MODEL	ANALOG BANDWIDTH	SIGNIFICANT BITS	ONE-SHOT MEMORY
HP 54200 A	50 Mhz	6	1024
TEK 7612 D	90 Mhz	6	2048
LeCroy 8828	100 Mhz	8	8k - 2M

Table III. Showing some of the available 200 MSPS digitizers and their characteristics.

Table III gives a comparison of the dual channel analyzers currently available with 200 MSPS capability. The LeCroy line seems to have the advantage in both significant bits and memory. There is evidence that the LeCroy 8901 CAMAC crate controller can maintain a throughput of at least 23.9 K bytes/sec and up to 430 K bytes/sec depending on the application (21). However the AEON 5488 crate controller was found to operate at rates of up to 600 K bytes/second and is considerably more versatile in operation. The AEON 5488 is compatable with LeCroy hardware (22).

A recent study at MONSANTO (23) comparing 200 MSPS A/D converters, showed the LeCroy 8828 to be superior to the Tecktronix 7612 in performance, maintenance, and flexibility for future upgrade. The performance tests involved a Sine-fit test, DC gain and linearity and an offset adjust test for missing code. The tests showed that the LeCroy 8828 was superior in the Sine-fit test, but the two units were comparable in the gain and linearity and offset adjust tests.

It has been brought to our attention (24) that LeCroy intends to bring a CCD based A/D to market which will exceed the 200 MSPS rate. At this time the design goals are for a 1.35 GSPS A/D with a 350 Mhz analog bandwidth and a one shot memory of 10,240 words and capable of

8 significant bits. LeCroy intends to manufacture this digitizer as a plug in unit compatable with all their existing hardware, mainframes, modular memories and existing software.

If the 1.35 GSPS A/D were realized and if transfer to memory problems can be solved, signals of up to 67 Mhz could be sampled at a density of 20 SPC. If 8 significant bits were realized, FFT analysis could be feasible at these frequencies. This might allow dual channel FFT analysis of all the CNI services in ICNIA at least in the 24 Mhz IF, without the necessity of being restricted to only repetitive signals. It should be noted that 8 significant bits may not be adequate for all FFT analysis applications and the effect of finite word length should be examined on a case by case basis (10, 11, 25).

Assuming that suitable A/D's are available a possible configuration for a near real time Dual Channel FFT Analyzer is shown in Figure 17. A suitable clock will be needed to synchronize the fast A/D's, and fast data transfer techniques will be needed to unload the A/D one-shot memories to the computer. The proposed 1.35 GSPS A/D of LeCroy will take one sample every 0.75 ns and could fill its 10,240 word one-shot memory in 7.6 u s. It seems that the two major problems of a system of this nature will be data transfer and storage. Using Direct Memory Access (DMA) through the General Purpose Input/ Output Processor (GPIOP) for the AP120B Array Processor may be the fastest data transfer method at this time. However, use of the GPIOP is not as convenient as other methods of data transfer.

X. LITERATURE SEARCH

In the Spring of 1985, a literature survey was conducted at Gannon to find articles describing the use of Dual Channel FFT Analysis in the evaluation of communication systems. This survey yielded no published reports on applications of that nature.

One possible reason for this is the fact that the highest frequency Dual Channel FFT Analyzer commercially available, the HP3562A, covers a maximum frequency of only 100 Khz. Another possible reason is the specificity of the conventional communications systems evaluation procedures being used and the availability of hardware designed for that purpose.

XI. SUGGESTED USES OF DUAL CHANNEL FFT ANALYSIS FOR COMMUNICATION SYSTEM EVALUATION

The first and most obvious suggested use of this system for communication system evaluation would be the use of the dual channel FFT system as a single channel analyzer. There are many recommended communications system evaluation measurements that can be done with single channel spectrum analysis. These measurements such as harmonic distortion, linearity, roll off, noise figure etc., have been explained in great detail elsewhere (8, 9, 26, 27, 28). If the communication equipment hardware is available, it may be more convenient to use a conventional analog Spectrum Analyzer to make these measurements. However, if the communication equipment hardware is not available locally, the appropriate output signals can be recorded at the site of the hardware and these recorded and digitized signals can be transferred to the computer hosting the FFT analysis software for processing.

This single channel FFT analysis approach need not be done in real time. Another suggested application of the dual channel approach to communication system evaluation consists in comparison of the Frequency Response Function (FRF) of the unit under test with a 'standard' or 'expected' FRF. For evaluation purposes maximum allowable deviations from the 'standard' FRF may be defined differently in different frequency ranges. Mean square deviations can be calculated automatically in each frequency range and used as a figure of merit for convenient evaluation decisions.

The 'standard' FRF for the CNI systems in ICNIA can be generated in several ways. The FRF may be able to be generated analytically from system design specifications for hardware that is not yet completed, or generated from system models that may be computerized.

SPICE is a method of modeling CNI circuits for such an application. For CNI hardware that is available the 'standard' FRF can be measured by using the dual channel FFT analysis or by other conventional methods, as long as the correspondence between the dual channel FFT approach and the conventional method is established and understood by the user.

A possible evaluation technique for the CNI system to be integrated in ICNIA could be the comparison of the measured FRF of the CNI service in ICNIA to the measured FRF of that CNI service now in use as a stand alone system. This evaluation technique of comparing FRF's is not dependent on the method of measuring the FRF. If however, noise is a problem, the dual channel FFT approach yields a choice of HA, H1 or H2 for determining the best estimate of the FRF to be used for a given CNI service. In general the FRF is a complex function consisting of amplitude and phase. Comparison of the measured to the 'standard' can be accomplished by examining their ratio at each frequency. The magnitude of the ratio will indicate relative gain, and the phase of the ratio will indicate relative phase shift, at each frequency. Again various evaluation criteria can be established in different frequency bands.

An additional suggestion for possible communication system evaluation application of the dual channel FFT analysis is a study of system linearity by using the Coherence (COH), Coherent Output Power (COP) and the Non-coherent Output Power (NCP) as discussed above in Section VIII. One would expect some cross-talk between the various systems in ICNIA since it seems that many of the CNI services in ICNIA will be connected to the same data buss. In the instance of spurious frequencies in the output of a CNI service, the cause might be able to be traced using a combination of the COH, COP and NCP.

16.37

Here the application has gone beyond mere evaluation and enters the realm of diagnostics (19, 20).

Furthermore the Signal to Noise Ratio at each frequency is also available from the dual channel FFT analysis approach as shown in Equation 22 of Table II (19).

All of the above suggestions for using the dual channel FFT analysis assume that the appropriate digitized signals are available. If a restriction of only having the low frequency (100 kHz) dual channel FFT analysers available were enforced, one could still evaluate transmitter-receiver systems by sampling the audio input at the transmitter and the audio output of the receiver. If on the other hand, higher frequency A/D with enough significant bits become available, the audio at the input of the transmitter could be compared with at least the IF of the transmitter output and the IF of the receiver input could be compared to the audio output. Also, the RF and/or the IF signals could be first down-converted to baseband for comparison with the information band inputs and outputs of trans-mitters and receivers, if the high frequency A/D converters are not adequate for these purposes. As discussed in Section IX, the A/D conversion rate and the number of significant bits available are two of the limiting factors involved in FFT analysis.

XII. LIMITATIONS

The dual channel FFT analyzer facility discussed in this report has some limitations that should be pointed out. There has been no provision made for windowing (5, 19). Windowing will not be difficult to add to the existing facility. There is no provision at this time for getting measured data to the Harris computer for processing. There is some expectation that the Harris computer will have telephone modem I/O ports available in the near future. This would be a possible data transfer mechanism at least in the near term.

The suggested communication evaluation approaches for the dual channel FFT analyzer discussed in Section XI are untested and unconventional, excepting of course for the single channel approach which is similar to the use of a Spectrum Analyzer.

The paucity of high speed A/D converters with enough significant bits is a critical factor in limiting the high frequency applications of the FFT analysis approach. Even the 1.35 GSPS A/D planned by LeCroy promises only 8 significant bits. Furthermore, even if the 8 significant bits are sufficient for adequately accurate FFT analysis, the timing precision and data transfer rate problems have yet to be resolved.

XIII. RECOMMENDATIONS

The recommendations included in this section are a result of many informative discussions with the staff of AAAI-4. Furthermore, most of these recommendations cannot be considered as original but simply a re-statement of suggestions and plans made by the AAAI-4 staff and the author during the period of this research effort.

1. The individual or individuals from the contractor who are responsible for the data reduction specifications for IESS should be identified and contacted to learn what data will be available from IESS on which evaluations can be based. Some questions that need to be answered are: Will the actual signals in baseband, IF and RF, be available in digitized form? Will the digitized signals on the data busses be available? Will the recording of the input signals and the output signals be coherent, so that relative phase between the input and the output is preserved? What conventional communication system evaluation methods are anticipated and/or recommended by the data reduction specifications? What new or unconventional communication system valuation methods are anticipated and/or recommended by the data reduction specifications? Are all the CNI systems of ICNIA to be evaluated by the same methods? Will IESS have a Fourier Analysis capability? Will all or some of the data reduction be done on a higher level than those methods discussed in this report?

2. It is recommended that an attempt be made to obtain operational units of each CNI service that is to be integrated in ICNIA, to study, characterize and evaluate each service now in use as a stand-alone system. This information will allow AAAI-4 to prepare for the evaluation of these CNI services as they will perform in ICNIA. Typical expected inputs and their

corresponding outputs may then be archieved for future comparison to those of each service in ICNIA.

3. If some or all of the operational units of the CNI services to be integrated in ICNIA cannot be obtained for study as mentioned above, recordings of typical inputs and outputs should be requested for analysis. Any computer models that might exist for these services would be valuable for generating data of this nature.

   The evaluations of the existing CNI services need not be done only by dual channel FFT analysis but conventional methods of evaluation should also be used.

4. To familiarize the staff of AAAI with the application of dual channel FFT analysis to communication systems as discussed in Section XI, it is recommended that one of the commercially available Dual Channel FFT Analyzers be obtained to practice evaluation and diagnostic techniques on existing CNI services that will be integrated in ICNIA. This will prepare AAAI-4 for the evaluation problems that will be faced on the arrival of IESS.

XIV. ACKNOWLEDGEMENTS

XV. REFERENCES

1. ICNIA Technical Proposal in Response to: F33615-83-C-1001.

2. IESS Technical Proposal in Response to: F33615-83-R-1109.

3. Griesacker, P. B., "Dual Channel FFT System Analysis Facility For Evaluating Integrated Communication, Navigation, and Identification Systems", AFOSR Technical Proposal, USAF/SCEEE Research Initiation Program 1984.

4. Bendat, J. S., and Piersol, A. G., "Random Data: Analysis and Measurement Procedures", Wiley-Interscience, NY, 1971.

5. Bendat, J. S., and Piersol, A. G., "Engineering Applications of Correlation and Spectral Analysis", Wiley-Interscience, NY, 1980.

6. Papoulis, A., "Circuits and Systems, A Modern Approach", Holt, Rinehart and Winston, Inc., NY, 1980.

7. Lathi, B. P., "Modern Digital and Analog Communications Systems", CBS College Publishing, NY, 1983.

8. Military Standard, "Measurement of Electromagnetic Interference Characteristics" MIL-STD-462, 31 July 1967.

9. Military Standard, "Electromagnetic Emission and Susceptability Requirements for the Control of Electromagnetic Interference" MIL-STD -461B, 1 April 1980.

10. Oppenheim, A. V. and Schafer, R. W., "Digital Signal Processing", Prentice-Hall, Englewood Cliffs, NJ, 1975.

11. Rabiner, L. R. and Gold, B., "Theory and Application of Digital Signal Processing", Prentice-Hall, Inc., NJ, 1975.

12. Biering, H. and Pedersen, O. Z., "System Analysis and Timedelay Spectrometry" Parts I & II, A. Bruel & Kjaer Publication, Marlborough, MA, 1983.

13. Thrane, N., "The Discrete Fourier Transform and FFT Analyzers", Bruel & Kjaer Technical Review, Nos. 1 and 2, 1983.

14. Mitchell, L. D. "Improved Methods for The FFT Calculation of the Frequency Response Function", Journal of Mechanical Design, April 1982, Vol. 104.

15. Cawley, P., "The Reduction Bias Error in Transfer Function Estimates Using FFT Based Analysers," M.S.A. - Session, ASME Conf., Dearborn, MI, Sept. 1983.

16. Upton, R., "Innovative Functions for Two-Channel FFT Analyzers", Sound and Vibration, Instrumentation Reference Issue, March (1984) 18-25.

17. Griesacker, P. B., "Digital Signal Approaches for Analysis and Evaluation of Communication Systems", AFOSR Technical Report,

USAF/SCEEE Summer Faculty Program, 1984.

18. "Programs for Digital Signal Processing" edited by the Digital
    Signal Processing Committee, IEEE Acoustics, Speech and Signal
    Processing Society, IEEE Press, NY 1979.

19. Herlufsen, H., "Dual Channel FFT Analysis (Part I)" Bruel and
    Kjaer Technical Review, No. 1 - 1984.

20. "Measuring the Coherence Function with the HP3582A Spectrum
    Analyzer", Hewlett Packard Association Note 245-2.

21. Telford, S. J., "Performance of Camac I/O with an HP A600"
    Prepared for Submittal to HP 1000 International Users Group
    Conference, Fort Worth, Texas, October 1983. UCRL-89129 Pre-
    print.

22. Telford, S. J. Priv. Comm.

23. "Technical Evaluation of 200 MHZ Waveform Digitizers" Tester
    Design and Test Systems Engineering Departments, Monsanto
    Research Corporation, Maimisburg, Ohio. March 1985.

24. Knick, D., Monsanto Research Corp., Priv. Comm.

25. Peled, A., and Liv, B., "Digital Signal Processing", John Wiley
    & Sons, N.Y., 1976.

26. Schrock, C. B., "FM Broadcast Measurements Using the Spectrum
    Analyzer", Tektronics Application Note 26AX-3582-3, Tektronics,
    Inc., 1981.

27. Schrock, C. B., "AM Broadcast Measurements Using the Spectrum
    Analyzer", Tektronics Application Note 26AX-3266, Tektronics,
    Inc., 1976.

28. "Spectrum Analysis SWEPT Frequency Measurements and Selective
    Frequency Counting With A Tracking Generator" HP Application Note
    150-3, Hewlett Packard, 1976.

```
PROGRAM DFFT

EXTERNAL   CDIV, DATIME, DONEPL, FFT842, I1MACH, LOGS., LUNITS,
&          PLOTIT, RECPOL
INTEGER   I1MACH
COMPLEX   CDIV
INTRINSIC  AIMAG, CMPLX, CONJG, DATAN, DBLE, FLOAT,
&          INDEX, LEN, MIN, REAL, SQRT
INTEGER   MXPNTS, MXTITLE
PARAMETER (MXPNTS=1024, MXTITLE=16)
COMPLEX   ALLCARR(MXPNTS,MXTITLE),
&         XTOT(MXPNTS), YTOT(MXPNTS),
&         XTOTFFT(MXPNTS), YTOTFFT(MXPNTS),
&         SXXTOT(MXPNTS), SYYTOT(MXPNTS),
&         SXYTOT(MXPNTS), SYXTOT(MXPNTS),
&         HOTOT(MXPNTS),
&         H1(MXPNTS), H2(MXPNTS), HA(MXPNTS),
&         COH(MXPNTS), COP(MXPNTS), NCP(MXPNTS), SNR(MXPNTS)
EQUIVALENCE   (ALLCARR(1,01),XTOT),
&             (ALLCARR(1,02),YTOT),
&             (ALLCARR(1,03),XTOTFFT),
&             (ALLCARR(1,04),YTOTFFT),
&             (ALLCARR(1,05),SXXTOT),
&             (ALLCARR(1,06),SYYTOT),
&             (ALLCARR(1,07),SXYTOT),
&             (ALLCARR(1,08),SYXTOT),
&             (ALLCARR(1,09),HOTOT),
&             (ALLCARR(1,10),HA),
&             (ALLCARR(1,11),H1),
&             (ALLCARR(1,12),H2),
&             (ALLCARR(1,13),COH),
&             (ALLCARR(1,14),COP),
&             (ALLCARR(1,15),NCP),
&             (ALLCARR(1,16),SNR)
COMMON /COMARR/   ALLCARR

LOGICAL   EXIST, PLOTTD, XPOLAR, YPOLAR
INTEGER   FORMN, I, IR, NCAPT, NPNTS, OLU, RECORDS,
&         TERMLU, TITLEN, XLU, YLU, XNPNTS, YNPNTS
REAL      CNTRAY(MXPNTS), TEMR(MXPNTS), TEMI(MXPNTS)
DOUBLE PRECISION  DTEMR(MXPNTS), DTEMI(MXPNTS)
DOUBLE PRECISION  RECIPR
COMPLEX   XF, YF,
&         XFFT(MXPNTS), YFFT(MXPNTS),
&         SXXAVE, SYYAVE, SXYAVE, SYXAVE,
&         COHT

INTEGER   MXFILLEN
PARAMETER (MXFILLEN = 8)
CHARACTER *(MXFILLEN)  XFILE, YFILE, OFILE
CHARACTER *30  DATSTR
CHARACTER *40  XFORMT, YFORMT, OFORMT, OFORMD
CHARACTER *80  ANSWER, COMMNT, JUNK
CHARACTER *1   REPLY

INTEGER   M,U
```

```fortran
      CHARACTER*32  F

      DOUBLE PRECISION  PI, RTODR
      COMMON /COZERO/  DVZERO, PRZERO
      DOUBLE PRECISION  DVZERO, PRZERO
      COMMON /COLOGS/ LOG0, LOG0CT
      DOUBLE PRECISION  LOG0
      INTEGER  LOG0CT

      INTEGER  MXCAPT, MXFORM, MXLEN
      PARAMETER (MXCAPT=9, MXFORM=6, MXLEN=58)
      CHARACTER *(MXLEN)  CAPTION(MXCAPT), FORM(MXFORM),
     &                    TITLE(MXTITLE), XLABEL(2)
      INTEGER  DOMAIN(MXTITLE)

      DATA   FORM/
     &           'Real part',
     &           'Imaginary part',
     &           'Magnitude',
     &           'Log of Magnitude',
     &           'Phase (radians)',
     &           'Phase (degrees)'/
      DATA   TITLE/
     &           'Average X input over N records - x(t)',
     &           'Average Y input over N records - y(t)',
     &           'FFT of average X input - X(f)',
     &           'FFT of average Y input - Y(f)',
     &           'Auto Spectrum of X input - Sxx',
     &           'Auto Spectrum of Y input - Syy',
     &           'Cross Spectrum - Sxy',
     &           'Cross Spectrum - Syx',
     &           'Transfer Function - HO',
     &           'Transfer Function - HA',
     &           'Transfer Function - H1',
     &           'Transfer Function - H2',
     &           'Coherence Function - COH',
     &           'Coherent Output Power - COP',
     &           'Non-Coherent Power - NCP',
     &           'Signal-to-Noise Ratio - SNR'/
      DATA   DOMAIN /2*1,14*2/
      DATA   XLABEL /'Time (n * DELTA.t)', 'Frequency (n * DELTA.f)'/


      PI = 4 * DATAN(1D0)
      RTODR = 180 / PI
      PRZERO = FLOAT(I1MACH(10)) ** (I1MACH(12)/2)
C     For double precision use:
C     PRZERO = DBLE(I1MACH(10)) ** (I1MACH(15)/2)
CC    PRINT *, '==  PRZERO =',PRZERO
      LOG0 = -4
      DO 9 I=1,MXPNTS
         CNTRAY(I) = FLOAT(I)
9     CONTINUE
      CALL LUNITS('GET','TERM',TERMLU)

10    OFORMD = '(2(3X,E15.7))'
12    WRITE (TERMLU,13)
13    FORMAT('   Enter X channel filename:')
```

16.46

```
      READ (TERMLU,'(A)',ERR=12,END=990)  XFILE
      CALL LUNITS('GET','DISK',XLU)
      OPEN (UNIT=XLU,FILE=XFILE,STATUS='OLD')
16    READ (XLU,'(A)')  XFORMT
      IF (XFORMT(1:1).EQ.'*')  GOTO 16
      IF (XFORMT(1:1).EQ.'(')  THEN
        READ (XLU,*)  XNPNTS
       ELSE
        READ (XFORMT,*)  XNPNTS
      ENDIF
      IF (XNPNTS.LE.0 .OR. XNPNTS.GT.MXPNTS)  THEN
        WRITE (TERMLU,19)  XNPNTS, MXPNTS
19      FORMAT(' *** ERROR ***'
     &         /'According to the file, it contains ',I16,' samples.'
     &         /'(This number should be between 1 and ',I6,')')
      GOTO 990
      ENDIF

20    WRITE (TERMLU,21)
21    FORMAT('   Is the data in polar form? (default is yes)')
      READ (TERMLU,'(A)')  REPLY
      XPOLAR = REPLY.NE.'N' .AND. REPLY.NE.'n'

30    WRITE (TERMLU,33)
33    FORMAT('   Enter Y channel filename:')
      READ (TERMLU,'(A)',ERR=30,END=990)  YFILE
      CALL LUNITS('GET','DISK',YLU)
      OPEN (UNIT=YLU,FILE=YFILE,STATUS='OLD')
36    READ (YLU,'(A)')  YFORMT
      IF (YFORMT(1:1).EQ.'*')  GOTO 36
      IF (YFORMT(1:1).EQ.'(')  THEN
        READ (YLU,*)  YNPNTS
       ELSE
        READ (YFORMT,*)  YNPNTS
      ENDIF
      IF (YNPNTS.LE.0 .OR. YNPNTS.GT.MXPNTS)  THEN
        WRITE (TERMLU,39)  YNPNTS, MXPNTS
39      FORMAT(' *** ERROR ***'
     &         /'According to the file, it contains ',I36,' samples.'
     &         /'(This number should be between 1 and ',I6,')')
      GOTO 990
      ENDIF

40    WRITE (TERMLU,41)
41    FORMAT('   Is the data in polar form? (default is yes)')
      READ (TERMLU,'(A)')  REPLY
      YPOLAR = REPLY.NE.'N' .AND. REPLY.NE.'n'

50    WRITE (TERMLU,51)
51    FORMAT('   Enter number of records to average (integer):')
      READ (TERMLU,*,ERR=50,END=990)  RECORDS
      IF (RECORDS .LE. 0)  GOTO 50

      NPNTS = MIN(XNPNTS,YNPNTS)
      WRITE (TERMLU,73)  RECORDS, NPNTS, XFILE, YFILE
73    FORMAT('   Process ',I4,' record(s), of ',I4,' samples each.'
     &       /'   X file name: ',A,',   Y file name: ',A,'.'
     &       /'   Is this correct? (Y/N)')
```

```fortran
         READ (TERMLU,'(A1)')  REPLY
         IF (REPLY.EQ.'N' .OR. REPLY.EQ.'n')  THEN
            CALL LUNITS('CLOSE','',XLU)
            CALL LUNITS('CLOSE','',YLU)
            GOTO 10
         ENDIF

CC       PRINT*, '==Zero totals'
         WRITE (TERMLU,101)
101      FORMAT('   Reading files, and doing calculations...')
         DO 109 I=1,NPNTS
            XTOT(I) = 0
            YTOT(I) = 0
            HOTOT(I) = 0
            SXXTOT(I) = 0
            SYYTOT(I) = 0
            SXYTOT(I) = 0
            SYXTOT(I) = 0
109      CONTINUE

         DO 149 IR=1,RECORDS

CC       PRINT *,'==read next survey'
         IF (XFORMT(1:1) .EQ. '(')    THEN
            READ (XLU,XFORMT)  (DTEMR(I),DTEMI(I),I=1,XNPNTS)
          ELSE
            READ (XLU,*)  (DTEMR(I),DTEMI(I),I=1,XNPNTS)
         ENDIF
CC       IF (XPOLAR)  PRINT *, '== calling RECPOL'
         IF (XPOLAR)  CALL RECPOL('PR',NPNTS,DTEMR,DTEMI,DTEMR,DTEMI)
         DO 115 I=1,NPNTS
            XTOT(I) = XTOT(I) + CMPLX(DTEMR(I),DTEMI(I))
CC          PRINT *, 'XTOT(I) == ', XTOT(I)
115      CONTINUE
         CALL FFT842(0,NPNTS,DTEMR,DTEMI)
         DO 119 I=1,NPNTS
            XFFT(I) = CMPLX(DTEMR(I),DTEMI(I))
CC          PRINT *, 'XFFT(I) == ',XFFT(I)
119      CONTINUE

         IF (YFORMT(1:1) .EQ. '(')    THEN
            READ (YLU,YFORMT)  (DTEMR(I),DTEMI(I),I=1,YNPNTS)
          ELSE
            READ (YLU,*)  (DTEMR(I),DTEMI(I),I=1,YNPNTS)
         ENDIF
         IF (YPOLAR)  CALL RECPOL('PR',NPNTS,DTEMR,DTEMI,DTEMR,DTEMI)
         DO 125 I=1,NPNTS
            YTOT(I) = YTOT(I) + CMPLX(DTEMR(I),DTEMI(I))
125      CONTINUE
         CALL FFT842(0,NPNTS,DTEMR,DTEMI)
         DO 129 I=1,NPNTS
            YFFT(I) = CMPLX(DTEMR(I),DTEMI(I))
CC          PRINT *, 'YFFT(I) == ',YFFT(I)
129      CONTINUE

CC       PRINT *,'==Calculate spectra'
         DO 139 I=1,NPNTS
            XF = XFFT(I)
```

16.48

```
                YF = YFFT(I)
CC              PRINT *, '== XF=', XF
CC              PRINT *, '== ABS(XF)= ',ABS(XF)
                HOTOT(I) = HOTOT(I) + CDIV(YF,XF)
CC              PRINT*,'=  SXXTOT'
                SXXTOT(I) = SXXTOT(I) + CONJG(XF) * XF
CC              PRINT*,'==  SYYTOT'
                SYYTOT(I) = SYYTOT(I) + CONJG(YF) * YF
CC              PRINT*,'==  SXYTOT'
                SXYTOT(I) = SXYTOT(I) + CONJG(XF) * YF
CC              PRINT*,'==  SYXTOT'
                SYXTOT(I) = SYXTOT(I) + CONJG(YF) * XF
139     CONTINUE

149     CONTINUE
        CALL LUNITS('CLOSE','DISK',XLU)
        CALL LUNITS('CLOSE','DISK',YLU)

CC      PRINT *, '==Compute averages from totals'
CC      PRINT *,'==and all the other sequences.'
        RECIPR = 1. / DBLE(RECORDS)
        DO 159 I=1,NPNTS
            XTOT(I) = XTOT(I) * RECIPR
            YTOT(I) = YTOT(I) * RECIPR
            HOTOT(I) = HOTOT(I) * RECIPR
            SXXAVE = SXXTOT(I) * RECIPR
            SXXTOT(I) = SXXAVE
            SYYAVE = SYYTOT(I) * RECIPR
            SYYTOT(I) = SYYAVE
            SXYAVE = SXYTOT(I) * RECIPR
            SXYTOT(I) = SXYAVE
            SYXAVE = SYXTOT(I) * RECIPR
            SYXTOT(I) = SYXAVE
CC      PRINT *, 'SXXAVE == ', SXXAVE
CC      PRINT *, 'SYYAVE == ', SYYAVE
CC      PRINT *, 'SXYAVE == ', SXYAVE
CC      PRINT *, 'SYXAVE == ', SYXAVE
            H1(I) = CDIV(SXYAVE,SXXAVE)
CC          PRINT *, 'H1(I) == ',H1(I)
            H2(I) = CDIV(SYYAVE,SYXAVE)
CC          PRINT *, 'H2(I) == ',H2(I)
            HA(I) = SQRT(CDIV(SYYAVE,SXXAVE))
CC          PRINT *, 'HA(I) == ',HA(I)
            COHT = CDIV(H1(I),H2(I))
            COH(I) = COHT
CC          PRINT *, 'COH(I) == ',COH(I)
            COP(I) = COHT * SYYAVE
CC          PRINT *, 'COP(I) == ',COP(I)
            NCP(I) = (1 - COHT) * SYYAVE
CC          PRINT *, 'NCP(I) == ',NCP(I)
            SNR(I) = CDIV(COHT,1-COHT)
CC          PRINT *, 'SNR(I) == ',SNR(I)
159     CONTINUE

CC      PRINT *, '==Do FFT of average'
        DO 165 I=1,NPNTS
            DTEMR(I) = REAL(XTOT(I))
            DTEMI(I) = AIMAG(XTOT(I))
```

16.49
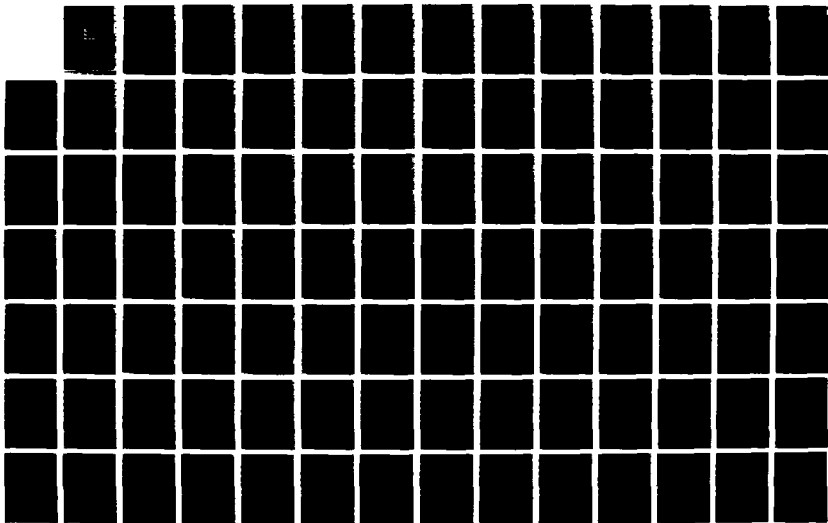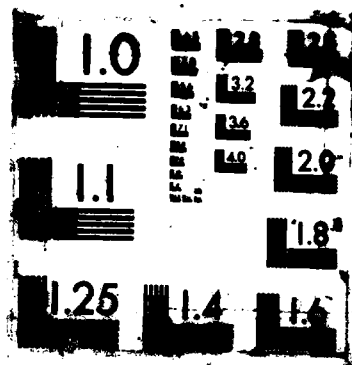
```
165     CONTINUE
        CALL FFT842(0,NPNTS,DTEMR,DTEMI)
        DO 169 I=1,NPNTS
           XTOTFFT(I) = CMPLX(DTEMR(I),DTEMI(I))
169     CONTINUE

        DO 175 I=1,NPNTS
           DTEMR(I) = REAL(YTOT(I))
           DTEMI(I) = AIMAG(YTOT(I))
175     CONTINUE
        CALL FFT842(0,NPNTS,DTEMR,DTEMI)
        DO 179 I=1,NPNTS
           YTOTFFT(I) = CMPLX(DTEMR(I),DTEMI(I))
179     CONTINUE


        PLOTTD = .FALSE.
CCC     GOTO 900
200     WRITE (TERMLU,201)  (I,TITLE(I),I=1,MXTITLE)
201     FORMAT('    Choose a data set:'
     &        /99(/8X,I2,' - ',A))
        WRITE (TERMLU,203)
203     FORMAT('    Or type Q to quit.')
        READ (TERMLU,'(A)',ERR=200,END=990)  ANSWER
        IF (ANSWER.EQ.'Q' .OR. ANSWER.EQ.'q')  GOTO 990
        READ (ANSWER,*,ERR=200,END=990)  TITLEN
        IF (TITLEN.LT.1 .OR. TITLEN.GT.MXTITLE)  GOTO 200


210     WRITE (TERMLU,211)
211     FORMAT('    Do you wish to record the data into a file?')
        READ (TERMLU,'(A1)',ERR=200,END=990)  REPLY
        IF (REPLY.EQ.'N' .OR. REPLY.EQ.'n')  GOTO 300
        IF (REPLY.NE.'Y' .AND. REPLY.NE.'y')  GOTO 200


220     WRITE (TERMLU,221)  LEN(OFILE)
221     FORMAT('    What would like to name the output file?'
     &        /'    (',I2,' characters maximum)')
        READ (TERMLU,'(A)',ERR=220,END=990)  OFILE
        INQUIRE (FILE=OFILE, EXIST=EXIST)
        IF (EXIST)  THEN
           WRITE (TERMLU,223)
223        FORMAT(4X,
     &            'The file already exists. Is it alright to replace it?')
           READ (TERMLU,'(A)',ERR=220,END=990)  REPLY
           IF (REPLY .NE. 'Y')  GOTO 220
        ENDIF
        CALL LUNITS('GET','DISK',OLU)
        OPEN (UNIT=OLU, FILE=OFILE)

230     WRITE (TERMLU,231)  LEN(COMMNT)
231     FORMAT(4X,
     &     'Type any comments that you would like written into the file;'
     &     /4X,
     &     'enter a single period on a line (".", to end the comments:'
     &     /8X,'(Limit:',I3,' characters per line)')
232     READ (TERMLU,'(A)',ERR=230,END=990)  COMMNT
        IF (COMMNT .NE. '.')  THEN
           WRITE (OLU,'(A)')  '* ' // COMMNT
```
16.50

```
            GOTO 232
         ENDIF

240      WRITE (TERMLU,241)  LEN(OFORMT), OFORMD
241      FORMAT('      Enter the format to be used,'
     &         /'          (',I2,' characters maximum)'
     &         /'      or type "*" for free format,'
     &         /'      or just hit RETURN to use  ',A)
         READ (TERMLU,'(A)',ERR=240,END=990)  OFORMT
         IF (OFORMT .EQ. '  ')  OFORMT = OFORMD
         IF (OFORMT .NE. '*')  THEN
            WRITE (JUNK,OFORMT,ERR=246)  1,0
            WRITE (OLU,'(A)')  OFORMT
            OFORMD = OFORMT
            GOTO 250
246         WRITE (TERMLU,247)  OFORMT
247         FORMAT(4X,A,' is an invalid format.')
            GOTO 240
         ENDIF

250      WRITE (TERMLU,251)
251      FORMAT('      By default the data will be written in POLAR form,'
     &         /'      unless you type R for rectangular form')
         READ (TERMLU,'(A)',ERR=250,END=990)  REPLY
         WRITE (OLU,*)  NPNTS
         IF (REPLY.EQ.'R' .OR. REPLY.EQ.'r')  THEN
            DO 255 I=1,NPNTS
               TEMR(I) = REAL(ALLCARR(I,TITLEN))
               TEMI(I) = AIMAG(ALLCARR(I,TITLEN))
255         CONTINUE
         ELSE
            DO 257 I=1,NPNTS
               DTEMR(I) = REAL(ALLCARR(I,TITLEN))
               DTEMI(I) = AIMAG(ALLCARR(I,TITLEN))
257         CONTINUE
            CALL RECPOL('RP',NPNTS,DTEMR,DTEMI,DTEMR,DTEMI)
            DO 259 I=1,NPNTS
               TEMR(I) = DTEMR(I)
               TEMI(I) = DTEMI(I)
259         CONTINUE
         ENDIF

         IF (OFORMT .EQ. '*')  THEN
            DO 265 I=1,NPNTS
               WRITE (OLU,*)  TEMR(I), TEMI(I)
265         CONTINUE
         ELSE
            DO 269 I=1,NPNTS
               WRITE (OLU,OFORMT)  TEMR(I), TEMI(I)
269         CONTINUE
         ENDIF
         ENDFILE (OLU)
         CALL LUNITS('CLOSE','DISK',OLU)

300      WRITE (TERMLU,301)
301      FORMAT('      Do you wish to have the data plotted?')
         READ (TERMLU,'(A1)',ERR=300,END=990)  REPLY
         IF (REPLY.EQ.'N' .OR. REPLY.EQ.'n')  GOTO 200
```

16.51

```
          IF (REPLY.NE.'Y' .AND. REPLY.NE.'y')  GOTO 300

310    WRITE (TERMLU,311)
311    FORMAT('     Choose one of the following:'/)
       WRITE (TERMLU,313)  (I,FORM(I),I=1,MXFORM)
313    FORMAT (8X,I1,'.     ',A)
       READ (TERMLU,*,ERR=310,END=990)  FORMN
       IF (FORMN.LT.1 .OR. FORMN.GT.MXFORM)  GOTO 310
       IF (FORMN .EQ. 1)  THEN
          DO 315 I=1,NPNTS
             TEMR(I) = REAL(ALLCARR(I,TITLEN))
315       CONTINUE
       ELSEIF (FORMN .EQ. 2)  THEN
          DO 319 I=1,NPNTS
             TEMR(I) = AIMAG(ALLCARR(I,TITLEN))
319       CONTINUE
       ELSE
          DO 321 I=1,NPNTS
             DTEMR(I) = REAL(ALLCARR(I,TITLEN))
             DTEMI(I) = AIMAG(ALLCARR(I,TITLEN))
321       CONTINUE
          CALL RECPOL('RP',NPNTS,DTEMR,DTEMI,DTEMR,DTEMI)
          IF (FORMN.EQ.3 .OR. FORMN.EQ.4)  THEN
             IF (FORMN .EQ. 4)  CALL LOGS('ML',NPNTS,DTEMR,DTEMR)
             DO 323 I=1,NPNTS
                TEMR(I) = DTEMR(I)
323          CONTINUE
          ELSEIF (FORMN .EQ. 5)  THEN
             DO 325 I=1,NPNTS
                TEMR(I) = DTEMI(I)
325          CONTINUE
          ELSEIF (FORMN .EQ. 6)  THEN
             DO 329 I=1,NPNTS
                TEMR(I) = DTEMI(I) * RTODR
                IF (TEMR(I) .LT. 0)  TEMR(I) = TEMR(I) + 360
329          CONTINUE
          ENDIF
       ENDIF

330    CALL DATIME(DATSTR)
       I = INDEX(DATSTR,'   ')
       WRITE (CAPTION(1),331)  XFILE, YFILE, DATSTR(:I-1)
331    FORMAT('X file: ',A,',   Y file: ',A,T48,A)
       WRITE (CAPTION(2),332)  TITLE(TITLEN), DATSTR(I+2:)
332    FORMAT(A,T48,A)
       WRITE (TERMLU,333)  CAPTION(1), CAPTION(2)
333    FORMAT('     The first two lines of the caption are: ',
      &     /2(/8X,A)/)
       NCAPT = 3
334    WRITE (TERMLU,335)  MXCAPT
335    FORMAT('     What would you like for the next line?',
      &                          ' (Max:',I2,' lines)'
      &     /'     Type a single period (".") to finish.')
       READ (TERMLU,'(A)',ERR=334,END=990)  CAPTION(NCAPT)
       IF (CAPTION(NCAPT) .NE. '.')  THEN
          NCAPT = NCAPT + 1
          GOTO 334
       ENDIF
```

```fortran
      NCAPT = NCAPT - 1
      WRITE (TERMLU,337)
337   FORMAT('    Plotting, please wait...')
      CALL PLOTIT('',NPNTS,CNTRAY,TEMR,XLABEL(DOMAIN(TITLEN)),
     &            FORM(FORMN),NCAPT,CAPTION)
      PLOTTD = .TRUE.
      GOTO 200


900   PRINT *, 'Which array would you like to see?'
      READ (*,*,ERR=900,END=990)  M
      PRINT *, 'FILENAME:'
      READ (*,'(A)')  F
      CALL LUNITS('GET','DISK',U)
      OPEN(UNIT=U,FILE=F)
      DO 909 I=1,NPNTS
         DTEMR(I) = REAL(ALLCARR(I,M))
         DTEMI(I) = AIMAG(ALLCARR(I,M))
         CALL RECPOL('RP',1,DTEMR(I),DTEMI(I),DTEMR(I),DTEMI(I))
         WRITE(U,'(2'//OFORMD//')')
     &                   REAL(ALLCARR(I,M)), AIMAG(ALLCARR(I,M)),
     &                   FLOAT(DTEMR(I)), FLOAT(DTEMI(I))
909   CONTINUE
      ENDFILE(U)
      CALL LUNITS('CLOSE','',U)
      GOTO 900

990   IF (PLOTTD)  CALL DONEPL
      STOP
      END



CINSERT D.REST



CINSERT FFT842.INS.F77


      COMPLEX FUNCTION CDIV(A,B)
      COMPLEX  A, B
      INTRINSIC  ABS

      COMMON /COZERO/  DVZERO, PRZERO
      DOUBLE PRECISION  DVZERO, PRZERO
      DATA  PRZERO /0/
      DATA  DVZERO /0/

      IF (ABS(B) .GT. PRZERO)  THEN
         CDIV = A / B
       ELSE
         IF (ABS(A) .GT. PRZERO)  THEN
            CDIV = DVZERO
          ELSE
            CDIV = 0
         ENDIF
      ENDIF
```

16.53

```
      RETURN
      END



      SUBROUTINE LOGS(CHOICE,N,IN,OUT)
      CHARACTER *2  CHOICE
      INTEGER  N
      DOUBLE PRECISION  IN(N), OUT(N)
      COMMON /COLOGS/ LOG0, LOG0CT
      DOUBLE PRECISION  LOG0
      INTEGER  LOG0CT
      INTRINSIC  LOG10
      INTEGER  I
      DATA LOG0/0/
      IF (CHOICE .EQ. 'ML')  THEN
          DO 19 I=1,N
             IF (IN(I) .NE. 0)  THEN
                OUT(I) = LOG10(IN(I))
              ELSE
                OUT(I) = LOG0
                LOG0CT = LOG0CT + 1
             ENDIF
19        CONTINUE
      ELSEIF(CHOICE .EQ. 'LM')  THEN
          DO 29 I=1,N
             OUT(I) = 10 ** IN(I)
29        CONTINUE
      ENDIF
      RETURN
      END



      SUBROUTINE RECPOL(CHOICE,N,IN1,IN2,OUT1,OUT2)
C
C RECPOL
C BY George Fytikas and Dave Platteter  for Dr. Paul B. Griesacker,
C     Gannon University, 1985.
C This routine will convert coordinates in one form into another.
C     The coordinates are given and returned in pairs of arrays.
C     N is the number of elements in each array.
C     To convert rectangular coordinates into polar coordinates:
C         CALL RECPOL('RP',n,realarray,imagarray,magarray,phasearray)
C     To convert polar coordinates into rectangular coordinates:
C         CALL RECPOL('PR',n,magarray,phasearray,realarray,imagarray)
C MODIFICATIONS:
C 3 June, 1985  [GAF]:  IN1 and IN2 arrays may be the same as OUT1
C     and OUT2 arrays (calling program may have new coordinates
C     "placed on top" of old ones).
C
      CHARACTER *2  CHOICE
      INTEGER  N
      DOUBLE PRECISION  IN1(N), IN2(N), OUT1(N), OUT2(N)
      INTRINSIC  ABS, ASIN, ATAN2, COS, SIN, SQRT
      INTEGER  I
      DOUBLE PRECISION  ASINP1, ASINM1, IN1T, IN2T
```

16.54

```
          ASINP1 = ASIN(1D0)
          ASINM1 = ASIN(-1D0)
          IF (CHOICE .EQ. 'RP')  THEN
              DO 19 I=1,N
                  IN1T = IN1(I)
                  IN2T = IN2(I)
                  IF (IN1T .EQ. 0)  THEN
                      OUT1(I) = ABS(IN2T)
                      IF (IN2T .EQ. 0)  THEN
                          OUT2(I) = 0
                       ELSEIF (IN2T .GT. 0)  THEN
                          OUT2(I) = ASINP1
                       ELSE
                          OUT2(I) = ASINM1
                      ENDIF
                   ELSE
                      OUT1(I) = SQRT(IN1T**2 + IN2T**2)
                      OUT2(I) = ATAN2(IN2T,IN1T)
                  ENDIF
19            CONTINUE
          ELSEIF (CHOICE .EQ. 'PR')  THEN
              DO 29 I=1,N
                  IN1T = IN1(I)
                  IN2T = IN2(I)
                  OUT1(I) = IN1T * COS(IN2T)
                  OUT2(I) = IN1T * SIN(IN2T)
29            CONTINUE
          ENDIF
          RETURN
          END




          INTEGER FUNCTION LENGTH(STR)
          CHARACTER *(*)  STR
          INTRINSIC  LEN
          INTEGER  I
          DO 9 I=LEN(STR),1,-1
            IF (STR(I:I) .NE. ' ')  GOTO 10
9         CONTINUE
10        LENGTH = I
          RETURN
          END




C     LUNITS
C
C     A subroutine that deals with system-dependent features of FORTRAN
C     logical units.
C     USAGE:
C     To get the system's logical unit for the terminal:
C         CALL LUNITS('GET','TERM',LUNIT)
C         Where the terminal's logical unit will be returned in LUNIT.
C     To find an available logical unit for a disk file:
C         CALL LUNITS('GET','DISK',LUNIT)
C         Where the available logical unit will be returned in LUNIT.
C     To close a logical unit (and tell LUNITS it is available):
```

```
C              CALL LUNITS('CLOSE',???,LUNIT)
C              ??? is any character expression (not examined, assumed 'DISK');
C              LUNIT is the logical unit to be closed.
C
      INTEGER FUNCTION LUNITS(ACTION,TYPE,LUNIT)
      CHARACTER *(*)  ACTION, TYPE
      INTEGER  LUNIT

      INTEGER  I

      COMMON /COUNIT/ TMUNIT, LDUNIT, LDUSED
      SAVE  COUNIT
      INTEGER  MXUNIT
C     The following is the first system-dependent line:
      PARAMETER (MXUNIT = 16)
      INTEGER  TMUNIT, LDUNIT(MXUNIT)
      LOGICAL  LDUSED(MXUNIT)
CC    SAVE  TMUNIT, LDUNIT, LDUSED
C     The next two lines are the only other system-dependent lines.
C     Currently set for the PRIME 750 computer.
      DATA  TMUNIT /1/
      DATA  LDUNIT /5,6,7,8,9,10,11,12,13,14,15,16,17,18,19,20/
      DATA  LDUSED /MXUNIT * .FALSE./


      IF (ACTION .EQ. 'GET')  THEN

         IF (TYPE .EQ. 'TERM')  THEN
            LUNIT = TMUNIT
            RETURN

         ELSEIF (TYPE .EQ. 'DISK')  THEN
            DO 3 I=1,MXUNIT
               IF (.NOT. LDUSED(I))  THEN
                  LUNIT = LDUNIT(I)
                  LDUSED(I) = .TRUE.
                  RETURN
               ENDIF
3           CONTINUE
            WRITE (TMUNIT,5)
5           FORMAT(//'*** ERROR ***'
     &             /'All available units are in use  (LUNITS)')
            LUNIT = -1
            RETURN

         ELSE
            WRITE (TMUNIT,9)  TYPE
9           FORMAT(//'*** ERROR ***'
     &             /'"',A,'" is an unrecognized type  (LUNITS)')
            LUNIT = -1
            RETURN
         ENDIF


      ELSEIF (ACTION .EQ. 'CLOSE')  THEN
         DO 11 I=1,MXUNIT
            IF (LDUNIT(I) .EQ. LUNIT)  THEN
               CLOSE (LUNIT)
```

16.56

```fortran
                      LDUSED(I) = .FALSE.
                      RETURN
                   ENDIF
11          CONTINUE
            WRITE (TMUNIT,13)  LUNIT
13          FORMAT(//'*** ERROR ***'
     &               /I15,' is not a valid logical unit  (LUNITS)')
            RETURN


        ELSE
            WRITE (TMUNIT,15)  ACTION
15          FORMAT(//'*** ERROR ***'
     &               /'"',A,'" is an unrecognized action request  (LUNITS)')
            RETURN
        ENDIF
        END




C     PLOTIT.F77
C
C------------------------------------------------------------------------
C     ROUTINES FROM THE DISSPLA SOFTWARE PACKAGE (VERSION 9.2)
C     BY ISSCO INC., ARE USED FOR ALL GRAPHICS-RELATED WORK.
C
C     (ORIGINALLY WRITTEN FOR THE PRlME 750 COMPUTER SYSTEM)
C
C  ORIGINAL AUTHORS:  GEORGE FYTIKAS AND DAVID PLATTETER
C            FOR DR. PAUL B. GRIESACKER   -  GANNON UNIVERSITY.
C  TRANSFORMED FROM GR.F77 TO PLOTIT.F77 BY GEORGE FYTIKAS, ON
C            13 JUNE, 1985.
C
C
C------------------------------------------------------------------------
C
        SUBROUTINE PLOTIT(HEADER,N,XRAY,YRAY,LXNAME,LYNAME,NLIN,LPKRAY)

        INTEGER  N, NLIN
        REAL   XRAY(N), YRAY(N)
        CHARACTER *(*)  HEADER, LXNAME, LYNAME, LPKRAY(NLIN)

        EXTERNAL   LENGTH, SPOPEN
        INTEGER   LENGTH
        EXTERNAL   AREA2D, BSHIFT, CROSS, CURVE, DONEPL, ENDPL, GRAF,
     &             LINES, LINEST, LSTORY, MARKER, NOBRDR,
     &             PNTRNX, RESET, SCLPIC, XNAME, YNAME
        INTEGER   LINEST
        INTRINSIC  MIN

        INTEGER   MAXLEN, MXLIN, WORDL, NWORDS
        PARAMETER (MAXLEN = 80, MXLIN = 9, WORDL = 4)
        PARAMETER (NWORDS = 3 + (MXLIN * (5 + MAXLEN/WORDL) ) )
        INTEGER   IPKRAY(NWORDS)

        INTEGER   I, IMAX, IT, IXNAME, IYNAME, MAXLIN, PLOTN
        REAL   SHIFT, XRMAX, YRMAX, XRMIN, YRMIN
        SAVE   PLOTN, SHIFT
```

16.57

```fortran
      DATA  PLOTN /0/
      DATA  SHIFT/-3/

      PLOTN = PLOTN + 1
      IF (PLOTN .EQ. 1)  THEN
CC       OPEN (UNIT=32,FILE='PLOTEMP')
         CALL SPOPEN(20,'',HEADER)
         ENDFILE (32)
         CALL PNTRNX
      ENDIF
      CALL RESET('ALL')
      CALL NOBRDR
      SHIFT = -SHIFT
CB    CALL BSHIFT(SHIFT,SHIFT)
      CALL AREA2D(6.,8.)
CB    CALL BSHIFT(SHIFT,SHIFT)

      CALL CROSS
      IXNAME = LENGTH(LXNAME)
      CALL XNAME(LXNAME,IXNAME)
      IYNAME = LENGTH(LYNAME)
      CALL YNAME(LYNAME,IYNAME)

C As to Mr Platteter's request:
C We are about to initialize the packing array
C      --  refer to DISSPLA Pocket Guide pp 22-23 (sections B-7.1 to B-7.5)
      IF (NLIN .GT. 0)  THEN
         IMAX = 0
         DO 69 I=1,NLIN
            IT = LENGTH(LPKRAY(I)) + 1
            IF (IT .GT. IMAX)  IMAX = IT
69       CONTINUE
         MAXLIN = LINEST(IPKRAY,NWORDS,IMAX)
C     If MAXLIN < NLIN then we got problems!
C     The following code does the actual packing into the array IPKRAY.
         DO 79 I=1,NLIN
            CALL LINES(LPKRAY(I)(:LENGTH(LPKRAY(I)))//'$',IPKRAY,I)
79       CONTINUE
         CALL LSTORY(IPKRAY,NLIN,0.,0.)
      ENDIF

      CALL BSHIFT(0.,0.30*(NLIN+1))
      CALL MARKER(15)
      CALL SCLPIC(.200)

      XRMAX = XRAY(1)
      XRMIN = XRAY(1)
      DO 89 I=2,N
         IF (XRAY(I) .GT. XRMAX)  XRMAX = XRAY(I)
         IF (XRAY(I) .LT. XRMIN)  XRMIN = XRAY(I)
89    CONTINUE

      YRMAX = YRAY(1)
      YRMIN = YRAY(1)
      DO 99 I=2,N
         IF (YRAY(I) .GT. YRMAX)  YRMAX = YRAY(I)
         IF (YRAY(I) .LT. YRMIN)  YRMIN = YRAY(I)
99    CONTINUE
```

16.58

```
            CALL GRAF(XRMIN,'SCALE',XRMAX,YRMIN,'SCALE',YRMAX)
            CALL CURVE(XRAY,YRAY,N,-1)
            CALL ENDPL(PLOTN)
CC          CALL DONEPL
            RETURN
            END



            SUBROUTINE SPOPEN(FUNIT,WHERE,HEADER)
            INTEGER  FUNIT
            CHARACTER *(*)  WHERE, HEADER

            EXTERNAL  LENGTH, MOVECH
            INTEGER  LENGTH
            EXTERNAL  ERRPR$, SPOOL$
            INTRINSIC  AND, INTS, NOT, OR

            INTEGER  HEADL, WHEREL
            INTEGER*2  BUFDIM
            PARAMETER (BUFDIM=1700)
            INTEGER*2  INFO(29), BUFFER(BUFDIM), CODE

            INFO(2) = FUNIT
            CALL MOVECH('         ',6,INFO(4),6)
CC~~        INFO(3) = :012000
            INFO(3) = :016000
            WHEREL = LENGTH(WHERE)
            IF (WHEREL .GT. 0)  THEN
               INFO(3) = OR(INFO(3),:000100)
               CALL MOVECH(WHERE,LENGTH(WHERE),INFO(13),16)
            ENDIF
            HEADL = LENGTH(HEADER)
            IF (HEADL .NE. 0)  THEN
               INFO(3) = AND(OR(INFO(3),:000040),NOT(:010000))
               CALL MOVECH(HEADER,HEADL,INFO(21),16)
            ENDIF
            CALL SPOOL$(INTS(2),0,0,INFO,BUFFER,BUFDIM,CODE)
            IF (CODE .EQ. 0)  THEN
CC             PRINT 1, INFO(8), INFO(9), INFO(10)
1              FORMAT(4X,4A2,'  opened.')
             ELSE
               CALL ERRPR$(INTS(2),CODE,HEADER,INTS(HEADL),'SPOPEN',INTS(6))
            ENDIF
            RETURN
            END



            SUBROUTINE MOVECH(FROM,FROML,TO,TOL)
            CHARACTER *1  FROM, TO
            INTEGER  FROML, TOL

            TO(:TOL) = FROM(:FROML)
            RETURN
            END
```

16.59

```fortran
C   DATIME
C   George A. Fytikas for Dr. Paul B. Griesacker.
C   14 June 1985
C   Written for the PR1ME 750 computer.
C   Returns date and time in "MM/DD/YY  HH:MM:SS" format.
C
      SUBROUTINE DATIME(STRING)
      CHARACTER *(*)  STRING

      EXTERNAL  CV$FDA, DATE$
      INTEGER*4  DATE$
      INTEGER*2  DOW
      CHARACTER*21  SYDATE

C     Date & time come in "YY-MM-DD.HH:MM:SS.DOW" format into SYDATE.
      CALL CV$FDA(DATE$(),DOW,SYDATE)
      STRING = SYDATE(4:5) // '/' // SYDATE(7:8) // '/' // SYDATE(1:2)
     &                    // ' ' // SYDATE(10:17)
      RETURN
      END
```

APPENDIX B

```
OK, SEG AFWAL>TEST>DCT
   Enter X channel filename:
T140
   Is the data in polar form? (default is yes)
Y
   Enter Y channel filename:
T151
   Is the data in polar form? (default is yes)
Y
   Enter number of records to average (integer):
1
   Process    1 record(s), of    4 samples each.
   X file name: T140    ,  Y file name: T151    .
   Is this correct? (Y/N)
Y
   Reading files, and doing calculations...
   Choose a data set:

        1 - Average X input over N records - x(t)
        2 - Average Y input over N records - y(t)
        3 - FFT of average X input - X(f)
        4 - FFT of average Y input - Y(f)
        5 - Auto Spectrum of X input - Sxx
        6 - Auto Spectrum of Y input - Syy
        7 - Cross Spectrum - Sxy
        8 - Cross Spectrum - Syx
        9 - Transfer Function - HO
       10 - Transfer Function - HA
       11 - Transfer Function - H1
       12 - Transfer Function - H2
       13 - Coherence Function - COH
       14 - Coherent Output Power - COP
       15 - Non-Coherent Power - NCP
       16 - Signal-to-Noise Ratio - SNR

   Or type Q to quit.
14
   Do you wish to record the data into a file?
Y
   What would like to name the output file?
   ( 8 characters maximum)
CP140151
   Type any comments that you would like written into the file;
   enter a single period on a line (".", to end the comments:
       (Limit: 80 characters per line)
COP XFIL=T140 YFIL=T151
.
   Enter the format to be used,
       (40 characters maximum)
   or type "*" for free format,
   or just hit RETURN to use  (2(3X,E15.7))

   By default the data will be written in POLAR form,
   unless you type R for rectangular form
```

16.61

Do you wish to have the data plotted?
Y
Choose one of the following:

        1.   Real part
        2.   Imaginary part
        3.   Magnitude
        4.   Log of Magnitude
        5.   Phase (radians)
        6.   Phase (degrees)
1
The first two lines of the caption are:

        X file: T140   ,   Y file: T151   10/08/85
        Coherent Output Power - COP   11:41:00

What would you like for the next line?   (Max: 9 lines)
Type a single period (".") to finish.
TEST PROBLEM DEMO
What would you like for the next line?   (Max: 9 lines)
Type a single period (".") to finish.
.
Plotting, please wait...

PLOT NO.   1 WITH THE TITLE

HAS BEEN COMPLETED.

PLOT ID. READS
PLOT 1   11.42.00   TUES   8 OCT, 1985   JOB=AFWAL   ,
ISSCO
 DISSPLA 9.2

DATA FOR PLOT

NO. OF CURVES DRAWN   1

HORIZ. AXIS LENGTH   6.0 INS.
VERT. AXIS LENGTH   8.0 INS.

HORIZ. ORIGIN 0.1000E+01
VERT. ORIGIN 0.0000E+00

HORIZ. AXIS LINEAR
STEP SIZE 0.5000E+00 UNITS/INCH

VERT. AXIS LINEAR
STEP SIZE 0.2812E-02 UNITS/INCH

        ....

```
      . LOCATION OF CURRENT PHYSICAL ORIGIN .
      . X=    1.50       Y=    1.12      INCHES .
      .       FROM LOWER LEFT CORNER OF PAGE    .
      . . . . . . . . . . . . . . . . . . . . . . . . . . . . . . . . . . . .



      Choose a data set:

            1 - Average X input over N records - x(t)
            2 - Average Y input over N records - y(t)
            3 - FFT of average X input - X(f)
            4 - FFT of average Y input - Y(f)
            5 - Auto Spectrum of X input - Sxx
            6 - Auto Spectrum of Y input - Syy
            7 - Cross Spectrum - Sxy
            8 - Cross Spectrum - Syx
            9 - Transfer Function - HO
           10 - Transfer Function - HA
           11 - Transfer Function - H1
           12 - Transfer Function - H2
           13 - Coherence Function - COH
           14 - Coherent Output Power - COP
           15 - Non-Coherent Power - NCP
           16 - Signal-to-Noise Ratio - SNR

      Or type Q to quit.
Q
 END OF DISSPLA 9.2 -- 2003 VECTORS IN 1 PLOTS.
 RUN ON 10/8/85 USING SERIAL NUMBER 999 AT ISSCO
 PROPRIETARY SOFTWARE PRODUCT OF ISSCO, SAN DIEGO, CA.
 977 VIRTUAL STORAGE REFERENCES; 5 READS; 0 WRITES.
 **** STOP

OK, COMO -END
```

16.63

```
CCCCCCCCCCCCCCCCCCCCCCCCCCCCCCCCCCCCCCCCCCCCCCCCCCCCCCCCCCCCCCCCCCCCCCCC
C                                                                      C
C   PROGRAM: CFFTA                                                     C
C                                                                      C
C   PURPOSE: A dual channel FFT system analyzer with averaging.       C
C            Input is obtained through the subroutine RECIN and        C
C            sent to the AP-120S for processing.  The data input       C
C            is simulated; data records are retrieved from             C
C            disk files rather than on-line samplers.                  C
C                                                                      C
C   AUTHOR: Michael R. Gray, 2Lt, AFWAL/AAAI-4, Ext 52766             C
C                                                                      C
C   COMPLETED: May 1985; Developed on a Harris model 800-13 computer   C
C                                                                      C
C   NOTE: It it the author's contention that an extensive header       C
C         section (i.e. comment block) is not the only way of making   C
C         the form and function of a software package understood       C
C         to others.  Explanation of the program logic is              C
C         interleaved within the source code statements.               C
C                                                                      C
CCCCCCCCCCCCCCCCCCCCCCCCCCCCCCCCCCCCCCCCCCCCCCCCCCCCCCCCCCCCCCCCCCCCCCCC

      IMPLICIT INTEGER(A-Z)      ! Every variable integer unless specified
      REAL TEMP,DATA(2048)       ! A temporary storage, data passing array
      CHARACTER*1 REPLY          ! Recieves replies from the user (Y or N)
      CHARACTER*40 XFORMT,YFORMT ! X data file format, Y data file format
      INTEGER*1 NAMES(17)        ! Variable used to obtain filenames
                                 ! from terminal
      INTEGER*1 XFILE(9),YFILE(9) ! X data file name, Y data file name
C
C  Common APADDR contains the addresses of data sets in the AP memory
C
      COMMON /APADDR/ INVBASE,XTBASE,YTBASE,XFBASE,YFBASE,SXXBASE,
     1     SYYBASE,SXYBASE,SYXBASE,HFBASE,HABASE,COPBASE,COHBASE,
     2     H1BASE,H2BASE,TEMPADR
C
C  Common DCOUNTS contains data set size defining parameters
C
      COMMON /DCOUNTS/ RECSIZ,RECSIZX2,HAFPL1,RECORDS,XSIZE,YSIZE
C
C  Common DSTORE contains the data which is passed to and from the AP
C
      COMMON /DSTORE/ DATA
C
C  Common FNAMES contains file defining parameters
C
      COMMON /FNAMES/ XLU,YLU,XFILE,YFILE,XFORMT,YFORMT
C
C  Common TERMLFN contains the Logical file number for the terminal
C
      COMMON /TERMLFN/ TERMLU
C
C  Data XLU is logical file number(LFN) for X file, YLU is LFN for
C  Y file, and TERMLU is LFN for terminal I/O(i.e. user response)
C
      DATA XLU/98/,YLU/99/,TERMLU/0/
C
CCCCCCCCCCCCCCCCCCCCCCCCCCCCCCCCCCCCCCCCCCCCCCCCCCCCCCCCCCCCCCCCCCCCCCCC
C                   Begin executable statements                        C
CCCCCCCCCCCCCCCCCCCCCCCCCCCCCCCCCCCCCCCCCCCCCCCCCCCCCCCCCCCCCCCCCCCCCCCC
C
C     DO UNTIL(correct parameter obtained)
```

```fortran
C
      REWIND(TERMLU)              ! Clear the terminal screen
      WRITE(TERMLU,20)
20    FORMAT(' ',' Enter X and Y channel filenames(separated by a'
     1  ,' comma):',/)
      READ(TERMLU,30) (NAMES(I),I=1,17)
30    FORMAT(2CA1)
      COMMA=0                     ! Set flag indicating comma not encountered
      YINDEX=1                    ! Set index for Y file name characters
      DO 60 INDEX=1,17            ! DO UNTIL: X and Y filenames separated
        IF((NAMES(INDEX).NE.',').AND.(COMMA.EQ.0)) THEN
          XFILE(INDEX)=NAMES(INDEX)
        ELSE IF(NAMES(INDEX).EQ.',') THEN
          COMMA=1
        ELSE
          YFILE(YINDEX)=NAMES(INDEX)
          YINDEX=YINDEX+1
        END IF
60    CONTINUE                    ! END DO UNTIL
C
      REWIND(TERMLU)              ! Clear the terminal screen
      WRITE(TERMLU,70) XFILE,YFILE
70    FORMAT(' ',' X-file: ',8A1,1X,'  Y-file: ',8A1,'.',
     1  '  Is this correct?(Y/N):')
      READ(TERMLU,80) REPLY
80    FORMAT(A1)
      IF((REPLY.NE.'Y').AND.(REPLY.NE.'y'))GO TO 10
C     END DO UNTIL
C
C     DO UNTIL(AP initialized without error)
90    CONTINUE
      REWIND(TERMLU)              ! Clear the terminal screen
      WRITE(TERMLU,100)
100   FORMAT(' ',' Initializing AP ...')
      CALL APASGN(1,1,STAT)       ! Check if AP is available
      IF(STAT.LT.0) THEN
        WRITE(TERMLU,110)
110   FORMAT(' ',' AP busy, waiting ...')
      END IF
      CALL APINIT(1,0,STAT)       ! Initialize the AP and clear
      CALL APWR                   ! Wait until AP initialization complete
      IF(STAT.LT.0)GO TO 90       ! Main data memory
C     END DO UNTIL
C
      CALL SETUP                  ! Initialize data channels
C
C  Initialize parameters dependent on record count and size
C
      RECSIZX2=RECSIZ+RECSIZ      ! RECSIZ times two
      RECSIZP2=RECSIZ+2           ! RECSIZ plus two
      HAFPL1=(RECSIZ/2)+1         ! Number of complex data elements
      TEMP=1.0/(REAL(RECORDS))    ! Record count inverse, for averaging
C
C  Initialize AP address pointers
C
      INVBASE=0                   ! Inverse of record count
      XTBASE=1                    ! X channel data
      YTBASE=XTBASE+RECSIZ        ! Y channel data
      XFBASE=YTBASE+RECSIZP2      ! X channel fourier transform
      YFBASE=XFBASE+RECSIZP2      ! Y channel fourier transform
      SXXBASE=YFBASE+RECSIZP2     ! Auto-spectra of X channel data
      SYYBASE=SXXBASE+RECSIZP2    ! Auto-spectra of Y channel data
      SXYBASE=SYYBASE+RECSIZP2    ! Cross-spectra: X(conj)Y
      SYXBASE=SXYBASE+RECSIZP2    ! Cross-spectra: Y(conj)X
      ...........................  ! ......................
```

16.65

```
      CCPBASE=HABASE+RECSIZP2      ! Coherent C/F power sequence
      CCHBASE=COPSASE+RECSIZP2     ! Coherence function sequence
      M1BASE=CCHBASE+RECSIZP2      ! Freq response(SXY/SXX)
      M2BASE=M1BASE+RECSIZP2       ! Freq response(SYY/SYX)
      TEMPADR=M2BASE+RECSIZP2      ! Temporary storage
C
      CALL APPUT(TEMP,INVBASE,1,2)  ! Put inverse of record count in AP
C
      REWIND(TERMLU)                          ! Clear the terminal screen
      WRITE(TERMLU,150) RECORDS,RECSIZ ! Let user know if RECSIZ was adjuste
150   FORMAT(' ',' Processing ',I4,' record(s) of ',I4
     1,' samples each ...')
C
C**********************************************************************
C            BEGIN AVERAGING DUAL CHANNEL FOURIER ANALYZER          *
C**********************************************************************
C
C     DO UNTIL(Specified number of records processed)
      DO 200 INDEX=1,RECORDS
C
        CALL APWR                  ! Wait for previous routine completion
        CALL RECCRD                ! X and Y records to AP
        CALL APWC                  ! Wait for data transfer completion
C
        CALL RFFTB(XTBASE,XFBASE,RECSIZ,1)   ! Transform X data (R->C)
        CALL RFFTSC(XFBASE,RECSIZ,3,1)       ! Scale the results (C->C)
        CALL RFFTB(YTBASE,YFBASE,RECSIZ,1)   ! Transform Y data (R->C)
        CALL RFFTSC(YFBASE,RECSIZ,3,1)       ! Scale the results (C->C)
C
        CALL ASPEC(XFBASE,SXXBASE,HAPPL1)  ! X auto-spectra (C->R)
        CALL ASPEC(YFBASE,SYYBASE,HAPPL1)  ! Y auto-spectra (C->R)
C
        CALL CSPEC(XFBASE,YFBASE,SXYBASE,HAPPL1) ! Cross-spectra XY(C->C)
        CALL CSPEC(YFBASE,XFBASE,SYXBASE,HAPPL1) ! Cross-spectra YX(C->C)
C
        CALL CVRCIP(XFBASE,2,TEMPADR,2,HAPPL1) ! Reciprocal of X(C->C)
        CALL CVMA(YFBASE,2,TEMPADR,2,HFBASE,2,
     1                    HFBASE,2,HAPPL1,1) ! Transfer sequence(C->C)
C
200   CONTINUE
C     END DO UNTIL
C
      CALL CLENUP        ! Disconnect data input channels
C
C  Divide by record count to get the averaged quantities
C
      CALL VSMUL(SXXBASE,1,INVBASE,SXXBASE,1,HAPPL1)    ! (R->R)
      CALL VSMUL(SYYBASE,1,INVBASE,SYYBASE,1,HAPPL1)    ! (R->R)
      CALL CVSMUL(SYXBASE,2,INVBASE,SYXBASE,2,HAPPL1)   ! (C->C)
      CALL CVSMUL(SXYBASE,2,INVBASE,SXYBASE,2,HAPPL1)   ! (C->C)
      CALL CVSMUL(HFBASE,2,INVBASE,HFBASE,2,HAPPL1)     ! (C->C)
C
C  Compute transfer sequence based on auto-spectra of X and Y
C
      CALL VCIV(SXXBASE,1,SYYBASE,1,HABASE,1,HAPPL1)
      CALL VSQRT(HABASE,1,HABASE,1,HAPPL1)
C
C  Compute transfer sequence based on X auto-spectra and cross-spectra
C
      CALL CFVDIV(SXYBASE,2,SXXBASE,1,M1BASE,2,HAPPL1)
C
C  Compute transfer sequence based on Y auto-spectra and cross-spectra
C
      CALL CVRCIP(SYXBASE,2,TEMPADR,2,HAPPL1)
      CALL CFVMUL(TEMPADR,2,SYYBASE,1,M2BASE,2,HAPPL1)
```

16.66

```
C   Compute coherence sequence (Using H1 and H2)
C
      CALL CVRCIP(H2BASE,2,TEMPACR,2,HAFPL1)
      CALL CVMUL(H1BASE,2,TEMPADR,2,CCHBASE,2,HAFPL1,1)
      CALL VSGRT(CCHBASE,1,CCHBASE,1,RECSIZP2)
C
C   Compute coherent output power sequence-wait for execution completion
C
      CALL CRVMUL(CCHBASE,2,SYYBASE,1,COPBASE,2,HAFPL1)
      CALL APWR
C
C*******************************************************************
C          END AVERAGING DUAL CHANNEL FOURIER ANALYZER            *
C*******************************************************************
C
      REWIND(TERMLU)              ! Clear terminal screen
      WRITE(TERMLU,290)
290   FORMAT(' ',' Do you want results displayed?(Y/N):'
     1,/,'   (Plots go to Textronics terminal.)')
      READ(TERMLL,30) REPLY
      IF((REPLY.EQ.'Y').OR.(REPLY.EQ.'y')) THEN
        CALL DISPLA(XFILE,YFILE)
      END IF
      REWIND(TERMLU)              ! Clear terminal screen
      WRITE(TERMLU,300)
300   FORMAT(' ',' Do you want results saved?(Y/N):')
      READ(TERMLL,30) REPLY
      IF((REPLY.EQ.'Y').OR.(REPLY.EQ.'y')) THEN
        CALL STORE
      END IF
C
      CALL APRLSE          ! Release the AP
C
      STOP
      END
C
CCCCCCCCCCCCCCCCCCCCCCCCCCCCCCCCCCCCCCCCCCCCCCCCCCCCCCCCCCCCCCCCCCCCCCC
```

APPENDIX D

GLOSSARY OF DATA FILE NAMES:

GENERAL NOTES:

o   All files will have names of eight characters or less.

o   All data will be stored in polar form (magnitude, phase).
     Phase is modulo 2*PI. Range: -PI <= PHASE <= +PI.

o   Input and output files and analytical frequency response
     sequences (FRF's) will need only one identifying number.

o   Calculated frequency response sequences, cross spectra,
     auto spectra, correlations, coherence sequences, etc.
     will need two identifying numbers, indicating the two
     sequences used in calculating them.

KEY:

FILENAMES FOR INPUT/OUTPUT SEQUENCES

First and second character (from RIGHT):
        Two-digit identifier
Third character (from RIGHT):
        One-digit classification number:
        0   Experimental data originating in time domain
        1   Analytical sequence originating in time domain
        2   Analytical sequence originating in frequency domain
        3   Analytical frequency response sequence originating
             in frequency domain.
        4-9 Unspecified as of 20 June, 1985
Fourth character (from RIGHT):
        F   Sequence currently in frequency domain
        T   Sequence currently in time domain
Fifth through eighth character (from RIGHT):
        Unspecified as of 20 June, 1985;
        may be used for identification/classification

FILENAMES FOR FRF's etc.

First through third character (from RIGHT):
        Identifying number of output sequence for FRF's,
        or second operand of products, as in cross spectra.
Fourth through sixth character (from RIGHT):
        Identifying number of input sequence for FRF's,
        or first operand of products, as in cross spectra.
Seventh and eighth character (from RIGHT):
        SA   Auto spectrum
        SC   Cross spectrum
        FR   Frequency response sequence (analytical)
        H1   Frequency response from auto spectrum of input
        H2   Frequency response from auto spectrum of output
        HA   Frequency response from auto spectra of input and output

```
HO    Frequency response from ratio of transforms
CO    Coherence sequence
CP    Coherent output power
NP    Non-coherent output power
SN    Signal-to-noise ratio
IR    Impulse response (IFFT of FR)
I1    Impulse response (IFFT of H1)
I2    Impulse response (IFFT of H2)
IA    Impulse response (IFFT of HA)
IO    Impulse response (IFFT of HO)
CT    Correlation calculated in Time domain
CF    Correlation calculated in Frequency domain
```

FILE FORMAT:

The top line of each data file contains 3 integers
in FORMAT(3(3X,I10)):
    the number of samples per record;
    the number of records;
    the number of comment lines immediately following (may be zero).

The next few line(s) are comments, that is, information
inserted by the user, and ignored by the computer.
The number of comment lines is given by the third integer
of the top line.

The first line after the comment lines contains the FORMAT to be
used for the data lines that follow (the data pairs or samples).
Typically, it will be: (2(3X,E15.7))
The format of this line itself is: (A40)

The next line contains the "record header" which is also present
at the beginning of each record (survey). It is treated like
a comment for the user's benefit, and thus ignored by the computer
when the file is read in. However, if a file is created
by a program, that program is required to write these
into the file (unless the user will insert them manually),
as their presence will be expected when another program
reads the file. It is suggested that two integers should be
included: the number of the current record, and the total
number of records in the file. Something along the line of
record number M out of N total records (FORMAT (2(3X,I10))).

Finally, a single record (survey) worth of data is written according
to the format specified above.

If there are multiple records, the first is written according to
the format specified above, and the rest will be prefaced with a
"record header" immediately followed by the data itself.

FILES:

16.69

T116.D	Sixteen-point reference sequence [1,1,1,0,0,0,0,0,0,0,0,0,0,0,1,1]
T140.D	Four-point reference sequence [1,1,0,0]
T141.D	Four-point reference sequence [0,1,1,0]
T142.D	Four-point reference sequence [0,0,1,1]
T143.D	Four-point reference sequence [1,0,0,1]
T144.D	IFFT of [F140 x FRF340]
T150.D	Four-point reference sequence [.3,.3,0,0]
T151.D	Four-point reference sequence [0,.3,.3,0]
T152.D	Four-point reference sequence [0,0,.3,.3]
T153.D	Four-point reference sequence [.3,0,0,.3]
T160.D	128 point AC Square wave, 8 cycles, amplitude +/- 0.5 (First rise at n=0)
T161.D	T160.D * 0.3
T162.D	T160 + SIN8.0 + SIN16.0 + SIN24 + SIN32
T163.D	T160 + SIN8.PI + SIN16.PI + SIN24 + SIN32
T164N.D	20 records T162.D and 20 records T163.D + 1% URN each record
T166.D	T160.D * FRF with antiresonance at N=23
T168.D	T160.D * FRF with resonance at N=23
T160N.D	40 records of T160 + 1% URN
T170.D	128 point reference sequence, 8 cycle square wave, amplitude = 1.0, first rise at n=0, DC
T171.D	128 point reference sequence, 8 cycle square wave, amplitude = 0.3,(T170 * .3) first rise at n=8
T172.D	T171 + SIG8
T175.D	128 point reference sequence, 16 cycle square wave, amplitude = 1.0, first rise at n=0, DC
T180.D	Eight-point reference sequence [1,1,0,0,0,0,1,1]
T316.D	IFFT of F316
T370.D	IFFT of F370
N10T170.D	10 records of T170 with 1% uniform random noise added
N10T171.D	10 records of T171 with 1% uniform random noise added
X10T170.D	10 records of T170 (repeated with no noise)
X10T171.D	10 records of T171 (repeated with no noise)
F116.D	FFT of T116
F140.D	FFT of T140
F141.D	FFT of T141
F142.D	FFT of T142
F143.D	FFT of T143
F144.D	F140 x FRF340
F160.D	FFT of T160
F161.D	FFT of T161
F162.D	FFT of T162
F163.D	FFT of T163
F166.D	FFT of T166
F168.D	FFT of T168
F170.D	FFT of T170
F171.D	FFT of T171 (Residing in TEST)
F175.D	FFT of T175
F316.D	Symmetrized version of F116 (Residing in TEST)
F370.D	Symmetrized version of F170
FRF340.D	Four point reference FRF

1984 USAF-SCEEE RESEARCH INITIATION PROGRAM

Sponsored by the

AIR FORCE OFFICE OF SCIENTIFIC RESEARCH

Conducted by the

SOUTHEASTERN CENTER FOR ELECTRICAL ENGINEERING EDUCATION

FINAL REPORT

FAR-INFRARED ABSORPTION PROFILES FOR DISTRIBUTED
SHALLOW DONORS IN GaAs-GaAlAs HETEROSTRUCTURES

Prepared by: Ronald L. Greene

Far-Infrared Absorption Profiles for Distributed
Shallow Donors in GaAs-GaAlAs Heterostructures

Final Report

Ronald L. Greene
University of New Orleans
New Orleans, Louisiana

ABSTRACT

The results of calculations of multiple-well effects
upon the energies of shallow donors, and their influence
upon far-infrared absorption profiles is reported. The
binding energies of the ground and first few excited states
are significantly affected by the finite width of the
barrier when the donor is located near an interface or
within a barrier layer. For typical barrier widths, the
excited states are affected for all donor positions. The
profiles show several peaks, the strongest corresponding to
donors located at the centers of a well or a barrier.

17.1

I. INTRODUCTION

The objective of the research described in this report was the calculation of absorption line profiles for shallow donors in GaAs-$Ga_{1-x}Al_xAs$ quantum-well structures. Two major extensions to our previous calculations were examined. These extensions were 1) realistic treatment of the finite width of the $Ga_{1-x}Al_xAs$ barrier layers of typical heterostructures, and 2) inclusion of higher excited states in the absorption profiles. We found that each of these contribute significantly to the final absorption profiles. (The "we" in this report refers to myself and Pat Lane, a physics graduate student at the University of New Orleans.)

The most significant results of this research are that shallow donor binding energies can be lowered significantly by the presence of neighboring wells, even for barriers several hundred Angstroms in thickness; and that donors located at the center of a $Ga_{1-x}Al_xAs$ barrier should be characterized by an absorption peak lower in energy, but otherwise similar to that due to donors located at the center of a GaAs well.

II. MULTIPLE WELL EFFECTS

In this section we report calculations of the binding energies for the ground state (1s-like) and low lying excited states ($2p_{\pm}$-like) of a hydrogenic donor associated

17.2

with the first subband level. Our model consists of a donor
atom placed in a periodic square well potential. The
subband energy levels are those of the periodic square well.
Results have been obtained for various values of the quantum
well width and potential barrier width and height. We have
considered the cases of the impurity ion located at the
center of a GaAs well, at the center of a $Ga_{1-x}Al_xAs$
barrier, and at various locations in between, including the
barrier-well interface. (This section has been adapted from
a manuscript by Pat Lane and myself which has been submitted
for publication.)

General Theory

Using the effective mass approximation, the Hamiltonian
of a hydrogenic donor in a $GaAs-Ga_{1-x}Al_xAs$ heterostructure
with a uniform magnetic field applied along the growth axis
can be expressed in dimensionless form as

$$H = \frac{1}{m^*} \nabla^2 - \frac{2}{r} + \gamma L_z + \frac{1}{4}\gamma^2 + V_B(z) \quad . \tag{1}$$

The effective Bohr radius in GaAs, $a_o^* = \hbar^2\epsilon/m^*e^2$, is the
unit of length and the effective Rydberg, $R^* = e^2/2\epsilon a_o^*$, is
the unit of energy. Using the GaAs values for the effective
mass and the dielectric constant, $a_o^* = 98.7$ Å and $R^* = 5.83$
meV. The quantity γ in Eq. (1) is a dimensionless measure
of the magnetic field, essentially the ratio of the magnetic
contribution to the energy to the effective Rydberg.[1] $V_B(z)$

excited states are a decrease in the central peak and a corresponding increase in the peak associated with the well centered at z = 2.0. The probability density of the ground state is more strongly affected by the interfacial position of the impurity. The probability of the electron being found in the 1.5<z<2.5 well is nearly as large as that for the m=±1 excited state. More surprisingly, there is a significant probability associated with the -2.5<z<-1.5 well. This is a manifestation of the p_o-like symmetry of the on-edge ground state, as discussed earlier.

Probability densities for heterostructures with small wells and barriers show larger effects, of course. For example, for L=b=0.5a$_o^*$, significant peaks arise in the next nearest wells.

II. ABSORPTION PROFILES

Theory

The theory of absorption of light by atomic systems can be found in standard texts on quantum mechanics.[10] We assume that the donors are well separated so that they do not interact with each other. Since the effective Bohr radius of a shallow donor in GaAs is about 100 Å, and the donors are constricted still further by the applied magnetic field and the quantum wells, this is not a very restrictive approximation for lightly-doped samples ($<10^{16}$ cm^{-3}). We

17.4

also assume that the temperature is low enough that all donors are initially in their ground states. As noted earlier, we take the z-axis along the growth direction for the heterostructure, and consider incident light polarized in the x-direction with intensity I_o.

The power absorbed in electric dipole transitions from a set of initial state (i) to all possible final states (f) is given by

$$P(\omega) = \frac{4\pi^2 e^2 \omega I_o}{h^2 c} \sum_{i,f} |<f|x|i>|^2 \, p_i \delta(\omega - E_{fi}/\hbar). \qquad (7)$$

where ω is the angular frequency of the incident light and E_{fi} is the energy difference between a given final state and the initial state --- $E_{fi} = E_f - E_i$. The quantity p_i is the probability that the donor electron is initially in the state i. Since we are interested in the shape of the absorption profile rather than its absolute expression, we calculate the so-called line shape function defined by

$$I(\omega) = \omega \sum_{i,f} |<f|x|i>|^2 p_i \delta(\omega - E_{fi}/\hbar) . \qquad (8)$$

All the frequency dependence of the absorption profile is contained in $I(\omega)$.

For a bulk semiconductor the sum over i reduces to a single term since the ground state energies of all isolated donors are the same. However, for a quantum well system the ground state energy of a given donor depends on its location

17.5

relative to the quantum well. The sum over i, then, is actually a sum over all the possible positions of the donor impurity. These positions may be considered to be continuously distributed since the donor is many times larger than the lattice spacing. Furthermore, since the energy of a donor is dependent upon only its z-coordinate (z_i), the sum over i may be replaced by an integral over z_i. The probability p_i in this case becomes the linear density of donors, $\lambda(z_i)$. Thus the line shape function is simplified to

$$I(\omega) = \omega \sum_f \int_{\infty}^{\infty} dz_i \lambda(z_i) |<f|x|i>|^2 \delta(\omega - E_{fi}/\hbar) . \quad (9)$$

Because of the cylindrical symmetry of the problem, the initial (ground) states are states of zero angular momentum projection along the z-axis (m=0 states as noted earlier). The matrix elements of the x operator vanish for all final states except those for which m=±1. In addition, we assume that the frequency of incident radiation is such that only the two lowest states for each m value contribute to $I(\omega)$ in the region of interest. The sum over final states is then reduced to a few terms.

For the results presented in the next section we replaced the δ-functions in Eq. (9) with narrow Lorentzians:

$$\delta(\omega) = \frac{\Gamma/\pi}{\omega^2 + \Gamma^2} . \quad (10)$$

This is a numerical approximation, although it mimics to some degree the effects of other broadening mechanisms that have been neglected in obtaining the expression for $I(\omega)$. In any case, we chose the width Γ to be small enough as to have very little effect upon the final profile. This was checked by comparison of results with several values for Γ.

Results and Discussion

We have performed calculations of the line shape function $I(\omega)$ for a uniform distribution of donors and for various combinations of well width ($0.5 < L < 1.5$), barrier width ($0.5 < b < 3.0$), and magnetic field strength ($0.0 < \gamma < 1.0$). All cases have several features in common. Each shows two sets of strong peaks for the lowest energy $m=0$ to $m=\pm 1$ transitions at the energies corresponding to donors located at the center of a well and the center of a barrier. These occur because of the large density of states associated with these locations.[9] For $\gamma = 0.0$, the $m=\pm 1$ transitions are degenerate, whereas for $\gamma > 0.0$ they are separated by 2γ. The (low energy) peak(s) associated with donors at the center of a barrier is (are) significantly stronger than that (those) for donors at the center of a well.

Two weaker sets of peaks occur which correspond to ground to second $m=\pm 1$ excited states ($3p_{\pm}$-like). For most cases these "peaks" do not rise very much above the general background due to their small dipole matrix elements.

In Tables 1-6 I present the $m=0$ to $m=-1$ transition

17.7

energies of donors located at the centers of a barrier or well for a variety of L, b, and γ values. The aluminum fraction is $x=0.3$, and the barrier height is $0.6 \Delta E_g$, where ΔE_g was given earlier. The symbol Δ_{1b} (Δ_{1w}) represents the transition energy for ground to first $m=-1$ excited state for a donor at the center of a barrier (well). The symbol Δ_{2b} (Δ_{2w}) represents the similar transition from ground to second $m=-1$ excited state. For $\gamma>0$ there will be similar energies shifted by 2γ from the values shown in the tables. In all cases strong peaks occur at energies very near Δ_{1b} and Δ_{1w} for uniformly distributed donors.

Also shown in Tables 1-6 are the energies for the lowest $m=0$ to $m=-1$ transition for donors located at an interface between GaAs and $Ga_{1-x}Al_xAs$. This column is labelled Δ_{1i}. Although there is no peak associated with this location for a uniform donor distribution, there is some evidence to suggest that impurities may accumulate at the interfaces between semiconductors. Such an accumulation would produce a local peak in $\lambda(z_i)$ of Eq. (9), and a corresponding peak in the absorption spectrum.

The experimental situation is still not completely clear. Jarosik, et al.[11] have reported good agreement between their far-infrared magnetospectroscopy data and the single-well results of Greene and Bajaj[1] for the donor at the center of the well. Our present calculations should also be in good agreement since the multiple well effects are not very important for such donors in moderate to large

wells and barriers (L, b > a_o^*). The experiments used GaAs-$Ga_{1-x}Al_xAs$ samples doped with donors at or near the center of the GaAs wells, so that it is unlikely that they would have seen a spectral feature associated with donors in a barrier. Similar experiments with doped $Ga_{1-x}Al_xAs$ layers should be of interest in an experimental study of confinement effects.

17.9

REFERENCES

1. Ronald L. Greene and K. K. Bajaj, Phys. Rev. B 31, 913 (1985).

2. R. C. Miller, A. C. Gossard, D. A. Kleinman, and O. Munteanu, Phys. Rev. B 29, 3740 (1984).

3. R. C. Miller, D. A. Kleinman, and A. C. Gossard, Phys. Rev. B 29, 7085 (1984).

4. H. Okimura, S. Misawa, S. Yoshida, and S. Gonda, Appl. Phys. Lett. 46, 377 (1985).

5. For a summary of other experimental work on band offsets see W. I. Wang and F. Stern, in Proceedings of the Twelfth Annual Conference on the Physics and Chemistry of Semiconductors, ed. by R. S. Bauer [J. Vac. Sci. Technol. 3, 1280 (1985)].

6. H.J.Lee, L.Y.Juravel, J.C. Woolley, and A. J. Springthorpe, Phys. Rev. B 21, 659 (1980).

7. S. Huzinaga, J. Chem. Phys. 42, 1293 (1965).

8. S. Chaudhuri, Phys. Rev. B 28, 4480 (1983).

9. Ronald L. Greene and K. K. Bajaj, submitted for publication.

10. See, for example, Leonard I. Schiff, Quantum Mechanics, 3rd Ed. (New York: McGraw-Hill, 1968).

11. N. C. Jarosik, B. D. McCombe, B. V. Shanabrook, J. Comas, John Ralston, and G. Wicks, Phys. Rev. Lett. 54, 1283 (1985).

FIGURE CAPTIONS

Figure 1.   Binding energy of the ground state of a shallow
donor in a superlattice as a function of donor position.
The aluminum fraction is $x = 0.3$, and $L = 1.0a_o$.

Figure 2.   Binding energy of the lowest $m = \pm 1$ excited
states of a shallow donor in a superlattice as a function of
donor position.   The aluminum fraction is $x = 0.3$, and
$L = 1.0a_o$.

Figure 3.   Probability density of the ground state (solid
line) and lowest $m = \pm 1$ states (dashed line) for the donor
impurity at the center of a GaAs well.

Figure 4.   Probability density of the ground state (solid
line) and lowest $m = \pm 1$ states (dashed line) for the donor
impurity at an edge of a GaAs well.

Figure 1.

17.12

Figure 2.

17.13

ELECTRON POSITION

PROBABILITY DENSITY

Figure 3.

17.14

PROBABILITY DENSITY

ELECTRON POSITION

Figure 4.

17.15
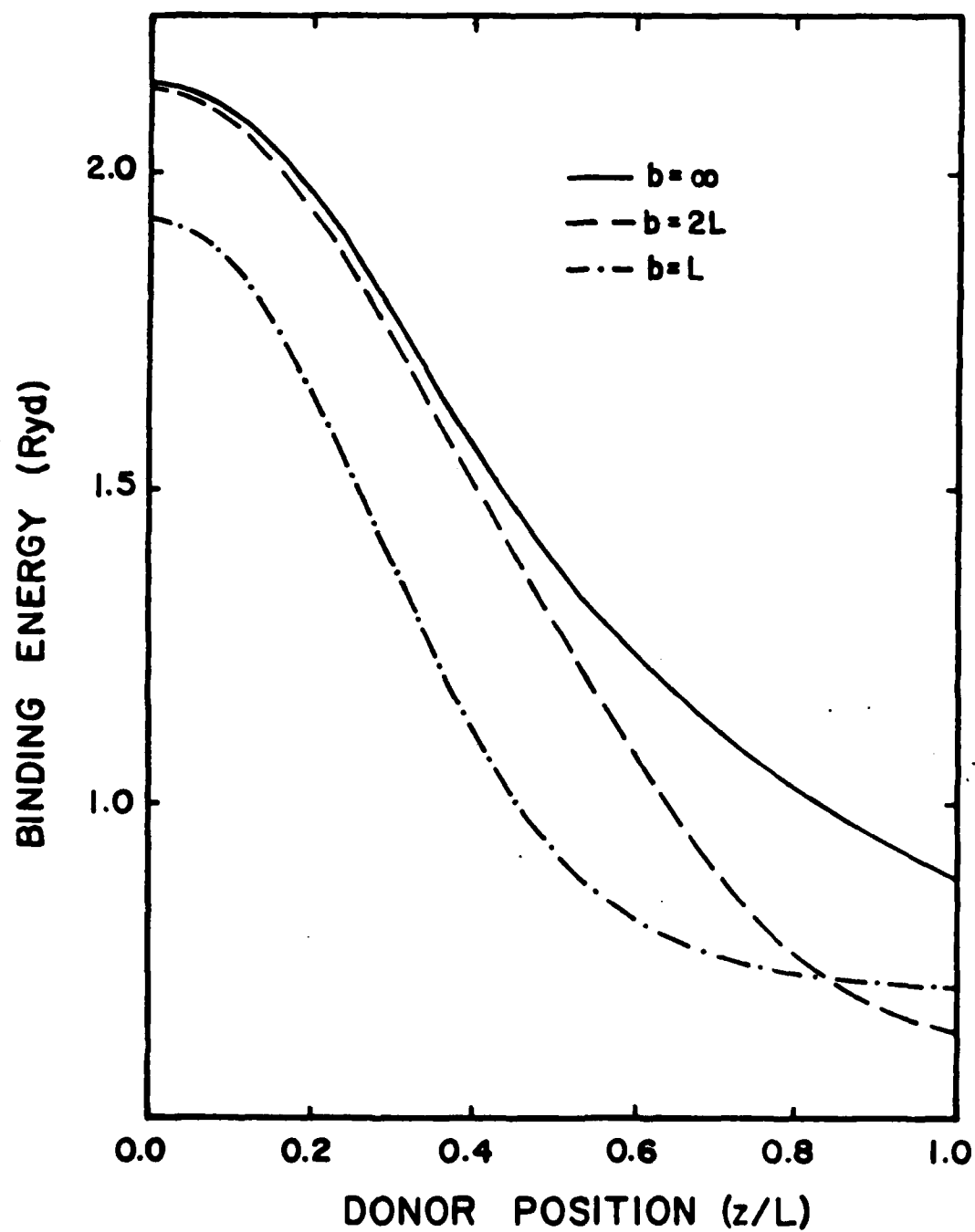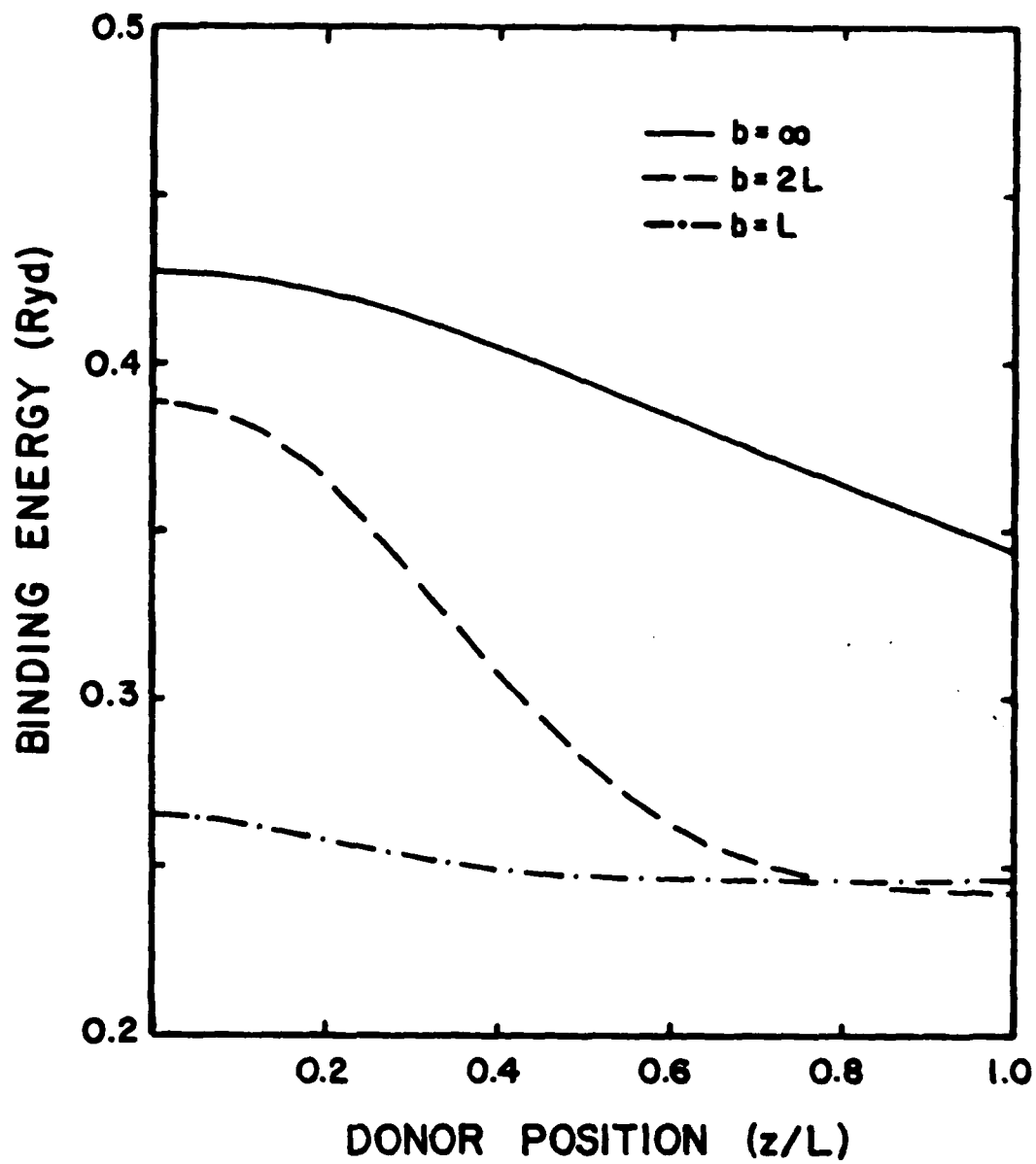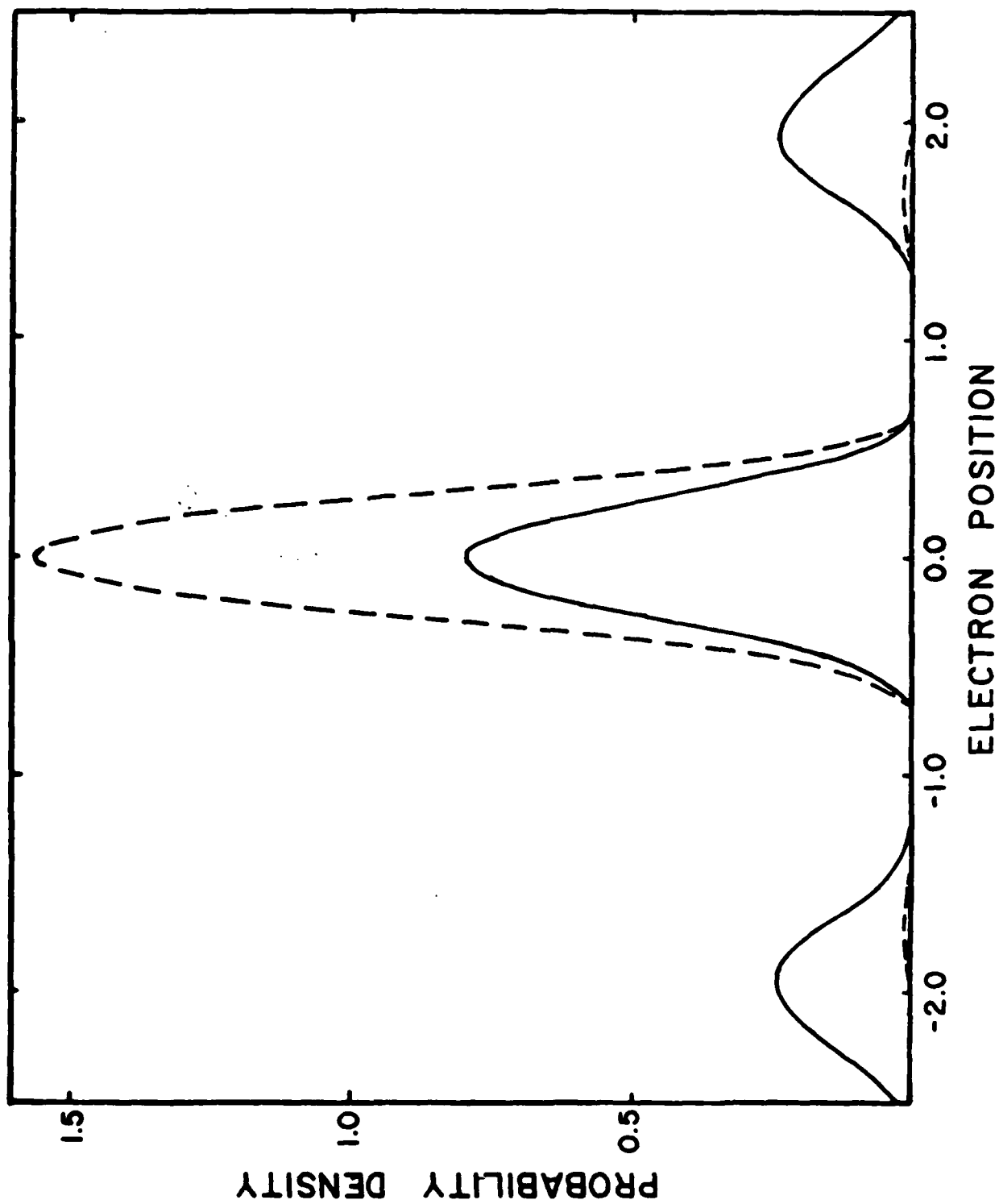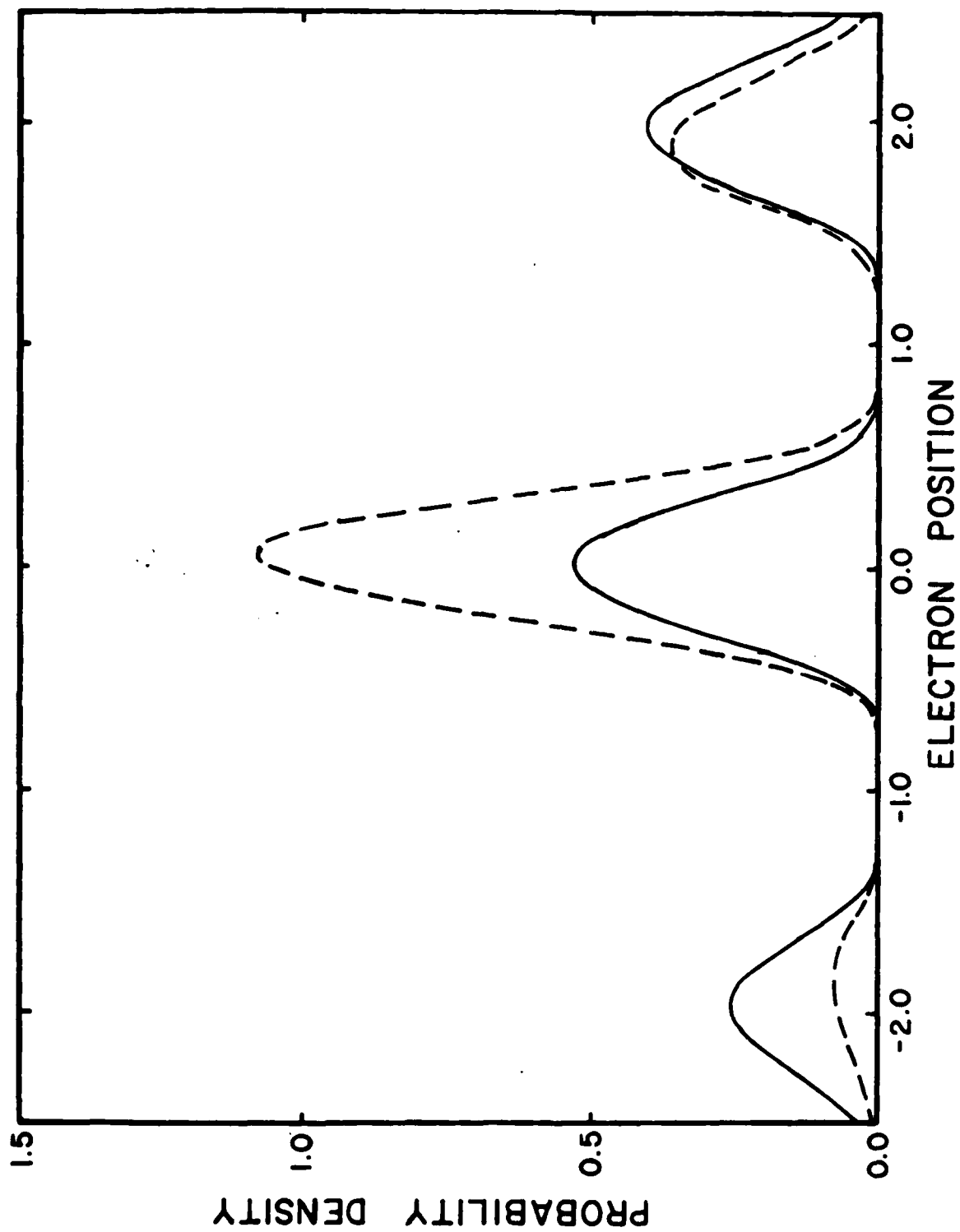
L(A)	b(A)	Δ_{1b}	Δ_{2b}	Δ_{1w}	Δ_{2w}	Δ_{1i}
50	50	0.64	0.78	1.07	1.21	0.74
50	100	0.59	0.73	1.92	2.07	1.06
100	50	0.58	0.72	1.42	1.56	0.63
100	100	0.47	0.61	1.66	1.81	0.68
100	200	0.37	0.51	1.73	1.96	1.01
150	150	0.37	0.51	1.53	1.74	0.61
150	300	0.23	0.36	1.50	1.76	0.74

Table 1. Transition energies for donors located at the center of a barrier (Δ_{1b} and Δ_{2b}), center of a well (Δ_{1w} and Δ_{2w}), and the interface (Δ_{1i}). The magnetic field strength is $\gamma = 0.0$. Energies are in GaAs effective Rydbergs (5.83 meV).

L(A)	b(A)	Δ_{1b}	Δ_{2b}	Δ_{1w}	Δ_{2w}	Δ_{1i}
50	50	0.57	0.89	1.01	1.33	0.67
50	100	0.51	0.83	1.85	2.18	0.99
100	50	0.50	0.82	1.35	1.68	0.55
100	100	0.39	0.70	1.57	1.88	0.60
100	200	0.27	0.56	1.62	1.99	0.91
150	150	0.28	0.57	1.42	1.77	0.53
150	300	0.15	0.42	1.39	1.80	0.64

Table 2. Transition energies for donors located at the center of a barrier (Δ_{1b} and Δ_{2b}), center of a well (Δ_{1w} and Δ_{2w}), and the interface (Δ_{1i}). The magnetic field strength is $\gamma = 0.2$. Energies are in GaAs effective Rydbergs.

L(A)	b(A)	Δ_{1b}	Δ_{2b}	Δ_{1w}	Δ_{2w}	Δ_{1i}
50	50	0.57	1.00	1.03	1.48	0.68
50	100	0.49	0.92	1.86	2.30	1.01
100	50	0.49	0.92	1.37	1.82	0.55
100	100	0.37	0.78	1.57	1.95	0.61
100	200	0.24	0.60	1.58	2.10	0.88
150	150	0.24	0.62	1.38	1.82	0.53
150	300	0.13	0.48	1.36	1.93	0.61

Table 3. Transition energies for donors located at the center of a barrier (Δ_{1b} and Δ_{2b}), center of a well (Δ_{1w} and Δ_{2w}), and the interface (Δ_{1i}). The magnetic field strength is $\gamma = 0.4$. Energies are in GaAs effective Rydbergs.

L(A)	b(A)	Δ_{1b}	Δ_{2b}	Δ_{1w}	Δ_{2w}	Δ_{1i}
50	50	0.57	1.12	1.07	1.61	0.69
50	100	0.49	0.99	1.88	2.39	1.04
100	50	0.49	1.02	1.41	1.95	0.55
100	100	0.35	0.85	1.57	2.03	0.62
100	200	0.21	0.63	1.57	2.21	0.87
150	150	0.22	0.65	1.37	1.99	0.53
150	300	0.11	0.51	1.35	2.06	0.60

Table 4. Transition energies for donors located at the center of a barrier (Δ_{1b} and Δ_{2b}), center of a well (Δ_{1w} and Δ_{2w}), and the interface (Δ_{1i}). The magnetic field strength is $\gamma = 0.6$. Energies are in GaAs effective Rydbergs.

L(A)	b(A)	Δ_{1b}	Δ_{2b}	Δ_{1w}	Δ_{2w}	Δ_{1i}
50	50	0.58	0.82	1.12	1.73	0.72
50	100	0.48	1.06	1.90	2.48	1.08
100	50	0.49	1.09	1.44	2.06	0.56
100	100	0.33	0.91	1.59	2.13	0.63
100	200	0.20	0.66	1.58	2.34	0.86
150	150	0.21	0.68	1.37	2.10	0.54
150	300	0.10	0.58	1.36	2.19	0.59

Table 5. Transition energies for donors located at the center of a barrier (Δ_{1b} and Δ_{2b}), center of a well (Δ_{1w} and Δ_{2w}), and the interface (Δ_{1i}). The magnetic field strength is $\gamma = 0.8$. Energies are in GaAs effective Rydbergs.

L(A)	b(A)	Δ_{1b}	Δ_{2b}	Δ_{1w}	Δ_{2w}	Δ_{1i}
50	50	0.59	1.28	1.16	1.85	0.74
50	100	0.48	1.11	1.93	2.53	1.12
100	50	0.49	1.15	1.48	2.17	0.57
100	100	0.33	0.97	1.61	2.23	0.64
100	200	0.19	0.70	1.59	2.45	0.86
150	150	0.20	0.72	1.38	2.21	0.54
150	300	0.09	0.67	1.37	2.31	0.59

Table 6. Transition energies for donors located at the center of a barrier (Δ_{1b} and Δ_{2b}), center of a well (Δ_{1w} and Δ_{2w}), and the interface (Δ_{1i}). The magnetic field strength is $\gamma = 1.0$. Energies are in GaAs effective Rydbergs.

17.18

Final Technical Report

TO: Southeastern Center for Electrical Engineering Education

AS: Contractor for

                        United States Air Force (AFOSR)
                        Contract F49620-82-C-0035
                        Subcontract Number 84 RIP 18

Title: "Effect of Pole Pieces on the Axial Magnetic Field in Traveling
         Wave Tubes:

Principal Investigator:

                        Dr. James D. Patterson
                        Professor Physics and Space Sciences
                        Florida Institute of Technology
                        Melbourne, FL 32901

Signature: *James D. Patterson*

Date: *30 October 1985*

Abstract

Magnetostatic field calculations were done for   permanent magnets surrounded by permeable media and vacuum. Geometries were selected so as to be relevant to the actual geometries of traveling wave tubes. Most of the calculations were on two dimensional analogs of the actual three dimensional situation in traveling wave tubes. As much as possible we did four calculations for each magnet geometry. These four cases were the magnets with and without permeable magnetic shims and with and without spatial fluctuations in the strengths of the magnets. Our main objective was to get an idea of how the shims would smooth out changes in magnetic field and its spatial fluctuation.   In all cases we assumed the shims were not saturated. As an adjunct to the report, we summarized the basic magnetostatics, some numerical techniques, some relevant properties of actual magnets, and some appropriate references.

The results we have are presented as graphs, equipotential plots, elevation (or potential) plots and field plots. Several things became apparent to us in the course of doing this work. The first was that the problem is large. Realistic field calculations for a variety of magnetic structures appropriate to travelling wave tubes would be a very large problem. Another was that small pieces of the problem were addressable, but the whole problem would be a major project. What we have in mind here is that a problem as to how permeable material could modify the near axis field from the TWT structures is manageable. We have some examples in this report. But to go ahead from there and predict how small variations in magnetic properties would affect the behavior of a given tube is a very large project and one for which experimental results near at hand would be handy to have. We thus recommend planning small projects or large well equipped projects (if the subject is of sufficient

18.2

practical importance). We feel that a project of intermediate scope is harder
to justify. Another fact quickly became apparent. We found
that the writing of programs to efficiently solve the equations of magneto-
statics is a rather major undertaking and if one can find canned programs
that are well adapted to the problem at hand, then one is well advised to
make good use of them.

Many of our results are in terms of potentials rather than fields, simply
because the potential is an easier quantity to deal with than its gradient.

We find, of course, that the shims can act to smooth out the fields,
but to be more quantitative our numerical results must be consulted.

I. Introduction

Two general problems were considered at the beginning of this project.

A. <u>What questions were answerable?</u> This problem resolved itself into two
problems. One was what questions were answerable in principle? The second was
what questions were answerable in the amount of time available and with the
resources at hand? In principle, one can not compute the magnetic field with
arbitrary accuracy. This is not only because of the necessity of performing
numerical analysis - but also because the variations in the properties of the
magnets were not known except that the magnetization of the magnets as a
function of position could be expected to vary by 20% or so. Thus, the type
of questions that need to be answered are:

1. how is the near axial field modified by fluctuations in the
    magnetization of the ring magnets of the TWT's?

2. how is this field modified by the Pole Pieces?

Both questions (1) and (2) can be answered with some degree of accuracy.

B. <u>The other problem was: of those questions that can be answered which
ones are worth answering?</u>   For example, suppose the ring magnets were pre-
cisely characterized, and suppose the numerical methods were completely accurate
and efficient, would an exact calculation of the axial magnetic field be of use?
Academically it would, of course. But practically speaking what one is in-
terested in is the motion of the electrons and their motion is affected by
many things besides the magnetic field. The cathode which supplies the electrons
provides a beam whose properties greatly affect the operation of the tube. The
electrons interact with each other and it is hard to see how a random, non-
periodic fluctuation in the magnetic field (which causes an average force on

18.4

the electron whose magnitude is less than typical forces due to electron-electron interaction forces) would be terribly important. Similarly, the electron beam interacts with the helical coil. Again magnetic force fluctuations smaller than inter-electron forces should not be too important.

Experimentally we know that the gaps in the magnet rings can have important effects on the motion of the electrons and the operation of the traveling wave tube. The gaps arise when the rings are cut in half in order to be assembled on the TWT. The first thing the tube "shimmers" do is to twist the magnets around so that the gaps are not aligned. Shimming refers to adjusting or adding to the pole pieces (or shims) to change the magnetic field.

We start in the next section with a statement of objectives and then follow with a brief summary of the properties of traveling wave tubes as they pertain to our calculation. We follow that with a brief summary of magnetic properties of magnets. We summarize the kinds of calculations that can be made. We present the results of our calculations and summarize what we have learned from them. We then make recommendations for future work.

II. Objectives

The objective is to gain clear insight into the nature of actual near axis fields and thus, to get a feel for what must be done in the manufacture of TWT's in order to reduce the necessity of "shimming" the magnets for proper tube behavior.
(G2)

We will solve the equations of magnetostatics in geometries as near to the actual one as we can manage and report these results. For technical reasons, 2D calculations are much easier and since we can learn a considerable amount from them we will do a fair amount of 2D analysis. Some 3D work was also done. After discussing the analysis, we summarize the remaining problems and indicate what would be most useful to work on.

18.5

III. General Discussion - Approaches and Problems
(A 11 - A 12)
A. General Discussion

Travelling wave tubes, (TWT's) use electron beams, which interact continuously with the electromagnetic (EM) wave to amplify microwaves over a broad range of frequencies. Fig. 1 shows the idea in a schematic way. The axial speed of the EM wave along the helix is slow enough so the electron's speed can be adjusted to be almost the same. The EM wave acts to "bunch" electrons and bunches of electrons in turn act to amplify the EM wave. Magnets are used to constrain the electron beam near the axis of the helix for proper functioning of the tube. Permanent periodic magnets (PPM) of opposite polarity placed side by side around the axis of tube are used because of their small size, light weight and because they require no input power. The PPM structure is useful because only the rms axial field is required for electron focussing and the reversal of the direction of the field doesn't matter, although fluctuation in the magnitude of the field does cause scalloping of the electron beam. PPM's are particularly good for airborne use. The typical PPM structure, see Fig. 1, is a collection of ring magnets separated by magnetic shims of high permeability (typically a steel). There is very little stray magnetic field with this structure. The shims are also called pole pieces. The problem is that the magnets as manufactured are not uniform. Thus the TWTs require individual adjustment to operate properly and this costs money. We need to study the effect of non uniformities on the tube operation. There are really three aspects to this problem. The first is how the field varies along and near the axis after it goes through the pole pieces (E1-E7), after that one needs to know how the resulting field affects the electron trajectories. (C1-C6) . Then we need to know how the operation of the tube is modified by inhomogeneities. We will concentrate mainly on the first problem; namely how to calculate the field near the axis and how to

18.6
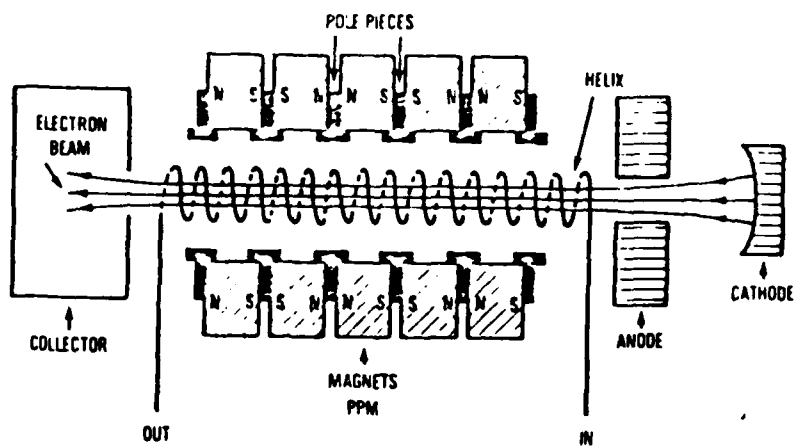
Figure 1. Schematic of Simplified TWT showing PPM focussing.

estimate the effect on the field of the inhomogeneities. As already mentioned, the magnets are cut in half to assemble them on the TWT and this introduces a gap. The gap produces an important inhomogeneity, of course. Typically $SmCo_5$ magnets are used because they have a large remanent magnetization and large coercive force and thus produce large fields which are relatively con-
stant under the presence of demagnetization fields. (G 1)

The helix structure used in the TWT is a slow wave circuit which inter-acts efficiently with an electron beam over a large frequency band. The power output can be limited, however, by heat dissipation. A large part of this heat dissipation involves interception of the beam by the helix. This can increase when the rf signal is applied to the traveling-wave tube. (A6) The magnets are, of course, important for focussing. Defocussing can be caused by rf bunching of the beam. The generated heat must be removed and dielectric support rods are often used for this purpose. However, the heat transfer involves two interfaces (metal to ceramic) and these can cause thermal resistance. One technique involves brazing the helix to the rods and another involves a pressure fit. (A2) It does not seem to be settled as to which is best.

The major problem with TWT manufacture is a typical practical problem with manufacturing anything. The TWTs cost too much and are not reliable enough. (A4, A8) Part of this problem is due to random variations in the focussing magnets. This can often be corrected by manual shimming which will add cost. One approach to the problem is to automate the manufacture and test-ing of the magnets. Hughes (B1) has developed a magnetic measurement system to reject those ring magnets that have excessive inhomogeneities.

18.8

There are other problems connected with the magnets, of course. (G1)
Not only may they have spatial inhomogeneities, but they may also vary
in time and with temperature. The magnets need to be stable at high tem-
perature in a repulsive PPM mode. Alloying can partially correct
this problem. Low oxygen processing can aid the stability. The problem of
variation with time and related shelf life problems don't appear to be
settled yet.

Gittins (A 11) has a good summary of the basic analysis of TWTs. One
equation relates (for the first pass band) the peak value of the magnetic
field and the period.

$$L = C_1 \, \sqrt{V}/B_m \qquad (1) \begin{cases} L = \text{period of magnet system} \\ V = \text{beam voltage} \qquad C_1 = \text{constant} \\ B_m = \text{peak value of axial magnetic field} \end{cases}$$

This is a condition of stable focussing. The stop band begins when the
radius increases without limit.
Another equation gives the value of the field for most efficient focussing. The
Brillouin field B_b is the minimum field needed.

$$B_b = C_2 \sqrt{\frac{I}{\sqrt{V}}} \frac{1}{a} \qquad (2) \begin{cases} a = \text{average radius of electron beam} \\ I = \text{beam current.} \end{cases}$$

This keeps the amplitude of 'scalloping' of the electron beams a minimum.
In practice a focussing field of perhaps twice the size is important.

A small period L is nice because it reduces the "ripple" in the
amplitude of the electron beam. However, by (1) the smaller the period L
the larger the field that is required. (E5) Increasing the magnetic field has
desirable features but it can lower the efficiency, (A3) in special cases.

For proper useful operation and amplification, TWT's need long, high
current density electron beams. (E4) Space change repulsion then tends to
spread out the beam. The magnetic field is used to hold the beam together.

Centrifugal effects also play a role. Good electron gun design is also important.

The role of temperature needs further discussion. Temperature can cause important effects on periodic permanent-magnetic structures. It is possible to compensate for this variation by use of magnetic shunts with temperature dependent reluctance. (A6) We already mentioned the role of alloying in temperature compensation. We also mentioned that one finds in typical magnets better stability at high temperature if one has magnets processed where there is low oxygen concentration.

Moats (C1) has given a nice summary of how variations of field strength can affect tube behavior. He has done calculations of beam trajectories with PPM focussing, but under non-ideal conditions. He was particularly interested in knowing what deviations from non ideal conditions the TWT would tolerate. Moats considered variations in magnetic field as due, for example, to thermal effects and random variations from magnet to magnet. Moats mentions that there were other effects that could well be more important. For example, beam injection at an angle or off center. Moats concluded that variations of magnetic field strength by 10% might be acceptable but that if shimming needs to be avoided then variations by 1.5% or less are needed.

B. <u>Magnetostatics</u>

We now begin a more explicit discussion of how to calculate the magnetic field. In general we must solve the basic equation of magnetostatics. From Appendix A-1 we have

$$\vec{\nabla} \cdot \vec{B} = 0 \qquad \text{(B 1)}$$

$$\vec{\nabla} \times \vec{H} = 0. \qquad \text{(B 2)}$$

We first set this up in an analytical way and then show how a discrete numerical scheme can be used.

Eqn (B2) implies there exists a ϕ such that $\vec{H} = -\vec{\nabla}\phi.$ (B 3)

Since

$$\vec{B} = \mu_0 (\vec{H} + \vec{M}) \qquad \text{(B 4)}$$

and since we assume in all cases that

$$\vec{M} = \vec{M}_0 + \chi \vec{H} \qquad \text{(B 5)}$$

where M_0 and χ are constant,

we can write

$$\vec{B} = \mu_0 \left[(1+\chi) \vec{H} + \vec{M}_0 \right]$$

then

$$\vec{\nabla} \cdot \vec{B} = \mu_0 (1+\chi) \vec{\nabla} \cdot \vec{H} = 0$$

or by *(B3)*

$$\nabla^2 \phi = 0. \qquad \text{(B 6)}$$

So the basic equation we must solve is Laplace's equation.

We also need to discuss what happens at a boundary where the properties change. Consider a boundary between regions 1 and 2 as shown in Figure <u>2</u>.
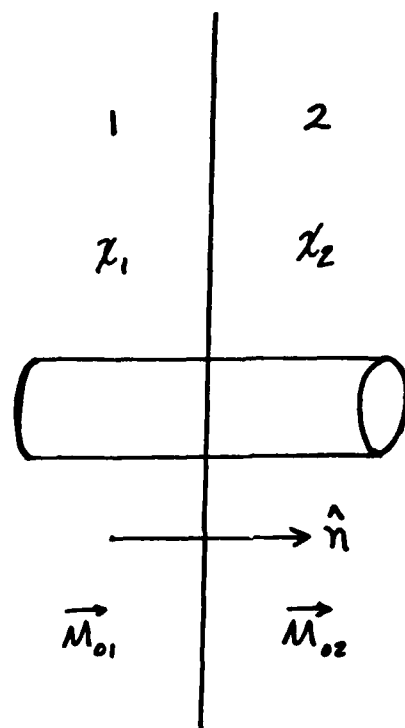
Figure 2. Boundary between Regions 1 and 2. A Gaussian Surface is also shown.

Since $\vec{\nabla} \cdot \vec{B} = 0$ we know

$$\vec{\nabla} \cdot \vec{H} = -\vec{\nabla} \cdot \vec{M} = -\chi \vec{\nabla} \cdot \vec{H} \underbrace{=}_{\vec{\nabla} \cdot \vec{M}_o} \vec{\nabla} \cdot \vec{M}_o$$

applying Gauss' theorem to the pillbox shown, ($\neq 0$ since M_0 changes across boundary)

$$(1+\chi) \vec{\nabla} \cdot \vec{H} = -\vec{\nabla} \cdot \vec{M}_o$$

or

$$(1+\chi_2) H_{n2} - (1+\chi) H_{n1} = -(M_{on2} - M_{on1})$$

$$(1+\chi_2) \frac{\partial \phi}{\partial n_2} - (1+\chi_1) \frac{\partial \phi}{\partial n_1} = M_{on2} - M_{on1} . \qquad \text{(B 7)}$$

If we require ϕ to be continuous then $\vec{\nabla} \times \vec{H} = 0$ is satisfied across the boundary.

We can summarize the situation as follows: In regions where the current density is zero and where the M = χH + Mo with χ and Mo constant, the magnetostatic potential ϕ satisfies

a. Laplaces Equation $\nabla^2 \phi = 0$ in regions of constant χ

b. ϕ continuous (and finite) everywhere.

c. The normal derivative of ϕ across a surface changes by the increment of constant magnetization.

$$(1+\chi_2) \frac{\partial \phi}{\partial n_2} - (1+\chi_1) \frac{\partial \phi}{\partial n_1} = M_{on2} - M_{on1}$$

d. If further we assume all sources are confined to a finite region we can also require ϕ vanishes at least as fast as r^{-2} as $r \to \infty$.

Next we show how to make a discrete numerical scheme out of this.

C. Numerical Techniques

1. Our Techniques

We now begin to discuss some numerical techniques. We start in two dimensions and define a grid as shown in Figure 3. We assume the magnetization is in the x direction. From $\nabla \cdot B = 0$, $\vec{H} = -\vec{\nabla}\phi$ (so $\vec{\nabla} \times \vec{H} = 0$), $\vec{B} = \mu o\ (\vec{H+M})$ and $\vec{M} = \vec{M}_0 + \chi\vec{H}$ we have

$$\vec{\nabla} \cdot (\nu \vec{H}) = -\vec{\nabla} \cdot \vec{M_o} \qquad (C\ 1)$$

where $\nu = 1 + \chi = \mu/\mu o$. We apply this to the Square shown

$$\int \vec{\nabla} \cdot \nu \vec{H}\, dA = -\int \vec{\nabla} \cdot \vec{M_o}\, dA \qquad (C\ 2)$$

$$\int \nu \vec{H} \cdot \hat{n}\, dl = -\int \vec{M_o} \cdot \hat{n}\, dl \qquad (C\ 3)$$

where $\hat{n}$ is normal to the perimeter of the square.

Thus

$$\overline{\nu \frac{\partial \phi}{\partial x}}\Big|_{+x} - \overline{\nu \frac{\partial \phi}{\partial x}}\Big|_{-x} + \overline{\nu \frac{\partial \phi}{\partial y}}\Big|_{+y} - \overline{\nu \frac{\partial \phi}{\partial y}}\Big|_{-y} = \overline{M}_{o,+x} - \overline{M}_{o,-x} \qquad (C\ 4)$$

see the figure for the notation.

We can clearly approximate this by

$$\frac{\nu_{i+1,j+1} + \nu_{i+1,j}}{2} \frac{\phi_{i+1,j} - \phi_{i,j}}{h} - \frac{\nu_{i,j+1} + \nu_{i,j}}{2} \frac{\phi_{i,j} - \phi_{i-1,j}}{h}$$

$$+ \frac{\nu_{i,j+1} + \nu_{i+1,j+1}}{2} \frac{\phi_{i,j+1} - \phi_{i,j}}{h} - \frac{\nu_{i,j} + \nu_{i+1,j}}{2} \frac{\phi_{i,j} - \phi_{i,j-1}}{h}$$

$$= \frac{M_{i+1,j+1} + M_{i+1,j}}{2} - \frac{M_{i,j+1} + M_{i,j}}{2}. \qquad (C\ 5)$$

18.14
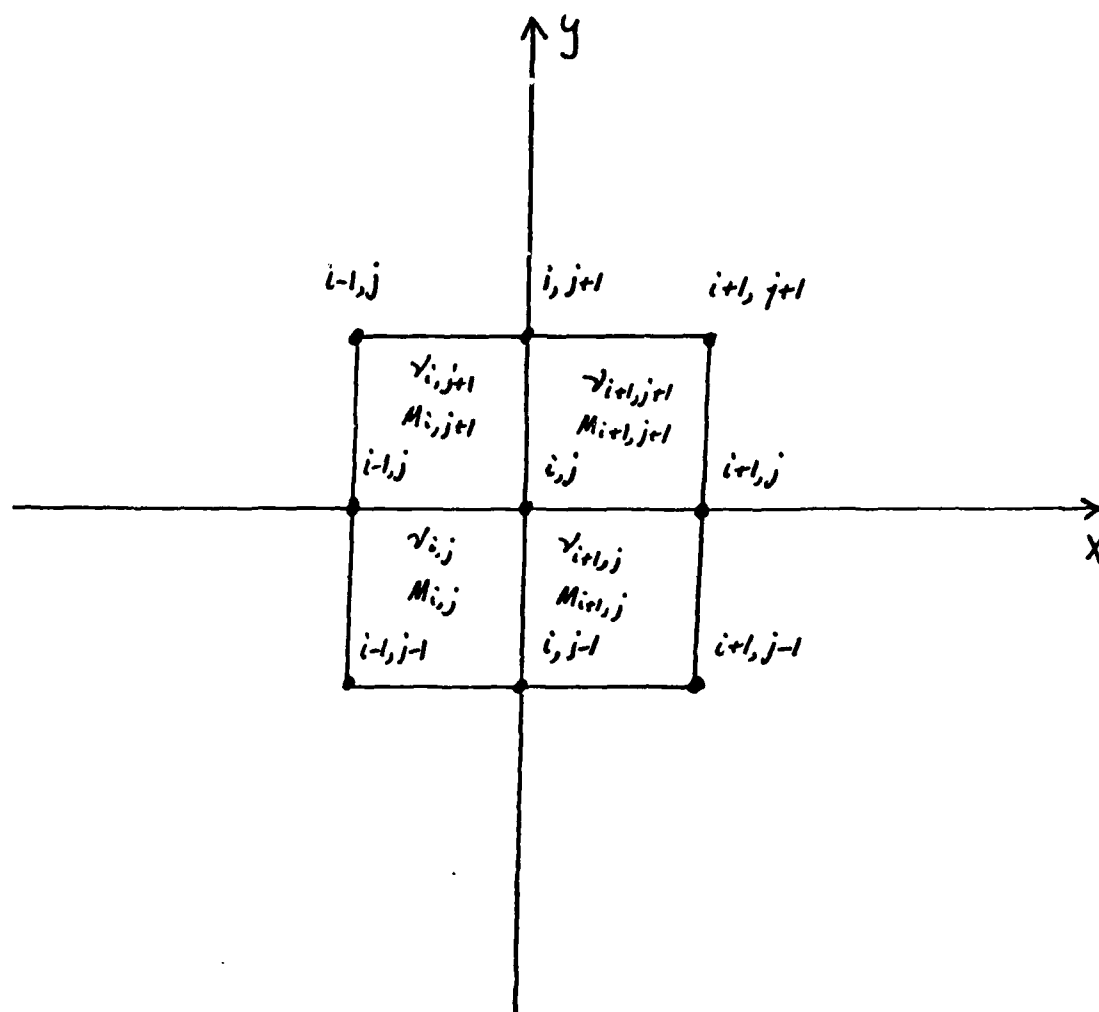
Figure 3. Grid of points for a Two Dimensional Calculation.

18.15

Let us define

$$R_{ij} = 2\left[\nu_{i+1,j} + \nu_{i,j+1} + \nu_{i+1,j+1} + \nu_{i,j}\right]. \qquad \text{(C 6)}$$

Then we have

$$\phi_{i,j} = -\frac{h\left[M_{i+1,j+1} + M_{i+1,j} - (M_{i,j+1} + M_{i,j})\right]}{R_{ij}}$$

$$+ \frac{(\nu_{i+1,j+1} + \nu_{i+1,j})\phi_{i+1,j} + (\nu_{i,j+1} + \nu_{i,j})\phi_{i-1,j} + (\nu_{i,j+1} + \nu_{i+1,j+1})\phi_{i,j+1} + (\nu_{i,j} + \nu_{i+1,j})\phi_{i,j-1}}{R_{ij}}$$

Method A   (C 7)

There are various ways this set of equations be solved for the unknown

$\phi_{i,j}$.

There is a slightly better calculational method. This is developed below, it

is based on the fact that we can estimate an x derivative in the following way

$$\frac{\partial \phi}{\partial x} = \vec{\nabla}\phi \cdot \hat{x} \qquad \text{(C 8)}$$

so an x derivative is approximately

$$\frac{\phi_{i+1,j+1} - \phi_{i,j}}{\sqrt{2}\, h}\; \frac{1}{\sqrt{2}} = \frac{\phi_{i+1,j+1} - \phi_{i,j}}{2h} \qquad \text{(C 9)}$$

Thus we write
$$\tfrac{1}{3}\left\{\left(\frac{\phi_{i+1,j-1} - \phi_{i,j}}{2h}\right)\nu_{i+1,j} + \left(\frac{\phi_{i+1,j} - \phi_{i,j}}{h}\right)\left(\frac{\nu_{i+1,j+1} + \nu_{i+1,j}}{2}\right) + \left(\frac{\phi_{i+1,j+1} - \phi_{i,j}}{2h}\right)\nu_{i+1,j+1}\right\}$$

$$+ \tfrac{1}{3}\left\{\left(\frac{\phi_{i+1,j+1} - \phi_{i,j}}{2h}\right)\nu_{i+1,j+1} + \left(\frac{\phi_{i,j+1} - \phi_{i,j}}{h}\right)\left(\frac{\nu_{i+1,j+1} + \nu_{i,j+1}}{2}\right) + \left(\frac{\phi_{i-1,j} - \phi_{i,j}}{2h}\right)\nu_{i,j+1}\right\}$$

$$+ \tfrac{1}{3}\left\{\left(\frac{\phi_{i-1,j} - \phi_{i,j}}{2h}\right)\nu_{i,j+1} + \left(\frac{\phi_{i-1,j} - \phi_{i,j}}{h}\right)\left(\frac{\nu_{i,j+1} + \nu_{i,j}}{2}\right) + \left(\frac{\phi_{i-1,j-1} - \phi_{i,j}}{2h}\right)\nu_{i,j}\right\}$$

$$+ \tfrac{1}{3}\left\{\left(\frac{\phi_{i-1,j-1} - \phi_{i,j}}{2h}\right)\nu_{i,j} + \left(\frac{\phi_{i,j-1} - \phi_{i,j}}{h}\right)\left(\frac{\nu_{i,j} + \nu_{i+1,j}}{2}\right) + \left(\frac{\phi_{i+1,j-1} - \phi_{i,j}}{2h}\right)\nu_{i+1,j}\right\}$$

$$= \frac{M_{i+1,j+1} + M_{i+1,j} - M_{i,j+1} - M_{i,j}}{2}$$

(C 10)

18.16

Let us define

$$R_{ij} = 4\left(\nu_{i,j} + \nu_{i+1,j} + \nu_{i,j+1} + \nu_{i+1,j+1}\right).$$

(C 11)

We can then write

$$\phi_{i,j} = -\frac{3h}{R_{ij}}\left[M_{i+1,j+1} + M_{i+1,j} - M_{i,j+1} - M_{ij}\right]$$

$$+ \Big[\left(\nu_{i+1,j+1} + \nu_{i+1,j}\right)\phi_{i+1,j} + \left(\nu_{i,j} + \nu_{i,j+1}\right)\phi_{i+1,j}$$

$$+ \left(\nu_{i,j+1} + \nu_{i+1,j+1}\right)\phi_{i,j+1} + \left(\nu_{i,j} + \nu_{i+1,j}\right)\phi_{i,j-1}$$

$$+ 2\nu_{i+1,j+1}\,\phi_{i+1,j+1} + 2\nu_{i+1,j}\,\phi_{i+1,j-1}$$

$$+ 2\nu_{i,j+1}\,\phi_{i-1,j+1} + 2\nu_{i,j}\,\phi_{i-1,j-1}\Big]\Big/R_{ij},$$ Method B.

(C 12)

It can be seen that this is a little more complicated than the previous method. Let us carry out the previous method in three dimension. We obtain

$$\left(\nu_{i+1,j+1,k+1} + \nu_{i+1,j,k} + \nu_{i+1,j+1,k} + \nu_{i+1,j,k+1}\right)\left(\phi_{i+1,j,k} - \phi_{i,j,k}\right)$$

$$\left(\nu_{i,j+1,k+1} + \nu_{i+1,j+1,k+1} + \nu_{i,j+1,k} + \nu_{i+1,j+1,k}\right)\left(\phi_{i,j+1,k} - \phi_{i,j,k}\right)$$

$$\left(\nu_{i,j,k+1} + \nu_{i,j+1,k+1} + \nu_{i+1,j+1,k+1} + \nu_{i+1,j,k+1}\right)\left(\phi_{i,j,k+1} - \phi_{i,j,k}\right)$$

$$\left(\nu_{i,j,k} + \nu_{i,j+1,k} + \nu_{i,j+1,k+1} + \nu_{i,j,k+1}\right)\left(\phi_{i-1,j,k} - \phi_{i,j,k}\right)$$

$$\left(\nu_{i,j,k+1} + \nu_{i+1,j,k+1} + \nu_{i,j,k} + \nu_{i+1,j,k}\right)\left(\phi_{i,j-1,k} - \phi_{i,j,k}\right)$$

$$\left(\nu_{i,j+1,k} + \nu_{i+1,j+1,k} + \nu_{i+1,j,k} + \nu_{i,j,k}\right)\left(\phi_{i,j,k-1} - \phi_{i,j,k}\right)$$

$$= M_{i+1,j+1,k+1} + M_{i+1,j,k} + M_{i+1,j+1,k} + M_{i+1,j,k+1}$$

$$- M_{i,j,k} - M_{i,j+1,k} - M_{i,j+1,k+1} - M_{i,j,k+1}, \text{ with } h = 1.$$

(C 13)

(D 3)

2. The Greenfield Program

We also used a two dimensional "canned" program called "Greenfield 2" which we purchased from Quantic Laboratories Inc. of Winnipeg, Canada. A User's Manual is available so we only briefly discuss this program.

The primary technique that Greenfield 2 uses is the boundary element method. It uses a Green function which in turn utilizes actual source distributions and boundary source distributions chosen so as to satisfy both boundary and interface conditions.

We assume our magnets are uniformly magnetized and of fixed magnetization, thus they can be replaced by a surface "pole" or "charge" density whenever the magnetization changes perpendicular to a surface. (that is, when its normal component changes). Greenfield 2 doesn't treat the case of a (2D) surface "charge" density so we use instead thin rectangles filled with "charge" to simulate the surface "charge" density.

The advantage of the boundary element method is that it only has nodes on surfaces and interfaces and so allows the computer to handle larger problems. Nevertheless there is only a limited number of nodes that can be used so the accuracy and complexity of the problem that can be treated is limited. (There is a maximum number of 150 boundary elements). The examples considered in this report are about as complicated as can be conveniently treated by Greenfield.

IV. Results

We have results for programs we wrote ourselves and we have results
obtained by use of some "canned" programs.

A. Two Dimensional

1. Greenfield

We start by discussing the results of the "canned" programs. This
program is the Greenfield 2 program discussed in the previous section.

Figure 4 shows the geometry that we used. It is obviously intended
to model the TWT geometry except that we have two dimensions rather than three
and we can model only a finite number of shims and magnets.

In Figs. 5 and 6 we have plotted some numerical results obtained from
Greenfield. Arbitrary units are used. Fig. 5 shows how shims modify the
potential and H_x along the center of the tube. The variation in the magnetic
field as a function of x is reduced due to the presence of the shims. In
Figure 6, we plot H_x and H_y vs y for fixed x.. The plots compare the variation
of H_y at a central location for the cases of with and without shims. They also
compare the variation of H_x at an edge of the shims for the two cases. In
general we see the shims increase the value of the field and also seems to
increase   the field variations at the edge.

18.19

FIELD IN X DIRECTION   4.408
FIELD IN Y DIRECTION   8.826E-3
? PV
LOCATE THE POINT
5.9 3.7
THE POTENTIAL IS 0.9357
?

POINT SOLUTION
PV - POTENTIAL SOLVE
FV - FIELD SOLVE
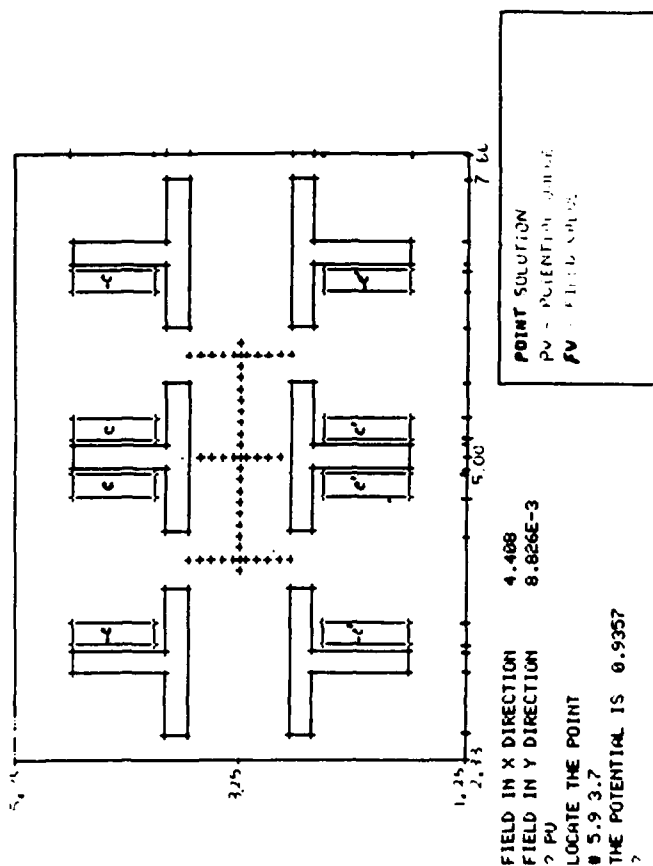
Figure 4. Two Dimensional Geometry for Mimicking a TWT. Only Relative Dimensions and Units are Important. The Rectangles have Magnetic density of "charge" C,C¹. Two Rectangles with Opposite "charges" thus Mimic a Magnet. The "T" Shaped Figures are the Permeable "Shims." The Center of the Figure is at x=5, y=3.25.
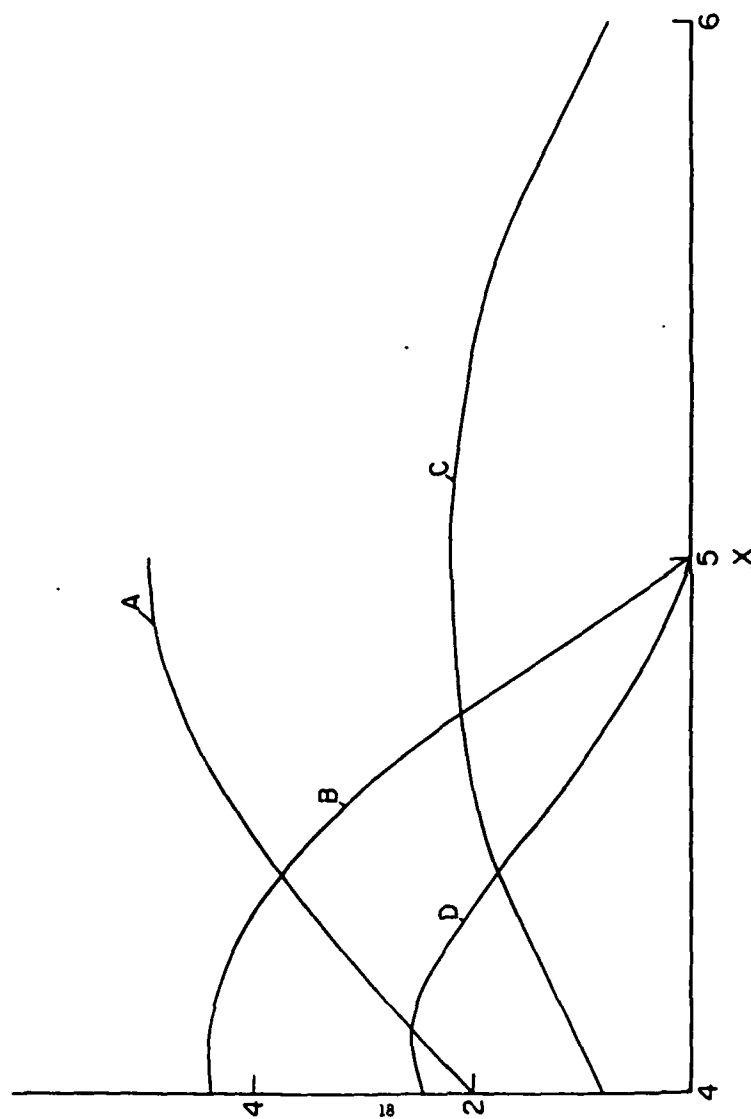
X
Fig. 5

Variations in potential ϕ and Horizontal Magnetic Field H_x (for
$y = 3.25$) vs. x. A = ϕ for No Shims and No Magnet Fluctuations.
B=$|H_x|$ for No Shims and No Magnet Fluctuations. C = ϕ for Shims
but no Magnet Fluctuations. D =$|H_x|$ for Shims but No Magnet
Fluctuations. The Relative Permeability of the Shims is 200.

$c=c^1=100$
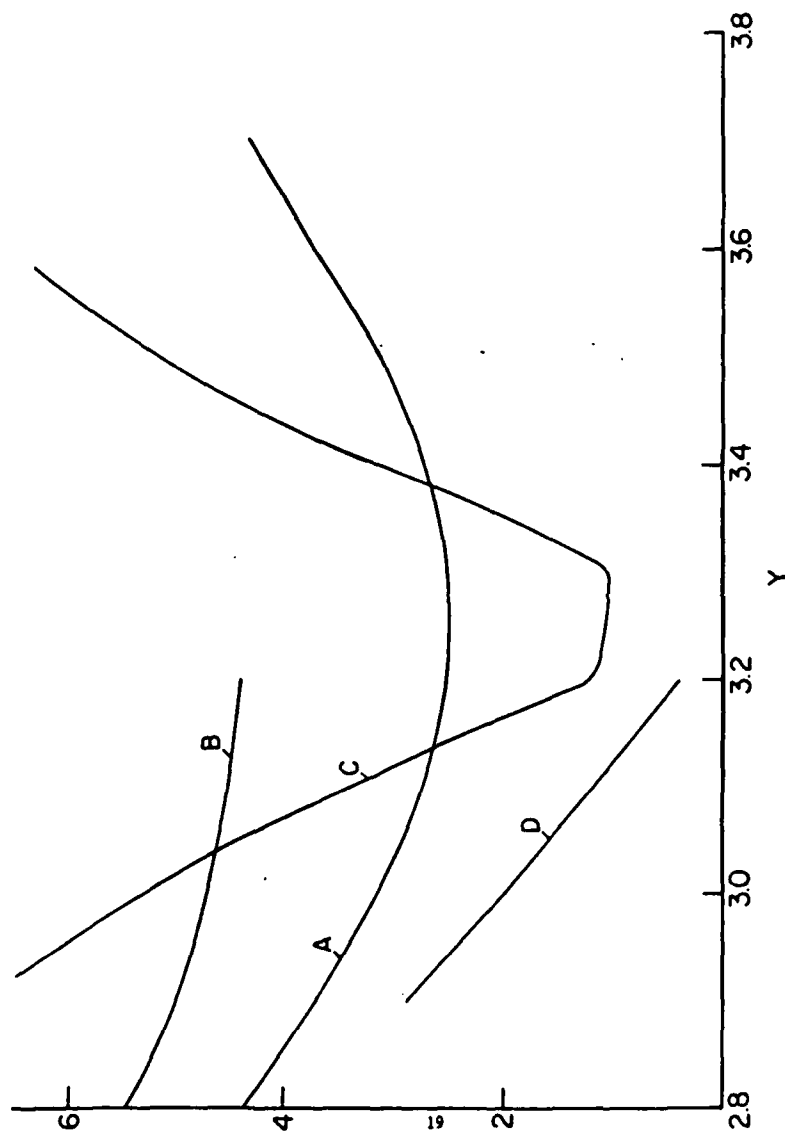
Y
Fig. 6

Variations in Vertical and Horizontal Magnetic Field vs. y for

fixed x. A = $|H_x|$ for x = 4.1 and shims, but no Fluctuations.

B = $|H_x|$ for x = 4.1 and no shims and no Fluctuations.   C = $(10|H_y|)$

for x = 5 and shims with No Fluctuations.   D = $|H_y|$ for x = 5

and no shims and no Fluctuations.   C = C^1 = 100.   The Relative

Permeability of the Shims is 200.

Notation for Captions of Figures 7 through 17

1. By TH-4 we mean no shims and no fluctuations and the "charges" are
    $C = C^1 = 100$.

2. By TH-5 we mean no shims and fluctuations with the "charges
    chosen as $C = 120$, $C^1 = 80$.

3. By TH we mean shims and no fluctuations. The relative permeability of
    the shims being 200.

4. By CP we mean shims and fluctuations with $C = 120$, $C^1 = 80$ and the
    relative permeability of the shims being 200.

The notation is purely an accident of labelling at the time the calculations
were done.

	No Shims	Shims
No Flucts.	TH-4	TH
Flucts.	TH-5	CP

Table I

We now show some of the results available in color graphics using Green-field. In Figs. 7 through 17, we simply compare the four cases shown in Table I. The magnets are arranged in opposition as for a TWT. As can be seen for each of the four cases we display both an equipotential contour plot and a elevation plot (which attempts to show in perspective the potential versus x and y coordinates). In many cases we also give a field plot in which an arrow represents the magnetic field (length proportional to strength). However, this part seems not to be accurate in all cases. Since we cannot add enough shims and magnets to model a long TWT it is only the part near the center of the figure that we will use. Thus the distortions at the edges of the figure should not be regarded as typical of interior fields. Figs. 7-9 show how things look with no fluctuations and no shims. Fig.9 shows the fields. They look more or less as we would expect if one considers that the field plots are not very accurate.

In Figs. 10-12 we introduce no shims, but we do make the magnets at the top stronger than the magnet at the bottom. Although this causes some changes there does not appear to be an enormous effect for the fields near the center and along a horizontal axis. In Figs. 13-15, we have shims but no fluctuations in the magnets. In Figs. 16, 17 we have both shims and fluctuations in the magnets.

By looking at Figs. 7, 10, 13 and 16 we see a steady progression for the four cases. One way to visualize the effect of the shims is to think of the field as being "squeezed" into regions away from the shims. It is apparent from Fig. 16, however, that, even with shims, the effect of varying the magnets is not negligible.
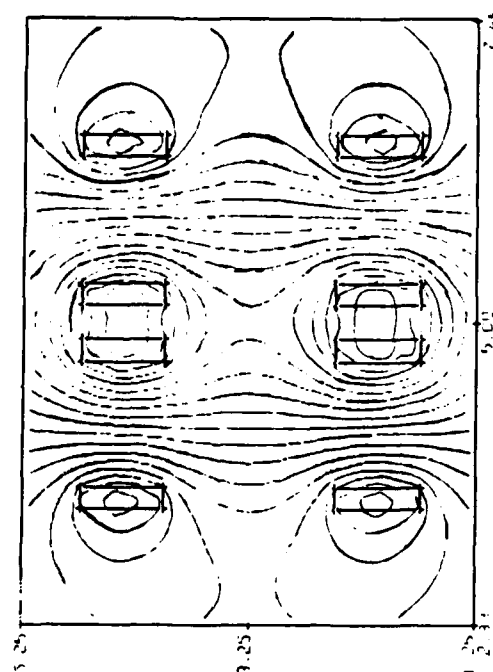
CONTOUR PLOT

CN--CONTOURS WITHOUT LABELS

ENTER THE GRID DENSITY (1..3)
2
ENTER THE NUMBER OF CONTOURS (2..50)
18

Figure 7. Equipotential Plots for TH-4. (See p. 20, 21).
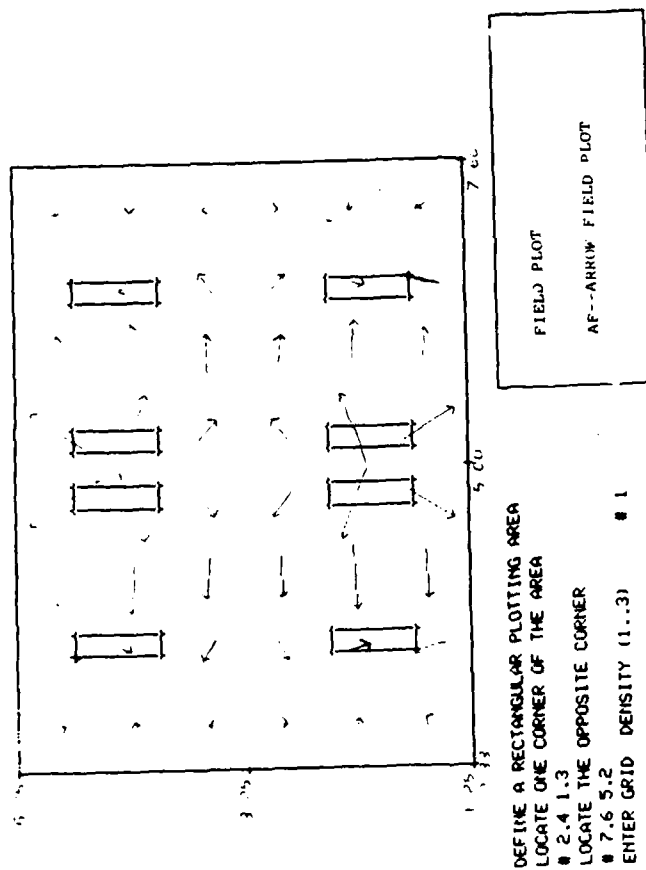
Figure 9. A Field Plot for TH-4. The length of the arrow is proportional to the Strength.
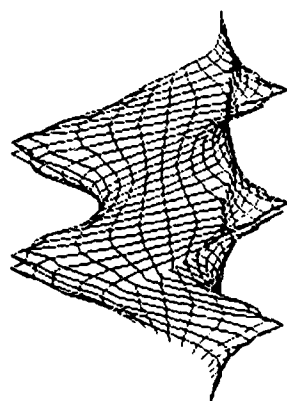
Figure 8. A Representation of Potential vs x and y for TH-4.

CONTOUR PLOT

CN--CONTOURS WITHOUT LABELS

ENTER THE GRID DENSITY (1..3)
2
ENTER THE NUMBER OF CONTOURS (2..50)
18
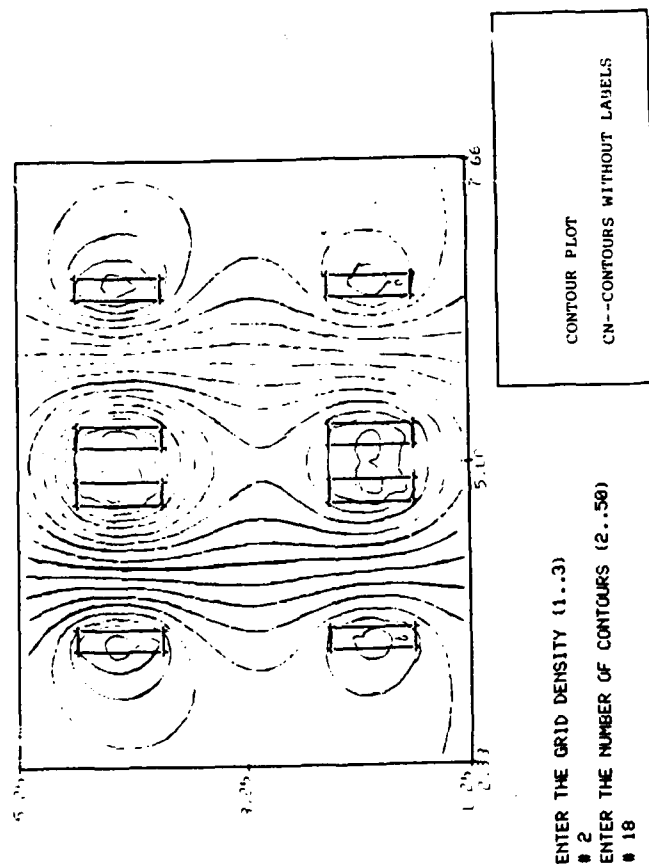
Figure 10. Equipotential Plots for TH-5.

18.30
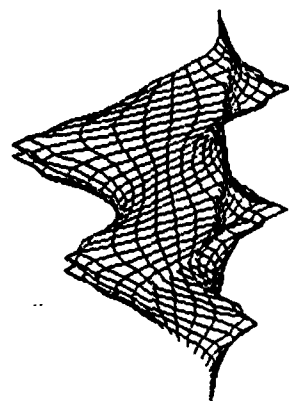
Figure 11. A Representation of Potential vs. x and y for Th-5.

DEFINE A RECTANGULAR PLOTTING AREA
LOCATE ONE CORNER OF THE AREA
2.4 1.3
LOCATE THE OPPOSITE CORNER
7.6 5.2
ENTER GRID DENSITY (1..3)   # 1
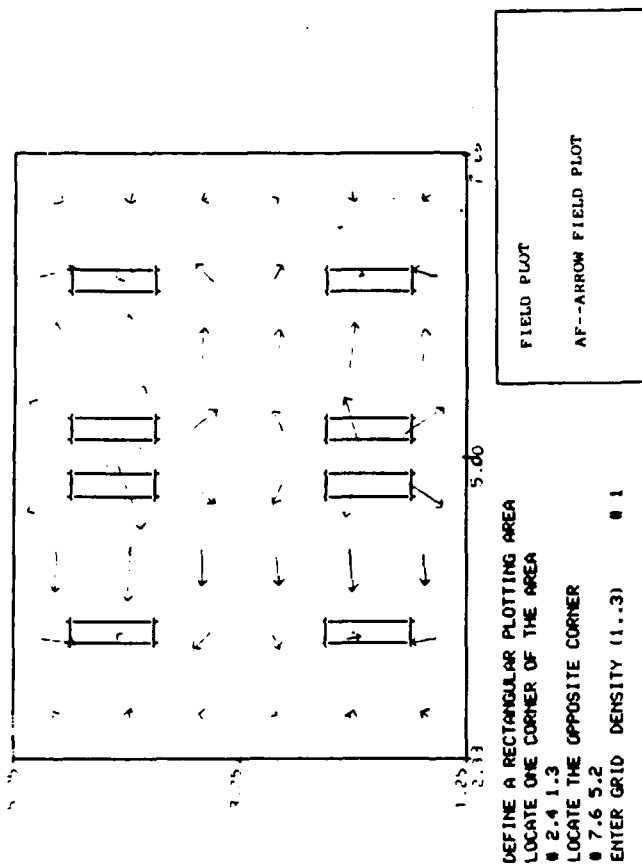
Figure 12. A Field Plot for TH-5.
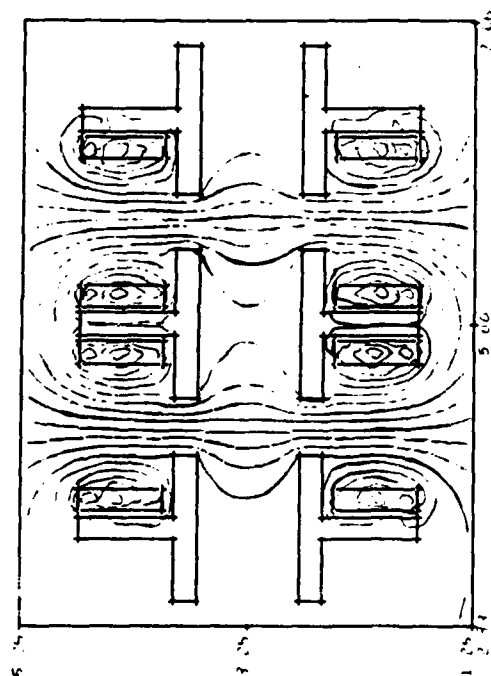
CONTOUR PLOT
CN--CONTOURS WITHOUT LABELS

ENTER THE GRID DENSITY (1..3)
@ 2
ENTER THE NUMBER OF CONTOURS (2..50)
@ 18

Figure 13. Equipotential Plots for TH
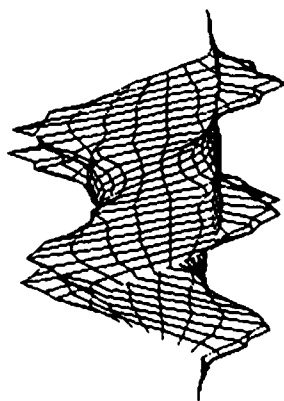
Figure 14. A Representation of Potential vs. x and y for TH.

18.33

FIELD PLOT

A--ARROW FIELD PLOT

ENTER GRID DENSITY (1..3)   # 1
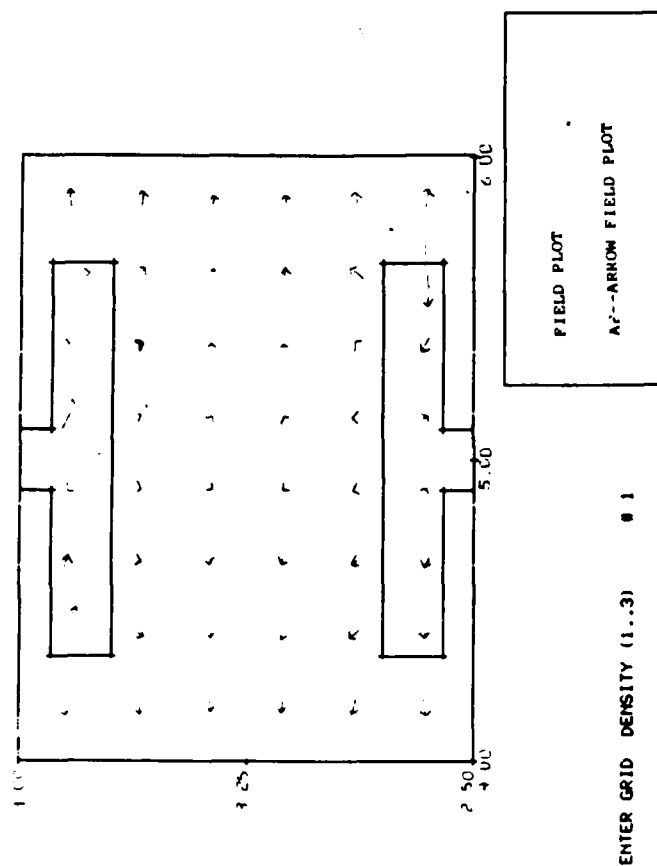
Figure 15. A Field Plot for TH.
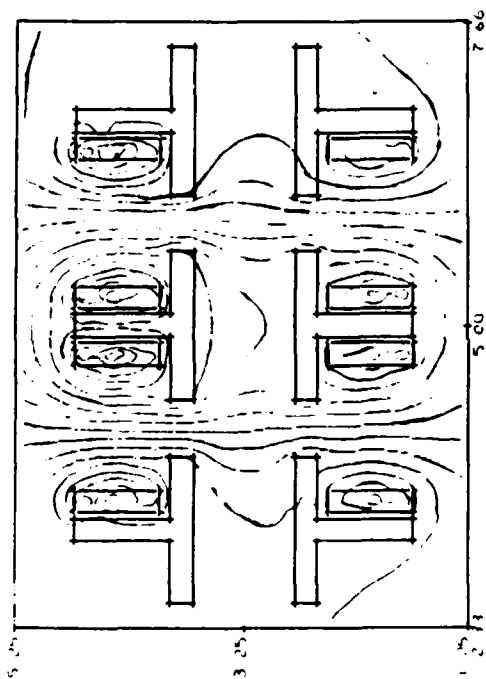
Figure 16. Equipotential Plots for CP.

18.36
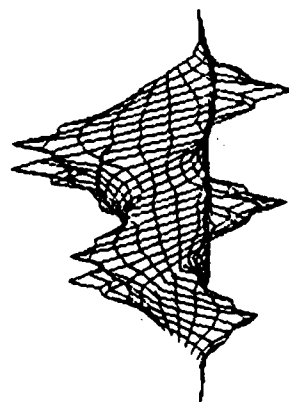
Figure 17. A Representation of Potential vs. x and y for CP

In figs. 18-20 we again treat the case of shims and varying magnetization. The variation in the magnetization is now greater than before. Figs. 21-23 show another variation in the magnetic field, but here the top magnets arise from ± 60, ± 140 "magnetic charges" and the bottom magnets arise from ± 140, ± 60 "magnetic charges." The second case doesn't seem to produce such a large field variation near the center.

In Figs. 24 and 25 we consider two magnets, the top one being stronger than the lower one. We look at the field on the right and consider the effect on the field of inserting a block of relative permeability 200. The arrow plots show that the field is "straightened" out somewhat by the effect of the permeable medium. By this I mean it is made somewhat more horizontal near the center.

In Figs. 26—28, we show several equipotential plots for a dielectric material of high dielectric constant placed between two plates of a capacitor. The potential difference between the plates creates an electric field. Mathematically, it is the same problem as placing a permeable media in a magnetic field. Note the bending of the equipotential lines. This is expected for a high material of high dielectric constant. An approximate representation of fields in shown in Fig. 29. The field in the region of high dielectric constant is reduced as it should be.
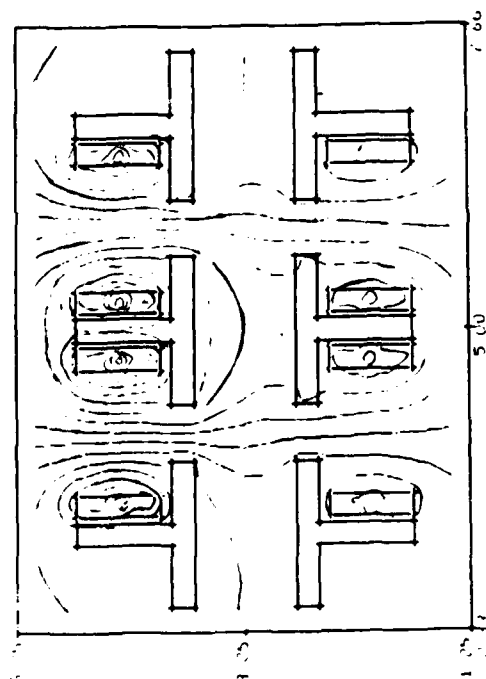
ENTER THE GRID DENSITY (1..3)
● 2
ENTER THE NUMBER OF CONTOURS (2..50)
● 18

CONTOUR PLOT
CN—CONTOURS WITHOUT LABELS

Figure 18. Equipotential plot for C=140 and C^1= 60 with the relative permeability of the others at 200.
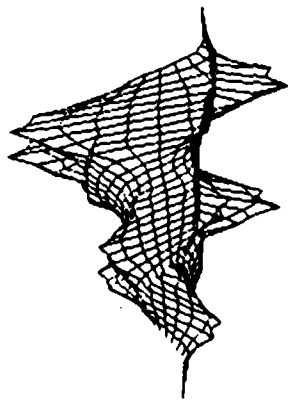
Figure 19. A Representation of the Potential vs x and y for the case of Fig. 15.

DEFINE A RECTANGULAR PLOTTING AREA
LOCATE ONE CORNER OF THE AREA
LOCATE THE OPPOSITE CORNER
ENTER GRID DENSITY (1..3)   # 1

FIELD PLOT

AF--ARROW FIELD PLOT
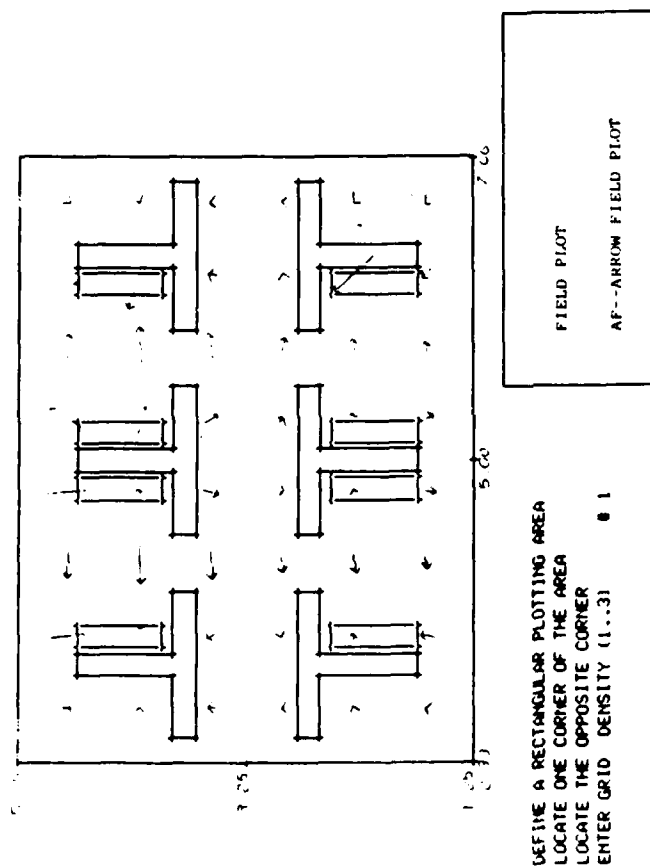
Figure 20. A Field Plot for the case of Fig. 15.

DEFINE A RECTANGULAR PLOTTING AREA
ENTER THE GRID DENSITY (1..3)
2
ENTER THE NUMBER OF CONTOURS (2..50)
18

CONTOUR PLOT

CN--CONTOURS WITHOUT LABELS
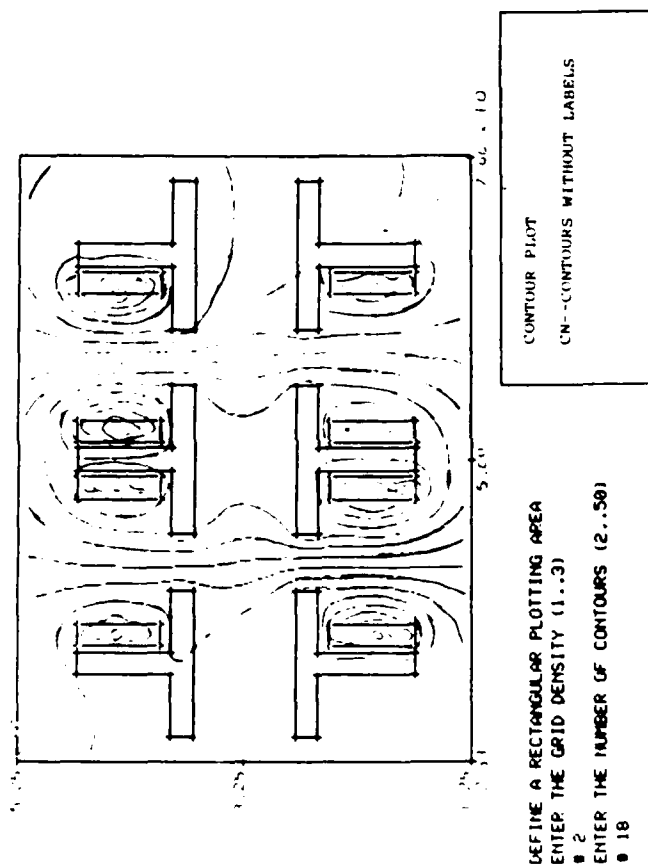
Figure 21. Equipotential Plot for the "charges" on the upper Rectangles being -60, 60, 140, -140, and on the lower rectangles being -140, 140, 60, -60. The Relative Permeability of the Shims is 200.
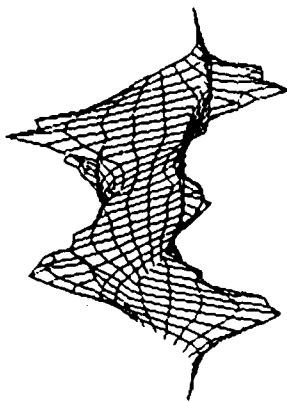
Figure 22. A Representation of the Potential vs x and y for the case of Fig. 18.
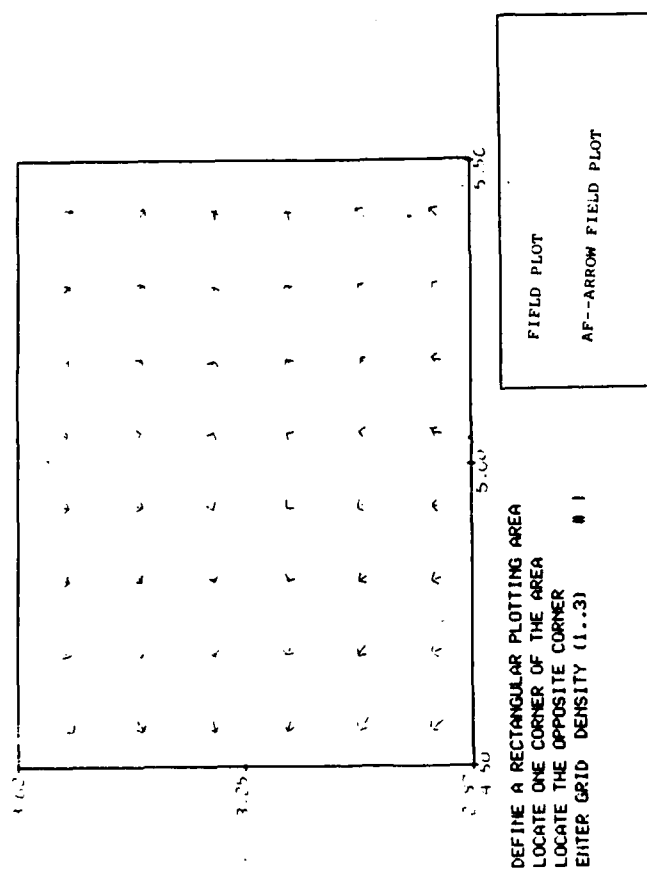
Figure 23. A Field Plot for the case of Fig. 18.
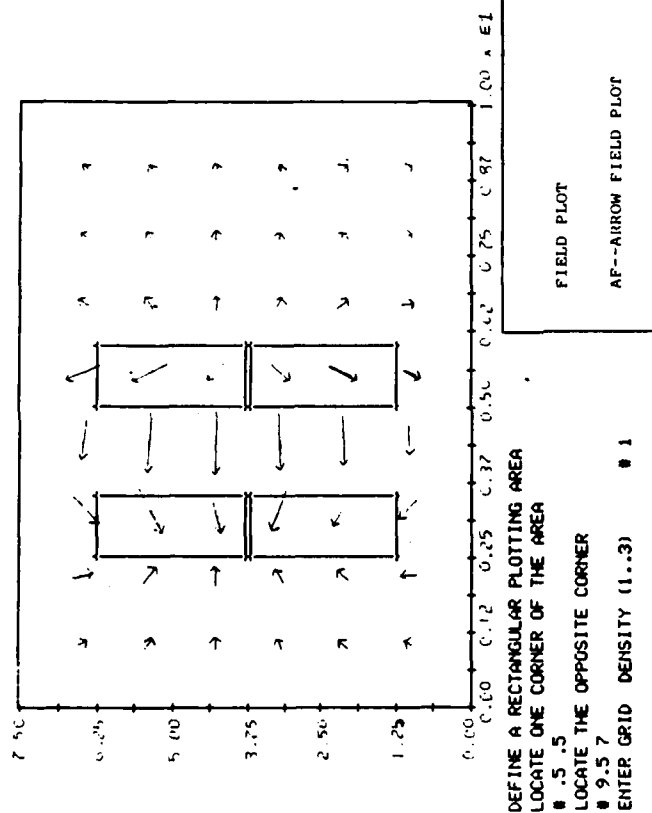
Figure 24. The Upper charges are -120, 120 and the Lower charges are -80, 80.

Field Plot.

DEFINE A RECTANGULAR PLOTTING AREA
LOCATE ONE CORNER OF THE AREA
#.5 .5
LOCATE THE OPPOSITE CORNER
#9.5 7
ENTER GRID DENSITY (1..3)   # 1

FIELD PLOT

AF--ARROW FIELD PLOT
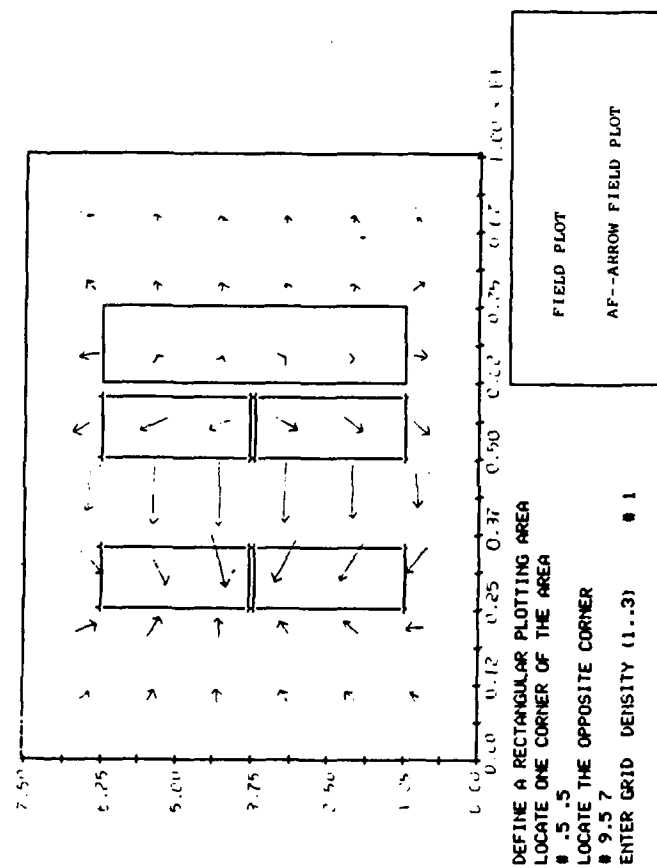
Figure 25.   Same as Fig. 21 but a Permeable Medium of Relative Permeability

200 is added.
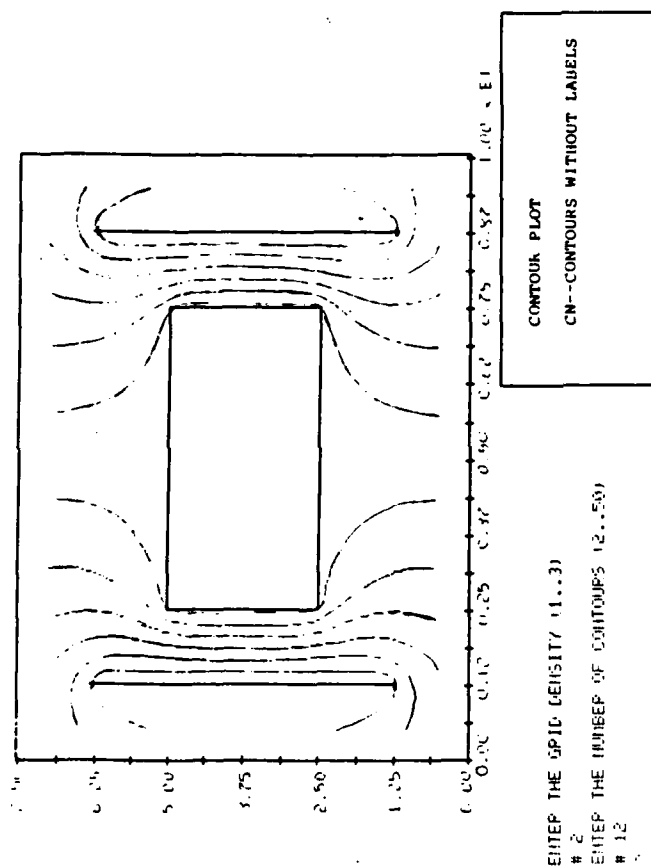
Figure 26. Equipotential Plot. There is a 20 volt difference between the plates. The Rectangle has a Relative Dielectric Constant of 200.
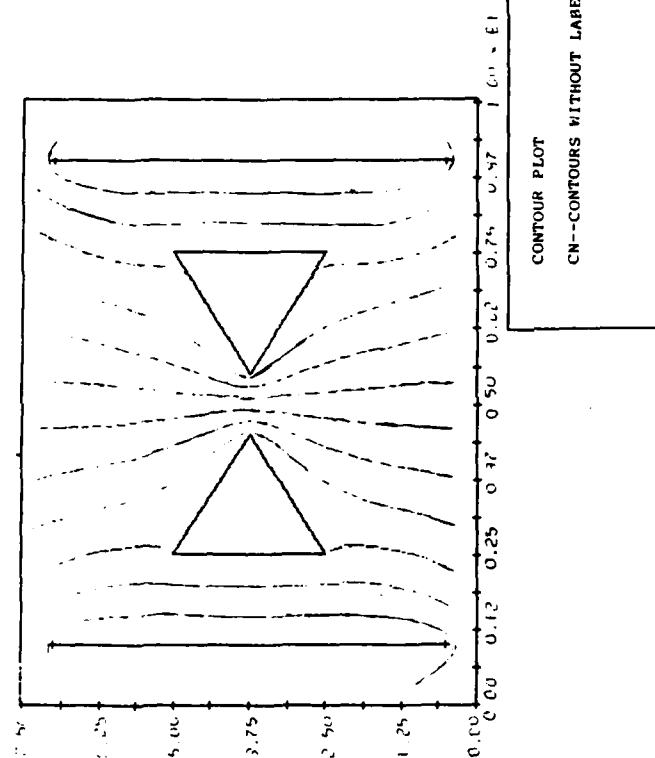
Figure 27. Equipotential Plot. There is a 50 volt difference between plates. The triangle has a relative dielectric constant of 200.
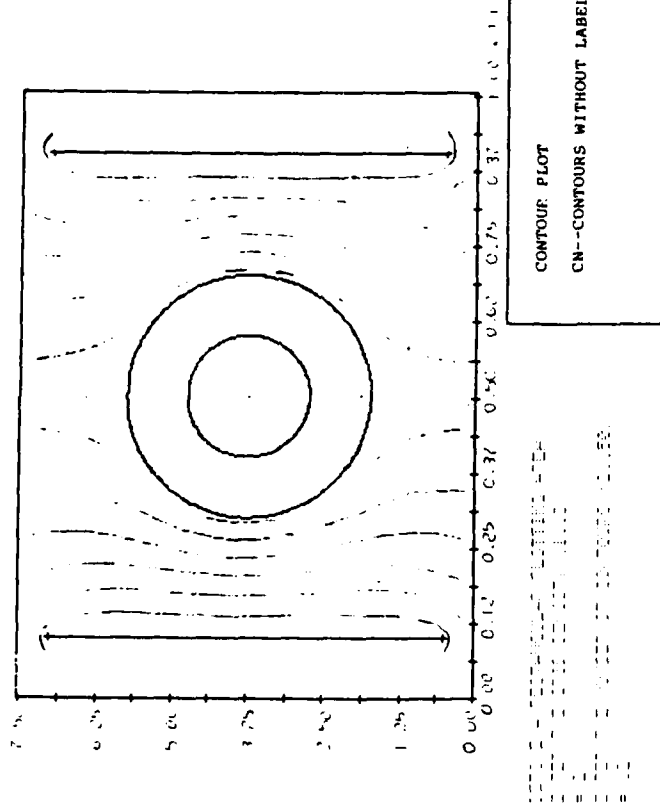
Figure 28. Equipotential Plot. There is a 50 volt difference between the relative dielectric constant of the Annular Ring. The plates is 200.
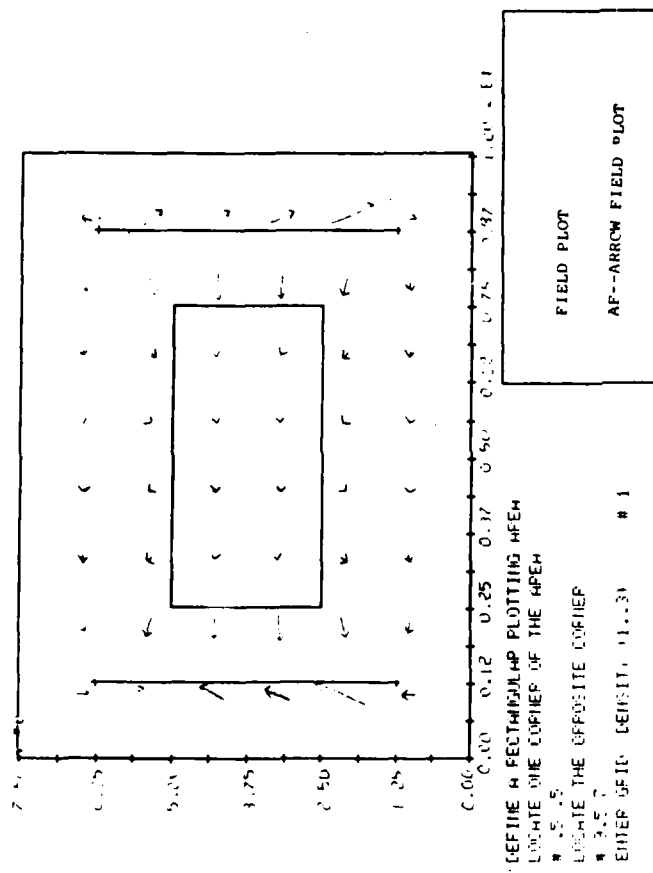
Figure 29. Approximate Field Plot for the Case of Fig. 23.

2. Handwritten Programs

In Figs. 31-34 we present some results of our own program. The geometry used is shown in Fig. 30. This is not intended to model a TWT. MA1, MA2, MB1 and MB2 are the magnetizations of the magnets and Mu is a region of relative permeability $\nu = Mu \equiv \mu/\mu_0$ ($\neq$ 1 in general). We then look at the effect on ϕ vs x of varying the magnetization at fixed μ, of varying the boundaries at fixed μ and of changing μ. In general we see that the fractional changes in the potential are not as large as the fractional changes in the magnetization. The effect of increasing Mu is clearly shown in Fig. 33. Fig. 34 shows the effect of fluctuating magnetization is damped out some by increasing Mu.

In Table II, p. 53, we list some numbers which help us compare the effect of magnetic permeability on fluctuation of the magnetization. The numbers were calculated using method B. See *p. 14* . We chose X=I=8 and MB1=-.9, MB2=-.1.1, Ma1=1.0 and MA2=.9. M1 was chosen as 13 (this located how far the boundary was from the origin). We assumed the shims were not saturated and had the constant permeability ν.
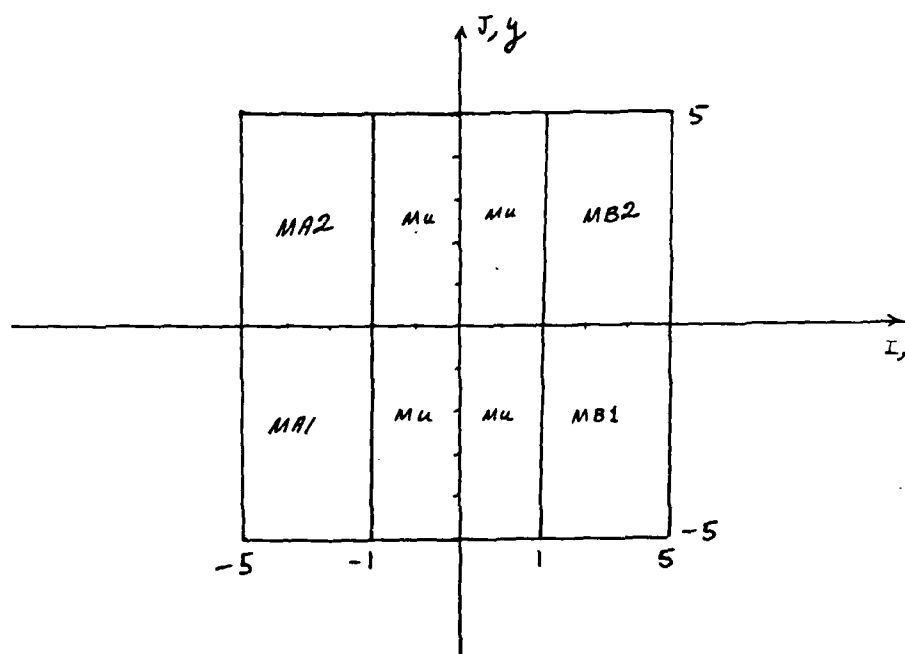
Figure 30. Geometry for some Two Dimensional Calculations.
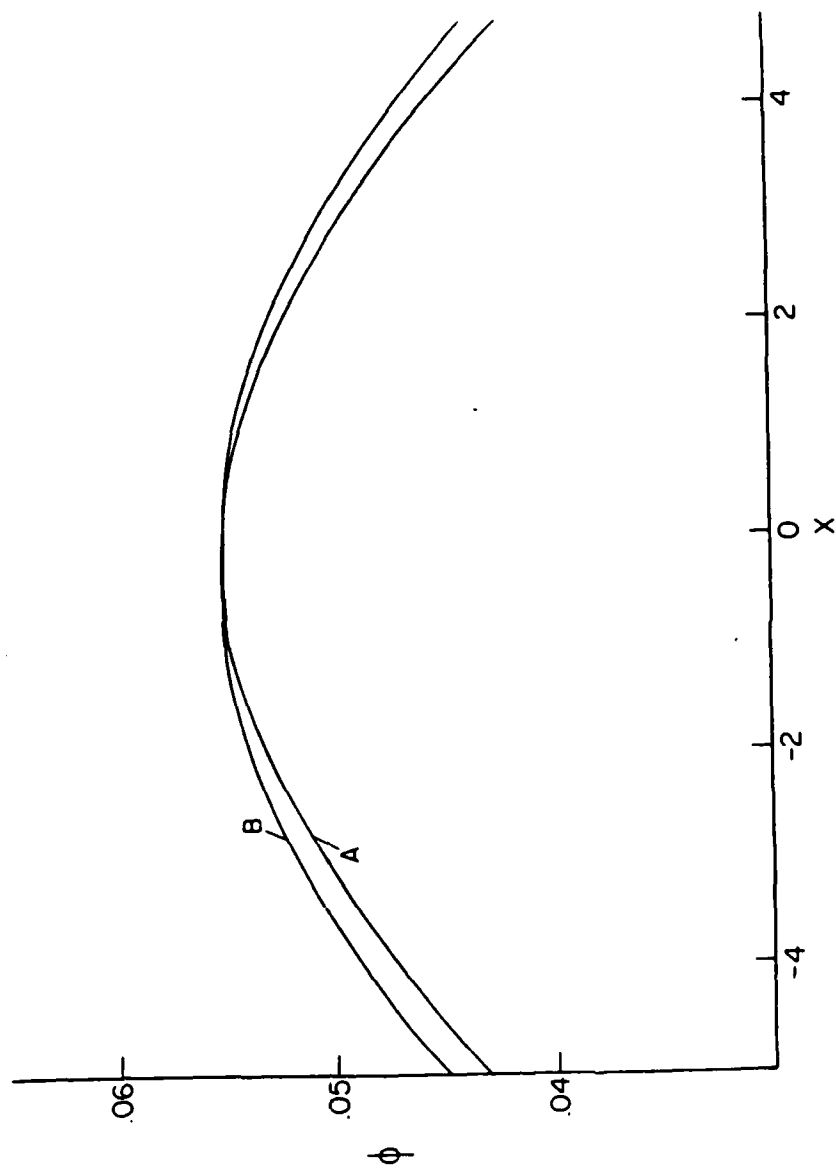
Fig. 31

Effect of Varying Magnetization on φ vs x for y = 20. Mu = 1.5.

A has MB1 = MB2 =-1, MA1 = MA2 =1 and B has MB1 =-.9, MB2=-1.1,

MA1 =1.1, MA2 =.9. 2D. Method B used with M1 = 25.
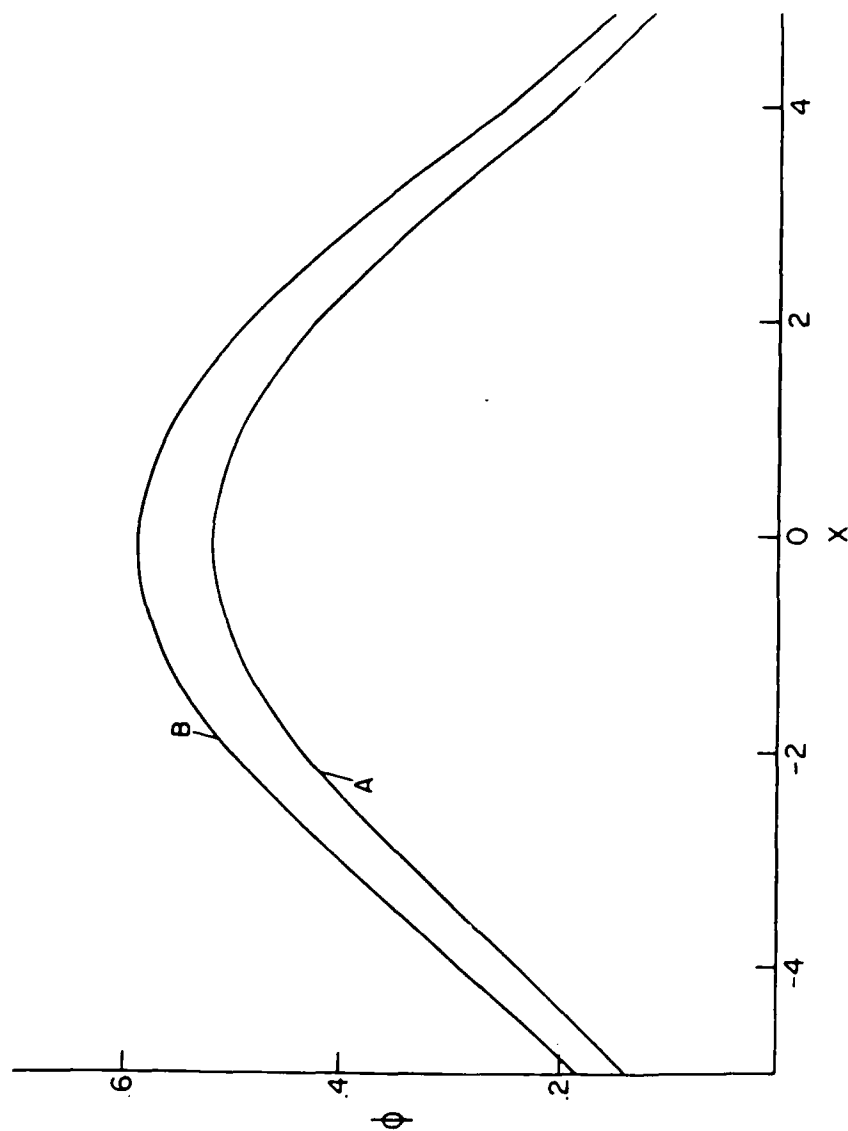
Fig. 32

Effect of changing zero potential boundary on φ vs x for y =8.

Mu = 2. A has MB1 = .9, MB2 = -1.1, MA1 = 1.1, MA2 = .9
=2.
and Mu_A = M1 = 13. B has the same but M1 = 25.   2D

X
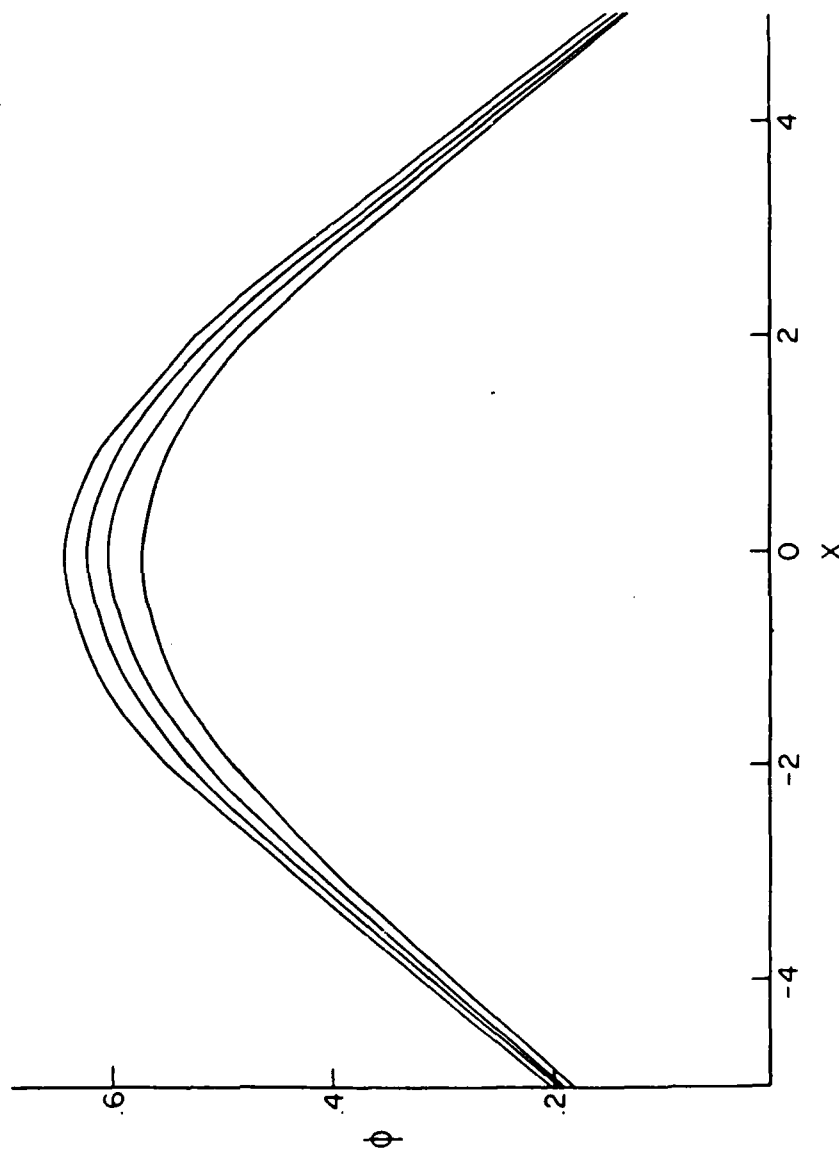
Fig. 33

Effect of changing Relative Permeability Mu on ϕ vs x for y = 8.

All can have MB1 =-.9, MB2 = -1.1, MA1 = 1.1 and MA2 =.9 with M_1=25.

2 D. The lower for the lower ϕ
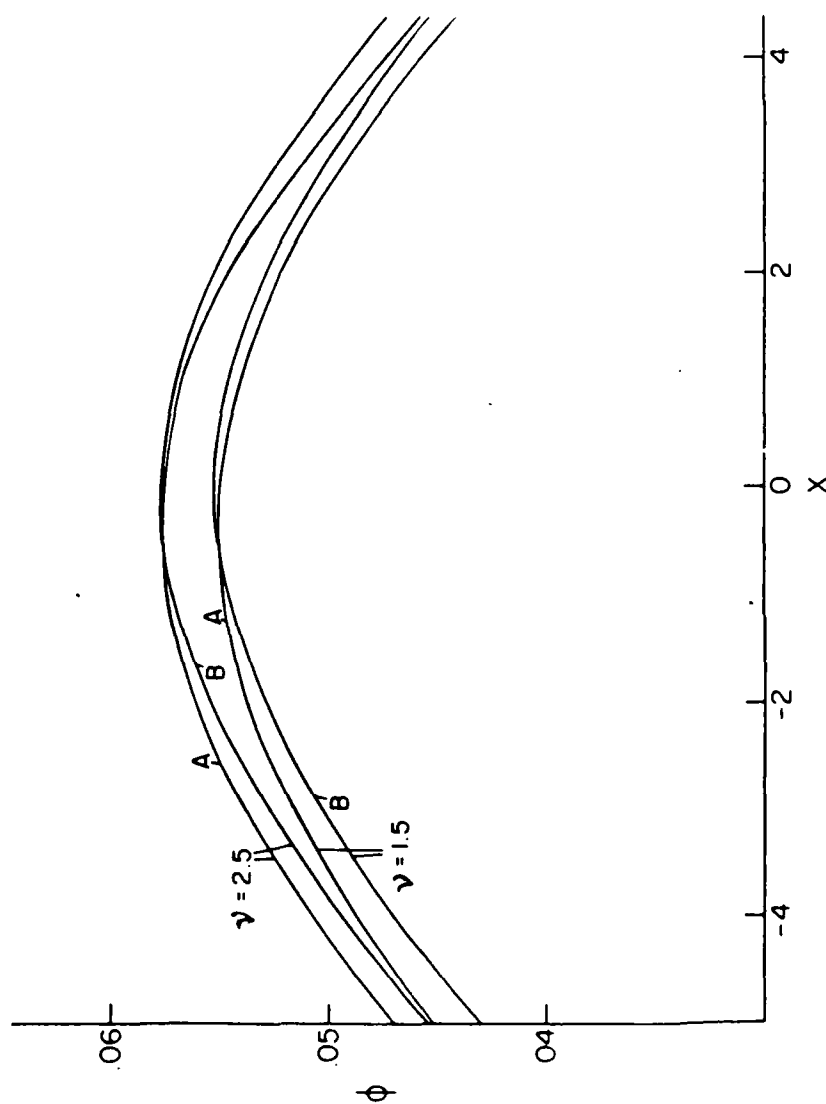
Fig. 34

Effect of Fluctuating Magnetization for Different Mu on φ vs. x

for y =20. A: has MB1 = -.9, MB2 =-1.1, MA1=1.1 and MA2=.9.   B

has MB1 = MB2 =-1 and MA1 = MA2 = 1.   2D

CHANGE IN FIELDS								
$\nu = 1$					$\nu = 2$			
J	φ	Differences	Difference of Differences		J	φ	Differences	Difference of Differences
-2	.2131				-2	.2381		
-1	.2186	} .0055			-1	.2441	.0060	
0	.2197		.0017		0	.2454	}	.0017
1	.2165				1	.2421	} .0077	
2	.2093	} .0072			2	.2344		

Table II

Figure 35. Geometry for a Rectangular TWT.

18.61
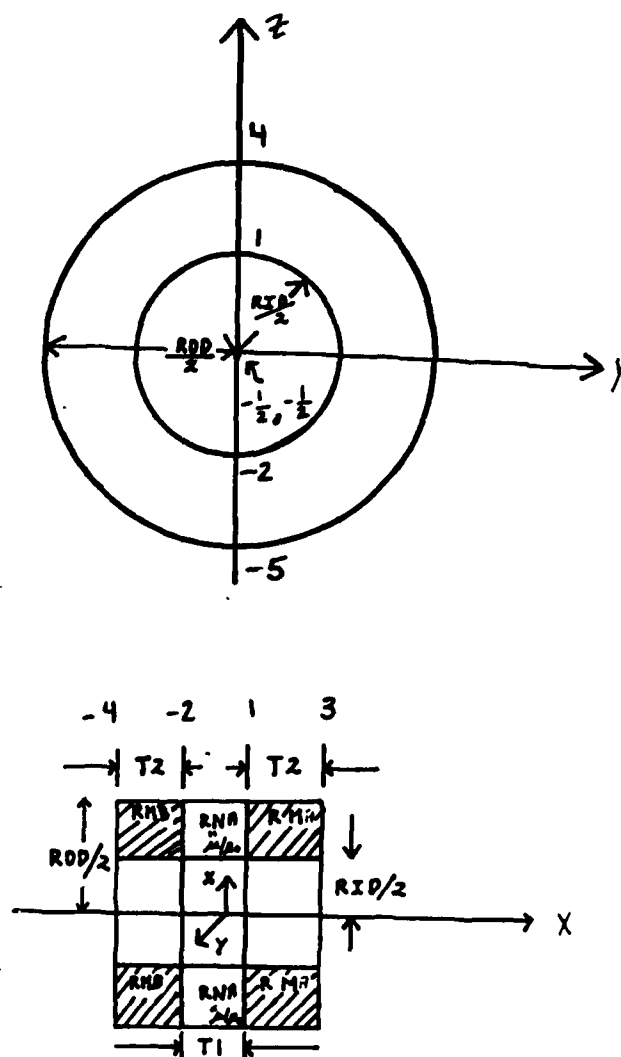
Figure 36. Simplified Geometry for a Ring TWT.

18.62
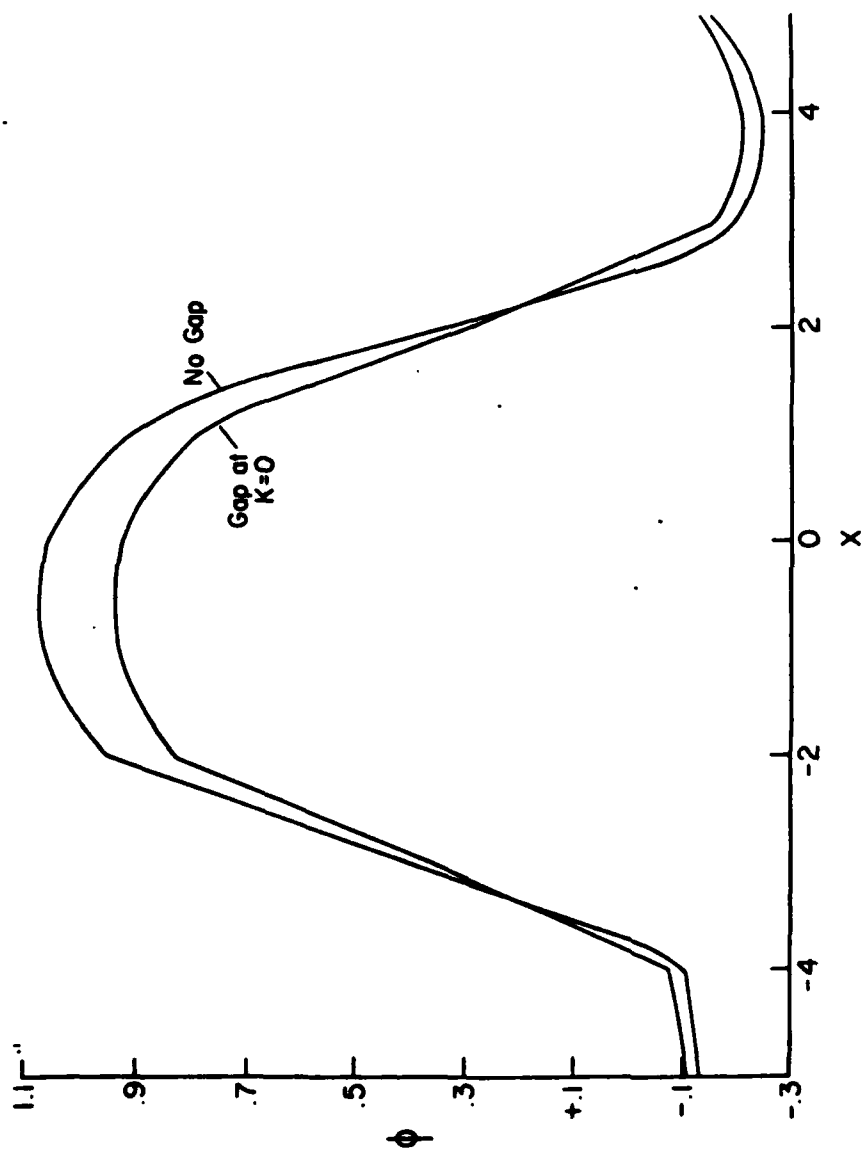
Fig. 37

Effect of Gap on Potential for Rectangular (3D) Wave Guide.

J = K = 0   φ vs. x   RMA = 1.0   RMA = -1.5.   RMB = 1.5
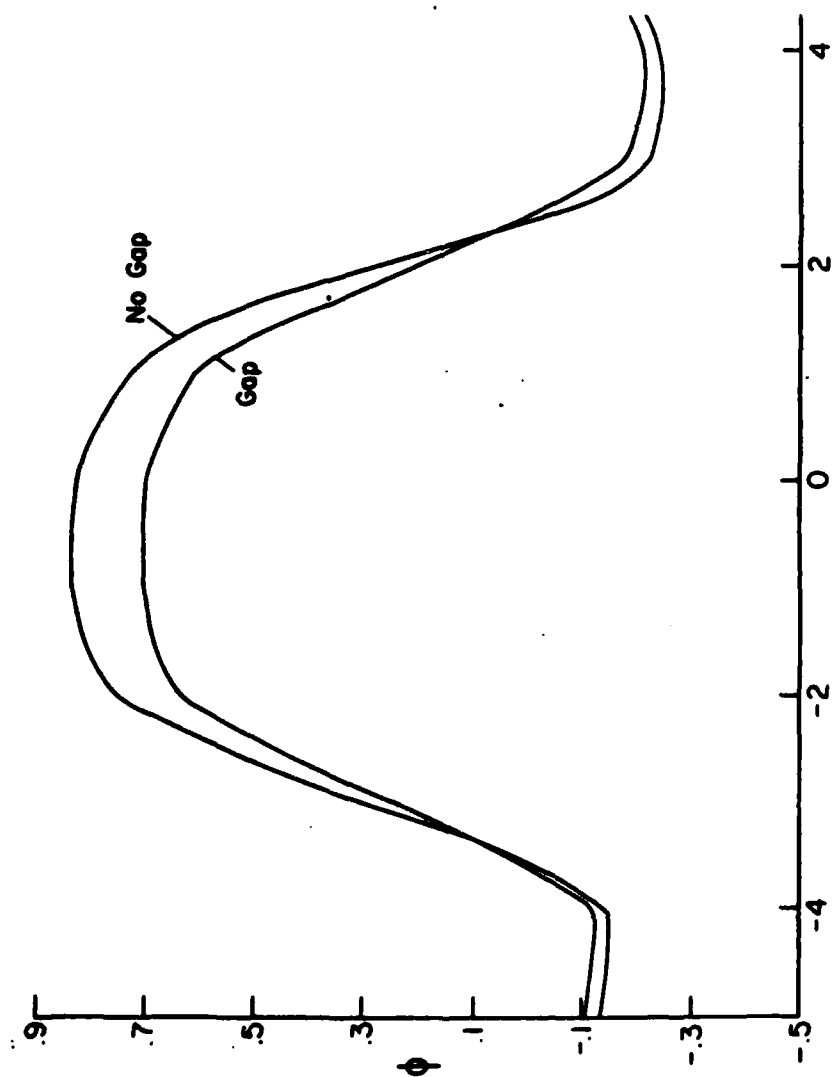
Fig. 38

Effect of Gap on Potential for (3D) "Ring", TWT, RNA = 1.0, RMA =-1.5
RMB = 1.5
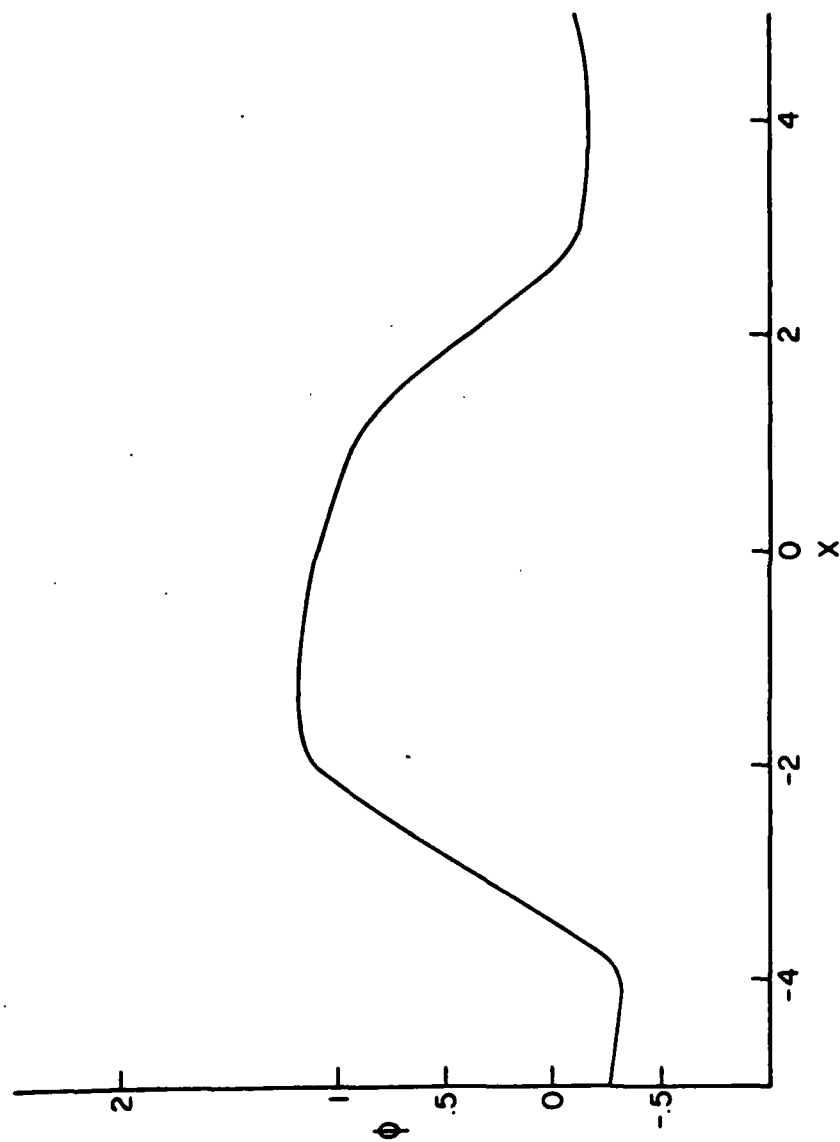
Figure 39. Effect on Potential For Magnetization Fluctuation (3D).

"Ring" TWT. RMA = 1.0, RMA = -1.5 RMB = 2.5
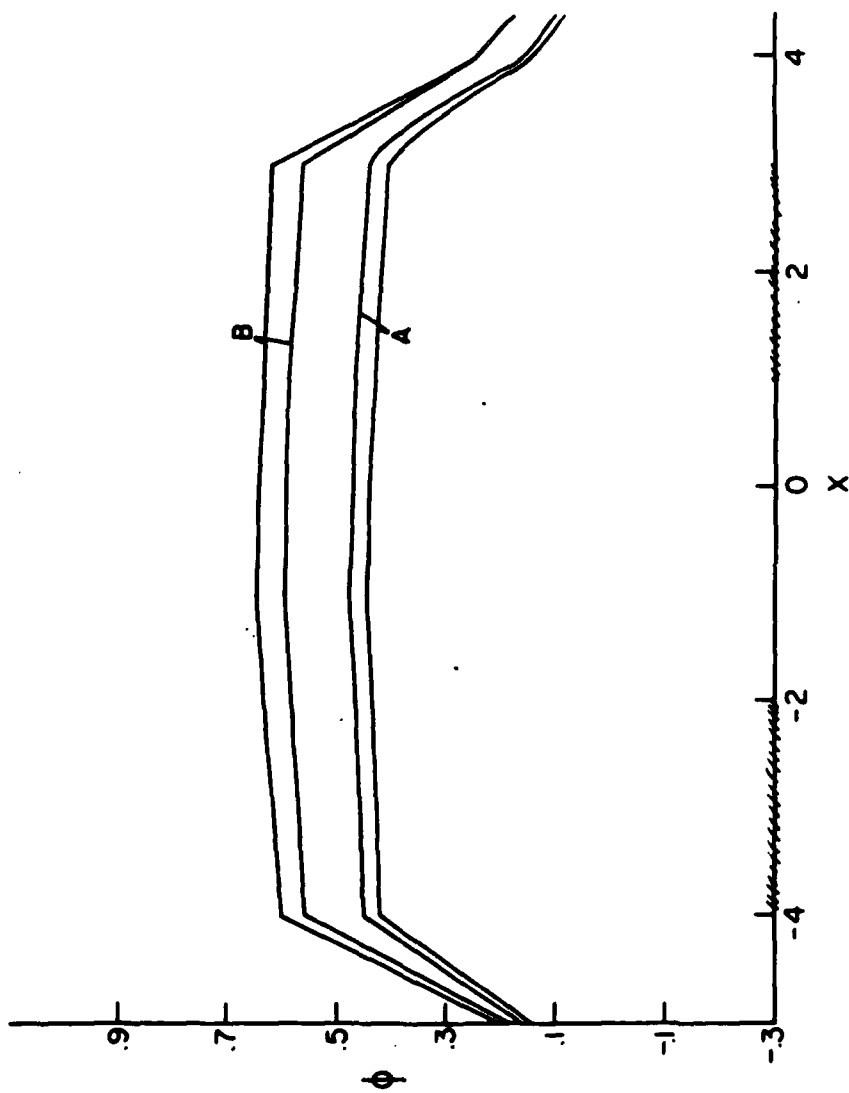
Fig. 40

Effect of High Permeability for Rectangular Case (3D).   K = J = 0

φ vs. x.   RNA = 200 A has RMA = -1.5, RMB = 1.5   B has RMA =-1.5,

RMB = 2.5.   For both A and B upper curve is with no gap.
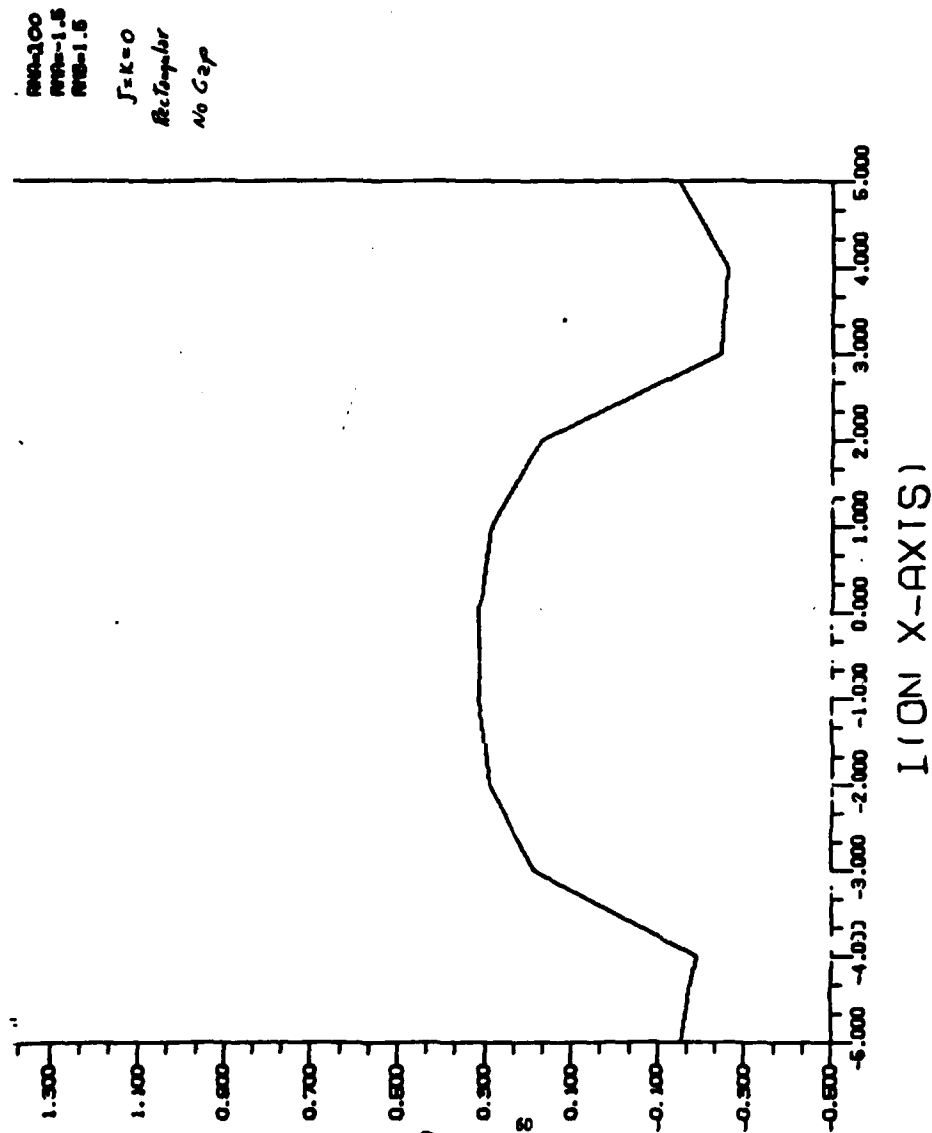
Figure 41. High Permeability 3D Rectangular Wave Guide. No gap.
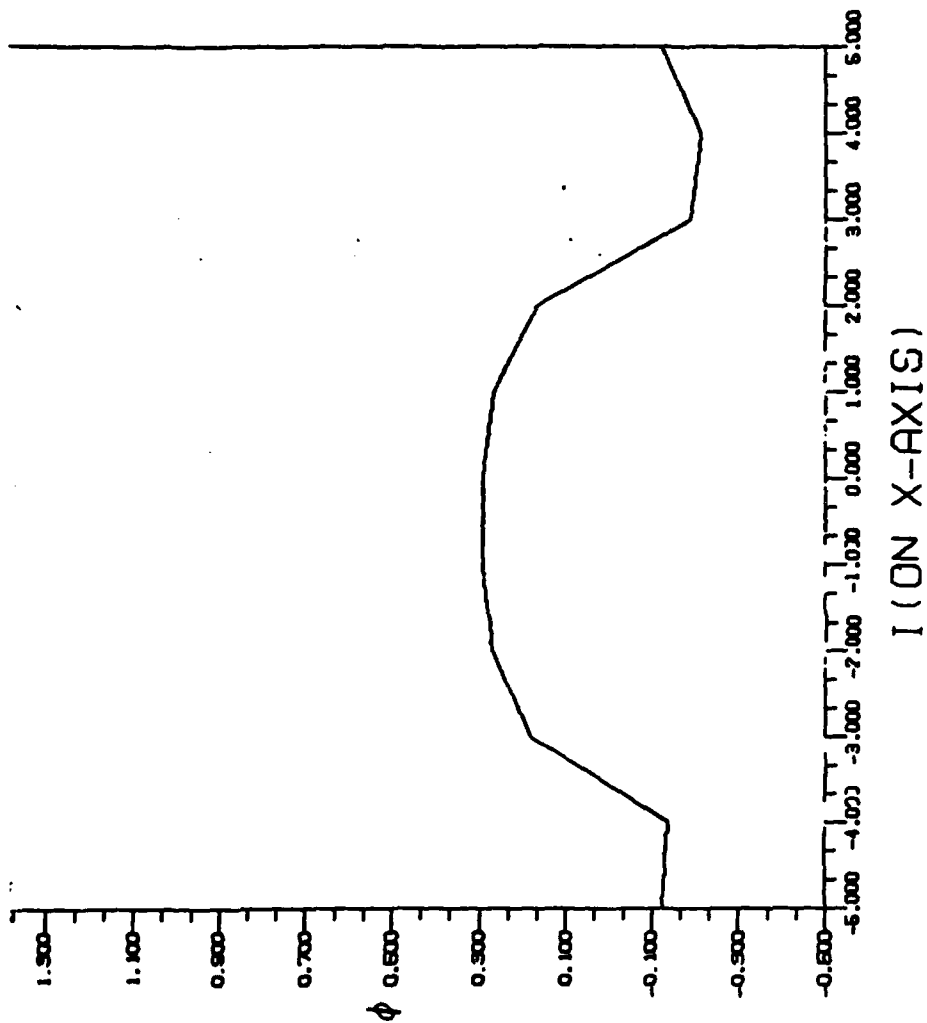
Figure 42. High Permeability 3D Rectangular Wave Guide with Gap.
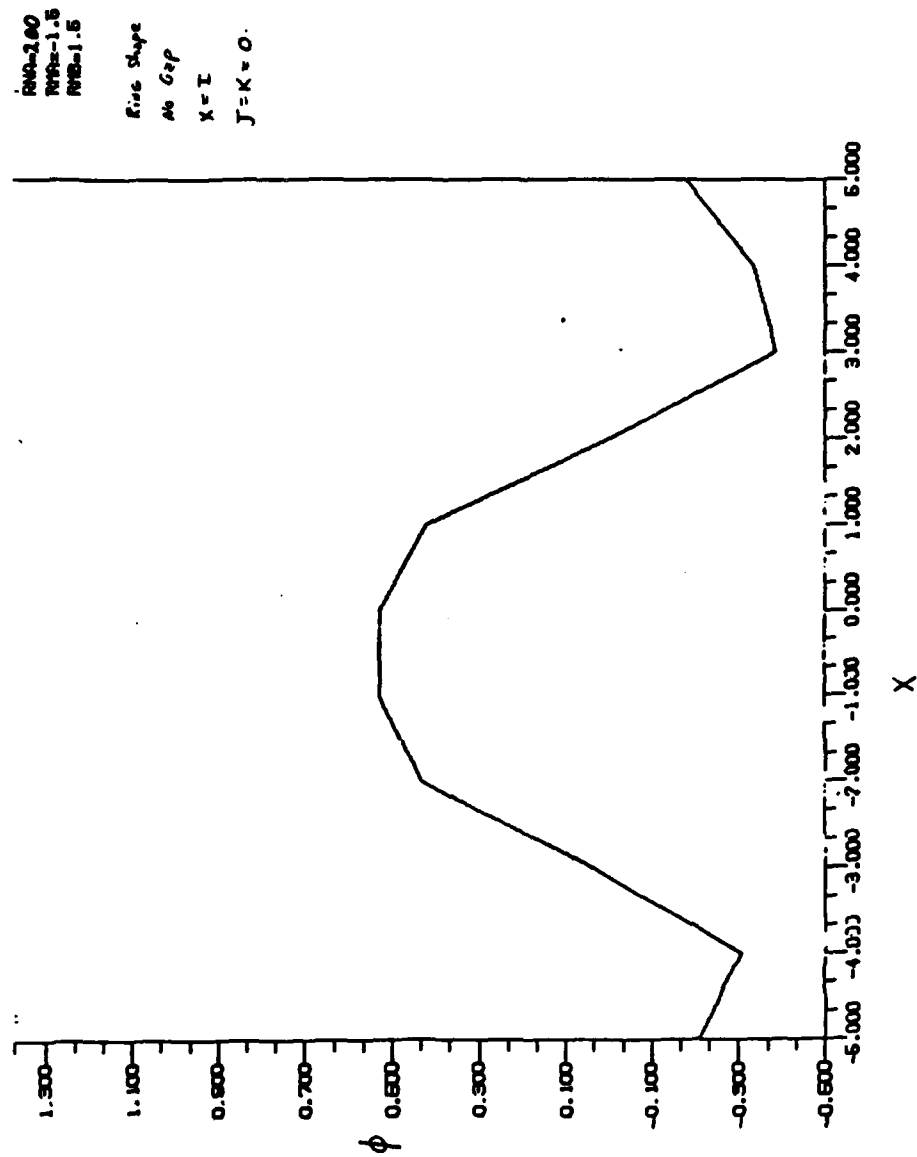
Figure 43. High Permeability 3D Ring Wave Guide. No Gap and ϕ vs X.
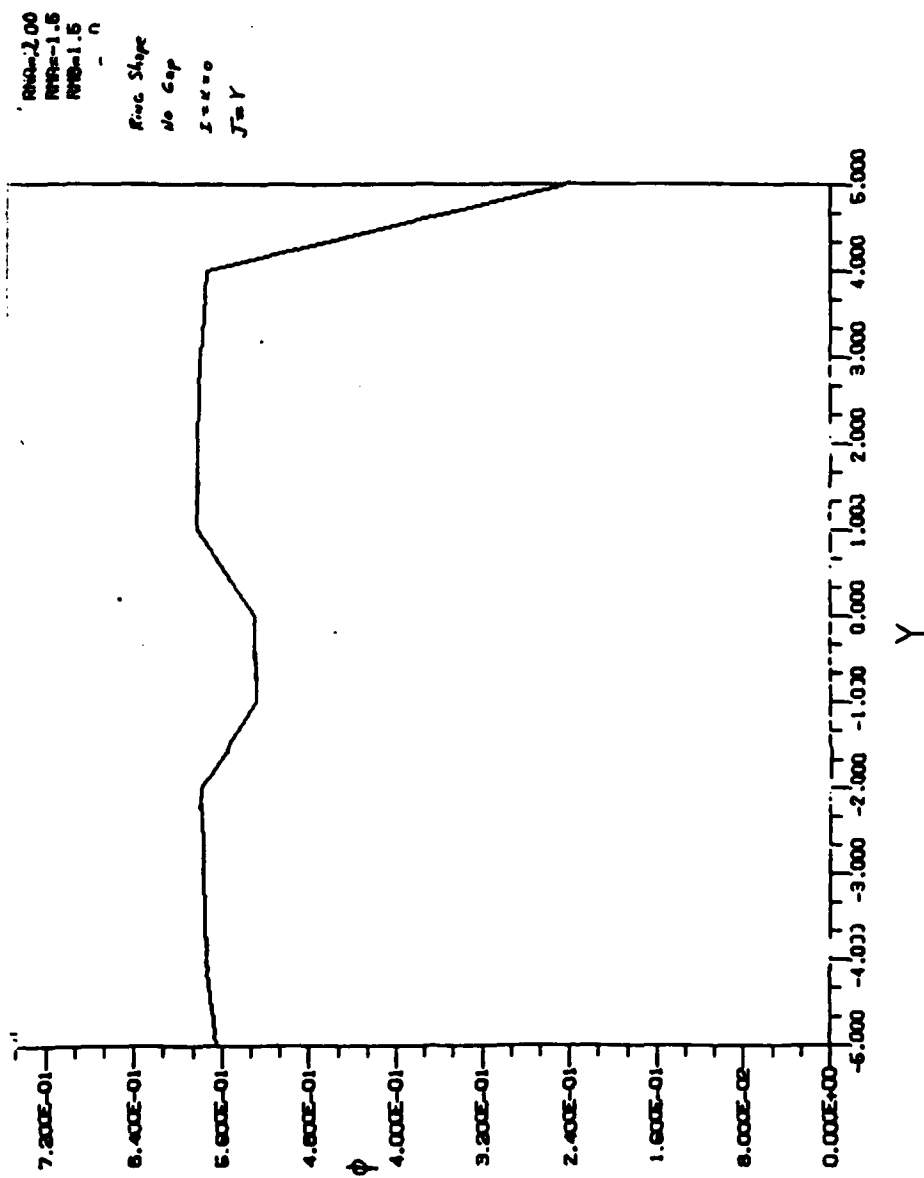
Figure 44. High Permeability 3D Ring Wave Guide. No Gap and φ vs y.
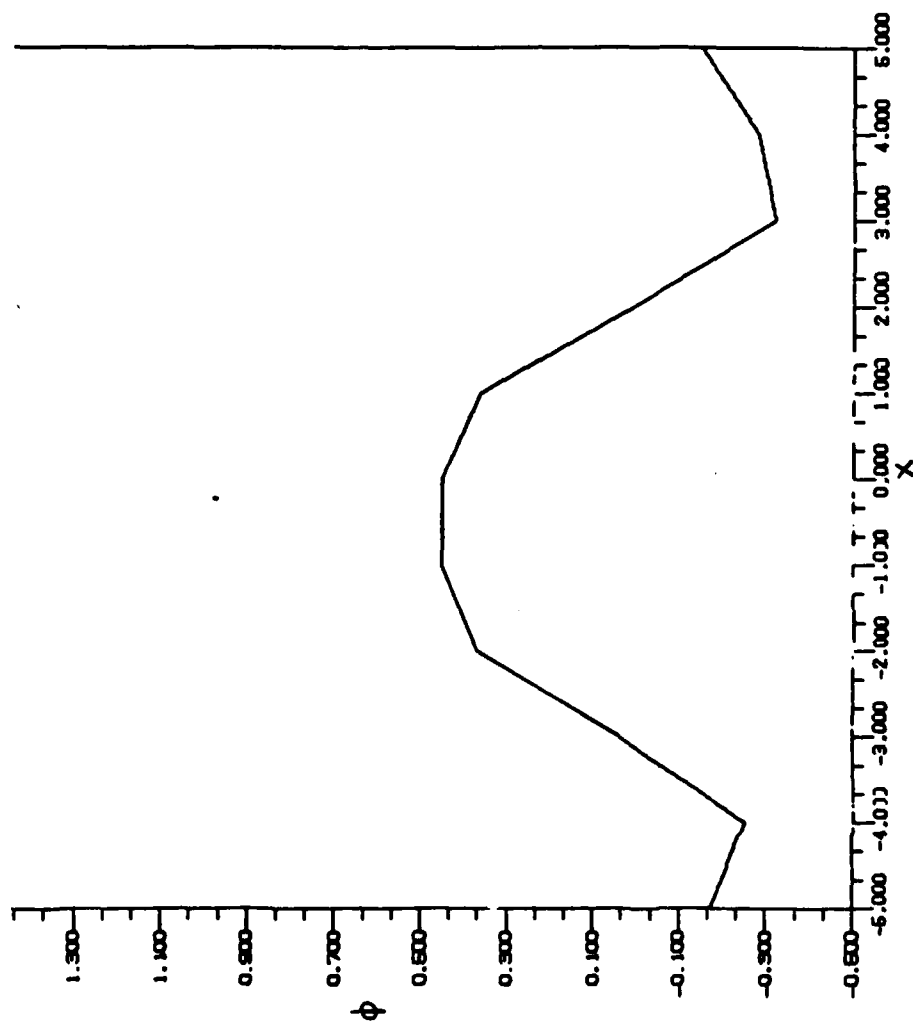
High Permeability 3D Ring Wave Guide with Air Gap.

Fig. 45

Normalizing these changes by the average field we have

$$\gamma = 1, \qquad \frac{.0017}{(.0055 + .0072)/2} = .2677$$

$$\gamma = 2, \qquad \frac{.0017}{(.0060 + .0077)/2} = .2482$$

This indicates the normalized change in field is damped out somewhat by increasing γ, but the change is not spectacular.

B. Three-Dimensional

In Figures 35-39 we show some three 3 D results. In the y=z=0 plane, the magnet region is shown by the shading (Figure 40). In Figure 37 we see that a gap at K = 0 can introduce considerable variation in ϕ. This shows up for both the "rectangular" and the " ing" wave guide, figure 38. Figure 39 shows the case of a fairly large magnetization fluctuation.

Figure 40 treats rectangular case with RNA = 200 (= the relative permeability). The case is rather artificial because permeable material is placed everywhere between the magnets including where the holes of the magnets are. The main point of the calculation is to demonstrate the capability of doing the calculation.

Figs 41-45 examine the case where the permeable material is placed only between the magnets and not where the electron beam is but for -3 <I< 2 in Figs. 41 and 42. This case is more realistic, but the flux tends then to be confined where the permeable materials are. The case is not realistic in that there are no flanges on the shims. That is, the rectangular case has a rectangular shim and the ring case has an annular ring for a shim. I = J = K = 0 is a central location. Slight asymmetries are due to asymmetries in boundary conditions.

All the 3D calculations must be viewed as somewhat preliminary. We would hope to have somewhat more realistic and useful calculations in the future.

18.72

V. Recommendations

It is a bit hard to know what to recommend. Originally we hoped to have several examples of field mappings so one could immediately calculate particle trajectories in realistic fields. This ended up being overly ambitious and so we studied more qualitative questions mostly in two dimensions. The main questions we studied had to do with the effect of the magnetically permeable shims and how their presence would modulate the fluctuations in the magnetization. We found that the shims would increase the field value and modulate it. Not enough calculations were done in 3D to have a realistic field available for calculating electron trajectories.

So should further calculational work be done? The answer to that question depends on the level of effort that could usefully be expended. To provide accurate field calculation in three dimensions for realistic examples of travelling wave tubes <u>could</u> require several man years of effort and several hundred thousand dollars worth of money. A cheaper alternative is the purchase of software and its adaption to the problem at hand. But the expenditure for software plus salaries would still be in the range of $50,000 to $100,000. I don't know if this would be a cost effective expenditure of money. Only the Air Force knows how important TWT's are to them. From the standpoint of basic physics it probably is not worth it.

Even if such a job were completed there would still be two further steps. One would be the calculation of particle trajectories in realistic fields and the second would be the calculation of the overall behavior of the tube under actual operating conditions. Here one is looking at a very considerable effort. There is a stage at which a complete analysis of a device is useful - when many such devices will be manufactured and when changes will

18.73

be often made so that it is inconvenient to take evaluative measurements all the time. Perhaps TWT's are at that stage.

The effort of Hughes to measure magnetic fluctuations of the magnets seems to be one step in the right direction.

My basic recommendation is that further small studies with limited objectives - which ask qualitative questions such as how do shims even out the inhomogeneites in the magnets - could be useful. A very large effort might be useful - depending on how cost-effective it is. I don't believe a medium scale effort is worthwhile. Such an effort would appear to be larger than needed to do relevant scientific work but not large enough for settling practical questions. In fact the calculations are sufficiently involved that should the results be of high importance and frequently requested it would probably make sense for some group to set up shop just to handle the problems. Once the programs are in place and once the operators are experienced in their use it would not take long to crank out new results. One should not, however, set up shop unless he has access to a rather powerful computer. Also, I feel that some programs should be locally generated even if heavy use will be made of canned programs. This is primarily so one will have a feeling for what is possible and what sort of errors may be present.

VI. Summary

We did "canned" (Greenfield) and "homegrown" two-dimensional calculations. We examined the effect of the shims and of magnetic inhomogeneities. We did a few similar calculations in three dimensions. We presented the basic ideas and mathematics of the calculation as well as numerical results. We also presented summary ideas of magnetostatic calculations, magnet properties and TWT properties.

We gathered some evidence for how the shims smooth out the field inhomogeneities, but completely realistic calculations were beyond our capabilities.

We recommend funding small narrowly focused projects as they arise and if they have some scientific merit and very large projects if they are needed for practical answers. We do not recommend intermediate size projects that likely would not answer scientific or practical questions.

18.75

VII. Personnel Involved

A. Principal Investigator

Dr. James D. Patterson
Professor of Physics and Space Sciences
Florida Institute of Technology
Melbourne, FL 32901

B. Graduate Students

Research Assistant

Kwang OK Park - did most of the computer runs on our handwritten two and
three dimensional programs.

Consultant and Part time Work

U. Shripathi Kamath - tried to develop a finite element program on his own.
He was not successful. However, some of his com-
ments were useful in an indirect and general way.

VIII. References

A. General References:

1. James W. Hansen (Hughes): "Eliminate Confusion in TWTA Specifications" Microwaves and RF, Vol. 23, No. 7, p. 91, July 1984.

2. Bud Pallakoff (Teledyne): "Broadband, High-Power Devices", Microwave Journal, February 1985, p. 69.

3. R.W. Herriott (Litton): "Advances in Airborne Radar TWT's Assure Their Continued Role," Microwave Systems News, Vol. 14, no. 8, p. 41, 1984.

4. Michael Kachmar (Editor): "A First Step Towards Reproducible TWT's", Microwaves and RF, Vol. 24, No. 7, p. 49, July, 1985.

5. Rudolf Kompfner, "The Invention of the Traveling-Wave Tube," San Francisco Press, 1964.

6. C. Louis Cuccia (RCA), "Periodically Focused Traveling-Wave Tubes," Radio Corporation of America, Electron Tube Division, Harrison, N.J. 1959.

7. Armand Staprans, Earl William McCune, and Jack A. Ruetz (Varian), "High-Power Linear -Beam Tubes" Proc. IEEE Vol. 61, No. 3, p. 299 March 1973.

8. Working Group, "TWT Development Problems", Defense Science and Electronics", Vol. 3, No. 4 p. 67 July, 1984.

9. J.R. Pierce (Bell), "Microwaves", Scientific American, p. 43, Aug. 1952.

10. Hughes TWT and TWTA Handbook, Electron Dynamics Division, Hughes Aircraft Company, Torrance, California.

11. J.F. Gittins, "Power Travelling Wave Tubes," American Elsevier Pub. Co. New York, 1965.

B. Magnetic Properties:

1. Donald Burnham, Gary R. Ralson, and Fred Wohlman, Jr., "Communications TWT Magnet Stack Measurement Station" (Hughes) Eighth International Workshop on Rare-Earth Magnets, Dayton, Ohio, 1985.

B. Magnetic Properties, con't:

2. Joseph J. Becker (General Electric), "Permanent Magnets",
   Scientific American, p. 92 Dec. 1970.

3. Frederic Keffer, "The Magnetic Properties of Materials", p. 222
   Sept. 1967, Scientific American.

4. Richard M. Bozorth, "Magnetic Materials," p. 68, Jan. 1955,
   Scientific American.

5. J.J. Becker, (General Electric) "Rare-Earth-Compound Permanent Magnets,"
   J. Appl. Physics, Vol. 41, No. 3, P. 1055 March, 1970.

6. D. Das, K. Kumar, and R.T. Frost and C.W. Chang (Draper Laboratory and
   General Electric Co.), "Samarium/Cobalt Magnets," NASA Tech. Briefs,
   Spring, 1984, Vol. 8, No. 3, MFS-27006.

7. W.J. Harrold (Raytheon), Permanent Magnets in Microwave Devices,"
   Technical Report No. PT-3224,Raytheon Company, 190 Willow St.
   Waltham, MA 02154.

8. Karl J. Strnat (U. Dayton), "Recent Developments in the Field of
   Rare Earth Magnets and Their Uses in the U.S.A," Proc. 6th Int.
   Workshop on Rare Earth-Cobalt Permanent Magnets, Ed, by J. Fidler,
   Tech. U. of Vienna, p. 479.

9. Karl J. Strnat (U. Dayton), "Rare-Earth Permanent Magnets: Develop-
   ment Trends and Their Implications for the Industry," from The Rare
   Earths in Modern Science and Technology, Vol. 2, Edited by Gregory J.
   McCarthy, James J. Rhyne and Herbert B. Sibler, Plenum Publ. Corp.,
   1980.

10. Karl J. Strnat, "Rare-Earth Magnets in Present Production and Develop-
    ment", J. of Magnetism and Magnetic Materials Vol. 7, p. 351 (1978)

11. H.A. Leupold, E. Potenziani, A. Tauber (Army) and H. F. Mildrum
    (U. Dayton), "High Coercivity 2:17 Cobalt Rare-Earth Magnets",
    J. Appl. Phys. Vol. 55 Not. 6, p. 2097, 15 March 1954.

12. Donald E. Polk (ONL) "Permanent Magnet Materials: An Opportunity to
    Reduce Cobalt Consumption", Naval Research Reviews, Vol. 34, p. 25
    (1982).

13. R. Wolfram (Siemens), "Application of Cobalt-REPM in Focusing of
    TWT's", Proc. 6th Intl. Workshop Rare Earth-Co. Perm Mas. (ed. by
    J. Fidler), Tech. U. of Vienna, 1982 p. 143.

14. Ch. G. Gnehm and J.P. Habere, "Homogeneity of Rare-Earth-Colbalt Magnets," Proc. 6th Intl. Workshop on Rare Earth-Co Perm. Mag. (Edited by J. Fidler), Tech. U. of Vienna, 1982, p. 329.

15. E.A. Nesbitt and J.H. Wernick (Bell Labs), "Rare Earth Permanent Magnets," Academic Press, New York, 1973.

C. Particle Beams

1. Robert R. Moats (Northrop), "Calculations of Beam Trajectories under Non-Ideal Conditions of PPM Focusing", Preprint.

2. A.M. Clogston and H. Heffner (Bell Labs), "Focusing of an Electron Beam by Periodic Fields", J. Appl. Physics Vol. 25, No. 4, p. 435 (1954).

3. J.D. Lawson, "The Physics of Charged-Particle Beams", Clarendon Press, Oxford, 1977.

4. Peter T. Kirstein, Gordon S. Kino and William E. Waters, "Space-Charge Flow", McGraw-Hill Book Co.

5. W.J. Kleen, "Electronics of Microwave Tubes", New York, Academic Press, Inc. New York, 1958.

6. J.R. Pierce, "Theory and Design of Electron Beams", D. Van Nostrand Co., Inc. New York, 1954.

D. Calculation of Fields:

1. Herbert A. Leupold (Army), "Design Considerations in the Employment of Rare Earth-Cobalt Permanent Magnets as Flux Sources", U.S. Army Electronics Research and Development Command, Fort Monmouth, N.J., Tech. Report Delet-TR-82-9.

2. "Canned" Programs can be purchased from Vector Fields Ltd., Kemp Hall Bindery, Osney Head, Oxford, OX2 DEE, U.K.

3. Also "Canned" program can be purchased from Quantic Laboratories Inc., Winnipeg, Canada. We used their Greenfield program.

4. Another "canned" program can be purchased from AOS Magnetic Analysis Program, 8901 No. Kildeer Court, Milwaukee, WI 53209.

5. O.C. Zienkiewicz, John Lyness, and D.R.J. Owen (U.K.) "Three-Dimensional Magnetic Field Determination Using a Scalar Potential-A Finite Element Solution," IEEE Transaction on Magnetics Vol. Mag, -13, No. 5, p. 1649, Sept. 1977.

D. Calculation of Fields, cont:

6. M.V.K. Chari and A. Konrad, J. D'Angelo M.A., Palmo (General Electric) "Finite Element Computation of Three-Dimension Electrostatic and Magnetostatic Field Problems", Trans. On Magnetics., Vol. Mag-19, No. 6, p. 2321 Nov. 1983.

7. S.J. Farlow, "Partial Differential Equations for Scientists and Engineers", John Wiley and Sons, New York, 1982.

8. O.C. Zienkiewicz, and K. Morgan, "Finite Elements and Approximation", John Wiley and Sons, New York, 1983.

E. Focussing of Electron Beams:

1. J.R. Pierce, Spatially Alternating Magnetic Field for Focusing Low-Voltage Electron Beams", J. Appl. Physics, Vol. 24, No. 9, p. 1247 (1953).

2. Kern K.N. Chang, (RCA), "Beam Focusing by Periodic and Complementary Fields" Proc. of the I.R.E. Vol. 43, p. 62, Jan. 1955.

3. J.T. Mendel (Bell Labs), "Magnetic Focusing of Electron Beams,"

4. J.T. Mendel, C.F. Quate and W.H. Yocum, (Bell) "Electron Beam Focusing with Periodic Permanent Magnetic Fields", Proc. of the I.R.E. Vol. 42, p. 800 (1954)

5. J.E. Sterrett and H. Heffner (Stanford), "The Design of Periodic Magnetic Focusing Structures", I.R.E. Trans. Electron Devices, Vol. ED-5 p. 35, Jan. 1958.

6. F. Sterzer and W.W. Siekanowicz (RCA), "The Design of Periodic Permanent Magnets for Focusing of Electron Beams" R.C.A. Review Vol. 18, p. 39 (1957)

7. Mario Corsi, A. Diligenti and G. Saladi, "Graphical Method for Optimum Design of Periodic Magnetic Focusing Structures", IEEE Transaction on Electron Devices Vol. Ed-21, No. 1, p. 2 Jan. 1974.

18.80

F. Powerful Magnets with Nd.

1. Arthur L. Robinson, "Powerful New Magnet Material Found, Science Vol. 223, p. 920 (1984).

2. J.F. Herbst and J.J. Croat (General Motors) and W.B. Yelon (Missouri) "Structural and Magnetic Properties of $Nd_2Fe_{14}B$", J. Appl. Phys. vol. 57 No. 1, p. 4086 (1985).

G. Related Reports and Proposals by Author:

1. "Permanent Periodic Magnets and the Reproducibility of Traveling Wave Tubes" J.D. Patterson Final Report to SCEEE 24 August 1984, Contract No. F49620-82-C-0035.

2. "Effect of Pole Pieces on the Axial Magnetic Field in Traveling Wave Tubes," J.D. Patterson, Proposal to SCEEE 15 Oct., 1984.

IX Appendices

A. Review of Relevant Magnetostatics

1. Basic Quantities

We use here S.I. units. see Jackson Classical Electrodynamics for a discussion of units.(p. 816)

First we set the notation. Let B be the magnetic induction or the magnetic flux density. Let M be the magnetization or the magnetic moment/volume. We then define the magnetic field intensity as

$$\vec{H} = \vec{B}/\mu_0 - \vec{M} \tag{A 1}$$

where $\mu_0 = 4\pi \times 10^{-7}$ in S.I. units. Both $\vec{H}$ and $\vec{M}$ nave units of amps/m. In the absence of external currents or of displacement current, we can write two of Maxwell's equations as

$$\vec{\nabla} \cdot \vec{B} = 0 \tag{A 2}$$

$$\vec{\nabla} \times \vec{H} = 0. \tag{A 3}$$

These are the basic equations of magnetostatics.

We now want to apply these to actual ferromagnetic materials. Such materials have two relevant properties. (i) Below a certain temperature, called the Curie Temperature, the material spontaneously magnetizes. See Fig. A 1 (ii) A spontaneously magntized material splits into domains (regions with different directions of magnetization). Domains cause the phenomena of hysteresis. See Fig. A 2.
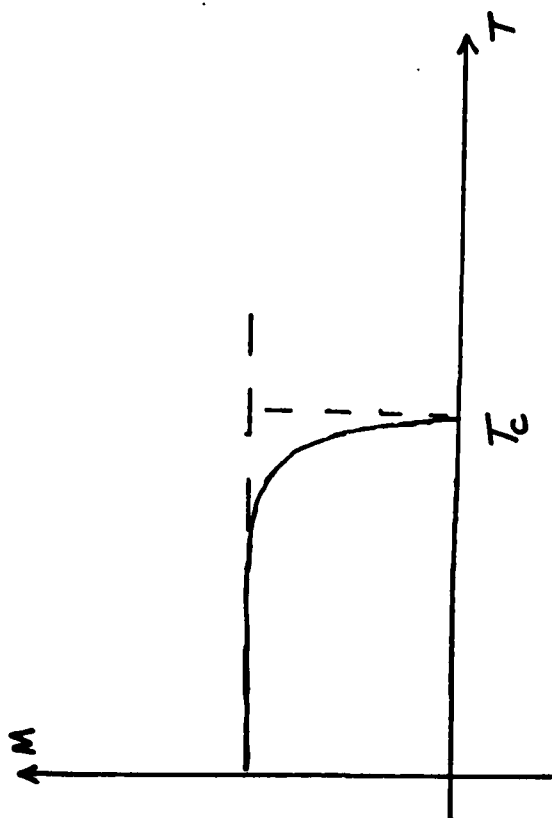
Figure A 1: Spontaneous Magnetization vs T at H=0. M_s is the Saturation Magnetization at $T = 0$ and T_c is the Curie Temperature.

18.83

Fig. A2 (a)

Fig. A2 (b)
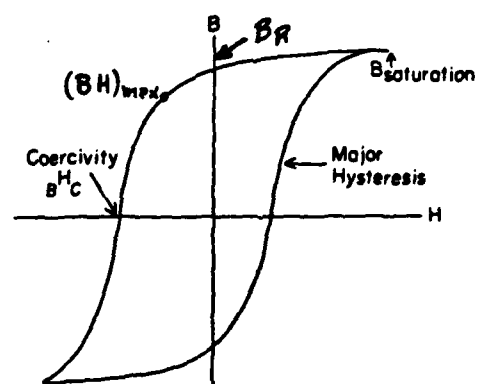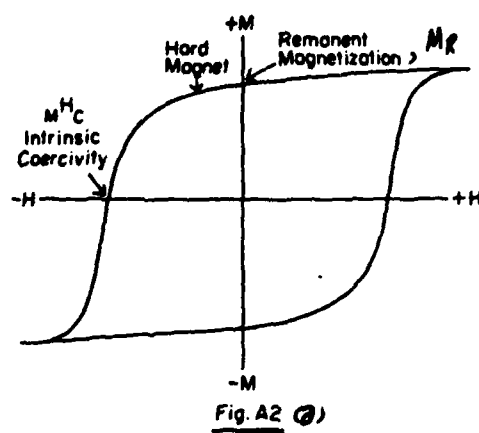
Figure A 2: Hysteresis (a) M vs H for $T < T_C$. (b) B vs H for $T < T_C$, $_MH_C$ is called the Intrinsic Coercivity. $_BH_C$ is called the Coercivity. M_R is called the Remanent Magnetization or Remanence. B_R is called the Retentivity. (BH) max is the maximum energy product.

2. The Magnetic Circuit ^(D1)

These equations can be used when we want some fairly crude estimates. By Ampere's law, when displacement currents can be neglected, we have

$$\oint_c \vec{H} \cdot d\vec{l} = I_{enclosed\ by\ c} . \qquad \text{(A 4)}$$

The quantity $\oint \vec{H} \cdot d\vec{l}$ is sometimes called the magnetomotive force (m.m.f.) by analogy to the electromotive force.

The m.m.f. is regarded as responsible for the production of flux through the magnetic circuit. In analogy to the resistance in Ohm's law, a quantity R, the reluctance is defined by

$$\mathcal{R} = \frac{\oint \vec{H} \cdot d\vec{l}}{\int \vec{B} \cdot d\vec{A}} = \frac{m.m.f.}{\phi} , \qquad \text{(A 5)}$$

where ϕ is the flux. R^{-1} is called the permeance.

An example should clarify the applications. Consider a <u>thin</u> toroidal solenoid wrapped on a material with permeability μ. The cross section is A. There are N turns of wire uniformly wound on it. The wire carries Current I.

Ampere's law gives

$$H = NI/L . \qquad \text{(A 6)}$$

We consider materials for which

$$B = \mu H = \mu\, NI/L . \qquad \text{(A 7)}$$

The reluctance is

$$R = \frac{HL}{BA} = \frac{HL}{\mu HA} = \frac{L}{\mu A} . \qquad \text{(A 8)}$$

Series and parallel combinations can be analyzed just as for D.C. circuits.

Series $\Phi = \dfrac{m.m.f}{\dfrac{\ell_1}{\mu_1 A_1} + \dfrac{\ell_2}{\mu_2 A_2} + \cdots}$ (A 9)

Parallel $\Phi = \dfrac{m.m.f.}{1/\left(\dfrac{\mu_1 A_1}{\ell_1} + \dfrac{\mu_2 A_2}{\ell_2} + \cdots \right)}$ (A 10)

The difficulty with this sort of analysis is that flux tends to leak out and hence the analysis lends to inexact results.

The discussion of permanent magnets is a little more complicated. We will consider $SmCo_5$ like magnets with a magnetization that we can regard as constant. Then

$$B = \mu_0 (H + M_s)$$ (A 11)

and thus (A 12)

$$_B H_c = - M_s$$

with (A 13)

$$B_r = \mu_0 M_s$$

We define

$$\mu_a \equiv \left| \frac{B_r}{_B H_c} \right| = \mu_0 ,$$

by A12 and A13.

Consider a situation like that shown in the Figure A 3.

18.86
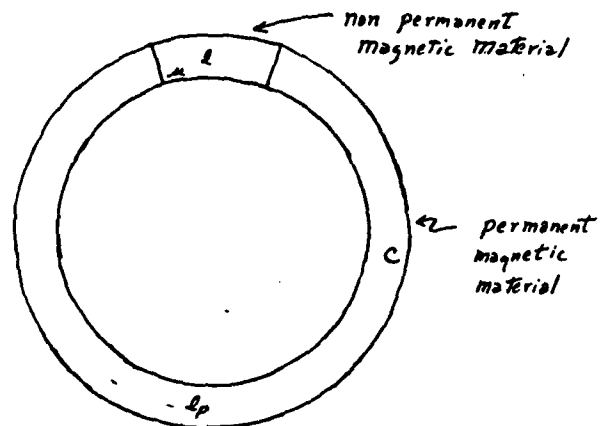
Figure A 3: Example of Magnetic Circuit
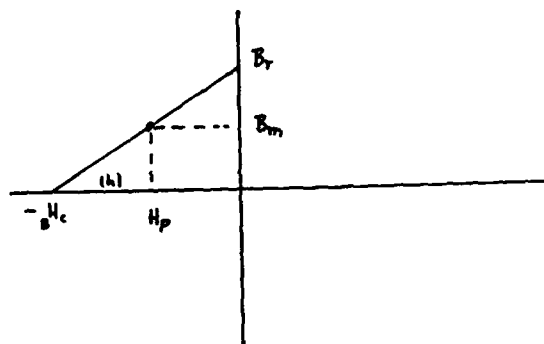
Figure A 4: Operating Point and Related Matters for Sm Co_5 ring of Fig. A3

Around a closed loop C

$$\oint H\,d\ell = 0$$

so

$$H_p\,\ell_p + H\ell = 0$$

or

$$-H_p\,\ell_p = H\ell = \frac{B\ell}{\mu} = \frac{BA\ell}{A\mu} = \Phi R,$$

where R is the reluctance. H_p is the operating point of the magnet. Refer to Figure A 4.

Note

$$\frac{B_r}{|_sH_c|} = \frac{B_m}{|h|} = \mu_\partial$$

So

$$_BH_c = |h| + |H_p| = \frac{B_m}{\mu_\partial} - H_p = \frac{B_m}{\mu_\partial} + \frac{\Phi R}{\ell_p}$$

or

$$_BH_c\,\ell_p = \Phi R + \frac{B_m\,\ell_p\,A_p}{\mu_\partial\,A_p} = \Phi(R + R_m)$$

where

$$R_m = \frac{\ell_p}{\mu_\partial\,A_p}$$

We interpret $_BH_c\,\ell_p$ as the m.m.f. of the permanent magnet so

$$m_p = {}_BH_c\,\ell_p = \frac{B_r}{\mu_\partial}\,\ell_p$$

$$\Phi = \frac{m_p}{R + R_m}\tag{A 14}$$

is analogy of Ohm's law.

18.88

Example $SmCo_5$

$$B_r \cong 10^4 \, gauss = 1 \; Tesla$$

$$R = \frac{L}{\mu A}$$

$$\Phi = \frac{B_r \ell_p / \mu_0}{\frac{L}{\mu A} + \frac{\ell_p}{\mu_0 A}} = \frac{B_r A}{\frac{\mu_0}{\mu} \frac{L}{\ell_p} + 1}$$

$$\Phi = \frac{\overline{\Phi}_r}{\frac{\mu_0}{\mu} \frac{L}{\ell_p} + 1}$$

$$B = \frac{B_r}{\frac{\mu_0}{\mu} \frac{L}{\ell_p} + 1} \longrightarrow B_r \quad as \; \frac{\mu}{\mu_0} \longrightarrow \infty$$

18.89
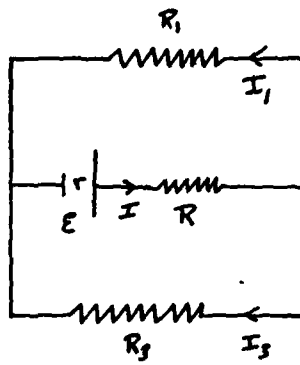
Figure A 5: Electrical Circuit
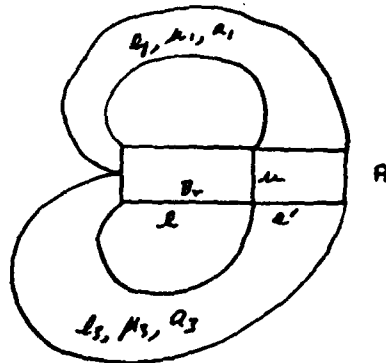
Figure A 6: Equivalent Magnetic Circuit   for Fig. A5

18.90

We now consider the cases of Figs. A 5 and A 6.

BASIC EQUATIONS

1. $I = I_1 + I_3$

2. $\varepsilon = (r+R)I + R_1 I_1$

3. $\varepsilon = (r+R)I + R_3 I_3$

$$R_1 I_1 = R_3 I_3$$

$$I_1 = I_3 \, R_3/R_1$$

$$I = I_3 + I_3 \, R_3/R_1$$

$$\varepsilon = (r+R)\left[1 + R_3/R_1\right] I_3 + R_3 I_3$$

$$\varepsilon = \left\{ \left(\frac{r+R}{R_1}\right)\left[R_1 + R_3\right] + R_3 \right\} I_3$$

$$I_3 = \frac{\varepsilon}{R_3 + (R_1 + R_3)\left(\frac{r+R}{R_1}\right)}$$

18.91

Transcribe to Magnetic Case:

$$\mathcal{E} \rightarrow B_r \ell / \mu_0 \qquad R = \ell' / \mu A \;,\quad R_1 = \frac{l_1}{\mu_1 a_1} \;,\quad R_3 = \frac{l_3}{\mu_3 a_3}$$

$$I_3 \rightarrow \bar{\Phi}_3 \qquad\qquad r = \frac{1}{\mu_0 A} \;, \quad \ldots$$

$$B_3 = \frac{\bar{\Phi}_3}{a_3} = \frac{B_r \left[A / a_3 \right]}{\left(\frac{A}{a_3} \right)\left(\frac{l_3}{\ell} \right)\left(\frac{\mu_0}{\mu_3} \right) + \left[\left(\frac{\mu_0}{\mu_1} \right)\left(\frac{l_1}{\ell} \right) + \left(\frac{\mu_0}{\mu_3} \right)\left(\frac{l_3}{\ell} \right)\left(\frac{a_1}{a_3} \right) \right] \left[\dfrac{1 + \left(\frac{\mu_0}{\mu} \right)\left(\frac{\ell'}{\ell} \right)}{\left(\frac{l_1}{\ell} \right)\left(\frac{\mu_0}{\mu_1} \right)} \right]}$$

We now apply to a case with fairly realistic numbers.

$$\frac{A}{a_3} \cong 5 \;,\quad \frac{l_3}{\ell} = 5 \;,\quad \frac{\mu_0}{\mu_3} \cong 1 \;,\quad \frac{\mu_0}{\mu_1} = 1$$

$$\frac{a_1}{a_3} \cong \frac{1}{5} \;,\quad \frac{\mu}{\mu_0} = 200 \;,\quad \frac{\ell'}{\ell} = 1 \;,\quad \frac{l_1}{\ell} = 5$$

We find:

$$B_3 \cong \frac{5 B_r}{25 + 6/5} \cong B_r / 5$$

3. Maximum Coercivity and Energy Product.

The maximum coercivity is the anisotropy field if assume notation would produce largest coercivity.

$$E_A = K_1 \sin^2\theta = -H_A M \cos\theta + \text{constant.}$$ (A 15)

The torques due to each should balance

$$2K_1 \sin\theta \cos\theta = H_A M \sin\theta.$$

For small angles $\cos\theta \cong 1$ so

$$H_A = 2K_1/M.$$ (A 16)

The maximum energy product

$$BH = \mu_0 (H^2 + HM)$$

requires

$$\frac{d}{dH}(BH) = 0$$

$$2H + M + H\frac{dM}{dH} = 0$$

$$H = -\frac{1}{2}\left(M + H\frac{dM}{dH}\right) = -\frac{1}{2}(M + \chi H)$$

$$-BH = -\frac{\mu_0}{4}\left[M^2 + H^2\chi^2 + 2MH\chi - 2M^2 - 2\chi HM\right]$$

$$= -\frac{\mu_0}{4}\left[H^2\chi^2 - M^2\right] \geq \frac{\mu_0 M^2}{4} \geq \frac{\mu_0 M_s^2}{4}$$

(A17)

18.93

4. <u>Comparison of Magnetic Force on Electron with Typical Electron - Electron</u>

   <u>Force.</u>

Consider an electron accelerated by a voltage of V=1500 volts. By energy
conservation, the kinetic energy is

$$\frac{1}{2} m v^2 = e V$$

so the velocity v of the electron is

$$v = \sqrt{\frac{2eV}{m}}$$

where e is the magnitude of the electron charge and m is the electron mass.
Substituting, we find:

$$v \cong 2.3 \times 10^7 \ m/s$$

$$\frac{v}{c} \cong \frac{1}{13}$$

where c is the speed of light.

The maximum force on such an electron in a magnetic flux density of 1000 gauss =
.1 Tesla is

$$F = q v B$$

which comes out

$$F \cong 3.7 \times 10^{-13} \ N.$$

To get an estimate for a typical force due to electron-electron
interactions, it is convenient to start with the beam current   I.

$$I = (n \ e \ v) A$$

where n is the number of electrons per unit volume, v is their average velocity
and A is the cross sectional area.

18.94

Applying Gauss' law to a cylindrical segment of current of length ℓ and radius r

$$E\,(2\pi r\ell) = \frac{1}{\varepsilon_0}\,(ne)(A)(\ell)$$

where E is the radial electric field. Thus

$$E = \frac{1}{2\pi\varepsilon_0}\,\frac{Ane}{r}.$$

Thus a typical electric force arising from the electron-electron interactions is

$$F = eE = \frac{1}{2\pi\varepsilon_0}\,\frac{(Ane)e}{r}$$

But since $\qquad nev = I/v \qquad$ we have

$$F = \frac{1}{2\pi\varepsilon_0}\,\frac{Ie}{vr}$$

Assuming I = 1mA, and y = .001 m we obtain for $v \cong 2.3 \times 10^{+7}$ m/s

$$F \cong 1.25 \times 10^{-16}\,N$$

Thus

$$\frac{F_{Mag}}{F_{Elect}} \cong \frac{3.7 \times 10^{-13}}{1.25 \times 10^{-16}} \cong 3100$$

In general we have

$$F_E = \frac{1}{2\pi\varepsilon_0}\,\frac{Ane^2}{r} = \frac{1}{2\pi\varepsilon_0}\,\frac{Ie}{vr}$$

$$F_M = evB$$

Thus $\hfill$ (A 18)

$$\frac{F_M}{F_E} = \frac{evBr}{mI/(4\pi\varepsilon_0)} \quad.$$

Using $I = \frac{1}{2}$ mA and r = .001 meter we run out a few examples:

V	B	computed F_M/F_E
1500 V	.1 T	2927 ($\cong$ 3000 as before)
1000 V	.0145 T	283
500 V	.01	97.6

The moral of this story is that magnetic forces can certainly be important.

(B1-B14, F1-F2)

B. Review of Relevant Properties of Magnets

Some typical values for Sm Co$_5$ are

Max Energy Density (BH)$_{max}$ = 190 KP$_a$ (24 MGO$_e$)

Retentivity B_R = 980 mT (9.8 kG)

Intrinsic Coercivity $_M H_c$ = 960 kA/m (12kO$_e$)

(see e.g. K.J. Strnat   J. Mag. Mag. Mat. 7, 351 (1978).

The Curie temperatures of SmCo$_5$ magnets are typically over 1000 K.

By contrast ALNICO 8 (Fe$_{36}$ Ni$_{15}$ Al$_7$ Co$_{36}$ Ti$_6$)

(BH)$_{max}$ = 40 kP$_a$ (5.1 MGO$_e$)

B_R = 850 mT =(8.5 kG)

$_M H_c$ = 130 kA/m = 1.6 kA

(D.E. Polk, Naval Res. Rev. XXXIV, 24 (1982), and

Sm$_2$ (Co,Fe, Cu, Zr)$_{17}$

(BH) max = 175 kP$_a$ = (22 MGOe)

B_R = 1060 mT = (10.6 kG)

$_m H_c$ = 560 kA/m = (7kOe)

18.96

(D.E. Polk, Op. Cit).

Some typical Curie temperatures (T_c) and saturation magnetizations M_s are:

	T_c	M_s (0°K)
Fe	1043 K	174 mT(1.740 kG)
Ni	627K	51.0 mT (.510kG)
Co	1388 K	144.6 mT(1.446 kG)
Gd	292K	206.0 mT(2.060 kG)

(C. Kittel, Intro.to S.S. Phys., Wiley, 1976, p. 465).

Permeabilities are highly variable. Initial permeabilities of various materials can be for example:

	Initial ($\frac{\mu}{\mu_o}$)	max ($\frac{\mu}{\mu_o}$)
mild steel	120	2000
permalloy	8000	100,000
Nickel	110	600

(see e.g. S. Chikazumi, "Physics of Magnetism", Wiley, 1964.).

C. Review of Relevant Travelling Wave Tube Properties - dimensions/magnetic properties (E1-E7)

Some Typical Sizes used in TWT PPM's

Inner Radius	Outer Radius	Thickness
3.71 m m	6.73 m m	1.78 m m
(.146 inches)	(.265 inches)	(.070 inches)

18.97

Some Typical Values for Magnetic Parameters Used in <u>TWT PPM's</u>

Remanence Br	Coercive Force mHc	Intrinsic Coercive Force	(BH) max Energy Product	H_K
1 T (10 kG)	800 kA/m(10kOe)	1500kA/m(18kOe)	200kPa≈25MGOe)	1100kA/m(14kOe)

These are Ball-Park Figures

D Some Analytical Solutions

Only special geometries allow an exact solution. This is the reason for the importance of numerical results. We summarize a few results here.

a. Field of uniformly magnetized sphere (J.D. Jackson, Classical Electro-
dynamics, p. 194)

The magnetic field inside the sphere of radius a is

$$\vec{H}_{in} = -\frac{1}{3}\vec{M} \qquad\qquad (A\ 19)$$

The magnetic induction inside the sphere is

$$\vec{B}_{in} = \frac{2\mu_0 \vec{M}}{3} \qquad\qquad (A\ 20)$$

Outside the sphere the magnetic potential is

$$\phi = \frac{M a^3}{3}\frac{\cos\theta}{r^2}$$

$$\vec{H}_{out} = -\vec{\nabla}\phi$$

$$\vec{B}_{out} = \mu_0 \vec{H}_{out}.$$

18.98

b. <u>Uniformly Magnetized Sphere in a Constant</u>

   <u>External Field</u> (Page and Adams, "Principles of Electricity", D. Van

Nostrand, 1958 3rd ed. p. 122, Jackson, p. 197).

   We use the results of Part a. By Superposition if the external fields

is $\vec{B}_o = \mu_o \vec{H}_o$;

$$\vec{B}_{in} = \vec{B}_o + \frac{2}{3}\mu_o \vec{M}$$

$$\vec{H}_{in} = \vec{B}_o/\mu_o - \frac{1}{3}\vec{M}.$$

Suppose $\vec{M}$ results from the applied field and $\vec{M}$ is not from a permanent magnet.

   Then

$$\vec{B}_o + \frac{2}{3}\mu_o \vec{M} = \mu_o \left(\frac{\vec{B}_o}{\mu_o} - \frac{1}{3}\vec{M}\right)$$

   So

$$\vec{M} = \frac{3\left(\mu/\mu_o - 1\right)\vec{B}}{2\mu_o + \mu} \qquad . \qquad (A\ 21)$$

c. <u>Permeable Cylinder in an External Field</u> (Page and Adams, p. 125).

   Let H_o be field perpendicular to axis of cylinder.

   The ratio of the field inside the cylinder (inner radius a, outer radius b)

to the field outside the cylinder is

$$r = \frac{1}{\left[1 + \frac{1}{4}\frac{(\mu/\mu_o - 1)^2}{(\mu/\mu_o)}\left(1 - a^2/b^2\right)\right]} \qquad (A\ 22)$$

See Jackson, p. 199 for a similiar calculation of a sphere in a field.

Note as $\mu/\mu_o \to \infty \ , \ r \to 0$

Thus we have magnetic shielding.

PROGRESS REPORT

ON NSF AND AIR FORCE GRANT AWARDS

(1)   NSF MEA-8304711, "Developing a Prototype
        Microcomputer Network for Implementing a
        Manufacturing Resource Planning System in Small
        Manufacturing Companies." - Final Report

(2)   NSF MEA-8401075/DMC-8505375, "Salary Support for
        Developing a Prototype Microcomputer Network for
        Implementing a Manufacturing Resource Planning
        System in Small Manufacturing Companies."

(3)   AFOSR/SCEEE, SUBCON #84 RIP 19, "Enhancing
        MPC-DSS to include Automatic Rescheduling and
        Adaptive Performance Measures". - Final Report

            Principal Investigator: Philip S. Chong

                    October 31, 1985

1. PRELIMINARIES

1.1   List of Grant Awards Related Support from NSF and the
       Air Force/SCEEE for which the author is the principal
       investigator include:

(a)   NSF Grant Award (Equipment) SPE-8263255; $10,500;
       Oct/ 1982 - Oct. 1984 at North Dakota State
       University. "Developing a Prototype Decision
       Support System for Classroom Use in Introductory
       Industrial Engineering Courses." - Completed Oct.
       1984.

(b)   NSF Grant Award (Equipment) MEA-8304711; $13,720;
       (matching); July 1983-Sep. 1985 at North Dakota
       State University, "Developing a Prototype Micro-
       computer Network for Implementing a Manufacturing
       Resource Planning System in Small Manufacturing
       Companies."

(c)   NSF Grant Award MEA-8401075; $38,530; July 1984-
       May 1985 at North Dakota State University.
       Transferred Grant Award DMA-8505375; $31,000;
       June, 1985 to present at Worcester Polytechnic
       Institute. "Salary Support for Developing a
       Prototype Micro-Computer Network for Implementing
       Manufacturing Resource Planning System in Small
       Manufacturing Companies."

(d)   AFOSR/SCEEE Grant Award SUBCON #84 RIP 19;
       $12,000. (matching); Nov. 1984 - Nov. 1985
       at Worcester Polytechnic Institute, "Enhancing
       MPC-DSS to Include Automatic Rescheduling and
       Adaptive Performance Measures."

1.2   ## Introduction

The reason for writing one progress report to cover
three separate current grant awards is chiefly be-
cause the work and accomplishments of each of the
proposal grants are intimately related and complement-
ary. The awards of the latter grants, for example,
can be attributed primarily to the accomplishments
and results of the earlier awards, and almost all of
the earlier work is continued and expanded into the
latter awards. To briefly provide a perspective,
SPE-8263255 provided two IBM personal computer
systems for the development of a manufacturing
planning and control decision support system MRP-
DSS for classroom use. This was successfully tested
in classroom environments, and the project is
completed.

A logical extension to the above research was to expand the capabilities of MRP-DSS significantly so that it can be implemented in a small manufacturing company. This involves the development of a prototype microcomputer network. MEA-834711 provided the funds to purchase two more IBM personal computers, one hard disk and networking capability for four users. MEA-8401075 which became DMC-8505375 after the principal investigator left North Dakota State University to join Worcester Polytechnic Institute, provided the salary support to implement the above research.

The Air Force of Scientific Research (AFOSR) and Southeastern Center for Electrical Engineering Education (SCEEE) sponsored SUB CON #84 RIP 19, which provided the support to enhance MRP-DSS to include Automatic Rescheduling and Adaptive Performance Measures. Several implementations at various Air Force installations were considered as a result.

1.3   <u>Research Accomplishments</u>

Research accomplishments to date from prior grant awards are many, varied and significant. They can be broadly classified into the following categories:

(a)   Development of Instructional Material

(b)   Industrial Implementation

(c)   Research Developments and New Awards

(d)   Presentations, conference proceedings, reports and journal publications

A.   Development of Instructional Materials- Innovative instructional materials were developed for the classroom which include games, experiments, demonstration data, mannuals and tutorials. Two articles -"Manufacturing Resource Planning Games" was featured in Production and Inventory Management Review, August, 1985 [1] and "System combines Manufacturing Resource Planning and Decision Support Approach" was featured in Industrial Engineering Journal, October, 1985 [2] - resulted in many inquiries from companies including AT&T Network Systems, MicroDyne Corporation, Sperry Univac, William Wright Co., and Silas Mason, as well as Universities such as Bradley, University of Tulsa, North Texas State University, Wilfred Laurier University of Ontario, University of Tennessee at Chatanooga University of Baltimore and others.

To date, 12 Universities and Colleges have adopted MRP-DSS for their classroom use including:

    (i)   California State University, Long Beach

    (ii)   Lehigh University

    (iii)   Northeastern University

    (iv)   West Virginia University

    (v)   Bradley University

    (vi)   North Carolina State University

    (vii)   University of Central Florida

    (viii) Worcester Polytechnic Institute

    (ix)   North Dakota State University

    (x)   Belmont College, Tennesee

    (xi)   Laurier Wilfred University, Ontario

    (xii)   University of Tennessee at Chatanooga

Many larger companies which are using mainframe or micro-computer systems, viewed the potential use of MRP-DSS as a low-cost training tool for their employees. The feedback from the users of MRP-DSS as a training tool has been extremely positive and encouraging.

B.   Industrial Implementation:

To date, several companies and organizations have received copies and/or implemented MRP-DSS, including:

    (i)   Alloway Manufacturing Company, Fargo, North Dakota

    (ii)   North Dakota State University Food Service, Fargo, North Dakota

    (iii)   McDonnell Douglas, Master Link Division Hopkinton, Massachusetts

    (iv)   The U.S. Air Force:

          • Tyndall AFB, Florida

          • Kelly AFB, Texas

- San Antonio Real Property Management Activity

- Logistics Management Center, Montgomery, Alabama

(v)   Mason & Hanger Company, Kentucky

Under the USAF Summer Faculty Research Program (SFRP)
sponsored by the Air Force Office of Scientific Research
(AFOSR) and the Air Force Logistics Management Center
(AFLMC), the principal investigator spent the summer of
1984 at AFLMC, Montgomery, Alabama, for ten weeks to study
in conjunction with AFLMC researchers, potential applications
of MRP-DSS to the Air Force. Potential applications in-
cluded the use of MRP-DSS for civil engineering work orders,
depot aircraft maintenance, base transportation vehicles,
maintenance vehicles, maintenance, food-service and
hospitals.

An agreement was signed betwen the Air Force and the
principal investigator to provide the Air Force with the
source code of MRP-DSS for such applications. Subsequent
to the summer of 1984, the Air Force Office of Scientific
Research/SCEEE provided a follow-on award, "Enhancing MRP-
DSS to include Automatic Rescheduling and Adaptive perform-
ance Measures", $12,000.; Nov. 1984 - present. The
responses from industrial users have also been very positive
and encouraging.

C.   Research Developments and New Awards

Highlights of the Research include enhancements made to
MRP-DSS and the development of MRP-DSS on a microcomputer
network. Several research accomplishments and enhance-
ments on MRP-DSS are significant.

> (i)   The system is extremely user-
> friendly and user-interactive.
> For example, Innovative Screen
> displays are used to increase user
> interactiveness.
>
> (ii) The user has complete control over every
> phase of the planning and decision making
> process including data entry and re-
> trieval, data analysis, model building,
> sensitivity analysis (what ifs) and other
> processing and application needs. For
> example, the intermediate steps of
> decision making is accessible to the user
> for data manipulation.
>
> (iii) Results of any experimentation on changes
> to the data is clearly evident and visible
> to the user on the screen, without having
> to print out hard copies of reports.

(iv)   "Intelligence" is built into the system
       to offer recommendations to alternative
       courses of actions, including rescheduling.
       For example, if capacity is exceeded,
       the system will provide suggestions for
       rescheduling certain shop or sales
       orders. It is found that, although auto-
       matic rescheduling is possible, the issues
       surrounding automatic rescheduling is
       complex because there are many courses
       of action a planner could take. Unless
       some measures of weight are defined for
       the different courses of actions, auto-
       matic rescheduling is not possible yet.
       The methodology that is used instead, is
       to provide the planner suggestions or
       recommendations to courses of reschedul-
       ing actions and their implications and let
       the planner decide on the appropriate
       action to take. The same approach is
       also used for the estimation of peform-
       ance measures. The performance measure-
       ments that were used include the
       deviations between planned and actual
       cost per part, lead time and quantity
       usage/delivery. The user is given the
       opportunity to scan those deviations and
       update the planned measures with the
       actual where they are significant and
       appropriate. Sample screen displays and
       reports relating to the work in (iv) are
       shown in figures V.6 to V.10 of the Users
       Manual in the Appendices. The work in
       (iv) is primarily supported by the Air
       Force Grant. The principal investigator
       made a presentation of the work in
       progress to the Air Force Logistics
       Management Center, particularly to Major
       Douglas Blazer and Captain Craig Carter
       on July 24, 1985.

(v)   The micro-computer network is able to
       respond with minimal performance
       deterioration when several users are using
       the system.

(vi)   Security and several levels of priviledge
       protection for several users are designed
       into the network system. Details of all
       the modules are given in the users manual
       and in several journal publications [1],
       [2], [3] - See appendices.

19.7

New awards include the three NSF funded grants stated earlier, implementation contracts with Alloway Manufacturing Company $3,000; NDSU food service, $4,500; and the Air Force Logistics Management Center, and a follow-on award from Air Force Office of Scientific Research/SCEEE, "Enhancing MRP-DSS to include Automatic Rescheduling and Adaptive performance measures", $12,000; November 1984 - present.

D.   Presentations, conference proceedings, reports and journal publications:

Presentations include the following:

(i)   "Manufacturing Planning Decision Support System" ORSA/TIMS Orlando meeting, Nov. 7-9, 1983

(ii)   "Developing a prototype microcomputer network for implementing a Manufacturing planning and control system in small manufacturing companies," 11th NSF Grantees Conference. Carnegie-Mellon University, May 21 - 24, 1984 (with proceedings)

(iii)   "Introducing Manufacturing Planning and Control Decision Support System" Seminar and Exhibits. North Dakota State University, March 7 - 8, 1984

(iv)   "MPC-DSS" Department of Management, Worcester Polytechnic Institute, March 7 - 8, 1984

(v)   "Manufacturing Resource Planning and Development Activities" to Management Department's Board of Advisors meeting October 15, 1984

(vi)   "MRP-DSS" Dept. of Industrial and Systems Engineering, Northeastern University - on invitation of Prof. Yang Park, November 8, 1984

(vii)   "MRP-DSS" Dept. of Business Administration Clark University - on invitation of Prof. Bharat Ruparel

(viii) "Designing a Prototype Manufacturing Planning and Control Decision Support

19.8

System" at CAD/CAM, Robotics and Auto-
mation Institute and Conference, Feb.
11 - 15, 1985 (with proceedings)

(ix)   "MRP-DSS Software" at John Bath Co., of
        Worcester, MA, November 6th and November
        27, 1984

(x)   "MRP-DSS" at British Thermal Unit
        Company, Chelmsford, MA, May 31, 1985

(xi)   "MRP-DSS" at Norton Co., Worcester, MA,
        May 8, 1985

(xii)   Designing a prototype "MRP-DSS" 12th NSF
        Grantees Conference. University of
        Wisconsin, Madison, May 14-17, 1985

Reports include:

(i)   Annual Progress Reports to NSF grants;
        1983, 1984, 1985

(ii)   "Investigating the potential application
        of an integrated Resource Management
        System to Various Air Force Environments".
        Final Report, 1984 USAF/SCEEE Summer
        Faculty Research Program

(iii)   "Materials Management System for the Air
        Force" with Major D. Blazer, AFLMC report,
        1984

(iv)   MRP-DSS Users Mannual, 1984/85

Journal Publications include:

(i)   "Manufacturing Resource Planning Games"
        Production and Inventory Management
        Review, August, 1985

(ii)   "System Combines Manufacturing Resource
        Planning and Decision Support Approach",
        Industrial Engineering Journal October,
        1985, Vol 17 No 10

(iii)   "A Manufacturing Resource Planning Decision
        Support System (MRP-DSS) for small Manu-
        facturing Companies and for Training and
        Classroom Use". Under review by
        Manufacturing Systems Journal

(iv)   "Note: A Dispute on James R. Evans "An
        Efficient Implementation of the Wagner-

Whitin Algorithum for Lot-Sizing"
JOM Vol. 5 No.2 under review by Journal
of Operations Management — accepted for publication

(v)   "A Manufacturing Resource Planning Decision
      Support System on a Micro-Computer based
      Network" under preparation

(vi) "BIDPLAN - a manufacturing planning
      game" under preparation

(vii) "MRP Systems Design and Developmental
      Issues" - under preparation

References

[1]   Chong, P.S. "Manufacturing Resource Planning Games",
        Production and Inventory Management Review, August,
        1985.

[2]   Chong, P.S. "System Combines Manufacturing Resource
        Planning and Decision Support Approach", October, 1985,
        Vol 17, No 10.

[3]   Chong, P.S. "MRP-DSS Users Manual", copyright 1985.

APPENDICES

JOURNAL

PUBLICATIONS

AND

USERS MANUAL

19.12

System Combines Manufacturing Resource Planning And Decision Support Approach

By Philip S. Chong
Worcester Polytechnic Institute

This article will propose a framework for the design and development of a manufacturing resource planning decision support system (MRP-DSS) and describe a prototype MRP-DSS as implemented on the IBM Personal Computer (PC). Traditionally, MRP systems were designed primarily as data processing systems. The benefits of a decision support system approach have been well documented. The need to re-address the design of manufacturing resource planning systems in light of decision support system methodology is urgent.

For successful implementation of DSS for MRP, several features of DSS must be maintained:

☐ The system must be extremely user-friendly and user-interactive.

☐ The user must have complete control over every phase of the planning and decision-making process, including data entry and retrieval, data analysis, model building, sensitivity (what if) analysis and other processing and application needs.

☐ Results of any experimentation or changes in the data must be clearly evident and visible to the user with-

What constitutes a manufacturing resource planning decision support system? Several key characteristics will be discussed.

Definition of resources and their relationship structure: The system must enable the user to define the pertinent manufacturing resources and related parameters such as parts, stations, machines, employees, operations, capacities, costs and planning horizon.

The two primary relationship documents in any manufacturing company are the multi-level bill of materials and the route sheet/process chart. The system must allow the user to enter the relationship structure between resources such as the parent-child relationship and usage rate, the sequence of processing/operations, and routings to machines and stations.

A model for planning/decision-making: Once a structure between resources is established, a model for planning or decision-making can be designed. In general, any manufacturing company will need an operating plan or schedule as well as a financial plan or schedule, and the two are intimately related. The planning model shown in Figure 1, consisting of a sequence of intermediary steps, is quite well established (see

ing"). In a DSS environment, the user must have access to every step of the planning model.

A model for control: Without proper control procedures (operating within a dynamic environment such as manufacturing), the planning procedures are likely to fail. Logically, planning and control functions go hand-in-hand, since:

● Planning uses initial estimates of data based on design. Then the estimates should be modified by actual past performance as revealed over time and through experience.

● Control captures the actual performance over time, which is used not only to provide the status of orders at any time, but also to provide the basis for estimates that are fed back to the planning function.

A control model has to be able to capture the dynamics of activities over time in a manufacturing environment. Three types of "orders" are proposed:

☐ Purchase orders—these relate to parts purchased from vendors or suppliers and track the quantity and promised date of delivery.

☐ Sales orders—these relate to parts or products sold to customers or clients and track the quantity and promised date of delivery.

☐ Shop orders—these relate to parts released to the shop floor and track the status of the orders as they are routed from one work center or station to another.

The assignment of order numbers to the above three types of orders allows materials and labor to be charged to each order, much as with a charge account. To receive or issue parts from the stockroom, an order number will be required. In the case of a shop order, a labor or machine reporting function will be required to track the number of labor or machine hours incurred on the shop order.

Figures 2 through 4 display flow chart models of purchase, shop and

Figure 1: Planning/Decision Making Process Model

onstrate how they relate to the planning model.

Evaluation and performance measures: The overall framework is quite complete now, but there is a need to measure the performance of a manufacturing environment over time. Performance measures may include the following:

□ Planned cost versus actual cost per part.
□ Planned lead time versus actual lead time.
□ Planned quantity of parts versus actual usage/delivery.

The actual performance measures can be retrieved from the control model and compared with the planned model. Updates of the planned measures can then be used in the planning model.

MRP-DSS on IBM PC

In recent years, the microcomputer has begun providing opportunities for small businesses to acquire some of the computing power and capabilities hitherto reserved for the larger companies. For many years, microcomputers have had such limitations as lower computational speed, smaller memory and disk capacities and lack of applications software. However, these limitations are being reduced at a rapid rate.

Most of the new microcomputers have a 16-bit processor, in addition to having larger memory and disk capacities than previous models. A prototype MRP-DSS has been designed and developed on the IBM PC with a hard disk. The prototype is a highly sophisticated and powerful tool, and contains all the necessary characteristics of MRP-DSS described earlier.

MRP-DSS modules

As it currently stands, MRP-DSS consists of 23 modules. All 23 modules have been designed, coded, tested and documented. The modules are divided into three categories:

Figure 2: Purchase Control Model
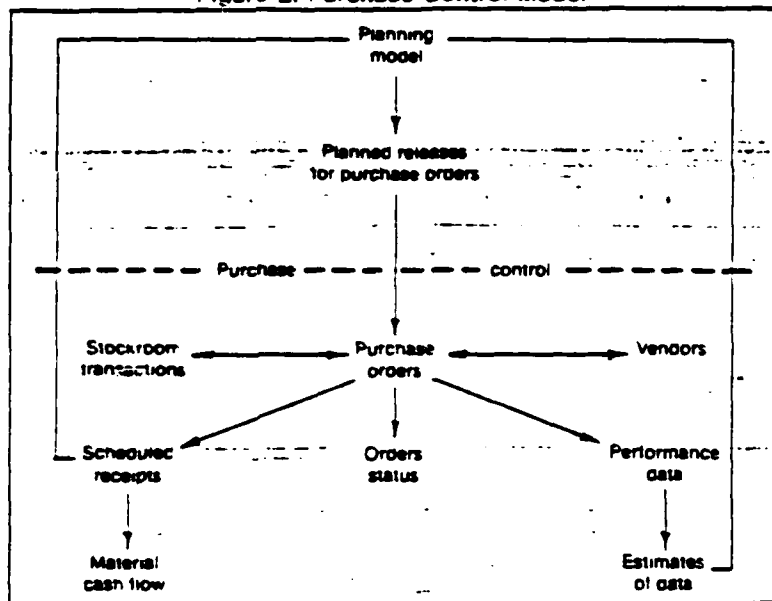
resources, control and planning. The categories of modules are described briefly as follows:

Resources:

(A) "INI"—*data initial/sort/print utility* is a utility module which allows file size definition, sorting of part numbers and printing of part and station data.

(B) "BOM"—*bill of materials* allows the user to enter or view part numbers, description, low-level code, child-parent relationship, usage rate

and part explosion and implosion.

(C) "INV"—*part inventories/cost data* allows the user to enter or view on-hand inventory levels, safety stock level, lot sizing methods used, material, labor and overhead and unit costs, storage area, and sales list price of parts.

(D) "STA" — *station definition/ load control* allows the user to enter or view station or work center number, description, available labor man-hours, labor and overhead rates, and

Planning model

Planned releases
for shop orders

— — — Shop — — — | — — Control — — —

Stockroom transactions → Shop orders ← Labor/machine reporting

Scheduled receipts — Orders status — Performance data

Released loads — Shop order scheduling — Estimates of data

Load cash flow

Figure 4: Sales Control Model

Planning model

— — — Sales — — — — — Control — — —

Stockroom transactions → Sales orders ← Clients

Master production schedule — Order status — Performance data

Sales cash flow — Estimates of data

---

both released and planned labor load profile over the planning horizon.

(E) "EMP"—*employee data control* allows the user to enter or view data relating to an employee or operator such as an ID number, name, address, labor rate and scheduled hours of work per week.

(F) "MAC"—*machine data control* allows the user to enter or view data relating to machines such as an ID number, description, station location and operator ID, if any.

(G) "OPE"—*operations and process data control* allows the user to enter or view data relating to operations or processes such as an ID number, description, machine and station connected with the operation, if any.

(H) "LEA" — *lead time/process routing/assembly planning* allows the user to enter or view data relating to the operations and process routing associated with each part. It also estimates lead time based on batch size, unit operation and processing times, set-up times and others.

control:

(I) "SHO"—*shop order control* allows the user to enter or view shop orders. The shop order authorizes the shop to begin manufacture of parts, including withdrawal of components from stores, and expenditure of labor. Data entered include part and number of units to make, date started and promised, and current status of the job.

(J) "SAC"—*sales accounts/clients control* allows the user to enter or view data relating to a sales account or client, including ID number, description, address and others.

(K) "SAL"—*sales order control* allows the user to enter or view sales orders. The sale order authorizes withdrawal of end items or products to fulfill a sale. Data entered include part and number of units sold, date of sale, and date promised, the client ID to and unit sale price.

(L) "VEN"—*vendor accounts control* allows the user to enter or view data relating to a vendor account, including ID number, description, address and others.
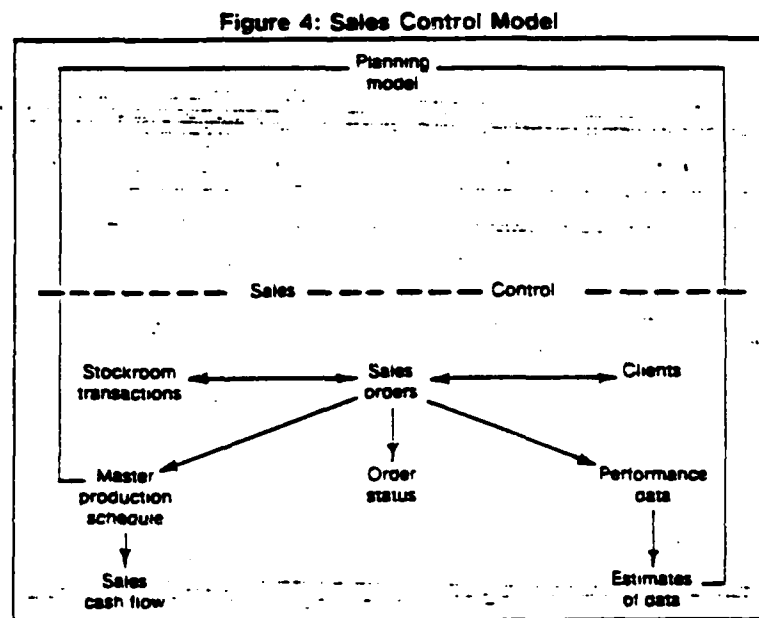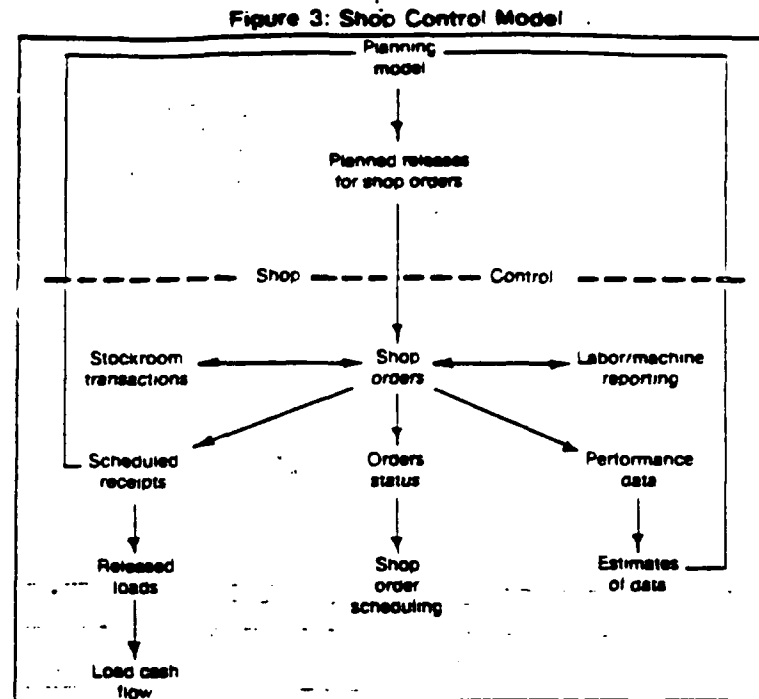
(M) "PUR"—*purchase orders control* allows the user to enter or view purchase orders. The purchase order authorizes the receipt of purchased parts to stores. Data entered include part and number of units purchased, date of purchase and date promised.

the vendor purchased from and unit purchase price.

(N) "STO" — *storeroom transaction control* allows the user to enter or view store transactions. Data entered include part and number of units issued or received, date of transaction, referenced purchase, and shop or sale order ID number. As each transaction occurs, the inventory level or status is updated.

Figure 5: Precedence Running Sequence of Modules with Feedback

(O) "LAB"—*labor reporting control* allows the user to enter or view labor reports. The labor report records the number of hours expended on a shop order by an operator and keeps track of the status of the shop order. Data entered include shop order ID number, date of report, number of hours incurred, operator ID number, units made and scrap.

(P) "HOR"—*date/orders, processing/planning horizon update* processes all the sales orders, and based on their promised dates, updates the master production schedule. Likewise, it processes all the purchase and shop orders and based on their promised dates, updates the planned scheduled receipts. Late orders are also accumulated and stored away.

Planning:

(Q) "MPS" — *master production schedule* allows the user to enter or view data in the master production schedule. The MPS can also be updated by sales orders entered in (K) via planning horizon update (P). Data include the number of units per week specific to every end or service part over a planning horizon of up to 52 weeks.

(R) "POR"—*order releases and schedule receipts* allows the user to enter or view data in the order release schedule and order receipts schedule. Generally, the order releases are the results of material requirements planning (T). Scheduled receipts can be updated by purchase orders entered in (M) and shop orders entered in (I). Data include the number of units per week over a planning horizon of up to 52 weeks specific to each part.

(S) "COS"—*product costing* processes the materials, labor and overhead costs incurred based on route sheet and bill of materials. Data to "roll up" are assumed to have been entered in the modules described earlier.

(T) "MRP" — *material require-*

ments planning processes all the data that are entered via the modules described earlier. Starting with the master production schedule, it performs the netting process through the bill of materials, taking into account on-hand inventories, lead time and scheduled receipts; performs economic lot size tradeoffs where called upon; flags for late order releases where they occur; and evolves the schedule of order releases

over the planning horizon for every part. The order releases are stored and can be viewed from (R).

(U) "CRP"—*capacity requirements planning* translates the order releases from "MRP" (T) of manufactured parts into labor or manhours (load profile) incurred in each station over the planning horizon. Total cost of labor on regular and overtime is generated for each station or work center.

Figure 6: Input/Output Relationships Between Modules and Data Files

(V) "ACT"—*summary actions to do* provides the user with a summary of all the impending actions that require attention as a result of running the application programs. The actions include orders due to be released as either shop or purchase orders this week, sales orders due this week, late sales, purchase and shop orders, and reschedules, in the form of either expediting or de-expediting certain orders.

(W) "COM"—*combination runs* allows the user to run any number of four application programs (P), (S), (T) and (U) consecutively and automatically without user intervention. This is especially useful when the application modules require an extended period of processing time and is best done at the end of the working day.

An overall flowchart is shown in Figure 5. It displays the principal relationship between modules, specifically the precedence running sequence of the modules. Obviously, the flow is never completely unidirectional, and several feedback loops are shown.

Modules and data files

The typical relationship between modules is one of data transfer, whereby the output from one module is stored in the data file and is used subsequently as input to another module. The data files in the system can be grouped into 12 major groups as follows:

☐ PAR.DAT—Part related data.
☐ STA.DAT—Station related data.
☐ EMP.DAT—Employee data.
☐ MAC.DAT—Machine data.
☐ OPE.DAT—Operations/process data.
☐ SHO.DAT—Shop orders data.
☐ SAC.DAT—Sales account/client data.
☐ SAL.DAT—Sales order data.
☐ VEN.DAT—Vendor data.
☐ PUR.DAT—Purchase order

data.
☐ STO.DAT—Stores transaction data.
☐ LAB.DAT—Labor report data.

Figure 6 shows the input/output relationships between the modules and the data files. The modules are shown twice—first in the left column, writing into the data files, and again in the right hand column, read-

ing from the data files.

Screen displays and reports

Figures 7 through 11 show several sample screen displays and reports. Figure 7 shows the main menu. Figures 8 and 9 show how a bill of materials is entered into the system and displayed to the user. Notice the tree-structure-like format for enter-

Figure 7: Screen Display of MRP-DSS Main Menu

Figure 8: Screen Display of Module B—Bill of Materials

ing the parent-child relationship.

Figures 10 and 11 show how work station data are entered and a load profile may be graphically displayed on the screen. Interaction between the user and the system is encouraged primarily via the screen.

The system's design philosophy is to discourage the use of hard copies, even though hard copies of all screens and reports may be made if necessary. The reader is referred to the MRP-DSS users manual for a complete discussion and exhibition of the screen displays and reports (Chong, "For further reading").

Multi-user networking

Many schemes can be used to provide for a multi-user network within which functional planners or engineers will interact using the modules and share a common data base on a hard disk. A functionally promising and cost effective multi-user scheme that the author found is Advanced Digital Corp.'s multi-user PC (personal computer) system, which uses PC-Slave processor boards.

The PC-Slave processor board is a high speed 16-bit computer on a single PC card that includes CPU memory, serial I/O ports and PC-bus interface. By connecting a "dumb" terminal to the PC-Slave board, a fully compatible second PC is created. In the same manner, other PC-Slave boards/terminals may be connected to the host PC.

The host PC performs disk and peripheral functions for the PC-Slaves. Each PC-Slave can have a terminal and its own printer. A multi-user environment will allow functional station planners or engineers to interact within the network using the modules and share a common data base.

Four functional stations are proposed: the production planner, design and manufacturing engineers, master production scheduler and

Figure 9: Hardcopy Report of an Indented Bill of Materials

Figure 10: Screen Display of Module 4—Station and Load Data

DATE: 03-19-1984   (STA)   (F10 - MAIN MENU)

inventory planner. Their primary areas of responsibility and the modules held under their charge are listed below.

—PRIMARY STATION
  TITLE: PRODUCTION PLANNER

FUNCTION: MANUFACTURING ACTIVITY
  PLANNING
MODULES: MPS, MRP, CRP, POR, STA,
  EMP, SHO, LAB, ACT
—SECONDARY STATION # 1
TITLE: MASTER PRODUCTION
  SCHEDULER

19.18

Figure 11: Screen Display of Station Load Profile

FUNCTION MASTER PRODUCTION
SCHEDULE PLANNING
MODULES SAL, SAC, MPS, PUR, HOR,
VEN POR ACT
— SECONDARY STATION #2
TITLE: DESIGN & MFG. ENGINEER
FUNCTION ENG. & PRODUCTION DATA
PLANNING
MODULES: BOM, LEA, MAC, OPE, STA,
EMP
— SECONDARY STATION #3
TITLE: INVENTORY PLANNER
FUNCTION: INVENTORY PLANNING
MODULES: STO, INV, POR, ACT

A typical layout of a small manu-
facturing company with proposed
network configuration connecting
the four functional areas is shown in
Figure 12.

Implementation

To date, several small manufac-
turing companies have implemented
and tested MRP-DSS. All the imple-
mentations have been in test facilities
where many developmental issues
were worked out in an applied envi-
ronment. Implementation normally
took place over several phases—
beginning with BOM(B), followed
by related modules leading to COS
(S), MRP (T) and CRP (U). The
responses have been enthusiastic and
overwhelmingly positive.

For further reading:

Chong. P.S., "MRP-DSS Users Manual,"
copyright 1985.
IBM Inc., "Communications Oriented Pro-
duction Information and Control System"
(COPICS), Vol. 1-8.
Turban. E., "Decision Support Systems
(DSS): A New Frontier for Industrial Engi-
neering," *Computers & Industrial Engi-
neering Journal,* Vol. 7, No. 1, 1983.
Vollman. T.E., Berry, W.L. and Whybark,
D.C., "Manufacturing Planning and Con-
trol System," Richard D. Irwin Inc., 1984.
Wight. O., "The Executive's Guide to Suc-
cessful MRPII," Oliver Wight Education
Associates Inc.
Williams. J.L., "Decision Support Systems in
Production Planning," *P & IM Review*
Nov., 1982.

Figure 12: Network Configuration as Applied to a
Typical Small Manufacturing Company
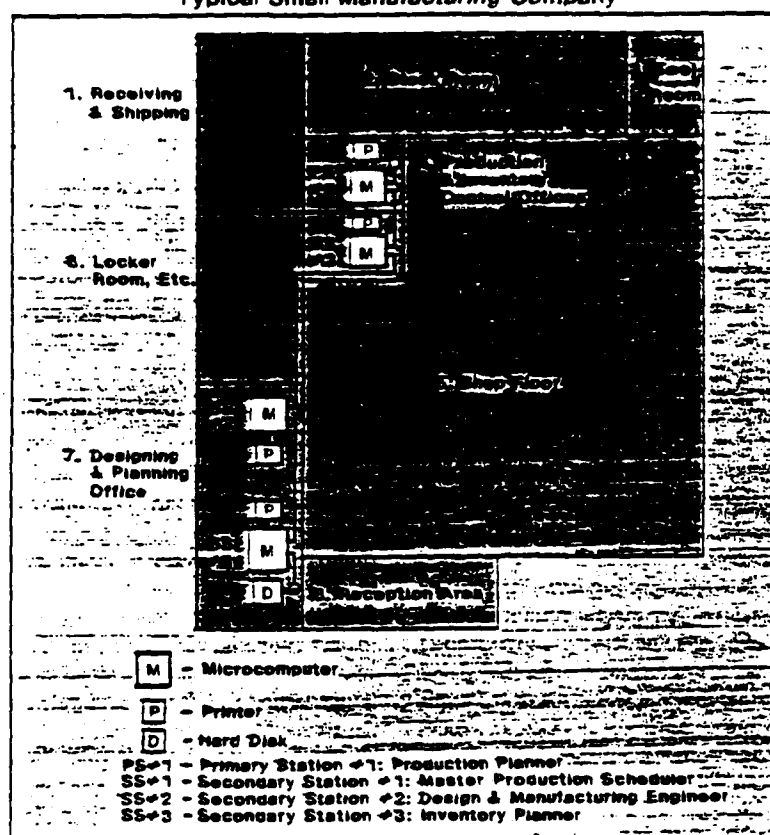
Philip S. Chong is currently an associate profes-
sor in the department of management, Worcester
Polytechnic Institute. He was assistant and asso-
ciate professor in the department of industrial
engineering and management at North Dakota
State University from 1977-1984. He received his
BS in mechanical engineering from the University of
Singapore and MS and PhD degrees in industrial
engineering and operations research from the Un-
iversity of Massachusetts. Chong is an active
researcher and consultant in the area of manufacturing planning and
control systems. He is the developer of a manufacturing resource planning
decision support system (MRP-DSS) on the IBM personal computer.

USERS MANUAL

FOR

MANUFACTURING RESOURCE PLANNING

DECISION SUPPORT SYSTEM

MRP-DSS Version 2.0

by

Dr. Philip S. Chong

copyright c 1985   Philip S. Chong

CONTENTS

INTRODUCTION

THE MRP-DSS

The Manufacturing Resource Planning Decision Support System
(MRP-DSS) is a highly integrated, user friendly and user interactive
software package developed for the IBM Personal Computer for small-to
medium-size manufacturing companies. It can be used to help plan and
control their manufacturing resources such as materials, labor, money,
capacity and machines and others. MRP-DSS is a derivative of two
widely-used planning and control tools, namely Manufacturing Resource
Planning (MRPII) and Materials Requirements Planning (MRPI), which are
generally implemented on a mainframe or medium-size computers at larger
manufacturing companies. MRP-DSS has many unique features and they
include:

- The system is extremely user-friendly and user-interactive.

- The user has complete control over data entry and retrieval,
data analyses, model building, sensitivity (what if) analysis and other
processing and application needs.

- The results of any experimentation or changes to the data are
clearly evident to the user.

WHO CAN BENEFIT FROM MRP-DSS

MRP-DSS can be used by any manufacturing company who would like to
run their business more efficiently. Using established and proven
techniques for manufacturing planning and control, combined with its
user-friendly and interactive features MRP-DSS can help a manufacturing
company achieve increased productivity levels in a short time after
implementation.

The size of a manufacturing company's data base may be determined
in many ways. It can be measured in terms of number of parts in
inventory, number of work stations, machines, employees, operatons,
number of store transactions, shop orders, purchase orders and sales
orders. Although MRP-DSS may be used for any size company depending
upon the size of the hard storage disk drive for data, the system is
limited by the speed of a microcomputer. The recommended guidelines for
the user's company size are:

- Maximum of 9,999 part numbers. (100 on demo)
- Maximum of 80 work stations. (20 on demo)
- Maximum of 9,999 record for all other items such as employees,
  machines, operations, transactions and orders. (50 on demo)

THE SYSTEM REQUIREMENTS

The minimum requirement for the MRP-DSS system to work is one IBM
Personal Computer with two disk drives and at least 198K of memory. For
all practical purposes, a hard disk drive will be needed for the system
to work efficiently. For example, with a 10 Megabyte hard disk drive,
the system will be able to accommodate a business of the following size:

- 4000 inventory parts or part numbers.
- 50 work stations.
- 2000 records for all other items.

   To determine the size of a hard disk needed for a company, a rough estimate of storage size should be calculated. The number of records for each category listed in the following table should be multiplied by the factor in the table, which is the number of bytes used per record. The sum of all the multiplications is a rough estimate of the total storage needed for the data.

STORAGE BYTE TABLE

RECORD	NUMBER OF BYTES/RECORD
Part Number	2400
Station Number	530
Store Transaction	120
Sales Order	160
Shop Order	160
Purchase Order	160
Client Account	160
Vendor Account	160
Operations Record	170
Machine Record	170
Employee Record	180
Labor Reporting	110

   A simple example would be a company with 25 part numbers and 20 work stations. The total storage *needed would be* (25*2400) + (20*530) = 61,000 bytes. All others are calculated in the same fashion.

ORGANIZATION OF THE MANUAL

   The organization of this manual will be in alphabetical order, from Modules A to Z, with each letter corresponding to a different module. This is the same order the modules appear on the main menu. This is the preferred way in which to enter data also. It does not have to be followed exactly, but some of the latter modules need data from earlier modules to work properly.

   In the main context of the manual, an overview of the main menu appears, followed by the description of the individual modules.

HELPFUL HINTS TO USE THE PROGRAM

1. The main menu will be the first menu displayed on the screen when the program is loaded. It has all the names of the modules in MRP-DSS. The menu is subdivided into three categories: (i) RESOURCES - MODULES A to H; (ii) CONTROL - MODULES I to P; (iii) PLANNING - MODULES Q to W. To load the particular module into memory so it can be utilized, the user needs only to depress the corresponding letter key on the keyboard. See Figure 1 for an example of the main menu.

2. After the key is pressed, the module is automatically loaded into memory and the screen will display the module that was loaded. The module is now ready to be executed. The individual modules will be explained later in this text. This is done for all the module, thus it will not be mentioned within the text of the individual modules.

3. The F10 key is used to return the user to the main menu display. The material on the screen at the time is not saved to disk until the next record or screen for the particular module is called. Thus, to avoid losing input data when returning to the main menu display, bring the next record onto the screen for whichever file you happen to be in. When this is done, your data will be written to disk, and the main menu display may be called up without fear of losing your data. From the main menu, the user may also exit the program to the IBM DOS system at anytime by depressing the ESC key.

4. The date entered at the start-up will appear in every screen at the bottom left hand side. For ease of reading, data information is always highlighted on the screen.

5. When an editing change option has been selected, the cursor will highlight the particular area to be changed. To make a change, just retype the correct information over the wrong data and this will change it on the screen and on the data disk.

6. Certain modules have the ability to print out lists of data. After these are completed, the computer prompts the user to enter any key to continue.

7. For number key entries, the user can use either the numbers on the top row of the keyboard or the numerical pad on the right hand side of the board. If the numerical pad is used, the Num Lock key will have to be pressed every time a new module is called to allow the numbers to be operational.

8. Before any data can be entered to the data diskette (or hard disk), the diskette must be initialized by the program. This is done by pressing the A key in the main menu and then the 1 key in the Data Initialization/Sort/Print module. For further details, see Data Initialization/Sort/Print chapter of this manual.

9. The modules interact with one another, thus a change in one module will be reflected in other modules.

10. There are no commands needed to save data when it is entered. The only requirement is the next record or screen must be displayed in order for the data to be saved. The data is automatically written and saved to the data disk.

11. In some modules, the information moves by on the screens very rapidly. To suspend the screen for viewing, press the Ctrl and Num Lock keys simultaneously. To continue the scrolling of information, press any key.

12. After data has been entered and the session with the system is over, BACKUP your data disk. This is a safety precaution and your only guarantee to make sure all of the work is not lost in case of a major problem (such as fire, erasing or original disk, etc.)

THE MAIN MENU

The Main Menu, or COMSET is the driving force for all the modules. All of the program options are listed on the main menu (see figure 1). The user needs only to press the corresponding letter next to the module wanted. It will automatically be loaded into memory. After the module is loaded, the screen will display the name of the module in memory and prompt the user to press any key to continue.

For a hard disk user, the hard disk must be partitioned off, part for the program and part for the data. The user should assign the program part of the hard disk (about 1 Megabyte) as Drive A and the rest of the hard disk as Drive B for data storage. An IBM DOS 2.0 is needed. For example, if the hard disk is drive C, copy all programs and data files to the hard disk. Then use DOS 2.0's ASSIGN command as follows: ASSIGN A=C, B=C. This will cause both programs and data to be accessed on disk C. When the DOS prompt is displayed (A>) the Main Menu may be called by the command COMSET. The date is required to be entered (in the form MM/DD/YY), then the menu will be loaded and will appear on the screen. There are twenty-three modules in the package. They are divided into three catagories: Resources, Control and Planning.

On-line help is available at the main menu. By pressing the F1 key, the help menu is activated. The user can then query for help by pressing the key that corresponds to the module that the user needs help with. A brief description of the module and its functions will be presented on the screen.

For applications not available or for a definite need, write or call the author:

Phil S. Chong, Ph.D.
Department of Management
Worcester Polytechnic Institute
Worcester, Massachusetts 01609
Telephone (617) 793-5182

Each individual module will now be described in detail. See figure 1 for display of main menu.

MODULE A - DATA INITIALIZATION/SORT/PRINT

This module is used to initialize the data diskette and to reserve the storage capacity on the diskette in Drive B for all of the data you plan to enter.

The module also does a major sort of the data, a minor sort of the data, prints out an alphanumeric sorted parts list, prints a parts list by record number and prints a 'ist of work stations by record number. These are the seven options available and will be described in greater detail in the following paragraphs. They are implemented by the number keys 1 to 7. If you are working with the sample data set, skip option 1 and move onto option 2.

1 - DATA FILES INITIALIZATION

This does the actual initialization of the data disk. When this key is pressed, the screen displays all twelve data files needed to be initialized. The initialization process erases existing data, then allocates enough storage space for each type of file. Do not allocate too much space for each file since there is a limited amount of storage on the disk. Thus, the ending record number should exceed the actual number of records by only a small amount. Be careful to save enough storage since if there is no space, data cannot be saved.

The twelve data files to be initialized are:

1. All associated item files
2. All associated station files
3. Storeroom transaction file
4. Sales order file
5. Shop order file
6. Employee data file
7. Purchase order file
8. Sales account file
9. Vendors accounts file
10. Operations/process file
11. Machine data file
12. Labor reporting file.

Each of these files must be initialized, with the beginning record for each set at 1, and the ending record number just above the actual number of records the user plans to enter. The cursor moves from begin to end records, then down the columns.

The user is then prompted to press the F1 key to begin the initialization. When the process is completed, the computer will respond with "Initialization of all files completed". It then prompts the user to enter any key to continue. The main menu will appear on the screen, and the system is ready to accept data.

*************************************WARNING*************************************
Only do this the first time the program is ever executed. The initialization module erases the data within the range of records specified every time it is run. Thus, if there is any type of data on the diskette within the range at the time, it will be erased and cannot be retrieved.
****

The file size may be increased, however. This is done by re-initializing the data disk with the beginning record one more than the old ending record, and the ending record set at the desired level. For example, if the initial ending record is 1000, and the user needs 1000 more records, for the reinitialization, the user's beginning record should be set at 1001 and the ending record at 2000. All other record initialization fields should be left blank, unless those fields need to be increased also. If they do, the same procedure should be used. Be sure to make a BACKUP copy of the data set before doing a reinitialization, for insurance against loss of data.

2 - Major SORT BY PART NUMBERS

This option performs a major sort of the part number data. It does an alphanumeric sort from scratch on the data. It assumes the data has never been sorted before. This should only be used once, after five to ten part numbers have been entered, since it can be very time consuming if there are many part numbers in the data file. Even when new parts are added, they will remain sorted.

3 - MINOR SORT BY PART NUMBERS

This option does a minor sort on the part number data. This assumes the data has been sorted before, It realigns and reestablishes the sort links, and speeds up response time to access or search for data. It should be used when response time becomes very slow.

4 - PRINT LIST OF PARTS BY RECORD NUMBER

This allows the user to view, with or without the printer on, a selective list of items in the data files, including inventory status and cost data, by record number. The user will be prompted to enter the beginning and the ending record numbers which are to be listed.

5 - PRINT SORTED LIST OF PARTS

This allows the user to view, with or without the printer on, a selective list of items in the data files, including inventory status and cost data, in alphanumeric sort order. The user does not have to do a sort before using this option, just enter the range of records that are to be listed. Even if new part number have been added, the sort will not have to be done, since they will automatically be place in sorted order.

6 - PRINT LIST OF STATIONS BY RECORD NUMBER

The user may view, with or without the printer on, a selective list of stations including man hours for each shift in the station. All that is required is the beginning and ending records of the stations to be listed.

7 - CHANGE COMPANIES NAME

The user may enter the company's name and address, which will appear at the heading of every printed copy that will be created by MRP-DSS.

See figure A.1 - A.5 for screen displays and reports.

MODULE B - BILL OF MATERIALS

The Bill of Materials module should be the first module used after
the data initialization module since this is where all the part number
data is entered on to the data diskette. The data that is required for
each part is the part number, description, low level code, item type,
the part's children and usage rate for each, and the part's parents and
usage rate.

When the program is loaded, the screen displays two choices; one to
enter part number, the second to enter record number. The part number
is the part classification number and the record number is the storage
location for this data on the data diskette. Depending upon which is
entered, there are four possible screens to be displayed. The four are:

- If a new part number is entered, the screen will display a note
indicating a new part is entered, request the user to press any key to
continue. A blank BOM worksheet will be displayed where the user has a
choice of many different ways to enter data.

- If an old part number (a record previously created) is entered,
the screen will display the worksheet with all of the data that has been
entered before.

- If a valid record number is entered, a record number within the
range initialized in the Data Initialization/Sort/Print module(A), is
entered, the worksheet and all of the associated data will be displayed
on the screen.

- If an invalid record number is entered, one which is outside of
the initialized range, the screen will tell the user that the maximum
record number has been exceeded and will prompt the user to try again.

Any of the two ways of accessing the worksheet is fine. The cursor
is used to choose between entering the Part Number or the Record Number.
When one is decided upon, move the cursor to the choice and type in the
corresponding part or record number data. The computer will respond in
one of the four ways previously discussed.

For the user who is entering data, the easiest way to enter the
part number is to let the computer search through the memory files to
see if the part is an old or new record. After the search is completed,
the computer will respond as in the above paragraph, depending upon the
part being a new or old record.

Whichever method of accessing the worksheet is used, if a valid one
is chosen, the worksheet will be displayed on the screen. On top of the
worksheet are the part number, part description, low level code, type of
item, and record number fields. The low level code tells the user at
which level the part is.

The type of item tells the user if the part is an end item, a
component item, or a service item. A service item is one which could be
either an end item or a component of another item.

19.28

The next two sections of the worksheet are the child and parent relationships, respectively, along with the usage rates of each.

The last section of the worksheet is the editing choices to change any of the above sections. Each editing feature has a particular key stroke associated with it. To choose a certain edit choice, the user needs only to press the corresponding key, and the cursor will be highlighted in that section. The changes can be typed in, with the cursor being moved by the return key. When all changes to the section are completed, press and hold the return key until the cursor moves off the screen. The module is now ready for another command. The following is a list and description of all the editing choices for this module.

A – CHANGE PART DEFINITION

This allows the editing of the parts characteristics: part description, low level code, and item type at the top of the worksheet. After the A key is pressed, the part description is highlighted, and can be changed. The cursor will move horizontally automatically if all the allowable spaces for the particular characteristic are used up. Otherwise the user must move the cursor manually. The low level code ranges from 0 to 99, for the level the part is at in the BOM structure. There are three item types to choose from. The first is the end item or final product. The second is a service item, which can be sold individually or as a component item for another product. The last is for a component item.

B – CHANGE PARTS CHILDREN

This option allows editing of the parts children section. Editing is done the same as in A above, except the cursor moves from the part number to the usage rate, then to the next child. The BOM is created by placing numbers into the children fields for each parent item. As this is selected, a search through all the files is done to see if the child is a new part or not. If it is a new part, a new file is automatically created by the module to store the data. There is a maximum number of fifty(50) children per part possible. If there are more than 50 children records, the user will be prompted and the children data will not be saved on the diskette. If a part has more then fifty children, a fictitious part can be created as the parent of all of the previous children. This part will become a child of the original real parent, thus allowing at least 49 more children to be entered. In this interpretation, the real children actually become grandchildren, with the part numbers for children 50 and 51 XXXX and YYYY respectively. A fictitious part number AAAA* is created and all of the children for part AAAA except 51 will be placed as children in the new parts BOM. The fictitious parent's(AAAA) BOM as children. Thus, part AAAA has two children, AAAA* and YYYY, and 50 grandchildren, which are actually it's children. See figure B.2 for a drawing of the suggested system.

Both the records of the artificial parts and of the original part and the relationship between the real and artificial parts need to be flagged. Either that or have a separate artificial part numbering system to provide easy recognition to keep the real and arificial parts separate.

19.29

The new child record can be viewed by using the MOVE(M) option or by using the CURSOR DOWN until the record is displayed. After the links are established, the low level code and the parent/child will be placed onto the sheet by the program. If a part's child is changed, the old part child will be replaced by the new part child, althouth the record of the child replaced will still be there. Data can be entered to any of the fields, using the editing techniques being described.

C - CHANGE PARTS PARENTS

The user is allowed to do editing of the parts parents and usage rates with this option. Editing is done the same as in B above. The same problem of a maximum number of 50 parents possible exists with the parent section also. It can be over come in the similar manner as the children problem is dealt with. A fictitious parent should be created with all of the real part's parents as parents for the fictitious part. The real part will then have as a parent, the fictitious part, as well as the ability to have up to 49 more. The first 50 parents of the real part are in actuality now it's grandparents, creating an extra BOM level. See figure B.6 for a drawing of this system.

The BOM can be created by using this option instead of the children relationship, but the user would have to start at the lowest part level, or the highest low level code number. The preferred way is still to enter the part's children.

D - DELETE PARTS

This option deletes the part from memory and the data diskette. The computer checks to make sure the user wants to delete the part number by asking "Are you sure?" A yes answer will delete the part. A no answer stops the process and waits for another editing feature to be chosen. If a part is deleted, the empty record becomes the next record to be filled with new part data.

E - LISTS PARTS CHILDREN

This allows the user to lists all the children of the part in question, along with the part description, usage rate, unit of measure, and purchase or make decision from the Part Inventory/Cost Data module (c). The user may also specify either the batch or lot size, which will vary the usage rate.

F - LISTS PARTS PARENTS

This option lists all the parents of the part in question, as well as the characteristics described in option E above.

G - BEGIN CHILD/PARENT DISPLAY

This allows changing of the beginning parent/child number in the parts children and parents section. Scrolling of last/next child/parent subsets is done without having to do it one by one.

H - COMPLETE EXPLOSION
This shows the complete explosion of the part and part's children, grandchildren, etc., with descriptions, usage rates and units of measure with or without the printer on.

I - COMPLETE IMPLOSION
This shows the complete implosion of a part and the part's parent, grandparents, etc., with descriptions, usage rates and units of measure with or without the printer on.

The next five edit choices are available for all modules in which they apply. For example, some modules do not have scrolling left or right.

CURSOR L - LAST CHILD/PARENT
Allows scrolling to the left for the last child/parent. If child 1 or parent 1 is in the farthest left position, a "parent/child" error will be displayed on the screen. Nothing happens with this error, it is just a reminder the user cannot proceed any farther in that particular direction.

CURSOR R - NEXT CHILD/PARENT
Allows scrolling to the right for the next parent/child relationship. A "parent/child" error occurs if the user tries to go past parent 50 or child 50.

CURSOR DOWN - NEXT RECORD
Allows the user to proceed to the next record in the data file. A record error will occur if the user tries to surpass the record limit set in the data initialization module.

CURSOR UP - LAST RECORD
Allows scrolling to the previous record in the data file. A record error will occur if Record number 1 is on the screen at the time.

M - MOVE TO ANOTHER RECORD
Allows the user to move onto another part to view, edit, or delete it from memory. When this command is used, the part number record number choice menu is displayed on the screen.

See Figures B.1 - B.6 for screen displays and reports.

MODULE C - PARTS INVENTORY/COST DATA

The part inventory and cost data module is used for inventory management information. All inventory data on each part is listed in this module.

After the module is loaded, the user needs to enter either the part number or record number to display a file on the screen. The computer may respond in one of two ways. They are:

-If an invalid part or record number is entered, the user is prompted to try again.

-If a valid record or part number is entered, the Parts Inventory/Cost Data worksheet is displayed for the particular part or record number asked for. Each record has three output sections.

On top of the display is the part characteristic section. This section has the part number, part description, low level code, item type and record number in it.

The middle section consists of all the part cost and part data. The cost data includes the unit cost per part, material costs, labor costs, overhead costs, set up costs per batch, and the suggested list price for the part.

The part data contains the lot size technique, the storage location code, purchased or manufactured part, number of units on hand, number of safety stock units, units allocated for and the unit of measure.

The last section is the edit choice section to change any of the above data. The editing choices are:

L - TO CHANGE LOT SIZE METHOD
This allows the user to define the lot sizing technique for reordering of parts. There are eight techniques to choose from in this module. The following is a list of the techniques.

1. Fixed order quantity.
2. Economic order quantity.
3. Lot for lot.
4. Fixed period ordering.
5. Least unit cost.
6. Least total cost.
7. Part period balancing.
8. Wagner Whitin method.

An asterisk will mark the present method. If the fixed period order is chosen, the user has to specify the period, in weeks, between orders. If the Fixed Order Quantity methos is chosen, the user is asked to supply the amount desired for each order, which must be a multiple of the fixed order quantity.

All of these techniques used are well documented in many different text books, thus they will not be explained. They all use trade off techniques between order or set up costs and carrying costs except for choices 1,3 and 4. The last choice, number 8, the Wagner Whitin method, is a more complicated method and uses considerable more time to calculate the order points than do the other methods.

C - TO CHANGE INVENTORY DATA
This permits changing of the inventory data. The data to be changed is shown in the middle section of the display screen and discussed above. Some general guidelines for data entry in this module include:

- For a manufactured part, the unit, material, labor and overhead costs should not be entered into this module, since it is possible to perform a cost roll up by entering the appropriate data into the Ldtime/Proc Rout/Assy (H) and the Station Definition/Load Control(D) modules, then running a Product Costing (S) module. Starting with the purchased parts, the Product Costing (S) module accumulates costs for each product as the module moves up through the BOM. Other entries to be made for a manufactured part include:

(a) The suggested list price can be entered for end item parts or service items only.
(b) An M should be placed into the purchases or make field.
(c) A storage location can be entered if there is one.
(d) The units on hand should remain empty, since the Storeroom Transaction (N) module should be used to enter this data. Control for the on hand stock should be completed through the Storeroom module.
(e) The safety stock may be changed, but care must be taken such, that if there are fewer on hand than the safety stock requires and a Materials Requirements Planning(T) module is run, order releases will be sent out.
(f) Another problem to watch out for is the units allocated for field. This should only be a temporarily used field, only when certain parts are committed to an order but are not withdrawn yet.
(g) The unit of measure needs to be entered and is used throughout the entire program for units.

- If the part is a purchased part, the purchase price should be entered into the unit cost as well as the material cost field. The other cost fields should be left blank. However, the user may consider the ordering cost as a set up cost and place it in that field. The storage place needs to be entered if there is one. Units on hand, units of safety stock, units allocated for and unit of measure are the same as for a manufactured part.

M - MOVE TO ANOTHER RECORD
This allows the user to move onto another display. The record number, part number menu appears after selection.

CURSOR UP - LAST RECORD
Displays the previous record in the file.

<u>CURSOR DOWN - NEXT RECORD</u>
Displays the next record in the file.

<u>P - JOB QUOTATION</u>
This option will provide the user with a complete job quotation, by summarizing all of the incurred costs. When chosen, the next screen will prompt the user to enter the needed data. The part numbers and code numbers have been provided. The batch size, lead time in days, company's name and cost mark-up (in percent) must be entered or the default values will be used. A summary of the costs can be viewed with the printer either on or off.

See Figures C.1 - C.4 for screen displays and reports.

MODULE D - STATION DEFINITION/LOAD CONTROL

The work station/load definition control module defines the work stations and the planned and released loads per week form each work station. When the module is loaded, the user must specify either the record number or the work station number desired to be displayed on the screen. The station number is the station definition number and the record number is the storage location for this data on the data disk. There are four possible displays that can occur form this. The four are:

- If a new station is entered, the screen will display a note stating such, then ask the user to press any key to continue. A blank Station Definition/Load Control worksheet will be displayed on the screen. Data may be entered through any of the editing features to be described.

- If an old station number is entered, one which has already been created, the station worksheet will all of the associated data will be displayed on the screen.

- If a valid record number, one within the range initialized in the Data Initialization/Sort/Print module(A), is chosen, the screen will display the corresponding station data for the record.

- If a invalid record number, one which is outside of the initialized range, is entered, the computer will tell the user to please try again.

Either the station number or the record number could be selected. The cursor is used to choose between the two. When one is decided upon, move the cursor to the choice and type in the corresponding data. If a station number is entered, the computer will search the data records to see if this part has been entered before. If it has, the record containing the data will be displayed on the screen. If there is not a match for this in the memory, the computer will respond with "New Station", then prompt the user to enter any key. The Station Definition/Load Control worksheet will be displayed on the screen. The worksheet may then be filled using the editing features to be described below. See figure D.1 for display of the worksheet.

If a record number is entered, the particular record worksheet will be shown on the screen. If the record number is outside of the range initialized in the Data Initialization module, the screen will display "maximum record number requested", and then prompt the user to enter again.

For the user who is entering data, the best and easiest way to prevent duplicate entries is to enter the station number, allowing the computer to search the memory files for the station number. Whether it is an old or new station number, the computer will respond as described above.

After a valid station number or record number has been entered, the worksheet will be displayed on the screen. There are three sections to the worksheet; the station definition section, the load section and the edit choice section.

The station definition part consists of the station code, the station description, available man-hours per week, record number, labor costs per shift per man-hour (possible three shifts) and the overtime premium in percentage.

The load section lists the beginning of the week date, the planned loads in man hours per week and the released loads in man hours per week. Following this are lists of weekly cash flow including labor cost, overhead cost and total costs.

The following list contains the editing features available for this module. The cursor is moved by the Return key for all editing options.

A - TO CHANGE STATION CHARACTERISTICS
This allows the user to change the station definition characteristics described above. For the overhead percentage, the number should be multiplied by 100. For example, for 15% overhead, the user should enter 15 rather than .15. All of the costs are used in the Product costing module(S) to calculate the unit cost for a product.

The man hours per shift are calculated by multiplying the each worker times the number of hours worked in a week, then adding all of the man hours together for a total.

B - TO CHANGE PLANNED LOADS
This changes the planned loads per week. The user is allowed to change the load in manhours for a planning horizon of up to 52 weeks. It is not necessary to change both the planned and released loads this way since the loads being displayed are the result of the Capacity Requirements Planning(T) module being run. This translates the order releases and scheduled receipts from the Order Releases and Scheduled Receipts(R) module into manhours required at each station using infomation covering the orders, routings, processes and operations in each station.

C - CHANGES RELEASED LOADS
This allows the user to change the released loads per week. It also has a 52 week planning horizon. See option B above for other stipulations.

G - GRAPHICS DISPLAY
This allows the display of a bar chart of the total man-hour load for the entire 52 week planning horizon.

W - TO SELECT STARTING DATE OF THE WEEK DISPLAY
This changes the beginning week display. The user may specify the starting week in the form MM/DD/YY. Seven weeks can be displayed on the screen at one time. Use the cursors to see other weeks.

M - MOVE TO ANOTHER RECORD
This allows the user to move onto another station. The station number, record number menu appears on the screen.

CURSOR LEFT - LAST WEEK
Scrolls left to the previous week's display.

CURSOR RIGHT - NEXT WEEK
Scrolls right to the next week's display.

CURSOR UP - LAST RECORD
Moves to the previous station record.

CURSOR DOWN - NEXT RECORD
Moves to the following station record.

See Figure D.1 - D.3 for screen displays and reports.

MODULE E - EMPLOYEE DATA CONTROL

This module is used to enter data about the employees into the employee file for every worker.

The first menu to be displayed has five menu options. The options are called by pressing the single digit number next to each option. The five are:

1. To open a new employee record.
2. To list the employee records in chronological order.
3. To list by state of residence.
4. To edit, close or view an individual record.
5. To return to the last record.

1 - TO OPEN A NEW EMPLOYEE RECORD
To open a new employee record allows the user to enter data into the records for a new employee. When this option is selected, a new page is displayed. On the display is room to enter data about the employee and editing commands to change the data. The data fields include employee number, employee name, telephone number, age, sex, job description, hourly pay rate, hours worked per week, record number and space for additional comments about the person.

The editing features are:

C - TO CHANGE DATA
This allows the user to change the data in the table. The cursor is moved by the RETURN key, with changes typed directly into the fields. Data field may be skipped over, but it is recommended to fill all fields if possible.

M - MOVE TO ANOTHER RECORD
The user may move onto another record. The employee number, record number menu will be displayed on the screen.

R - RETURN TO THE USER'S MENU
Returns the user to the Employee Data Control main menu.

CURSOR UP - LAST RECORD
Displays the previous employee record(last record).

CURSOR DOWN - NEXT RECORD
Displays the next record.

2 - TO LIST THE EMPLOYEE RECORDS IN CHRONOLOGICAL ORDER
The user may list the employee records in chronological order. When this option is chosen, the computer prompts the user to type in the beginning and ending record numbers. This allows the user to look at only a subset of records, rather than the whole data set, with or without the printer on.

19.38

3 - TO LIST BY STATE OF RESIDENCE

This option allows the user to list the employee records by state of residence. The beginning and ending record numbers must be specified, along with the state code(a two letter code for each state). The user may specify the printer to be on or off for the listing.

4 - TO EDIT/CLOSE OR VIEW INDIVIDUAL RECORD

This allows the user to view, edit or close an existing individual order. The record number or employee number is required. The screen displays the same table as is seen and described in option 1 above. The editing features are also the same.

5 - TO RETURN TO LAST RECORD

This allows the user to return to the most recent, past record, This command is quicker than using the Move(M) option, then entering the record number. The past record is automatically retrieved and displayed on the screen.

See Figure E.1 - E.3 for screen displays and reports.

MODULE F - MACHINE DATA CONTROL

This module is used to enter data for every piece of machinery into the files.

The first menu to be displayed has seven menu options. The options are called by pressing the single digit number next to each option. The seven options are:

1. To open a new machine record.
2. To list the machine records in chronological order.
3. To list by machine number.
4. To list by operator number.
5. To list by station number.
6. To edit, close or view an individual record.
7. To return to the last record.

1 - TO OPEN NEW MACHINE RECORD
This option opens a new machine record by allowing the user to enter data into the records for a new machine. When the option is selected, a new page is displayed. On the display is room to enter data about the machine and editing commands to change the data. The data fields consist of machine number, machine description, date opened (MM/DD/YY), operator name, operator number, station number, station description, a comment block for comments about the machine and record number.

The editing features are:

C - TO CHANGE DATA
This option allows the user to change data on the screen. Before data can be entered into the operator and station fields, these records must have been created previously through the Station Definition/Load Control(D) and Employee Data Control(E) modules. If the records have not been created, the data entered to these fields will not be saved. The user will have to create the fields before data will be accepted. If the records have been created and a correct station or employee number is entered, the corresponding station description and employee name will be generated automatically.

M - MOVE TO ANOTHER RECORD
Moves onto another record. The machine number, record number menu will be displayed on the screen.

R - TO RETURN TO THE USER'S MENU
This option returns the user to the Machine Data Control main menu.

CURSOR UP - LAST RECORD
Displays te last machine (last record).

CURSOR DOWN - NEXT RECORD
Displays the next machine(next record).

2 - TO LIST THE MACHINE RECORDS IN CHRONOLOGICAL ORDER

This allows the user to list the machine data records in chronological order. When the option is chosen, the computer prompts the user to type in the beginning and ending record numbers. This allows the user to look at only a subset of records, rather than the whole data record, with or without the printer on.

3 - TO LIST BY MACHINE NUMBER

The user may list the records by machine number. The beginning and ending record numbers must be specified, along with the machine number. The user may do this with or without the printer on.

4 - TO LIST BY OPERATOR NUMBER

This option lists the machine records by operator number. The beginning and ending record numbers must be specified again. The operator number must also be entered and the printer needs to be specified on or off.

5 - TO LIST BY STATION NUMBER

This lists the machine data records by the station number. Again, the beginning and ending record numbers are required. Also, the station number is needed. The user again may have the printer on or off.

6 - TO EDIT/CLOSE/VIEW INDIVIDUAL RECORDS

The user may view, edit or close an existing individual order. The record number or machine number is required. The screen displays the same table as is seen and described in option 1 above. The editing features are also the same.

7 - TO RETURN TO LAST RECORD

This allows the user to return to the most recent, past record. This command is quicker than using the Move(M) option, then entering the record number. The past record is automatically retrieved and displayed on the screen.

See Figures F.1 - F.3 for screen displays and reports.

19.41

MODULE G - OPERATIONS AND PROCESS DATA CONTROL

The Operations and Process Data Control module is used to enter data into operations and process data records for every operation and process type used in the system.

The first menu to be displayed has seven menu options. The options are called by pressing the single digit number next to each option. The cursor is moved by the RETURN key, which also is used to enter the data. The seven options are:

1. To open a new process/operations record.
2. To list the process/operations records in chronological order.
3. To list by process operation number.
4. To list by machine number.
5. To list by station number.
6. To edit, close or view an individual record.
7. To return to the last record.

1 - TO OPEN NEW PROCESS/OPERATIONS RECORD
This option opens a new process/operations record by allowing the user to enter data into the records for a new process/operation. When the option is selected, a new page is displayed. On the display is room to enter data about the process/operation and editing commands to change the data. The data fields consist of process/operation number, process/operation description, date opened, machine number, machine description, station number, station description, a comment block for comments about the machine and record number.
The editing features are:

C - TO CHANGE DATA
The user may change data in the table. If the machine and station records have not been created before by using the Station Definition/Load Control (D) and Machine Data Control (F) modules, the data entered into these fields will not be saved. The records must be created first by using the two aforementioned modules. If the records have been created, and correct station and machine numbers entered, the station description and machine name will automatically be entered to the correct fields by the computer.

M - MOVE TO ANOTHER RECORD
Moves onto another record. The process/operation number, record number menu will be displayed on the screen.

R - TO RETURN TO THE USER'S MENU
Return the user to the Process and Operations Data Control main menu.

CURSOR UP - LAST RECORD
Displays the previous operations record.

CURSOR DO~N - NEXT RECORD
Displays the next operations record.

2 - TO LIST THE PROCESS/OPERATIONS RECORDS IN CHRONOLOGICAL ORDER

This allows the user to list the process/operations data records in chronological order. ~hen the option is chosen, the computer prompts the user to type in the beginning and ending record numbers. This allows the user to look at only a subset of records rather than the whole data record, with or without the printer on.

3 - TO LIST BY PROCESS/OPERATION NUMBER

The data records are listed by process/operation number. The beginning and ending record numbers, and the process/operation number are required to continue the option. The user may view this with or without the printer on.

4 - TO LIST BY MACHINE NUMBER

The user may list the operation records by machine number. The beginning and ending record numbers must be specified, along with the machine number. Again, the user may view with or without the printer on.

5 - TO LIST BY STATION NUMBER

This option lists the process/operation data records by the station number. Again, the beginning and ending record numbers are required. Also, the station number is needed. The printer needs to be specified either on or off.

6 - TO EDIT/CLOSE/VIE~ INDIVIDUAL RECORDS

This allows the user to view, edit or close an existing individual order. The record number or process/operation number is required. The screen displays the same table as is seen and described in option 1 above. The editing features are also the same.

7 - TO RETURN TO LAST RECORD

The user may return to the most recent, past record. This command is quicker than using the Move(M) option, then entering the record number, The past record is automatically retrieved and displayed on the screen.

See Figures G.1 to G.5 for screen displays and reports.

MODULE H - LEAD TIME/PROC ROUT/ASSEMBLY PLANNING

The Lead Time/Proc Rout/Assembly Planning module is used to enter data aboout product routings, lead times, process and assembly procedures.

After the module is loaded, the user needs to enter either the part number or record number to display a record on the screen. There are two possible responses to the data input. They are:

- If a invalid part or record number is entered, the screen will request the user to try again.

- If a valid part or record number is entered, the screen will display the record requested. Each record has three output sections.

On top of the display is the part characteristic section. This section has the part number, part description, low level code, item type and record number in it.

The middle section consists of the work station sequence(order of operations), the work station number (a maximum of 50 stations possible), machine number, operation number, unit operation time in hours, batch setup/tear down time, batch transportation time (moving time), batch queue time (waiting time) before and after an operation, batch size and the lead time in hours. The lead time will automatically be calculated after all the other data has been entered.

The last section is the edit choice section to change any of the above data. The cursor is moved by the RETURN key. The editing choices are:

A - TO CHANGE LEAD TIME COMPONENTS
This allows the user to change the lead time components. These are described in the middle section above. The machine, station and operator records must be established previous to entering data into the fields or the data will not be saved. These records must be created by the Machine Data Control(F), Station Definition/Load Control(D) and Operations Data(G) modules respectively. If the records are not created, the user will have to create them before the data will by accepted.

B - TO CHANGE BATCH SIZE
This allows the user to change the batch size. When the batch size is changed, the lead time will be computed again and displayed.

R - TO REORDER SEQUENCE
The user may change the ordering of the work stations so if the order of visitation is not in numerical sequence, the stations will be listed in the order in which they visit the work stations. By using the A edit choice, to change Lead Time Components, and changing the entry in the Work Station Sequence, the switch will be made ofter pressing the R key.

M - MOVE TO ANOTHER RECORD
Move onto another record. The record number, part number menu
appears after selection.

CURSOR LEFT - LAST STATION
Scrolls left to display the last work station.

CURSOR RIGHT - NEXT STATION
Scrolls right to display the next work station.

CURSOR UP - LAST RECORD
Displays the previous record in the record.

CURSOR DOWN - NEXT RECORD
Displays the next record in the record.

P - TO PRINT ROUTE SHEET
This allows the user to produce the route sheet with description of
the operation, machine and work station, with or without the printer on.
This can also be used as an error checking device, since with the
information printed, erroneous entries can be spotted easier.

See Figures H.1 - H.2 for screen displays and reports.

19.45

MODULE I - SHOP ORDER CONTROL

The shop order control module contains the shop order data. This module is used to control all shop orders and provide the status of any shop order.

There are eight menu options to choose from. The eight are:

1. To open a new shop order.
2. To list the shop orders in chronological order.
3. To list by current station numbers.
4. To list by part number.
5. To edit, close or view an individual order.
6. To return to the last order.
S To store away old orders to file.
R To restore old orders from file.

To call any of these options from the Shop Order Control menu, the user needs to press the corresponding number next to each option.

1 - TO OPEN A NEW SHOP ORDER
This allows the user to open a new shop order. The shop order table appears on the screen with a choice of editing features. There are many fields in the table that need data placed into them. These fields are: the shop order number; the date the order is opened entered as DD/MM/YY, promised and closed; the part number; the part description; number of units ordered; current station; current station description and a comment block for anything else.

The cursor is moved by the RETURN key, with changes typed directly into the fields. The editing features are:

C - TO CHANGE DATA
The user may change the data in the table. The station number must be created before data can be entered, otherwise the data will not be saved. The station number is created by using the Station Definition/Load Control (D) module.

M - MOVE TO ANOTHER RECORD
Moves onto another record. The shop number, record number menu will be displayed on the screen.

R - RETURN TO THE USER'S MENU
This option returns the user to the Shop Order Control main menu.

CURSOR UP - LAST RECORD
Displays the previous order(last record).

CURSOR DOWN - NEXT RECORD
Displays the next order(next record).

2 - TO LIST THE SHOP ORDERS IN CHRONOLOGICAL ORDER

This allows the user to list the shop orders in chronological order. When the option is chosen, the computer prompts the user to type in the beginning and ending record numbers. This allows the user to look at only a subset of records, rather than the whole data set, with or without the printer on.

3 - TO LIST BY CURRENT STATION NUMBER

The user may list the shop orders by current work station. The beginning and ending record numbers must be specified along with the station number. The total units of the shop order are calculated and the date promised is displayed. The user may have the printer on or off.

4 - TO LIST BY ITEM NUMBER

This lists the shop orders by item number. The beginning and ending record numbers are needed again, along with the item number. Total units of the shop order are calculated, along with the data promised are displayed. The user had the choice of the printer being on or off.

5 - TO EDIT/CLOSE/VIEW INDIVIDUAL RECORDS

This allows the user to view, edit or close an existing individual order. The record number is required, then a table the same as the one discribed in choice 1 is displayed on the screen. The editing features are also the same.

6 - TO RETURN TO THE LAST ORDER

This allows the user to return to the most recent, past order. This command is quicker than using the *Move(M)* option, *then entering the* record number. The past record is automatically retrieved and displayed on the screen.

The shop orders can be transformed into planned scheduled receipts via the Planning Horizon Update(P) module.

S - TO STORE AWAY OLD ORDERS TO FILE

This allows the user to store either all orders to file or only closed orders to file.

R - TO RESTORE OLD ORDERS FROM FILE

This allows the user to restore an old order from files specified by the user.

See Figures I.1 to I.3 for screen displays and reports.

MODULE J - SALES ACCOUNT/CLIENTS CONTROL

The sales account/clients control module stores all the sales accounts or client number data.

There are five menu options to choose from. The five are:

1. To open a new sales account or client.
2. To list the sales accounts in chronological order.
3. To list by state in which client resides.
4. To edit or view an account.
5. To return to the last account.

To chose any of these five options, press the corresponding number next to each option.

1 - TO OPEN A NEW SALES ACCOUNT OR CLIENT
The user may open a new sales account or client record. The sales account/client table appears on the screen with a fields requiring data. The fields are: the account number; the date the account is opened, address, city, state, zip, contact person, telephone number; client account description and a comment block.

The cursor is moved by the RETURN key with changes typed directly into the fields. The editing features are:

C - TO CHANGE DATA
This allows the user to change data in the table. The date should be in the MM/DD/YY form.

M - MOVE TO ANOTHER RECORD
Moves onto another record. The sales number, record number menu will be displayed on the screen.

R - TO RETURN TO THE USER'S MENU
This lets the user return to the Accounts/Client Control main menu.

CURSOR UP - LAST RECORD
Displays the previous account(last record).

CURSOR DOWN - NEXT RECORD
Displays the next account(next record).

2 - TO LIST THE SALES ACCOUNTS IN CHRONOLOGICAL ORDER
The user may lists the sales accounts in chronological order. When the option is chosen, the computer prompts the user to type in the beginning and ending record numbers. This allows the user to look at only a subset of records, rather than the whole data set, with the printer on or off.

3 - TO LIST BY STATE IN WHICH CLIENT RESIDES
This option lists the sales accounts by state of residence. The beginning and ending record numbers must be specified, along with the state code(a two letter code for each state). The total units of the sales orders and the total sales dollars for the orders are calculated for each account. The user may specify the printer to be either on or off.

4 - TO EDIT/CLOSE/VIEW INDIVIDUAL ACCOUNTS
This allows the user to view, edit or close an existing individual account. The record number is required, then a table the same as the one described in choice 1 is displayed on the screen. The editing features are also the same.

5 - TO RETURN TO THE LAST RECORD
This allows the user to return to the most recent, past order. This command is quicker than using the Move(M) option, then entering the record number. The past record is automatically retrieved and displayed on the screen.

See Figures J.1 - J.3 for screen displays and reports.

MODULE K - SALES ORDER CONTROL

This module keeps track of all the sales orders received by the company. There are eight menu options to choose from. The eight are:

1. To open a new sales order.
2. To list the sales orders in chronological order.
3. To list by sales account number.
4. To list by item number.
5. To edit, close or view an order.
6. To return to the last order.
S. To store away old orders to file.
R. To return old orders form file.

To call these from the menu, the user only needs to press the corresponding number next to the option.

1 - TO OPEN A NEW SALES ORDER
This option allows the user to open a new sales order. The sales order table appears on the screen, with a choice of editing features. The table is made up of ten fields, each requiring some type of input. The fields are: The sales number; the date the sale is opened, promised and closed; the part number; the part description; number of units ordered; price per unit; total price; client account number; client account description and a comment block for anything else deemed necessary.

The cursor is moved by the RETURN key, with changes typed directly into the fields. The editng features are:

C - TO CHANGE DATA
The user may change the data in the table with this option.

M - MOVES TO ANOTHER RECORD
Moves onto another record. The sales number, record number menu will be displayed on the screen.

R - TO RETURN TO THE USER'S MENU
This option returns the user to the Sales Order Control main menu.

CURSOR UP - LAST RECORD
Displays the last order (next record).

CURSOR DOWN - NEXT RECORD
Displays the next order (next record).

2 - TO LIST THE SALES ORDERS IN CHRONOLOGICAL ORDER
The user may list the sales orders in chronological order. When this option is chosen, the computer prompts the user to type in the beginning and ending record numbers and whether the orders in the list are closed, opened or both. This allows the user to look at only a subset of records, rather than the whole data set, with or without the printer on. The list may also be represented graphically on the screen.

19.50

3 - TO LIST BY SALES ACCOUNT NUMBER
This allows the user to list the sales records by sales account number. Again, the beginning record numbers, ending record numbers, the sales account numbers and the type of account must be specified. The total units of the sales order and the total sales dollars for the order are calculated and the promised date is displayed. The user has the choice of viewing with or without the printer. Also, an option exists for a graphical representation of the list.

4 - TO LIST BY ITEM NUMBER
The user may list the sales by item number. The beginning and ending record numbers are needed again, along with the item number and type of item. Total units of the sale and the total sales dollars are calculated and displayed, along with the promised date. The printer may be set either on or off and there is an option for graphic representation as well.

5 - TO EDIT/CLOSE/VIEW INDIVIDUAL ORDERS
This allows the user to view, edit or close an existing individual order. The record number is required, then a table exactly like the one described in choice 1 is displayed on the screen. The editing features are also the same.

6 - TO RETURN TO THE LAST RECORD
This allows the user to return to the most recent, past order. This command is quicker than using the Move (M) option, then entering the record number. The past record is automatically retrieved and displayed on the screen.

S- TO STORE AWAY OLD ORDERS TO FILE
This allows the user to store some or all of the orders to file. The following three options appear on the next screen:

1- To store all orders to file.
2- To store only closed orders to file.
3- To return to the user's menu.

1- TO STORE ALL ORDERS TO FILE
This option will store all orders to file, once you have provided the name of the file that is to be stored.

2- TO STORE ONLY CLOSED ORDERS TO FILE
This option will store closed orders, while keeping available opened orders. The user must provide the name of the file that is to be stored.

3- TO RETURN TO THE USER'S MENU
This option will return the user back to the Sales Order Control main menu.

R- TO RESTORE OLD ORDERS FROM FILE
This option retrieves a previously stored order from file. All the user must do is enter the name of the file that is to be restored.

The sales orders can be transformed into the Master Production Schedule (Q), by the Planning Horizon Update (P) module.

See Figures K.1 - K.3 for screen displays and reports.

19.51

MODULE L - VENDOR ACCOUNT CONTROL

The vendor account control module stores all the vendor account numbers and description data.

There are five menu options to choose from. The five are:

1. To open a new vendor account.
2. To list the vendor accounts in chronological order.
3. To list by state in which vendor resides.
4. To edit, close or view an account.
5. To return to the last account.

To choose any of these five options, press the corresponding number next to each option.

1 - TO OPEN A NEW VENDOR ACCOUNT
This allows the user to open a new vendor account record. The vendor account table appears on the screen, with a choice of editng features. The table has many different fields requiring data. The fields are: the vendor/purchase number, the date opened, the client account description, the street address number, city, state, zip code, contact person, telephone number, a comment section and record number. See figure L.1.

The cursor is moved by the RETURN key, with changes typed directly into the fields. The editing features are:

C - TO CHANGE DATA
This allows the user to change the data in the table. The date should be in the MM/DD/YY form.

M - MOVE TO ANOTHER RECORD
Moves onto another record. The vendor number, record number menu will be displayed on the scsreen.

R - RETURNS TO THE USER'S MENU
Returns the user to the Vendor Account Control main menu.

CURSOR UP - LAST RECORD
Displays the last account (last record).

CURSOR DOWN - NEXT RECORD
Displays the next account (next record).

2 - TO LIST THE VENDOR ACCOUNTS IN CHRONOLOGICAL ORDER
This lists the vendor accounts in chronological order. When this option is chosen, the computer prompts the user to type in the beginning and ending record numbers. This allows the user to look at only a subset of records, rather than the whole data set, with the printer on or off.

3 - TO LIST BY STATE IN WHICH VENDOR RESIDES

This lists the sales accounts by state of residence. The beginning and ending record numbers must be specified, along with the state code (a two letter code for each state). The total units of the sales orders and the total sales dollars for the orders are calculated for each account. The user may specify the printer to be on or off. See figure L.3.

4 - TO EDIT/CLOSE/VIEW INDIVIDUAL ACCOUNTS

This allows the user to view, edit or close an existing individual order. The record number or vendor account number is required. A table the same as the one described in choice 1 is displayed on the screen. The editing features are also the same.

5 - TO RETURN TO THE LAST RECORD

This allows the user to return to the most recent, past order. This command is quicker than using the Move (M) option, then entering the record number. The past record is automatically retrieved and displayed on the screen.

See Figures L.1 - L.3 for screen displays and reports.

19.53

MODULE M - PURCHASE ORDER CONTROL

The purchase order control module contains the purchase order data. There are eight menu options to choose from.

1. To open a new purchase order.
2. To list the purchase orders in chronological order.
3. To list by vendor account numbers.
4. To list by item number.
5. To edit, close or view an individual account.
6. To return to the last order.
S. To store away orders to file.
R. To return orders orders from file.

To call any of these from the Purchase Order Control menu, the user needs to press the corresponding number next to each option.

1 - TO OPEN A NEW PURCHASE ORDER

The purchase order table appears on the screen, with a choice of editing features. There are many fields in the table that need data placed into them. These fields are: the sales number; the date the sale is opened, promised and closed; the part number; the part description; number of units ordered; price per unit; total price; vendor account number; vendor account description and a comment block for anything else deemed necessary.

The cursor is moved by the RETURN key, with changes typed directly into the fields. The editing features are:

C - TO CHANGE DATA

This allows the user to change the data within the table. The date should be in the MM/DD/YY form.

M - MOVES TO ANOTHER RECORD

This allows the user to move to another record. The sales number menu will be displayed on the screen.

R - RETURNS TO THE USER'S MENU

Returns the user to the Purchase Order Control main menu.

CURSOR UP - LAST RECORD

Displays the next order (next record).

CURSOR DOWN - NEXT RECORD

Displays the next order (next record).

2 - TO LIST THE PURCHASE ORDERS IN CHRONOLOGICAL ORDER

This option lists the purchase orders in chronological order. When this option is chosen, the computer prompts the user to type in the beginning and ending record numbers and identify the type of order as either open, closed or all. This allows the user to look at only a subset of records, rather than the whole data set, with the printer on or off. The data may also be shown graphically.

3 - TO LIST BY VENDOR ACCOUNT NUMBER

This option allows the user to list the purchases by vendor account numbers. Again the beginning and ending record numbers must be specified, along with the vendor account number and type of order. The total units of the purchase order and the total cost in dollars for the purchase order is calculated and the promised date is shown. This may be viewed graphically with the printer either on or off.

4 - TO LIST BY ITEM NUMBER

This allows the user to list the sales orders by item number. The beginning and ending record numbers are needed again, along with the item number and type of order. Total units of the purchase and the total cost in dollars of purchase order are calculated and the promise date is also shown. The user may again view the data graphically, with or without the printer.

5 - TO EDIT/CLOSE VIEW INDIVIDUAL RECORDS

This option allows the user to view, edit or close an existing individual order. The record number is required, then a table like the one described in choice 1 is displayed on the screen. The editing features are also the same as choice 1.

6 - TO RETURN TO THE LAST ORDER

This allows the user to return to the most recent, past order. This command is quicker than using the Move (M) option, then entering the record number. The past record is automatically retrieved and displayed on the screen.

S- TO STORE AWAY ORDERS TO FILE

This option allows the user to store all or a fraction of the orders to file. The screen will display the following choices:

1. To store all orders to file.
2. To store only closed orders to file.
3. To return to the user's menu.

1- TO STORE ALL ORDERS TO FILE

To store all of the orders to file, all the user must do is provide the name of the file that is to be stored.

2- TO STORE ONLY CLOSED ORDERS TO FILE

This option will store only closed options and keep the remaining open orders. Again, all the user must do is provide the name of the file that is to be stored.

3- TO RETURN TO THE USER'S MENU

This option returns the user to the Purchase Orders Control main menu.

R- TO RESTORE OLD ORDERS FROM FILE

This option will return frim storage any previously stored purchase order. All the user must provide is the name of the file that is to be restored.

Purchase orders may be transformed into planned scheduled receipts by the Planning Horizon Update module (P).
See Figures M.1 to M.4 for screen displays and reports.

MODULE N - STOCKROOM TRANSACTION CONTROL

The stockroom transaction control module controls the stockroom or on-hand inventory. Every time a part is taken from or added to the inventory, this module adjusts the on-hand inventory level accordingly. The on-hand inventory level may be viewed via the Part Inventory/Cost Data module (C). There are nine menu options to choose from. The nine are:

1. To open a new individual part transaction.
2. To open a new parts list transaction.
3. To list the transactions in chronological order.
4. To list the transactions by part number.
5. To list the transactions by order number.
6. To edit, close or view transaction.
7. To return to the last transaction.
S. To store old transactions to file.
R. To restore old transactions from file.

To call these from the menu, the user only needs to press the corresponding number next to the option.

1 - TO OPEN A NEW INDIVIDUAL PART TRANSACTION

This option allows the user to open a new individual part transaction. The stockroom transaction table appears on the screen, along with a choice of editing features. The table is made up of fields which reqire data inputs. The fields are: The transaction number; the date the transaction occurs; the part number; the part description; number of units ordered; stock issue or receipt; a reference order number for either sales (S), manufacturing (M) or purchasing (P); a comment block for additional comments and the record number.

For editing purposes, the cursor is moved by pressing the Return key. The editing features are:

C - TO CHANGE DATA

To change the data in the table. The date should be in the MM/DD/YY form.

M - MOVE TO ANOTHER RECORD

Moves onto another record. The transaction number, record number menu will be displayed on the screen.

R - RETURN TO THE USER'S MENU

Returns the user to the Stockroom Transaction Control main menu.

CURSOR UP - LAST RECORD

Displays the last transaction (last record).

CURSOR DOWN - NEXT RECORD

Displays the next transaction (next record).

2 - TO OPEN A NEW PARTS LIST TRANSACTION

This option allows the user to add to or remove from inventory a multipart transaction, with all the parts lists being incremented or decremented at the same time. An example would be removing all of the component parts necessary to make an end item from inventory. All component parts making up this item would have heirinventory levels decremented dependent upon the usage rate of each to the parent item. If there are five component parts, there will be five transaction records created.

3 - TO LIST THE TRANSACTIONS IN CHRONOLOGICAL ORDER

This option allows the user to list the transactions in chronological order. When this option is chosen, the computer prompts the user to type in the beginning and ending record numbers. This allows the user to look at only a subset of records rather than the whole data record, with or without the printer on.

4 - TO LIST THE TRANSACTIONS BY PART NUMBER

This option allows the user to list the transactions by part number. When chosen, the computer will prompt the user to enter the beginning and the ending record numbers along with the part number. The listing can be made with th e printer either on or off.

5 - TO LIST THE TRANSCATIONS BY ORDER NUMBER

This option allows the user to list the transactions by order number. When chosen, the computer will prompt the user to enter the beginning and ending record numbers, type of transaction that is to be listed and the order number. The list may be viewed with the printer either on or off.

6 - TO EDIT/CLOSE OR REVIEW AN ACCOUNT

This allows the user to view, edit or close an existing individual order. The record number is required, then a table exactly like the one described in choice 1 is displayed on the screen. The editing features are also the same.

7 - TO RETURN TO THE LAST ORDER

This allows the user to return to the most recent, past order. This command is quicker than using the Move (M) option, then entering the record number. The past record is automatically retrieved and displayed on the screen.

S - TO STORE OLD TRANSACTIONS TO FILE

This option allows the user to store some or all of the transactions to file. The following options appear on the next screen:

1. To store all transactions to file.
2. To store a range of tranactions to file.
3. To return to user's menu.

The user may choose any of the options by moving the cursor with the return key.

1 - TO STORE ALL TRANSACTIONS TO FILE

To store all of the transactions to file, all the user must provide is the name of the file that is to be stored.

2 - TO STORE A RANGE OF TRANSACTIONS TO FILE

To store a partial list of transactions to file and keep the remaining files, all the user must provide is the range of records that is to be stored. Specifically, the user must enter the beginning record and the ending record number.

3 - TO RETURN TO THE USER'S MENU

This option returns the user to the Storeroom Transaction Control main menu.

R - TO RETURN TRANSACTIONS FROM FILE

This option will return from file any previously stored storeroom transactions. All the user must do is provide the name of the file that is to be restored.

See Figures N.1 to N.3 for screen displays and reports.

MODULE O - LABOR REPORTING CONTROL

The Labor Reporting Control module is used to enter data pertaining to labor reports (hours of labor) for specific shop orders.

The first menu to be displayed has twelve menu options. The options are called by pressing the single digit number next to each option. The cursor is moved by the Return key, which also is used to enter the data. The twelve options are:

1. To open a new labor report record.
2. To list the labor report records in chronological order.
3. To list by shop order number.
4. To list by part number.
5. To list by operation number.
6. To list by machine number.
7. To list by station number.
8. To list by employee number.
9. To edit, close or view an individual record.
10. To return to the last record.
S. To store old records to file.
R. To restore old records from file.

1 - TO OPEN A NEW LABOR REPORT

This option opens a new labor reporting record by allowing the user to enter data into the records for a new labor report. When the otion is selected, a new page is displayed. On the display is room to enter data about the labor report and editing commands to change the data. The data fields consist of the labor report number, the date, the reference shop order number, the part number, part description, operation number, operaton description, machine number, machine description, station number, station description, employee number, employee name, labor hours reporting and a regular or overtime work specification.

The next section is the editing section. The editing features are:

C - TO CHANGE DATA

To change the data in the table. All of the fields must have records already created through other modules before using this module. If the records do not exist, any data entered into the fields will not be saved. For all of the records which are there, after a valid number has been entered, the corresponding description will automatically be entered by the computer.

M- MOVES TO ANOTHER RECORD

Moves onto another record. The labor report number, record number menu will be displayed on the screen.

R - RETURN TO THE USER'S MENU

Returns the user to the Labor Report Control main menu.

<u>CURSOR UP - PREVIOUS RECORD</u>
Displays the previous report (last record).

<u>CURSOR DOWN - NEXT RECORD</u> .
Displays the next report (next record)..

<u>2 - TO LIST THE LABOR REPORT RECORDS IN CHRONOLOGICAL ORDER</u>
This lists the process/operations data records in chronological
order. When the option is chosen, the computer prompts the user to type
in the beginning and ending record numbers. This allows the user to
look at only a subset of records, rather than the whole data record,
with or without the printer on. The total labor costs are calculated
for the product. The option to display the list graphically also
exists.

<u>3 - TO LIST BY SHOP ORDER NUMBER</u>
This option allows the user to list the data records by shop order
number. The beginning and ending record numbers, and the shop order
number are required to continue the option. The user has the option of
viewing the listing with or without the printer on. A graphic
representation is also available.

<u>4 - TO LIST BY THE PART NUMBER</u>
This lets the user view with the printer on or off, the list of
labor records by part number. The beginning and ending record numbers
are required, along with the part number. A graphic display of the list
is also optional.

<u>5 - TO LIST BY OPERATION NUMBER</u>
This allows the user view with or without the printer, the labor
records by operation number. Again, the beginning and ending record
numbers are needed. The operation number is also needed. The listing
may also be shown graphically.

<u>6 - TO LIST BY MACHINE NUMBER</u>
This allows the user to list labor records by machine number. The
beginning and ending record numbers must be specified, along with the
machine number. The user has a choice of viewing with the printer on or
off. The listing may also be displayed graphically.

<u>7 - TO LIST BY STATION NUMBER</u>
This allows the user to list the labor report data records by the
station number. Again, the beginning and ending record numbers are
required. Also, the station number is needed. The user must specify
the printer to be on or off. The listing may also be displayed
graphically.

<u>8 - TO LIST BY EMPLOYEE NUMBER</u>
This lets the user view the labor records by employee number. The
beginning and ending record number and the employee number must be
specified. The user again has the choice to have the printer on or off.
The listing may also be shown graphically.

9 - TO EDIT/ CLOSE/VIEW INDIVIDUAL RECORDS

This allows the user to view, edit or close an existing individual report. The record number of labor report number is required. The screen displays the same table as is seen and described in option 1 above. The editing features are also the same.

10 - TO RETURN TO THE LAST RECORD

This allows the user to return to the most recent, past record. This command is quicker than using the Move (M) option, then entering the record number. The past record is automatically retrieved and displayed on the screen.

S - TO STORE OLD RECORDS TO FILE

This allows the user to store all reports or range of reports to file specified by the user.

R - TO RESTORE OLD RECORDS FROM FILE

This allows the user to restore old reports from files specified by the user.

See figure 0.1 to 0.4 for screen displays and reports.

MODULE P - DATE/ORDERS PROC/PLAN HORIZON UPDATE

The purpose of this module is to update or post the Master Production Schedule and Scheduled Receipts schedule, with all the new sales, shop and purchase order data which have been received. This module will capture the dynamics of the planning horizon by updating all sales, purchase and shop orders. It is also used to collect performance statistics such as late orders, sales and purchase prices, leadtime, scrap rate and labor costs.

When the module is loaded, the user must enter the date and press the Return key to continue. The display on the screen will be the Date/Orders Proc/Plan Horizon Update worksheet. See figure P.1.

The worksheet has only one section to it. The beginning and ending record numbers must be entered for each of the following categories:

1. Sales order processing
2. Shop order processing
3. Purchase order processing
4. Labor Report processing

The beginning and ending record numbers are the range of record numbers to be processed. The module will process the range of records specified for the sales orders and update the Master Production Schedule. Likewise, it will process the range of records specified for the shop and purchase orders and update the Scheduled Receipts Schedule.

In addition to updating the Master Production Schedule and the Receipts Schedule, performance statistics such as late orders, sales and purchase prices, leadtime, scrap rate and labor cost are collected and may be viewed from the Summary Actions To Do module (V).

The F1 key is used to proceed with the processing. When the process is completed, the computer will respond with "processing completed" and prompts the user to enter any key. The main menu will be displayed then.

After processing, the output may be viewed in the Master Production Schedule module (Q) and the Order Releases and Receipts Schedule module (R) for the sales orders and shop and purchase orders, respectively, and the Summary Actions To Do module (V) for performance statistics.

19.63

MODULE Q - MASTER PRODUCTION SCHEDULE

The Master Production Schedule module sets the gross requirements per week for each part number over a planning horizon of up to 52 weeks.

When the module is loaded, the user must enter the part or record number to proceed further. The user must enter data into either of the fields, using the Return key to move the cursor and to enter the data. The display on the screen will be the Master Production Schedule worksheet. See figure Q.1.

The worksheet is divided into three different sections; the part characteristic section, gross requirements section and the editing section. The part characteristics section consists of the part number, part description, low level code, item type and record number.

The middle section displays the week beginning date and the gross requirements per week for the particular part number.

The final section is the editing features section. The following is a list of the editing features for the module. The cursor is moved by pressing the Return key.

C - TO CHANGE GROSS REQUIREMENTS
This allows the user to change the gross requirements per week.

G - GRAPHICS DISPLAY
This allows the display of a bar chart for the Master Production Schedule over the entire 52 weeks planning horizon.

W - TO SELECT THE STARTING WEEK DATE
This lets the user select the starting week date for display, in the form MM/DD/YY.

M - MOVE TO ANOTHER RECORD
This allows the user to move onto another record. The record number, part number menu will appear on the screen.

CURSOR LEFT - LAST WEEK
Scrolls left to show last week's data.

CURSOR RIGHT - NEXT WEEK
Scrolls right to display next week's data.

CURSOR UP - PREVIOUS RECORD
Displays the previous record.

CURSOR DOWN - NEXT RECORD
Displays the next record.

P - PRINT LIST
This allows the user to view the production schedule for a particuliar part for a full year with the printer either on or off.

The Master Production Schedule may derive it's schedule from the sales orders entered in the Sales Order (L) module via the Planning Horizon Update module (P).

See figure Q.1 to Q.3 for screen displays and reports.

MODULE R - ORDER RELEASES AND RECEIPT SCHEDULE

This module allows the user to see the planned releases and scheduled receipts per week for each part number. The output from this module may be used as input to the Capacity Requirements Planning (T) module to transform the data into manhour requirements or load profile in each station. The order releases are the basis for creating shop and purchase orders.

The part or record number menu appears on the screen next. The user must enter data into either of the fields, using the Return key, to move the cursor and to enter the data. The display on the screen will be the Order Releases and Receipt Schedule worksheet table. See figure R.1.

The table is divided into three different sections; the part characteristic section, release and receipt section and the editing section. The part characteristics section consists of the part number, part description, low level code, item type and record number.

The week beginning date, along with the planned releases and scheduled receipts per week are listed in the next section.

The final section is the editing features section. The following list is all of the editing features for the module. The cursor is moved by pressing the Return key.

R - TO CHANGE ORDER RELEASES
This allows the user to change order releases.

S - TO CHANGE SCHEDULE RECEIPTS
This allows the user to change the schedule receipts.

G - GRAPHICS DISPLAY
This allows the display of bar charts for both the schedules of order releases and receipts over the entire 52 weeks planning horizon.

W - TO SELECT STARTING WEEK DATE
Lets the user select the starting week date, in the form, MM/DD/YY.

M - MOVE TO ANOTHER RECORD
This lets the user move onto another record. The record number, part number menu will appear on the screen.

CURSOR LEFT - LAST WEEK
Scrolls left to show last week's data.

CURSOR RIGHT - NEXT WEEK
Scrolls right to display next week's data.

CURSOR UP - PREVIOUS RECORD
Displays the previous record.

CURSOR DOWN - NEXT RECORD
Displays the next record.

P - PRINT LIST
This option allows the user to view the planned order releases for each part for a full year, with the printer either on or off.

The planned scheduled receipts may be derived from Purchase (N) and Shop (J) Order modules via the Planning Horizon Update module (P). The planned order releases are the output from the Materials Requirements Planning (S) module.

See Figure R.1 - R.4 for screen displays and reports.

MODULE S - PRODUCT COSTING

This module calculates the cost of the parts being made. When the program is loaded, the first screen to appear is the parameter definition option. There are two parameters the number of stations and number of items. See figure S.1.

The number of stations pertains to the number of work stations existing in the station record.

The number of parts is the number of parts existing in the bill of materials records files.

The results are printed out quickly across the screen. Each item or part number is printed first, followed by four different costs. The four costs are the cost of materials labor, overhead and the total unit cost. The total unit cost, is the additon of the three above costs.

To suspend the screen for viewing, press the Ctrl and Num Lock keys simultaneously. To release the screen, press any key and the scrolling will continue.

This module is dependent upon other modules for the data used to calculate the total costs of the product. It uses a cost roll up method, starting from the purchased parts working up the entire BOM, with the final products accumulating labor costs, material costs and overhead costs. It is dependant upon the Bill of Materials (B), Parts Inventory/Cost Data (C), Station Definition/Load Control (D), and Ldtime/Poc Rout/Assy Planning (H) modules for data in order to work. Thus, all of these modules must have data entered into them before the Product Costing module will run correctly.

MODULE T - MATERIALS REQUIREMENTS PLANNING

This module calculates all of the material requirements needed to meet the Master Production Schedule. The requirements are in order releases per week, over the planning horizon.

When the module is loaded, the Materials Requirements Planning (MRP) main menu is displayed. There are five choices on this menu. The choices are:

1. To define the parameters.
2. To recompute the low level codes.
3. To select items for MRP processing.
4. To proceed with MRP processing.
5. To view MRP output for an individual item.

1 - TO DEFINE THE PARAMETERS
This allows the user to define the parameters, has four parameters which must be defined for the module to work. These parameters are the number of items, the number of weeks, and the carrying cost in annual percentage. See figure T.1.

The number of items pertains to the number of part numbers to do the processing on.

The number of words is the number of weeks th user wants to do the process for, up to 52 weeks.

The cost percentage should be multiplied by 100 if it is fractional. For example, for 15%, the user should enter 15, rather than .15.

The user has two more options to choose from under option one. The E key will allow the user to change the paratmeters, while the P key will bring the MRP main menu back onto the screen.

2 - TO RECOMPUTE THE LOW LEVEL CODES
This allows the user to automatically recompute the low level codes of all the parts in the file, based on the product structure.

3 - TO SELECT ITEMS FOR MRP PROCESSING
This allows the user to select the items for MRP processing. The part or record number for each item is needed. If more than one item is wanted, just keep entering part or record numbers until all items are entered. All children and grandchildren of the parts selected will be stored for processing also. When this is done, press the F1 key to end the data input. The items will be stored away until the 4 key discussed next, is pressed. The MRP main menu will then be displayed.

4 - TO PROCEED WITH MRP PROCESSING
This option lets the user proceed with the MRP processing. It computes the order releases for the items selected in option 3 above. If no items were selected using option 3, then all items will be processed. The user has the choice to have the printer on or off.

The output generated has three sections to it (see figure S.2).
The first section displays the lot sizing data for the coverage of the
net requirements. It has the lot size technique, the number of periods,
the net requirements for each period and the planned order per period.
A total for the net requirements and planned orders is also calculated.
The lot sizing method is chosen in the Parts Inventory/Cost Data (C)
module. If no lot sizing method is chosen, the module will default to
use the lot for lot method.

The next section of the output consists of many items. The are:

1. Number of set ups.
2. Set up costs.
3. Number of parts per week.
4. Total carry costs.
5. Total set up and carry costs.
6. Total set up and carry costs, including on hand and
   safety stock.
7. Item number.
8. Lead time.
9. Number on hand.
10. Amount of safety stock.
11. Amount allocated for.
12. Late release.
13. Recommend rescheduling.

A late release would be a part which should have been released
already. These parts are candidates for expediating or whose parent's
orders should be rescheduled to a later date.

The last section of the output displays the gross requirements for
each parent item, each service order, the total orders, the schedules
receipts, the amount available, the net requirements, the planned order
releases and the planned order receipts per week. The planned order
releases and receipts from this module are displayed in the Order Release
and Receipt Planning(R) module.

5 - TO VIEW MRP OUTPUT FOR AN INDIVIDUAL ITEM
This allows the user to view the MRP processing for an individual
item. The record number, part number menu appears and data is entered to
continue the processing.

See figure T.1 - T.3 for screen displays and reports.

MODULE U - CAPACITY REQUIREMENTS PLANNING

The capacity requirements planning module determines the capacity requirements for each individual work stations. It takes the order release calculated by the MRP(T) module and translates them into manhours based on the lead time and routing data received from the Ldtime/Proc Rout/Assy Planning (H) module. The results may be viewed in the Station Definition/Load Control (D) module.

The first screen to appear when the module is loaded is the parameter definiton option(see figure U.1). The parameters to be defined are the number of stations, number of items and number of weeks. The number of stations are the number of work stations in the station record. The number of items are the number of parts in the part inventory records. The number of weeks is the planning horizon, the number of weeks the process will look at, with a maximum of 52 weeks possible.

There are two editing features available. The E key allows editing of the parameters, while the P key proceeds with the actual calculations.

The computer calculates for a while, then automatically prints out the results (see figure U.2). The work station and work station code numbers are printed first. After those numbers, the week beginning date, which is the same specified above, is printed next.

Under the date is the number of released loads (based on scheduled receipts) during the week and the number of planned loads (based on planned order releases) for the week. A total load cost for each station is then calculated and displayed.

Each work station is shown in this manner. The screen scrolls very fast, displaying each station individually. After the final work station has been displayed, a total cost for all stations combined is calculated and displayed. A "processing has completed" response will also be on the screen, with a prompt to the user to enter any key to continue. After this is done, the user is returned to the Main Menu, ready for additonal instructions.

MODULE V - SUMMARY ACTIONS TO DO

This module lists a summary of action items to be done. These items are the results of the four application modules, Product Costing(S), Date/Orders Proc/Plan Horizon Update(P), MRP (T) and Capacity Requirements Planning (U) being run. They give a list of recommended actions to do.

The first screen to appear is the Summary Actions main menu. See figure V.1. There are nine choices on it. The choices are:

1. Items requiring order releases this week or earlier.
2. Items whose shop or purchase orders are promised this week or earlier.
3. Items whose sales orders are promised this week or earlier.
4. Items whose scheduled receipts are recommended for rescheduling.
5. Parts deviation report for planned versus actual prices.
6. Parts deviation report for planned versus actual leadtime.
7. Parts deviation report for planned versus actual scrap and safety stock.
8. Stations where overloads exist.
9. Station deviation report for planned versus actual labor cost.

1 - TO VIEW THOSE ITEMS REQUIRING ORDER RELEASES THIS WEEK OR EARLIER
This allows the user to view with or without the printer, a list of order releases due this week and a list of order releases due last week or earlier. The user may select between purchase orders or shop orders. The tables have the part number, the description, the number of orders and the unit of measure for each release.

2 - TO VIEW SHOP/PURCHASE ORDES PROMISED THIS WEEK OR EARLIER
This option lists with the printer on or off, shop or purchase orders promised this week or earlier. There are two tables listed, one for this weeks data and the other for the earlier weeks data, with the same information as in the tables described in option one above.

3 - TO VIEW ITEMS WHOSE SALES ORDERS ARE PROMISED THIS WEEK OR EARLIER
This option allows the user to view a list, with or without the printer, of sales orders promised this week or earlier. AGAIN, TWO TABLES ARE DISPLAYED, ONE FOR THIS WEEK AND THE OTHER FOR THE EARLIER ORDERS. The information is the same as in option one above.

4 - TO VIEW ITEMS WHOSE SCHEDULED RECEIPTS ARE RECOMMENDED FOR RESCHEDULING
This allows the user to display a list, with or without the printer, of scheduled receipts which are recommended for rescheduling. The item number, description, number of orders and unit of measure are listed for each receipt.

5 - TO VIEW PARTS DEVIATION REPORT FOR PLANNED VERSUS ACTUAL PRICES

The user may compare the actual prices with the planned prices of a specified set of parts. The user must specify the range of records that is to be considered and the data may be viewed with the printer on or off. The actual prices are collected from Module P - Date/Orders Proc/Horizon Update. The user may specify to have either the sale or purchase prices of items. After the information is displayed, the user is requested to replace the current planned with the actual data if desired.

6 - TO VIEW PARTS DEVIATION REPORT FOR PLANNED VERSUS ACTUAL LEADTIME

The user must indicate whether it is sale, purchase or shop leadtimes and the range of records in the parts file. The printer may be set either on or off while viewing. The screen will display for each part, performance statistics relating to the planned or estimated leadtime in days, the average leadtime from order opening to the date when promised and the average leadtime from order opening to the date when closed. The user will be asked if the estimated/planned leadtime will be replaced by either the promised or closed leadtime.

7 - TO VIEW PARTS DEVIATION REPORT FOR PLANNED VERSUS ACTUAL SCRAP AND SAFETY STOCK

The user will be able to compare the actual safety stock with the recommended safety stock. All the user must enter is whether it is scrap or safety stock for a made or purchased part, the range of records to be considered and whether or not the printer is to be on or off. Performance statistics relating to the number of parts scrapped and good, percentage defective, safety stock and recommended safety stock level. The user may replace the current safety stock level with the recommended level.

8 - TO VIEW WHETHER OVERLOADED STATIONS EXIST

To list the overloaded stations, the user must identify the range of records to be considered in the stations file and whether or not the printer should be on or off. If overloaded stations exist, MRP-DSS will provide rescheduling recommendations if they are desired. The recommendations will include parent parts which will be affected and potential sale orders for rescheduling.

9 - TO VIEW STATION DEVIATION REPORT FOR PLANNED VERSUS ACTUAL LABOR COSTS

The user will be able to compare actual labor costs with planned labor costs, once the desired records have been specified. This may be done with or without the printer. The user may replace the planned labor costs with the actual average labor costs for each station.

See figure V.1 to V.5 for screen displays and reports.

MODEL ₩ - COMBINATION RUNS

This module is designed to allow the user to make combination runs of the four processing modules; Product Costing(S), Date/Order Processing/Plan Horizon Update(P), Materials Requirements Planning(T) and the Capacity Requirements Planning(U).

On entering the module, a list of the four production run modules is given, along with two other columns to answer yes(Y) or no(N) to ; Do you wish to ren the module? and Do you want the printer on? See figure ₩.1.

For an example, the user may want to run the Product Costing module with the printer on, and the Material Requirements Planning module with the printer on. The table would look like the following:

I - Product Costing	Y	N
P - Date/Proc Order/ Plan Update	Y	N
S - Materials Requirements Planning	Y	N
T - Capacity Requirements Planning	Y	N

The Fl key needs to be pressed to begin the processing.

Since all four processing modules tend to take a long time to execute, this module is designed to allow the user to run any combination of these four, without user intervention. This allows the user to do this at times which are convenient when the computer is used very little (at night for example). The processing can be completed and hard copy outputs generated to look at. A summary of the recommended actions can be viewed in the Summary Action To Do Module(U). Updated cost data can be seen in the Part Inventory/Cost Control module (C). Updated Order Releases and Receipts Scheduled module (R). Updated labor, manhours load profile can be seen in the Station Definition/Load Control(D).

A hard copy of all the parts including cost data may be obtained from the Data Initialization/Sort/Print module(A).

```
┌─────────────────────────────────────────────────────────────────────┐
│        · MANUFACTURING RESOURCE PLANNING DECISION SUPPORT SYSTEM      │
├──────────────────────────────────┬────────────────────────────────────┤
│           RESOURCES              │              CONTROL               │
├──────────────────────────────────┼────────────────────────────────────┤
│  A - DATA INITIAL/SORT/PRINT UTILITY │  I - SHOP ORDERS CONTROL         │
│  B - BILL OF MATERIALS DATA      │  J - SALES ACCOUNTS/CLIENTS CONTROL │
│  C - PART INVENTORIES/COST DATA  │  K - SALES ORDERS CONTROL          │
│  D - STATION AND LOAD DATA       │  L - VENDOR ACCOUNTS CONTROL       │
│  E - EMPLOYEE DATA               │  M - PURCHASE ORDERS CONTROL       │
│  F - MACHINE DATA                │  N - STOREROOM TRANSACTION CONTROL │
│  G - OPERATIONS & PROCESS DATA   │  O - LABOR REPORTING               │
│  H - LDTIME/PRCSS ROUT/ASSY DATA │  P - DATE/ORDERS PROC/HORIZON UPDATE│
├──────────────────────────────────┴────────────────────────────────────┤
│                          P L A N N I N G                              │
├─────────────────────────────────────────────────────────────────────┤
│  Q - MASTER PRODUCTION SCHEDULE         T - MATERIALS REQUIREMENTS PLANNING │
│  R - ORDER RELEASES/RECEIPTS SCHEDULE   U - CAPACITY REQUIREMENTS PLANNING  │
│  S - PRODUCT COSTING                    V - SUMMARY ACTIONS TO-DO           │
│                                         W - COMBINATION PROCESSING MODULE   │
├─────────────────────────────────────────────────────────────────────┤
│  COMMAND:                                                             │
└─────────────────────────────────────────────────────────────────────┘

DATE: 03-12-1984      <ESC KEY-TO DOS>     <F1 - HELP>      <F10 - MAIN MENU>
```

Figure 1: Main Menu

19.75

```
┌──────────────────────────────────────────────────────────────────────┐
│                                                                        │
│  MODULE A - DATA FILES INITIALIZATION/PART NUMBERS SORT/PRINT UTILITY  │
│                                                                        │
├──────────────────────────────────────────────────────────────────────┤
│                                                                        │
│              1 - DATA FILES  INITIALIZATION                            │
│                                                                        │
│              2 - MAJOR SORT BY PART NUMBERS                            │
│              3 - MINOR SORT BY PART NUMBERS                            │
│                                                                        │
│              4 - PRINT LIST OF PARTS BY RECORDS                        │
│              5 - PRINT LIST OF PARTS BY SORT ORDER                     │
│                                                                        │
│              6 - PRINT LIST OF STATIONS BY RECORDS                     │
│                                                                        │
│              7 - CHANGE COMPANY'S NAME                                 │
│                                                                        │
├──────────────────────────────────────────────────────────────────────┤
│                                                                        │
│         ENTER CHOICE:                                                  │
│                                                                        │
└──────────────────────────────────────────────────────────────────────┘

TE: 03-12-1984                              (INI)      (F10 - MAIN MENU)
```

Figure A.1

19.76

```
                    DATA FILES INITIALIZAION

                    BEGIN    ENDIN                              BEGIN    ENDIN
                    RECORD   RECORD                             RECORD   RECORD

ALL ASSOC.ITEM FILES:    1      100    PURCHASE ORDER FILE:        1       50

ALL ASSO.STATION FILES:1        20    SALES ACCOUNTS FILE:         1       50

STOREROOM TRANSN FILE: 1        50    VENDORS ACCOUNTS FILE:       1       50

SALE ORDER FILE:        1       50    OPERATIONS/PROCESS FILE:     1       50

SHOP ORDER FILE:        1       50    MACHINE DATA FILE:           1       50

EMPLOYEE DATA FILE:     1       50    LABOR REPORTING FILE:        1       50


          ENTER BEGINNING AND ENDING RECORD

          ENTER F1 TO BEGIN INITIALIZATION


DATE: 03-12-1984                          (INI)      (F10 - MAIN MENU)
```

Figure A.2

| REC# | ITEM# | DESCRIPTION | | | | | U/MEAS | ONHAND | SAFETY | ALLOC |
	U/COST	M/COST	L/COST	O/COST	S/PRICE	U/COST*ON-HAND		PURC/MADE	
1	ZZZZZZ	CODE NAME: WAGON 1					EA	100.00	25.00	0.00
	35.46	21.12	9.80	4.54	70.00		3545.99	M		
2	MMMMMM	STEERING SUB-ASSEMBLY					EA	100.00	25.00	0.00
	14.78	8.18	4.40	2.20	15.00		1478.00	M		
3	SSSSSS	BODY SCREWS					EA	880.00	50.00	0.00
	0.02	0.02	0.00	0.00	0.02		17.60	P		
4	HNNNNN	HEXAGON NUTS					EA	30.00	25.00	0.00
	0.05	0.05	0.00	0.00	0.05		1.50	P		
5	LWWWWW	LOCK WASHERS					EA	880.00	59.00	0.00
	0.02	0.02	0.00	0.00	0.02		17.60	P		
6	AAAAAA	WAGON BODY					EA	100.00	30.00	0.00
	11.80	7.80	2.67	1.33	11.00		1180.00	M		
7	XXXXXX	REAR AXLE SUB-ASSEMBLY					EA	100.00	25.00	0.00
	7.03	4.42	1.87	0.75	7.25		703.33	M		
8	SHHHHH	SQUARE HOLE WASHER					EA	970.00	100.00	0.00
	0.02	0.02	0.00	0.00	0.02		19.40	P		
9	CPPPPP	COTTER PIN					Ea	0.00	0.00	0.00
	0.04	0.04	0.00	0.00	0.05		0.00	P		
10	EEEEEE	STEERING ARM					EA	50.00	25.00	0.00
	3.00	3.00	0.00	0.00	3.00		150.00	P		
11	DDDDDD	STEERING TURNTABLE					EA	50.00	25.00	0.00
	0.75	0.75	0.00	0.00	0.75		37.50	P		
12	CBBBBB	CARRIAGE BOLT					EA	100.00	25.00	0.00
	0.05	0.05	0.00	0.00	0.05		5.00	P		
13	HHHHHH	HANDLE SAFETY CAP					EA	1000.00	25.00	0.00
	0.05	0.05	0.00	0.00	0.05		50.00	P		
14	BBBBBB	WAGON HANDLE					EA	100.00	25.00	0.00
	2.00	2.00	0.00	0.00	2.00		200.00	P		
15	CCCCCC	WHEELS					EA	940.00	25.00	0.00
	1.00	1.00	0.00	0.00	1.00		940.00	P		
16	CNNNNN	CASTLE NUT					EA	1000.00	25.00	0.00
	0.15	0.15	0.00	0.00	0.15		150.00	P		

19.78

PARTS LISTING BY RECORD NUMBER
DATE: 03-12-1984

| REC# | ITEM# | DESCRIPTION | | | | | U/MEAS | ONHAND | SAFETY | ALLOC |
		U/COST	M/COST	L/COST	O/COST	S/PRICE	U/COST*ON-HAND	PURC/MADE		
17	HCCCCC	WHEEL HUB CAP					EA	940.00	50.00	0.00
		0.01	0.01	0.00	0.00	0.01	9.40	P		
18	MSSSSS	MACHINE SCREW					EA	1000.00	25.00	0.00
		0.05	0.05	0.00	0.00	0.05	50.00	P		
19	ACCCCC	ACORN NUT					EA	100.00	25.00	0.00
		0.03	0.03	0.00	0.00	0.03	3.00	P		
20	SHSSSS	SHEET STEEL STOCK					EA	85.00	25.00	0.00
		7.80	7.80	0.00	0.00	7.80	663.00	P		
21	FFFFFF	REAR AXLE BOLSTER					EA	85.00	24.00	0.00
		1.40	1.40	0.00	0.00	1.40	119.00	P		
22	HUNTIN	REAR AXLE BRACE					EA	70.00	25.00	0.00
		0.50	0.50	0.00	0.00	0.50	35.00	P		

TOTAL DOLLAR INVENTORY: 9375.31

Figure A.3

19.79

```
******************************************************************************
```

REC#	ITEM#	DESCRIPTION					U/MEAS	ONHAND	SAFETY	ALLOC
		U/COST	M/COST	L/COST	O/COST	S/PRICE	U/COST*ON-HAND		PURC/MADE	
6	AAAAAA	WAGON BODY					EA	100.00	30.00	0.00
		11.80	7.80	2.67	1.33	11.00	1180.00		M	
19	ACCCCC	ACORN NUT					EA	100.00	25.00	0.00
		0.03	0.03	0.00	0.00	0.03	3.00		P	
14	BBBBBB	WAGON HANDLE					EA	100.00	25.00	0.00
		2.00	2.00	0.00	0.00	2.00	200.00		P	
12	CBBBBB	CARRIAGE BOLT					EA	100.00	25.00	0.00
		0.05	0.05	0.00	0.00	0.05	5.00		P	
15	CCCCCC	WHEELS					EA	940.00	25.00	0.00
		1.00	1.00	0.00	0.00	1.00	940.00		P	
16	CNNNNN	CASTLE NUT					EA	1000.00	25.00	0.00
		0.15	0.15	0.00	0.00	0.15	150.00		P	
9	CPPPPP	COTTER PIN					Ea	0.00	0.00	0.00
		0.04	0.04	0.00	0.00	0.05	0.00		P	
11	DDDDDD	STEERING TURNTABLE					EA	50.00	25.00	0.00
		0.75	0.75	0.00	0.00	0.75	37.50		P	
10	EEEEEE	STEERING ARM					EA	50.00	25.00	0.00
		3.00	3.00	0.00	0.00	3.00	150.00		P	
21	FFFFFF	REAR AXLE BOLSTER					EA	85.00	24.00	0.00
		1.40	1.40	0.00	0.00	1.40	119.00		P	
17	HCCCCC	WHEEL HUB CAP					EA	940.00	50.00	0.00
		0.01	0.01	0.00	0.00	0.01	9.40		P	
13	HHHHHH	HANDLE SAFETY CAP					EA	1000.00	25.00	0.00
		0.05	0.05	0.00	0.00	0.05	50.00		P	
4	HNNNNN	HEXAGON NUTS					EA	30.00	25.00	0.00
		0.05	0.05	0.00	0.00	0.05	1.50		P	
22	HUNTIN	REAR AXLE BRACE					EA	70.00	25.00	0.00
		0.50	0.50	0.00	0.00	0.50	35.00		P	
5	LWWWWW	LOCK WASHERS					EA	880.00	59.00	0.00
		0.02	0.02	0.00	0.00	0.02	17.60		P	
2	MMMMMM	STEERING SUB-ASSEMBLY					EA	100.00	25.00	0.00
		14.78	8.18	4.40	2.20	15.00	1478.00		M	

19.80

REC#	ITEM#	DESCRIPTION				U/MEAS	ONHAND	SAFETY	ALLOC
		U/COST	M/COST	L/COST	O/COST	S/PRICE	U/COST#ON-HAND	PURC/MADE	
18	MSSSSS	MACHINE SCREW					EA	1000.00	25.00	0.00
		0.05	0.05	0.00	0.00	0.05		50.00	P	
8	SHHHHH	SQUARE HOLE WASHER					EA	970.00	100.00	0.00
		0.02	0.02	0.00	0.00	0.02		19.40	P	
20	SHSSSS	SHEET STEEL STOCK					EA	85.00	25.00	0.00
		7.80	7.80	0.00	0.00	7.80		663.00	P	
3	SSSSSS	BODY SCREWS					EA	880.00	50.00	0.00
		0.02	0.02	0.00	0.00	0.02		17.60	P	
7	XXXXXX	REAR AXLE SUB-ASSEMBLY					EA	100.00	25.00	0.00
		7.03	4.42	1.87	0.75	7.25		703.33	M	
1	ZZZZZZ	CODE NAME: WAGON 1					EA	100.00	25.00	0.00
		35.46	21.12	9.80	4.54	70.00		3545.99	M	

TOTAL DOLLAR INVENTORY: 9375.31

Figure A.4

```
*************************************************************************************
ABC COMPANY, TIMBER. TIMBUKTU 12345
MODULE A - 'INITIALIZATION/PRINT/SORT UTILITY
STATION LISTING BY RECORD NUMBER
DATE: 03-12-1984                                              PAGE #:   1

REC#   STAT#   DESCRIPTION              M-HRS SHIFT1 SHIFT2 SHIFT3
       $/M-HR   SHIFT1    SHIFT2    SHIFT3 OVERHEAD-PERCENT

   1   000001 STEEL STOCK FORMING STATION        100      50     30
               8.00     10.00    15.00     50.00

   2   000002 STEERING ASSEMBLY STATION          400     100    100
               8.00     12.00    15.00     50.00

   3   000003 AXLE ASSEMBLY STATION               40       0      0
               8.00      0.00     0.00     40.00

   4   000004 FINAL PRODUCT PACKAGING             40       0      0
               8.00      0.00     0.00     30.00
```

Figure A.5

```
                   MODULE B - BILL OF MATERIALS

PART NUMBER:      MMMMMM      DESCRIPTION:    STEERING SUB-ASSEMBLY
LO-LEVEL CODE:      1         TYPE: COMPONENT ITEM      RECORD NUMBER:   2

PARTS PARENTS       1        2        3        4        5        6        7
PARENT NUMBER    ZZZZZZ
USAGE RATE        8.00

PARTS CHILDREN      1        2        3        4        5        6        7
CHILD NUMBER ·   SHHHHH   EEEEEE   DDDDDD   CBBBBB   HHHHHH   BBBBBB   CCCCCC
USAGE RATE        2.00     1.00     1.00     1.00     1.00     1.00     2.00

A-CHANGE PARTS DEFINITION    M-MOVE ON TO ANOTHER ITEM    E-LIST PARTS CHILDREN
B-CHANGE PARTS PARENTS       CURSOR L-LAST CHILD/PARENT    F-LIST PARTS PARENTS
C-CHANGE PARTS CHILDREN      CURSOR R-NEXT CHILD/PARENT    G-BEGIN# CH/PA DISPLAY
D-DELETE PART                CURSOR U-LAST RECORD          H-COMPLETE EXPLOSION
                             CURSOR D-NEXT RECORD          I-COMPLETE IMPLOSION

ENTER CHOICE:
```

DATE: 03-12-1984   (BOM)   (F10 - MAIN MENU)

Figure B.1

19.83

IF EXCEED MAXIMUM NUMBER OF CHILDREN:

BEFORE:

```
       P1    P2    P3     ............................. Parents
         !____!____!____!____!____!
                  AAAA
     !--------------!--------------------!
       C1    C2    C3     ....C49   XXXX(50) YYYY(#51).  Children
```

AFTER:

```
       P1    P2    P3     ............................. Parents
         !____!____!____!____!____!
                  AAAA
       !--------------!--------------!
       AAAA* YYYY C52   C53     ...................... Children
   !------!--------------------!
   C1   C2    C3    C4    ........ XXXX(50) ........... Grandchildren
```

IF EXCEED MAXIMUM NUMBER OF PARENTS:

BEFORE:

```
       P1  P2  P3    .....  P50 P51 ................. Parents
         !___!___!___!___!___!___!___!___!
                  AAAA
     !--------------!--------------------!
       C1   C2   C3   C4    .......................... Children
```

AFTER:

```
       P1    P2    P3    .... P50 ..................... Grandparents
         !____!____!____!____!
             AAAA* P51   P52     ...................... Parents
               !____!____!____!____!
                  AAAA
       !--------------!--------------!
       C1   C2   C3   C4    .......................... Children
```

Figure B.2

```
****************************************************************************************
ABC COMPANY, TIMBER, TIMBUKTU 12345
MODULE B - BILL OF MATERIALS DATA
CHILDRENS PART LISTING - SINGLE LEVEL
DATE: 03-12-1984                                                 PAGE #:  1


ITEM MMMMMM   STEERING SUB-ASSEMBLY
BATCH SIZE:  1

PART#     DESCRIPTION                          USAGE       U/M   P/M
SHHHHH    SQUARE HOLE WASHER                  2.00000      EA     P
EEEEEE    STEERING ARM                        1.00000      EA     P
DDDDDD    STEERING TURNTABLE                  1.00000      EA     P
CBBBBB    CARRIAGE BOLT                       1.00000      EA     P
HHHHHH    HANDLE SAFETY CAP                   1.00000      EA     P
BBBBBB    WAGON HANDLE                        1.00000      EA     P
CCCCCC    WHEELS                              2.00000      EA     P
CNNNNN    CASTLE NUT                          1.00000      EA     P
HCCCCC    WHEEL HUB CAP                       2.00000      EA     P
MSSSSS    MACHINE SCREW                       1.00000      EA     P
ACCCCC    ACORN NUT                           1.00000      EA     P
CPPPPP    COTTER PIN                          1.00000      Ea     P
```

Figure B.3

19.85

```
****************************************************************************************
ABC COMPANY, TIMBER, TIMBUKTU 12345
MODULE B - BILL OF MATERIALS DATA
INDENTED BILL OF MATERIALS LISTING - MULTIPLE LEVELS
DATE: 03-12-1984                                              PAGE #:   1


EXPLOSION OF PART # ZZZZZZ   CODE NAME: WAGON 1
BATCH SIZE:   1

PART #                      DESCRIPTION                    USAGE      U/MEASURE
ZZZZZZ                      CODE NAME: WAGON 1             1.00000        EA
 SSSSSS                     BODY SCREWS                   8.00000        EA
 MMMMMM                     STEERING SUB-ASSEMBLY         8.00000        EA
  SHHHHH                    SQUARE HOLE WASHER            2.00000        EA
  EEEEEE                    STEERING ARM                  1.00000        EA
  DDDDDD                    STEERING TURNTABLE            1.00000        EA
  CBBBBB                    CARRIAGE BOLT                 1.00000        EA
  HHHHHH                    HANDLE SAFETY CAP             1.00000        EA
  BBBBBB        .           WAGON HANDLE                  1.00000        EA
  CCCCCC                    WHEELS                        2.00000        EA
  CNNNNN                    CASTLE NUT                    1.00000        EA
  HCCCCC                    WHEEL HUB CAP                 2.00000        EA
  MSSSSS                    MACHINE SCREW                 1.00000        EA
  ACCCCC                    ACORN NUT                     1.00000        EA
  CPPPPP                    COTTER PIN                    1.00000        EA
 LWWWWW                     LOCK WASHERS                  8.00000        EA
 AAAAAA                     WAGON BODY                    1.00000        EA
  SHSSSS                    SHEET STEEL STOCK             1.00000        EA
 XXXXXX                     REAR AXLE SUB-ASSEMBLY        1.00000        EA
  FFFFFF                    REAR AXLE BOLSTER             1.00000        EA
  HUNTIN                    REAR AXLE BRACE               2.00000        EA
  CCCCCC                    WHEELS                        2.00000        EA
  HCCCCC                    WHEEL HUB CAP                 2.00000        EA
 SHHHHH                     SQUARE HOLE WASHER            2.00000        EA
```

Figure B.4

19.86

```
**************************************************************************
ABC COMPANY, TIMBER, TIMBUKTU 12345
MODULE B -, BILL OF MATERIALS DATA
PARENTS PART LISTING - SINGLE LEVEL
DATE: 03-12-1984                                          PAGE #:   1


ITEM CCCCCC   WHEELS

PART#   DESCRIPTION                         USAGE      U/M    P/M
MMMMMM   STEERING SUB-ASSEMBLY              2.00000     EA     M
XXXXXX   REAR AXLE SUB-ASSEMBLY             2.00000     EA     M
```

Figure B.5

```
****************************************************************************
ABC COMPANY, TIMBER, TIMBUKTU 12345
MODULE B - BILL OF MATERIALS DATA
IMPLOSION OF PART LISTING - MULTIPLE LEVELS
DATE: 03-12-1984                                          PAGE *:   1


IMPLOSION OF PART # CCCCCC   WHEELS

PART #                  DESCRIPTION                        USAGE     U/MEASURE
CCCCCC                  WHEELS                             1.00000      EA
 MMMMMM                 STEERING SUB-ASSEMBLY              2.00000      EA
  ZZZZZZ                CODE NAME: WAGON 1                 8.00000      EA
 XXXXXX                 REAR AXLE SUB-ASSEMBLY             2.00000      EA
  ZZZZZZ                CODE NAME: WAGON 1                 1.00000      EA
```

Figure B.6

```
              MODULE C - PART INVENTORY/COST DATA

PART NUMBER:  ZZZZZZ       DESCRIPTION:   CODE NAME: WAGON 1
LO LEVEL CODE:   O         TYPE: END PART              RECORD NUMBER:  1

  PURCHASED(P) OR MADE(M)         M        LOT SIZE METHOD: LOT FOR LOT

  UNIT COST                 $  55.93      STORAGE LOCATION CODE

  MATERIAL COST             $  37.04      UNITS ON HAND               100.00
  LABOR COST                $  10.72      UNITS OF SAFETY STOCK        25.00
  OVERHEAD COST             $   8.17      UNITS ALLOCATED FOR           0.00

  SET-UP COST/BATCH         $   0.10      UNIT OF MEASURE                .EA

  SUGGESTED LIST PRICE      $ 100.00

L-CHANGE LOT SIZE METHOD   CURSOR UP-LAST RECORD      M-MOVE ON TO ANOTHER PART
C-CHANGE INVENTORY DATA    CURSOR DOWN-NEXT RECORD    P-JOB QUOTATION

ENTER CHOICE:
```

DATE: 03-12-1984   (INV)   (F10 - MAIN MENU)

Figure C.1

```
            LOT SIZE METHODS

     1 - FIXED ORDER QUANTITY
     2 - ECONOMIC ORDER QUANTITY
     3 - LOT FOR LOT*
     4 - FIXED PERIOD ORDERING
     5 - LEAST UNIT COST
     6 - LEAST TOTAL COST
     7 - PART PERIOD BALANCING
     8 - WAGNER WHITIN METHOD



   * - CURRENT METHOD

   LOT SIZE METHOD:


DATE: 03-12-1984                          <INV>    <F10 - MAIN MENU>
```

Figure C.2

```
JOB QUOTATION FOR THE MANUFACTURE OF PART NUMBER: ZZZZZZ
               CODE NAME: WAGON 1


          ENTER BATCH SIZE:   1

          LEAD TIME IN DAYS:   8

          COMPANY'S NAME: ABC COMPANY OF NEW YORK

          PRICE MARK-UP % OF COST:   10

          DO YOU WANT PRINTER ON (Y/N)?: N



DATE: 03-12-1984                          (INV)      (F10 - MAIN MENU)
```

Figure C.3

19.91

B QUOTATION FOR: ABC COMPANY OF NEW YORK
TE: 03-12-1984

E MANUFACTURE OF 1 EA ZZZZZZ CODE NAME: WAGON 1

E COST OF MANUFACTURE AS FOLLOWS:
E COST OF MATERIALS: $ 20.76
E COST OF LABOR: $ 9.80
E COST OF OVERHEADS: $ 4.54
E COST OF SETUPS: $ 0.53
E COST OF MARKUP: $ 3.56

E PRICE OF JOB $ 39.19

IT PRICE: $ 39.19

LIVERY DATE: 03-20-84

TE: 03-12-1984   ENTER ANY KEY...   (INV)   (F10 - MAIN MENU)

Figure C.4

19.92

```
                    MODULE D - STATION AND LOAD DATA

STATION CODE:  000001       DESCRIPTION:   STEEL STOCK FORMING STATION
AVAIL.M-H IN SHIFT 1/2/3 PER WEEK:     40  /   20  /    0  RECORD NUMBER:  1
LABOR COST-SHIFT 1/2/3 PER M-H:    $ 8.00 /$10.00 /$ 0.00  O-H PERCENT: 50.0


WEEK BEGINNING DATE     03/12    03/19    03/26    04/02    04/09    04/16    04/23
PLANNED  LOAD IN M-H       30       20       25       10        5        5        5
RELEASED LOAD IN M-H       15       10        5        0        0        0        0
TOTAL LOAD IN M-H          45       30       30       10        5        5        5
LABOR COST IN $        370.00   240.00   240.00    80.00    40.00    40.00    40.00
OVERHEAD COST IN $     185.00   120.00   120.00    40.00    20.00    20.00    20.00
TOTAL COST IN $        555.00   360.00   360.00   120.00    60.00    60.00    60.00


A-CHANGE STATION DEFINITION  D-DELETE STATION              CURSOR LEFT-LAST WEEK
B-CHANGE PLANNED LOADS       M-MOVE TO ANOTHER STATION      CURSOR RIGHT-NEXT WEEK
C-CHANGE RELEASED LOADS      G-GRAPHICS DISPLAY             CURSOR UP-LAST RECORD
W-STARTING WEEK DISPLAY      P-PRINT LIST                   CURSOR DOWN-NEXT RECOR

ENTER CHOICE:
```

DATE: 03-12-1984   <STA>   <F10 - MAIN MENU>

Figure D.1

19.93
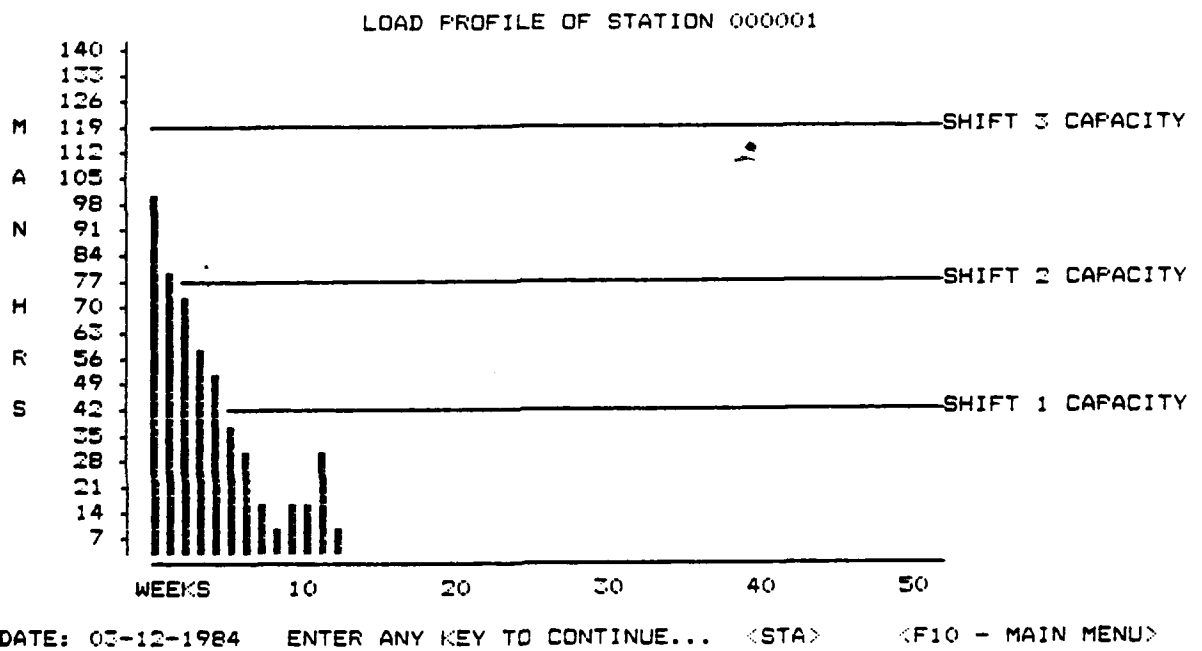
Figure D.2

```
••••••••••••••••••••••••••••••••••••••••••••••••••••••••••••••••••••••••••••••••••
ABC MANUFACTURING COMPANY. TIMBER. TIMBUKTU 12345
MODULE D - STATION AND LOAD DATA
STATION LOAD SCHEDULE LISTING
DATE: 01-01-1980                                              PAGE #:  1
STATION: 000001  STEEL STOCK FORMING STATION

STATION CAPACITY IN M-HRS SHIFT 1/2/3:  40  /  20  /  30
TOTAL STATION.CAPACITY:  90
```

WEEK	M-HRS-PLANNED	RELEASED	M-HRS-TOTAL	$M-HRS-TOTAL	$OVERHEADS	$TOTAL
01/01	25	15	40	320.00	160.00	480.00
01/08	30	10	40	320.00	160.00	480.00
01/15	35	5	40	320.00	160.00	480.00
01/22	40	0	40	320.00	160.00	480.00
01/29	45	0	45	370.00	185.00	555.00
02/05	50	0	50	420.00	210.00	630.00
02/12	55	0	55	470.00	235.00	705.00
02/19	0	0	0	0.00	0.00	0.00
02/26	0	0	0	0.00	0.00	0.00
03/05	0	0	0	0.00	0.00	0.00
03/12	0	0	0	0.00	0.00	0.00
03/19	0	0	0	0.00	0.00	0.00
03/26	0	0	0	0.00	0.00	0.00
04/02	0	0	0	0.00	0.00	0.00
04/09	0	0	0	0.00	0.00	0.00
04/16	0	0	0	0.00	0.00	0.00
04/23	0	0	0	0.00	0.00	0.00
04/30	0	0	0	0.00	0.00	0.00
05/07	0	0	0	0.00	0.00	0.00
05/14	0	0	0	0.00	0.00	0.00
05/21	0	0	0	0.00	0.00	0.00
05/28	0	0	0	0.00	0.00	0.00
06/04	0	0	0	0.00	0.00	0.00
06/11	0	0	0	0.00	0.00	0.00
06/18	0	0	0	0.00	0.00	0.00
06/25	0	0	0	0.00	0.00	0.00
07/02	0	0	0	0.00	0.00	0.00
07/09	0	0	0	0.00	0.00	0.00
07/16	0	0	0	0.00	0.00	0.00
07/23	0	0	0	0.00	0.00	0.00
07/30	0	0	0	0.00	0.00	0.00
08/06	0	0	0	0.00	0.00	0.00
08/13	0	0	0	0.00	0.00	0.00
08/20	0	0	0	0.00	0.00	0.00
08/27	0	0	0	0.00	0.00	0.00

19.95

STATION LOAD SCHEDULE LISTING
DATE: 01-01-1980   PAGE #: 2

WEEK	M-HRS-PLANNED	RELEASED	M-HRS-TOTAL	$M-HRS-TOTAL	$OVERHEADS	$TOTAL
09/03	0	0	0	0.00	0.00	0.00
09/10	0	0	0	0.00	0.00	0.00
09/17	0	0	0	0.00	0.00	0.00
09/24	0	0	0	0.00	0.00	0.00
10/01	0	0	0	0.00	0.00	0.00
10/08	0	0	0	0.00	0.00	0.00
10/15	0	0	0	0.00	0.00	0.00
10/22	0	0	0	0.00	0.00	0.00
10/29	0	0	0	0.00	0.00	0.00
11/05	0	0	0	0.00	0.00	0.00
11/12	0	0	0	0.00	0.00	0.00
11/19	0	0	0	0.00	0.00	0.00
11/26	0	0	0	0.00	0.00	0.00
12/03	0	0	0	0.00	0.00	0.00
12/10	0	0	0	0.00	0.00	0.00
12/17	0	0	0	0.00	0.00	0.00
12/24	0	0	0	0.00	0.00	0.00

TOTAL M-HRS: 310
TOTAL $M-HRS: 2540
TOTAL $OVERHEADS: 1270
TOTAL $$$: 3810

Figure D.3

19.96

```
                    MODULE E - EMPLOYEES DATA


      1 - TO OPEN NEW EMPLOYEE RECORD

      2 - TO LIST CHRONOLOGY OF EMPLOYEE RECORDS

      3 - TO LIST BY STATE OF RESIDENCE

      4 - TO EDIT/CLOSE/VIEW INDIVIDUAL RECORD

      5 - TO RETURN TO LAST RECORD



      ENTER EDIT CHOICE:
```

DATE: 03-12-1984   <EMP>   <F10 - MAIN MENU>

Figure E.1

```
                    MODULE E - EMPLOYEE DATA
 ┌─────────────────────────────────────────────────────────────────┐
 │ EMPLOYEE NUMBER:000001           DATE OPENED: 03/06/84            │
 │                                                                   │
 │ EMPLOYEE NAME:OLIVIA JONES                                        │
 │                                                                   │
 │ ADDRESS STREET #:2201 3 ST. SO.    CITY: SYDNEY                   │
 │                                                                   │
 │ STATE:AU     ZIP CODE:             TELEPHONE #: 234-9987          │
 │                                                                   │
 │ JOB DESCRIP:PRESS OPERATOR                 AGE: 37    SEX(M/F): F │
 │                                                                   │
 │ HOURLY RATE:$   8.00               HOURS PER WEEK:    40.00       │
 │                                                                   │
 │ COMMENTS: TWO OF A KIND                        RECORD NUMBER:  1  │
 ├─────────────────────────────────────────────────────────────────┤
 │ C-TO CHANGE DATA          R-RETURN TO USERS MENU   CURSOR UP-LAST RECORD │
 │ M-MOVE TO ANOTHER ACCOUNT  D-DELETE RECORD         CURSOR DOWN-NEXT RECORD │
 ├─────────────────────────────────────────────────────────────────┤
 │ ENTER CHOICE:                                                     │
 └─────────────────────────────────────────────────────────────────┘
```

DATE: 03-12-1984   <EMP>   <F10 - MAIN MENU>

Figure E.2

19.98

```
┌─────────────────────────────────────────────────────────────────┐
│                    MODULE F - MACHINES DATA                       │
├─────────────────────────────────────────────────────────────────┤
│ MACHINE   NUMBER:    000001           DATE OPENED: 03/06/84       │
│                                                                   │
│ MACHINE    DESCRIPTION: 100-TON DIE PRESS                         │
│                                                                   │
│ OPERATOR NUMBER:000001                                            │
│                                                                   │
│ OPERATOR'S NAME: OLIVIA JONES                                     │
│                                                                   │
│ STATION NUMBER: 000001                                            │
│                                                                   │
│ STATION DESCRIPTION: STEEL STOCK FORMING STATION                  │
│                                                                   │
│ COMMENTS: WATCH YOUR FINGERS!!!!            RECORD NUMBER:   1     │
├─────────────────────────────────────────────────────────────────┤
│ C-TO CHANGE DATA           R-RETURN TO USER'S MENU   CURSOR UP-LAST RECORD │
│ M-MOVE TO ANOTHER RECORD   D-DELETE RECORD           CURSOR DOWN-NEXT RECORD │
├─────────────────────────────────────────────────────────────────┤
│ ENTER CHOICE:                                                     │
│                                                                   │
└─────────────────────────────────────────────────────────────────┘
```

DATE: 03-12-1984   <MAC>   <F10 - MAIN MENU>

Figure F.2

19.99

```
********************************************************************************

MODULE F - MACHINES DATA
MACHINE LISTING BY RECORDS                              PAGE #:   1
DATE: 01-01-1980

REC#  M/C#    DATE-OPEN   DESCRIPTION                        EMPLY#
      NAME                             STAT#  STAT-DESCRIPTION


  1   000001 03/06/84    100-TON DIE PRESS                   000001
      OLIVIA JONES                     000001 STEEL STOCK FORMING STATION
      WATCH YOUR FINGERS!!!!

  2   000002 03/06/84    AIR INPACT WRENCH                   000002
      JOHN TRAVAOLA                    000002 STEERING ASSEMBLY STATION
      AIR POWERED ASSEMBLER WRENCH

  3   000003 03/06/84    AIR IMPACT WRENCH                   000003
      DANIEL FETTIG                    000003 AXLE ASSEMBLY STATION
      AIR POWERED ASSEMBLER WRENCH

  4   000004 03/06/84    MECHANICAL PRODUCT PACKAGER    000004
      STEVE DEAN                       000004 FINAL PRODUCT PACKAGING
      PACKAGER .
```

Figure F.3

19.100

```
          MODULE G - OPERATIONS AND PROCESS DATA


     1 - TO OPEN NEW PROC/OPER RECORD

     2 - TO LIST CHRONOLOGY OF RECORDS

     3 - TO LIST BY PROC/OPER NUMBER

     4 - TO LIST BY MACHINE NUMBER

     5 - TO LIST BY STATION NUMBER

     6 - TO EDIT/CLOSE/VIEW INDIVIDUAL ORDER

     7 - TO RETURN TO LAST RECORD


     ENTER EDIT CHOICE:

DATE: 03-12-1984                          <OPE>     <F10 - MAIN MENU>
```

Figure G.1

19.101

```
 _____
|           MODULE G - OPERATIONS AND PROCESS DATA              |
|_____|
| PROC/OPER  NUMBER: 000001        DATE OPENED: 03/06/84         |
|                                                                |
| PROC/OPER DESCRIPTION: STEEL STOCK FORMING                     |
|                                                                |
| MACHINE NUMBER: 000001                                         |
|                                                                |
| MACHIN DESCRIPTION: 100-TON DIE PRESS                          |
|                                                                |
| STATION NUMBER: 000001                                         |
|                                                                |
| STATION DESCRIPTION: STEEL STOCK FORMING STATION               |
|                                                                |
| COMMENTS: WATCH YOUR FINGERS!!!!          RECORD NUMBER:   1    |
|_____|
| C-TO CHANGE DATA        R-RETURN TO USER'S MENU  CURSOR UP-LAST RECORD  |
| M-MOVE TO ANOTHER ORDER  D-DELETE RECORD   CURSOR DOWN-NEXT RECORD|
|_____|
| ENTER CHOICE:                                                  |
|_____|
```

DATE: 03-12-1984   <OPE>   <F10 - MAIN MENU>

Figure G.2

```
*************************************************************************

MODULE G - OPERATIONS AND PROCESS DATA
OPERATIONS AND PROCESS LISTING BY RECORDS
DATE: 01-01-1980                                              PAGE #:   1

REC#   OPER#   DATE-OPEN   DESCRIPTION
       M/C#    M/C-DESCRIPTION
       STA#    STATION-DESCRIPTION
       COMMENTS

   1   000001 03/06/84 STEEL STOCK FORMING
       000001 100-TON DIE PRESS
       000001 STEEL STOCK FORMING STATION
       WATCH YOUR FINGERS!!!!

   2   000002 03/06/84 STEERING ASSEMBLY STATION
       000002 AIR INPACT WRENCH
       000002 STEERING ASSEMBLY STATION
       PNEUMATICS IN ACTION!!!

   3   000003 03/06/84 REAR AXLE ASSEMBLY
       000003 AIR IMPACT WRENCH
       000003 AXLE ASSEMBLY STATION
       PNEUMATICS

   4   000004 03/06/84 PRODUCT PACKAGING
       000004 MECHANICAL PRODUCT PACKAGER
       000004 FINAL PRODUCT PACKAGING
       PROCESS USES CARDBOARD
```

Figure G.3

19.103

```
┌─────────────────────────────────────────────────────────────────────┐
│        MODULE H - LEAD TIME / PROCESS ROUTING / ASSEMBLY DATA         │
├─────────────────────────────────────────────────────────────────────┤
│ PART NUMBER:  ZZZZZZ      DESCRIPTION:   CODE NAME: WAGON 1            │
│ LO-LEVEL CODE:    0       TYPE: END ITEM            RECORD NUMBER:  1  │
├─────────────────────────────────────────────────────────────────────┤
│ WORK STATION SEQUENCE          1          2        3        4        5 │
│ WORK STATION NUMBER         000004                                     │
│ MACHINE NUMBER              000004                                     │
│ OPERATION NUMBER            000004                                     │
│ UNIT OPER. TIME(HRS)          0.108                                    │
│ BATCH SETUP/TEAR TIME         0.016                                    │
│ BATCH TRANSPORT TIME          0.016                                    │
│ BATCH QUE TIME B/AFTER        0.000                                    │
│                                                                        │
│ BATCH SIZE:    50            LEAD TIME IN HOURS      40                 │
├─────────────────────────────────────────────────────────────────────┤
│ A-CHANGE L-TIME COMPONENTS  M-MOVE TO ANOTHER ITEM    CURSOR UP-LAST RECORD   │
│ B-CHANGE BATCH SIZE         CURSOR LEFT-LAST STATION  CURSOR DOWN-NEXT RECORD │
│ R-REORDER SEQUENCE          CURSOR RIGHT-NEXT STATION P-PRINT ROUTE SHEET     │
├─────────────────────────────────────────────────────────────────────┤
│ ENTER CHOICE:                                                          │
└─────────────────────────────────────────────────────────────────────┘
```

DATE: 03-12-1984   <LTR>   <F10 - MAIN MENU>

Figure H.1

19.104

```
*********************************************************************

MODULE E - EMPLOYEES DATA
EMPLOYEE LISTING BY RECORDS
DATE: 01-01-1980                                    PAGE #:   1

REC#  EMPLY# NAME                          STREET          CITY    STATE
      JOB DESCRIPTION                TELE#        AGE   SEX
      COMMENTS                       HR-RATE  HOURS

   1  000001 OLIVIA JONES              2201 3 ST. SO.      SYDNEY   AU
      PRESS OPERATOR               234-9987        37    F
      TWO OF A KIND                8.00  40.00

   2  000002 JOHN TRAVADLA              23 ST NO.          L.A.     CA
      STEERING ASSEMBLER           234-9987        32    M
      LET'S RODEO !!               8.00  40.00

   3  000003 DANIEL FETTIG             1445 9ST. SO.       FGO.     ND
      REAR AXLE ASSEMBLER          232-0317        22    M
      PNEUMATIC LAUGH INC.         8.00  40.00

   4  000004 STEVE DEAN               8805 NO. HAPSIRE RD.JAMAICA   HW
      FINAL PRODUCT PACKAGING      234-5534        33    M
      PACKAGER DOES MOST OF THE WORK.  8.00  40.00
```

Figure E.3

19.105

```
                    MODULE F - MACHINES DATA

        1 - TO OPEN NEW MACHINE RECORD

        2 - TO LIST CHRONOLOGY OF RECORDS

        3 - TO LIST BY MACHINE NUMBER

        4 - TO LIST BY OPERATOR NUMBER

        5 - TO LIST BY STATION NUMBER

        6 - TO EDIT/CLOSE/VIEW INDIVIDUAL RECORD

        7 - TO RETURN TO LAST ORDER


        ENTER EDIT CHOICE:
```

DATE: 03-12-1984   <MAC>   <F10 - MAIN MENU>

Figure F.1

19.106

```
*********************************************************************************

MODULE H - LEAD TIME/PROCESS ROUTING/ASSEMBLY DATA
ROUTE/OPERATIONS/ASSEMBLY SHEET
DATE: 01-01-1980                                                    PAGE #:   1

***ITEM NUMBER: ZZZZZZ CODE NAME: WAGON 1

SEQUENCE OP-CODE OPERATION DESCRIPTION
         MC-CODE MACHINE DESCRIPTION
         ST-CODE STATION DESCRIPTION
         UNIT OP-TIME    S/U-TIME    TRANSPORT-TIME    QUEUE-TIME
         (HRS)           (HRS)       (HRS)             (HRS)

   1     000004 PRODUCT PACKAGING
         000004 MECHANICAL PRODUCT PACKAGER
         000004 FINAL PRODUCT PACKAGING
            0.11          0.02          0.02            0.00
```

Figure H.2

```
┌─────────────────────────────────────────────────────────────┐
│              MODULE I - SHOP ORDERS CONTROL                   │
├─────────────────────────────────────────────────────────────┤
│                                                               │
│        1 - TO OPEN NEW SHOP ORDER                             │
│                                                               │
│        2 - TO LIST CHRONOLOGY OF SHOP ORDERS                  │
│                                                               │
│        3 - TO LIST BY CURRENT STATION NUMBER                  │
│                                                               │
│        4 - TO LIST BY ITEM NUMBER                             │
│                                                               │
│        5 - TO EDIT/CLOSE/VIEW INDIVIDUAL ORDER                │
│                                                               │
│        6 - TO RETURN TO LAST ORDER                            │
│                                                               │
│        S - TO STORE AWAY OLD ORDERS TO FILE                   │
│                                                               │
│        R - TO RESTORE OLD ORDERS FROM FILE                    │
│                                                               │
├─────────────────────────────────────────────────────────────┤
│        ENTER EDIT CHOICE:                                     │
└─────────────────────────────────────────────────────────────┘
```

DATE: 03-12-1984   <SHO>   <F10 - MAIN MENU>

Figure I.1

19.108

```
                MODULE I - SHOP ORDERS CONTROL

SHOP ORDER NUM:000001 DATE OPENED:PROMED:CLOSED: 03/06/84 : 03/12/84 :

PART NUMBER:ZZZZZZ  PART DESCRIPTION: CODE NAME: WAGON 1

NUMBER OF UNITS:  100.00

CURRENT STATION NUMBER:    000004

CURRENT STATION DESCRIPTION:FINAL PRODUCT PACKAGING

COMMENTS:                                         RECORD NUMBER:  1

C-CHANGE DATA              R-RETURN TO USER'S MENU    CURSOR UP-LAST ORDER
M-MOVE TO ANOTHER ORDER                              CURSOR DOWN-NEXT ORDER

ENTER CHOICE:
```

DATE: 03-12-1984   <SHO>   <F10 - MAIN MENU>

Figure I.2

19.109

```
************************************************************************

MODULE I - SHOP ORDERS CONTROL
SHOP ORDERS LISTING BY RECORDS .
DATE: 03-12-1984                                      PAGE #:   1

REC# SHOP-O# DATE-OPEN PROMISED CLOSED   ITEM# ITEM-DESCRIPTION
     *OF-UNITS CURRENT-STATION#-DESCRIPTION
     COMMENTS '

   1 000001  03-06-84 03-13-84            ZZZZZZ CODE NAME: WAGON 1
      100.00    000004 FINAL PRODUCT PACKAGING


   2 000002  03/06/84 03/13/84            ZZZZZZ CODE NAME: WAGON 1
      100.00    000004 FINAL PRODUCT PACKAGING


   3 000003  03/06/84 03/20/84            ZZZZZZ CODE NAME: WAGON 1
      100.00    000004 FINAL PRODUCT PACKAGING


   4 000004  03/06/84 03/13/84            MMMMMM STEERING SUB-ASSEMBLY
      100.00    000002 STEERING ASSEMBLY STATION


   5 000005  03/06/84 03/13/84            AAAAAA WAGON BODY
      100.00    000001 STEEL STOCK FORMING STATION
```

Figure I.3

```
┌──────────────────────────────────────────────────────────────┐
│                                                                │
│          MODULE J - SALES ACCOUNTS / CLIENTS CONTROL           │
│                                                                │
├──────────────────────────────────────────────────────────────┤
│                                                                │
│                                                                │
│      1 - TO OPEN NEW SALE ACCOUNT OR CLIENT                    │
│                                                                │
│      2 - TO LIST CHRONOLOGY OF SALE ACCOUNTS                   │
│                                                                │
│      3 - TO LIST BY STATE                                      │
│                                                                │
│      4 - TO EDIT/CLOSE/VIEW INDIVIDUAL ACCOUNT                 │
│                                                                │
│      5 - TO RETURN TO LAST ACCOUNT                             │
│                                                                │
│                                                                │
├──────────────────────────────────────────────────────────────┤
│                                                                │
│      ENTER EDIT CHOICE:                                        │
│                                                                │
│                                                                │
└──────────────────────────────────────────────────────────────┘

DATE: 03-12-1984                          <CLI>    <F10 - MAIN MENU>
```

Figure J.1

```
╔══════════════════════════════════════════════════════════════╗
║         MODULE J - SALES ACCOUNTS / CLIENTS CONTROL            ║
╟──────────────────────────────────────────────────────────────╢
║ SALE OR CLIENT ACCOUNT NUMBER:000001   DATE OPENED: 03/06/84   ║
║                                                                ║
║ CLIENT ACCOUNT DESCRIPTION:SELL'S  HARDWARE IN FGO.            ║
║                                                                ║
║ ADDRESS STREET # :2201 SO UNIV. DR.        CITY: FGO.          ║
║                                                                ║
║ STATE: ND                   ZIP CODE: 58103                   ║
║                                                                ║
║ CONTACT PERSON: J.T.                TELEPHONE #: 232-8903      ║
║                                                                ║
║ COMMENTS:  APPLE DAY                       RECORD NUMBER:  1   ║
╟──────────────────────────────────────────────────────────────╢
║   C - TO CHANGE DATA               CURSOR UP - LAST RECORD     ║
║   M - MOVE ON TO ANOTHER ACCOUNT   CURSOR DOWN - NEXT RECORD   ║
║   R - RETURN TO USER'S MENU                                    ║
╟──────────────────────────────────────────────────────────────╢
║ ENTER CHOICE:                                                  ║
╚══════════════════════════════════════════════════════════════╝
```

DATE: 03-12-1984   <CLI>   <F10 - MAIN MENU>

Figure J.2

19.112

```
****************************************************************************

MODULE J - CLIENTS OR SALES ACCOUNTS CONTROL
SALES ACCOUNTS LISTING BY RECORDS
DATE: 03-12-1984                                              PAGE #:  1

REC# S-ACC# DESCRIPTION                      STREET          CITY    STATE
     CONTACT                TEL#      COMMENTS

  1 000001  SELL'S  HARDWARE IN FGO.         2201 SO UNIV. DR.   FGO.    ND
     J.T.                232-8903   APPLE DAY

  2 000002  CASTLE HARRY'S WAGON WHEELS      3409 NO HE. RD.     INUIT   AL
     JOHN McWHIRTER      999-8765-234 GOOD CUSTOMER ALWAYS PAYS BILLS

  3 000003  CHARLIE BAILEY GEN'L STORE INC.  5601 SO. JAM ROAD   ABERDEEN SD
     JOHN BENDACO        333-9876   DONT PICK UP CHANGE

  4 000004  RED LITE WHEELS INC.             9175 NO RED RD.     PERTH   AU
     BOBBY JOEL          999-FAMOUS  ALLEN TOWN
```

Figure J.3

19.113

```
                     MODULE K - SALES ORDERS CONTROL

        1 - TO OPEN NEW SALE ORDER

        2 - TO LIST CHRONOLOGY OF SALE ORDERS

        3 - TO LIST BY SALES ACCOUNT

        4 - TO LIST BY ITEM NUMBER

        5 - TO EDIT/CLOSE/VIEW INDIVIDUAL ORDER

        6 - TO RETURN TO LAST ORDER

        S - TO STORE AWAY OLD ORDERS TO FILE

        R - TO RESTORE OLD ORDERS FROM FILE


        ENTER CHOICE:
```

DATE: 03-12-1984   <SAL>   <F10 - MAIN MENU>

Figure K.1

```
                    MODULE K - SALES ORDERS CONTROL

SALE ORDER NUM:000001 DATE OPENED:PROMED:CLOSED: 03/06/84 : 03/13/84 :

PART NUMBER:ZZZZZZ   PART DESCRIPTION: CODE NAME: WAGON 1

NUMBER OF UNITS:  100.00 UNIT PRICE:    70.00   TOTAL PRICE:    7000.00

CLIENT ACCOUNT NUMBER:      000001

CLIENT ACCOUNT DESCRIPTION:SELL'S  HARDWARE IN FGO.

COMMENTS: LIL RED WAGON                       RECORD NUMBER:  1

  . C - TO CHANGE DATA                  CURSOR UP - LAST ORDER
    M - MOVE ON TO ANOTHER ORDER        CURSOR DOWN - NEXT ORDER
    R - RETURN TO USER'S MENU

ENTER CHOICE:
```

DATE: 03-12-1984   <SAL>   <F10 - MAIN MENU>

Figure K.2

```
****************************************************************************

MODULE K - SALES ORDERS CONTROL
SALES ORDERS LISTING BY RECORDS
DATE: 03-12-1984                                              PAGE #:  1

REC# SALE-ORD# DATE-OPEN  PROMISED  CLOSED    PART
     ITEM-DESCRIPTION                  #OF-UNITS    U-COST   SALES-ACCT#
     ACCT-DESCRIPTION                  COMMENTS

  1 000001    03/06/84   03/13/84              ZZZZZZ
    CODE NAME: WAGON 1                 100.00      70.00   000001
    SELL'S  HARDWARE IN FGO.           LIL RED WAGON

  2 000002    03/06/84   03/20/84              ZZZZZZ
    CODE NAME: WAGON 1                 100.00      70.00   000002
    CASTLE HARRY'S WAGON WHEELS        CASTLES IN THE SAND

  3 000003    03/06/84   03/27/84              ZZZZZZ
    CODE NAME: WAGON 1                 200.00      65.00   000003
    CHARLIE BAILEY GEN'L STORE INC.    CUSTOMER IS A GOOD BUYER

  4 000004    03/27/84   04/03/84              ZZZZZZ
    CODE NAME: WAGON 1                 100.00      56.00   000004
    RED LITE WHEELS INC.               PRODUCER OF KEYSTONE KLASSICS

  5 000005    03/28/84   04/04/84              ZZZZZZ
    CODE NAME: WAGON 1                 100.00      58.95   000004
    RED LITE WHEELS INC.               ROXANNE: PUT ON THE RED LITE
```

Figure K.3

CASH FLOW OF SALES BY SEQUENTIAL RECORD

```
13020 ┤
12369 ┤
11718 ┤
D11067 ┤
10416 ┤
O 9765 ┤
9114 ┤
L 8463 ┤
7812 ┤─────────────────────────────────────AVERAGE DOLLAR$
L 7161 ┤
6510 ┤
A 5859 ┤
5208 ┤
R 4557 ┤
3906 ┤
S 3255 ┤
2604 ┤
1953 ┤
1302 ┤
651 ┤
```
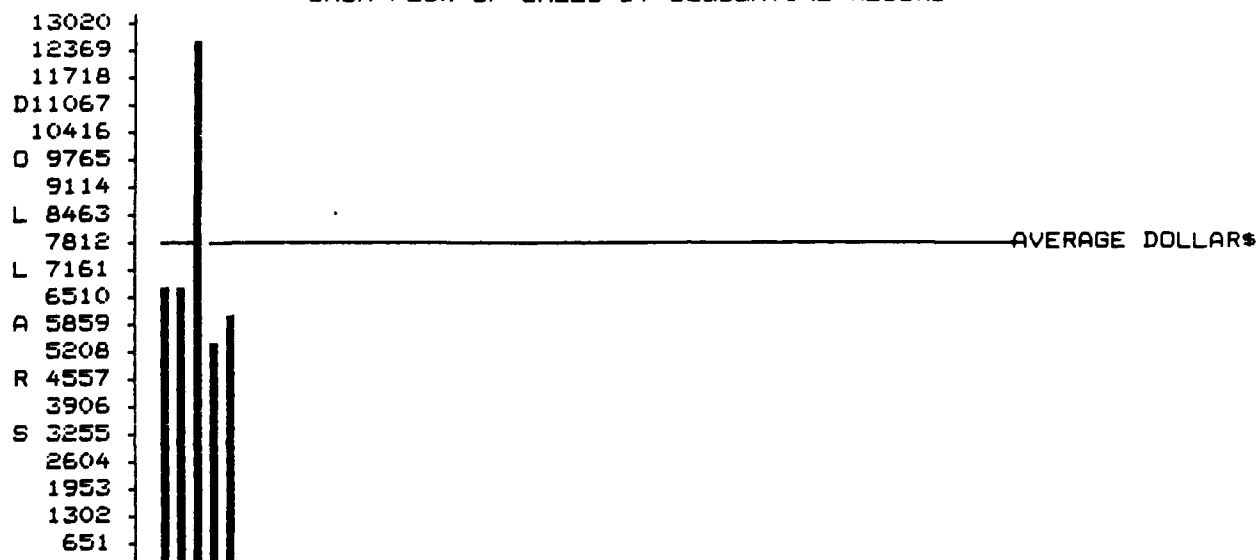
THE NEXT 52 SEQUENTIAL RECORDS BEGINNING RECORD # 1

DATE: 03-12-1984   ENTER ANY KEY TO CONTINUE...   (SAL)   (F10 - MAIN MENU)

Figure K.4

19.117

```
┌────────────────────────────────────────────────────────────────┐
│              MODULE L - VENDOR ACCOUNTS CONTROL                  │
├────────────────────────────────────────────────────────────────┤
│                                                                  │
│      1 - TO OPEN NEW VENDOR ACCOUNT                              │
│                                                                  │
│      2 - TO LIST CHRONOLOGY OF VENDOR ACCOUNTS                   │
│                                                                  │
│      3 - TO LIST BY STATE                                        │
│                                                                  │
│      4 - TO EDIT/CLOSE/VIEW INDIVIDUAL ACCOUNT                   │
│                                                                  │
│      5 - TO RETURN TO LAST ACCOUNT                               │
│                                                                  │
│                                                                  │
├────────────────────────────────────────────────────────────────┤
│                                                                  │
│      ENTER EDIT CHOICE:                                          │
│                                                                  │
└────────────────────────────────────────────────────────────────┘
```

DATE: 03-12-1984   <VEN>   <F10 - MAIN MENU>

Figure L.1

```
                MODULE L - VENDOR ACCOUNTS CONTROL

VENDOR ACCOUNT NUMBER: 000001          DATE OPENED: 03/06/84

VENDOR ACCOUNT DESCRIPTION:BETHAL    STEEL INC.

ADDRESS STREET # :2309 SO. APPLE RD.      CITY: PHIL.

STATE:PN                    ZIP CODE: 55021

CONTACT PERSON: CURT MIDTHUN        TELEPHONE #: 238-9912

COMMENTS:   SHEET STEEL SUPPLIER                     RECORD NUMBER:  1

   C - TO CHANGE DATA                 CURSOR UP - LAST RECORD
   M - MOVE ON TO ANOTHER ACCOUNT     CURSOR DOWN - NEXT RECORD
   R - RETURN TO USER'S MENU

ENTER CHOICE:
```

DATE: 03-12-1984   <VEN>   <F10 - MAIN MENU>

Figure L.2

19.119

```
**********************************************************************

MODULE L - VENDORS ACCOUNTS CONTROL
VENDORS ACCOUNTS LISTING BY RECORDS
DATE: 03-12-1984                                         PAGE #:  1

REC# VENDOR# DESCRIPTION              STREET           CITY    STATE
     CONTACT              TEL#        COMMENTS

  1 000001 BETHAL   STEEL INC.        2309 SO. APPLE RD.   PHIL.      PN
    CURT MIDTHUN          238-9912    SHEET STEEL SUPPLIER


  2 000002 PARTCO OF MINNESOTA        7703 SO HENNIPIN AV. MPLS.      MN
    STEVE MARTIN          232-JOKE    THE MAN WITH TWO (2) BRAINS


  3 000003 PAPERFAB OF SOUTH DAKOTA   3409 SO 12 ST.       SIOUX FLS. SD
    JOHN HABERLACK    34082877618     SUPPLIER OF CARDBOARD FOR PKGING


  4 000004 AMERICAN MATERIALS INC.    20982 WEST 2ND ST.   BREMEN     WG
    HELMUT KOHL           ABC-TTYER   SUPPLIER OF BOLTS. NUTS. ETC.


  5 000005 PREFAB OF WISCONSIN        9984 2ND ST NO.      BOWMAN     ND
    JEFF SHEEP            345-9128    SUPPLIER OF PRE-FB WAGON PARTS.
```

Figure L.3

19.120

```
                MODULE M - PURCHASE ORDERS CONTROL

       1 - TO OPEN NEW PURCHASE ORDER

       2 - TO LIST CHRONOLOGY OF PURCHASE ORDERS

       3 - TO LIST BY VENDORS ACCOUNT

       4 - TO LIST BY ITEM NUMBER

       5 - TO EDIT/CLOSE/VIEW INDIVIDUAL ORDER

       6 - TO RETURN TO LAST ORDER

       S - TO STORE AWAY OLD ORDERS TO FILE

       R - TO RESTORE OLD ORDERS FROM FILE


       ENTER CHOICE:

DATE: 03-12-1984                          <PUR>    <F10 - MAIN MENU>
```

Figure M.1

19. 121

```
                 MODULE M - PURCHASE ORDERS CONTROL

PURCHASE ORD #:000001 DATE OPENED:PROMED:CLOSED: 03-06-84 : 03-13-84 :

PART NUMBER:SSSSSS  PART DESCRIPTION: BODY SCREWS

NUMBER OF UNITS: 1000.00 UNIT PRICE:     0.02   TOTAL PRICE:      20.00

VENDOR ACCOUNT NUMBER:     000002

VENDOR ACCOUNT DESCRIPTION:PARTCO OF MINNESOTA

COMMENTS: BODY SCREWS                              RECORD NUMBER:   1

  C - TO CHANGE DATA                  CURSOR UP - LAST ORDER
  M - MOVE ON TO ANOTHER ORDER        CURSOR DOWN - NEXT ORDER
  R - RETURN TO USER'S MENU

ENTER CHOICE:
```

DATE: 03-12-1984   <PUR>   <F10 - MAIN MENU>

Figure M.2

```
*****************************************************************************

MODULE M - PURCHASE ORDERS CONTROL
PURCHASE ORDERS LISTING BY RECORDS
DATE: 03-12-1984                                              PAGE #:   1

REC# PUR-O# DATE-OPEN PROMISED CLOSED   PART#-DESCRIPTION
     #OF-UNITS UNIT-COST  VENDOR#-DESCRIPTION
     COMMENTS ·

   1 000001 03/06/84 03/13/84           SSSSSS BODY SCREWS
     1000.00    0.02      000002 PARTCO OF MINNESOTA
     BODY SCREWS

   2 000002 03/06/84 03/06/84           HNNNNN HEXAGON NUTS
     1000.00    0.05      000002 PARTCO OF MINNESOTA
     HEXAGON NUTS

   3 000003 03/06/84 03/06/84           LWWWWW LOCK WASHERS
     1000.00    0.02      000005 PREFAB OF WISCONSIN
     LOCK WASHERS

   4 000004 03/06/84 03/06/84           SHSSSS SHEET STEEL STOCK
     1000.00   · 7.80     000001 BETHAL   STEEL INC.
     3/32" THICK STEEL STOCK

   5 000005 03/06/84 03/06/84           SHHHHH SQUARE HOLE WASHER
     %10000.00    0.02     000002 PARTCO OF MINNESOTA
       SQUARE HOLE WASHERS

   6 000006 03/06/84 03/06/84           CPPPPP COTTER PIN
     1000.00    0.03      000004 AMERICAN MATERIALS INC.
     COTTER PINS

   7 000007 03/06/84 03/06/84           EEEEEE STEERING ARM
     1000.00    3.00      000005 PREFAB OF WISCONSIN
     WAGON STEERING ARMS

   8 000008 03/06/84 03/06/84           DDDDDD STEERING TURNTABLE
     1000.00    0.75      000005 PREFAB OF WISCONSIN
     WAGON STEERING TURNTABLES

   9 000009 03/06/84 03/06/84           CBBBBB CARRIAGE BOLT
     1000.00    0.05      000002 PARTCO OF MINNESOTA
     CARRIAGE BOLTS

  10 000010 03/06/84 03/06/84           HHHHHH HANDLE SAFETY CAP
     1000.00    0.05      000002 PARTCO OF MINNESOTA
     HANDLE SAFETY CAP
```

Figure M.3

19.123

CASH FLOW OF PURCHASES BY SEQUENTIAL RECORD

```
10020
 9519
 9018
 8517
 8016
 7515
 7014
 6513
 6012
 5511
 5010
 4509
 4008
 3507
 3006
 2505
 2004 ─────────────────────────────────────── AVERAGE DOLLAR$
 1503
 1002
  501
```
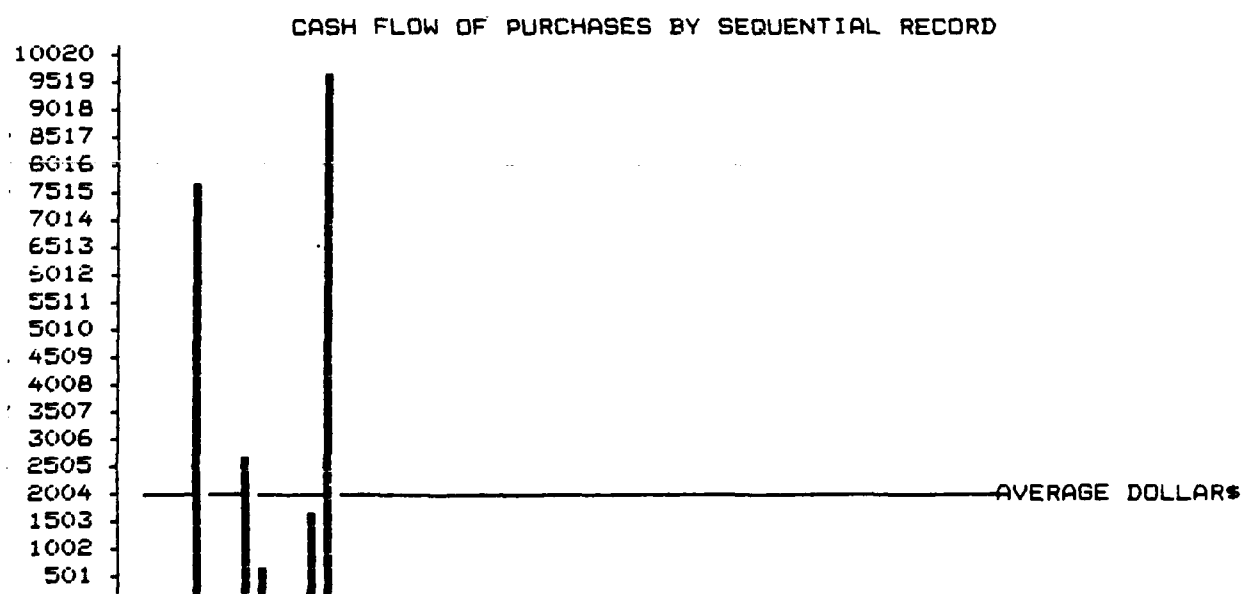
THE NEXT 52 SEQUENTIAL RECORDS BEGINNING RECORD # 1

TE: 03-12-1984   ENTER ANY KEY TO CONTINUE...   (PUR)   (F10 - MAIN MENU)

Figure M.4

19.124

```
              MODULE N - STOREROOM TRANSACTION CONTROL


  1-OPEN NEW INDIVIDUAL PART TRANSACT.    6-EDIT/VIEW INDIVIDUAL TRANSACTION

  2-OPEN NEW PARTS LIST TRANSACTION       7-RETURN TO LAST TRANSACTION

  3-LIST CHRONOLOGY OF TRANSACTIONS       S-STORE AWAY OLD TRANSACTIONS TO FILE

  4-LIST TRANSACTIONS BY PART NUMBER      R-RESTORE OLD TRANSACTIONS FROM FILE

  5-LIST TRANSACTIONS BY ORDER NUMBER


      ENTER EDIT CHOICE:


DATE: 03-12-1984                              <STO>    <F10 - MAIN MENU>
```

Figure N.1

```
        ************PART TRANSACTION************

TRANSACT NUMBER:000001              DATE: 03/06/84

PART NUMBER:SSSSSS   PART DESCRIPTION: BODY SCREWS

NUMBER OF UNITS:   120.00

STOCK ISSUE=I,RECEIPT=R:R

REFERENCE ORDER NUMBER FOR SALES=S,MANUF=M,PURCH=P:P      NUMBER: 000001

COMMENTS:STORES                                  RECORD NUMBER:   1

    C - TO CHANGE DATA                    CURSOR UP - LAST TRANSACT
    M - MOVE ON TO ANOTHER TRANSACT       CURSOR DOWN - NEXT TRANSACT
    R - RETURN TO USER'S MENU

    ENTER CHOICE:
```

DATE: 03-12-1984   <STO>   <F10 - MAIN MENU>

Figure N.2

```
REC# TRANX# DATE      ITEM#-DESCRIPTION                    #OF-UNITS ISS(I)/RE
(R)      SALE/SHOP/PURCH-ORDER-REF COMMENTS

  1 000001 03/06/84 SSSSSS BODY SCREWS                     120.00      R
         P 000001                 STORES

  2 000002 03/06/84 HNNNNN HEXAGON NUTS                    120.00      I
         P 000002                 INVENTORY FOR COMPNT. PARTS

  3 000003 03/06/84 LWWWWW LOCK WASHERS                    120.00      I
         P 000003                 STORES FOR COMPONENT PARTS

  4 000004 03/06/84 SHSSSS SHEET STEEL STOCK                15.00      I
         P 000002                 STORES ARE FOR COMPNT. PARTS

  5 000005 03/06/84 FFFFFF REAR AXLE BOLSTER                15.00      I
         P 000002                 COMPNENT INVENTORY
ENTER ANY KEY TO CONTINUE...



DATE: 03-12-1984                         <STO>    <F10 - MAIN MENU>
```

Figure N.3

19.127

```
                    MODULE 0 - LABOR REPORTING

1 - TO OPEN NEW LABOR REPORT        6 - TO LIST BY MACHINE NUMBER

2 - TO LIST CHRONOLOGY OF REPORTS   7 - TO LIST BY STATION NUMBER

3 - TO LIST BY SHOP ORDER NUMBER    8 - TO LIST BY EMPLOYEE NUMBER

4 - TO LIST BY PART NUMBER          9 - TO EDIT/CLOSE/VIEW INDIVIDUAL REPORT

5 - TO LIST BY OPERATION NUMBER     0 - TO RETURN TO LAST REPORT

S - TO STORE OLD RECORDS TO FILE    R - TO RESTORE OLD REPORTS FROM FILE


   ENTER CHOICE:
```

DATE: 03-12-1984   <LAB>   <F10 - MAIN MENU>

Figure 0.1

19.128

```
                    MODULE D - LABOR REPORTING

LABOR REPORT NUMBER:000001        DATE: 03-06-84      REF SHOP ORDER#: 000002

PART      NUMBER:ZZZZZZ      PART   DESCRIPTION: CODE NAME: WAGON 1

OPERATION  NUM:000004      OPERATION DESCRIP: PRODUCT PACKAGING
MACHINE NUMBER:000004      MACHINE   DESCRIP: MECHANICAL PRODUCT PACKAGER
STATION NUMBER:000004      STATION   DESCRIP: FINAL PRODUCT PACKAGING

EMPLOYEE NUMBER:000004     EMPLOYEE  DESCRIP:STEVE DEAN
HOURS REPORTING:  40.00    REG(R)/OVERTIME(O):R           SHIFT 1/2/3:1
UNITS GOOD:   5.00         UNITS SCRAP:   1.00

COMMENTS:HSMOKIES!!!!!                                RECORD NUMBER:  1

C-CHANGE DATA             M-MOVE TO ANOTHER ORDER      CURSOR UP-LAST ORDER
                          R-RETURN TO USER'S MENU      CURSOR DOWN-NEXT ORDER

ENTER CHOICE:
```

DATE: 03-12-1984   (LAB)   (F10 - MAIN MENU)

Figure 0.2

19.129

```
********************************************************************************
ABC COMPANY, TIMBER, TIMBUKTU 12345
MODULE O - LABOR REPORTING CONTROL
LABOR REPORTS LISTING BY RECORDS
DATE: 03-12-1984                                              PAGE #:

REC# LAB-REP# DATE        SHOP-ORDER#  ITEM#-DESCRIPTION
     OPER#-DESCRIPTION
     MACHINE#-DESCRIPTION
     STATION#-DESCRIPTION
     EMPLOYEE#-DESCRIPTION
     REG(R)/OVT(O)  SHIFT  HOURS-REPORTED NUMBER-UNITS-GOOD  SCRAP

  1 000001  03-06-84   000002       ZZZZZZ CODE NAME: WAGON 1
    000004 PRODUCT PACKAGING
    000004 MECHANICAL PRODUCT PACKAGER
    000004 FINAL PRODUCT PACKAGING
    000004 STEVE DEAN
       R            1            40.00         5.00         1.00

  2 000002  03-06-84   000003       ZZZZZZ CODE NAME: WAGON 1
    000004 PRODUCT PACKAGING
    000004 MECHANICAL PRODUCT PACKAGER
    000004 FINAL PRODUCT PACKAGING
    000004 STEVE DEAN
       R            1            40.00         4.00         1.00

  3 000003  03-06-84   000004       MMMMMM STEERING SUB-ASSEMBLY
    000002 STEERING ASSEMBLY STATION
    000002 AIR INPACT WRENCH
    000002 STEERING ASSEMBLY STATION
    000002 JOHN TRAVAOLA
       R            1            40.00        10.00         1.00

  4 000004  03-06-84   000004       MMMMMM STEERING SUB-ASSEMBLY
    000002 STEERING ASSEMBLY STATION
    000002 AIR INPACT WRENCH
    000002 STEERING ASSEMBLY STATION
    000001 OLIVIA JONES
       R            2            40.00         5.00         0.00

TOTAL NUMBER OF GOOD UNITS:  24
TOTAL NUMBER OF SCRAP UNITS:  3
TOTAL LABOR HOURS REPORTED:  160
TOTAL COST OF LABOR HOURS: $  1280
```

Figure O.3

COST OF LABOR BY SEQUENTIAL RECORD

```
      340
      323
      306
D     289
      272
O     255
      238
L     221  ─────────────────────────────────────────────AVERAGE DOLLAR$
      204
L     187
      170
A     153
      136
R     119
      102
S      85
       68
       51
       34
       17
```

THE NEXT 52 SEQUENTIAL RECORDS BEGINNING RECORD # 1

DATE: 03-12-1984   ENTER ANY KEY TO CONTINUE...   (LAB)   (F10 - MAIN MENU)

Figure 0.4

19.131
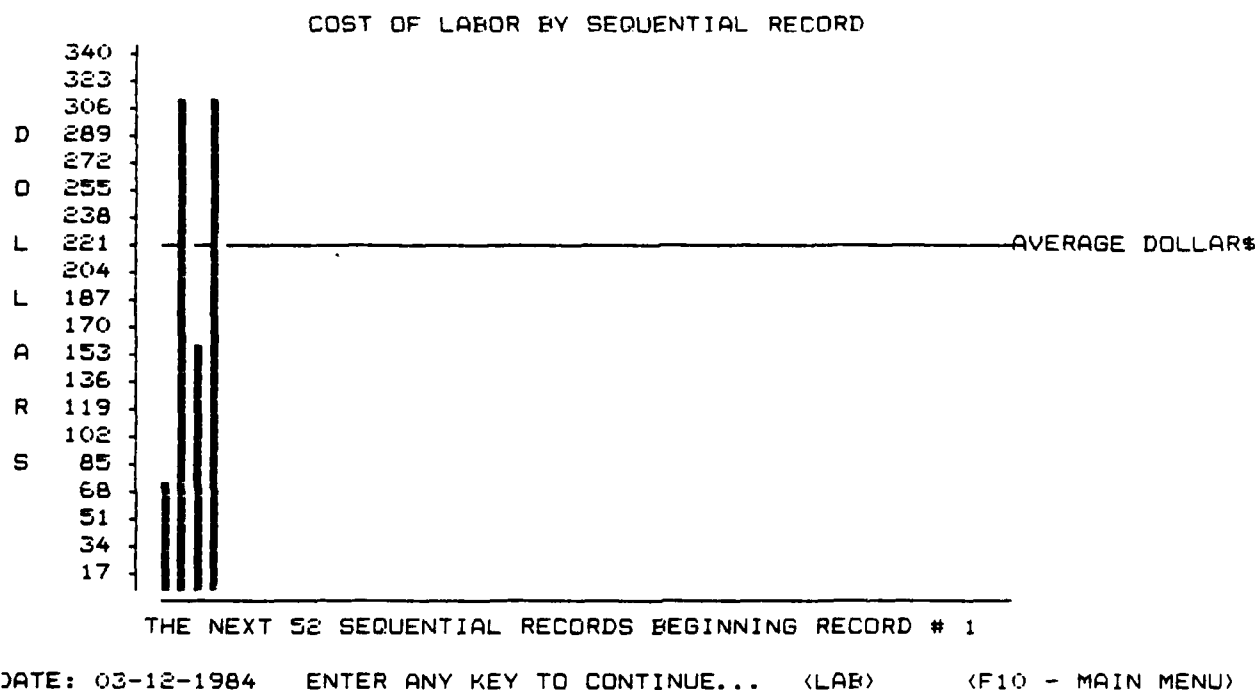
```
  _____
 |                                                                |
 |        MODULE P - DATE / ORDERS PROCESSING / HORIZON UPDATE     |
 |_____|
 |                                                                |
 |                                      BEGIN    ENDIN            |
 |                                      RECORD   RECORD           |
 |                                                                |
 |  TO PROCESS SALES ORDERS RECORDS:                              |
 |                                                                |
 |  TO PROCESS SHOP ORDERS RECORDS:                               |
 |                                                                |
 |  TO PROCESS PURCHASE ORDERS RECORDS:                           |
 |                                                                |
 |  TO PROCESS LABOR REPORTS RECORDS:                             |
 |                                                                |
 |_____|
 |                                                                |
 |         ENTER BEGINNING AND ENDING RECORD                      |
 |                                                                |
 |         ENTER F1 TO BEGIN INTIALIZATION                        |
 |_____|

 TE: 03-12-1984                        (HOR)     (F10 - MAIN MENU)
```

19.132

```
                MODULE Q - MASTER PRODUCTION SCHEDULE

PART NUMBER:  ZZZZZZ      DESCRIPTION:   CODE NAME: WAGON 1
LO-LEVEL CODE:    O       TYPE: END ITEM              RECORD NUMBER:   1


WEEK BEGIN DATE  03/12    03/19    03/26    04/02    04/09    04/16    04/23

GROSS REQUIRED  100.00   200.00   200.00   300.00   200.00   200.00   250.00

GROSS PROD. $  3625.98  7251.96  7251.96 10877.94  7251.96  7251.96  9064.95

GROSS SALES $  7000.00 14000.00 14000.00 21000.00 14000.00 14000.00 17500.00


CURSOR UP-LAST RECORD      CURSOR LEFT-LAST WEEK    C-CHANGE REQUIREMENTS
CURSOR DOWN-NEXT RECORD    CURSOR RIGHT-NEXT WEEK   W-SELECT START WEEK DISPLAY
M-MOVE TO ANOTHER ITEM     G-GRAPHICS DISPLAY

ENTER CHOICE:
```

DATE: 03-12-1984   <MPS>   <F10 - MAIN MENU>

Figure Q.1

MASTER PRODUCTION SCHEDULE OF PART ZZZZZZ
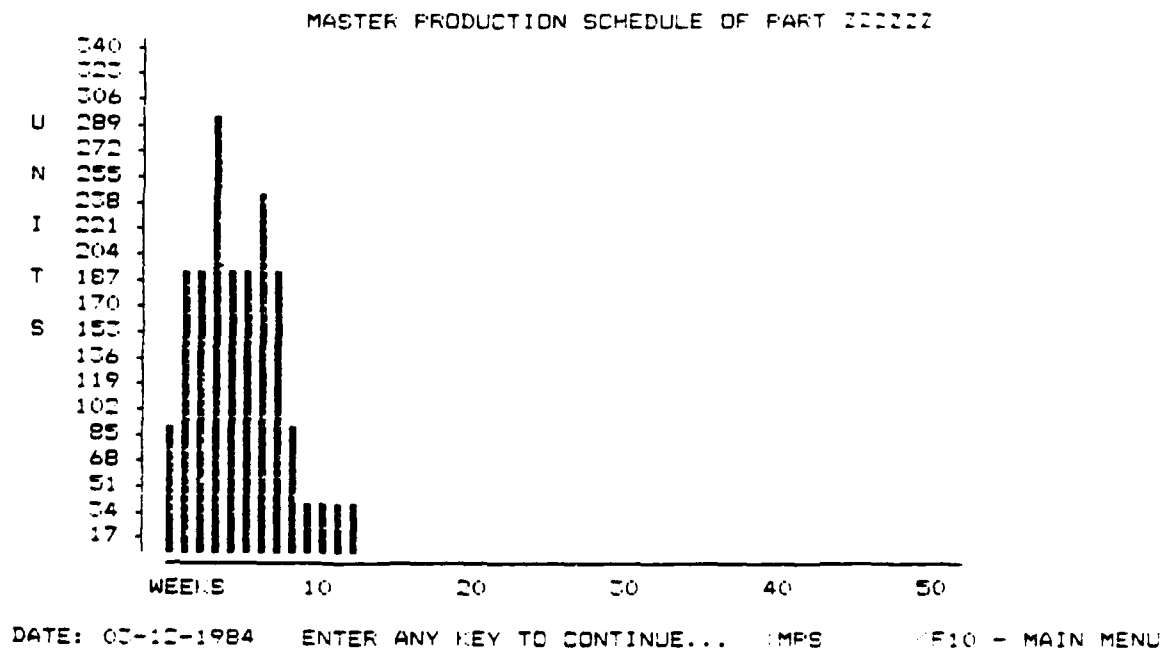
Figure Q.2

```
***************************************************************************
ABC COMPANY, TIMBER, TIMBUKTU 12345
MODULE G - MASTER PRODUCTION SCHEDULE
MASTER PRODUCTION SCHEDULE LISTING
DATE: 03-12-1984                                            PAGE #:  1


PART # : ZZZZZZ   CODE NAME: WAGON 1
UNIT PROD COST:  35.41989
UNIT SELLING PRICE:  70


    WEEK      GROSS-REQUIRED     GROSS-PROD$       GROSS-SALES$

    03/12         100.00          3541.99           7000.00
    03/19         200.00          7083.98          14000.00
    03/26         200.00          7083.98          14000.00

    04/02           0.00             0.00              0.00
    04/09           0.00             0.00              0.00
    04/16           0.00             0.00              0.00
    04/23           0.00             0.00              0.00
    04/30           0.00             0.00              0.00

    05/07           0.00             0.00              0.00
    05/14           0.00             0.00              0.00
    05/21           0.00             0.00              0.00
    05/28           0.00             0.00              0.00

    06/04           0.00             0.00              0.00
    06/11           0.00             0.00              0.00
    06/18           0.00             0.00              0.00
    06/25           0.00             0.00              0.00

    07/02           0.00             0.00              0.00
    07/09           0.00             0.00              0.00
    07/16           0.00             0.00              0.00
    07/23           0.00             0.00              0.00
    07/30           0.00             0.00              0.00

    08/06           0.00             0.00              0.00
    08/13           0.00             0.00              0.00
    08/20           0.00             0.00              0.00
    08/27           0.00             0.00              0.00

    09/03           0.00             0.00              0.00
    09/10           0.00             0.00              0.00
    09/17           0.00             0.00              0.00
    09/24           0.00             0.00              0.00

    10/01           0.00             0.00              0.00
    10/08           0.00             0.00              0.00
    10/15           0.00             0.00              0.00
    10/22           0.00             0.00              0.00
    10/29           0.00             0.00              0.00

    11/05           0.00             0.00              0.00
```

19.135

WEEK	GROSS-REQUIRED	GROSS-PROD$	GROSS-SALES$
11/12	0.00	0.00	0.00
11/19	0.00	0.00	0.00
11/26	0.00	0.00	0.00
12/03	0.00	0.00	0.00
12/10	0.00	0.00	0.00
12/17	0.00	0.00	0.00
12/24	0.00	0.00	0.00
12/31	0.00	0.00	0.00
01/07	0.00	0.00	0.00
01/14	0.00	0.00	0.00
01/21	0.00	0.00	0.00
01/28	0.00	0.00	0.00
02/04	0.00	0.00	0.00
02/11	0.00	0.00	0.00
02/18	0.00	0.00	0.00
02/25	0.00	0.00	0.00
03/03	0.00	0.00	0.00

```
TOTAL GROSS REQUIRED:  500
TOTAL GROSS PRODUCTION $:  17709.95
TOTAL GROSS SALES $:  35000
```

Figure Q.3

```
MODULE R - ORDER RELEASES AND RECEIPTS SCHEDLES

PART NUMBER:  ZZZZZZ       DESCRIPTION:    CODE NAME: WAGON 1
LO-LEVEL CODE:    0        TYPE: END ITEM              RECORD NUMBER:   1


WEEK BEGIN DATE  03/12   03/19   03/26   04/02   04/09   04/16   04/23

PLND RELEASES    328.00   0.00    0.00    0.00    0.00    0.00    0.00

SCHDLD RECPTS    100.00   0.00    0.00    0.00    0.00    0.00    0.00


   R - TO CHANGE ORDER RELEASES          CURSOR LEFT - LAST WEEK
   S - TO CHANGE SCHEDULED RECEIPTS      CURSOR RIGHT - NEXT WEEK
   W - SELECT STARTING WEEK DISPLAY      CURSOR UP - LAST RECORD
   M - MOVE ON TO ANOTHER ITEM           CURSOR DOWN - NEXT RECORD
   G - GRAPHICS DISPLAY

   ENTER CHOICE:


DATE: 03-12-1984                    <FOR>     <F10 - MAIN MENU>
```

Figure R.1

ORDER RECEIPTS OF PART ZZZZZZ

```
    120
    114
    108
U   102
     96
N    90
     84
I    78
     72
T    66
     60
S    54
     48
     42
     36
     30
     24
     18
     12
      6

     WEEKS      10        20        30        40        50
```

DATE: 03-12-1984   ENTER ANY KEY TO CONTINUE...   <POR>   <F10 - MAIN ME!

Figure R.2

19.138

ORDER RELEASES OF PART ZZZZZZ

Figure R.3

PART # : 222222

WEEK	PLANNED-ORDER RELEASES	SCHEDULED-RECEIPTS
03/12	125.00	100.00
03/19	200.00	0.00
03/26	0.00	0.00
04/02	0.00	0.00
04/09	0.00	0.00
04/16	0.00	0.00
04/23	0.00	0.00
04/30	0.00	0.00
05/07	0.00	0.00
05/14	0.00	0.00
05/21	0.00	0.00
05/28	0.00	0.00
06/04	0.00	0.00
06/11	0.00	0.00
06/18	0.00	0.00
06/25	0.00	0.00
07/02	0.00	0.00
07/09	0.00	0.00
07/16	0.00	0.00
07/23	0.00	0.00
07/30	0.00	0.00
08/06	0.00	0.00
08/13	0.00	0.00
08/20	0.00	0.00
08/27	0.00	0.00
09/03	0.00	0.00
09/10	0.00	0.00
09/17	0.00	0.00
09/24	0.00	0.00
10/01	0.00	0.00
10/08	0.00	0.00
10/15	0.00	0.00
10/22	0.00	0.00
10/29	0.00	0.00
11/05	0.00	0.00

PLANNED ORDER RELEASES/SCHEDULED RECEIPTS LISTING
DATE: 03-12-1984

WEEK	PLANNED-ORDER RELEASES	SCHEDULED-RECEIPTS
11/12	0.00	0.00
11/19	0.00	0.00
11/26	0.00	0.00
12/03	0.00	0.00
12/10	0.00	0.00
12/17	0.00	0.00
12/24	0.00	0.00
12/31	0.00	0.00
01/07	0.00	0.00
01/14	0.00	0.00
01/21	0.00	0.00
01/28	0.00	0.00
02/04	0.00	0.00
02/11	0.00	0.00
02/18	0.00	0.00
02/25	0.00	0.00
03/03	0.00	0.00

TOTAL PLANNED ORDER RELEASES: 325
TOTAL PLANNED SCHEDULED RECEIPTS: 100

Figure R.4

19.141

```
            MODULE S - PRODUCT COSTING


          NUMBER OF STATIONS:                    4

          NUMBER OF PARTS:                       23




    DO YOU WANT PRINTER ON (Y/N)?:N

    DO YOU WANT PAUSE AFTER EACH PART (Y/N)?: N


DATE: 03-12-1984                    <COS>    <F10 - MAIN MENU>
```

Figure S.1

```
**********************************************************************

MODULE S - PRODUCT COSTING
PRODUCT AND PART COSTING
DATE: 03-12-1984                                      PAGE #:   1

**********************************************************************

PART NUMBER : SHHHHH      RECORD #:   8

COST OF MATERIALS:                    0.02
COST OF LABOR:                        0.00
COST OF OVERHEAD:                     0.00
TOTAL UNIT COST:                      0.02

SET-UP COST:                          0.00
ACCUM SET-UP COST:                    0.00

**********************************************************************

PART NUMBER : CPPPPP      RECORD #:   9

COST OF MATERIALS:                    0.04
COST OF LABOR: ·                      0.00
COST OF OVERHEAD:                     0.00
TOTAL UNIT COST:                      0.04

SET-UP COST:                          0.00
ACCUM SET-UP COST:                    0.00

**********************************************************************

PART NUMBER : EEEEEE      RECORD #:  10

COST OF MATERIALS:                    3.00
COST OF LABOR:                        0.00
COST OF OVERHEAD:                     0.00
TOTAL UNIT COST:                      3.00

SET-UP COST:                          0.00
ACCUM SET-UP COST:                    0.00

**********************************************************************

PART NUMBER : DDDDDD      RECORD #:  11

COST OF MATERIALS:                    0.75
COST OF LABOR:                        0.00
COST OF OVERHEAD:                     0.00
TOTAL UNIT COST:                      0.75

SET-UP COST:                          0.00
ACCUM SET-UP COST:                    0.00
```

19.143

PRODUCT AND PART COSTING
DATE: 03-13-1984   PAGE #: 5

****

PART NUMBER : SSSSSS   RECORD #: 3

COST OF MATERIALS: 12.00
COST OF LABOR: 0.00
COST OF OVERHEAD: 3.00
TOTAL UNIT COST: 12.00

SET-UP COST: 12.00
ACCUM SET-UP COST: 10.00

****

PART NUMBER : HNNNNN   RECORD #: 4

COST OF MATERIALS: 10.00
COST OF LABOR: 0.00
COST OF OVERHEAD: 0.00
TOTAL UNIT COST: 10.00

SET-UP COST: 0.00
ACCUM SET-UP COST: 0.00

****

PART NUMBER : LWWWWW   RECORD #: 5

COST OF MATERIALS: 0.02
COST OF LABOR: 0.00
COST OF OVERHEAD: 0.00
TOTAL UNIT COST: 0.02

SET-UP COST: 0.00
ACCUM SET-UP COST: · 0.00

****

PART NUMBER : AAAAAA   RECORD #: 6

COST OF MATERIALS: 7.80
COST OF LABOR: 2.67
COST OF OVERHEAD: 1.33
TOTAL UNIT COST: 11.80

SET-UP COST: 0.13
ACCUM SET-UP COST: 0.13

19.144

```
**********************************************************************

PART NUMBER : XXXXXX     RECORD #:  7

COST OF MATERIALS:                    4.42
COST OF LABOR:                        1.87
COST OF OVERHEAD:                     0.75
TOTAL UNIT COST:                      7.03

SET-UP COST:                          0.13
ACCUM SET-UP COST:                    0.13


**********************************************************************

PART NUMBER : ZZZZZZ     RECORD #:  1

COST OF MATERIALS:                  180.56
COST OF LABOR:                        9.80
COST OF OVERHEAD:                     4.54
TOTAL UNIT COST:                    194.90

SET-UP COST:                          0.13
ACCUM SET-UP COST:                   40.53
```

Figure S.2

```
MODULE T - MATERIALS REQUIREMENTS PLANNING


    1 - TO DEFINE PARAMETERS

    2 - TO RECOMPUTE LO-LEVEL CODES

    3 - TO SELECT PARTS FOR MRP PROCESSING

    4 - TO PROCEED WITH MRP PROCESSING

    5 - TO VIEW MRP OUTPUT FOR INDIVIDUAL PART



    ENTER CHOICE:
```

DATE: 03-12-1984   <MRP>   <F10 - MAIN MENU>

Figure T.1

```
┌─────────────────────────────────────────────────────────────────┐
│                                                                   │
│            MODULE T - MATERIALS REQUIREMENTS PLANNING             │
│                                                                   │
├─────────────────────────────────────────────────────────────────┤
│                                                                   │
│     .        NUMBER OF PARTS:                    23               │
│                                                                   │
│              NUMBER OF WEEKS:                    5                │
│                                                                   │
│              CARRYING COST IN ANNUAL PERCENT:    18               │
│                                                                   │
├─────────────────────────────────────────────────────────────────┤
│                                                                   │
│     E - TO EDIT PARAMETERS         R - TO RETURN TO MRP USER'S MENU│
│                                                                   │
├─────────────────────────────────────────────────────────────────┤
│                                                                   │
│     ENTER CHOICE:                                                 │
│                                                                   │
└─────────────────────────────────────────────────────────────────┘

DATE: 03-12-1984                      <MRP>      <F10 - MAIN MENU>

                          Figure T.2
```

19.147

```
********************************************************************

    **********PART NUMBER********ZZZZZZ
    RECOMMEND RE-SCHEDULE RECEIPT IN WEEK   1
    ***LEAD TIME(WKS)** 1
    ***ON HAND********** 100
    ***SAFETY STOCK**** 25
    ***ALLOCATED FOR*** 0
    ***LATE RELEASES*** 0
    *** RECOMM RESCHED* 1

    *WEEK BEGINNING DATE**  03/12    03/19    03/26    04/02    04/09
    GROSS REQUIREMENTS FOR
    **END PART***ZZZZZZ    100.00   200.00   300.00   400.00   300.00
    **SERVICE ORDERS***      0.00     0.00     0.00     0.00     0.00
    **TOTAL ORDERS*****    100.00   200.00   300.00   400.00   300.00
    **SCHEDULED RECEIPT    100.00    12.00    23.00   123.00    12.00
    **ON-HAND BALANCE**    100.00   100.00    25.00    25.00    25.00
    **NET REQUIREMENTS*      0.00   113.00   277.00   277.00   288.00
    **PLND ORDR RECPTS*      0.00   113.00   277.00   277.00   288.00
    **PLND ORDR RELEASE    113.00   277.00   277.00   288.00     0.00
    ********************************************************************


    **********PART NUMBER********MMMMMM
    *****LATE ORDER IN WEEK*** 0 ***ORDER QUANTITY** 38
    ***LEAD TIME(WKS)** 1
    ***ON HAND********** 100
    ***SAFETY STOCK**** 25
    ***ALLOCATED FOR*** 0
    ***LATE RELEASES*** 38
    *** RECOMM RESCHED* 0

    *WEEK BEGINNING DATE**  03/12    03/19    03/26    04/02    04/09
    GROSS REQUIREMENTS FOR
    *PARENT PART*ZZZZZZ    113.00   277.00   277.00   288.00     0.00
    **SERVICE ORDERS***      0.00     0.00     0.00     0.00     0.00
    **TOTAL ORDERS*****    113.00   277.00   277.00   288.00     0.00
    **SCHEDULED RECEIPT      0.00     0.00     0.00     0.00     0.00
    **ON-HAND BALANCE**    100.00    25.00    25.00    25.00    25.00
    **NET REQUIREMENTS*     38.00   277.00   277.00   288.00     0.00
    **PLND ORDR RECPTS*    ******   277.00   277.00   288.00     0.00
    **PLND ORDR RELEASE    277.00   277.00   288.00     0.00     0.00
    ********************************************************************


    **********PART NUMBER********SSSSSS
    *****LATE ORDER IN WEEK*** 0 ***ORDER QUANTITY** 194
    ***LEAD TIME(WKS)** 1
    ***ON HAND********** 760
    ***SAFETY STOCK**** 50
    ***ALLOCATED FOR*** 0
    ***LATE RELEASES*** 194
    *** RECOMM RESCHED* 0

    *WEEK BEGINNING DATE**  03/12    03/19    03/26    04/02    04/09
    GROSS REQUIREMENTS FOR
    *PARENT PART*ZZZZZZ    904.00  2216.00  2216.00  2304.00     0.00
    **SERVICE ORDERS***      0.00     0.00     0.00     0.00     0.00
    **TOTAL ORDERS*****    904.00  2216.00  2216.00  2304.00     0.00
```

19.148

```
**SCHEDULED RECEIPT      0.00       0.00      0.00      0.00      0.00
**ON-HAND BALANCE**    760.00      50.00     50.00     50.00     50.00
**NET REQUIREMENTS*    194.00    2216.00   2216.00   2304.00      0.00
**PLND ORDR RECPTS*    ******    2216.00   2216.00   2304.00      0.00
**PLND ORDR RELEASE   2216.00    2216.00   2304.00      0.00      0.00
    *****************************************************************
```

```
***********PART NUMBER********HNNNNN
*****LATE ORDER IN WEEK*** 0 ***ORDER QUANTITY** 899
***LEAD TIME(WKS)** 1
***ON HAND********** 30
***SAFETY STOCK**** 25
***ALLOCATED FOR*** 0
***LATE RELEASES*** 899
*** RECOMM RESCHED* 0
```

```
*WEEK BEGINNING DATE** 03/12      03/19     03/26     04/02     04/09
GROSS REQUIREMENTS FOR
*PARENT PART*ZZZZZZ    904.00    2216.00   2216.00   2304.00      0.00
**SERVICE ORDERS***      0.00       0.00      0.00      0.00      0.00
**TOTAL ORDERS*****    904.00    2216.00   2216.00   2304.00      0.00
**SCHEDULED RECEIPT      0.00       0.00      0.00      0.00      0.00
**ON-HAND BALANCE**     30.00      25.00     25.00     25.00     25.00
**NET REQUIREMENTS*    899.00    2216.00   2216.00   2304.00      0.00
**PLND ORDR RECPTS*    ******    2216.00   2216.00   2304.00      0.00
**PLND ORDR RELEASE   2216.00    2216.00   2304.00      0.00      0.00
    *****************************************************************
```

```
***********PART NUMBER********LWWWWW
*****LATE ORDER IN WEEK*** 0 ***ORDER QUANTITY** 83
***LEAD TIME(WKS)** 1
***ON HAND********** 880
***SAFETY STOCK**** 59
***ALLOCATED FOR*** 0
***LATE RELEASES*** 83
*** RECOMM RESCHED* 0
```

```
*WEEK BEGINNING DATE** 03/12      03/19     03/26     04/02     04/09
GROSS REQUIREMENTS FOR
*PARENT PART*ZZZZZZ    904.00    2216.00   2216.00   2304.00      0.00
**SERVICE ORDERS***      0.00       0.00      0.00      0.00      0.00
**TOTAL ORDERS*****    904.00    2216.00   2216.00   2304.00      0.00
**SCHEDULED RECEIPT      0.00       0.00      0.00      0.00      0.00
**ON-HAND BALANCE**    880.00      59.00     59.00     59.00     59.00
**NET REQUIREMENTS*     83.00    2216.00   2216.00   2304.00      0.00
**PLND ORDR RECPTS*    ******    2216.00   2216.00   2304.00      0.00
**PLND ORDR RELEASE   2216.00    2216.00   2304.00      0.00      0.00
    *****************************************************************
```

```
***********PART NUMBER********AAAAAA
*****LATE ORDER IN WEEK*** 0 ***ORDER QUANTITY** 43
***LEAD TIME(WKS)** 1
***ON HAND********** 100
***SAFETY STOCK**** 30
***ALLOCATED FOR*** 0
***LATE RELEASES*** 43
*** RECOMM RESCHED* 0
```

```
*WEEK BEGINNING DATE** 03/12      03/19     03/26     04/02     04/09
GROSS REQUIREMENTS FOR
*PARENT PART*ZZZZZZ    113.00     277.00    277.00    288.00      0.00
**SERVICE ORDERS***      0.00       0.00      0.00      0.00      0.00
```

19.149

```
** _ REQUIREMENTS **   .....    .....    .....    .....      ..
**PLND ORDR RCPTS**   ......   277.00   277.00   288.00    0.00
**PLND ORDR RELEASE  277.00   277.00   288.00    0.00      0.00
**********************************************************************


***********PART NUMBER**********XXXXXX
*****LATE ORDER IN WEEK*** 0  ***ORDER QUANTITY** 38
***LEAD TIME(WKS)** 1
***ON HAND*********** 100
***SAFETY STOCK**** 25
***ALLOCATED FOR*** 0
***LATE RELEASES*** 38
*** RECOMM RESCHED* 0

*WEEK BEGINNING DATE** 03/12    03/19    03/26    04/02    04/09
GROSS REQUIREMENTS FOR
*PARENT PART*ZZZZZZ   113.00   277.00   277.00   288.00    0.00
**SERVICE ORDERS***     0.00     0.00     0.00     0.00    0.00
**TOTAL ORDERS*****    113.00   277.00   277.00   288.00    0.00
**SCHEDULED RECEIPT     0.00     0.00     0.00     0.00    0.00
**ON-HAND BALANCE**    100.00    25.00    25.00    25.00   25.00
**NET REQUIREMENTS*     38.00   277.00   277.00   288.00    0.00
**PLND ORDR RECPTS*   ******   277.00   277.00   288.00    0.00
**PLND ORDR RELEASE   277.00   277.00   288.00    0.00      0.00
**********************************************************************


***********PART NUMBER*******SHHHHH
***LEAD TIME(WKS)** 1
***ON HAND********* 970
***SAFETY STOCK**** 100
***ALLOCATED FOR*** 0
***LATE RELEASES*** 0
*** RECOMM RESCHED* 0

*WEEK BEGINNING DATE** 03/12    03/19    03/26    04/02    04/09
GROSS REQUIREMENTS FOR
*PARENT PART*MMMMMMM   554.00   554.00   576.00    0.00    0.00
**SERVICE ORDERS***     0.00     0.00     0.00     0.00    0.00
**TOTAL ORDERS*****    554.00   554.00   576.00    0.00    0.00
**SCHEDULED RECEIPT     0.00     0.00     0.00     0.00    0.00
**ON-HAND BALANCE**    970.00   416.00   100.00   100.00  100.00
**NET REQUIREMENTS*     0.00   238.00   576.00    0.00    0.00
**PLND ORDR RECPTS*     0.00   238.00   576.00    0.00    0.00
**PLND ORDR RELEASE   238.00   576.00    0.00    0.00      0.00
**********************************************************************


***********PART NUMBER*******CPPPPP
***LEAD TIME(WKS)** 0
***ON HAND********* 0
***SAFETY STOCK**** 0
***ALLOCATED FOR*** 0                        Figure T.3
***LATE RELEASES*** 0
*** RECOMM RESCHED* 0

*WEEK BEGINNING DATE** 03/12    03/19    03/26    04/02    04/09
GROSS REQUIREMENTS FOR
*PARENT PART*MMMMMMM   277.00   277.00   288.00    0.00    0.00
**SERVICE ORDERS***     0.00     0.00     0.00     0.00    0.00
**TOTAL ORDERS*****    277.00   277.00   288.00    0.00    0.00
**SCHEDULED RECEIPT     0.00     0.00     0.00     0.00    0.00
**ON-HAND BALANCE**     0.00     0.00     0.00     0.00    0.00
```

19.150

```
                    MODULE U - CAPACITY REQUIREMENTS PLANNING


        NUMBER OF STATIONS:                    4

        NUMBER OF ITEMS:                       23



        NUMBER OF WEEKS:                       5

        DO YOU WANT PRINTER ON (Y/N)?:   N

        DO YOU WANT PAUSE AFTER EACH STATION (Y/N)?: N
```

DATE: 03-12-1984   ‹CRF.   F:. - --. . -

Figure U.1
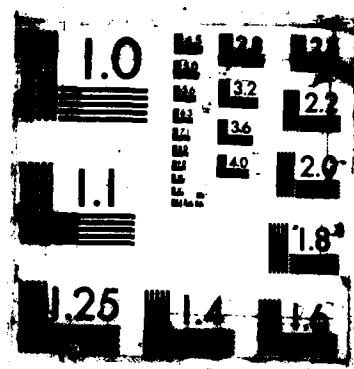
```
***************************************************************************

MODULE U - CAPACITY REQUIREMENTS PLANNING
CAPACITY REQUIREMENTS PLANNING
DATE: 03-12-1964

***************************************************************************

***STATION RECORD** 1
***STATION CODE****000001
***CAPACITY IN M-H* 160


**WEEK BEGIN DATE**     03/12    03/19    03/26    04/02    04/09
**RELEASED LOAD****       0.0      0.0      0.0      0.0      0.0
**PLANNED LOAD*****      92.3     92.3     96.0      0.0      0.0
**TOTAL LOAD********     92.3     92.3     96.0      0.0      0.0

TOTAL LOAD $ (DIR+OVH) IN STATION  1            3368.57
TOTAL OVERLOAD M-HOURS IN STATION  1              0.00


***************************************************************************

***STATION RECORD** 2
***STATION CODE****000002
***CAPACITY IN M-H* 40


**WEEK BEGIN DATE**     03/12    03/19    03/26    04/02    04/09
**RELEASED LOAD****       0.0      0.0      0.0      0.0      0.0
**PLANNED LOAD*****     152.4    152.4    158.4      0.0      0.0
**TOTAL LOAD******** 152.4*** 152.4*** 158.4***      0.0      0.0

TOTAL LOAD $ (DIR+OVH) IN STATION  2            7616.70***
TOTAL OVERLOAD M-HOURS IN STATION  2             343.15


***************************************************************************

***STATION RECORD** 3
***STATION CODE****000003
***CAPACITY IN M-H* 40


**WEEK BEGIN DATE**     03/12    03/19    03/26    04/02    04/09
**RELEASED LOAD****       0.0      0.0      0.0      0.0      0.0
**PLANNED LOAD*****      64.6     64.6     67.2      0.0      0.0
**TOTAL LOAD********  64.6***  64.6***  67.2***      0.0      0.0

TOTAL LOAD $ (DIR+OVH) IN STATION  3            2629.43***
TOTAL OVERLOAD M-HOURS IN STATION  3              76.51


***************************************************************************

***STATION RECORD** 4
***STATION CODE****000004
***CAPACITY IN M-H* 40


**WEEK BEGIN DATE**     03/12    03/19    03/26    04/02    04/09
**RELEASED LOAD****      10.8      1.3      2.5     13.3      1.3
```

19.152

```
 PLANNED LOAD*****     12.3     30.0     30.0     31.2     0.0
 TOTAL LOAD*******     23.1     31.3     32.5  44.6***      1.3

TOTAL LOAD $ (DIR+OVH) IN STATION  4          1405.31***
 ITAL OVERLOAD M-HOURS IN STATION  4                 4.56


TOTAL LOAD COSTS $ FOR ALL STATIONS          15020.01
```

Figure U.2

19.153

```
+------------------------------------------------------------------------+
|                                                                        |
|              MODULE V - SUMMARY ACTIONS TO-DO                          |
|                                                                        |
+------------------------------------------------------------------------+
|                                                                        |
|   1 - PARTS REQUIRING ORDER RELEASES THIS WEEK OR EARLIER              |
|   2 - PARTS WHOSE SHOP OR PURCHASE ORDERS ARE PROMISED THIS WEEK OR EARLIER |
|   3 - PARTS WHOSE SALES ORDERS ARE PROMISED THIS WEEK OR EARLIER       |
|   4 - PARTS WHOSE SCHEDULED RECEIPTS ARE RECOMMENDED FOR RESCHEDULE    |
|                                                                        |
|   5 - PARTS DEVIATION REPORT FOR PLANNED VS ACTUAL PRICES             |
|   6 - PARTS DEVIATION REPORT FOR PLANNED VS ACTUAL LEADTIME           |
|   7 - PARTS DEVIATION REPORT FOR PLANNED VS ACTUAL SCRAP AND SAFETY STOCK |
|                                                                        |
|   8 - STATION WHERE OVERLOAD EXIST                                     |
|   9 - STATION DEVIATION REPORT FOR PLANNED VS ACTUAL LABOR COST        |
|                                                                        |
+------------------------------------------------------------------------+
|                                                                        |
|        ENTER MENU CHOICE:                                              |
|                                                                        |
+------------------------------------------------------------------------+

}TE: 03-12-1984                          (ACT)      (F10 - MAIN MENU)
```

Figure V.1

```
******PURCHASE ORDERS TO BE RELEASED THIS WEEK*****

PART #       DESCRIPTION
EEEEEE       STEERING ARM                    ORDERS   UNIT/M
DDDDDD       STEERING TURNTABLE              25.00     EA
HUNTIN       REAR AXLE BRACE                 25.00     EA
ENTER ANY KEY TO CONTINUE...                55.00     EA
```

DATE: 03-12-1984

(ACT)   (F10 - MAIN MENU)

Figure V.2

19.155

```
******SHOP OR PURCHASE ORDERS DUE THIS WEEK***

ITEM #       DESCRIPTION                    ORDERS   UNIT/M
ZZZZZZ       CODE NAME: WAGON 1             100.00    EA

******SHOP OR PURCHASE ORDERS DUE LAST WEEK AND EARLIER***

ITEM #       DESCRIPTION                    ORDERS   UNIT/M
ZZZZZZ       CODE NAME: WAGON 1             200.00    EA
MMMMMM       STEERING SUB-ASSEMBLY          100.00    EA
SSSSSS       BODY SCREWS                   1000.00    EA
HNNNNN       HEXAGON NUTS                  1000.00    EA
LWWWWW       LUCK WASHERS                  1000.00    EA
HAWAWA       WAGON BODY                     100.00    EA
XXXXXX       REAR AXLE SUB-ASSEMBLY         100.00    EA
SHHHHH       SQUARE HOLE WASHER           10000.00    EA
CPPPPP       COTTER PIN                    1000.00    EA
EEEEEE       STEERING ARM                  1000.00    EA
DDDDDD       STEERING TURNTABLE            1000.00    EA
CBBBBB       CARRIAGE BOLT                 1000.00    EA
HHHHHH       HANDLE SAFETY CAP             1000.00    EA
BBBBBB       WAGON HANDLE                  1000.00    EA
CCCCCC       WHEELS                       10000.00    EA
SHSSSS       SHEET STEEL STOCK             1000.00    EA
```

Figure V.3

19.156

```
******SALES ORDERS DUE THIS WEEK***

ITEM #      DESCRIPTION                              ORDERS     UNIT/M
ZZZZZZ      CODE NAME: WAGON 1                       100.00     EA

******SALES ORDERS DUE LAST WEEK AND EARLIER***

ITEM #     : DESCRIPTION                             ORDERS     UNIT/M
ZZZZZZ      CODE NAME: WAGON 1                       100.00     EA
```

Figure V.4

```
******ITEMS RECOMMENDED FOR RESCHEDULE***

ITEM #     DESCRIPTION                        # OF RECEIPTS RESCHED
ZZZZZZ     CODE NAME: WAGON 1                     1
```

Figure V.5 ·

REC#	PART #-DESCRIPTION	PLANNED-PRICE	AVE-ACTUAL	REPLACE(Y/N)?
3	SSSSSS BODY SCREWS	0.020	0.020	N
4	HNNNNN HEXAGON NUTS	0.050	0.050	N
5	LWWWWW LOCK WASHERS	0.020	0.020	N
8	SHHHHH SQUARE HOLE WASHER	0.020	0.020	N
9	CPPPPP COTTER PIN	0.040	0.030	N
10	EEEEEE STEERING ARM	3.000	3.000	N
11	DDDDDD STEERING TURNTABLE	0.750	0.750	N
12	CBBBBB CARRIAGE BOLT	0.050	0.050	N
13	HHHHHH HANDLE SAFETY CAP	0.050	0.050	N
14	BBBBBB WAGON HANDLE	2.000	2.000	N

DATE: 03-12-1984   (ACT)   (F10 - MAIN MENU)

Figure V.6

C#	PART #-DESCRIPTION	LEAD-TIME-DAYS-(E)ST	AVE-(P)ROMISED	(C)LOSED	E/P/C?
3	SSSSSS BODY SCREWS	7	7	0	E
4	HNNNNN HEXAGON NUTS	7	0	0	E
5	LWWWWW LOCK WASHERS	7	0	0	E
8	SHHHHH SQUARE HOLE WASHER	7	0	0	E
9	CPPPPP COTTER PIN	0	0	0	E
10	EEEEEE STEERING ARM	7	0	0	E
11	DDDDDD STEERING TURNTABLE	7	0	0	E
12	CBBBBB CARRIAGE BOLT	7	0	0	E
13	HHHHHH HANDLE SAFETY CAP	7	0	0	E
14	BBBBBB WAGON HANDLE	7	0	0	E

TE: 03-12-1984   (ACT)   (F10 - MAIN MENU)

Figure V.7

19.160

REC#	PART #-DESCRIPTION	NUMBER-SCRP	GOOD	%DEF	SF(E)TY	(R)COM	E/R?
1	ZZZZZZ CODE NAME: WAGON 1	2	9	18.2	25.0	13.3	E
2	MMMMMM STEERING SUB-ASSEMBLY	1	15	6.3	25.0	6.7	E
6	AAAAAA WAGON BODY	0	0	0.0	30.0	0.0	E
7	XXXXXX REAR AXLE SUB-ASSEMBLY	0	0	0.0	25.0	0.0	E

DATE: 03-12-1984   (ACT)   (F10 - MAIN MENU)

Figure V.8

19.161

```
C# STATION #-DESCRIPTION                   WEEK-BEGIN AVAIL-MHRS REQ-MHRS

 4 000004 FINAL PRODUCT PACKAGING            03/12       20.00     22.00

 4 000004 FINAL PRODUCT PACKAGING            03/26       20.00     22.00
```

TE: 03-12-1984   RESCHEDULE RECOMMENDATIONS(Y/N)?:Y   (F10 - MAIN MENU)

Figure V.9

19.162

```
RESCHEDULE RECOMMENDATIONS FOR STATION: 000004 FINAL PRODUCT PACKAGING
OVERLOAD IN WEEK OF : 03/26

THE FOLLOWING PARTS WILL BE AFFECTED:
END        PART ZZZZZZ WEEK BEGINNING: 04/02
RESCHEDULE SALES ORDER #:000004 PART NUMBER: ZZZZZZ
CODE NAME: WAGON 1               PROMISED DATE: 04/03/84
PARTIAL OR ALL OF UNITS:  100
RESCHEDULE SALES ORDER #:000005 PART NUMBER: ZZZZZZ
CODE NAME: WAGON 1               PROMISED DATE: 04/04/84
PARTIAL OR ALL OF UNITS:  100




DATE: 03-12-1984        ENTER ANY KEY...        (ACT)       (F10 - MAIN MENU)
```

Figure V.10

19.163

C#	STATION #-DESCRIPTION	PLANNED-LABOR-COST	ACTUAL	REPLACE(Y/N)?
1	000001 STEEL STOCK FORMING STATION	8.00	0.00	N
2	000002 STEERING ASSEMBLY STATION	8.00	8.00	N
3	000003 AXLE ASSEMBLY STATION	8.00	0.00	N
4	000004 FINAL PRODUCT PACKAGING	8.00	8.00	N

TE: 03-12-1984   (ACT)   (F10 - MAIN MENU)

Figure V.11

19.164

```
           MODULE W - COMBINATION PROCESSING MODULE
_____

                                          YES/NO      PRINTER?
                                          (Y/N)        (Y/N)

RUN MODULE S - PRODUCT COSTING:

RUN MODULE P - PLANNING HORIZON UPDATE:

RUN MODULE T - MATERIALS REQUIREMENTS PLANNING:

RUN MODULE U - CAPACITY REQUIREMENTS PLANNING:

_____

        ENTER F1 TO BEGIN PROCESSING
_____

DATE: 03-12-1984                    (COM)    (F10 - MAIN MENU)
```

Figure W.1

19.165

END

DATE
FILMED

FEB.
1988